

AD-A044 413

WESTINGHOUSE ELECTRIC CORP PITTSBURGH PA ADVANCED ENE--ETC F/G 21/5
COMPACT CLOSED CYCLE BRAYTON SYSTEM FEASIBILITY STUDY.(U)

JUL 77 R E THOMPSON, G H PARKER, R L AMMON N00014-76-C-0706

UNCLASSIFIED

WAES-TNR-233

NL

OF 5
AD
A044413



AD-A0444413

12

WAES-TNR-233

JULY 1977

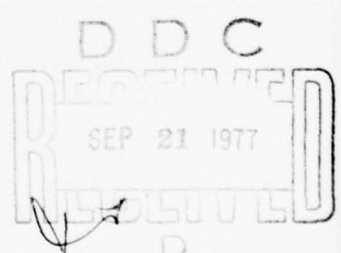


Advanced Energy Systems Division

**COMPACT CLOSED CYCLE
BRAYTON SYSTEM
FEASIBILITY STUDY**

FINAL REPORT - YEAR 1

**RESEARCH SPONSORED BY
OFFICE OF NAVAL RESEARCH
ARLINGTON, VIRGINIA 22217
UNDER CONTRACT
N00014-76-C-0706**



**WESTINGHOUSE ELECTRIC CORPORATION
Advanced Energy Systems Division
P.O. Box 10864
Pittsburgh, Pennsylvania 15236**

"Approved For Public Release; Distribution Unlimited"

"Reproduction in whole or in part
is permitted for any purpose of the
United States government."

SECURITY CLASSIFICATION OF THIS PAGE (When Data Entered)

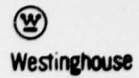
REPORT DOCUMENTATION PAGE		READ INSTRUCTIONS BEFORE COMPLETING FORM
1. REPORT NUMBER WAES-TNR-233	2. GOVT ACCESSION NO.	3. RECIPIENT'S CATALOG NUMBER
4. TITLE (and Subtitle) Compact Closed Cycle Brayton System Feasibility Study; Final Report - Year 1		5. TYPE OF REPORT & PERIOD COVERED Interim Final 20 May 1976 to 19 June 1977
7. AUTHOR(s) R. E. Thompson, G. H. Parker, R. L. Ammon, F. R. Spurrier, B. L. Pierce, L. E. Van Bibber of Westinghouse and A. Pietsch, E. A. Mock, B. J. Gray, B. B. Heath of AiResearch		6. PERFORMING ORG. REPORT NUMBER WAES-TNR-233
9. PERFORMING ORGANIZATION NAME AND ADDRESS Westinghouse Advanced Energy Systems Division P. O. Box 10864 Pittsburgh, Pennsylvania 15236		10. PROGRAM ELEMENT, PROJECT, TASK AREA & WORK UNIT NUMBERS
11. CONTROLLING OFFICE NAME AND ADDRESS Office of Naval Research 800 North Quincy Street Arlington, Virginia 22217		12. REPORT DATE July 1977
		13. NUMBER OF PAGES 423
14. MONITORING AGENCY NAME & ADDRESS (if different from Controlling Office)		15. SECURITY CLASS. (of this report) Unclassified
		15a. DECLASSIFICATION/DOWNGRADING SCHEDULE
16. DISTRIBUTION STATEMENT (of this Report) Approved for public release; distribution unlimited. Reproduction in whole or in part is permitted for any purpose of the United States government.		
17. DISTRIBUTION STATEMENT (of the abstract entered in Block 20, if different from Report)		
18. SUPPLEMENTARY NOTES		
19. KEY WORDS (Continue on reverse side if necessary and identify by block number) Gas turbine engines, marine surface propulsion, Brayton cycle, axial flow turbines, axial flow compressors, heat resistant alloys, high temperature materials tests, heat exchangers, bearings, gas bearings.		
20. ABSTRACT (Continue on reverse side if necessary and identify by block number) This report presents the results obtained from the first year of a three year study evaluating the feasibility of a closed Brayton cycle power conversion system for compact light weight naval propulsion plants. Because of the continuing nature of the program, this report is both a final report, for the tasks which were scheduled for completion in the first year, and a status report for those tasks which are scheduled for continuation into the second year of the program.		

ABSTRACT (Continued)

The contracted tasks for the first year have been accomplished as planned. The results confirm the validity of the technical and programmatic approach and indicate a high probability of successful demonstration of feasibility from the three year program. During this year, the studies have primarily been directed toward providing the technology research specifically directed toward Navy needs, which is necessary as a basis for concept definition and evaluation. These studies provide an integrated foundation for the subsequent efforts of the program.

The results to date are very encouraging. Reference case requirements have been established, including a unit output of 70,000 horsepower, turbine inlet gas temperature of 1700°F, and use of helium as the working fluid. Critical components such as bearings and compact heat exchangers have been evaluated and shown to have more than one suitable design solution. In each of these cases, the most desirable configuration has been selected for incorporation into the power conversion system design concept for further evaluation. The cross-counterflow tubular type of heat exchanger was selected for the design concept precooler and intercooler. The tube and shell type of heat exchanger was selected for the recuperator. Gas bearings were selected for inclusion in the design concept. Preliminary designs of the most critical portion of the turbomachinery rotor, the first stage turbine, have been derived. Material tests have provided data which are important to this study and also have provided significant extensions to the data available to the materials community. Interfaces with subsystems outside the power conversion system have been examined and considered in the design. An initial design concept has been defined for an integrated power conversion system which has the necessary characteristics and is appropriate for the most stringent requirements associated with the various energy sources, fossil or nuclear, which the Navy could desire to use.

ACCESSION NO.				
RTS	White Section <input checked="" type="checkbox"/>			
SGC	Gold Section <input type="checkbox"/>			
UNANNOUNCED				
JUSTIFICATION				
DT				
DISTRIBUTION/AVAILABILITY CODES				
Dist.	AVAIL. REG/R SPECIAL			
<table border="1"> <tr> <td>A</td> <td></td> <td></td> </tr> </table>		A		
A				



WAES-TNR-233
JULY 1977

COMPACT CLOSED CYCLE
BRAYTON SYSTEM
FEASIBILITY STUDY

FINAL REPORT - YEAR 1

RESEARCH SPONSORED BY
OFFICE OF NAVAL RESEARCH
ARLINGTON, VIRGINIA 22217
UNDER CONTRACT
N00014-76-C-0706

WESTINGHOUSE ELECTRIC CORPORATION
ADVANCED ENERGY SYSTEMS DIVISION
P. O. BOX 10864
PITTSBURGH, PENNSYLVANIA 15236

TABLE OF CONTENTS

	<u>Page No.</u>
1.0 INTRODUCTION	1-1
2.0 SUMMARY	2-1
2.1 GENERAL	2-1
2.2 SPECIFIC	2-1
3.0 COMPACT CLOSED CYCLE BRAYTON SYSTEMS	3-1
3.1 APPROACH TO FEASIBILITY STUDY	3-1
3.2 TOP LEVEL REQUIREMENTS	3-2
3.3 SECOND LEVEL REQUIREMENTS AND TRIAL DESIGN	3-5
3.4 CYCLE STUDIES	3-13
3.4.1 General	3-13
3.4.2 Nuclear System Parametric Studies	3-15
3.4.3 Fossil System Parametric Studies	3-31
3.5 CCCBS DESIGN CONCEPT	3-53
3.5.1 Design Concept (1st Definition)	3-55
3.5.1.1 General	3-55
3.5.1.2 Assembly	3-59
3.5.1.3 Design	3-63
3.5.2 Design Concept (2nd Definition)	3-83
3.6 REFERENCES	3-88
4.0 CRITICAL COMPONENT TECHNOLOGY EVALUATIONS	4-1
4.1 COMPACT HEAT EXCHANGERS	4-2
4.1.1 Gas to Gas (Recuperator) Heat Exchangers	4-2
4.1.1.1 Tube and Shell Recuperators	4-2
4.1.1.2 Plate-Fin Recuperator	4-10
4.1.1.3 Comparative Evaluation and Selection of Recuperator Type for CCCBS	4-20

TABLE OF CONTENTS (Continued)

	<u>Page No.</u>
4.1.2 Gas to Water (Precooler and Intercooler) Heat Exchangers	4-30
4.1.2.1 Shell and Tube Coolers	4-30
4.1.2.2 Finned Tube (Helical and Cross Counterflow)	4-31
4.1.2.3 Plate-Fin Cooler and Intercooler	4-41
4.1.2.4 Comparative Evaluation and Selection for CCCBS	4-44
4.2 HIGH PRESSURE (GAS GENERATOR) TURBINE	4-49
4.2.1 Blade State-of-the-Art	4-49
4.2.1.1 Materials-Currently Available	4-29
4.2.1.2 Materials-Expected Developments	4-54
4.2.1.3 Design	4-56
4.2.2 Disc State-of-the-Art	4-62
4.2.2.1 Materials-Currently Available	4-62
4.2.2.2 Materials-Expected Developments	4-64
4.2.2.3 Design	4-65
4.2.3 Concept Design for CCCBS	4-67
4.2.3.1 General	4-67
4.2.3.2 Blade Design	4-69
4.2.3.3 Disc Design	4-70
4.2.3.4 Stator Assembly	4-71
4.2.4 Aerodynamic Design Consideration	4-73
4.2.5 Blade Stress Analysis	4-80
4.3 BEARING EVALUATIONS	4-85
4.3.1 Oil Lubricated Bearings	4-85
4.3.1.1 Tilting Pad Thrust Bearings	4-88
4.3.1.2 Tilting Pad Journal Bearings	4-105
4.3.1.3 Lubrication System Design Consideration	4-116

TABLE OF CONTENTS (Continued)

	<u>Page No.</u>
4.3.2 Gas Bearings	4-120
4.3.2.1 Gas Bearing State-of-the-Art	4-122
4.3.2.2 Gas Bearing Characteristics	4-125
4.3.2.3 Gas Bearing Designs for CCCBS	4-132
4.3.2.4 Gas Bearing Recommendations	4-142
4.3.2.5 Auxilliary Equipment	4-142
4.3.2.6 Gas Bearing Technology Development	4-147
4.3.3 Comparative Evaluation and Selection	4-148
4.3.3.1 Bearing Comparisons	4-148
4.3.3.2 Conceptual Design Selection	4-153
4.4 REFERENCES	4-155
5.0 CCCBS/PROPULSION PLANT INTERFACES	5-1
5.1 ELECTRICAL POWER TRANSMISSION INTERFACE CONSIDERATIONS	5-1
5.1.1 General	5-1
5.1.2 Electrical Equipment System Considerations	5-6
5.1.2.1 AC Systems	5-7
5.1.2.2 DC Systems	5-13
5.1.2.3 AC/DC Systems	5-20
5.1.3 Candidate Propulsor Types	5-23
5.1.3.1 Types for Displacement Ships	5-24
5.1.3.2 Types for Lift Augmented Ships	5-25
5.1.4 Refrigeration System Configuration	5-26
5.1.5 Excitation Systems	5-28
5.1.6 Switchgear	5-29
5.1.7 Instrumentation	5-33
5.1.8 Size and Weight of Machines	5-34



Westinghouse

TABLE OF CONTENTS (Continued)

	<u>Page No.</u>
5.1.8.1 Superconducting Generator	5-36
5.1.8.2 Superconducting Motors	5-39
5.2 ENERGY SOURCE HEAT EXCHANGER INTERFACE CONSIDERATIONS	5-46
5.2.1 Heat Exchanger Design Considerations	5-46
5.2.2 Results of State-of-the-Art Survey	5-49
5.2.3 Conclusions	5-52
5.3 REFERENCES	5-56
6.0 MATERIALS TESTING AND EVALUATION	6-1
6.1 INTRODUCTION AND BACKGROUND	6-1
6.2 TEST EQUIPMENT AND PROCEDURE	6-2
6.2.1 Helium Gas Analysis	6-5
6.2.2 Test Procedure	6-6
6.3 ALLOY SELECTION, PROCUREMENT, AND CHARACTERIZATION	6-10
6.3.1 Alloy Selection	6-10
6.3.2 Procurement	6-13
6.3.2.1 Microstructure of Starting Material	6-13
6.3.2.2 Test Specimen Geometry	6-20
6.3.2.3 Tensile Properties of Test Materials	6-23
6.4 CREEP-RUPTURE TEST RESULTS AND EVALUATION	6-23
6.4.1 Alloy 713LC	6-26
6.4.2 Alloy IN 100	6-28
6.4.3 Alloy MAR-M509	6-33
6.4.4 Alloy MA-754	6-37
6.4.5 Alloy TZM	6-37
6.5 ACCOMPLISHMENTS	6-37
6.6 REFERENCES	6-42

TABLE OF CONTENTS (Continued)

	<u>Page No.</u>
APPENDIX A - Brayton Cycle Analysis	A-1
APPENDIX B - Frontal Area Characteristic of Tube and Shell Recuperators	B-1
APPENDIX C - First Stage Rotor Blade Stress Analysis Computer Printouts	C-1



Westinghouse

LIST OF ILLUSTRATIONS

<u>Figure</u>		<u>Page</u>
1.1	Generalized Logic of Program	1-3
1.2	Program Tasks and Schedule	1-4
1.3	System Scope CCCBS Study	1-5
2.1	CCCBS Design Concept (2nd Definition)	2-3
3.1	Trial Design Assembly	3-6
3.2	Helium Working Gas Flow Path	3-7
3.3	Power Conversion Heat Exchanger Envelopes	3-11
3.4	Bearing Loads	3-12
3.5	Lightweight Nuclear Powerplant	3-16
3.6	Brayton Cycle Temperature Entropy Diagrams	3-19
3.7	System Weight Comparison of Cycles	3-22
3.8	Reactor Power Input Comparison of Cycles	3-23
3.9	Gas to Gas Heat Exchanger Capacity Comparison of Cycles	3-25
3.10	Gas to Liquid Heat Exchanger Capacity Comparison of Cycles	3-26
3.11	Turbo-Compressor Capacity Comparison of Cycles	3-27
3.12	40,000 HP Helium Turbomachinery	3-32
3.13	12,000 HP Engine Match Point	3-34
3.14	12,000 HP Engine Core	3-35
3.15	12,000 HP Engine	3-36
3.16	Xe-He Gas Mixtures	3-37
3.17	Heat Source Performance Versus Specific Weight	3-39
3.18	Fossil Fueled Intercooled	3-40
3.19	Fossil Fueled Nonintercooled	3-41
3.20	Intercooled	3-42
3.21	Nonintercooled	3-43
3.22	Fossil Fueled Intercooled	3-45

LIST OF ILLUSTRATIONS (Continued)

<u>Figure</u>		<u>Page</u>
3.23	Fossil Fueled Nonintercooled	3-46
3.24	70,000 HP Engine Summary	3-47
3.25	70,000 HP Engine Match Point	3-49
3.26	70,000 HP Engine Core	3-50
3.27	70,000 HP Engine Heat Source	3-51
3.28	70,000 HP Engine	3-52
3.29a	CCCBS Design Concept (1st Definition) Sheet 1	3-56
3.29b	CCCBS Design Concept (1st Definition) Sheet 2	3-57
3.30a	CCCBS Design Concept (2nd Definition) Sheet 1	3-84
3.30b	CCCBS Design Concept (2nd Definition) Sheet 2	3-85
4.1	Surface Compactness Versus Tube Diameter	4-3
4.2	Typical Types of Tube to Header Joints (Reference 2)	4-5
4.3	Proportional Frontal Area Versus Reynolds Number for Axial Flow in Tubes	4-7
4.4	Recuperator Module Concept Using Hex Ended Tubing	4-9
4.5	Recuperator Module	4-12
4.6	1000-2000 HP Closed Brayton Engine	4-13
4.7	12,000 HP Engine Core	4-14
4.8	Compact Engine Packaging	4-15
4.9	Curved Recuperator Module Construction	4-16
4.10	Exploded View Annular Recuperator/Cooler Assembly	4-17
4.11	Recuperator Assembly Envelope	4-19
4.12	Recuperator Packaging	4-21
4.13	Flow Path Through Heat Exchangers	4-22
4.14	Unwrapped View of the Recuperator	4-23
4.15	Detail of Module Tube Ending and Heater	4-32

LIST OF ILLUSTRATIONS (Continued)

<u>Figure</u>		<u>Page</u>
4.16	Pre-Cooler Detail of Module Headering	4-33
4.17	Layout of Precooler and Intercooler - Hexagonal Modular Concept	4-34
4.18	Finned Tubes	4-37
4.19	Cooler/Intercooler	4-39
4.20	Cooler/Intercooler Packaging	4-40
4.21	Flow Path Through Heat Exchangers	4-42
4.22	Unwrapped View of the Cooler	4-43
4.23	Stress Rupture Data (Larson-Miller Plot) for Selected Nickel Base Alloys	4-50
4.24	Stress Rupture Data for Selected Refractory Alloys	4-55
4.25	Variation of Centrifugal Stress with Hub/Tip Ratio	4-57
4.26	Variation of Bending Stress with Blade Chord	4-61
4.27	5 Stage HP Turbine	4-68
4.28	Correlation of Measured Turbine Stage Efficiencies	4-75
4.29	High Pressure Turbine Row IR-Base Station	4-78
4.30	High Pressure Turbine Row IR-Tip Station	4-79
4.31	Extended Blade Root and Platform	4-81
4.32	Kingsbury Tilting Pad Thrust Bearing	4-90
4.33	Thrust Bearing with Directed Lubrication	4-92
4.34	Limits of Safe Operation	4-94
4.35	Effect of Shaft Speed and Load on Maximum Babbitt Temperature (10-1/2 Inch Thrust Bearing)	4-95
4.36	Effect of Load and Shaft Speed on Power Loss (10-1/2 Inch Double Thrust Bearing)	4-99
4.37	Lube Oil Distribution to Active and Inactive Elements of 267 mm (10-1/2 Inch Bearing)	4-100
4.38	Waukesha Tilting Pad Journal Bearing	4-106
4.39	Kingsbury Tilting Pad Journal Bearing	4-108
4.40	Pioneer Tilting Pad Journal Bearing (Fluid Pivot)	4-110

LIST OF ILLUSTRATIONS (Continued)

<u>Figure</u>	<u>Page</u>
4.41 Orion Tilting Pad Journal Bearing	4-112
4.42 Foil Bearing Applications	4-123
4.43 Brayton Rotating Unit-Foil (BRU-F)	4-124
4.44 540,000 RPM Foil Bearing System	4-126
4.45 BRU-F Foil Bearing Machine Shock Tests	4-129
4.46 70,000 HP CBC Engine Bearing Support Schematic	4-133
4.47 Gas Bearings	4-134
4.48 Journal Bearing Design	4-136
4.49 Thrust Bearing Design	4-138
4.50 Gas Generator L.P. Compressor Thrust and Journal Bearings	4-143
4.51 Gas Generator L.P. and H.P. Speed Journal Bearings	4-144
4.52 Gas Generator/Power Turbine Journal Bearings	4-145
4.53 Power Turbine Journal and Thrust Bearings	4-146
 5.1 70 KHP (52.5 MVA) Generator 13.8 KV	5-37
5.2 70 KHP (52.5 MVA) Generator 13.8 KV	5-38
5.3 50,000 HP Motor	5-40
5.4 50,000 HP Motor	5-41
5.5 5000 HP Motor 1500 RPM, 13.8 KV	5-43
5.6 5000 HP Motor 1500 RPM, 13.8 KV	5-44
 6.1 Schematic Diagram of Modified Ultra-High Vacuum Creep Units	6-3
6.2 Photograph of Modified Ultra-High Vacuum Creep Units	6-4
6.3 Schematic Diagram of Ultra-High Purity Helium Creep Test Unit	6-8
6.4 Microstructure of As-Cast Alloy 713LC	6-15
6.5 Microstructure of As-Cast IN100	6-16
6.6 Microstructure of As-Cast MAR-M509	6-17
6.7 Microstructure of MA 754	6-18



Westinghouse

LIST OF ILLUSTRATIONS (Continued)

<u>Figure</u>		<u>Page</u>
6.8	Microstructure of Stress-Relieved TZM	6-19
6.9	Creep-Rupture Specimen Geometries for Various Test Materials	6-21
6.10	Photographs of Creep-Rupture Test Specimens	6-22
6.11	Creep Rupture Life of Alloy 713LC	6-27
6.12	Creep-Rupture Curves for As-Cast Alloy 713LC	6-29
6.13	Creep-Rupture Curves for As-Cast Alloy 713LC	6-30
6.14	Creep-Rupture Curves for As-Cast Alloy 713LC	6-31
6.15	Stress Rupture Life of IN 100	6-32
6.16	Creep-Rupture Curves for As-Cast IN 100	6-34
6.17	Creep-Rupture Life of MAR-M-509	6-35
6.18	Creep-Rupture Curves for As-Cast MAR-M-509	6-36
6.19	The Creep-Rupture Life of MA 754	6-38
6.20	Creep-Rupture Life of TZM	6-39
6.21	Creep-Rupture Curves for Stress Relieved TZM	6-40

LIST OF TABLES

<u>Table</u>		<u>Page</u>
3.1	State Points and Component Efficiencies	3-9
3.2	Cycle Analysis Assumptions	3-18
3.3	Cycle Parameters at the Selected Pressure Ratios	3-28
3.4	Brayton Cycle Comparative Evaluations	3-29
4.1	Shell and Tube Recuperator Geometry	4-8
4.2	Evaluation Criteria for Recuperators	4-24
4.3	Physical Size and Weight Impact of Recuperator on Powerplant	4-26
4.4	Recuperator Concept Evaluations	4-28
4.5	Precooler and Intercooler Shell and Tube Geometry	4-35
4.6	Cooler Concept Evaluations	4-46
4.7	Contributions to Total Turbine Rotor Expansion 17 Inch Tip Diameter Closed Brayton Cycle First Stage Rotor	4-63
4.8	High Pressure Turbine Stage 1 Blade Geometry	4-77
4.9	Oil Flow and Head Removal Requirements	4-117
4.10	Hydrostatic Bearing System	4-135
4.11	Hydrodynamic Foil Bearings 100 PSI Ambient Pressure	4-140
4.12	Improved Integrated Foil Journal Bearing Design	4-141
4.13	Evaluation Criteria for Bearings	4-149
4.14	Oil Bearing/Gas Bearing Trade-off Study	4-150
5.1	Basic Design Considerations	5-48
5.2a	Metallic Heat Exchangers from Various Technologies	5-50
5.2b	Metallic Heat Exchangers from Various Technologies	5-51
5.3	State-of-the-Art of Ceramic Heat Exchangers (Continuous Flow Types)	5-53
5.4	Heat Source Heat Exchanger State-of-the-Art	5-54



Westinghouse

LIST OF TABLES (Continued)

<u>Table</u>	<u>Page</u>
6.1 Typical Helium Gas Analysis	6-9
6.2 Selected Alloys and Nominal Compositions	6-11
6.3 Chemical Analysis of Test Material	6-14
6.4 Tensile Properties of Test Materials	6-24
6.5 Creep-Rupture Data for Selected CCCBS Materials at 1700°F	6-25

1.0 INTRODUCTION

This report presents the results obtained from the first year of a three year study evaluating the feasibility of a closed Brayton cycle power conversion system for compact light weight naval propulsion plants. Because of the continuing nature of the program, this report is both a final report, for the tasks which were scheduled for completion in the first year, and a status report for those tasks which are scheduled for continuation into the second year of the program.

The first year studies have defined the reference requirements, provided detailed considerations of critical component technologies, defined critical interface conditions that must be considered, accomplished significant materials testing in helium, and provided initial definitions of the Compact Closed Cycle Brayton System (CCCBS) design concept. These results are valuable in themselves and also in that they indicate the probability of successful demonstration of feasibility, the program objective.

The overall objective of the program is to conduct the analytical study and experimental research required to evaluate and to demonstrate feasibility of a closed Brayton cycle power conversion system for a low volume, light weight marine propulsion plant. The objective is also to insure relevance of power conversion system study results to all candidate applications, including recognition of the various energy sources which the Navy could desire to use in the future.

In order to accomplish the very broad objective while minimizing program cost and efforts, the program has been carefully planned and structured to provide the results that are necessary through evaluations in response to one combined set of most stringent, representative requirements. The technology evaluations are therefore more than sufficient for applications with less stringent requirements. In this way, detailed studies of one configuration provide results which meet or exceed the necessary conditions for feasibility assessments of a wide range of potential closed Brayton cycle power conversion system applications.

The generalized logic of the three year program is illustrated in Figure 1.1. The logic recognizes that it is basic to determination of feasibility that evaluations be conducted in the context of a set of requirements which are representative of those which would be placed upon the power conversion system in actual use. All efforts which provide the inputs to the end evaluations must be accomplished in the context of the same set of requirements if the results are to be valuable and are to make maximum uses of the resources applied. The overall technical approach of the program is designed to provide the baseline, continually integrated studies and integrated evaluations that are necessary to fulfill the program objective.

The tasks which comprise the program are shown in Figure 1.2. The first year tasks are directed toward definition of requirements, critical technology and interface assessments, and critical material tests leading to the initial definition of the power system design concept to be used for evaluation of feasibility.

The scope of the power conversion system for this study, illustrated in Figure 1.3, excludes specific energy sources, specific loads, and specific heat rejection subsystems. However, consideration is given in this study to the reasonable ranges of conditions for each of these interfaces to insure that the study results meet or exceed the conditions which may be required.

The stated objective requires that consideration be given throughout the study to what is required to achieve a compact, light weight powerplant. This in turn requires a very compact power conversion system. Satisfactory derivation of a compact light weight powerplant can only be accomplished through consideration of the total system as a whole rather than as an assembly of components. Thus, although portions of the total closed Brayton system are outside the scope defined for detail study, total system considerations are included as necessary to properly define and evaluate the compact closed cycle Brayton power conversion system of this study.

This study has been accomplished under the guidance of Mr. J. A. Satkowski, Director Power Programs of the Material Sciences Division of the Office of Naval Research and LCDR W.R. Seng

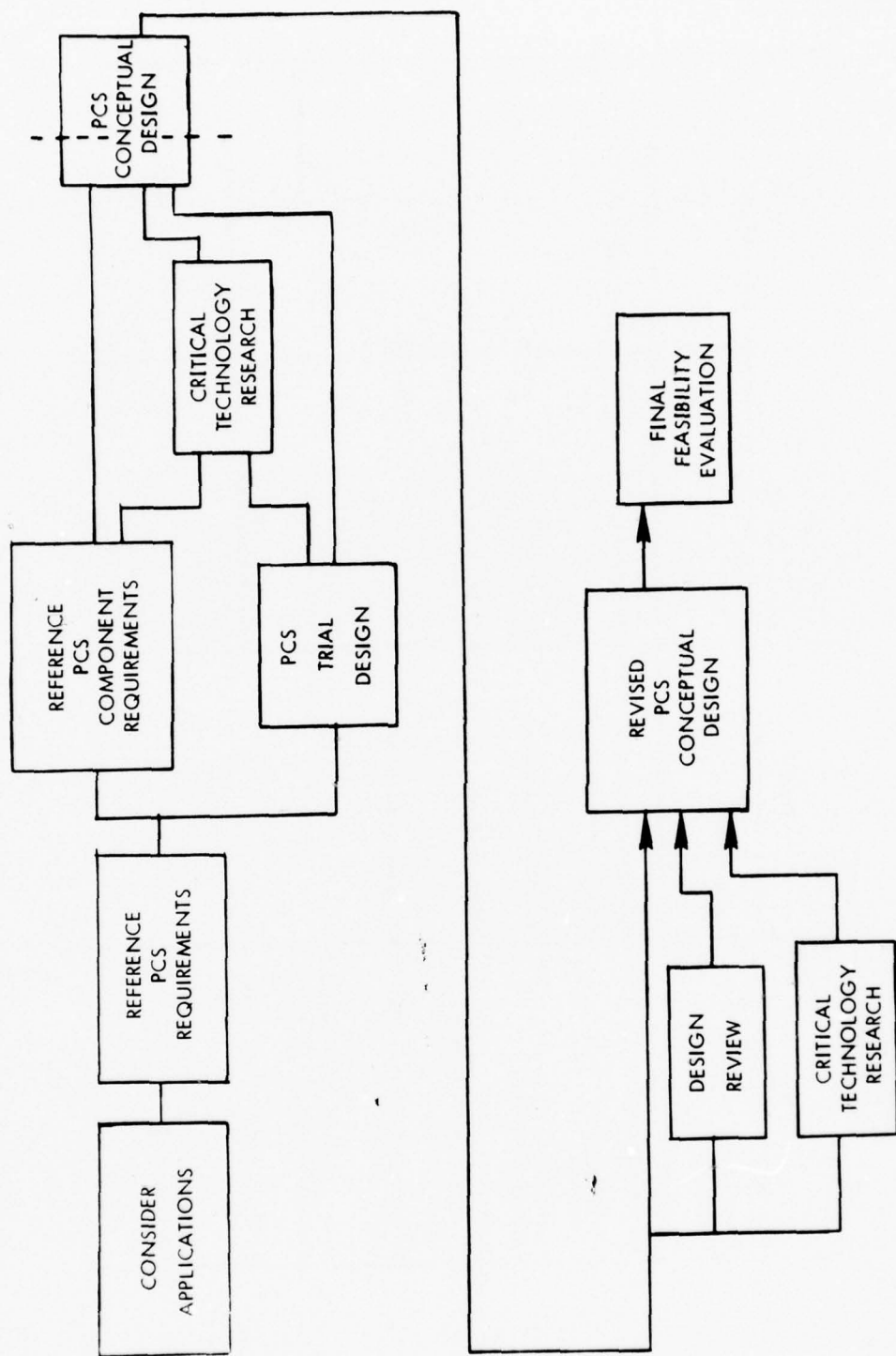
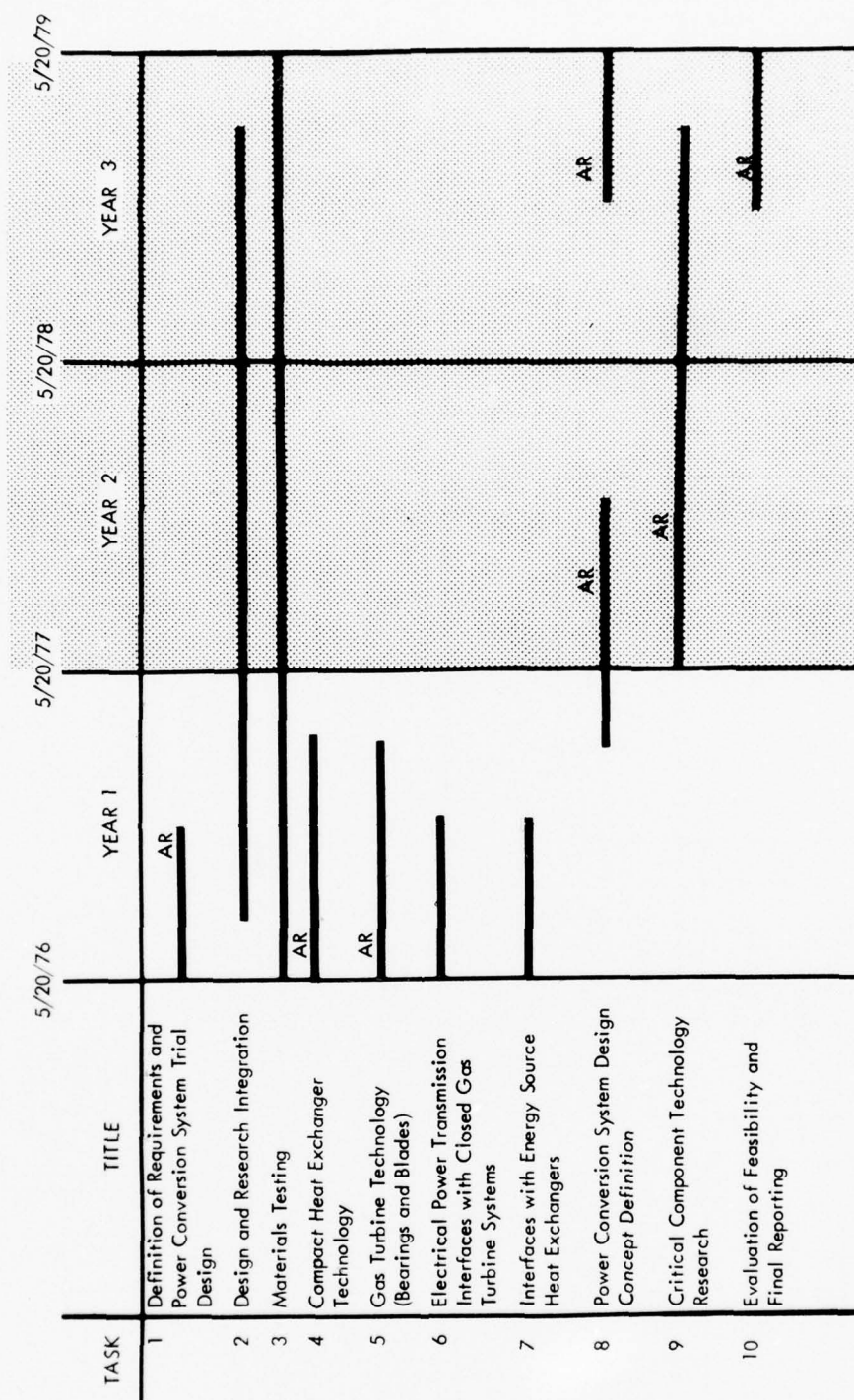


Figure 1.1 Generalized Logic of Program



Westinghouse



AR - INDICATES TASKS WITH MAJOR AEROSPACE CONTENT

Figure 1.2 Program Tasks and Schedule

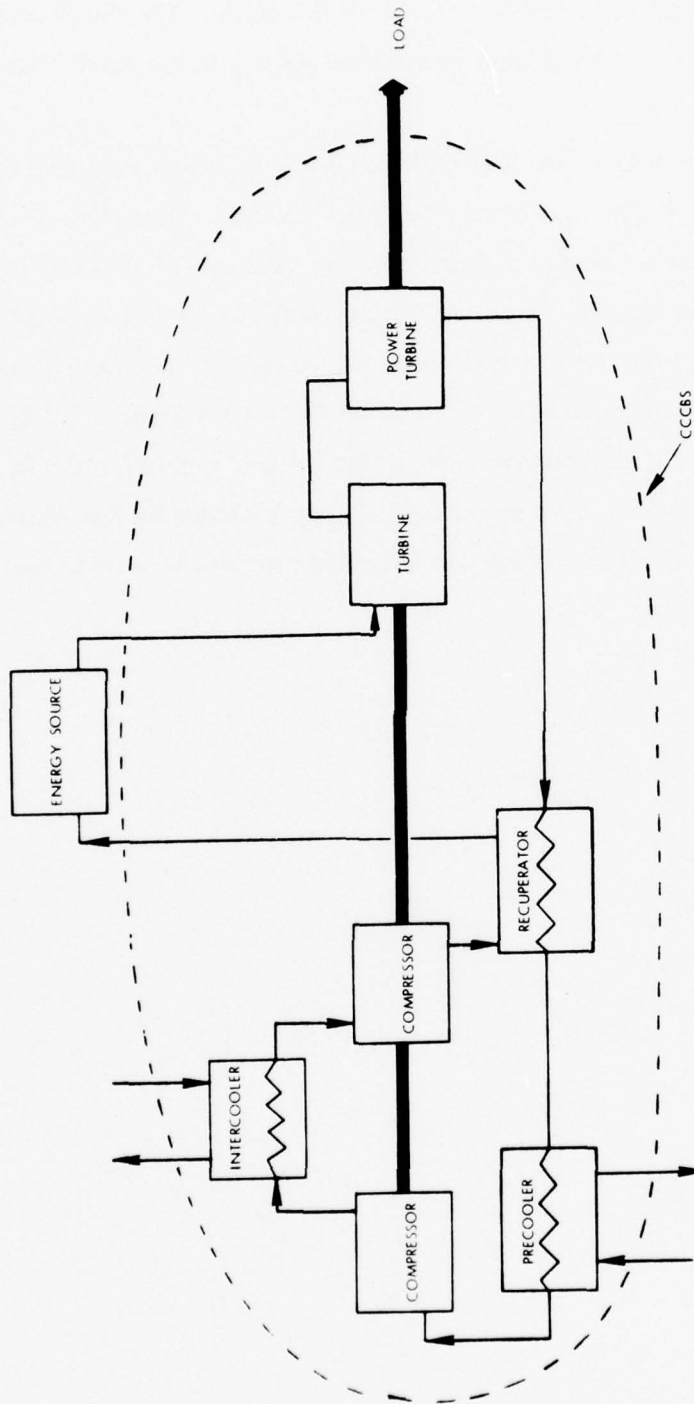


Figure 1.3 System Scope CCCBS Study



Westinghouse

who has served as the ONR Scientific Officer for this study. The direction and technical input of Mr. Satkowski and LCDR Seng have contributed greatly to the results that have been achieved.

The study has been directed by the Westinghouse Advanced Energy Systems Division with Mr. R. E. Thompson as Project Manager. The study has been accomplished by a team including the Garrett Corporation's AiResearch Manufacturing Company of Arizona, where Mr. A. Pietsch served as Project Manager, and various Westinghouse Divisions with appropriate applicable expertise. Specific contributions to this report by AiResearch include the system optimizations of Section 3.4.3, the heat exchanger studies of Sections 4.1.1.2 and 4.1.2.2, the gas bearing studies of Section 4.2.2.2, and contributions to the integrated evaluations in these areas. Specific contribution to the report as Section 5.0, was provided by the Westinghouse Electro-Mechanical Division. Other Westinghouse Divisions provided support in their areas of specific expertise during the study.

2.0 SUMMARY

2.1 GENERAL

The contracted tasks for the first year have been accomplished as planned. The results confirm the validity of the technical and programmatic approach and indicate a high probability of successful demonstration of feasibility from the three year program.

During this year, the studies have primarily been directed toward providing the technology research specifically directed toward Navy needs, which is necessary as a basis for concept definition and evaluation. These studies provide an integrated foundation for the subsequent efforts of the program.

The results to date are very encouraging. Critical components such as bearings and compact heat exchangers have been evaluated and shown to have more than one suitable design solution. In each of these cases, the most desirable configuration has been selected for incorporation into the power conversion system design concept for further evaluation. Preliminary designs of the most critical portion of the turbomachinery rotor, the first stage turbine, have been derived. Material tests have provided data which are important to this study and also have provided significant extensions to the data available to the materials community. Interfaces with subsystems outside the power conversion system have been examined and considered in the design. An initial design concept has been defined for an integrated power conversion system which has the necessary characteristics and is appropriate for the most stringent requirements associated with the various energy sources, fossil or nuclear, which the Navy could desire to use.

2.2 SPECIFIC

Some specific highlights are as follows:

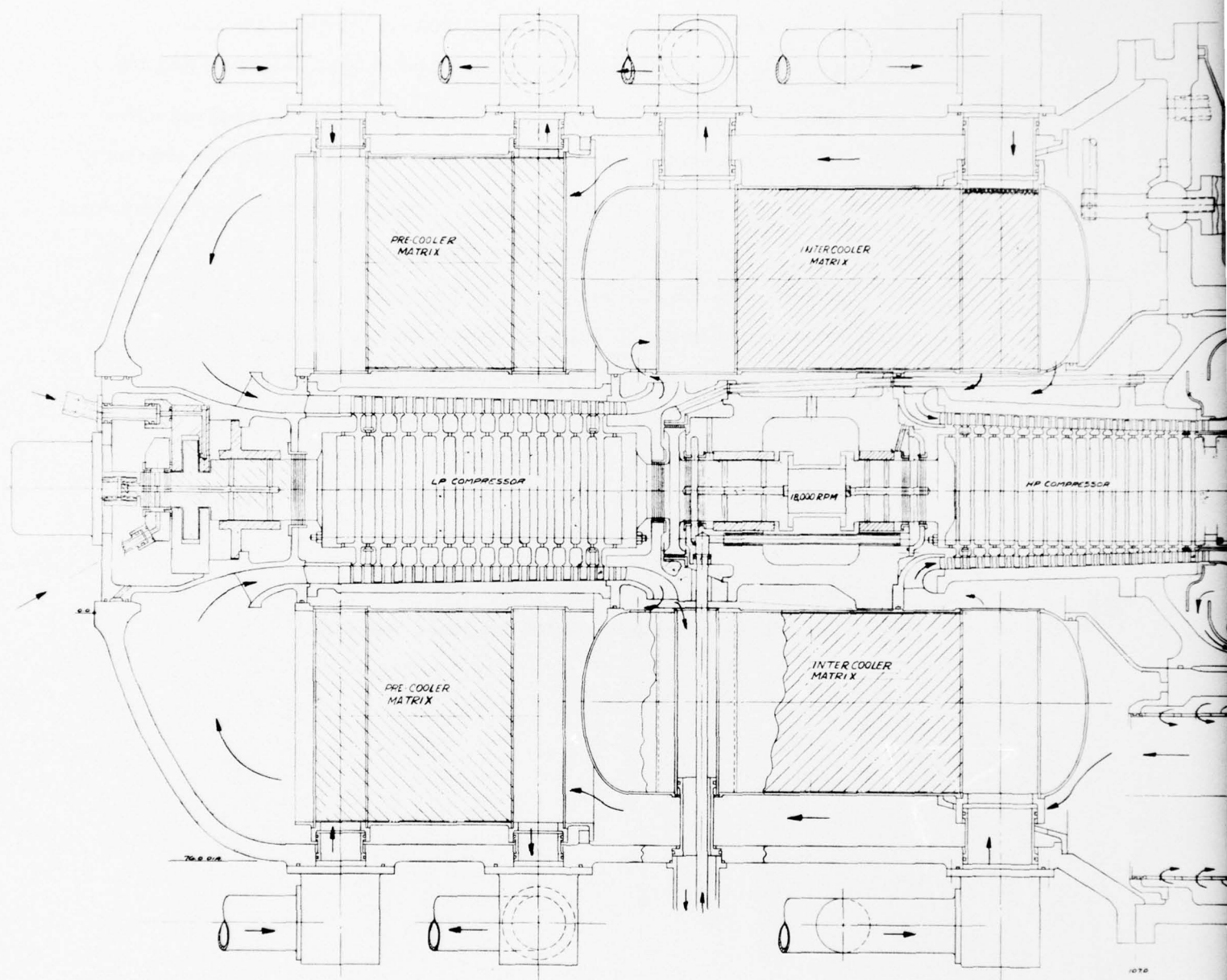
- Representative most stringent requirements have been defined and coordinated with ONR to form a basis for the studies. Among the reference requirements



Westinghouse

are a unit output of 70,000 horsepower, turbine inlet gas temperature of 1700°F and use of helium as the working fluid.

- The recuperated and intercooled cycle has been shown to be most attractive for the anticipated Navy requirements, and is also the most severe test of feasibility.
- Two preliminary iterations of a power conversion system design concept have been derived for further maturing during years two and three. Figure 2.1 shows the Design Concept (2nd Definition) status. The design concept has attractive characteristics and appears to have a high probability of supporting ultimate conclusions of feasibility.
- Various configurations of compact heat exchangers have been studied and it has been shown that there are several alternates, each of which could fulfill the requirements. The apparent suitability of more than one type of heat exchanger enhances the feasibility of the power conversion system. For the precooler and intercooler, cross-counterflow finned tube exchangers have been selected for incorporation into the design concept for evaluation. For the recuperator, the shell and tube configuration has been selected.
- Both gas bearings and oil lubricated tilting pad bearings have been studied and found to be capable of fulfilling the requirements. Gas bearings have been selected for incorporation into the design concept.
- A turbomachinery rotor concept providing the necessary passive thrust balancing has been defined and incorporated into the design concept for further evaluation.
- The most critical turbomachinery rotating stage has been studied and an un-cooled turbine blade configuration defined.



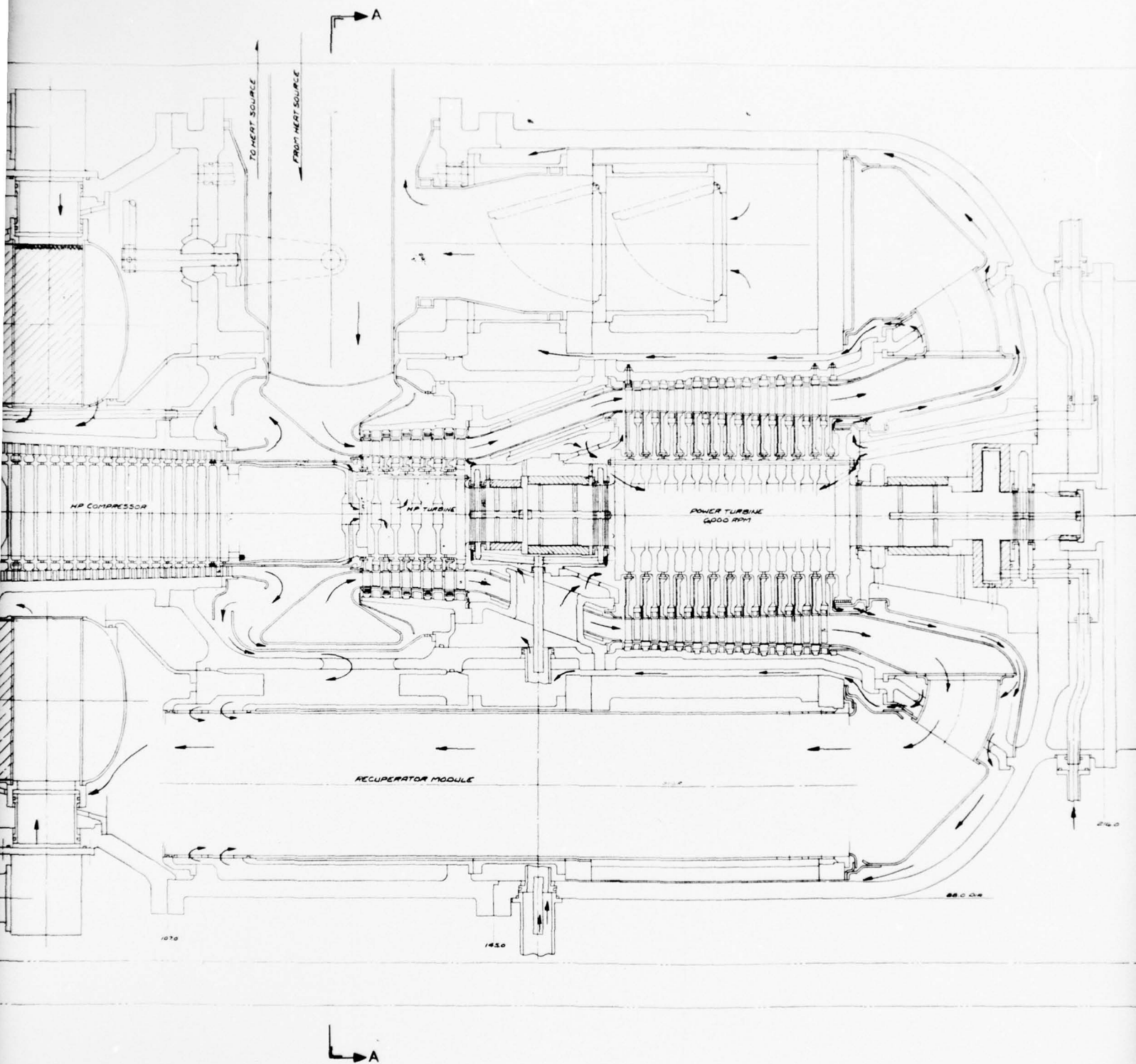


Figure 2.1 CCCBS Design Concept (2nd Definition)

9



Westinghouse

- Interface considerations of importance that could be expected with use of candidate electrical power transmission systems have been identified and scoped.
- Interfaces and considerations of importance that could be expected with use of fossil fueled energy source heat exchangers have been identified and scoped.
- Creep rupture material tests in ultra-pure helium at turbine inlet temperatures have provided important indications of the probability of suitable material availability. 28,924 total hours of creep-rupture testing on five candidate materials have been accomplished in ultra-pure helium at temperatures up to 1700°F. These data are supplemented by 22,023 total hours of testing in air at temperatures up to 1700°F. These tests provide baseline data for subsequent testing with candidate impurities. These data also provide valuable new additions to the data available to the materials community.
- No deleterious effects of the helium environment on the creep-rupture behavior of the materials tested have been observed.

3.0 COMPACT CLOSED CYCLE BRAYTON SYSTEMS

As discussed in Section 1.0, the feasibility study of the CCCBS is being accomplished over a three year period and is being performed within the context of the most stringent powerplant requirements which can reasonably be foreseen. These requirements provide the foundation for the program, and are summarized in Sections 3.2 and 3.3. Cycle parametric studies have been accomplished and are documented in Section 3.4. Definition of the CCCBS Design Concept is in process and the status of the design is shown in Section 3.5.

3.1 APPROACH TO FEASIBILITY STUDY

Top level requirements placed upon the power conversion system have been identified considering the various applications of the power conversion system which could occur as well as typical powerplant/ship interfaces. The philosophy used to guide the determination of requirements is that they must be representative of the ranges which reasonably can be expected, and they must be sufficiently stringent to adequately test the realism of a closed Brayton system for potential naval propulsion applications. Also imposed on these studies is the philosophy or constraint that the design must be based on existing technology or technology which is already being developed. This requirement is practical because of the broad spectrum of technologies already developed or under development. This constraint leads to confidence in the evaluation and demonstration.

An early "Trial Design" of the power conversion system was necessary because representative requirements were also needed for each of the major components of the power conversion system. These second level requirements must consider the component interactions which result from integration of the components into a total power conversion system which is responsive to the top level requirements. The trial design provides the framework for these considerations by translating the top level requirements into a design concept which identifies the interactions and also identifies those parameters and features which are critical to the demonstration of feasibility. The trial design was only derived to the detail necessary to

support definition of component requirements and to establish the critical technology areas. The trial design also provided the basis for the later more detailed "Design Concept" definition.

3.2 TOP LEVEL REQUIREMENTS

In order to accomplish the objective of the program, feasibility must be evaluated in the concept of a coherent set of representative top level requirements. These requirements must be representative of those which could reasonably be expected to be placed upon CCCBS plants for naval propulsion applications. The requirements must also be sufficiently stringent to support generalized conclusions regarding feasibility. Based upon these considerations, a set of top level requirements were defined and coordinated with ONR. The major requirements are itemized and discussed below.

Reference Application - Surface Effect Ship

The needs of various types of naval vessels that could make use of compact, lightweight powerplants were considered. Because the study is directed toward compact, lightweight powerplants, emphasis was placed upon the advanced vessel types for which powerplant compactness and/or lightweight are important parameters. Surface Effect Ships (SES), hydrofoil and advanced displacement ships are the major types of vessels given emphasis.

The limitations placed upon the powerplant by the vessel are most demanding for the SES application. This particular application tends to be very limiting with regard to space, weight, accessibility and load variability. It also requires consideration of power conversion system matching with electric power or mechanical power transmission systems. Indications are that powerplants which fulfill the requirements of SES applications would also meet or exceed the requirements of other applications. Therefore, the SES was selected as the reference application with the recognition that the CCCBS design studies must not include features which would exclude other applications.

Unit Power Conversion Assembly Output - 70,000 SHP

Studies have indicated that unit power for the various applications can be expected to range from 20,000 to 100,000 SHP with the more likely unit power required in the range of 60,000 to 100,000 SHP. The needs of the high performance ships appear to favor unit powers toward the high end of the range. To make the results of this study most generally applicable, the unit power selected for study should be appropriate for the high power range, but also should be reasonably scalable to lower powers. It was determined that a unit power level of 70,000 SHP would fulfill these criteria and would also provide the benefit to this study of direct infusion of the results of prior Westinghouse funded studies.

In addition to unit power level, it was also determined that the CCCBS power conversion assembly must be capable of operation in the configuration of two power conversion assemblies coupled in parallel to a single energy source. Such a configuration has been found to be needed for some installations such as large SES. Because such an installation imposes more stringent conditions on the CCCBS evaluations, this configuration capability was established as a requirement.

It was also established that, for general applicability, the CCCBS evaluations must include provisions to accept fixed and variable speed loads.

Specific Weight of Power Conversion System - 2 lb/SHP

The most restrictive weight limitations are placed by the SES application. On the order of 15 lb/SHP has been determined to be a reasonable value for the total weight of powerplant and fuel. Of this amount, on the order of 2 lb/SHP is a reasonable, but stringent, upper limit for the CCCBS power conversion system. However, it must be recognized that the feasibility of the CCCBS is enhanced if the specific weight is lower than this value and the study should emphasize attainment of lower weight.

Lifetime - 10,000 Equivalent Full Power Hours (40,000 Operating Hours)

The most stringent lifetime requirement was determined through consideration of the need for the CCCBS to be compatible with any of the various energy sources that the Navy may desire to use. Application with a nuclear energy source would place the most stringent lifetime requirement upon the CCCBS power conversion assembly because of the long reactor lifetimes that are possible and the desire for the power conversion assembly to have a comparable lifetime.

Studies have shown that reactor lifetimes of 10,000 Equivalent Full Power Hours (EFPH) can be planned for naval applications. The duty cycle is, of course, a function of the ship and its normal mission. Since some applications can have a normal duty cycle approximating 25 percent, the CCCBS evaluations must also consider that the total operating time to achieve 10,000 EFPH may be as high as 40,000 hours.

Shock - MIL-S-901C (Navy)

The system shall be suitable for qualification in accordance with the requirements of MIL-S-901C (Navy).

Heat Rejection - To Seawater at 85° F

All candidate applications can utilize seawater for heat rejection, with the exception of Air Cushion Vehicles (ACV). However, the ACV is considered to be a special case with the least likelihood of actual implementation with a CCCBS. Therefore, heat rejection shall be considered to be to seawater. For these feasibility evaluations, a conservatively high seawater temperature of 85° F shall be used as the most stringent requirement.

3.3 SECOND LEVEL REQUIREMENTS AND TRIAL DESIGN

To amplify the top level requirements discussed above, a set of second level requirements has been established at the component level. These requirements are reviewed below in conjunction with a brief description of the trial design which aided in specifying the component requirements.

Integrated Assembly

To achieve the compactness needed for low specific weight, an integrated assembly of the turbo-machinery and heat exchangers is needed. The trial design as shown in Figure 3.1 illustrates this integrated assembly.

The flow path of the working gas is illustrated in simplified form in Figure 3.2. High temperature gas from the heat source enters the module through the inner pipe of a concentric duct and enters the high pressure inlet plenum. The high pressure turbine extracts the work necessary to drive both low and high pressure compressors which are of the axial type for high efficiency. After leaving the high pressure turbine, the gas flows to the low pressure turbine (power turbine) where the work necessary to drive the load is extracted. A free power turbine was specified because of the requirement to be able to interface with either fixed or variable speed loads. The gas then enters the low pressure side of the recuperator and is subsequently cooled in the precooler. The gas is then compressed in the low pressure compressor, cooled in the inter-cooler and further compressed in the high pressure compressor. The high pressure gas from the compressor then flows through the high pressure side of the recuperator, where it is heated by the energy extracted from the low pressure side gas. The heated gas then passes into a collector manifold from which it is piped through two check valves in series to the outer annulus of the concentric duct to the heat source.

Working Fluid and Pressure Level - Helium, 1500 psia Turbine Inlet Pressure

Fossil fired closed Brayton systems tend to optimize with mixtures of inert gases (e.g., helium-xenon) while direct gas cooled nuclear systems require the use of helium. Based upon the study



Westinghouse

TURBINE - COMPRESSOR - HEAT EXCHANGE PACKAGE

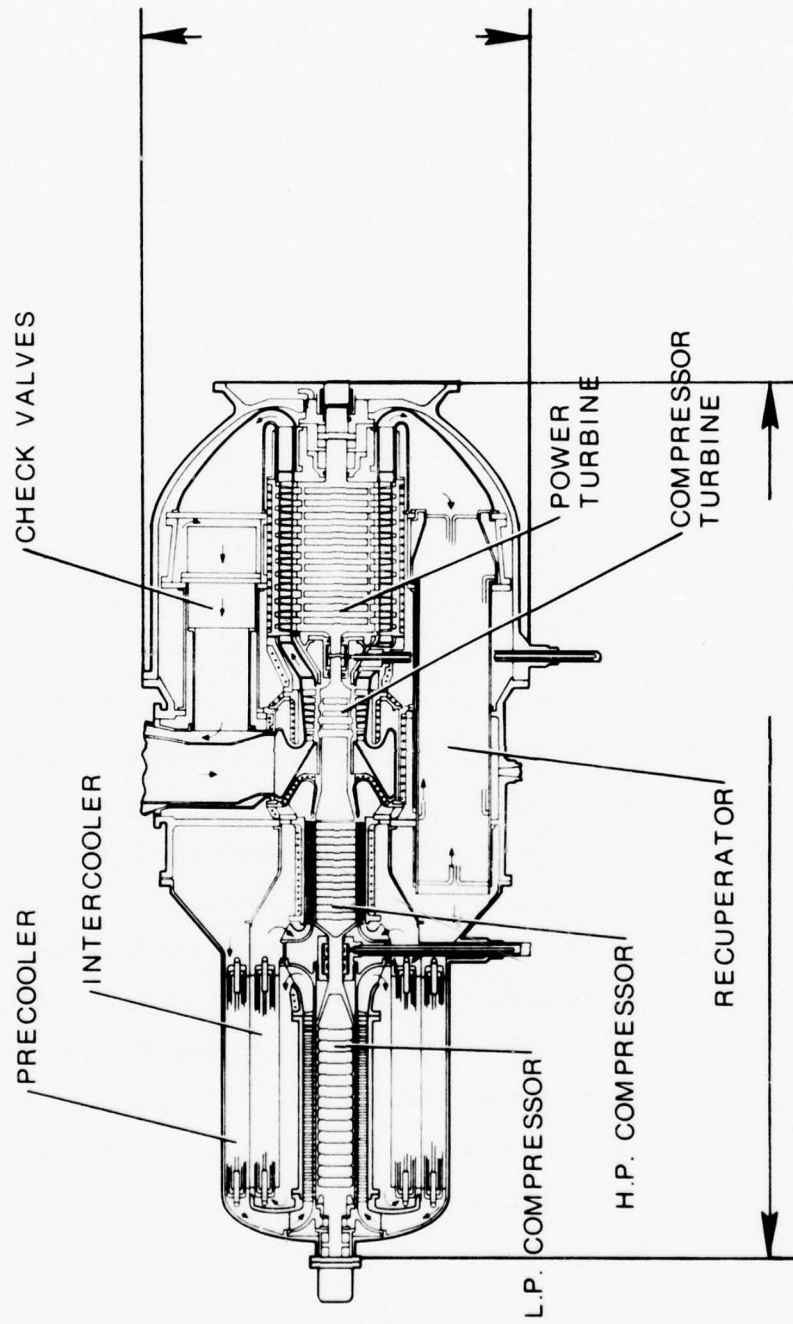


Figure 3.1 Trial Design Assembly

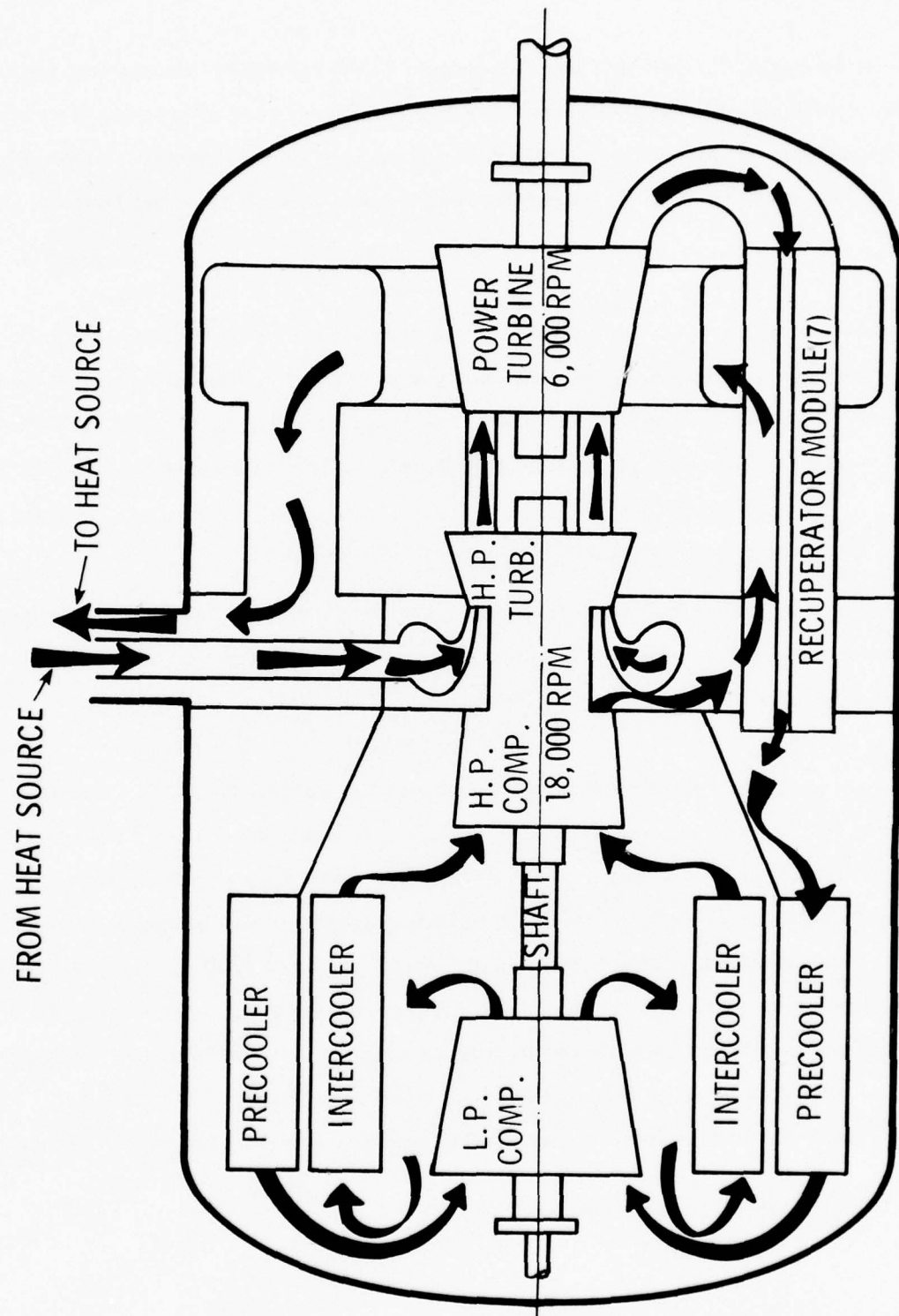


Figure 3.2 Helium Working Gas Flow Path

guidelines for use of the most stringent requirement in the feasibility evaluations, helium was specified as the working fluid. Helium cycle turbomachinery must incorporate more compressor and turbine stages and helium is the more difficult working fluid to contain. The results of the CCCBS studies will then meet or exceed the requirements imposed by mixed inert gas working fluids.

The requirement for compactness dictates the use of as high a system pressure as is practical. Considerations of the compressor, turbine, seals, and of prior studies during the MGCR closed Brayton cycle turbomachinery program (Reference 1) indicate that 1500 psia is a relatively high, yet achievable, turbine inlet pressure level. Therefore, 1500 psia was established for the studies.

State Points and Component Efficiencies

The temperatures, pressures, helium flow rates, and component efficiencies are specified in Table 3.1. These values were derived from work on the trial design and parametric studies and form a basis for the component requirements.

Special note is given to the selection of the turbine inlet temperature (TIT). Cycle efficiency considerations dictate the use of the highest practical temperature. Based on expected materials properties, it was concluded that a design turbine inlet temperature on the order of 1700°F pushes but does not exceed the state-of-the-art for uncooled turbine blades and stators in inert gases. A gas cooled nuclear heat source could supply helium at 1700°F. Based on the results of the state-of-the-art survey and reasonable design practices using superalloys, fossile energy sourc heat exchangers can be expected to produce working fluid gas temperatures less than 1700°F. Therefore, a reference design TIT of 1700°F was selected as the most stringent goal. The latitude exists to reduce the turbine inlet temperature for extended off-design point (part-power) operations.

TABLE 3.1
STATE POINTS AND COMPONENT EFFICIENCIES

	TEMPERATURES - °F		INLET	PRESSURE - PSIA	COMPONENT	EFFICIENCY - %
	INLET	OUTLET				
ENERGY SOURCE	805	1730		1580	-	-
TURBINE	1700	1275		1500	90	
POWER TURBINE	1275	960		840	90	
RECUPERATOR	935	435		470	80	
	280	810		1600		
PRECOOLER	435	100		460	98	
COMPRESSOR	100	305		450	85	
	100	280		875		

NOMINAL 135 LB/ SEC HELIUM FLOW RATE,
 150 MW(t) HEAT SOURCE
 70,000 HP OUTPUT

Heat Exchanger Envelope

Figure 3.3 summarizes the envelope dimensions that were specified as a result of the trial design work. These dimensions were used in the evaluations of recuperators and coolers that are discussed in Section 4.1.

Bearing Loads

Figure 3.4 illustrates the bearing loads that were specified as a result of the trial design work. These loads were used in the bearing evaluation studies discussed in Section 4.3.

SPACE AVAILABLE, INCLUDING HEADERING

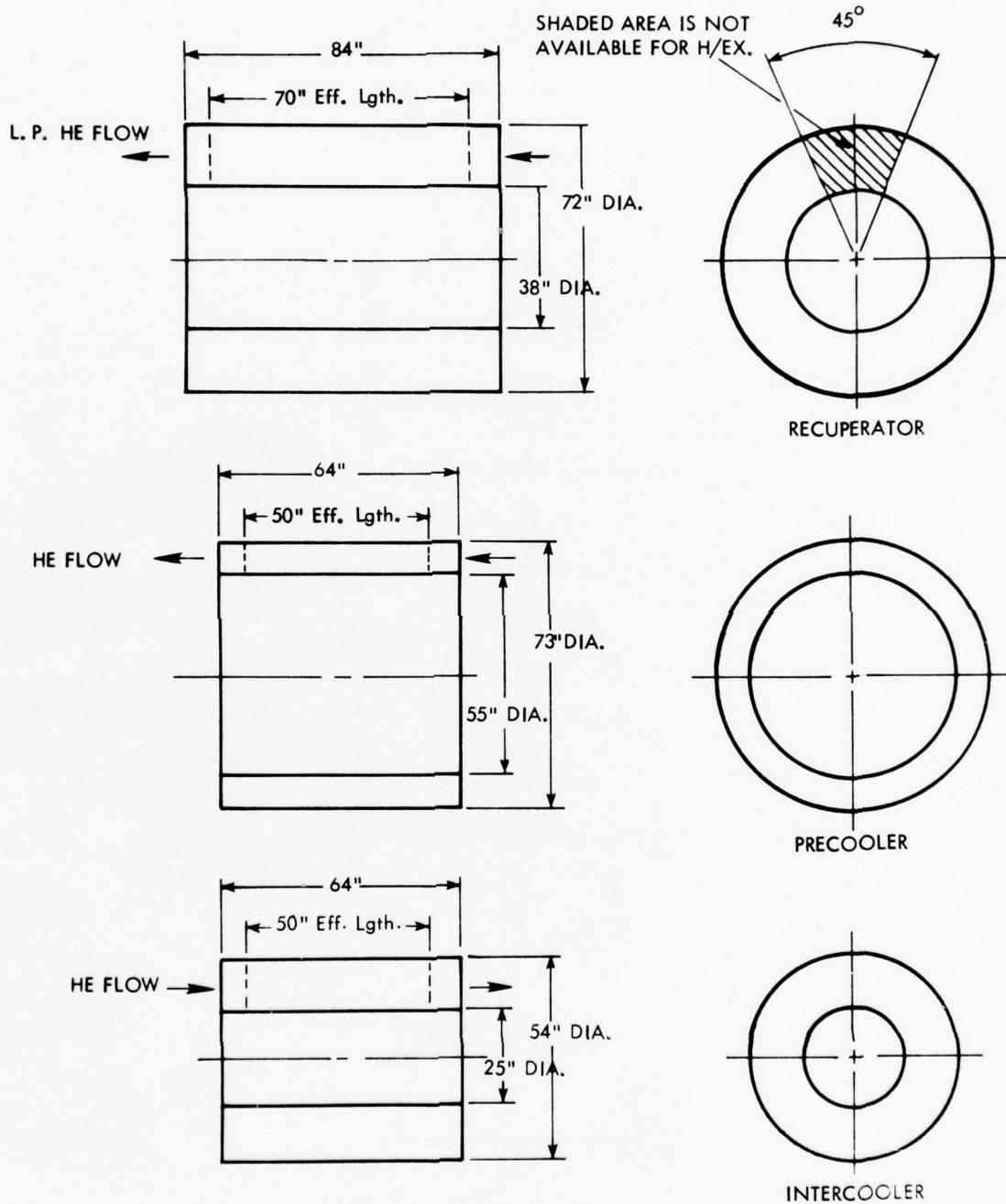


Figure 3.3 Power Conversion Heat Exchanger Envelopes

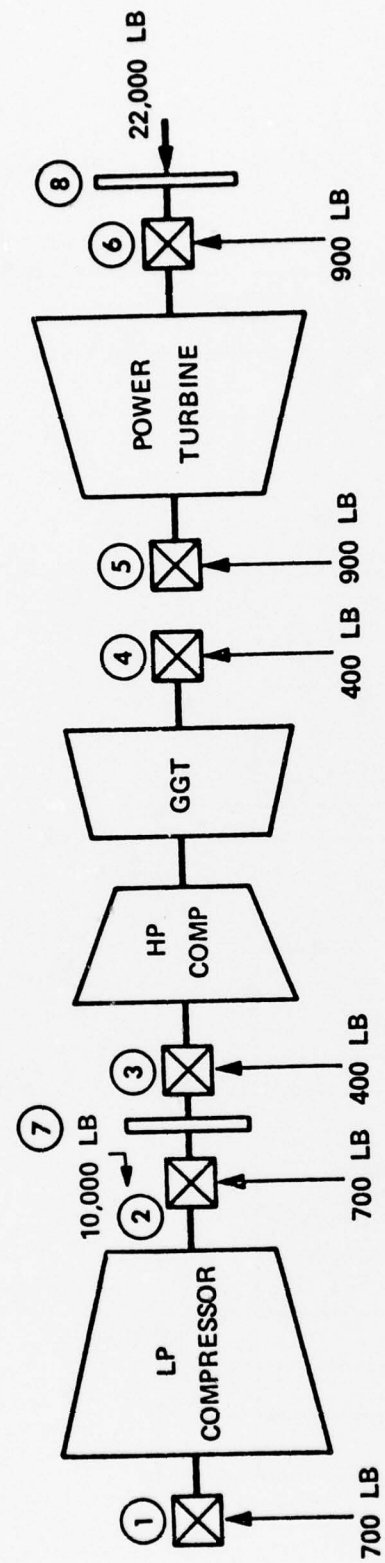


Figure 3.4 Bearing Loads

3.4 CYCLE STUDIES

3.4.1 General

Cycle studies were performed considering both nuclear and fossil energy sources. The primary purpose of these studies was to determine the CCCBS configuration to be studied; i.e., simple cycle, recuperated, or recuperated-intercooled. Additionally, these parametric studies were accomplished to provide broad perspective and visibility regarding the effects of cycle optimizations. These analyses also aided in the definition of the most stringent CCCBS requirements. In Section 3.4.2, a summary of the trends that developed in analyzing the nuclear CCCBS option is presented. Results of cycle study utilizing a fossil fueled energy source are presented in Section 3.4.3.

Based upon the early cycle study results, and the results of prior Westinghouse and AiResearch studies, it was apparent that the nuclear system application would place the most stringent requirements upon the CCCBS. Both fossil and nuclear system studies indicated the desirability to conduct the CCCBS feasibility studies based upon a recuperated-intercooled cycle. It was therefore determined that the most useful application of efforts in the nuclear system would be parametric studies around the selected CCCBS design point, and in the fossil system studies would be in considering the potential gains in performance through the use of high performance energy source exchangers.

Of the inert gases, helium has been shown to be the most desirable working fluid for nuclear systems. For many reasons, helium is an excellent choice as working fluid for a fossil fired closed gas turbine as well. In addition, gas cooled reactor and fossil fired gas turbine system temperatures, pressures and mass flow rates can be very compatible. Thus, accomplishment of the CCCBS feasibility studies using helium is warranted.

Certain considerations also indicate the desirability, in some applications, to optimize fossil fired systems using a mixed inert gas working fluid. In order to give visibility to some of these considerations, a portion of the fossil fired cycle studies built upon the results of earlier



Westinghouse

MARAD sponsored studies to illustrate the application of CCCBS technology to advanced fossil fired systems using a mixed gas working fluid. For these cycle studies, it was judged to be most effective to adapt the MARAD results even though there are some configuration differences from the CCCBS. The results are valid, however, as indications of potential capabilities for advanced fossil fired systems utilizing the gas turbine technologies evaluated in the overall CCCBS study.

3.4.2 Nuclear System Parametric Studies

This Section presents the results of cycle analyses for reactor driven compact closed cycle Brayton power conversion systems. In defining representative interface characteristics that can be expected of advanced nuclear energy source, as they relate to a closed Brayton cycle power conversion system, the lightweight nuclear reactor configuration given in Reference 2 is used. In the 200 to 400 MW (t) range the nuclear subsystem weight is estimated by the following relationship:

$$W_T \approx 82460 (Q)^{0.353} \quad (1)$$

where W_T is in pounds and Q in the reactor thermal rating in megawatts. The nuclear subsystem (NSS) weight includes the reactor, lateral support structure, reflector, support plates, pressure vessel, shielding and part of the containment vessel (See Figure 3.5).

The pressure loss through the reactor subsystem (shield inlet to plug shield exit) is approximated by:

$$\Delta P = \frac{51.2}{\rho} \left(\frac{W}{Q} \right)^2 \quad (2)$$

where ΔP is in lbs/in^2 , ρ is the inlet helium density in lbs/ft^3 and W is the flow rate in lbs/sec . This approximation is predicated on a fixed set of core variables such that the core flow area is proportional to reactor power and is also appropriate for the range of 200-400 MW (t).

The plant lifetime 40,000 hours between major overhauls at 25% duty cycle of 10,000 effective full power hours (EFPH) establishes neutron fluence levels in the various reactor components. The reactor materials are affected by both fluence level and temperature level. Since the reactor inlet fluid is used to cool the components, the maximum reactor



Westinghouse

COMPONENTS INCLUDED IN
WEIGHT RELATIONSHIP
(EQUATION 1)

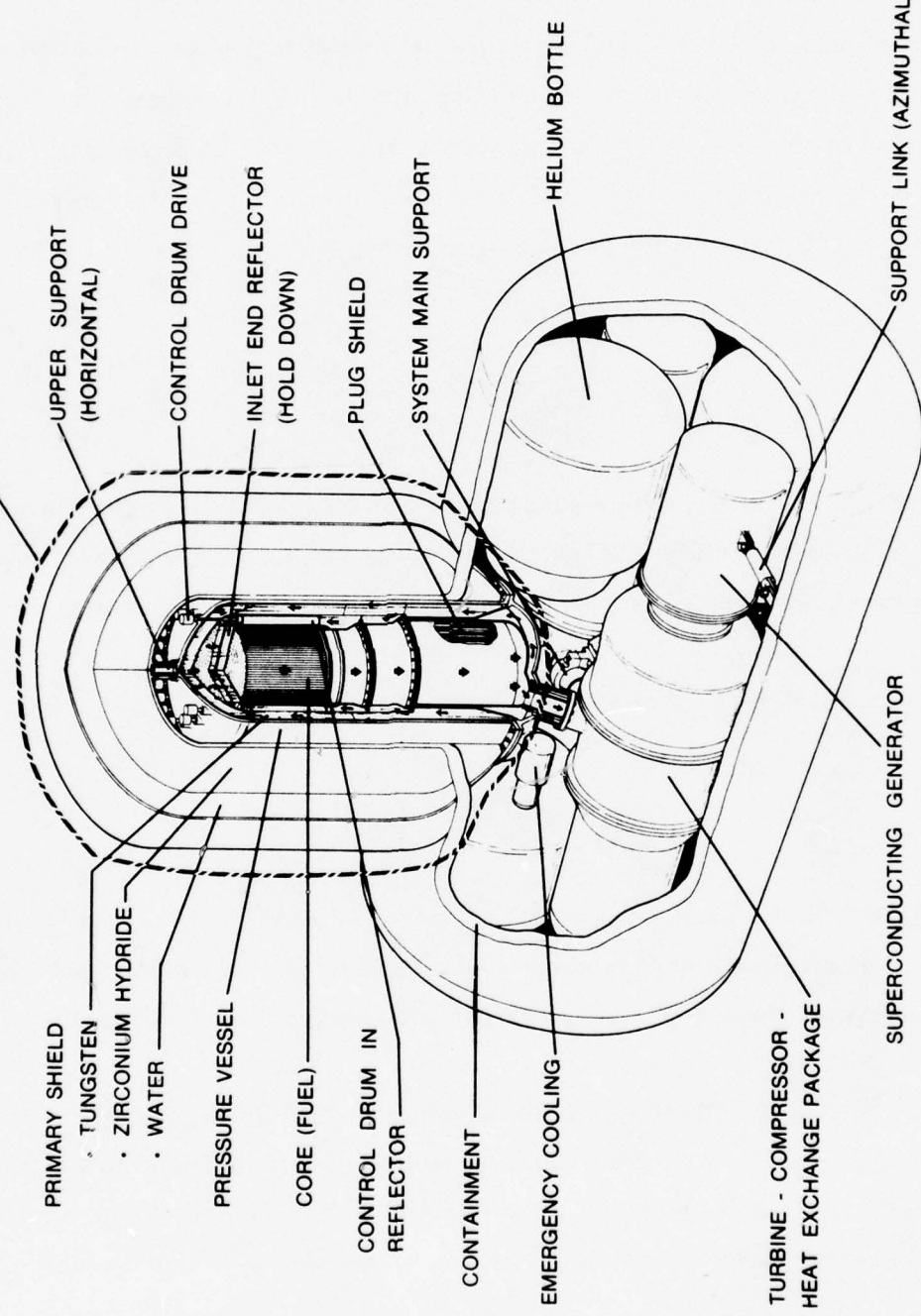


Figure 3.5 Light Weight Nuclear Powerplant

inlet temperature that should be considered in parametric studies is 1000°F. At temperatures below 1000°F, the effects on materials due to temperature levels and fast neutron irradiation is projected to be acceptable.

The assumptions used in this Brayton cycle analysis are given in Table 3.2. Both the compressor and turbine efficiencies are conservatively set about 2 percent less than that obtained in the MGCR program (Reference 1). The assumption of no bleed flows, (only for the parametric studies) produces slightly higher cycle efficiencies, but should have negligible effect on the comparisons of the different Brayton cycles. The cooling water inlet temperature of 95° allows an approach temperature difference of 10°F with the seawater inlet temperature of 85°F. In this study the pressure loss in the heat exchanger increases as heat exchanger effectiveness increases (see Appendix A) and the pressure loss increases as more heat exchangers types (adding intercooling for example) are added to the cycle.

In estimating the weight trends of the various Brayton cycle powerplants, two major weights were considered; the nuclear subsystem and the turbo-compressor heat exchanger containment vessel. These two components normally make up about 70 percent of the total powerplant weight. For the fixed output power assumption, the power transmission and auxiliaries weights are constant and make up about 20 percent of the powerplant weight. This then leaves the turbo-compressor heat exchange package and control gas storage that make up the remaining 10 percent of the powerplant weight which is variable, but this variation is small and is neglected in these parametric studies.

In this study six types of Brayton cycles were investigated. The temperature entropy diagrams for the six cycle types are shown in Figure 3.6. In all cycle types, two turbo-compressor units are assumed to be located in the containment with the heat exchangers wrapped around the turbo-compressor units. The heat exchangers are assumed to effectively utilize 75 percent of the annulus area around the Turbo-compressors. The spacing between the turbo-compressor units is assumed to be 12 inches and with a 6 inch clearance between the turbo-compressor unit and



Westinghouse

TABLE 3.2
CYCLE ANALYSIS ASSUMPTIONS

- Compressor Efficiency 85%
- Turbine Efficiency 90%
- Cooling Water Inlet Temperature 95°F
- Turbine Flow Equals Compressor Flow (no bleed flows)
- Pressure losses in the heat exchangers are proportional to their effectiveness
- In water cooled heat exchangers the capacity rate ratio equals 0.18
- Auxiliaries require 1% of the output power
- In heat exchangers the ratio of flow rate to free flow area is constant and the ratio of flow rate to wetted perimeter is constant
- The overall heat transfer conductance is constant for each type of heat exchanger
- Helium is the working fluid
- Intercooled cycles have equal high and low compressor pressure ratios
- Output power (net) of 140,000 HP (total of power conversion modules)
- Two turbo-compressor heat exchanger units located inside steel containment

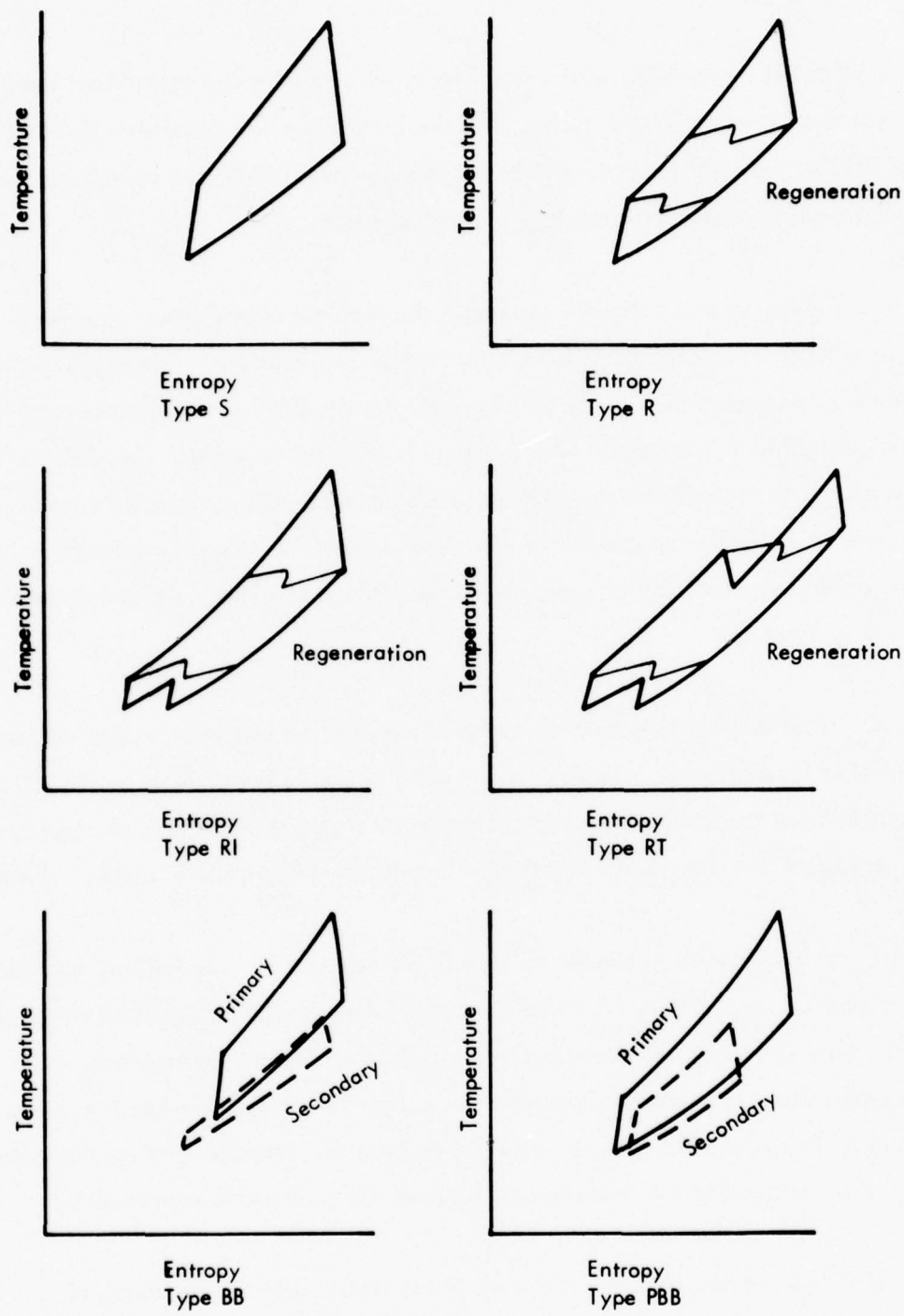


Figure 3.6 Brayton Cycle Temperature Entropy Diagrams

the containment inner wall. In the first four types of cycles the cylindrical length of the containment is assumed to be 216 inches. For the Bi-Brayton and Precooled Bi-Braxton systems (BB and PBB), the cylindrical length is 144 inches. In all cases the containment is assumed to be a right circular cylinder with 2 to 1 ellipical heads.

Figure 3.6 (Type S) schematically represents the simplest closed cycle arrangement with the gas going first through the compressor then through the heat source (reactor) where energy is added, then expanded through the turbine and, finally, back to the compressor through a heat exchanger called a "precooler" where energy is rejected to a sink. The addition of regeneration is one of the primary means by which the simple Brayton cycle can be made more efficient. Regeneration is simply the transfer of heat from the turbine exhaust gas to the compressor discharge gas before that gas has energy externally supplied. This is shown schematically in Figure 3.6, Type R.

The addition of intercooling reduces the work required for compression and thus more energy is available for shaft work, and also allows more effective use of regeneration at higher pressure ratios than would be feasible with the recuperated (Type R) cycle, thereby reducing component sizes as well as the flow rate. This cycle (Type RI) is schematically shown in Figure 3.6.

The next cycle, Type RT, is similar to Type RI differing in that the helium, after passing through the recuperator, is partially expanded through a turbine. The helium then passes through the heat source and through the power turbine. This cycle feature is that the pressure level at peak cycle temperature is reduced. However, the energy source pressure loss increases, which causes a reduction in cycle efficiency as compared to Type RI. Proponents of such a system cite potential advantages of lowered pressure level at the peak cycle temperature.

In the Bi-Brayton cycle (BB), the net work of the simple primary Brayton cycle is used to compress the secondary gas, which is then heated in the intermediate heat exchanger (removes reject heat from the primary gas) before passing to the power turbine and precooler. In this

cycle, the power turbines, generators and precoolers are located externally to the containment vessel. This then minimizes the components inside the containment, and does not introduce cooling water inside the containment. This cycle uses a form of pneumatic power transmission similar to one of the forms studied for the Naval Ship Research and Development Center (Reference 3). The next cycle (PBB) is the Bi-Brayton cycle with precooling added to the primary loop. This adds a component (precooler) inside the containment, but reduces compression work which increases cycle efficiency.

The characteristics of these cycles for various turbine pressure ratios, heat exchanger effectivenesses and turbine inlet temperatures are given in Appendix A. The above cycles can be compared on the basis of some of their functional requirements, these requirements are divided into four major categories:

1. System Weight
2. Input Energy Requirement (Fuel)
3. Heat Transmission Capacity (Heat Exchangers)
4. Work Conversion Capacity (Turbomachinery)

The totals for each category for a given turbine inlet temperature of 1700°F are given in Figures 3.7 through 3.11. The curves are plotted with heat exchanger effectiveness for the various cycles that produce the lowest system weight and the curves are terminated at a reactor inlet temperature of 1000°F if encountered. The recuperated cycles (R , RI and RT) have the characteristics of increasing reactor inlet temperature at low pressure ratios as the pressure ratio is decreased, while the non-recuperated cycles have an increasing reactor inlet temperature as pressure ratio increases. The pre-cooled Bi-Brayton (PBB) cycle has the lowest system weight.

Figure 3.8 shows the relationship of the reactor heat input versus turbine pressure ratio for the various cycles. The curves are as expected, with the recuperated and intercooled (RI) cycle requiring the lowest heat input.

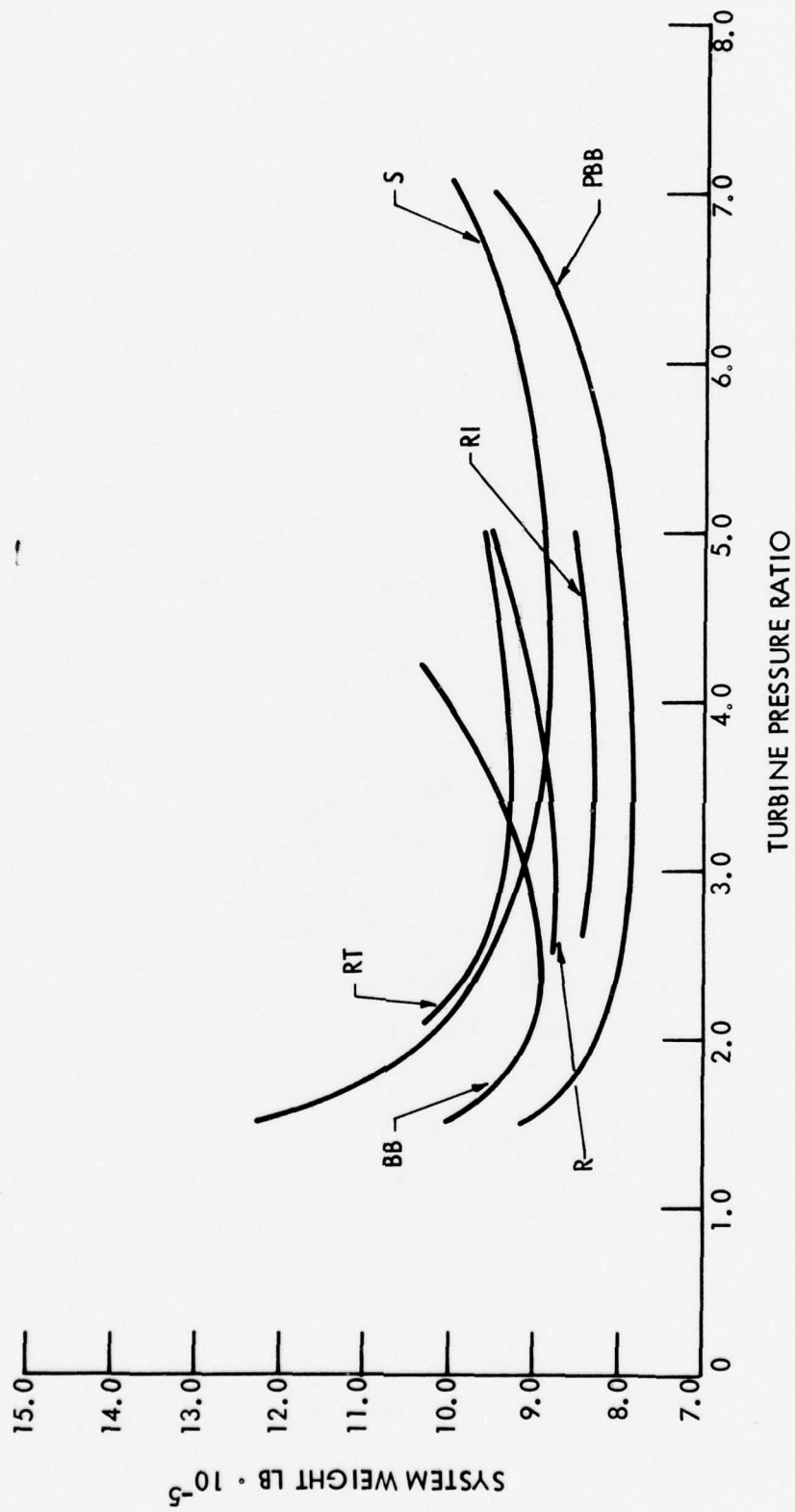


Figure 3.7 System Weight Comparison of Cycles

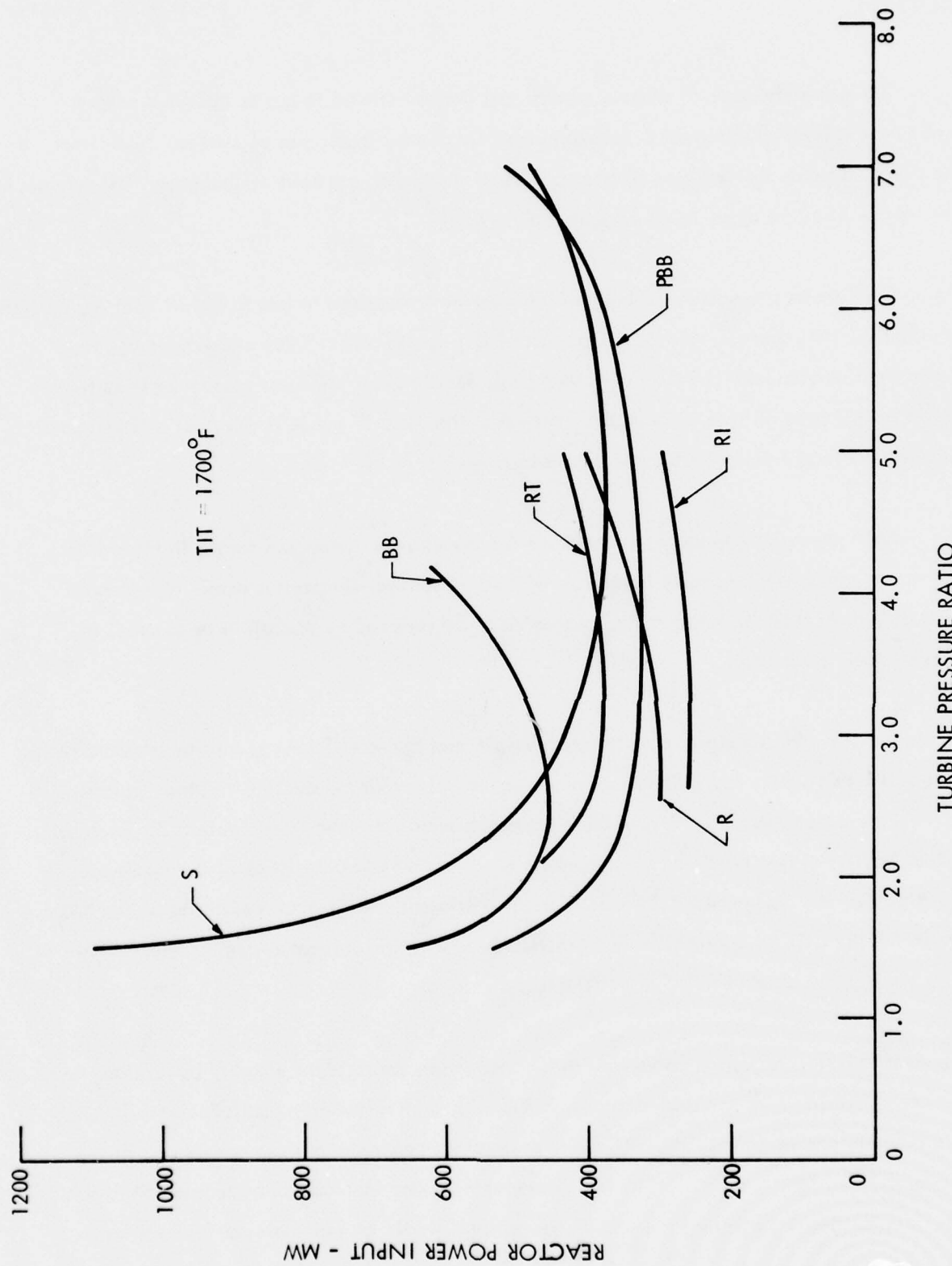


Figure 3.8 Reactor Power Input Comparison of Cycles

Figure 3.9 shows the amount of heat which must be transmitted in gas to gas (recuperator intermediate heat exchangers) heat exchangers for the various types of cycles. Note that the simple Brayton cycle (Type S) does not have any gas to gas heat exchangers. The recuperated (Type R) cycle drops to zero regeneration limit.

Figure 3.10 shows the amount of heat which must be transferred in gas to liquid heat exchangers (precoolers, intercoolers, reject). Since all of the cycles reject their waste heat in gas to liquid heat exchangers, the most efficient cycle should have the least amount of heat transferred in this type of heat exchanger. Note that the Type RI cycle is the most efficient and requires the least heat rejection of the various cycles.

The turbo-compressor capacity requirements for the various cycles are shown in Figure 3.11. The turbo-compressor capacity is the sum of all turbine and compressor work. The curves generally show that the turbo-compressor work to be reduced by operating at as small as pressure ratio as possible.

Considering the NSS weight, containment weight and cycle efficiency, turbine pressure ratios were selected slightly lower than the minimum weight/maximum cycle efficiency points. Some cycle parameters, for these selected pressure ratios, are shown in Table 3.3. Evaluation of the Brayton cycles consisted of comparing a number of characteristics of the cycles, each of which met the design point performance. The criteria used in the evaluation of the Brayton cycles for the CCCBS application are grouped in four major categories, which are: effect on ship, operability, cost and risk of development.

The effect on ship is broken down into three categories, powerplant weight, powerplant volume and compatibility with the ship as shown in Table 3.4. Availability, malfunction suitability, vulnerability and compatibility with other powerplant components were considered in the area of operability. In the area of cost, fuel, development and fabrication costs were considered. It is assumed that a sufficient number of powerplants would be built so that fuel costs are

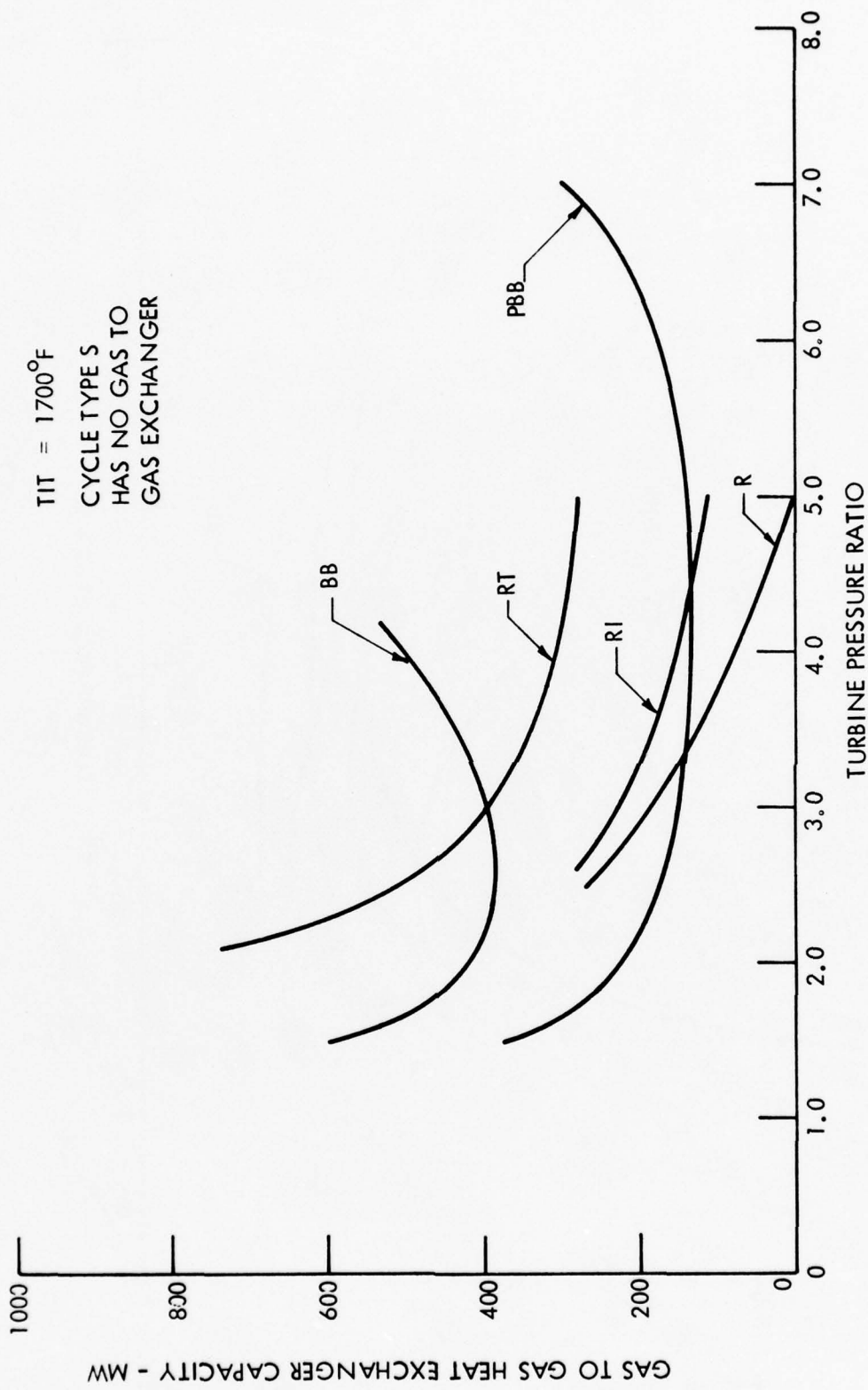


Figure 3.9 Gas to Gas Heat Exchanger Capacity Comparison of Cycles

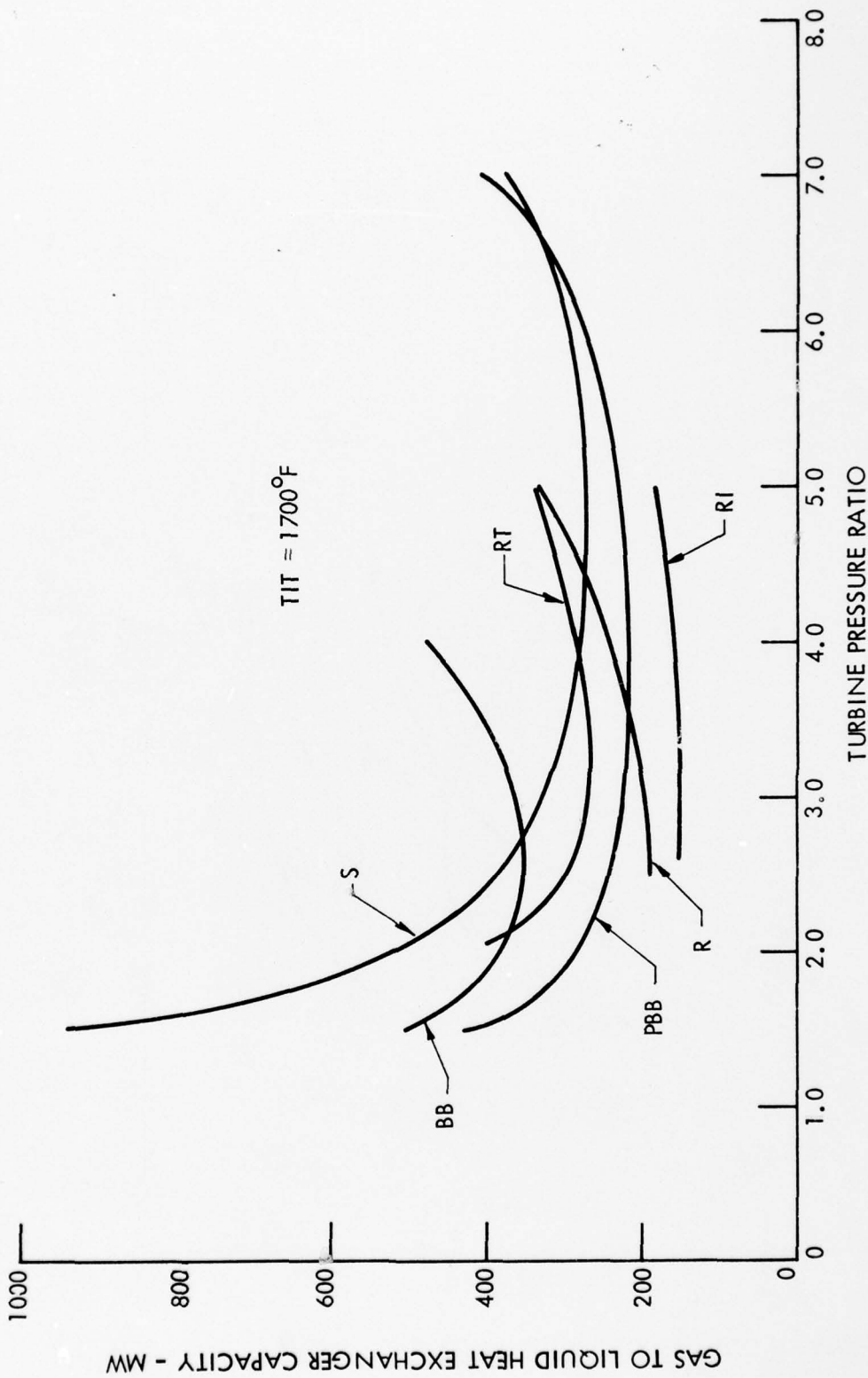


Figure 3.10 Gas to Liquid Heat Exchanger Capacity Comparison of Cycles

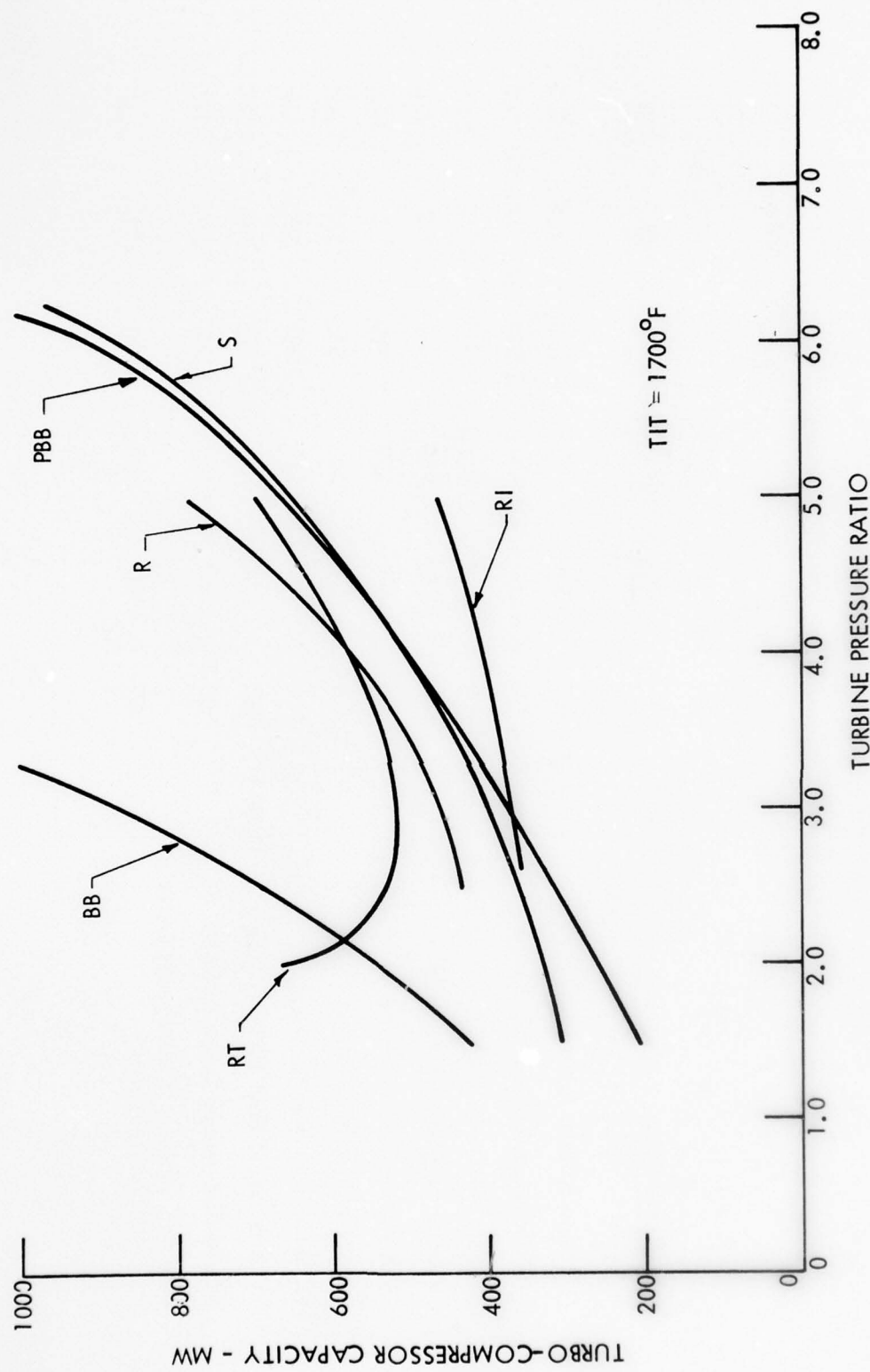


Figure 3.11 Turbo-Compressor Capacity Comparison of Cycles



Westinghouse

TABLE 3.3
CYCLE PARAMETERS AT THE SELECTED PRESSURE RATIOS

CYCLE TYPE	<u>S</u>	<u>R</u>	<u>RI</u>	<u>RT</u>	<u>BB</u>	<u>PBB</u>
Turbine Pressure Ratio	4.0	3.0	3.0	3.0	2.5	3.0
NSS and Containment Weight (lb)	884, 800	876, 100	831, 100	938, 200	897, 700	789, 000
Cycle Efficiency (%)	27.0	34.9	40.7	27.6	22.8	31.3
Reactor Inlet Temperature ($^{\circ}$ F)	633	970	946	886	770	476
Compressor Exit Temperature ($^{\circ}$ F)	633	519	278	310	770	476
Reactor Flow Rate (lb/sec)	277.6	314	261	355	377	208
Gas-To-Gas Heat Exchange	NA	185	228	399	389	154
Gas to Liquid Heat Exchange Capacity (MW)	282	194	151	272	352	228
Turbo-Compressor Capacity (MW)	500	460	364	517	690	375
Turbo-Compressor Containment Outer Diameter (inch)	157	185	178	190	173	150

TABLE 3.4
BRAYTON CYCLE COMPARATIVE EVALUATIONS

	Weighting Factor	CYCLE TYPE					
		S	R	RI	RT	BB	PBB
Powerplant Weight	10	50	60	80	30	50	100
Powerplant Volume	8	64	32	56	24	56	100
Compatibility with Ship	9	90	72	90	72	27	81
Availability	10	80	90	100	90	30	70
Malfunction Suitability	5	40	45	45	40	50	45
Vulnerability	6	60	54	54	54	42	42
Compatibility with other powerplant components	6	48	48	60	54	48	54
Fuel Cost	10	40	70	100	40	10	60
Development Cost	6	60	54	48	48	36	30
Fabrication Cost	6	60	60	60	54	42	42
Development Risk	6	60	60	60	36	36	36
Total		652	645	753	542	427	660



Westinghouse

significant to the life cycle costs. Since cycle Types S, R and RI have been built and operated the development risk is lower for these cycles.

In the overall evaluation the recuperated and intercooled (RI) Brayton cycle has about 100 points advantage over the next three cycle Types (S, R and PBB) which are grouped at about 650. Therefore the RI cycle type is recommended for the power conversion system design concept. Since the overall objective of the CCCBS study is to show the feasibility of a closed cycle Brayton Power conversion system for a low volume, lightweight marine propulsion plant, it is judged that the feasibility of cycle Types S, R and RT will also be shown because the components in these cycles represent simpler configurations than the recuperated-intercooled cycle.

3.4.3 Fossil System Parametric Studies

Powerplants based on metallic superalloy tube energy source heat exchanger technology have been investigated previously (Reference 4). Powerplants of 40,000, 60,000, and 80,000 HP were evaluated with maximum superalloy heater tube hot spot temperatures limited to 1650°F with the turbine inlet temperature limited to 1500°F. The powerplant designs were based on 20,000 HP heat exchanger modules so that two, three or four module sets were utilized to cover the powerplant range. Total powerplant specific weight was approximately 15.0 lb/HP with a full power specific fuel consumption of 0.341 lb/HP at an output power of 40,000 HP. Powerplant specific weight increased as the output power increased due to the heat exchanger modularization concept. The helium turbomachinery for a 40,000 HP unit (Reference 5) is shown in Figure 3.12 that has a turbine inlet temperature of 1500°F. This figure illustrates the commonality possible between nuclear and fossil fired closed Brayton turbomachinery. For the current CCCBS study the superalloy heat source concepts were thus judged to be adequately documented by the prior work.

Ceramic heat source technology for large naval powerplants has not been previously evaluated and was therefore selected for the present study to show future potential. An ANVCE study (Reference 6) utilized the MARAD superalloy heat source design as the 1980 technology and did not include weight optimized turbomachinery, and predicted that the powerplant specific weight would decrease to about 12.0 lb/HP at 40,000 HP for the year 2000 with a powerplant SFC of 0.3 lb/HP-hr. This appears to be a reasonable extrapolation but by the year 1990 the ceramic heat source technology will result in powerplant specific weights of 1.1 lb/HP based on use of a superalloy turbine. This demonstrates the quantum steps possible with marked changes in the heat source technology.

Two 70,000-HP fossil fired powerplant studies were conducted in these CCCBS studies. The first design study was based on a refractory metal turbine with an inlet temperature of 2250°F and utilized a silicon carbide tube heat source heat exchanger with a hot spot temperature of 2500°F. The second design study was based on a turbine inlet temperature of 1750°F, so

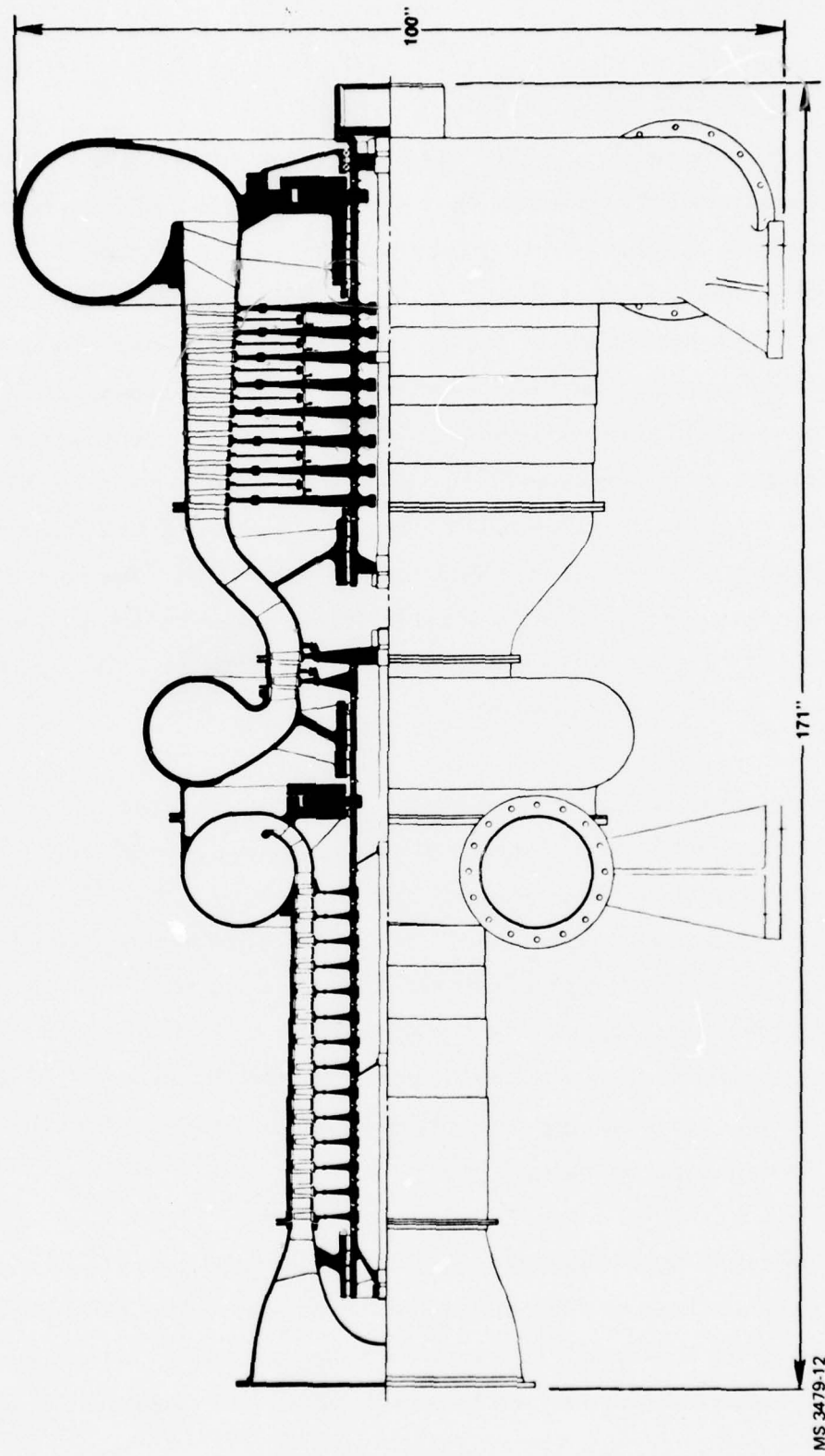


Figure 3.12 40,000 HP Helium Turbomachinery

that the fossil fired and nuclear powerplants would incorporate essentially the same turbine materials technology (superalloys). The silicon carbide heat source for the second design study was defined on the basis of maintaining the energy source heat exchanger hot spot tube temperature at 2500°F.

These design studies were initially based on a 12,000 HP engine design study conducted for another program. This low power engine study is presented below to show the basis for the 70,000 HP fossil fueled engine study presented in subsequent paragraphs.

12,000 HP Engine Design Base

In June 1975, a 12,000 HP fossil fueled closed-Brayton cycle engine design study was conducted. The 12,000 HP engine was designed for a ship propulsion cruise engine application in which minimum weight and volume were important. Figure 3.13 schematically shows the 12,000 HP engine design and Figure 3.14 shows the core engine layout.

Two heat source designs were defined for the 12,000 HP engine with combustion loop efficiencies of 0.85 and 0.92. The heat source heat exchanger had a silicon carbide tube hot spot temperature of 2500°F. The 0.85 efficient combustion heat source had a lower heater effectiveness, which resulted in a much lower heat source weight than the 0.92 efficient combustion loop heat source. Trade-off studies on weight, volume, and fuel consumption were made, and the 0.85 efficient combustion heat source was selected. Figure 3.15 shows the core engine matched to the 0.85 efficient combustion heat source.

70,000 HP Fossil Fuel Engine Design

The considerations for using xenon-helium mixtures versus helium in the fossil fired powerplant concepts is that xenon-helium mixtures can be tailored to the application for those powerplant configurations in which a low nuclear cross section is not a requirement. Figure 3.16 shows the variation in the number of compressor stages required as a function of the gas molecular weight. Figure 3.16 also shows that the penalties in heat transfer surface area can be kept



Westinghouse

CYCLE EFFICIENCY = 0.501
WORKING FLUID MOL WT = 20.183
PRESSURE LOSS PARAMETER, β = 0.940
GAS GENERATOR SPEED, RPM = 26,000
POWER TURBINE SPEED, RPM = 26,000

T = °F
P = PSIA
M = LB/SEC

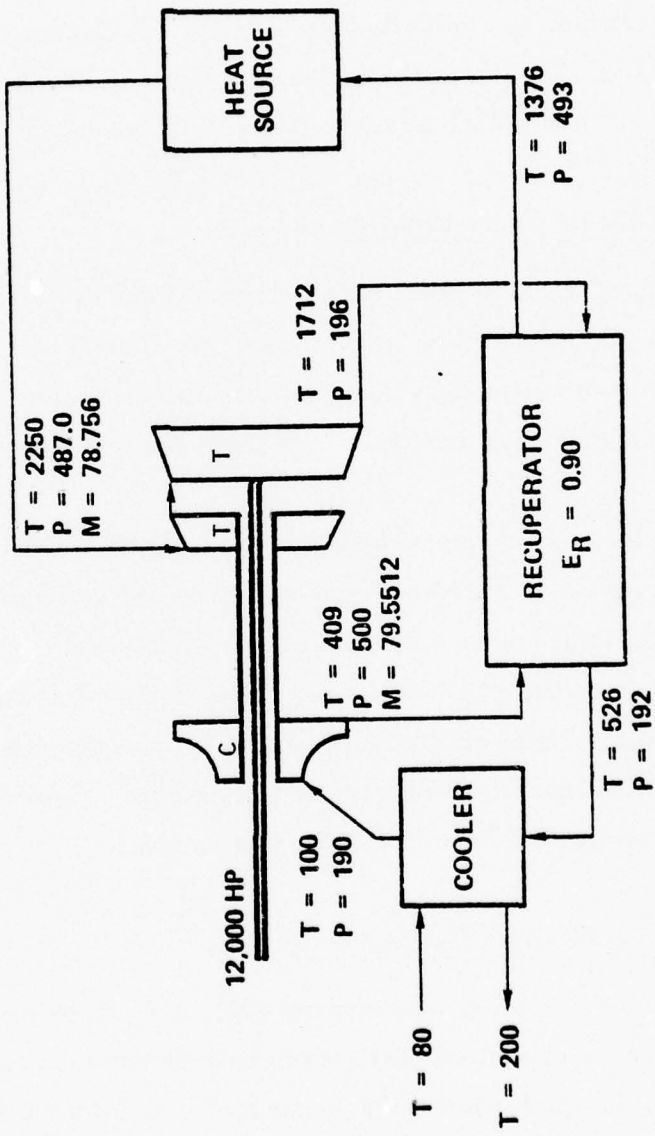


Figure 3.13 12,000 HP Engine Match Point

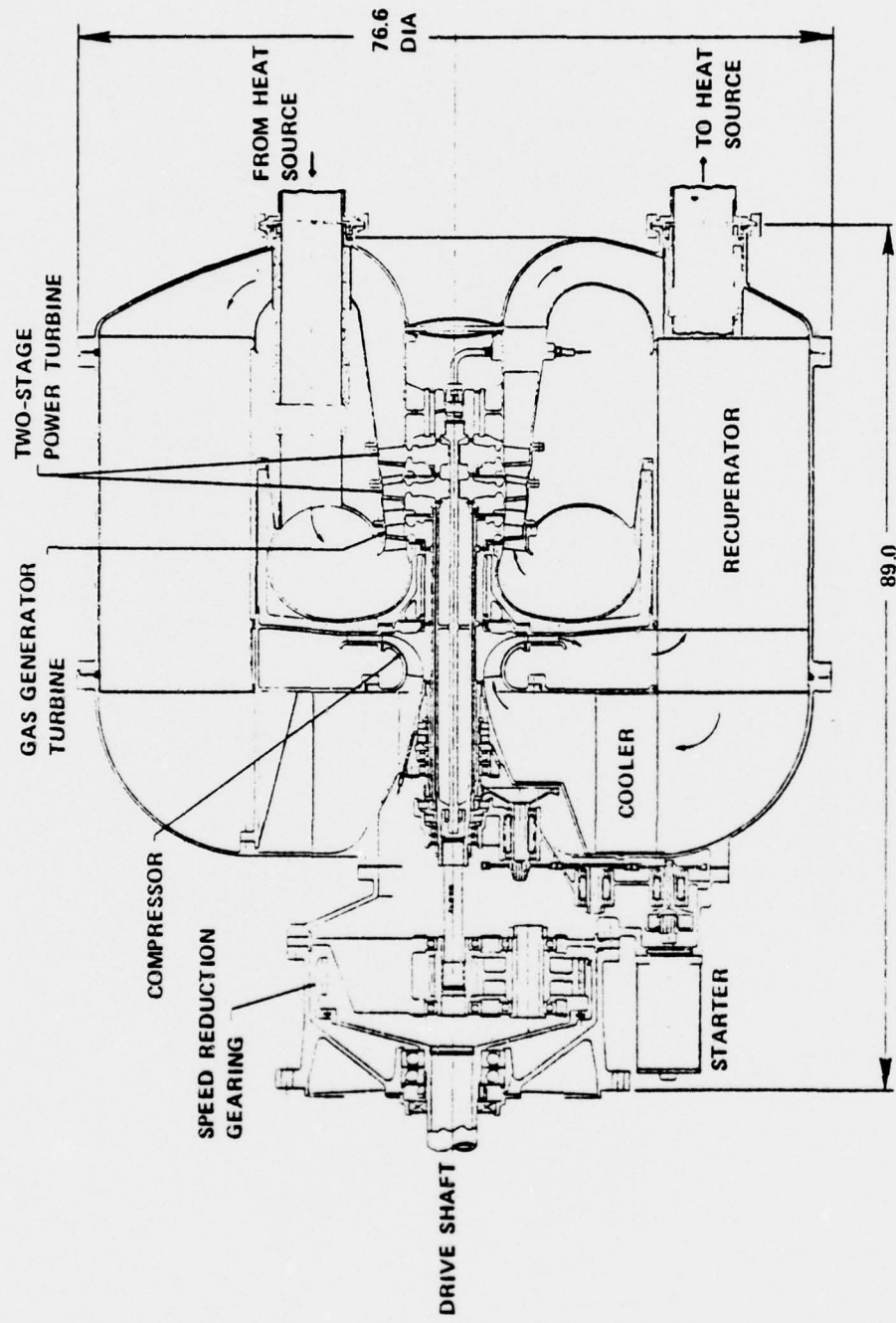


Figure 3.14 12,000 HP Engine Core



Westinghouse

SFC = 0.32 LB /HP-HR
INLINE HEAT SOURCE CONFIGURATION

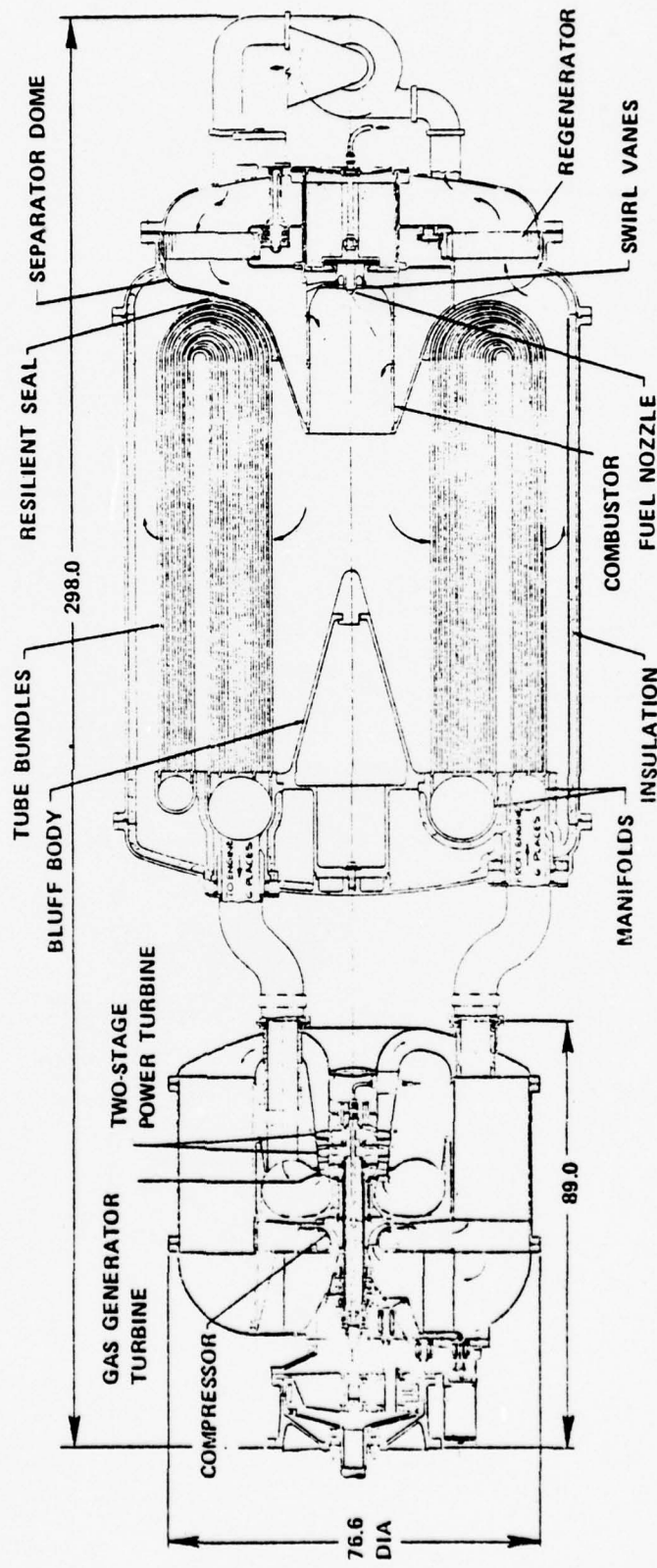


Figure 3.15 12,000 HP Engine

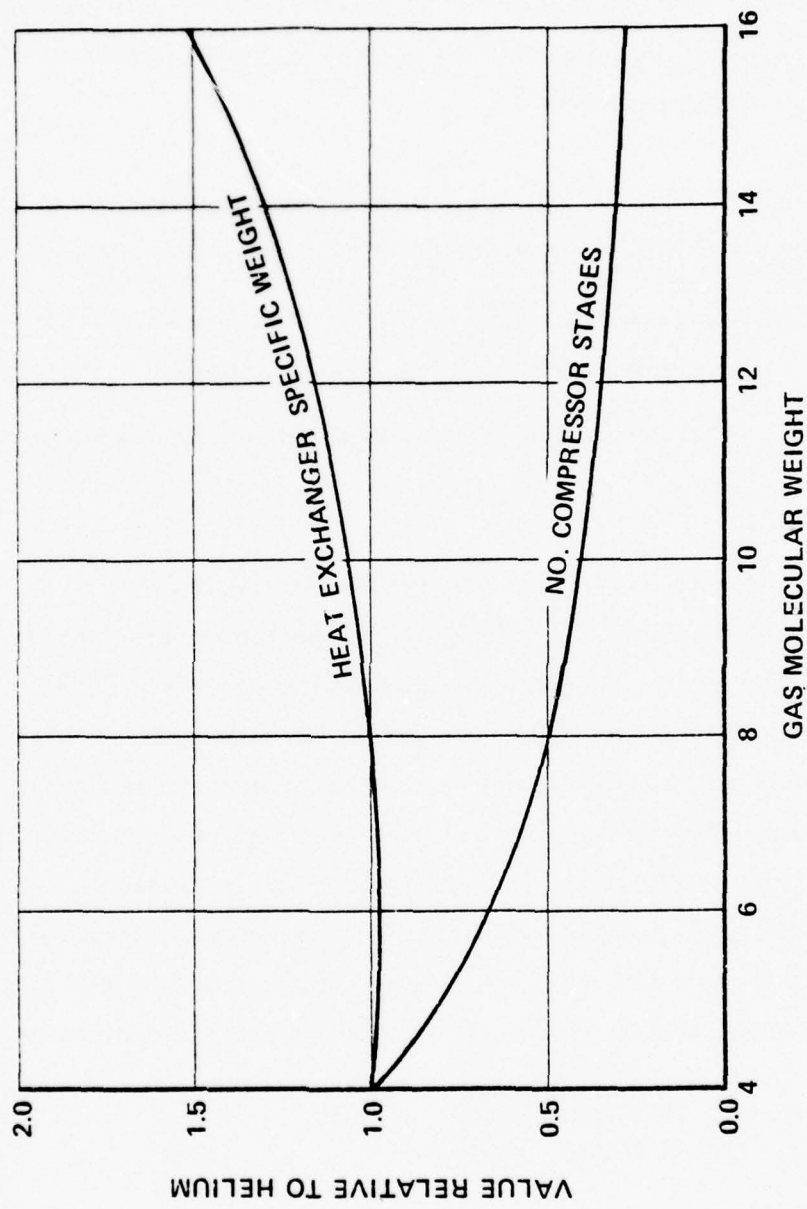


Figure 3.16 Xe-He Gas Mixtures



Westinghouse

small by using a xenon-helium mixture instead of a pure gas (such as neon). A molecular weight of 20.183 was selected for evaluation at the 70,000 HP level. The xenon-helium gas mixture molecular weight is frequently selected such that a single constituent monatomic gas (in this case neon) can be used for a majority of the engine turbomachinery development testing to effect cost reductions.

The initial 70,000 HP fossil fueled engine for this study was designed at a turbine inlet temperature (T_6) of 2250°F. In this design, two questions were addressed:

1. What combination of system weight and specific fuel consumption should be used to maximize the ship's range?
2. What is the weight/performance split between the engine and heat source?

Figure 3.17 shows the heat source predicted specific weight (based on the 12,000 HP design) as a function of the heat source efficiency. The heat source efficiency (η_{HS}) was varied from 0.84 to 0.92, and the heat source thermal output was varied from 20,000 to 140,000 kW_t. As the thermal output increases and η_{HS} decreases, the heat source specific weight decreases. Figures 3.18 and 3.19 are "shot gun" plots for both intercooled and nonintercooled engines in which recuperator effectiveness, compressor inlet pressure, compressor pressure ratio, compressor and turbine inlet temperature, and pressure loss parameter were all varied. These figures show the locus of the minimum specific weight core engine design versus cycle efficiency. These results (Figures 3.17 through 3.19) were combined to yield total powerplant specific weights (including fuel) of 10, 15, and 20 lb/HP with specific fuel consumption defined as:

$$SFC = \frac{0.1386}{\eta_{heat\ source} \times \eta_{cycle}}, \text{ lb/HP hr}$$

Figures 3.20 and 3.21 show the resulting range of the power plant as a function of cycle efficiency (η_{cy}) and heat source efficiency (η_{HS}), and assuming that the difference between

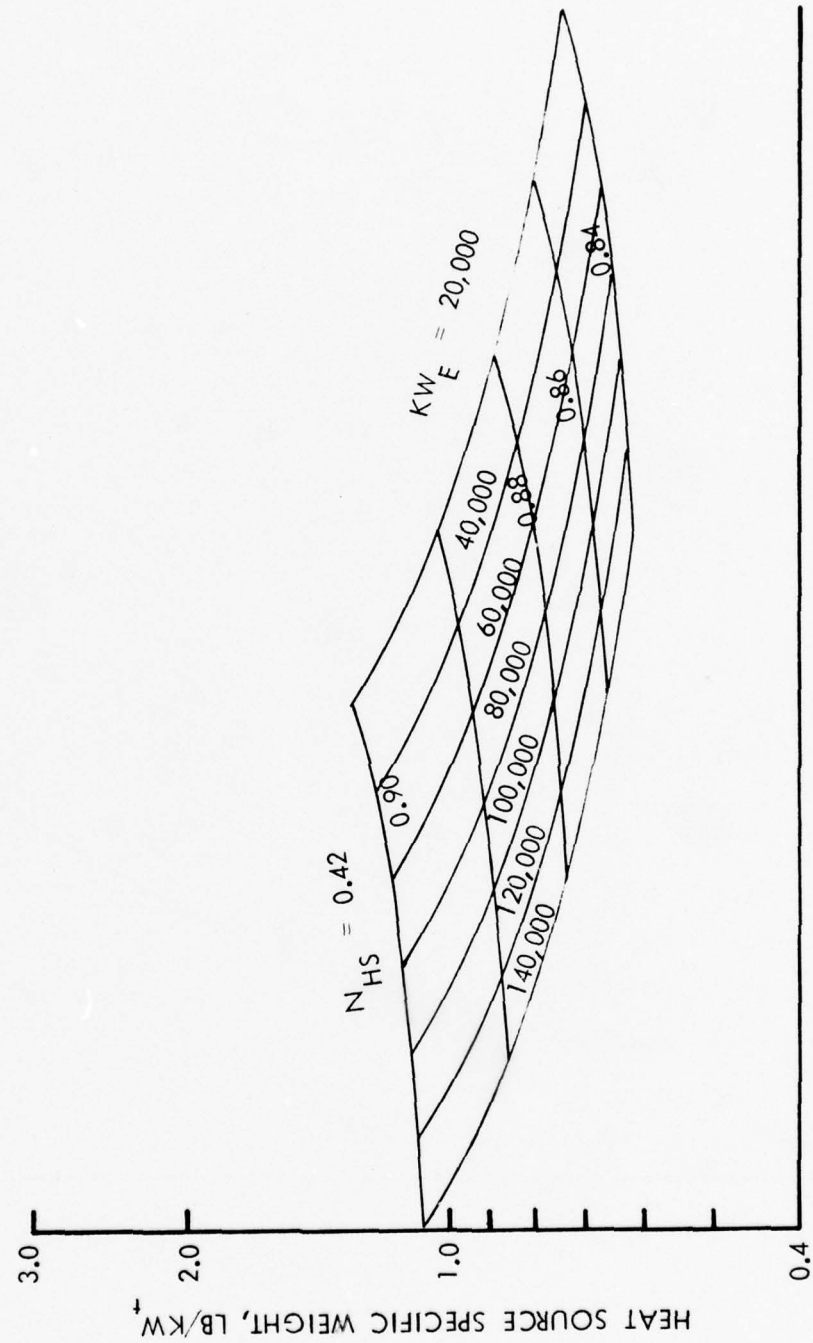


Figure 3.17 Heat Source Performance Versus Specific Weight

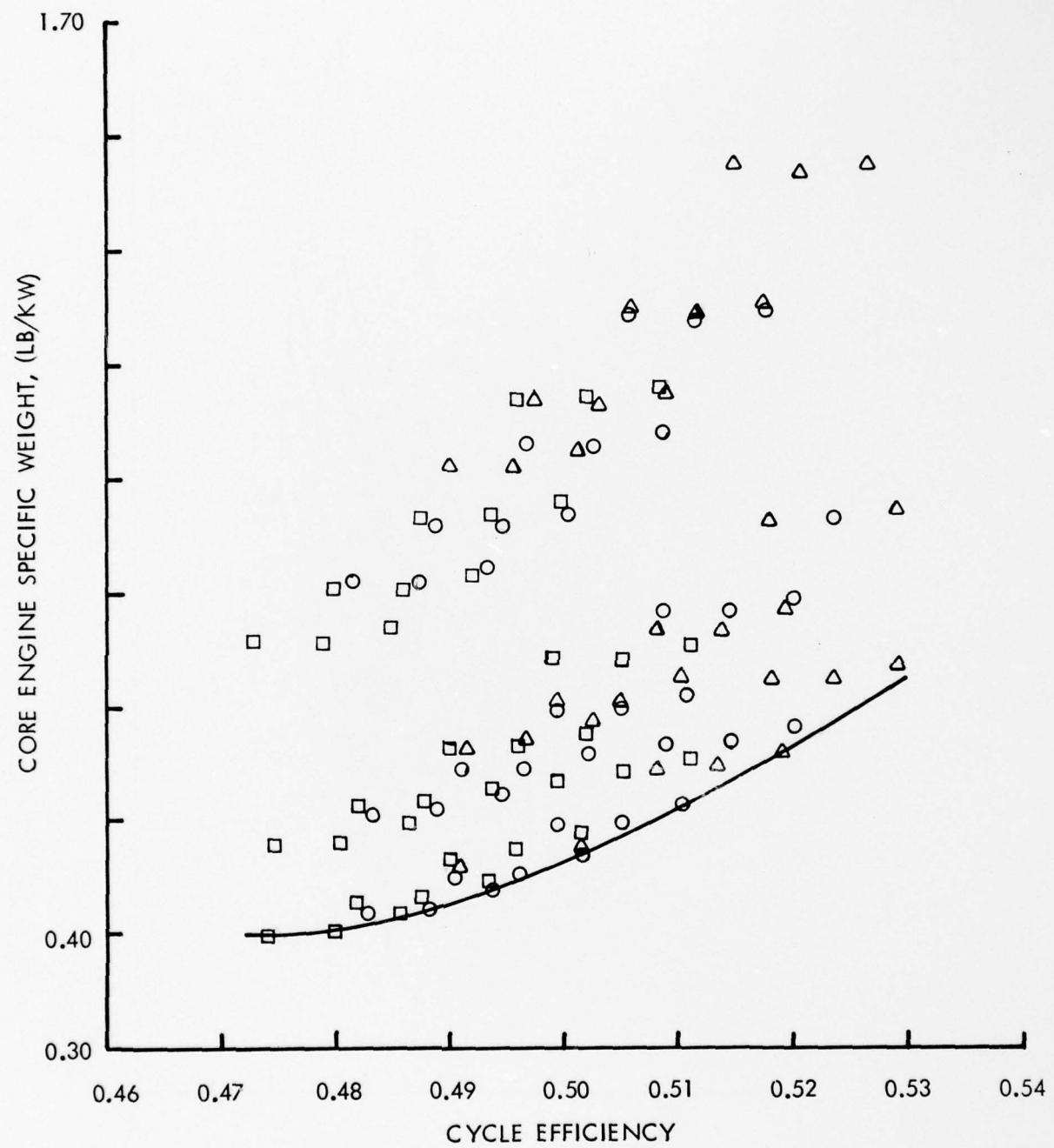


Figure 3.18 Fossil Fueled Intercooled

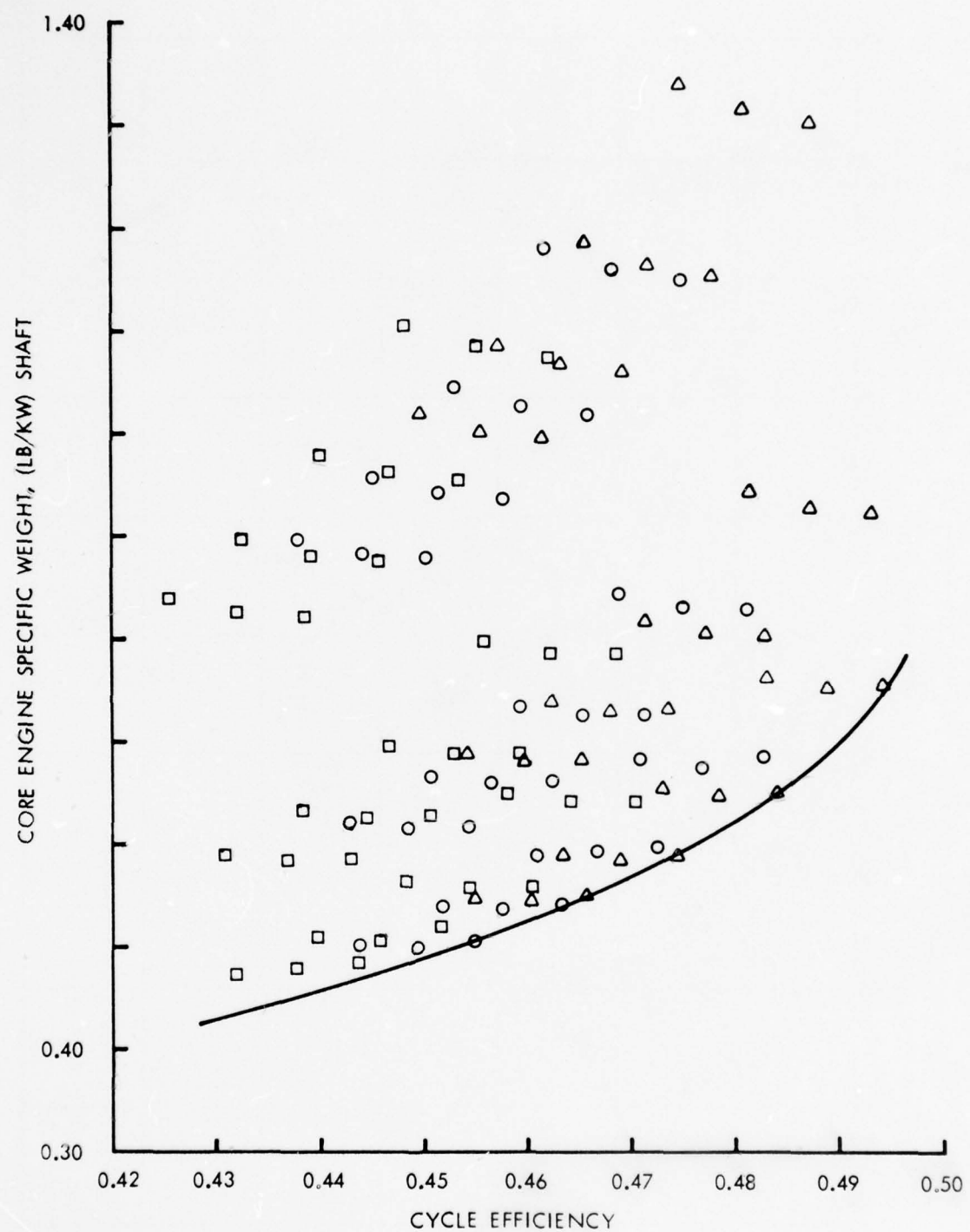


Figure 3.19 Fossil Fueled Non-Intercooled



Westinghouse

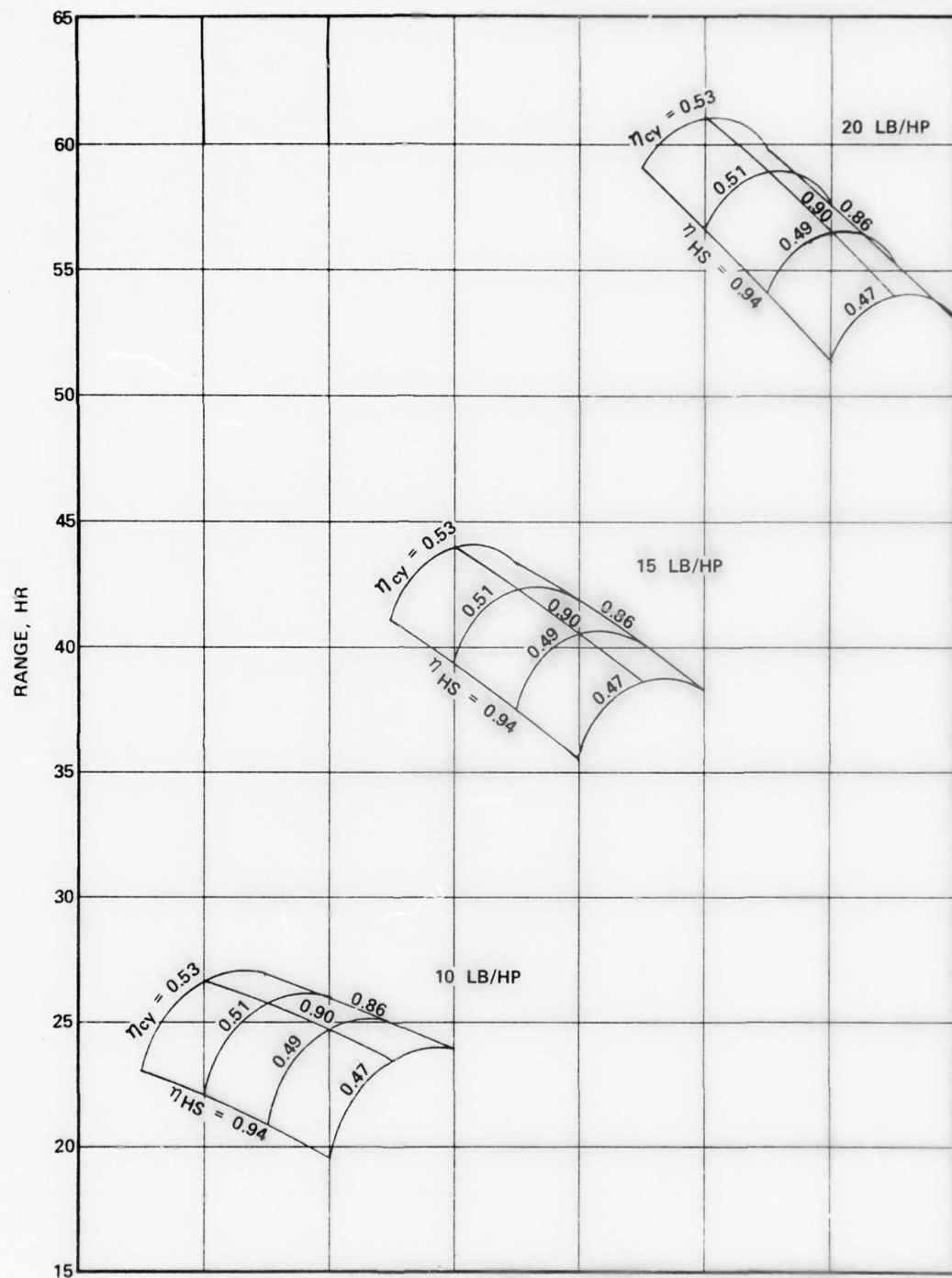


Figure 3.20 Intercooled

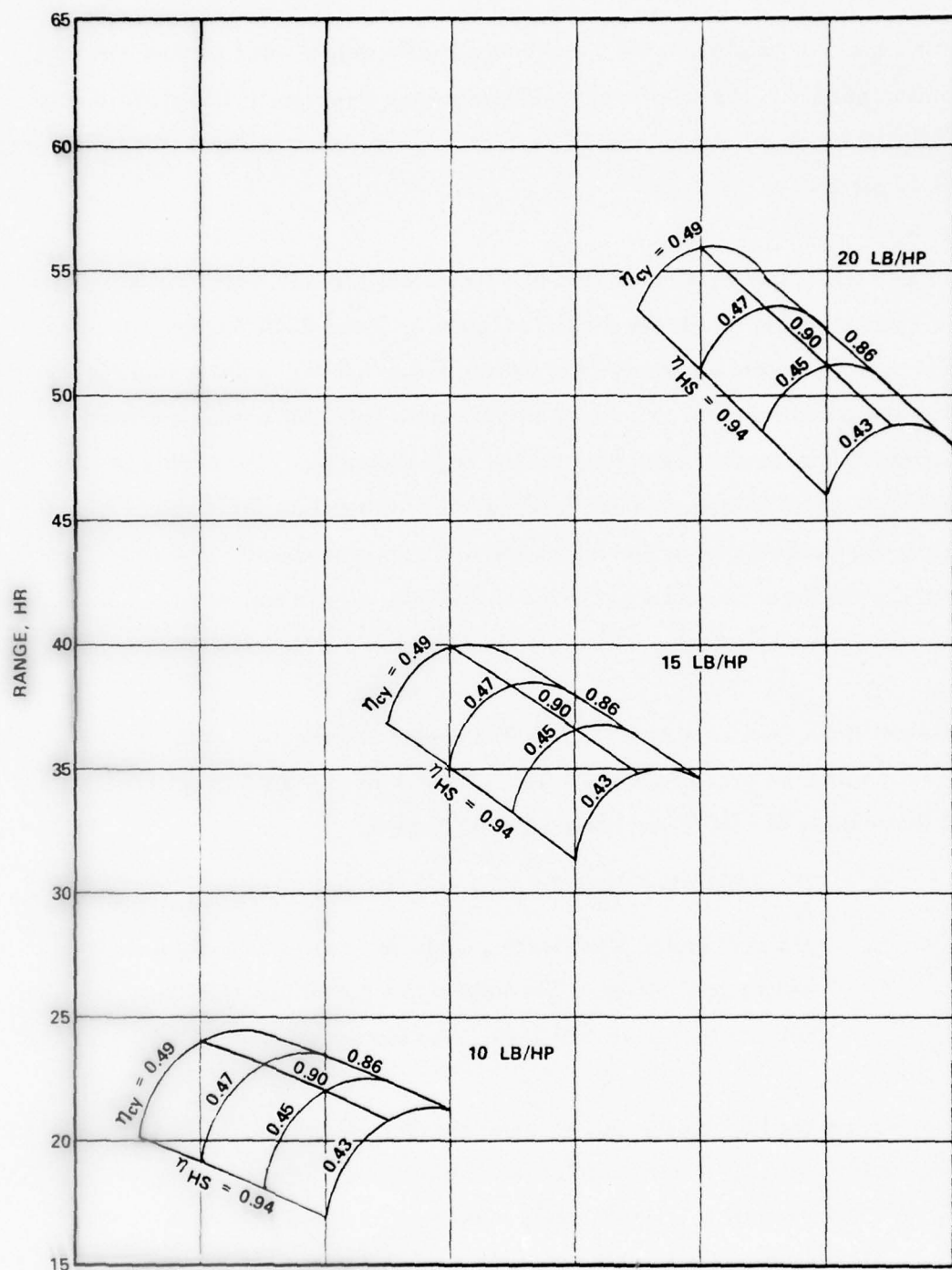


Figure 3.21 Non-Intercooled

the total specific weight and the powerplant specific weight was fuel consumed at the rate of the full power SFC. The significant conclusions from these results is that the heat source should be designed for an efficiency near 90 percent, and that intercooling increases the range by about 10 percent.

New "shot gun" plots were run for the two engine designs with higher cycle pressures the major change. These results are shown in Figures 3.22 and 3.23. Comparison of these results at, for example, a core engine specific weight of $0.5 \text{ lb/kW}_{\text{shaft}}$ shows that the intercooled engine will exhibit a cycle efficiency of 0.52 versus 0.475 for a nonintercooled engine. These results incorporate finned tube coolers and intercoolers. The engine designs noted on Figures 3.22 and 3.23 were selected for detailed investigations, including changing to plate-fin cross-counterflow coolers and intercoolers. The engine specific weight trade-offs were essentially the same but packaging of the finned tube coolers and intercoolers showed a clear cut advantage over packaging with plate-fin coolers and intercoolers.

Additional studies were conducted for an intercooled engine at a turbine inlet temperature of 1750°F with both xenon-helium (20.183 MW) and air as the working fluids. A turbine inlet temperature of 1750°F was chosen for two reasons:

- a. The CCCBS helium technology gained could be directly utilized.
- b. The heat source effectiveness could be lowered, thereby lowering its weight and volume, while maintaining the silicon carbide tubes at a hot spot temperature of 2500°F maximum.

Several engine and heat source designs were investigated. Figure 3.24 summarizes the results for the 2250°F and 1750°F turbine inlet temperature cases. The xenon-helium (20.183 MW) design at 1750°F results in a significantly lower weight system due to the heat source design. This reduction is due to the lower heat source pressure ratio and engine side heater effectiveness for the 1750°F case.

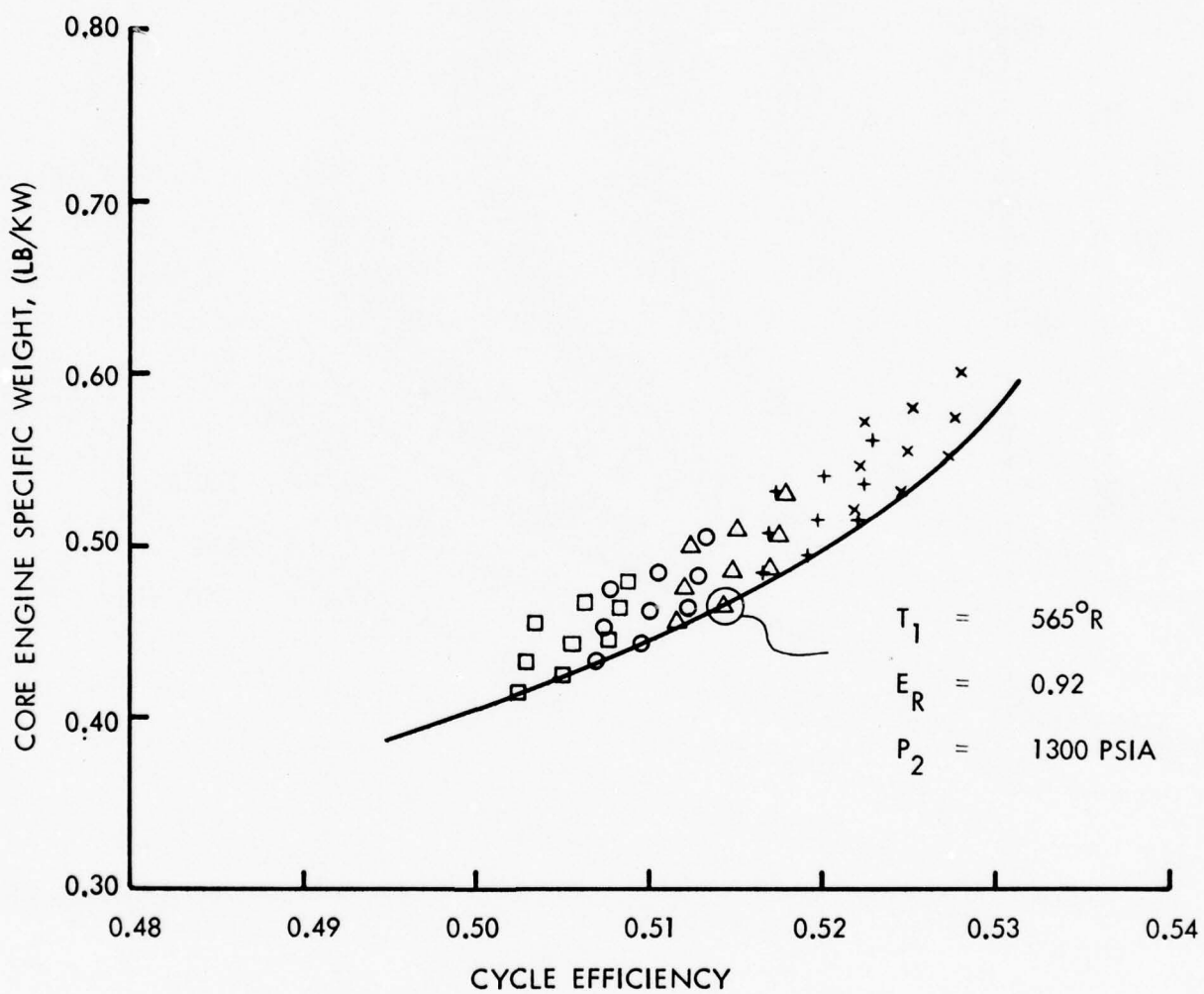


Figure 3.22 Fossil Fueled Intercooled

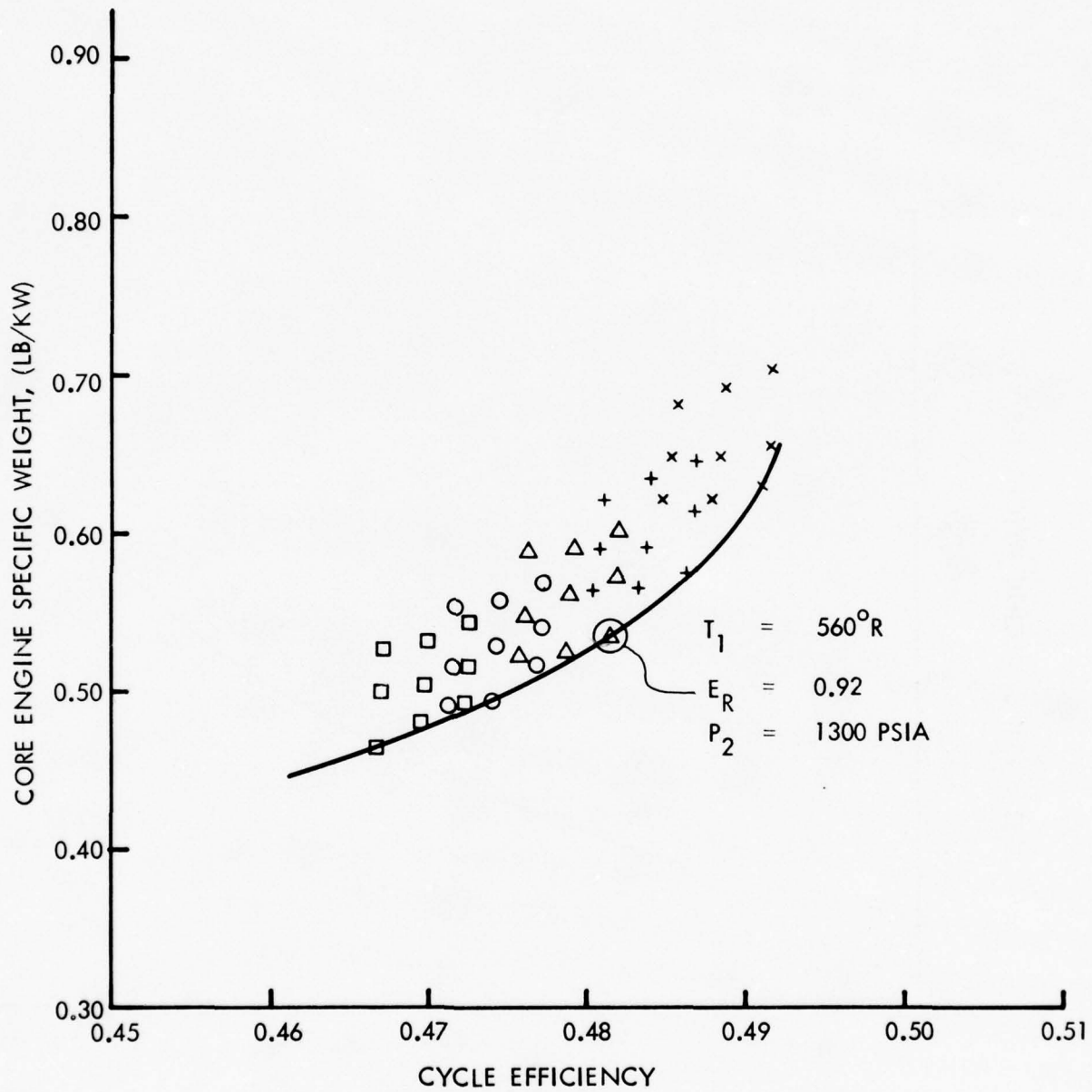


Figure 3.23 Fossil Fueled Non-Intercooled

	ENGINE WORKING FLUID		
	XeHe 20*	XeHe 20 **	AIR **
CYCLE EFFICIENCY	0.517	0.449	0.449
SHAFT SPEED, RPM	12,000	11,000	11,000
ENGINE SIDE HEATER EFFECTIVENESS	0.359	0.258	0.242
HEAT SOURCE PRESSURE RATIO	3.7	1.84	1.84
COMBUSTION LOOP EFFICIENCY	0.90	0.906	0.906
COMPONENT WEIGHTS AND VOLUME, LB & FT ³			
CORE ENGINE	25,400	-	33,600 & 437
HEAT SOURCE	126,000	-	40,700 & 784
ACCESSORIES AND MISCELLANEOUS	5,080	6,720 -	46,650 & 906
TOTAL WEIGHT AND VOLUME	156,480	81,020 & 1,221	10,800 -
ENGINE SPECIFIC WEIGHT, LB/HP	2.24	1.16	1.59
ENGINE SPECIFIC VOLUME, FT ³ /HP	-	0.017	0.021

*BASED ON T₆ = 2250°F
** BASED ON T₆ = 1750°F

Figure 3.24 70,000 HP Engine Summary

Figure 3.25 schematically shows the 1750°F 70,000 HP engine design, and Figure 3.26 shows the core engine layout. The recuperator was modeled as eight plate-fin pure counterflow curved modules. The cooler and intercooler were modeled as six-finned tube cross-counterflow curved modules with six liquid passes. The rotating group consists of two centrifugal compressors to take advantage of prior studies, a two-stage axial gas generator turbine (GGT) and a four-stage axial power turbine (PT). Axial compressors could be utilized in this engine design by replacing each of the single centrifugal stages with four axial stages and an axial to radial flow transitional diffuser.

The selected heat source design is shown on Figure 3.27. This design was modeled with silicon carbide tubes making two passes with a hot spot temperature of 2500°F. Figure 3.28 shows the approximate size of the ceramic heat source matched to the core engine.

The xenon-helium engine provides low estimated weight and volume. For certain applications, an air engine may be justified on the basis of reduced logistics support which could offset the weight and volume advantage that the xenon-helium (molecular weight = 20.183) exhibits.

CYCLE EFFICIENCY = 0.449
 WORKING FLUID MOL WT = 20.183
 PRESSURE LOSS PARAMETER, β = 0.94
 GAS GENERATOR SPEED, RPM = 11,000
 POWER TURBINE SPEED, RPM = 6,000

$T = ^\circ F$
 $P = PSIA$
 $M = LB/SEC$

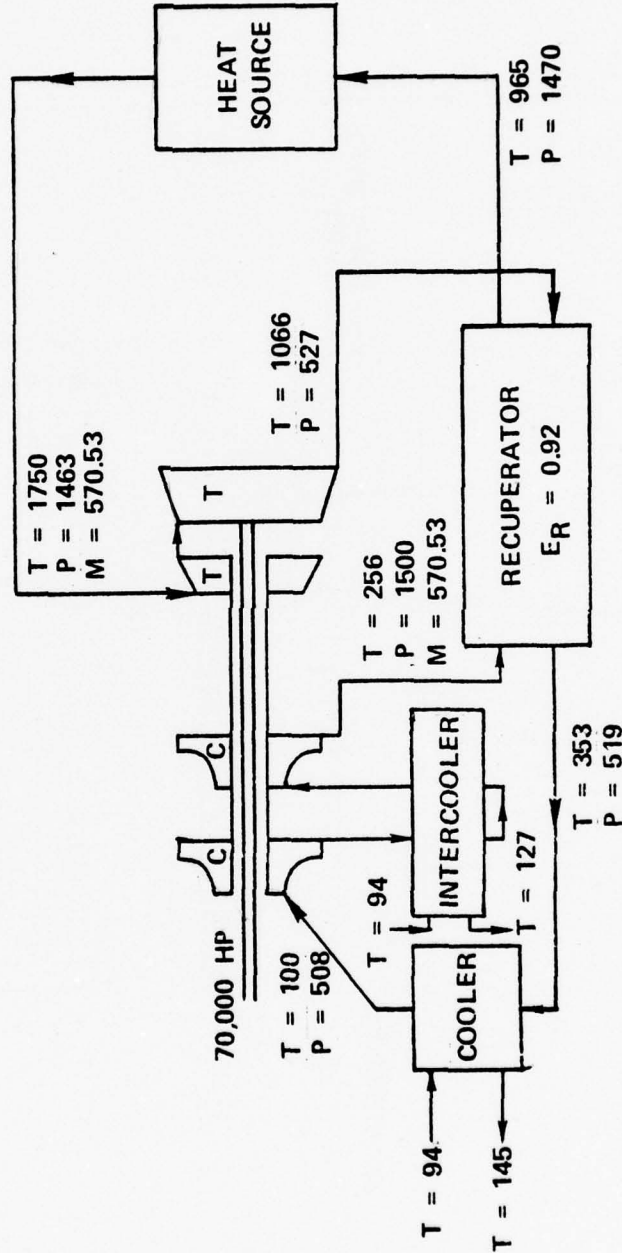


Figure 3.25 70,000 HP Engine Match Point



Westinghouse

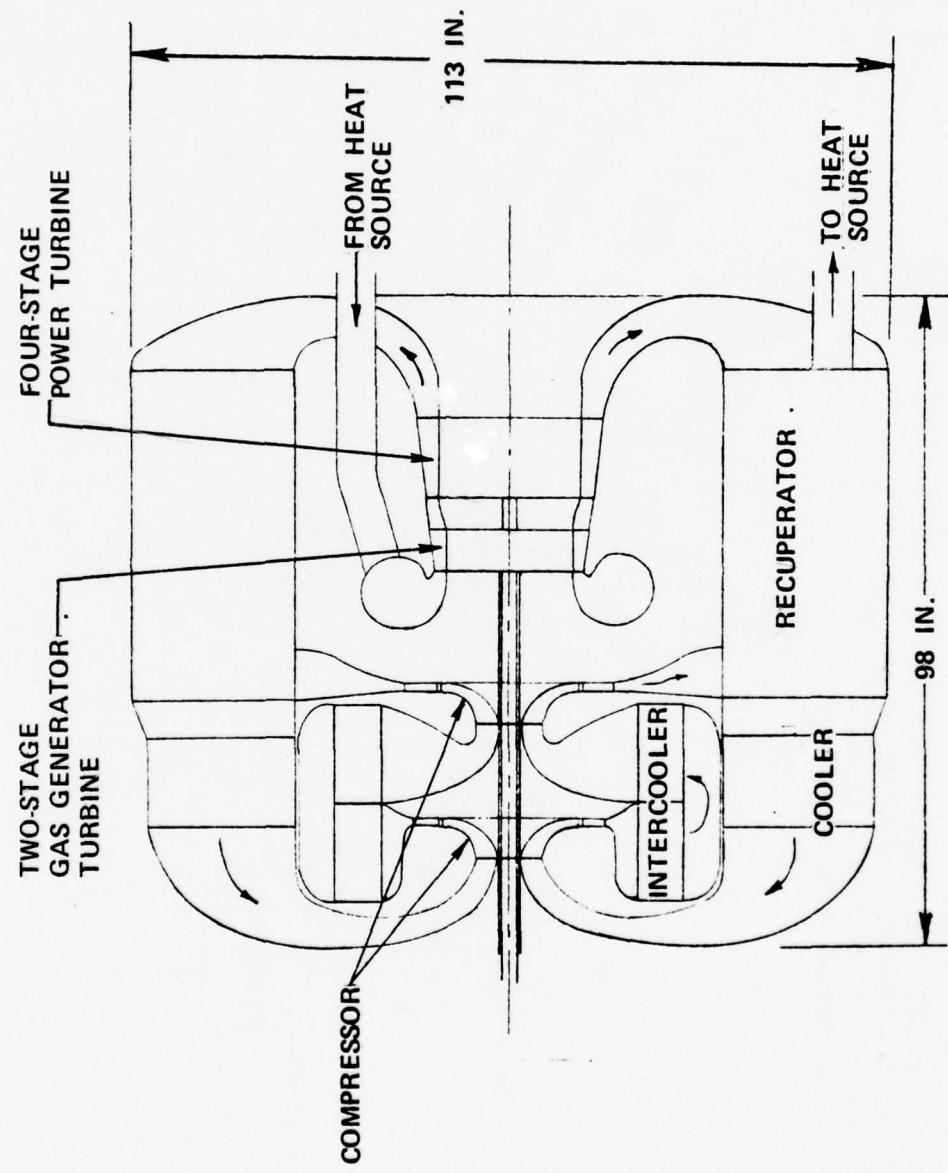


Figure 3.26 70,000 HP Engine Core

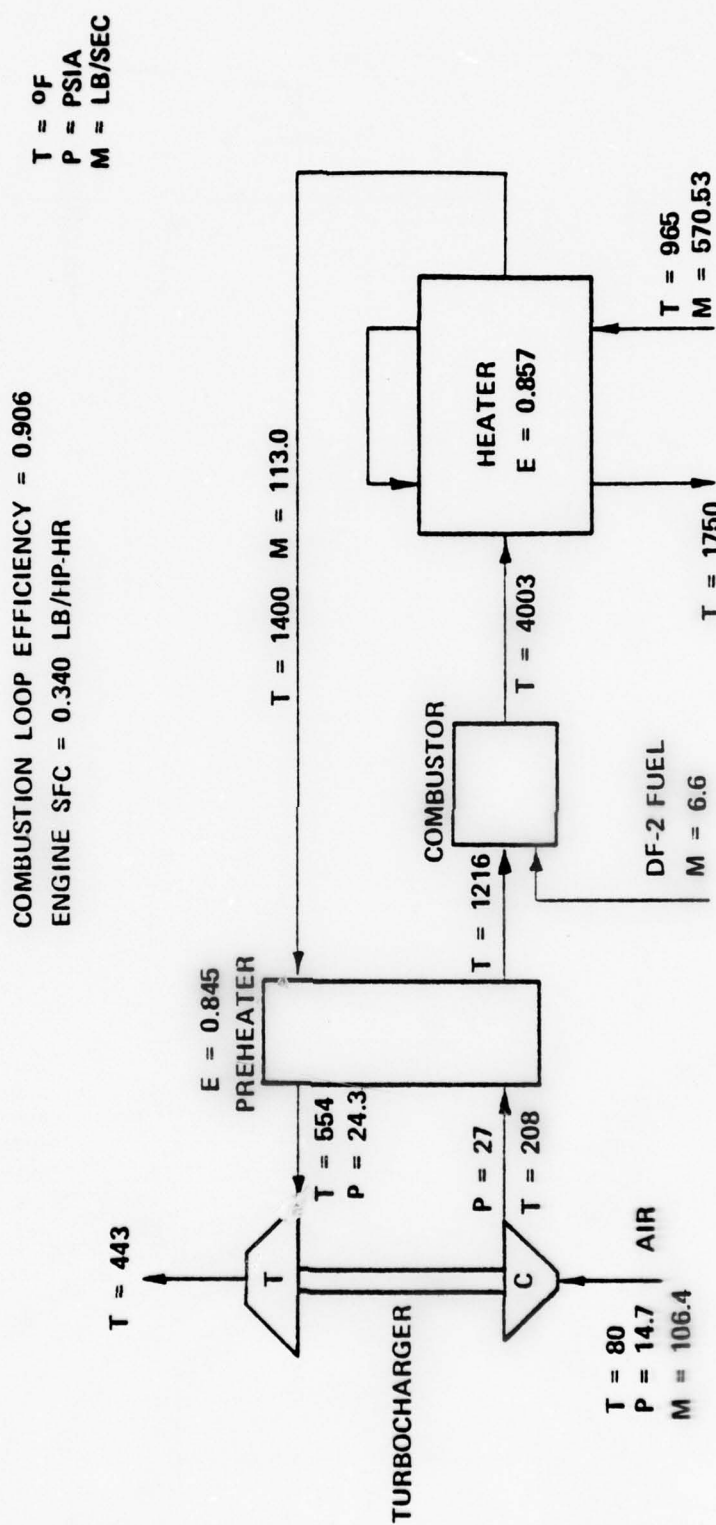


Figure 3.27 70,000 HP Engine Heat Source



Westinghouse

SFC = 0.34 LB/HP-HR
INLINE HEAT SOURCE CONFIGURATION

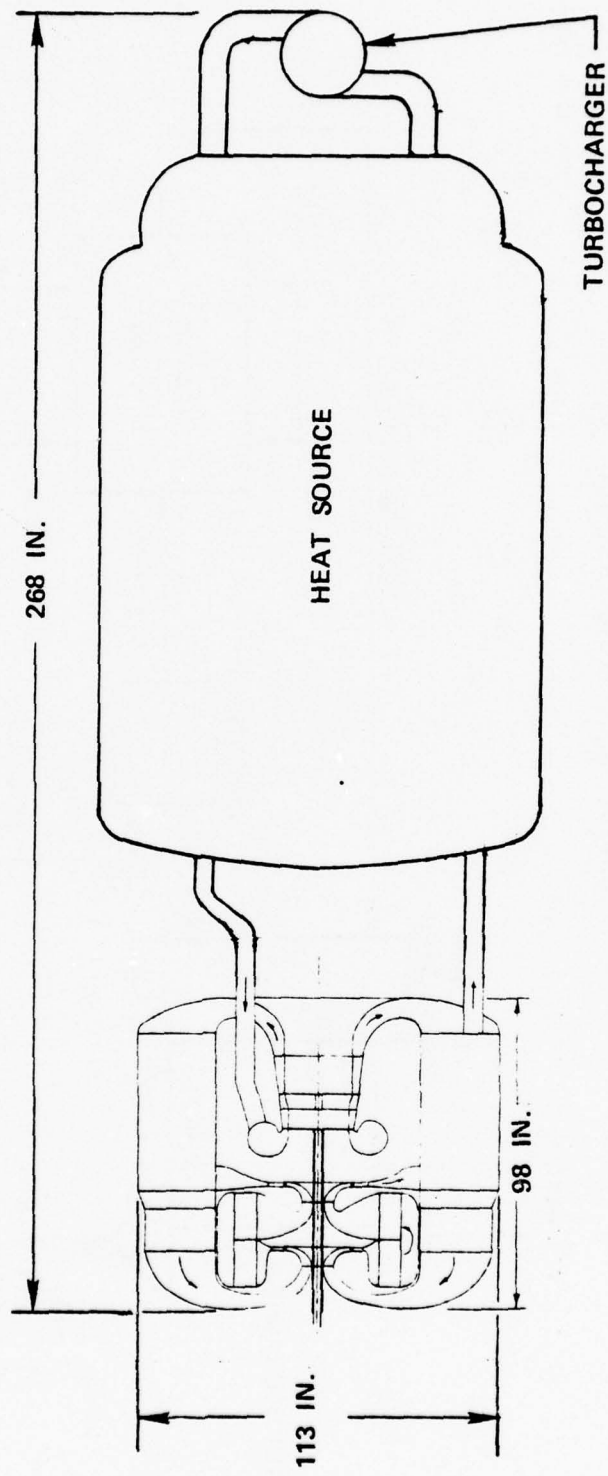


Figure 3.28 70,000 HP Engine

3.5 CCCBS DESIGN CONCEPT

The Design Concept definition is being conducted to define the specific power conversion design concept which will be used as a basis for feasibility evaluation. The results of all other tasks are used as input in defining the concept. The second programmatic purpose of early power conversion design concept definition is to provide a meaningful review of the program and of the early indications of results which can be expected.

Several terms are used in this report referring to different steps in the maturing of the design under evaluation. These are "Trial Design", "Design Concept (1st Definition)", and "Design Concept (2nd Definition)." These different terms have been used to identify discrete steps in the process of maturity.

The trial design is associated with the initial derivation of requirements and the detail required is only that necessary to support reasonableness and consistency of requirements. Because it appropriately fulfilled the top-level requirements which were derived, the trial design was taken to be that shown in Figure 3.1, which had been derived and studied in some detail by earlier in-house Westinghouse studies. This infused the earlier results to enhance the CCCBS study. It also meant that the "Trial Design" included more detail than required, which was beneficial to subsequent efforts.

The terms "Design Concept (1st Definition)" and "Design Concept (2nd Definition)" refer to two iterations of the more detailed power conversion system definition which have been accomplished in the first year's efforts under Task 8 of Figure 1.2. As shown in Figure 1.2, the design concept will continue to mature during the second year of the program. However, it has been judged that both the first and second iterations are important in themselves and

are therefore worthy of reporting. The "1st Definition" represented a major step in maturity from the Trial Design but was accomplished before the component comparison studies of heat exchangers and bearings were completed. The "2nd Definition" represents the status of the Design Concept at the end of the first year efforts with the selected bearings and heat exchanger types incorporated. This "2nd Definition" version will be further matured and evaluated during the second year efforts.

Some clarification of the turbine inlet temperatures used in the various tasks of this study is also desirable for clear understanding of the reported results. As stated in Section 3.3 a turbine inlet temperature of 1700°F was established as a goal which has reasonable probability of successful achievement with uncooled superalloy blades. However, prior to agreement upon this level as a goal, it had been necessary to initiate evaluations of the first stage turbine (Section 4.2) which, in order to maximize the output of this study, built upon the results of earlier Westinghouse studies that had been conducted for similar design conditions and configuration. The earlier studies had utilized a turbine inlet temperature of 1671°F and the CCCBS efforts therefore used this temperature and expanded upon the earlier results. When 1700°F was agreed upon as a goal, all cycle studies and other component studies could be accomplished at the new conditions without significant repetition of work. However, it was judged that the first stage turbine studies should be continued in more detail for the 1671°F conditions rather than in the shallower detail that would have been possible if much of the work had been redone at 1700°F . Thus, the first stage turbine studies and the turbine configurations of the early design concept iterations refer to 1671°F turbine inlet temperature. During the second year of the study, these results will be adapted to 1700°F turbine inlet gas temperature conditions.

3.5.1 Design Concept (1st Definition)

3.5.1.1 General

The "initial definition" of the concept design is illustrated in Figure 3.29. The flowpath is identical to that of the trial design described in Section 3.3. However, the concept design, developed as a result of the continued development of the trial design, incorporates component designs of greater maturity. The critical heat exchanger and turbomachinery components have been subjected to more design and analytical attention and the turbomachinery has been redesigned to achieve reduced stress levels and improved long life temperature capability. The design changes made in the turbomachinery and other components to improve their practical characteristics have resulted in some component geometry and size changes. In addition, major improvements have been made in the integration of the turbomachinery into the assembly which facilitate its incorporation into and removal from a powerplant. As a result, the accessibility of the turbomachinery for maintenance and overhaul has been enhanced. The concept design assembly has a maximum diameter of 93 inches, measured over the center frame bolting flanges, and its length is 19 feet. Two of the units are capable of being accommodated side-by-side in a nuclear containment vessel having a diameter of 18 feet.

The philosophy initially adopted in the design of the turbomachinery was to push but not exceed established or expected state of the art. This philosophy was followed in the trial design with the intent of minimizing development risk and cost. The 1700°F turbine inlet temperature, while sufficiently high to provide good cycle efficiency, permits the use of uncooled turbine blading thus avoiding the need for helium blade cooling development programs. Similarly, although compactness and light weight have been design goals, they have been achieved without compromising reliability and long life characteristics. Thus, although the construction of the rotor and stator assemblies is more characteristic of aircraft engine than industrial turbine practice, the bearing assemblies included in this first definition follow conventional industrial practice in the use of hydrodynamically lubricated bearings.



Westinghouse

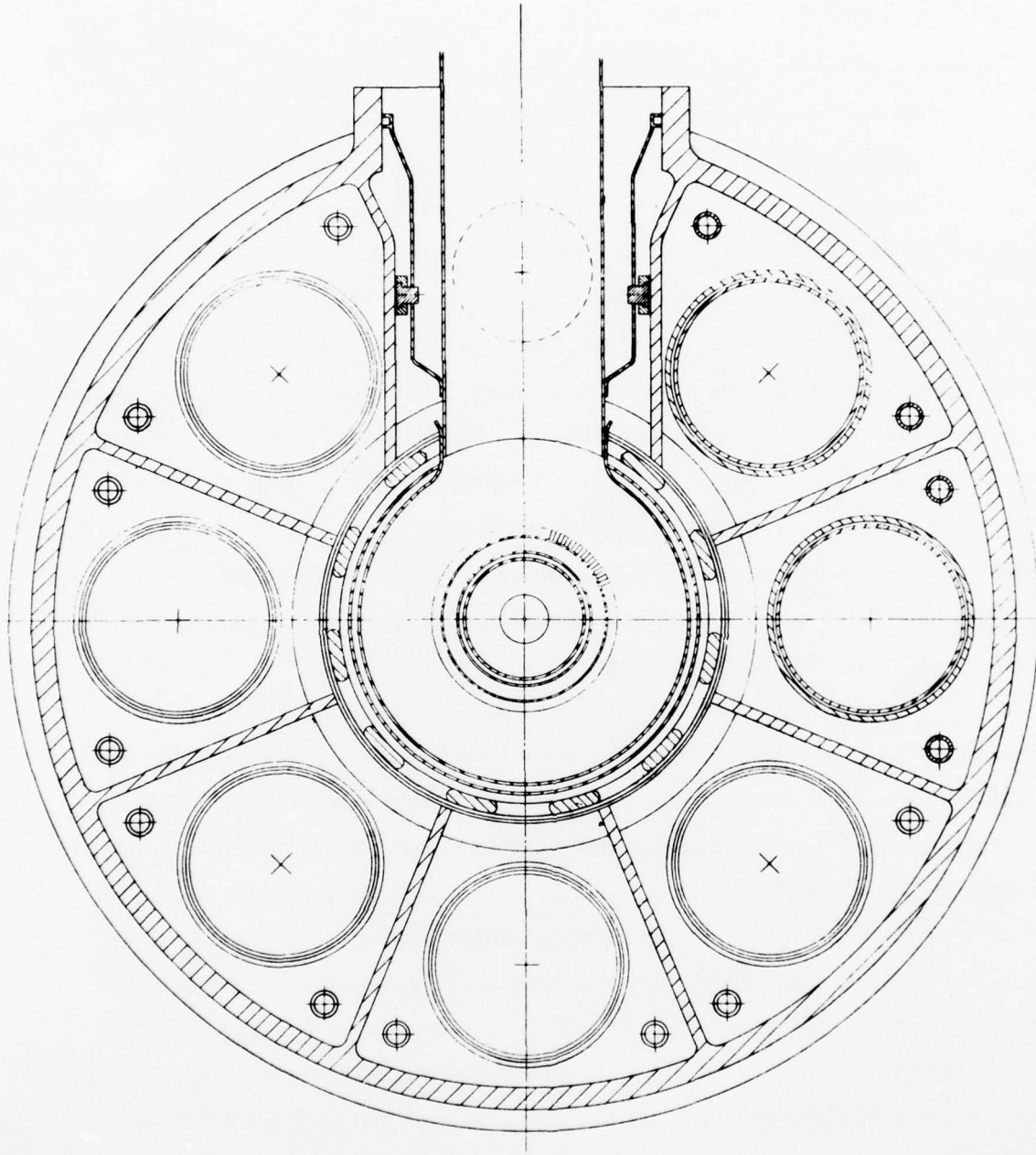
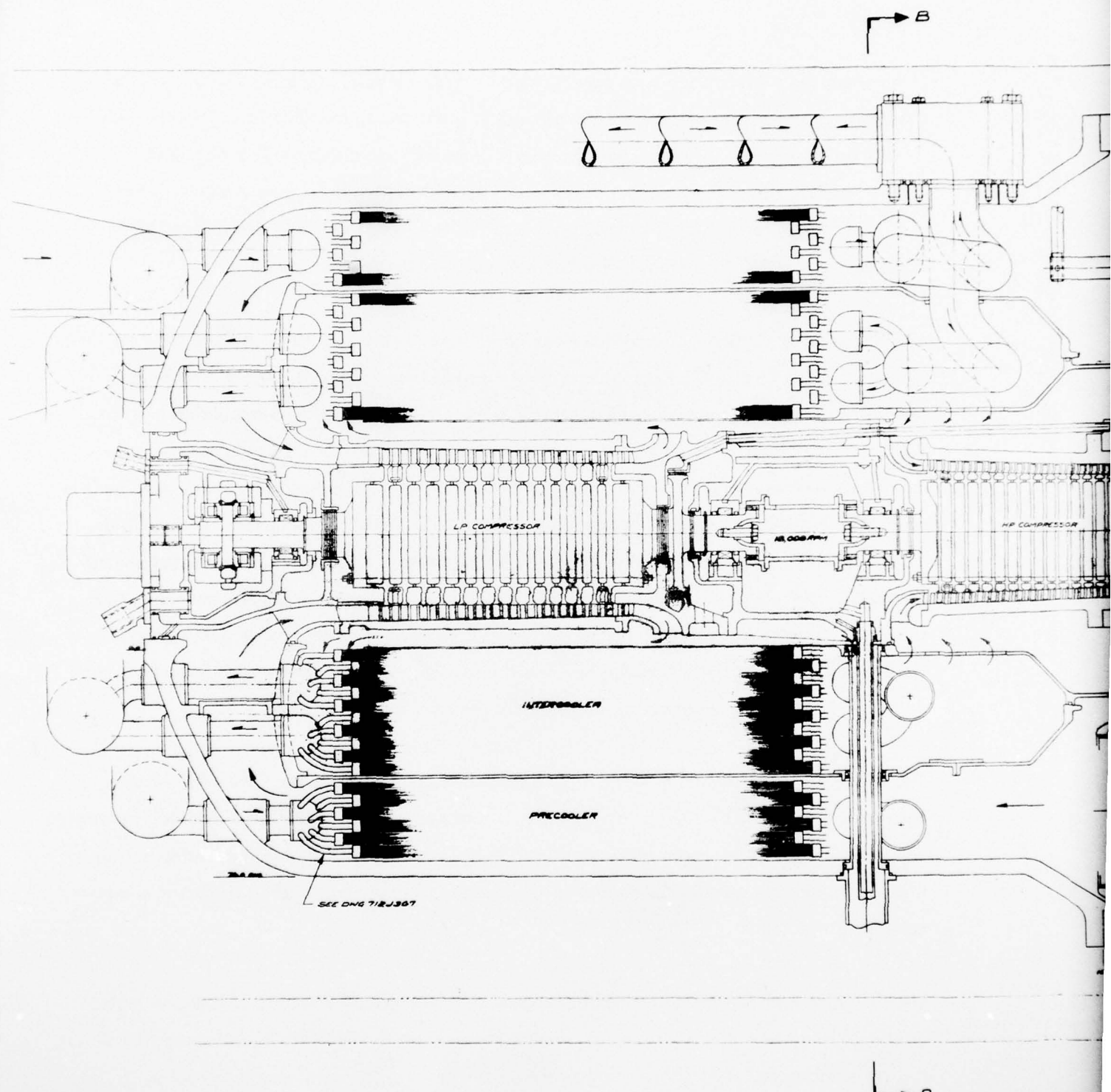


Figure 3.29a CCCBS Design Concept (1st Definition) Sheet 1



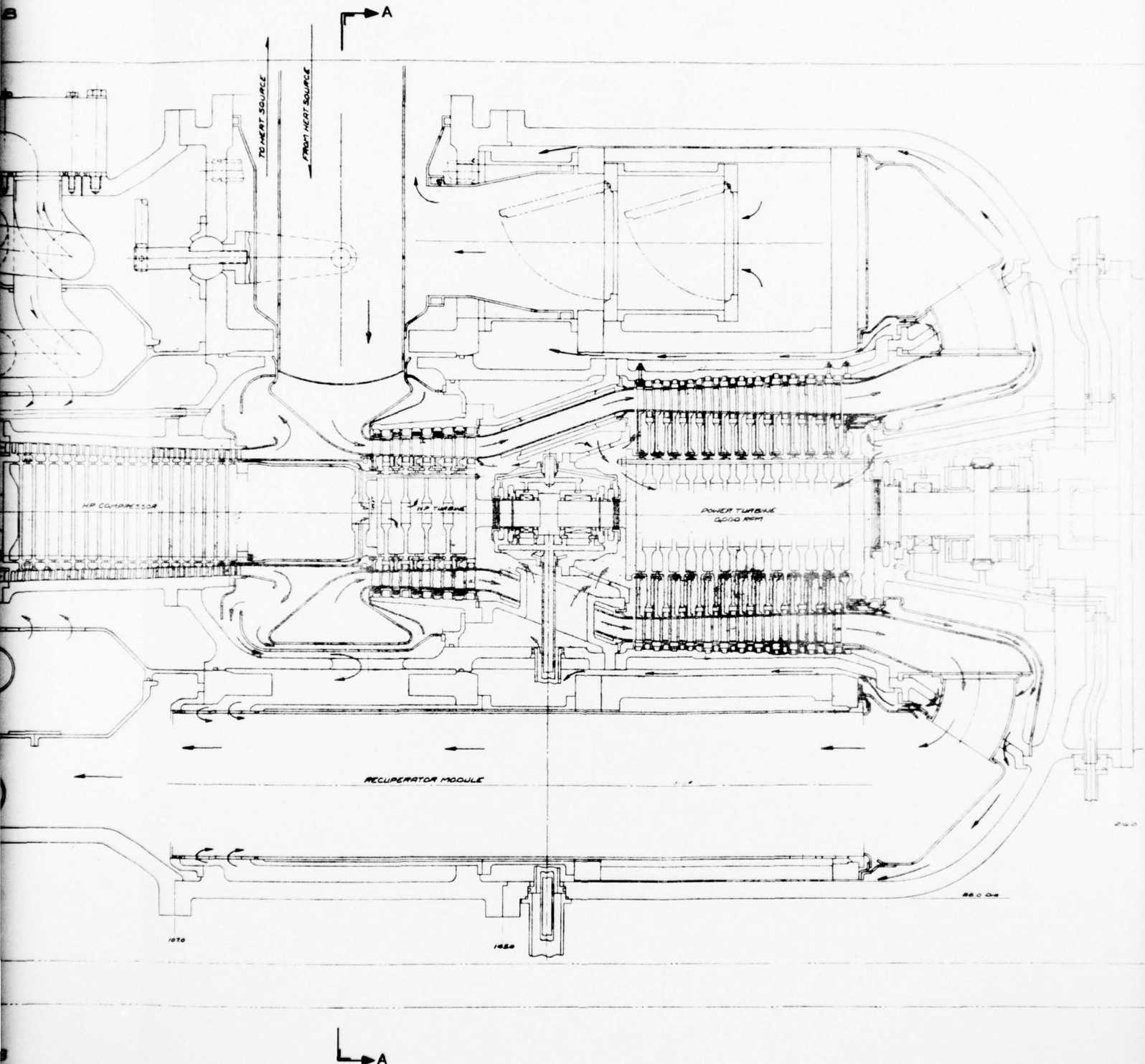


Figure 3.29b CCCBS Design Concept (1st Definition) Sheet 2



Westinghouse

rather than the anti-friction type employed in aircraft engines. As a result, the unscheduled shutdowns occasionally encountered in aircraft engines due to metal fatigue failures in balls, rollers and races will not be expected in the CCCBS turbomachinery. The high pressure compressor/turbine rotor speed has been set at 18,000 RPM. This speed along with an optimized high pressure turbine design has resulted in a conservatively stressed machine consistent with CCCBS operating life and turbine inlet temperature goals.

The design of the turbomachinery has been based upon technology developed in the Maritime Gas Cooled Reactor (MGCR) program suitably adapted to achieve lightweight and high reliability using current state-of-the-art practices. In the MGCR program (Reference 1) Westinghouse Electric Corporation was a subcontractor to General Dynamics for the turbomachinery development. Emphasis was placed on the development of turbomachinery operating on a regenerative, intercooled, closed gas turbine cycle with helium as the working fluid. Engine machinery concepts used in the MGCR designs were substantiated by a development program involving aerodynamic model tests (including full scale four stage compressor and two stage turbine tests), metallurgical testing in high purity helium and mechanical testing of lubrication and shaft sealing methods. Thus the MGCR program turbomachinery technology developments provide a proven design basis for the CCCBS turbomachinery.

The CCCBS power conversion assembly is designed as an integrated package whose major components can be individually assembled and checked and which can be completely assembled and checked out as an assembly. Consideration has been given to providing access to the turbomachinery for maintenance through providing for its removal and reinsertion into a power conversion assembly.

The CCCBS power conversion assembly consists of an integrated assembly of low and high pressure compressors and high pressure turbine rotating at 18,000 RPM, low pressure free power turbine rotating at 6,000 RPM (at full power), recuperator, precooler and intercooler. In this first definition of the design concept, the turbomachinery rotors are supported by oil lubricated

tilting pad bearings and the heat exchangers are of the tube and shell type. These components are assembled into a casing capable of withstanding full system pressure.

3.5.1.2 Assembly

Although local pressures throughout most of the power conversion assembly are lower than maximum system pressure, consideration of operation with one of two parallel units shut down dictates casing design conditions. Pressure throughout the inoperative unit will tend to approach full system pressure because of leakage through the shut-off valves. The complete power conversion assembly is therefore contained within a cylindrical pressure vessel made of low alloy steel, capable of accommodating the maximum system pressure. The pressure vessel is made in three sections, a center frame structure and forward and rear sections. The three sections are joined together by bolted flanges. Sealing of the flanges can be effected by metal or elastomer O-rings or alternately seal welded. The maximum temperature of the pressure vessel is approximately 400° F.

The forward section of the pressure vessel accommodates the intercooler and precooler in an annular arrangement around the turbomachinery.

The center frame structure consists of a relatively short cylindrical section of casing having two diaphragm members, one at each end, which extend radially inward towards the center. The diaphragm members have central holes which provide radial support for the turbomachinery casing. The two diaphragms are supported in the axial direction, one from the other, by eight essentially radial webs. Each of the diaphragms, in the spaces between the radial webs, is pierced by seven large diameter holes. These holes accommodate the seven recuperator modules. Only one of the diaphragms is pierced at the eighth inter-web location which accommodates the ducting connecting the powerplant with the heat source. A bolted flange penetration is provided on the exterior cylindrical portion of the center frame structure at this location. During operation, the center frame structure is pressurized by high pressure compressor outlet gas and serves as the recuperator high pressure inlet plenum. Sealing of the turbomachinery to the center frame is effected by elastomer O-rings, carried in grooves



Westinghouse

on the turbomachinery casing, which engage with prepared surfaces at the inner diameter of the center frame diaphragm members. The gas temperature at this location is approximately 300°F.

The recuperator modules are constructed in the form of long circular cylinders and are housed in SA533 tubular support members which extend axially from the center frame structure. The tubular members support a rectangular section SA533 toroidal pressure vessel which functions as the recuperator high pressure outlet plenum. During operation, the high pressure gas, after being heated on the shell side of the seven recuperator modules, is dumped into the toroidal vessel and flows around it to the eighth pipe location through which it passes into the outer annulus of the coaxial duct to the heat source.

The recuperator modules are inserted through the toroidal vessel into their tubular support members and fastened into position by means of bolted flanges at their hot ends. Relative thermal expansion between the recuperator module and the support members and between the tubing and the shell of the recuperator modules is accommodated by sliding joints sealed by elastomer O-rings at the cold ($\approx 300^{\circ}\text{F}$) end. In this arrangement, the tubular support members are separated from the recuperator modules by a thin layer of stagnant helium. On their outer diameters the tubular support members are exposed to the relatively cool gas inside the external pressure casing (originating from the power turbine balance piston labyrinth). Relative expansion effects between the tubular support members are therefore expected to be small resulting in a minimum of distortion.

At the eighth tubular support member, the collector pipe from the toroidal vessel passes through two check valves in series into a short inner pipe separate from the tubular support member. The inner pipe is sealed to the toroidal vessel and to the outer coaxial duct to the heat source by means of piston rings or other similar sealing devices. Piston rings, or similar devices, are also used to seal the separate coaxial duct component to the center frame structure. The piston rings allow the separate inner duct components to expand and contract

freely, under the influence of the hot gases they convey. The tubular support member and the center frame structure are exposed only to the relatively stagnant compressor outlet gas on their inner surfaces and to the cool gas inside the external pressure casing on their outer surfaces. The tubular support member at the delivery pipe location is therefore expected to experience essentially the same temperature conditions as the other seven tubular members at the recuperator module locations.

The rear section of the pressure vessel supports the interfacing load machinery (e.g., an electric generator) and the aft or power turbine outlet end of the turbomachinery. Under normal operating conditions the rear section of the pressure vessel locates the turbomachinery in the axial direction and provides support in the radial direction at the outlet end. The turbomachinery casing receives additional support in the radial direction from the center frame structure and from the forward section of the pressure vessel. The turbomachinery is free to slide axially at these locations to accommodate thermal expansion. Sealing of the turbomachinery to the pressure vessel components is effected by elastomer O-rings.

The turbomachinery assembly can be removed from the power conversion assembly as a unit together with the generator and the rear casing pressure vessel section. During this operation the rear section of the casing conveniently functions as a lifting fixture since the center of gravity of the turbomachinery, generator and rear pressure vessel section is located approximately at the attachment flange of the rear section of the vessel to the center frame structure. Jacking screws in the flange of the rear section are used to apply axial force to the turbomachinery to overcome the friction of the O-ring seals at the powerplant/turbomachinery interfaces. The turbomachinery, generator and rear assembly can then be removed axially from the assembly while suspended at the center of gravity from a crane or transporter device. The transporter device can be furnished as an integral part of the containment system in a nuclear plant, thus allowing transport of the turbomachinery inside the containment to a suitably located penetration. The protrusion of the rear pressure vessel casing through the containment penetration, while still supported from the transporter inside the containment,

would then allow a special lifting fixture to be bolted to the rear pressure vessel from outside the containment. The lifting fixture would be designed such that an external crane hook could apply its lift force over the center of gravity of the assembly, by suitably shaping and counterbalancing the lift fixture. Transfer of the assembly weight from the in-containment transporter to the external crane could then be completed. A system of stabilizer rails to prevent swinging would probably be desirable.

During removal of the turbomachinery from the powerplant, the internal flow path is separated at sliding joints in the low pressure recuperator entry plenum. The entry plenum is a sheet metal (18-8 stainless steel, or possibly, 2-1/4 Cr/Mo) vessel which receives the power turbine outlet gas from eight radial pipes which pass through the rear turbomachinery support structure. The sheet metal plenum confines the relatively warm ($\approx 950^{\circ}\text{F}$) turbine outlet gas as it enters the recuperator modules. The rear pressure vessel section is exposed to cooler ($\approx 400^{\circ}\text{F}$) gas originating from the power turbine balance piston labyrinth seal. This cooler gas also cools the power turbine casing before passing through the center frame structure in a number of transfer pipes and joining the main cycle flow path at entry to the precooler. The transfer pipes are sized so that the pressure drop of the balance piston leakage gas in traversing them is slightly greater than the pressure drop of the hot side recuperator flow path. This ensures that the leakage flow at the sliding joints of the recuperator entry plenum is from the cold gas outside to the hot gas inside the plenum thus minimizing the heating of the cooler gas adjacent to the pressure vessel.

The coaxial duct connecting the turbomachinery to the heat source is designed so that it can be retracted from the turbomachinery to facilitate the removal of the turbomachinery from the powerplant. A possible retractable support concept is illustrated in Figure 3.29. The retractable pipe is supported and located radially (with respect to the turbomachinery centerline) by a forked member which is pivoted in a spherical graphite ball located in one of the diaphragm members of the center frame structure. A push/pull rod, attached to the end of the forked member remote from the retractable pipe, penetrates the powerplant pressure vessel and is either fixed at an accessible point on the vessel or is attached to an actuator device. The

details of this area of the concept will obviously depend on the particular application. Retraction of the pipe could be effected by manual release and activation of the push/pull rod or by remote control.

The oil and gas service pipes are also designed to be retracted radially from the powerplant assembly prior to removal of the turbomachinery.

Access to the recuperators for removal is obtained by first removing the rear pressure vessel, turbomachinery and generator. The recuperator modules can then be unbolted at their hot end flanges and withdrawn axially from the powerplant assembly.

Access to the precooler and intercooler is obtained by removing the forward section of the powerplant pressure vessel.

3.5.1.3 Design

Mechanical Design

The construction of the turbomachinery is straight forward and employs current state-of-the-art practice. Figure 3.29 illustrates the mechanical design of the concept design turbomachinery. The concept design powerplant was initially developed to use oil lubricated turbomachinery bearings and counterflow precooler and intercooler. This is the arrangement illustrated in Figure 3.29. More recently in the study, gas bearings and multi-pass crossflow cooler have been adopted for the CCCBS Conceptual Design. These changes are described in detail in Section 3.5.2.

High Pressure Rotor Mechanical Design

The high pressure rotor consists of the high pressure turbine rotor and the high pressure compressor rotor which are rigidly joined together by a short length of large diameter hollow drive shaft. The resulting rigid rotor is supported at each end in tilting pad journal bearings. The design of the high pressure turbine rotor is described in detail in Section 4.2.



Westinghouse

The high pressure compressor rotor is straightforward and employs multiple discs joined together by through bolts and curvic couplings. The curvic couplings are machined onto cylindrical extensions at the front and rear of each disc and provide accurate radial alignment of the discs while transmitting the driving torque. The multiple through bolts provide sufficient clamping force to hold the rotor together. Alternative forms of construction are also possible. The multiple through-bolts could be replaced by a single centrally located bolt or, alternatively, the discs could be welded together.

The high pressure compressor rotor blades are attached to the discs using conventional dove-tails and grooves. The blade axial width dimensions vary from 0.6 inch at the compression inlet to 0.5 inch at the exit and result in acceptable gas bending stresses, in the region of 15,000 psi, while achieving a reasonably short compressor assembly. The stator vane axial widths are held constant at 0.4 inch, the smaller chord being permitted by the superior support provided by the shrouded arrangement. Rotor/stator axial gaps are 0.25 inch at all locations. The axial gap is required to accommodate length variations in the rotor and stator assemblies resulting from tolerance stack-up and differential thermal expansion. Obviously the location of the thrust bearing has a substantial effect on the amount of axial gap which must be provided at a given location to insure against rubs. In this respect a more central thrust bearing location, between the two compressors would be preferable to that shown in Figure 3.29. The thrust bearing location at the inlet end of the low pressure compressor, shown in the drawing, was chosen for the small thrust collar inner diameter made possible by the absence of any substantial driving torque. The inter-compressor location, although more desirable from the standpoint of minimizing axial gap, forces the use of a larger thrust collar inner diameter with its adverse surface speed implications.

Blade centrifugal stresses range from approximately 16,000 psi at inlet to 13,000 psi at exit. The design of the root fixings and discs has not been optimized but no problems are foreseen in this area due to the reasonably low mean blade speed (≈ 1150 feet/second) and

temperature (< 300° F). AISI type 403 stainless steel material is used extensively in combustion gas turbine compressor blades and discs and should be appropriate in the CCCBS at these conditions.

High Pressure Stator Mechanical Design

The high pressure stator consists of the high pressure turbine stator, the high pressure compressor stator and their interconnecting structure. The interconnecting structure is a rigid assembly formed by the compressor outlet/turbine inlet plenum casing and the high pressure turbine outlet diffuser casing.

The design of the high pressure turbine stator is described in detail in Section 4.2. The high pressure turbine stator is attached, by means of a flange at its outlet end, to a mating flange on the inlet end of the high pressure turbine outlet diffuser casing.

The high pressure turbine outlet diffuser casing is attached, by means of a flange at its outlet end, to a mating flange on the compressor outlet/turbine inlet plenum casing. A flange on the other end of the compressor outlet/turbine inlet plenum casing is attached to a mating flange on the high pressure compressor casing. Large diameter O-rings at the circumference of the casing engage with machined surfaces at the inner diameter of the powerplant center frame structure and separate the high pressure compressor outlet gas from the lower pressure gas entering the high pressure compressor and the low pressure gas in the powerplant cavity.

In addition to the circumferential mating flanges, all of the high pressure stator casings are provided with axial split flanges which allow half of the stator structure to be removed to facilitate inspection of the blading. The turbomachinery must be withdrawn axially from the power conversion assembly before the stator half casings can be removed.



Westinghouse

The high pressure compressor stator vanes are of the shrouded type. The vanes are brazed or welded into half ring members at the inner and outer diameters. The stator vane assemblies are assembled into grooves machined in the compressor casing. Details of this area of the design have not been defined but several options are available. The stator vane assembly inner half rings carry honeycomb or some other abradable material machined to provide a close clearance with labyrinth seal fins machined onto the rotor disc curvic coupling extensions. Materials used in the compressor stator vane assemblies will be chosen for compatibility with the method of fabrication employed. AISI Type 347 stainless steel is amenable to welding and brazing and is a good candidate for half rings and vanes.

The stator casings can be machined from ductile iron castings or low alloy steel weldments. The Ni-resist ductile iron materials are available in low expansion grades which are attractive from the standpoint of minimizing thermal distortion and stresses. However, the acceptability of cast casing materials will have to be evaluated in the light of the Navy shock requirement for the particular application being considered. Alternatively, the casings could be machined from 2-1/4 Cr-1Mo steel weldments.

The hot gas duct and scroll carrying the helium from the heat source to the high pressure turbine inlet is made from a superalloy material similar to Hastelloy X. Inconel 617 was considered a good candidate but has recently found to be vulnerable to corrosion in a helium environment. The hot gas duct and scroll is completely surrounded by the cooler compressor outlet gas flowing from the high pressure compressor diffuser outlet to the recuperator modules in the powerplant center frame. The cool gas leaves the turbomachinery compressor outlet/turbine inlet plenum casing through several holes in the casing and passes into the powerplant center frame region. It is possible that the design of these components will become more complex as more detailed analyses are performed. A double walled hot gas duct consisting of an essentially unstressed hot liner supported by a cooler structural member may be necessary. This approach would create a stagnant gas layer between the hot and cold members to reduce the conductive thermal gradients in the materials. Considerable attention will have to be

given to the design of the axial split seal arrangement used in the hot scroll and to the sliding seal between the hot gas inlet duct and the scroll. The sliding seals at ducting joints must be thoroughly evaluated to ensure freedom from galling and bonding in the high temperature helium environment. The application of special coating materials in the areas of sliding may be necessary.

The high pressure turbine outlet diffusor consists of a sheet metal assembly, in the form of an annular passageway penetrated by a number of airfoil section struts and a cooled structural casting or fabrication which is protected from the hot gas leaving the high pressure turbine by the sheet metal assembly. The structural assembly consists of an outer pressure casing and an inner ring member supported from it by a number of hollow radial struts. The housing for the high pressure turbine outlet journal bearing and the power turbine inlet journal bearing is supported from the inner ring member.

Cooling gas, tapped from the low pressure compressor outlet is piped to the annular region surrounding the high pressure turbine outlet diffuser and flows radially inward through the hollow struts in the structural assembly. The cooling gas circulates around the bearing housing and structural assembly.

The structural assembly casings, the sheet metal fairing assembly and the bearing housing casings are all designed to be split diametrically to facilitate the inspection of bearings and blading.

Low Pressure Compressor and Drive Shaft Mechanical Design

The low pressure compressor is similar in construction to the high pressure compressor and employs similar material combinations. The low pressure rotor is of multiple disc design using curvic couplings and through bolts and is supported on tilting pad journal bearings

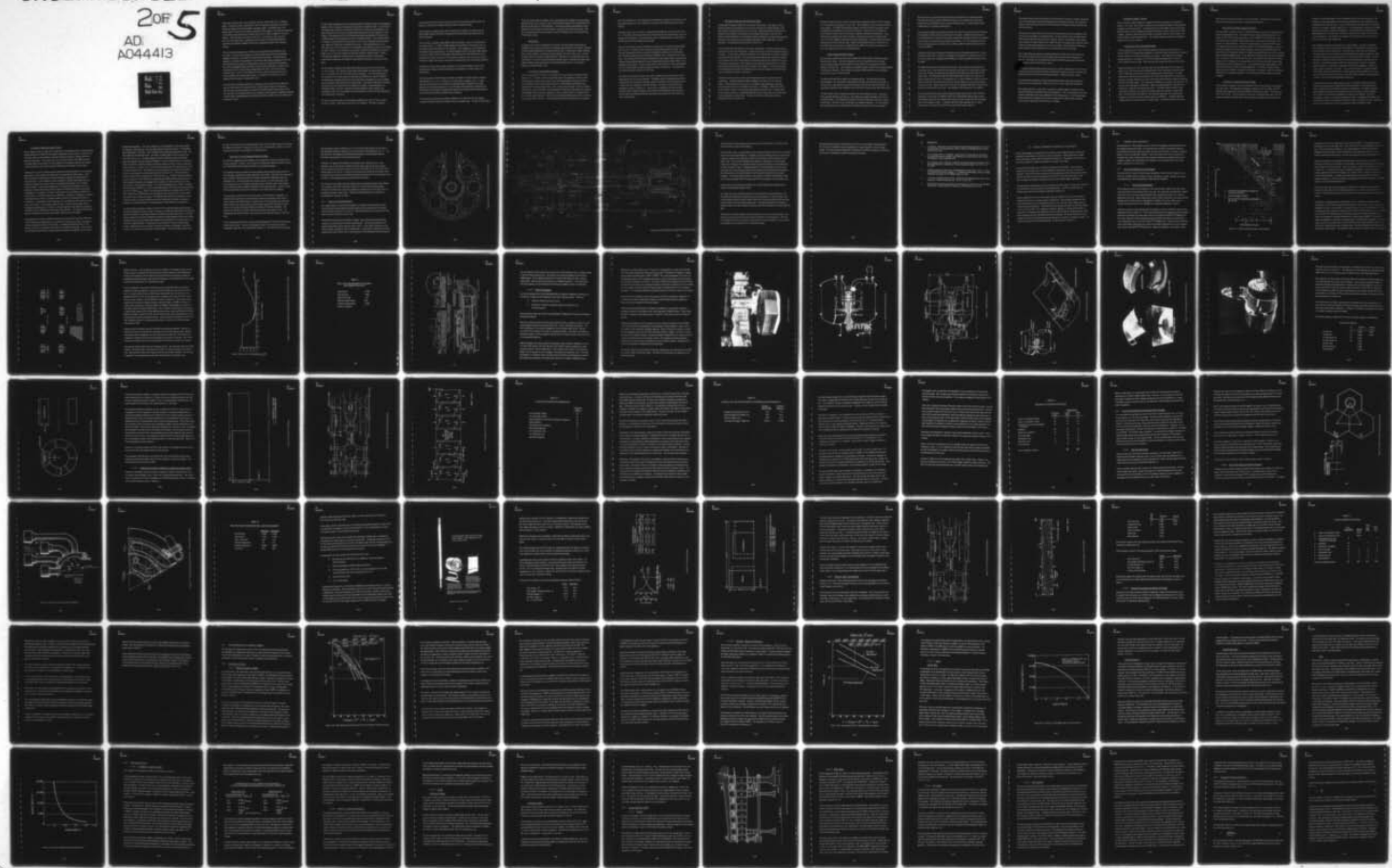
AD-A044 413 WESTINGHOUSE ELECTRIC CORP PITTSBURGH PA ADVANCED ENE--ETC F/6 21/5
COMPACT CLOSED CYCLE BRAYTON SYSTEM FEASIBILITY STUDY.(U)
JUL 77 R E THOMPSON, G H PARKER, R L AMMON N00014-76-C-0706

UNCLASSIFIED

WAES-TNR-233

NL

20F 5
AD
A044413



at the inlet and outlet ends. Also mounted on the rotor, at the outlet end, is a balance piston. The balance piston is pressurized on the face nearest the compressor rotor by high pressure gas tapped from the high pressure compressor outlet. The opposite face of the balance piston is exposed to low pressure compressor outlet pressure. The axial force generated by the balance piston reduces the net axial rotor force to a value acceptable to the thrust bearing. This is discussed more fully in Section 4.2. The leakage of the pressurizing gas across the balance piston is minimized by the provision of a multi-stage labyrinth seal at the outer diameter together with the use of abradable material on the stationary housing.

The low pressure compressor rotor is driven from the high pressure rotor through a short drive shaft. The drive shaft is designed to transmit axial load and to have self-aligning capability in addition to the ability to transmit the driving torque. The self-aligning capability is provided to accommodate the eccentricity and angular misalignment which can arise between the low pressure and high pressure rotors due to manufacturing tolerances. The axial load capability allows the shaft to transmit the net axial thrust, resulting in the high pressure rotor due to the pressure changes across the rotor, into the low pressure compressor rotor. This net thrust together with the low pressure compressor rotor thrust, further modified by the balance piston thrust, is carried by the thrust bearing which is located at the low pressure compressor inlet end.

The drive shaft self-aligning capability is achieved by the use of gear-tooth couplings at each end which transmit the torque but allow a small amount of angular misalignment. The axial load carrying capability is provided by spherical joints at each end which allow the axial load to be transmitted between the compressor rotors through the misaligned couplings. The gear-tooth coupling/spherical joint combination has been widely used in gas turbines over the past thirty years.

The drive shaft arrangement forms a convenient assembly interface and allows the independent assembly of the low pressure compressor and high pressure rotor/stator units. The lubrication of the gear-tooth couplings is conveniently achieved, since they are accommodated in the same housing as the low pressure compressor outlet bearing and the high pressure rotor inlet bearing. The replacement of the oil lubricated bearings by gas bearings will require that a shaft arrangement be developed which does not require lubrication. One design possibility is to employ a single journal bearing between the low pressure compressor and high pressure rotor supporting a rigid shaft connecting the two rotors. The bending flexibility in the shaft would then have to be sufficient to accommodate shaft misalignment without overstressing the shaft in fatigue. Care would have to be taken in assembling and handling the long and fragile rotor, to avoid overstressing the rigid small diameter connecting shaft. Possibly a flexing metal diaphragm coupling could be included having sufficient flexibility to accommodate misalignment and sufficient axial stiffness and strength to transmit the axial loads.

The low pressure compressor rotor blade axial widths vary from 0.9 inch at the inlet to 0.7 inch at outlet. The resulting maximum gas bending stresses are approximately 10,000 psi., or somewhat lower than in the high pressure compressor. The centrifugal stresses in the low pressure rotor blades range from approximately 28,000 psi at inlet to 20,000 psi at outlet and are somewhat higher than in the high pressure compressor due to the increased mean blade speed (1350 feet/second) and blade height. The design of the blade root fixings and discs has not been optimized but no problems are foreseen in the development of a satisfactory design. However, somewhat more detail attention will be needed in the optimization of the disc rim and blade root fixing geometry to minimize the disc stresses than in the high pressure compressor.

The stator vane axial widths in the low pressure compressor vary from 0.7 inch at inlet to 0.5 inch at outlet. Axial gaps are 0.25 inch at all locations. This value is probably



Westinghouse

over-generous for the low pressure compressor with the thrust bearing location shown, but results in a conservative (somewhat large) estimate of compressor length.

The low pressure compressor stator casing is attached by a flange at its outlet end to the outlet diffuser casing which also accommodates the balance piston high pressure and low pressure chambers.

The low pressure compressor outlet diffuser casing is attached, in turn, to the bearing and drive shaft housing. A number of drilled passages are provided in the housing to carry oil to the bearings and clean helium to the seal areas. Other passages carry the drainage oil and breather gas from the bearings. The drilled passages connect with supply tubes, sealed by O-rings, which traverse the intercooler outlet and precooler inlet flow regions of the powerplant to external connections on the powerplant pressure vessel. Provision is made to withdraw the supply tubes prior to removing the turbomachinery from the powerplant assembly.

The bearing and drive shaft housing is supplied with an axial split flange, like the other turbomachinery casings, allowing the bearings to be inspected or the drive shaft to be disconnected.

The bearing and drive shaft housing is attached by a flange to the high pressure compressor inlet casing which, in turn, is attached to the high pressure compressor casing. A large diameter O-ring seal at the circumference of the high pressure compressor inlet casing engages with a machined surface at the inner diameter of the intercooler and separates the flow leaving the low pressure compressor and entering the intercooler from the flow leaving the intercooler and entering the high pressure compressor.

The low pressure compressor inlet casing is attached to the inlet end of the low pressure compressor casing and supports the bearing housing and starter motor. O-rings at the periphery

of the inlet casing effect the sealing of the turbomachinery flow passages to the powerplant assembly and are used to confine a zone of purified helium between the turbomachinery flow path gas and the exterior of the powerplant. The bearing housing accommodates the high speed rotor thrust bearing and the low pressure compressor inlet end journal bearing. Both the thrust bearing and the journal bearing are of the tilting pad type in this first definition of the design concept.

Starter Motor

The starter motor drives the high speed rotor through a short quill shaft and provides the capability of accelerating the rotor to self sustaining speed during the initial phase of startup. In the gas bearing application, the starter motor may also be called upon to apply a braking force, during shutdown, to minimize the time required to bring the rotor to rest. The type of starter motor to be used has not been selected. Both electric and pneumatic options are conceivable. The use of the helium inventory control system for regulating the power output makes available a large stored volume of high pressure helium which could be used to energize a pneumatic starter motor.

Low Pressure Turbine Mechanical Design

The low pressure turbine is similar in construction to the high pressure turbine described in Section 4.2.1. However, the lower mean blade speed and temperature conditions of the twelve stage low pressure turbine result in the less stringent design conditions and allow the consideration of less strategic materials than the IN100 blading and MAR509 vanes considered for the high pressure turbine. Also, as previously mentioned, the use of rotating blade shrouds can be considered, to provide support in bending for high aspect ratio blading. The diaphragm stator construction employed in the low pressure turbine is extended inward to a relatively small diameter in order to minimize the seal leakage area and also to minimize the axial gas thrust on the rotor. The resulting small effective shaft diameter is acceptable



Westinghouse

since the requirements for rotor stiffness are less demanding in the power turbine than in the high pressure turbine due to the relatively low speed and short bearing span of the former machine.

The power turbine rotor is mounted on tilting pad journal bearings, one at each end of the rotor. The shaft at the turbine outlet end is extended through the thrust bearing to carry the coupling to the generator. The power turbine outlet end bearing housing is supported from the rear section of the powerplant pressure vessel.

The power turbine stator casing is attached at its outlet end to a conical structural member which, in turn, is attached to the rear section of the powerplant pressure vessel. This structural arrangement allows the complete turbomachinery assembly to be cantilevered from the pressure vessel rear section during its installation into or removal from the powerplant. The conical structural member is penetrated at eight equally spaced circumferential locations by eight radial pipes which convey the gas from the turbine outlet diffuser to the recuperator inlet plenum. The low pressure turbine outlet diffuser is a sheet metal assembly which is mounted inside the turbine casing and conical structural member thus protecting the casings and pressure vessel from the hot gas.

The outlet end of the power turbine rotor carries a balance piston which carries a multi-stage labyrinth seal on its outer diameter. The balance piston is pressurized by gas which is tapped from the low pressure compressor outlet and reduces the rotor axial thrust load to a value within the capability of the thrust bearing. The subject of thrust balancing is discussed more fully in Section 4.2. The gas which is supplied to the balance piston and which leaks through the balance piston labyrinth seal subsequently cools the power turbine casing and powerplant pressure vessel before rejoining the main flow path gas at entry to the precooler.

Bearings, Housings and Seals Mechanical Design

The bearings illustrated in Figure 3.29 are standard catalog items. The Kingsbury tilting pad thrust bearings are equipped with oil control rings around the outside diameter of the thrust collar to minimize power loss due to churning. While this standard high speed thrust bearing is fully capable of meeting the thrust and speed requirements, using the thrust balancing methods described, some additional bearing development to reduce pad temperature and power loss, possibly by the use of directed lubrication and/or offset pads, would be beneficial. These possibilities are discussed in Section 4.3.

The journal bearings illustrated are Orion tilting pad bearings. The load and speed requirements fall well within the manufacturer's catalog ratings and no need for bearing development is foreseen. Journal bearing loads are sufficiently low (≈ 100 psi) that no need for hydrostatic jacking at start-up is foreseen. The Orion tilting pad journal bearings incorporate floating ring oil seals on each side of the bearing to minimize the amount of oil ejected in the region of the bearing housing seals. This is believed to be a beneficial design feature in a machine which employs labyrinth seals and which is sensitive to oil leakage. The functional aspects of the bearings and the operating conditions to which they are exposed in the CCCBS power-plant are discussed more fully in Section 4.3.

The bearing housings employ a double seal arrangement to prevent oil loss at the shaft penetrations. The space between the seals is supplied with helium from the clean-up-system. The seal adjacent to the housing is a "windback" seal employing a multi-start screw thread which returns oil droplets to the housing. In addition, a steady buffer flow of clean helium is drawn into the housing preventing the loss of oil mist. The seal remote from the bearing housing is a multi-stage labyrinth seal to minimize the loss of clean helium to the turbomachinery working fluid. The operation of the oil and seal gas systems is discussed more fully in Section 4.3.



Westinghouse

The barrier helium gas which is drawn into the bearing compartments flows, with the scavenge oil, to a separator incorporated in the oil tank. After separation, the oil and gas are returned to the systems. The MGCR turbomachinery program included a lubricant test program which investigated the compatibility of lubricants with helium. Factors such as the tendency of oils to produce foam and vapor under practical operating conditions were examined. It was determined that paraffin base turbine lubricant, typified by names such as Teresso-43 and D.T.E. 797 were capable of satisfying the MGCR requirements. Since the MGCR and CCCBS requirements are functionally the same, insofar as the lubrication system is concerned, and the CCCBS lube and seal system is adapted from the MGCR, the MGCR test experience can be directly applicable to the CCCBS turbomachinery.

Heat Exchanger Mechanical Design

The recuperator modules are constructed as simple thin walled cylinders containing bundles of heat transfer tubing. The flow configuration is that of a counterflow heat exchanger with the turbine exhaust helium flowing in the tubes and with the compressor exit helium flowing on the shell side. The recuperator is composed of seven modules which are approximately 16.36 inches in diameter. Each module contains about 10700 tubes with an outer diameter of 0.120 inch and are 0.010 inch thick.

The tubes are formed at their ends into a hexagonal section. The tube ends are furnace brazed together. The tube bundle is also brazed at the ends to an external cylinder and a cold end ring. Filler pieces are used to fill the gaps at the tube and cylinder interface. No tube sheet is required in this arrangement since each tube carries the local axial tension force.

The tube module is free to expand and contract due to the floating end ring. O-rings are used to seal the floating cold end ring. The modules are located and sealed at the hot end by bolted flanges. This arrangement eliminates the need for tube sheets with their numerous drilled holes. However the hex-end forming is an additional operation. The conventional tube sheet approach can be substituted if manufacturing studies show this to be desirable.

The common duct structure located around the power turbine section is supported axially from the center frame by eight SA 533 pressure tubes, seven containing the recuperator modules and one containing the check valves and delivery pipe. The eight pressure tubes contain helium at compressor outlet pressure.

The recuperator modules are located axially from the common duct structure by bolted flanges which separate the high and low pressure sides of the system. Differential thermal growth, in the axial direction, between the recuperator modules and the pressure tubes is accommodated by the sliding O-ring seals at the cold ends of the modules. The O-rings separate the high and low pressure gases and are made of silicon rubber capable of operating at temperatures in excess of 400°F.

Differential thermal growth between the delivery pipe and the eighth pressure tube is accommodated by piston rings. The piston ring leakage is acceptable in this location since it will be very low because the leakage pressure difference is small (recuperator module plus check valve ΔP).

The radial pipe located in the center frame structure, which receives the heated gas from the delivery pipe, is also sealed from the compressor outlet gas in the center frame by piston rings which can slide to accommodate the thermal growth between the radial pipe and the center frame. The radial pipe carries the heated gas radially outward to a nozzle on the pressure casing whence it flows to the energy source. A coaxial Hastelloy X liner (or similar) passing through the radial pipe, delivers hot gas from the energy source to the high pressure turbine inlet scroll. Simple sliding joints in the liner accommodate differential thermal growth between the liner and the inlet scroll. Some leakage at the sliding joints is acceptable.

The hot gas from the heat source passes through the high pressure turbine, which drives the compressors, and into the low pressure turbine via an intermediate bearing support casing. After passing through the low pressure power turbine, the gas is ducted into the low pressure side of the recuperator module. A stainless steel liner system separates the hot turbine outlet gas from the pressure casing and turbine bearing and support assembly.



Westinghouse

The turbine outlet gas then flows axially forward through the recuperator modules, transferring heat to the tube bundle containing the high pressure compressor outlet gas. The cooled low pressure turbine outlet gas leaves the forward ends of the recuperator modules and enters the precooler annulus.

The precooler and intercooler are built up from the tube modules which are assembled within the annular flow passages accommodating them. The tube modules consist of small diameter stainless steel tubes spaced by spiral wire wrapping. The basic tube module in this arrangement consists of 91 tubes 0.100 inch ID x 0.120 inch OD on a triangular pitch forming a hexagonal array measuring approximately 1.41 inch across flats. The tube ends are brazed into small hexagonal header assemblies which are fed by single 5/8 inch OD tubes.

The 91 tube hexagonal modules are bundled together into groups of up to 33 modules and their 5/8 inch OD feed tubes are curved appropriately and brazed into hemispherical headers. The headers can be manufactured as small investment castings and are generally in compression under the high helium pressure.

The variously shaped module groups are bundled into annular configurations to suit the intercooler and precooler geometries and their hemispherical headers are bolted to manifold pipe assemblies at each end of the heat exchanger assembly. Sealing is by static o-rings.

The manifold pipe assemblies penetrate the powerplant pressure vessel and are joined by piping to the much larger pipes, isolation valves, etc. at the containment penetration.

The modular approach to construction is expected to simplify problems of quality control during manufacture and facilitate repair and replacement. The 91 tube modules can be leak checked individually before being assembled into 33 module groups. The 33 module groups being mechanically assembled into the heat exchanger can be checked before assembly and are readily replaceable without brazing or welding.

Aerodynamic Design - General

The low molecular weight of helium (4 compared with 29 for air) results in high acoustic velocity. As a result, Mach number constraints on the aerodynamic design of turbomachinery components are not encountered. The high specific heat and enthalpy change characteristic of helium tends to drive the design toward high blade speeds in order to minimize the number of stages. However, mechanical stress limitations ultimately limit the work per stage which can be handled in helium turbomachinery. The resulting numbers of stages are consequently larger than in air cycle machines.

High Pressure Turbine Aerodynamic Design

The high pressure turbine, having the highest operating temperature environment in the machine (1632°F first stage blade temperature), is the most critical turbomachinery component from the standpoint of the stress limitations on the design. The temperature and pressure conditions assumed in the design are 1671°F and 1487.9 psia respectively at inlet and 1277°F and 836.9 psia at outlet. The helium mass flow through the turbine is 130.6 lb/sec.

Design parameters were chosen to achieve high work per stage and so limit the number of stages to five, while limiting the centrifugal stresses in the rotor blade to value consistent with a 10,000 hour life using state of the art blade materials ($\approx 20,000$ psi). The load coefficient of 3.39 and the flow coefficient of 0.78 are both higher than the values corresponding to maximum efficiency in order to achieve the required work per stage and minimize flow area (and blade height). The compromise in efficiency is not great (\approx one percent). The resulting mean blade speed is 1200 ft/sec. Blade centrifugal stresses are minimized by the selection of a relatively high hub/tip ratio (0.81). This latter selection results in some compromise in efficiency, as a result of the less favorable tip clearance to blade height ratio, and this has been accounted for in the efficiency prediction. The resulting mean diameter is 15.28 inches and the rotational speed is 18,000 RPM. The blade heights are 1.608 and 2.33 for the first and last rows respectively. The turbine blading is of the free



Westinghouse

vortex type with 50 percent reaction at the mean diameter. The design and stress analysis of the first stage turbine is discussed in more detail in Section 4.2.

High Pressure Compressor Aerodynamic Design

The high pressure compressor is driven at 18,000 RPM directly from the high pressure turbine through a large diameter shaft. The temperature and pressure conditions assumed in the design are 99°F and 874.7 psia respectively at inlet and 281°F and 1610.5 psia at outlet. The thermodynamic properties of helium require that a large amount of mechanical work be done on it to raise its pressure. While the low temperature environment (<300°F) would have allowed the use of an increased mean diameter in the compressor blading, to achieve high work per stage and minimum number of stages, the resulting small blade height and high hub/tip ratio would have resulted in reduced compressor efficiency due to the increased effect of blade tip leakage losses. It was, therefore, decided to arbitrarily limit the hub/tip ratio to a value of .85 in order to limit tip losses. The resulting mean diameters and blade heights are 14.8 inches and 1.2 inches at inlet and 13.29 inches and 1.08 inches at outlet respectively for a flow coefficient of 0.5. The corresponding mean blade speeds are 1163 ft/sec and 1044 ft/sec at inlet and outlet respectively. The number of stages was then determined from the MGCR compressor data (Reference 1) adjusted to allow for the different blade speed and temperature conditions. The resulting high pressure compressor requires 18 stages.

Low Pressure Compressor Aerodynamic Design

The low pressure compressor is driven at 18,000 RPM from the high pressure rotor through a short drive shaft. The temperature and pressure conditions used in the design are 102°F and 448.1 psia respectively at inlet and 306°F and 878.4 psia at outlet. The helium mass flow is 134.7 lb/sec. Due to the higher volume flow, the required flow areas in the low pressure compressor are higher than in the high pressure compressor with the result that a

limitation on mean blade speed to achieve reasonable hub/tip ratio was not required. The limitation on mean blade speed in the low pressure compressor was set at 1350 ft/sec from considerations of mechanical stress. Using the MGCR data as the design basis, the resulting number of low pressure compressor stages was 14. A small adjustment in stage mean diameters was made to maintain a constant inner diameter. The resulting final mean diameters and blade heights are 17.42 inches and 1.74 inches at inlet and 16.96 inches and 1.28 inches at exit respectively. The constant inner diameter is 15.68 inches hub/tip ratios are 0.82 and 0.86 at inlet and exit respectively.

Both compressor designs employ symmetric free vortex blading. This type of compressor may subsequently be improved upon from the standpoint of minimizing the relatively large number of stages required using helium. Since the amount of work that each individual compressor stage can do is a function of the blade speed and the pressure coefficient, there is a desire to increase the pressure coefficient to minimize the number of stages. However, the pressure coefficient must be chosen such that overall performance characteristics are optimized. Increasing the pressure coefficient beyond this point results in a decreased level of efficiency. Other types of compressors may show less degradation in efficiency at high pressure coefficients. Currently, some work is being done on compressor designs having highly asymmetric blading with very high degrees of reaction (Reference 2). However, the 50 percent reaction blading was used in the CCCBS compressor concept definition in order to utilize the existing development background.

Testing performed on a four stage compressor model in the MGCR program and reported in Reference 3 demonstrated a blade path efficiency capability in the 87 to 88 percent range, surpassing the CCCBS assumed requirement of 85 percent. The MGCR compressor tests indicated the superiority of shrouded stator vanes over those of unshrouded design, both in efficiency and reduced susceptibility to boundary layer effects. The CCCBS compressors, therefore, both employ shrouded stator vanes. An additional advantage of the shrouded stator design is the additional mechanical support it provides to the vane, permitting the use of a reduced blade chord and a consequently reduced compressor length.



Westinghouse

Low Pressure Turbine Aerodynamic Design

The low pressure turbine is a free power turbine which was designed to drive a superconducting electric generator at 6,000 RPM. This speed is representative, but probably not optimum, for an electric drive and can probably be increased somewhat resulting in smaller turbine and generator components. On the other hand, for a mechanical drive, the 6,000 RPM speed is probably higher than desirable from the standpoint of the propeller reduction gear design. A mechanical drive power turbine speed of 3,600 RPM will be defined in later studies.

Designing for a low RPM, although generally beneficial from the standpoint of the operating stress levels, is detrimental to the achievement of compactness and light weight. As the RPM is reduced, the blade diameter must be increased to maintain the blade speed and stage work output. If the diameter increases necessary to maintain blade speed cannot be permitted, the stage work must be reduced, necessitating the provision of an increased number of stages. As a practical design aspect, the amount that the diameter can be increased (to maintain blade speed as RPM is reduced) is limited by other than purely space considerations. As diameter is increased, hub/tip ratio must be increased to maintain the axial velocity in an efficient range of flow coefficient. Eventually, as diameter is increased and blade length is reduced, tip clearance effects contribute an unacceptably large loss in efficiency. Consequently as RPM is reduced, both the diameter and the number of stages tend to be increased. The increased number of stages, of lower work per stage, allows the blade tangential speed to be reduced. Axial gas velocity can be reduced in proportion, maintaining the flow coefficient in the range of high efficiency. The reduced axial velocity results in increased flow area and longer blades, reducing the tip loss effect.

The temperature and pressure conditions assumed in the design of the free power turbine are 1277°F and 836.9 psia respectively at inlet and 957°F and 474 psia at outlet. The mass flow of helium through the machine is 130.6 lb/sec. In designing the power turbine, it was desired to limit the outer diameter of the casing to the region of three feet. This constraint was intended to ensure that the resulting design was reasonably compatible with the overall

powerplant arrangement. As a result, allowing for initial judgements of the space required for casing and stator structure, the mean blade diameter was set at 26 inches. The resulting mean blade speed is 681 ft/sec. Using 12 stages, the resulting load coefficient is 3.56. The flow coefficient was selected at 0.8. This results in blade heights of 2.35 inches at inlet and 3.39 inches at exit. The load coefficient and flow coefficient values are somewhat higher than optimum from the efficiency standpoint in order to reduce the size of the machine. These load and flow coefficient values for the power turbine are shown on a plot of measured turbine efficiency in Section 4.2.3. The power turbine design point falls approximately on the 92 percent efficiency line. This efficiency must be adjusted for leaving loss and tip leakage in the manner discussed for the high pressure turbine in Section 4.2.3. The axial leaving velocity is 544.6 ft/sec corresponding to 0.7 percent loss ($\eta_{LL} = 0.993$) if 50 percent diffusion recovery is assumed. (The relatively low exhaust energy resulting from the large area power turbine design is noteworthy and suggests that the design of its exhaust diffuser will be less critical than in the high pressure turbine.) If a clearance/diameter ratio of 0.0015 is assumed the tip clearance is 0.039 inch. Using a mean blade height of 2.87 inches, the clearance/blade area ratio is 0.027 ($\eta_{Leak} = 0.973$). The resulting net efficiency is therefore $0.92 \times 0.993 \times 0.973 = 0.89$ which is sufficiently close to the desired value to indicate that concept refinements should allow meeting of the goal. This estimate of the efficiency achievable in a well designed turbine, having the selected load and flow coefficients is believed to represent a reasonable compromise between the conflicting goals of high efficiency and compactness.

The blade profile development outlined in Section 4.2.1 for the high pressure turbine has not yet been performed for the power turbine. However, no problems are anticipated in the detailed design of the blading. More design latitude is available in the power turbine than in the high pressure turbine due to the lower temperature levels and rotational speed of the former machine. Centrifugal stress levels and blade metal temperatures are sufficiently low to permit the use of relatively untapered blading. A design option also available is the use of rotating blade shrouds. Rotating shrouds were not shown to confer any efficiency advantage, in the MGCR testing, if tip clearances were held below 0.0015 diameter. However, rotating shrouds could



Westinghouse

be useful in permitting the use of reduced blade chords due to the support they provide against first made blade vibration. A reduction in blade chord, although small in itself, can result in a significant reduction in the length of a 12 stage machine.

Inlet and Outlet Flow Passages Aerodynamic Design

The inlet flow passages and outlet diffusers of the compressor and turbine components have not been optimized. However, work to date has indicated that sufficiently efficient designs can be developed within the space provided in the powerplant assembly.

The compressor inlets are strutted converging passages having favorable pressure gradients. The main design requirement in these components is to provide a sufficiently fair and gradual flow curvature to assure the provision of a uniform total pressure distribution across the compressor inlet. The turbine inlets are normally less sensitive to flow distribution than the compressors due to the relatively high pressure drop in the first nozzle vanes together with the favorable pressure gradient associated with the expanding flow. However, certain minimum requirements must be met in its design of the turbine inlet flow passages.

The high pressure turbine inlet is an annular vessel or "scroll" fed by a single pipe. An important design requirement is that the pipe and vessel be made large enough that the dynamic head of the entering helium is a small portion of the total head, thus minimizing pressure losses in the annular vessel or scroll and assuring good flow distribution into the turbine. The turbine inlet pipe provided on the design is 14 inches in diameter. The resulting flow velocity in the pipe is 472 feet/sec and the Mach number is 0.07. The resulting dynamic head of the flow in the pipe is less than one half a percent of the total head.

The low pressure turbine inlet is an annular strutted passage which follows the high pressure turbine outlet diffuser. The area of the passage at inlet to the low pressure turbine is substantially larger than at the high pressure turbine exit. The velocity of the gas leaving

the high pressure turbine is 936 ft/sec ($M = 0.16$) and the dynamic head is two percent of the total head whereas the velocity into the power turbine is only 550 ft/sec ($M < .1$). The flow profiles in the passage should therefore be designed to provide efficient diffusion allowing for the presence of the air foil section struts.

In general, the design of the diffusers in the CCCBS is less critical than in air cycle machinery, due to the high sonic velocity in helium which result in low Mach numbers. The low pressure turbine outlet velocity is very low at 545 ft/sec ($M = 0.1$) and the exhaust diffuser design is not critical. In the particular design being considered, the diffuser outlet gas passes through the structural member supporting the outlet end of the power turbine casing via eight circular passages equally spaced around the centerline.

The compressor outlet diffusers are less critical than the high pressure turbine outlet diffuser. The compressor outlet Mach numbers are similar (0.16 and 0.13) but the flow passage dimensions are smaller due to the lower temperature conditions and, in the case of the HP compressor the higher pressure level. Sufficiently efficient diffusers can therefore be accommodated in the space provided.

3.5.2 Design Concept (2nd Definition)

The concept design is currently being modified to incorporate the finned tube cross flow intercooler and precooler designs and the gas bearings which were selected in the trade studies reported in Sections 4.1.1 and 4.1.2. Figure 3.30 illustrates the current status of the design at the end of the first contract year.

The precooler and intercooler are similar in design. Each cooler employs finned tubing arranged in a helical matrix around the turbomachinery. The tubing is headered in four equally spaced radial pipes at each end of the matrix. A "four-start" arrangement of the tubing provides compatibility with the header pipes. Cooling water is piped into the radial header pipes through "bobbin" and O-ring connectors, flows through the helical tubing and



Westinghouse

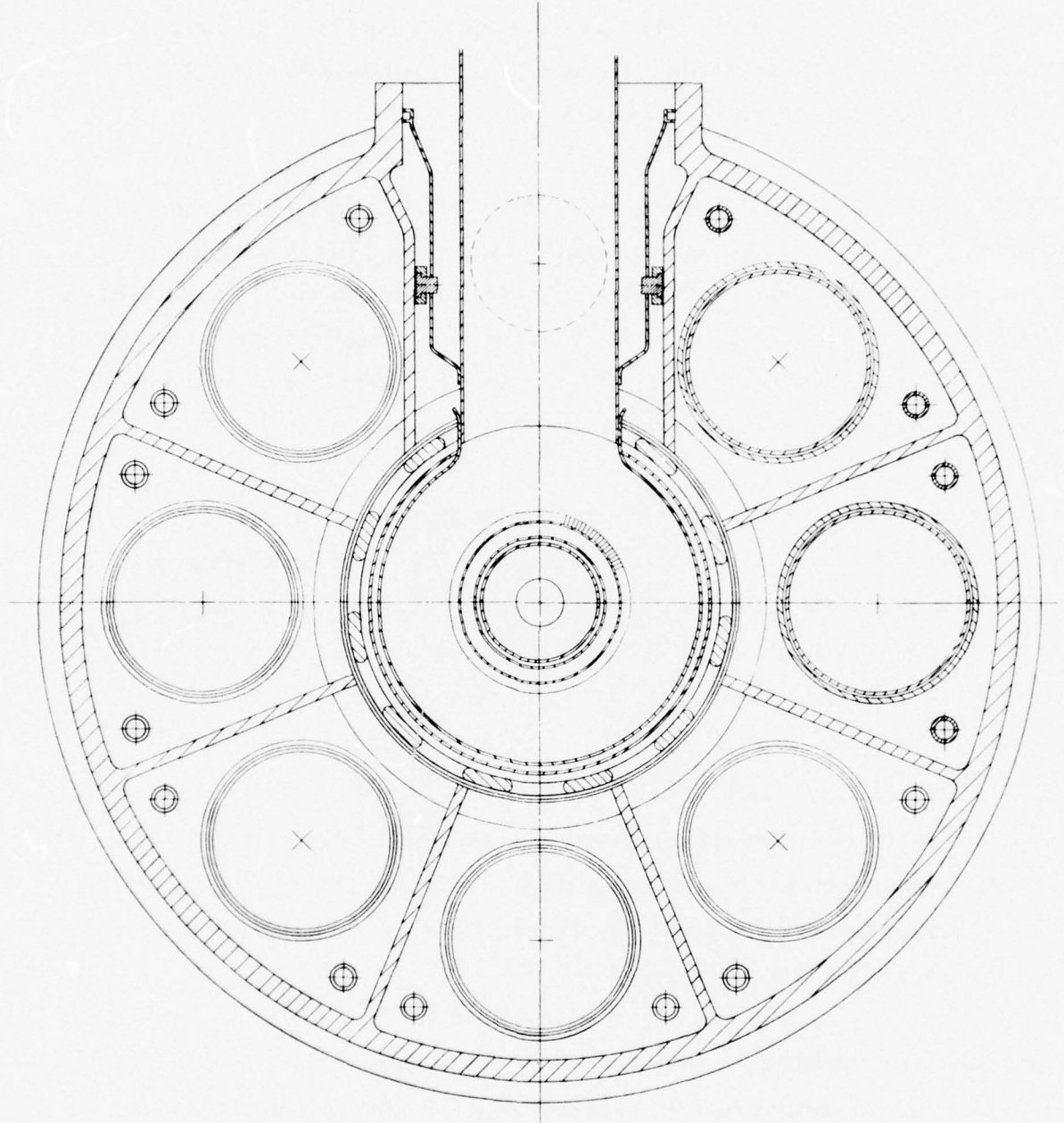
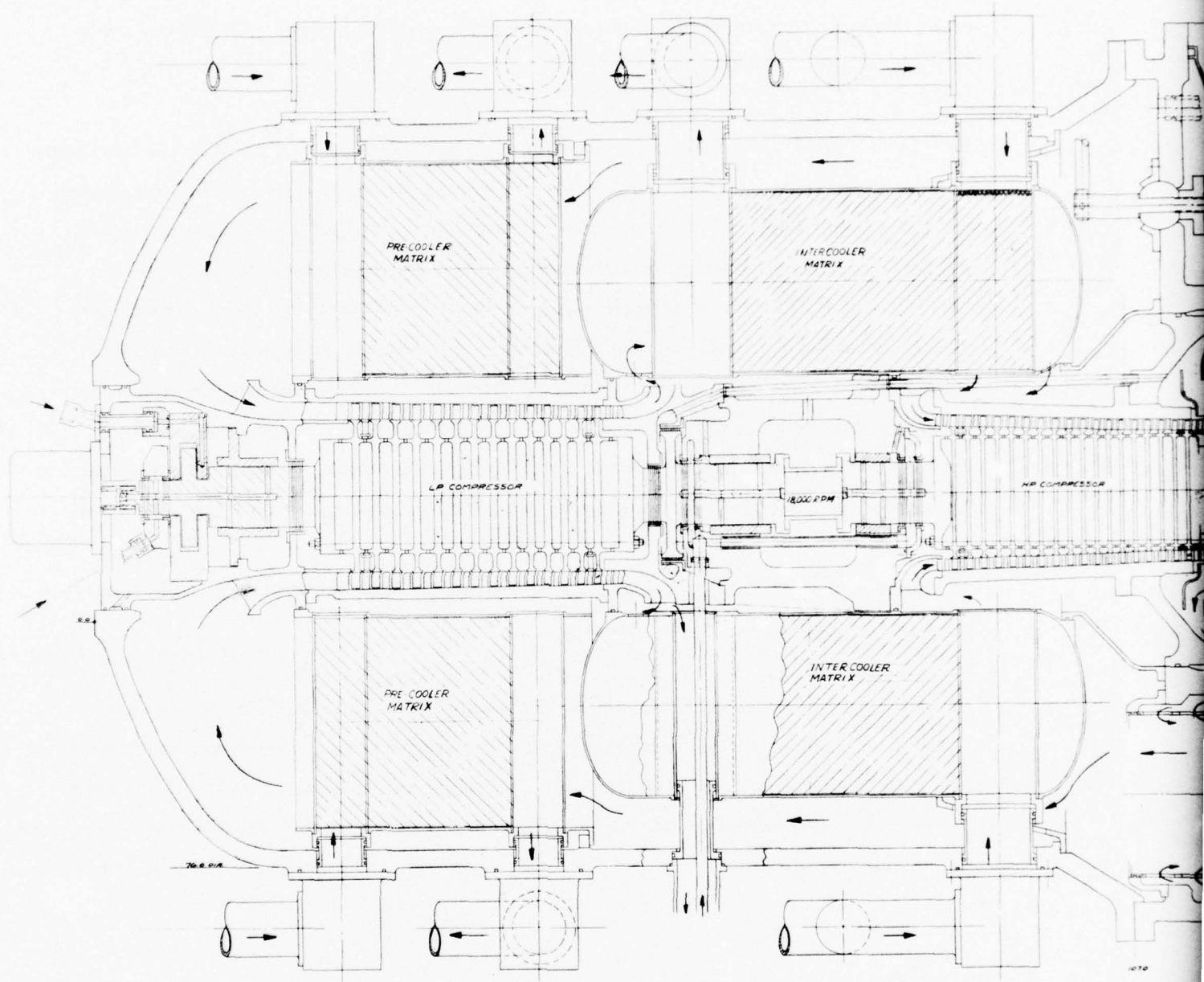


Figure 3.30a CCCBS Design Concept (2nd Definition) Sheet 1



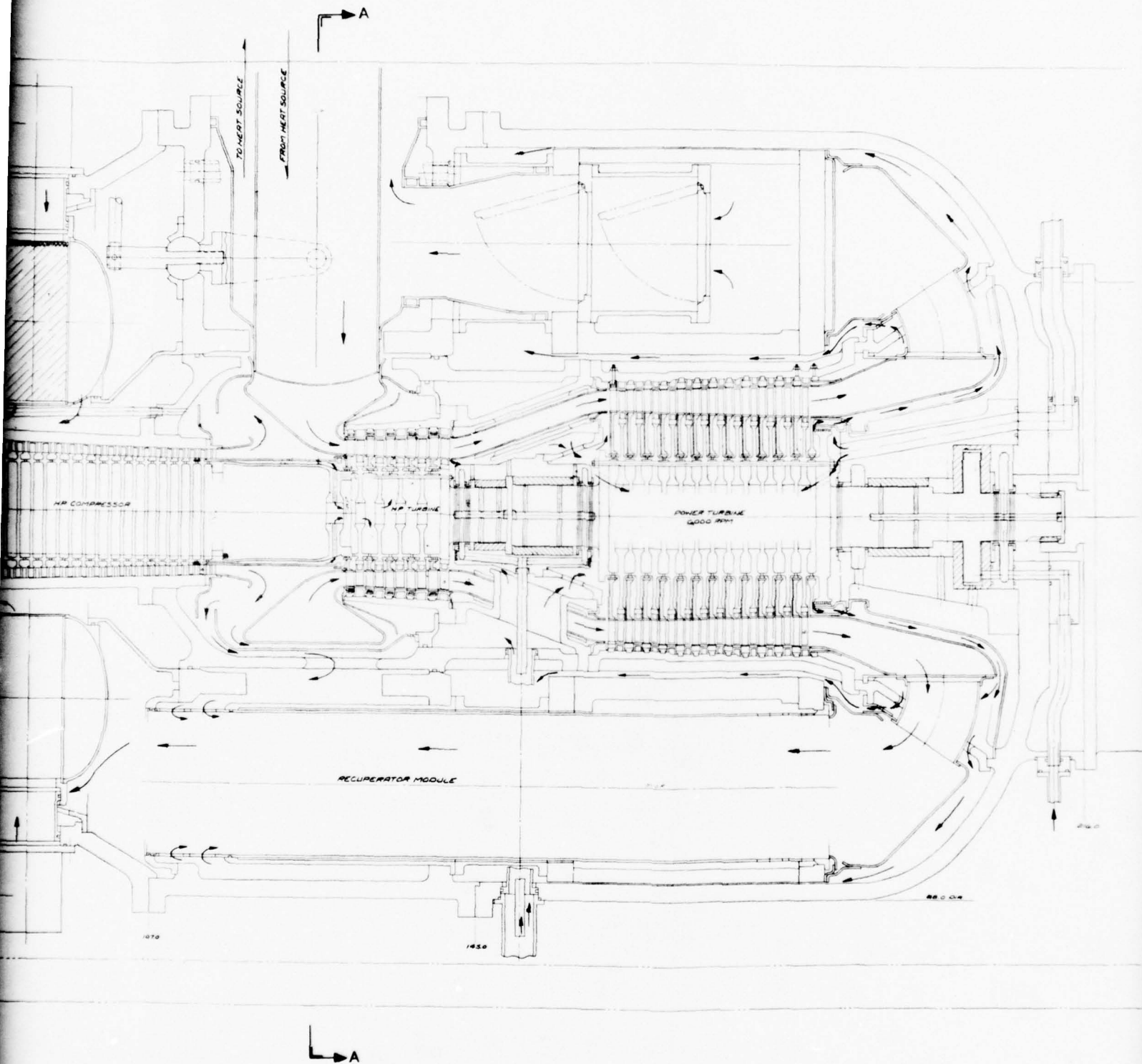


Figure 3.30b CCCBS Design Concept (2nd Definition) Sheet 2

leaves through the radial header pipes and connectors at the other end. The helium cycle gas flows axially across the finned tubing.

The intercooler matrix is accommodated within a cylindrical pressure shell which is terminated at each end in pressurized headers. The headers convey the helium gas from the low pressure compressor outlet into the intercooler and from the intercooler into the high pressure compressor inlet. The intercooler/header/vessel assembly is supported by a conical support member from a flange on the powerplant pressure vessel and is sealed to the turbomachinery by means of rubber O-rings. Complete separation of the higher pressure gas in the intercooler from the lower pressure gas entering the precooler is thus achieved while permitting the turbomachinery to be freely withdrawn from the assembly through the O-ring seal interfaces. The conical support member is penetrated by a number of large diameter holes which allow the passage of the low pressure gas from the recuperator to the precooler inlet.

The precooler and its header are integrated into a similar assembly and supported from a flange on the powerplant pressure vessel.

The coolers have been carefully located in the axial direction to avoid interference with the radial pipes supplying the pressurizing gas to the gas bearings. Pressurizing gas is fed to the bearings through the smaller diameter pipes which are accommodated inside the larger turbine cooling and balance piston supply pipes. The pressurizing gas enters the bearing rotating members via a small chamber surrounding the shaft and sealed by the double labyrinth seals.

The flexible drive shaft couplings have been deleted from the low pressure compressor drive shaft since they would not receive the required lubrication in this arrangement. This area of the design will require more study to ensure that the necessary flexibility can be provided at acceptable cyclic stress levels in an unlubricated design.

The gas journal bearings are fully described in Section 4.1.2 and employ the hydrodynamic foil concept with hydrostatic pressure augmentation to permit operation in the low speed regime. The thrust bearings are designed to be primarily hydrostatic in operation with backup provisions for hydrodynamic operation during engine transients.



Westinghouse

3.6 REFERENCES

1. V. Proscino, "Maritime Gas Cooled Reactor Project Engineering Report No. EC-167 on Development of Turbomachinery (Summary Report)," Westinghouse Gas Turbine Division, June 1963.
2. G. H. Farbman and R. E. Thompson, "Applications of Nuclear Rocket Technology to Lightweight Nuclear Propulsion and Commercial Nuclear Process Heat Systems," AIAA Paper 75-1261, September 1975.
3. R. E. Thompson and E. Venning, "Closed Cycle Pneumatic Power Transmission Study," Westinghouse Electric Corporation, Oceanic Engineering Report No. 75-41, July 31, 1975.
4. "Marine Closed Gas Turbine and LNG Refrigeration System Study - Part 1 - Closed Gas Turbine Marine Power Systems," U. S. Maritime Administration Contract 3-3600, AiResearch Document No. 74-310632, March 31, 1974.
5. F. Critelli, A. Pietsch and N. Spicer, "Closed Gas Turbine Engines for Future Marine Propulsion," Marine Technology, Vol. 13, No. 3, July 1976.
6. Standard Power Plant Characteristics for Advanced Naval Vehicles in the 1980-2000 Time Period. Working Paper 011 Enclosure to ANVCE Memo No. 103-76.

4.0 CRITICAL COMPONENT TECHNOLOGY EVALUATIONS

Several technologies were identified at the initiation of the CCCBS evaluations as being key component technologies for which early studies were required. These studies then provided input to the design concept definition reported in Section 3.5. The specific results of each of the critical component studies are reported in this section of the report.

Compact heat exchangers are very important components of the CCCBS. Various types of compact heat exchangers which can be considered for the CCCBS have been evaluated and compared. The results of these evaluations and the comparisons and heat exchanger type selections for the design concept are documented in Section 4.1. Gas-to-gas and gas-to-water heat exchangers are discussed separately because of their different design requirements.

The high pressure (gas generator) turbine, particularly the first stage, to a large extent determines the characteristics and configuration of the turbomachinery. This critical component was studied and the results of the studies are reported in Section 4.2.

Bearing capabilities can have a major impact upon the reliability which can be confidently expected for the power conversion system turbomachinery. Bearing design concepts can also effect the dimensions of the turbomachinery which in turn can have a major impact upon the compactness of the powerplant. The bearing and seal concepts also effect the auxiliary systems which must be provided. Early studies were therefore necessary to provide the data base for evaluations of turbomachinery capabilities and to provide the basis for subsequent design efforts. Both gas bearings and oil lubricated bearings were evaluated. The resulting assessments were compared and the most promising bearing type selected for inclusion in the design concept. The results of the studies and the bearing selection are documented in Section 4.3.



Westinghouse

4.1 COMPACT HEAT EXCHANGERS

The requirement for close-coupled integration of the heat exchangers and turbomachinery into one compact package results from system requirements to minimize containment dimensions, and therefore total system weight and volume, and also from the desire to minimize connecting piping in order to provide high reliability. This section reports the results of compact heat exchanger task studies including conclusions regarding technology availability, performance capability, weight, size, fabricability, and reliability. Heat exchanger selections are discussed in Sections 4.1.1.3 and 4.1.2.4.

4.1.1 Gas to Gas (Recuperator) Heat Exchangers

Over the last thirty years, the fixed boundary recuperator, of both tubular and plate-fin constructions, has been used for industrial, marine, locomotive, aircraft, vehicular and closed-cycle applications, and has demonstrated a high degree of reliability.

4.1.1.1 Tube and Shell Recuperators

The recuperator initially found acceptance in the large European industrial open and closed cycle gas turbines, introduced about thirty years ago. The recuperator was essentially a supplement to the cycle to provide reasonable specific fuel consumptions with the low component efficiencies of that era. These recuperators, of mainly tubular construction, were conservatively designed and have demonstrated a high degree of reliability and in many cases, have run virtually maintenance free for over 100,000 hours of operation (References 1 and 2).

A plot of the range of surface compactness (area density per unit of volume) for tubular surface geometries is shown in Figure 4.1. Plain tubular surfaces used in recuperators for large industrial and marine gas turbines had compactness values in the range of 30 to 80 ft^2/ft^3 (Reference 3). The current large plain tubular recuperators built for closed cycle helium gas turbine plants have compactness values in the order of 100 ft^2/ft^3 (Reference 4). Compact tubular geometries used for lightweight recuperative gas turbines for helicopter application have surface compactness values of about 400 ft^2/ft^3 (Reference 2). Reference 5 describes a very compact tubular

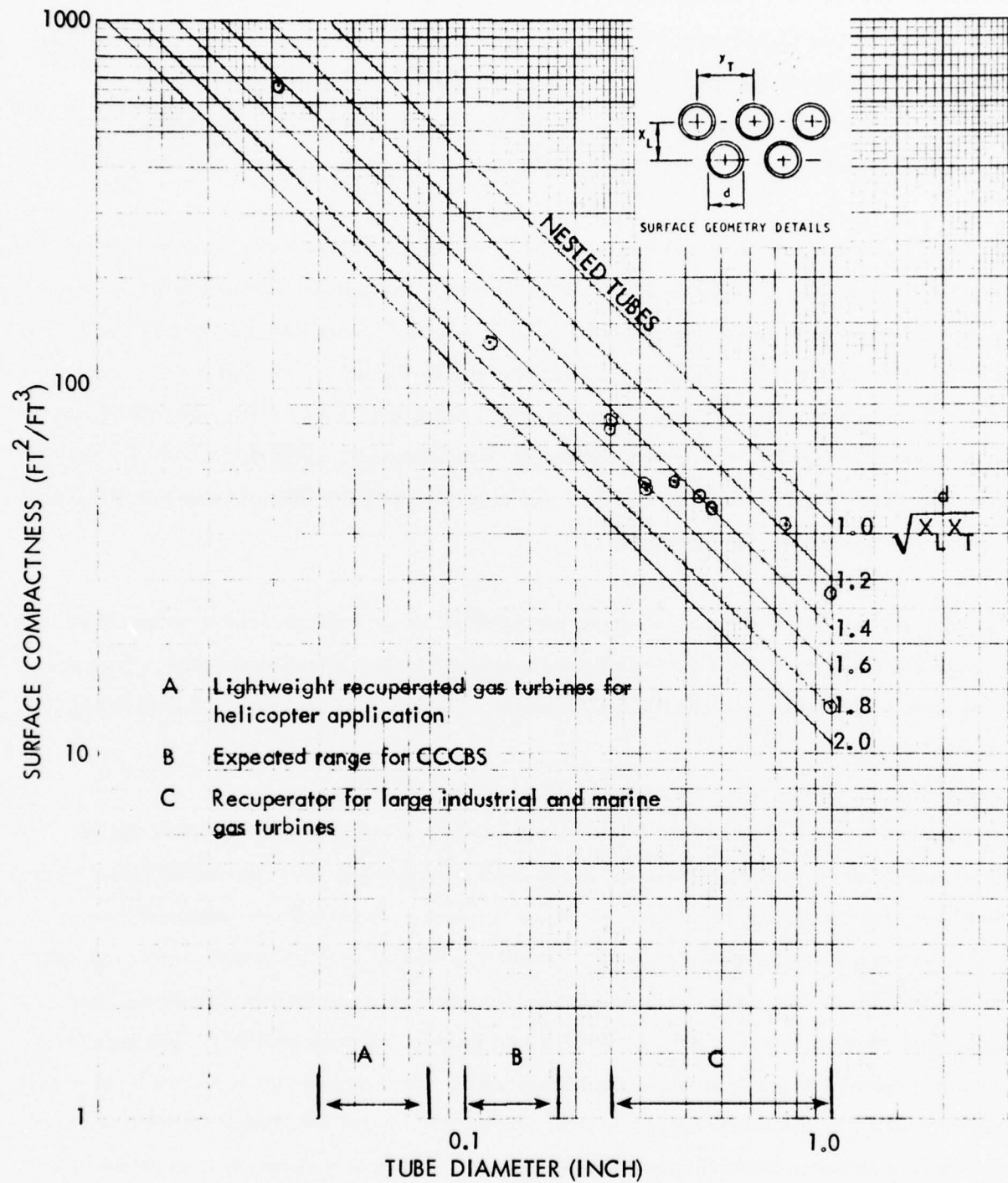


Figure 4.1 Surface Compactness Versus Tube Diameter

recuperator surface with a compactness value of almost 700 ft²/ft³. The expected range of compactness for this CCCBS application is from 150 to 250 ft²/ft³ (tube diameter 0.15 to 0.10 inch). Tubular recuperator specimens, in this range (diameter of 0.118 inch), have been assembled, brazed and tested. Pressure tightness tests were performed both before and after torsional and thermal fatigue testing. No leaks were detected in these tests (Reference 6).

Usually tubular designs are assembled into drilled header plates, however, the tubes can be designed to integrally form the header at the tube ends. The joining process can be done either using welding or brazing techniques. Typical end seals for tubular heat exchangers are shown in Figure 4.2. In the lightweight tubular recuperators developed for aircraft gas turbines, compact geometries and small tube diameters are utilized, and this virtually necessitates brazing the assembly together. Extremely lightweight designs can be achieved by utilizing very compact geometries, in which the tube ends are expanded into the form of hexagons and brazed together to form the header (Reference 2).

The tube and shell type of heat exchanger was selected as a candidate for the recuperator because it has the potential for the desired compactness and because it represents a type of construction that has been proved to have the structural integrity necessary for long life applications.

Compactness is required regardless of the energy source. In addition, an important design consideration of the CCCBS powerplant is the containment vessel which for safety reasons must completely surround a nuclear system. This vessel is heavy, surrounds the turbomachinery, heat exchangers and other components, and thus constrains the sizing of the power conversion assembly. For the CCCBS, the turbomachinery and the primary loop heat exchangers (precooler, intercooler and recuperator) have been integrated into a single compact assembly. Two parallel redundant assemblies are required in some applications. The recuperator is placed in an annular region around the free power turbine and the recuperator frontal area then determines the diameter of the turbomachinery/heat exchanger module. This module diameter then determines the containment vessel diameter. The recuperator frontal area has a significant effect on powerplant

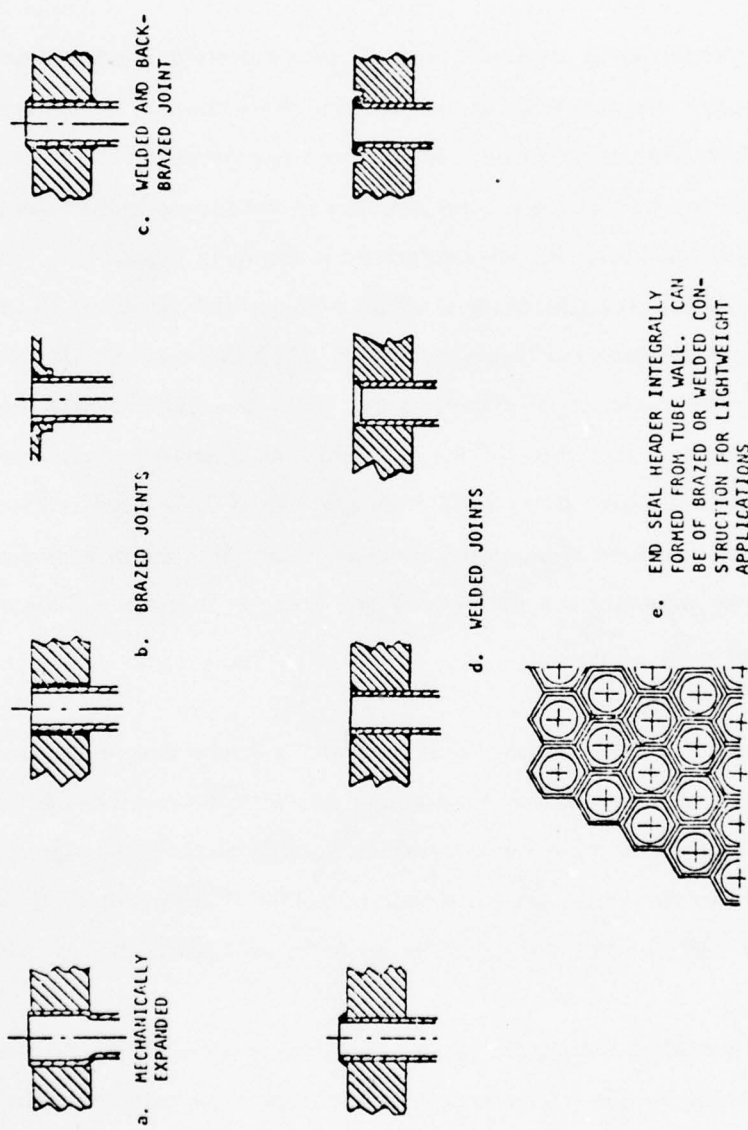


Figure 4.2 Typical Types of Tube to Header Joints (Reference 2)

weight and volume. If the recuperator outer annular diameter is increased one inch, the containment volume increases by 160 cubic feet and the weight increases by about 5900 pounds. As long as the recuperator overall length is less than 96 inches the containment vessel and turbomachinery/heat exchanger vessel weight and dimensions are not affected, since the vessel length is then determined by the turbomachinery length.

Since the recuperator cross sectional (frontal) area has a significant effect on powerplant weight and volume, the approach of the tube and shell concept was to minimize the frontal area. For a given helium flow rate, effectiveness and pressure loss, it can be shown from Appendix B that the frontal area is proportional to the square root of the ratio of the friction factor to Colburn modulus. This characteristic is shown in Figure 4.3. With a small relative roughness the frontal area minimizes at about a Reynolds Number of 15,000. Utilizing the Colburn factor evaluated at a Reynolds Number of 15,000 the tube diameter is a function of tube length and heat exchanger effectiveness. With an effective tube length of 70 inches and an effectiveness range of 0.8 to 0.9 the required tube diameter ranges from 0.080 to 0.180 inch. Based on the above, a tube ID of 0.100 inch and OD of 0.120 inch was selected for the initial trial design shell and tube recuperator concept. Using the above tube diameters, the tube and shell recuperator geometry was determined and is shown in Table 4.1 for a heat exchanger effectiveness of 0.86.

Figure 4.4 shows a schematic drawing of the shell and tube design approach. The flow configuration is that of a counterflow heat exchanger with the turbine exhaust helium flowing in the tubes and with the compressor exit helium flowing on the shell side. The recuperator is composed of 7 modules which are each approximately 16.36 inches in diameter. Each module contains about 10,700 tubes with an outer diameter of 0.120 inch and 0.010 inch thickness.

The tubes are formed at their ends into a hexagonal section. The tube ends are furnace brazed together. The tube bundle is also brazed at the ends to an external cylinder and a cold end ring. Filler pieces are used to fill the gaps at the tube and cylinder interface. No tube sheet is required in this arrangement since each tube carries the local axial tension force.

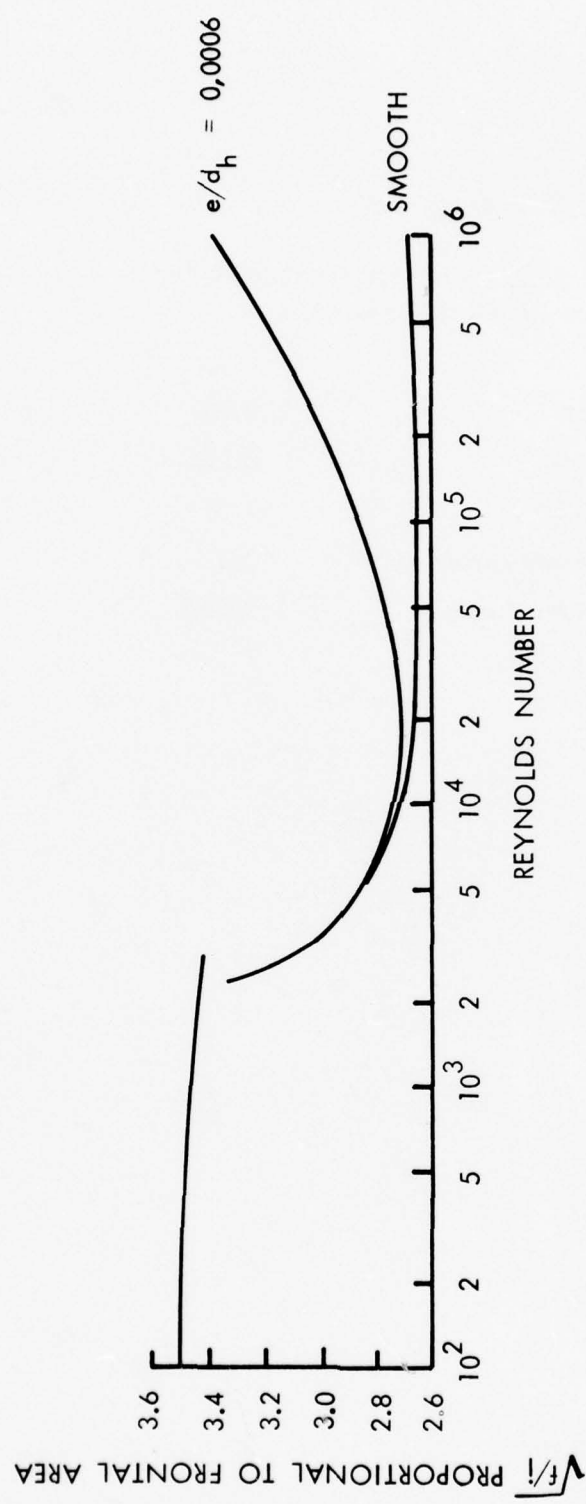


Figure 4.3 Proportional Frontal Area Versus Reynolds Number for Axial Flow in Tubes



Westinghouse

TABLE 4.1

SHELL AND TUBE RECUPERATOR GEOMETRY
(One 70,000 HP Turbo-Unit)

Tube ID-inch	0.100
Tube OD-inch	0.120
Pitch to OD ratio	1.20
Effective Length-inches	70.0
Number of tubes/module	10700
Number of Modules	7

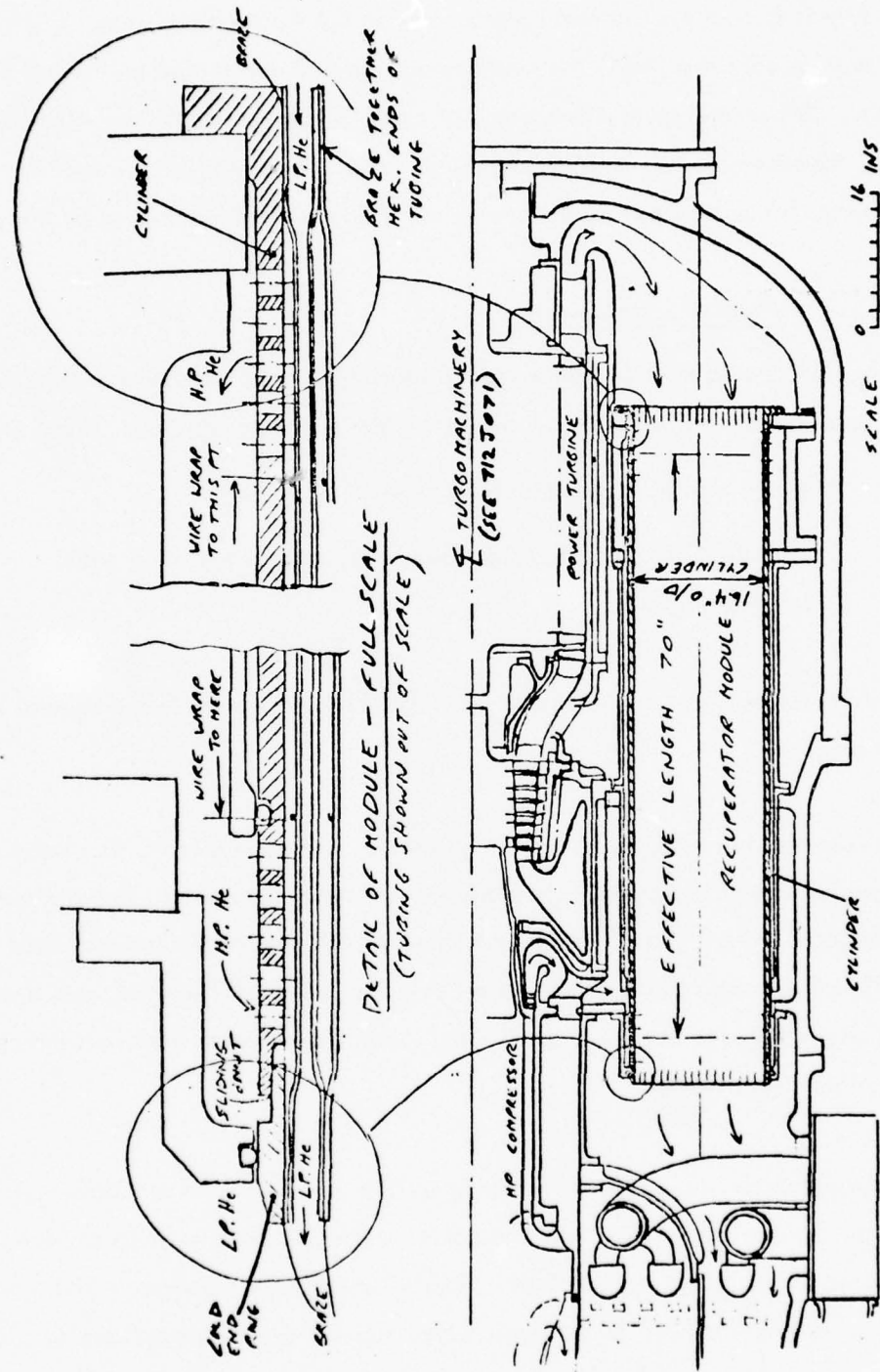


Figure 4.4 Recuperator Module Concept Using Hex Ended Tubing



Westinghouse

The tube module is free to expand and contract due to the floating end ring. O-rings are used to seal the floating cold end ring. The modules are located and sealed on the hot end by bolted flanges. This arrangement eliminates the need for tube sheets with their numerous drilled holes. However the hex-end forming is an additional operation. The conventional tube sheet approach can be substituted if manufacturing studies show this to be desirable.

4.1.1.2 Plate-Fin Recuperator

Two key technology issues must be addressed before the plate-fin recuperator technology can be seriously considered for the reference compact lightweight powerplant. These are:

- a. Thermal transients and thermal cycles
- b. Fabrication of compact recuperator designs for integration with the rotating group.

These technology issues have recently been addressed by AiResearch during several recuperator development programs.

Plate-fin recuperators have historically been needed to achieve competitive closed cycle gas turbine designs for applications requiring efficient, compact lightweight powerplants. The first closed Brayton cycle engines, designed for low power space applications, used conventional solid closure bars in the plate-fin recuperator designs. The result was competitive powerplant designs, but the recuperators imposed restrictive thermal transient and cycle limits on the powerplant operation.

Major development activities on plate-fin recuperators were initiated at AiResearch in 1972 to achieve high thermal cycle life under the severe thermal transients imposed by an open cycle gas turbine in vehicular applications. Basic changes were required in the mechanical design of the recuperator as well as changes in the braze alloys and braze cycle. The latest developments in recuperator design and fabrication techniques are illustrated by the modular high-temperature recuperator for industrial gas turbines in the 5,000 to 100,000 HP range

(Reference 7). These modules, shown in Figure 4.5, are designed for a usable life of 120,000 hours with 5,000 undelayed gas turbine start/stop cycles. The modules are designed to operate at gas turbine exit temperatures of 1100° to 1200°F. The current development activities are to include demonstration of the recuperator technology in a full scale thermal cycle test facility. This testing was initiated in June 1977. The details of these new recuperator mechanical design and fabrication techniques are considered proprietary information by AiResearch, but nevertheless, form an extremely significant plate-fin heat exchanger technology baseline for the reference powerplant. This technology baseline encompasses recuperator and liquid to gas heat exchangers.

Integration of the recuperator and rotating group was initially investigated at AiResearch for a variety of low-power closed Brayton engines in volume-limited underwater applications. Figure 4.6 shows an example of these early designs.

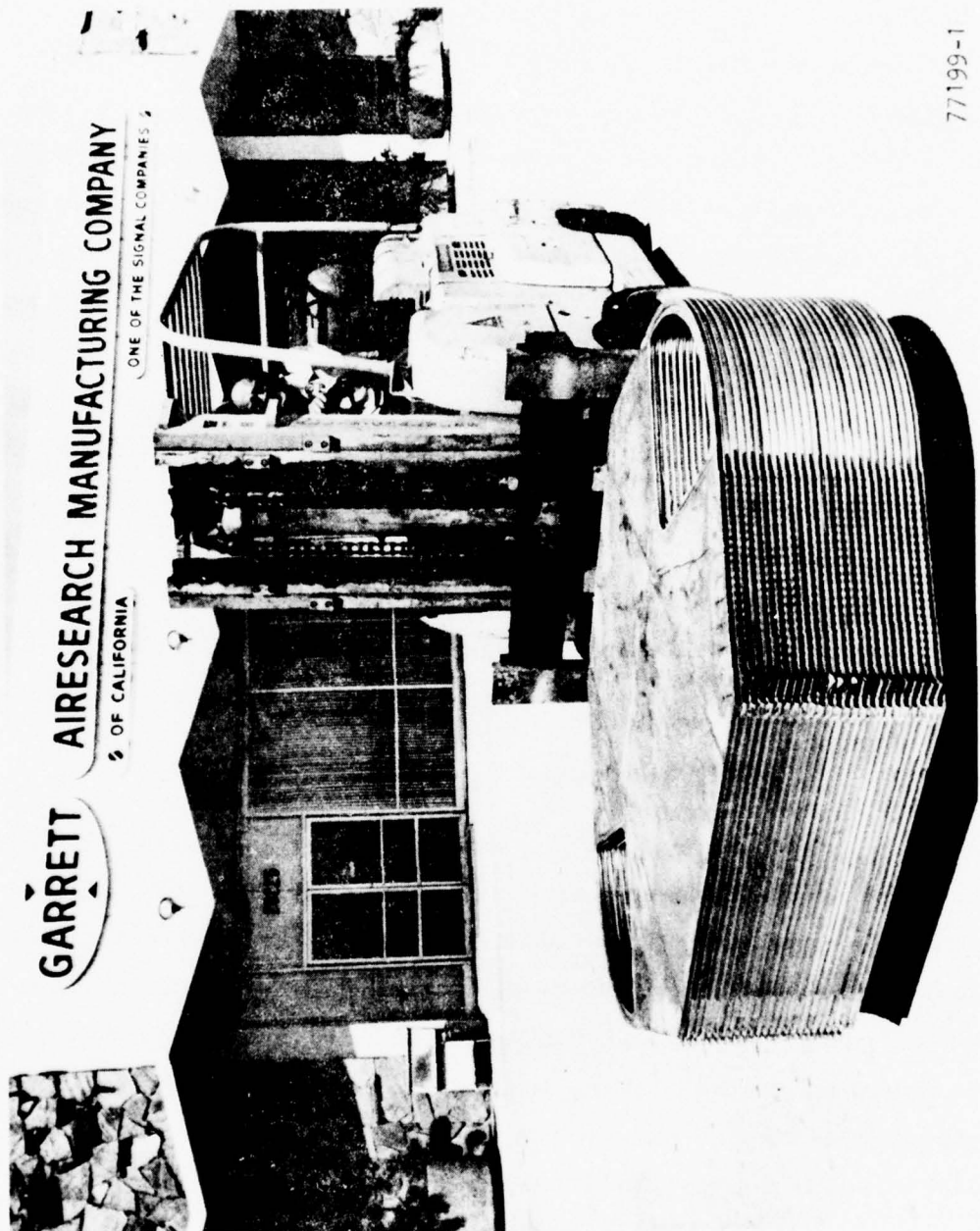
Additional studies were performed to determine the feasibility of this compact recuperator packaging concept for a high performance, high temperature, 12,000 HP engine. These studies resulted in a compact engine design, shown in Figure 4.7, which used six annular recuperator modules.

AiResearch developed the annular recuperator, shown in Figure 4.8 under Contract N00500-73-C-0112 for the Naval Ship Research and Development Center (NSRDC) in order to prove the validity of this recuperator packaging approach. Figure 4.9 shows the buildup of a single curved recuperator core which was constructed using existing fin designs. As shown in Figures 4.8 and 4.10, this design resulted in a cylindrical engine configuration with a minimum of interconnecting ducting and low overall engine volume. This recuperator has been operated at NSRDC as part of their compact closed Brayton engine evaluation program. Recuperator performance has equaled or exceeded the performance goals.

The annular plate-fin pure counterflow recuperator configuration was evaluated for the 70,000 HF compact closed cycle Brayton system. The results of the evaluation are presented in the following sections.



Westinghouse



77199-1

Figure 4.5 Recuperator Module

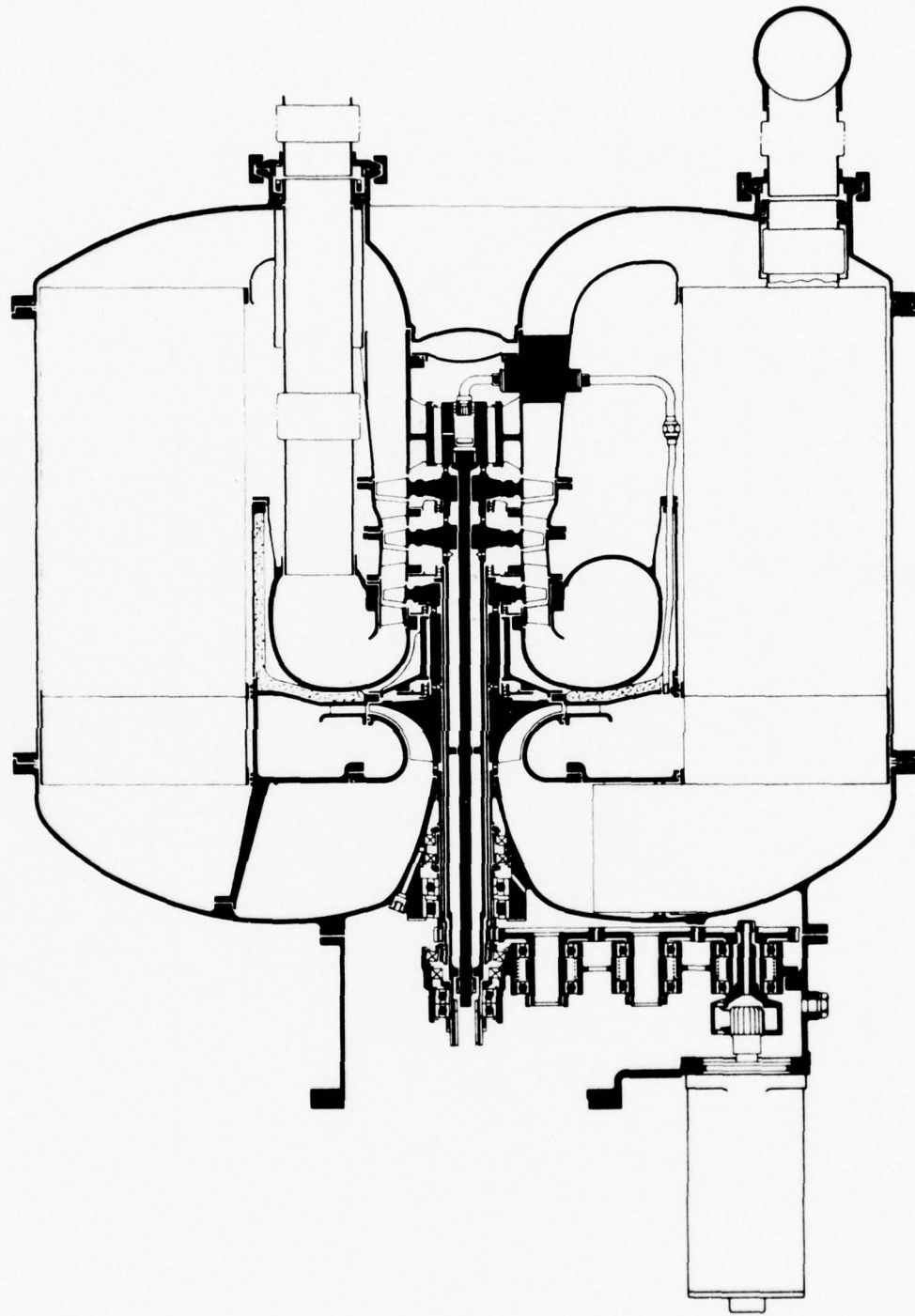


Figure 4.6 1000-2000 HP Closed Brayton Engine



Westinghouse

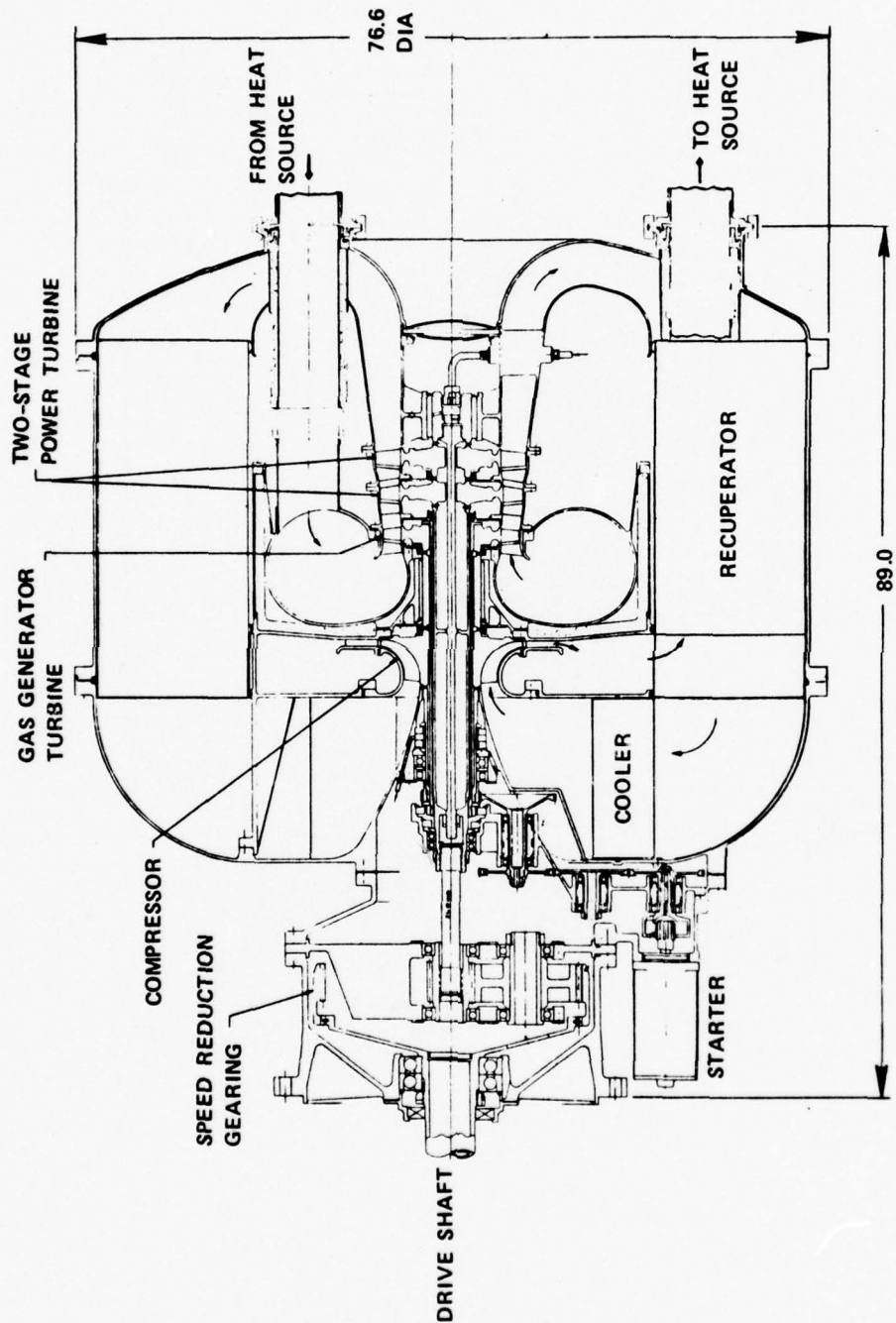


Figure 4.7 12,000 HP Engine Core

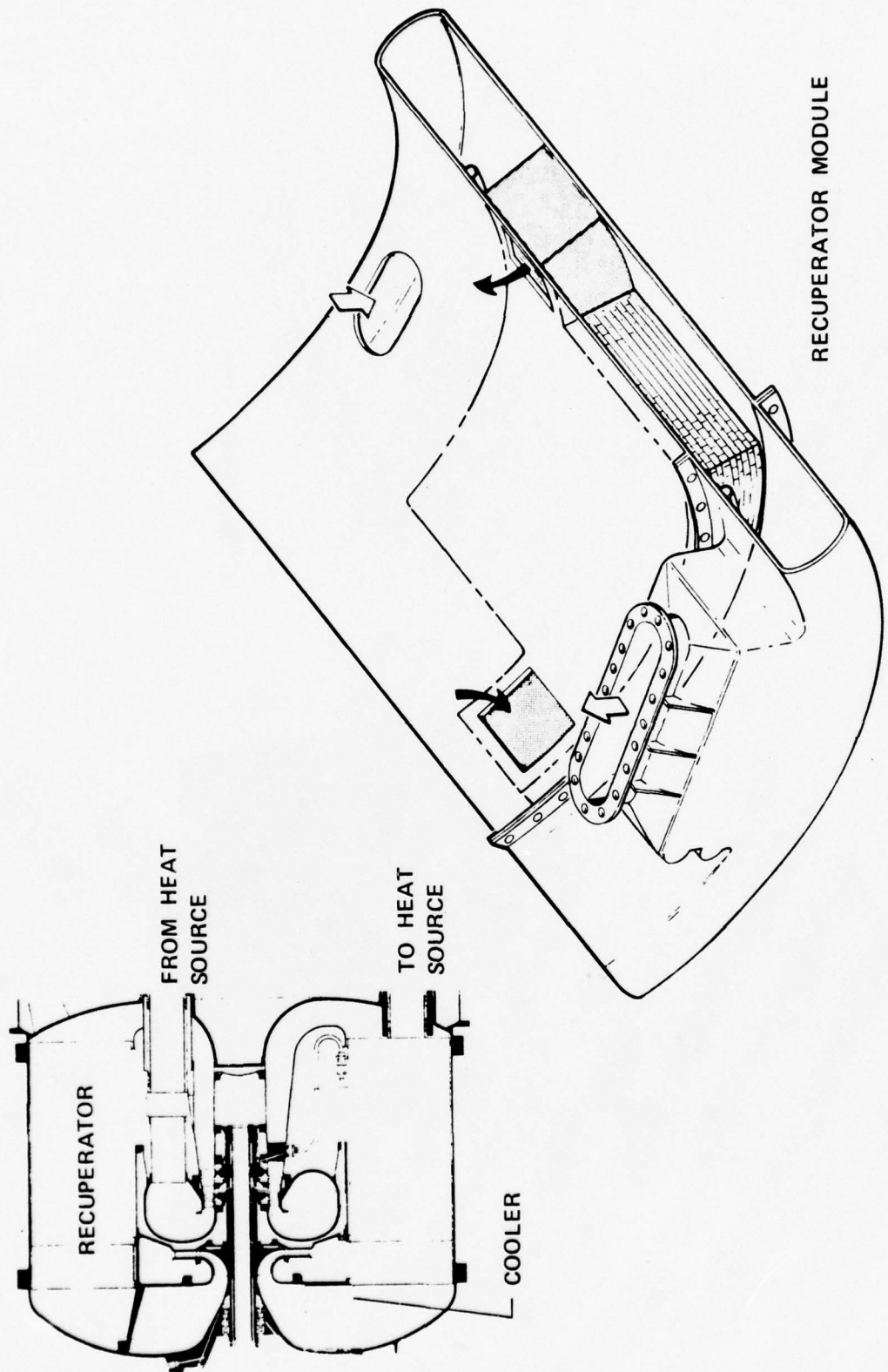


Figure 4.8 Compact Engine Packaging



Westinghouse

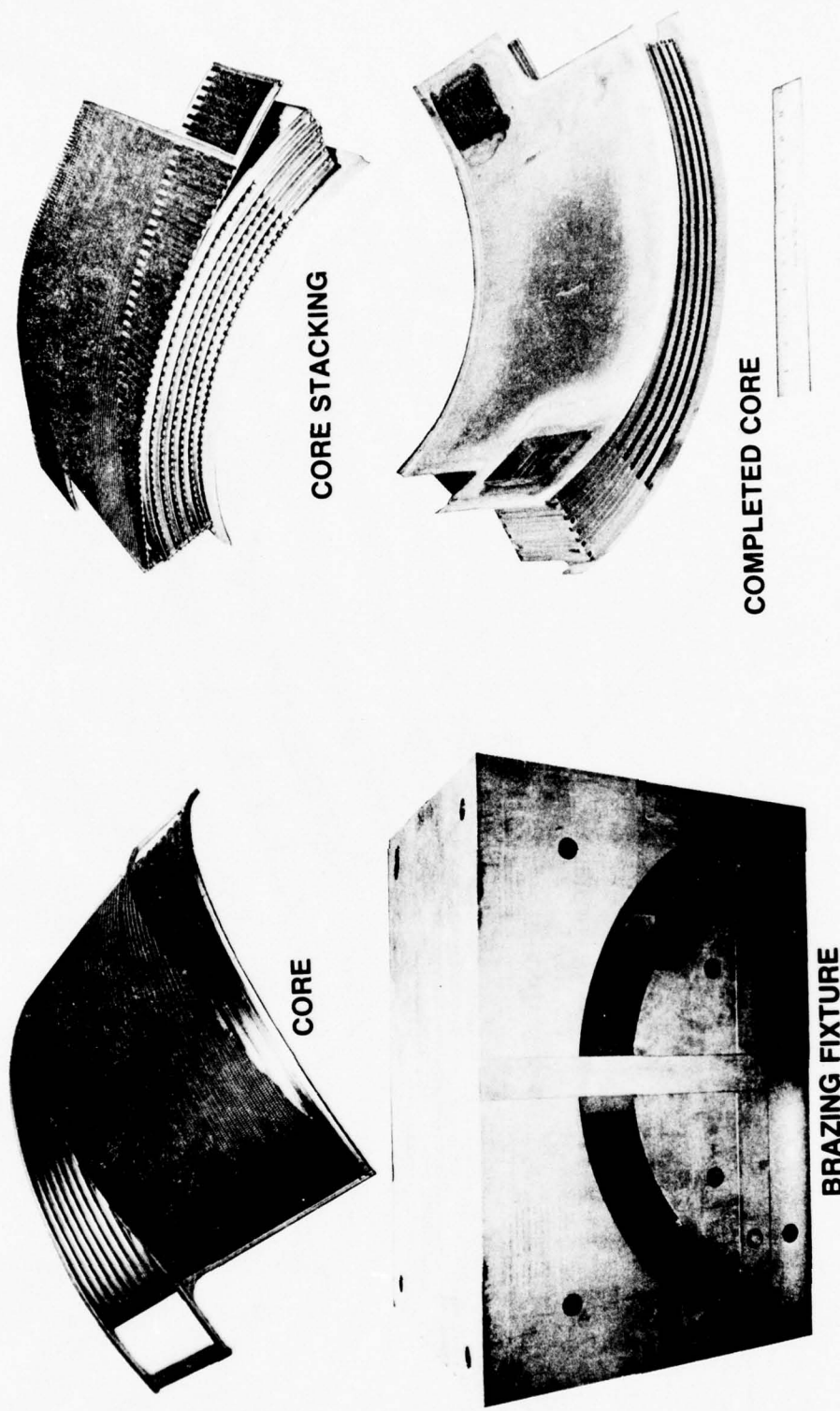


Figure 4.9 Curved Recuperator Module Construction

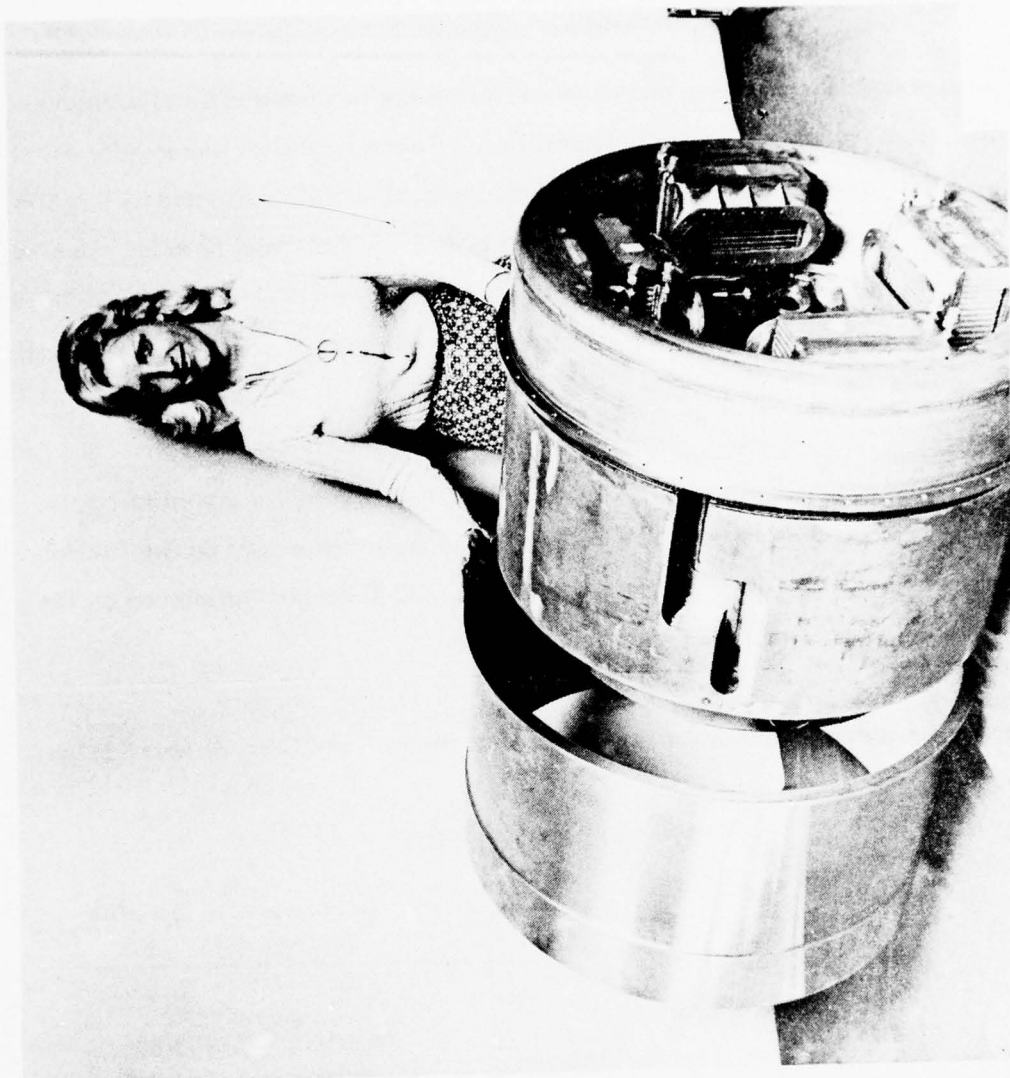


Figure 4.10 Exploded View Annular Recuperator/Cooler Assembly



Westinghouse

The plate-fin pure counterflow heat exchanger was modeled as six modules in an annular configuration as shown in Figure 4.11. The effectiveness, inside diameter, and total pressure drop ($\Delta P/P$) were set at the trial design values of 0.855, 38 inches, and 0.040, respectively.

The recuperator core fin geometry and material define the recuperator fin effectiveness and the overall dimensions for a given set of conditions. Several cases of rectangular offset fin geometries (including perforated plate-fin configurations) were investigated by varying fin spacing from 0.075 to 0.150 inch and the number of fins per inch from 12 to 22. Due to fin stress considerations, 0.006 inch thick stainless steel fins with a density of 0.28 lb/in^3 and a conductivity of $15.15 \text{ Btu/hr-ft-}^\circ\text{R}$ were used, and the minimum number of fins per inch on the high pressure side was limited to 16.

The friction factor and Colburn modulus used in the analysis are from actual test data. In order to ensure a conservative design, 0.20 and 0.10 margins were used on the friction factor and Colburn modulus data, respectively. In addition, a 0.10 margin was placed on the overall heat transfer and pressure drop of the design.

The plate-fin geometry, selected for the initial trial design conditions, is listed below:

PLATE-FIN GEOMETRY

	N_f	Thickness In.	Spacing In.
LP Side Fins	12	0.006	0.100
HP Side Fins	20	0.006	0.075
LP Side Header Fin	10	0.010	
HP Side Header Fins	10	0.010	
Splitter Plates		0.010	
Wrap-Up Material		0.100	
Braze Material		0.001	

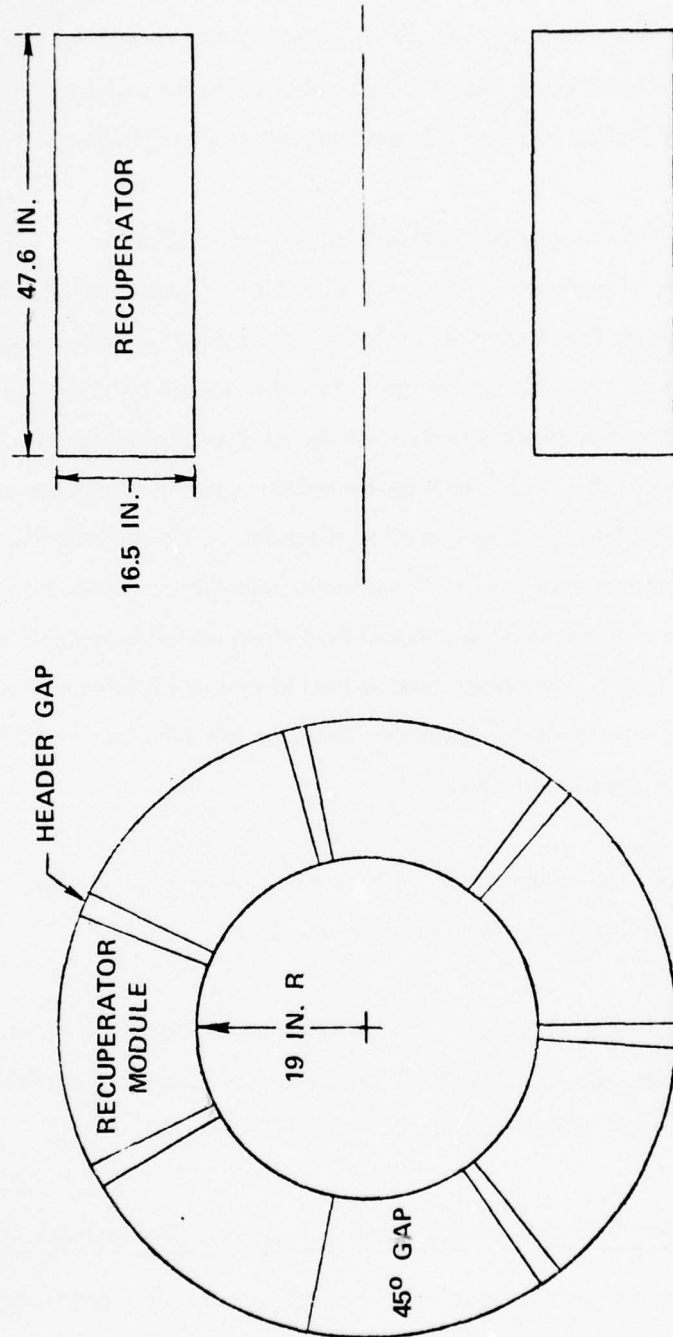


Figure 4.11 Recuperator Assembly Envelope



Westinghouse

This plate-fin geometry resulted in a recuperator design that packaged well within the recuperator envelope as shown in Figure 4.12. Total core volume, including end section but without inlet or discharge manifolds, is 62,84 ft³ with an estimated weight of 8,792 pounds. The overall length is 47.59 inches and the outside diameter is 71.02 inches.

The flow path through the recuperator is shown on Figures 4.13 and 4.14. Figure 4.14 is an unwrapped view of the recuperator at the mean diameter. Compressor discharge (HP) gas enters each recuperator module from the inside of the annulus and flows radially outward in a formed manifold. From this manifold, the gas enters the curved triangular end sections that distribute the flow to the counterflow section of the heat exchanger core. The gas flows along the counterflow section of the core and is collected by another triangular end section at the end of the cylinder. The triangular end section discharges into a manifold. A duct that delivers the heated gas to the heat source is connected to this manifold. The hot turbine exhaust (LP gas) enters the rear annular face of the recuperator, flows axially straight through, and exits from the front annular face. The recuperator is bolted at the LP inlet and is positioned at the LP exit by support structures which incorporate seals for the HP inlet and LP exit. Figure 4.13 illustrates packaging of the recuperator.

The plate-fin recuperator design should have high reliability under design operating conditions due to the thermal cycle design techniques to be employed.

The development and fabrication costs should be low due to the facilities and fabrication techniques previously developed, along with the availability of existing fin designs. The tooling required would need minor rework.

4.1.1.3 Comparative Evaluation and Selection of Recuperator Type for CCCBS

Evaluation of the design concepts consisted of comparing a number of characteristics of the two types of heat exchangers, each of which met the design point performance. The criteria used in the evaluation of the heat exchangers for the CCCBS application are shown in Table 4.2 and the overall ratings are shown in Table 4.4.

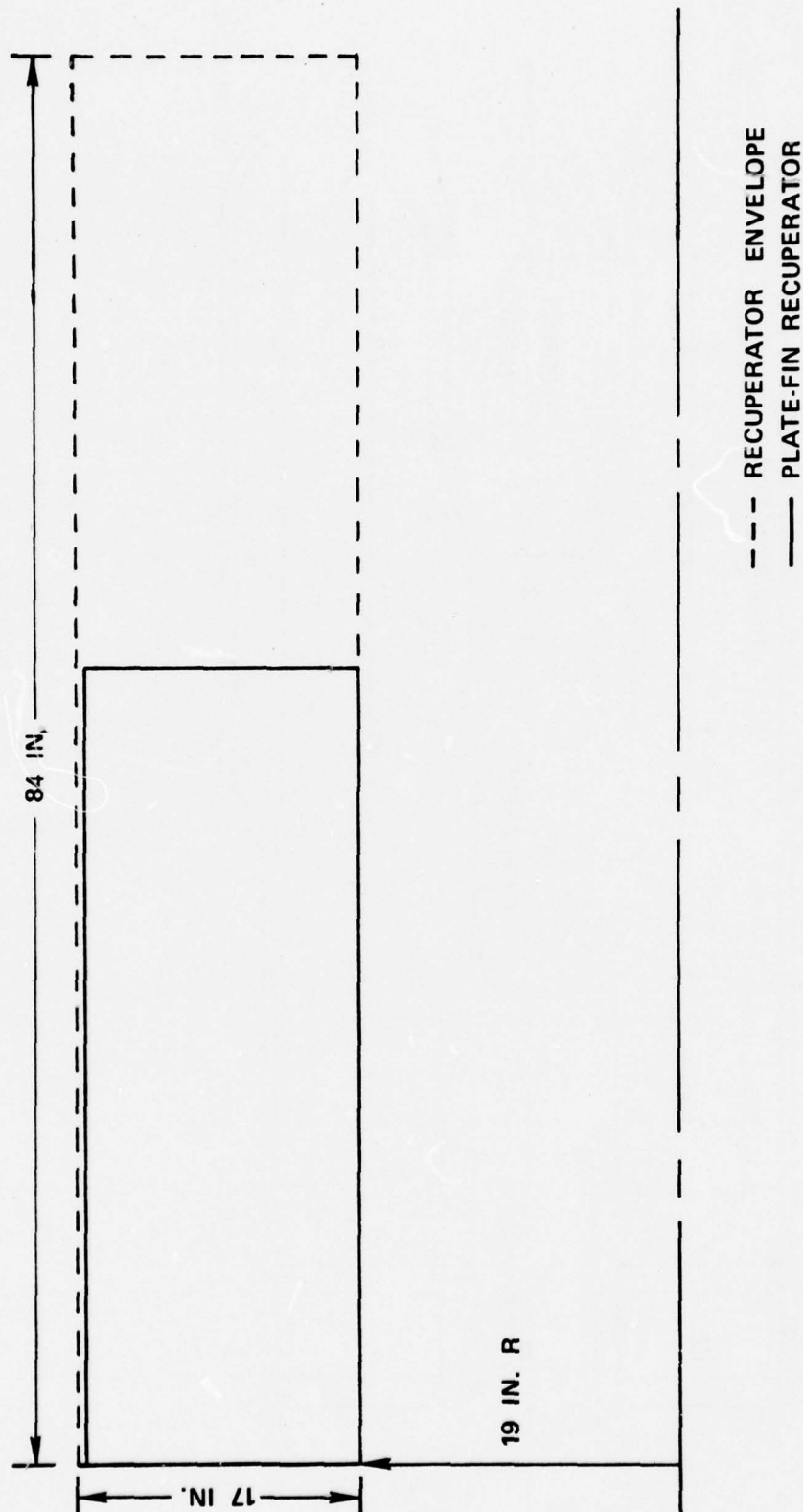


Figure 4.12 Recuperator Packaging

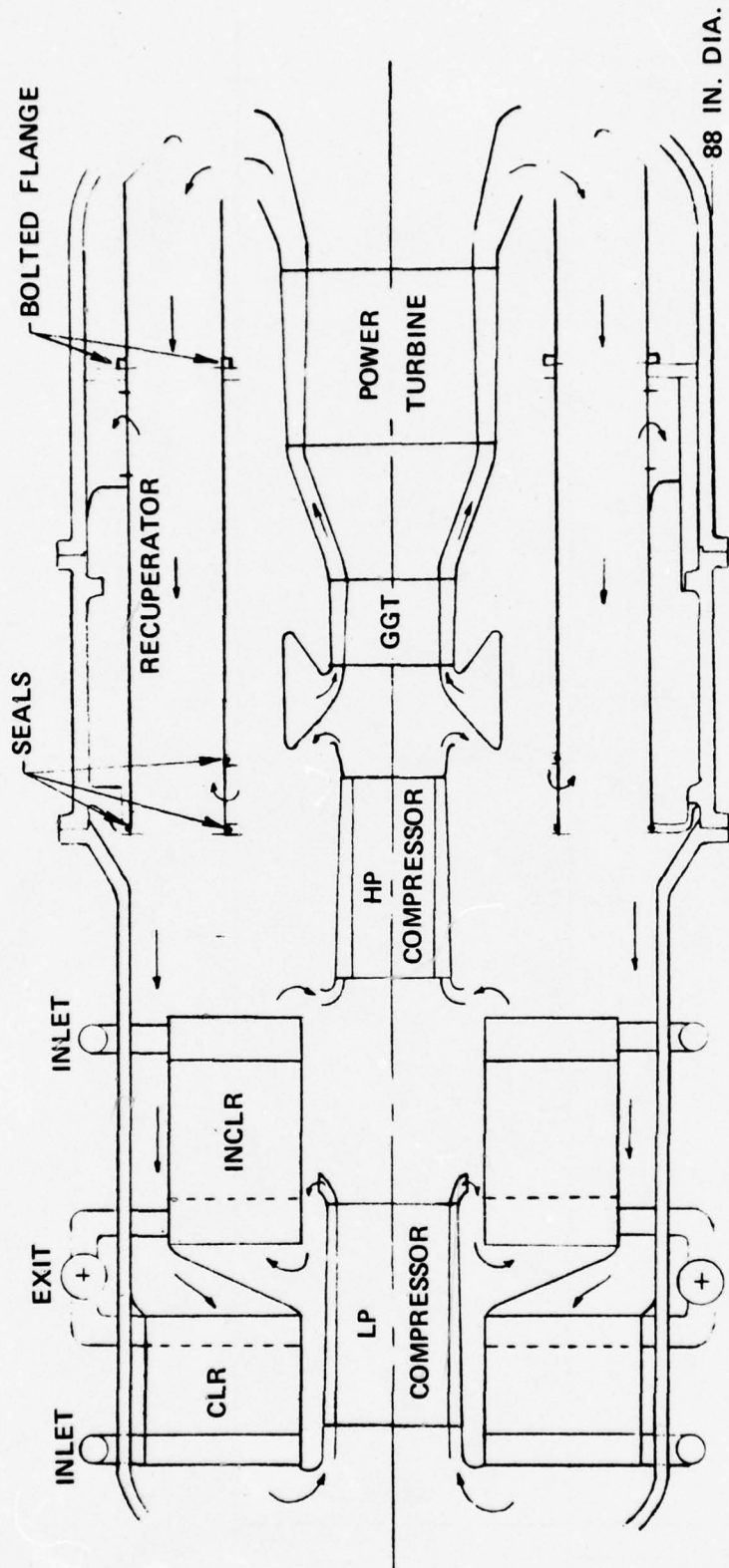


Figure 4.13 Flow Path Through Heat Exchangers

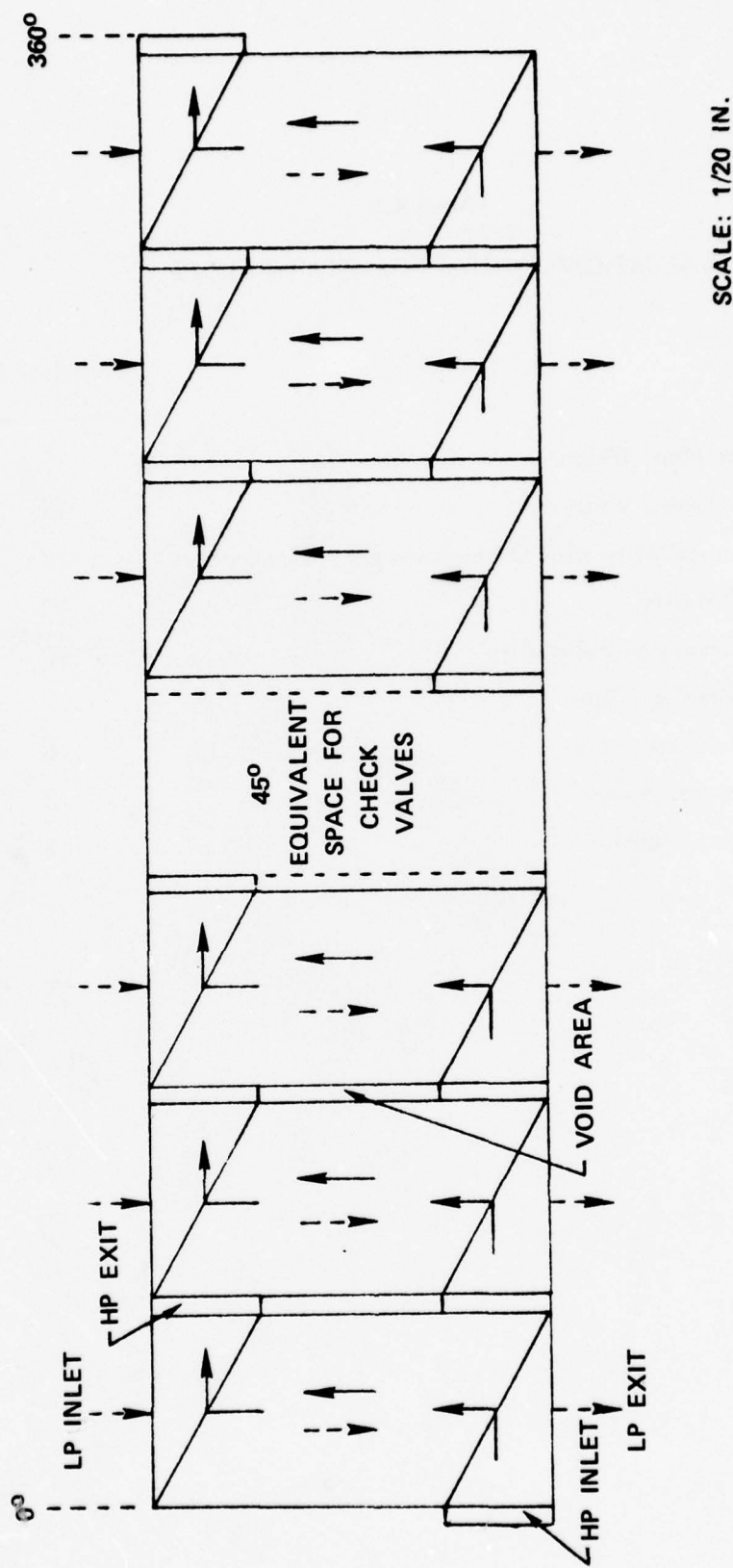


Figure 4.14 Unwrapped View of the Recuperator



Westinghouse

TABLE 4.2
EVALUATION CRITERIA FOR RECUPERATORS

	<u>Weighting Factor</u>
Low Powerplant Weight	10
Low Powerplant Volume	10
High Compatibility with Other Powerplant Components	10
High Reliability	10
High Malfunction Suitability	10
High Technology Base	7
Low Development Cost	6
Low Fabrication Cost	3
High Maintainability	2

Plate-fin heat exchanger configurations usually result in a small flow length with a relatively large frontal area. In contrast, the tube and shell designs usually produce relatively large flow lengths and small frontal areas. However, due to different packaging arrangements to achieve the desired modularization, the annulus area required is approximately the same for each. These trends can be noted in Table 4.3 in the physical size comparisons of the two concepts. The plate-fin concept has a slightly larger outer diameter and slightly larger pressure loss, both of which produce a small weight penalty. As seen in the table, the two concepts are about equal in the impact on powerplant weight and volume.

The plate-fin recuperator configuration results in a lower axial machine length requirement. However, in the configuration under study, the axial length of the power conversion is set by the turbomachinery rather than by the recuperator.

Compatibility with other powerplant components is taken to mean heat exchanger compatibility with the other trial design components or compatibility with new trial design configurations in the components. The main compatibility consideration is that of sealing between the compressor discharge and the recuperator and sealing between the recuperator and the heat source inlet. This sealing consideration is shared by the plate-fin and tube and shell recuperators. The tube and shell modules are circular in shape so that sealing is easily accomplished. The plate fin recuperator modules would be welded into a single annular assembly with O-Ring seals on the compressor end and bolted flange seal on the turbine end. The two types were rated equal.

Reliability is the probability that a device will perform its required function under given environmental conditions for a specific operating time within the prescribed limits of precision and accuracy. The areas of concern in the design of these recuperators are the brazed joints which, experience indicates, are the most likely place for failure if one were to occur. The number of inches of brazed joint exposed to significant pressure differences is considered to be one measure of the reliability of the design. The shell and tube concept has about 75,000 inches of brazed joint compared to approximately 72,000 inches exposed to significant ΔP for the plate fin concept.



Westinghouse

TABLE 4.3

PHYSICAL SIZE AND WEIGHT IMPACT OF RECUPERATOR ON POWERPLANT

	<u>Concept 1</u> <u>Shell & Tube</u>	<u>Concept 2</u> <u>Plate-fin</u>
Outside Annulus Diameter (inch)	70.7	71.0
Heat Exchanger Core Length (inch)	70.0	34.3
Overall Length (inch)	84.0	47.6
Total Heat Exchanger Weight (lb)	23,220	17,580

The tube and shell concept with its cold end floating ring allows the tube bundle to expand and contract independently of the shell so that thermal stresses and thermal strain cycling are low. In the plate-fin concept the modules are assembled into a single unit such that thermal stresses and thermal strain cycling can be low. Therefore, the two concepts were rated essentially equal.

The plate-fin recuperator is more susceptible to over stress failure within the core due to a high pressure difference spike. A failure of this type could be caused by either overpressurizing the system above the mechanical design maximum pressure or by an increased compressor pressure ratio at a high compressor discharge pressure. Recuperator failures of this type can be minimized by careful fabrication development. However, small areas within a module could have incomplete brazing not detected with non-destructive inspection and testing.

Again due to the free floating end ring, the tube and shell concept would be more tolerant of thermal stresses in the course of transients that might occur in emergencies or as a consequence of operator error. Therefore, tube and shell concept is judged to be better in malfunction suitability.

The plate-fin recuperator concept has been demonstrated in a variety of applications. Of particular note is the annular recuperator built for NSRDC and the 2000 pound recuperator core demonstrated by AiResearch for Westinghouse of Canada. The module is designed for 120,000 hours of operation with 5,000 undelayed gas turbine start/stop cycles, however this design is for relatively low pressure differences as compared to the CCCBS requirements. Existing plate-fin designs are incorporated in the recuperator plate-fin concept for the CCCBS.

The tube and shell type of heat exchanger was selected as a candidate for the recuperator because it represents a type of construction that has been proven to have the structural integrity necessary for long-life applications. The shell and tube technology base for high pressure differences is higher than the technology base for plate-fin construction. The shell and tube concept was judged to have the higher technology base for this application.

Development costs are expected to be reasonable for both concepts due to the extensive technology bases. Both concepts require forming operations (hex forming on tubes and fin forming of plates) and brazing operations. The concepts are judged to be about equal in this category.

Labor cost is estimated to be about 20 percent greater for the tube and shell concept. However, both types require forming operations, assembly into modules and brazing operations. With the tube and shell concept, since the braze is only on the end of the tube bundle, gaps remaining after initial furnace brazing operation could be treated with appropriate braze compound at each end and rebraced to seal. Small areas within a plate-fin module could have incomplete brazing possibly not detected with non-destructive inspection and testing. However, the flat stock required for the plate-fin concepts is more economical than the tubing required for the tube and shell concept, the plate-fin concept would have the advantage in this category.

Recuperator maintainability is assumed to mean module replacement if failure occurs. Since both concepts have about the same size of module, the concepts are judged to be equal in this category.

Table 4.4 shows the comparisons of the two candidate types of recuperators for each of the evaluation criteria. It is very important to note that both types meet the design requirements and that the feasibility of a compact closed cycle Brayton power conversion system should be demonstratable with either type.

As shown in Table 4.4, the two types are very close in their overall rating. However, one type must be selected for inclusion in the CCCBS Design Concept for further evaluations. The shell and tube type was selected based upon its slightly higher ranking and technology base.

TABLE 4.4
RECUPERATOR CONCEPT EVALUATIONS

	Weighting Factor	Rating Factors	
		Tube & Shell	Plate-Fin
Impact on Powerplant Weight	10	10	10
Impact on Powerplant Volume	10	10	10
Compatibility with other Powerplant Components	10	10	10
Reliability	10	10	10
Malfunction Suitability	10	10	8
Technology Base	7	10	8
Development Cost	6	10	10
Fabrication Cost	3	7	10
Maintainability	2	10	8
Total (Weighting x Rating)		671	642

Based on these results, it is recommended that the shell and tube recuperator concept be selected for the CCCBS conceptual design study. However, it is very important to note that both types of recuperators meet the design requirements and that the feasibility of a closed cycle Brayton power conversion system for this application could be demonstrated with either type of recuperator.

4.1.2 Gas to Water (Precooler and Intercooler) Heat Exchangers

The intercoolers and precoolers are units in which heat is transferred from a gas to a liquid. In most instances, for this type of exchanger, the heat-transfer coefficients on the gas-side are much lower than those on the liquid side, and hence finned surfaces are advantageous. However, with helium as the gas, the gas side heat transfer coefficients are within a factor of 2 or 3 of that on the liquid side, so that bare tubes may be effective. Therefore, for the intercoolers and precoolers, the shell and tube type of construction was selected as a candidate for the CCCBS. Four different types of precooler - intercooler heat exchanger concepts were carried through preliminary conceptual design and technical evaluation with the object to select the best concept for further design studies. The four candidate types (shell and tube, plate-fin, helical, and cross counterflow tubular) are described in this Section and the evaluation and selection procedure is presented.

4.1.2.1 Shell and Tube Coolers

Shell and tube gas to liquid heat exchangers technology is well developed. Small tubular (0.206 inch tube diameter intercoolers were in use over twenty years ago (Reference 3). A considerable amount of experience has been obtained with closed cycle gas turbine plants that utilize tubular intercoolers and precoolers (Reference 1).

Three counterflow shell and tube concepts were initially generated for the study. Of these three concepts, the modular concept was selected for comparison against the other types (non-modular) of heat exchangers, since it was judged to represent a practical approach to the design of heat exchangers having a very large number of small tubes.

The basic tube module in this arrangement consists of 91 tubes 0.100 ID x 0.120 OD on 0.148 triangular pitch (Figure 4.15) forming a hexagonal array measuring approximately 1.41 inches across flats. The tube ends are brazed into small hexagonal header assemblies which are fed by single 5/8 inch OD tubes (Figure 4.16).

The 91 tube hexagonal modules are bundled together into groups of up to 33 modules (Figure 4.17) and their 5/8 inch OD feed tubes are curved appropriately and brazed into hemispherical headers measuring approximately 4.5 inches OD. The headers can be manufactured as small investment castings and are generally in compression under the high helium pressure.

The variously shaped module groups are bundled into annular configurations to suit the inter-cooler and precooler geometries and their hemispherical headers are bolted to manifold pipe assemblies at each end of the heat exchanger assembly. Sealing is by static O-rings.

The manifold pipe assemblies penetrate the powerplant pressure vessel and are joined by piping to the much larger pipes, isolation valves, etc. at the containment penetration.

The modular approach to construction is expected to simplify problems of quality control during manufacture and facilitate repair and replacement. The 91 tube modules can be leak checked individually before being assembled into 33 module groups. The 33 module groups being mechanically assembled into the heat exchanger can also be checked before assembly and are readily replaceable without brazing or welding.

The geometry for the counterflow shell and tube concept is given in Table 4.5.

4.1.2.2 Finned Tube (Helical and Cross Counterflow)

AiResearch has successfully designed and fabricated a Brayton Heat Exchanger Unit Alternate Design (BHXU-Alternate) under a NASA contract. The BHXU-alternate consisted of a recuperator, heat sink heat exchanger (HSHX), and gas ducting system (Reference 8).

A helical-wound finned tube core design was selected for the gas-to-liquid HSHX. This design

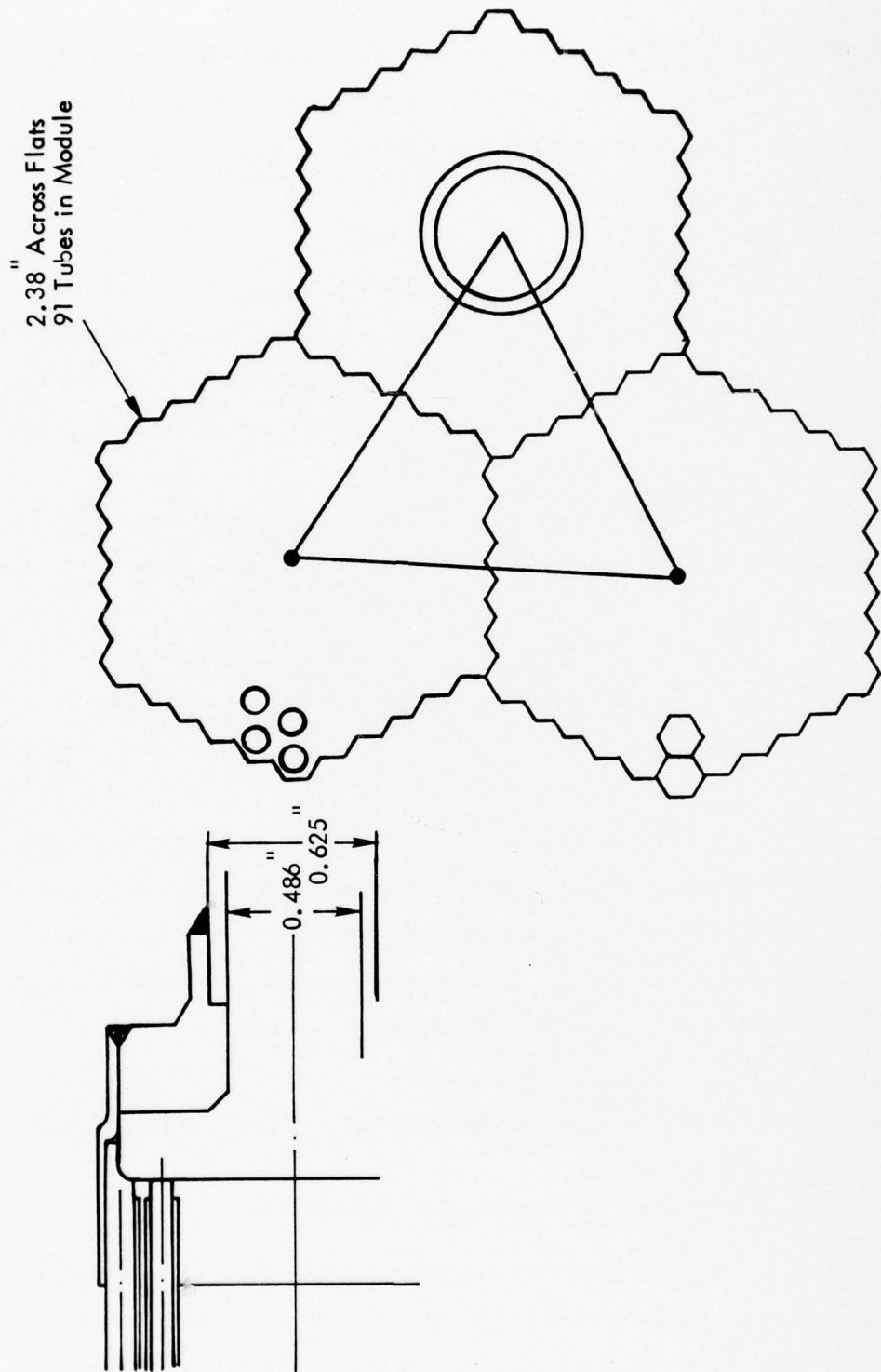


Figure 4.15 Detail of Module Tube Ending and Header

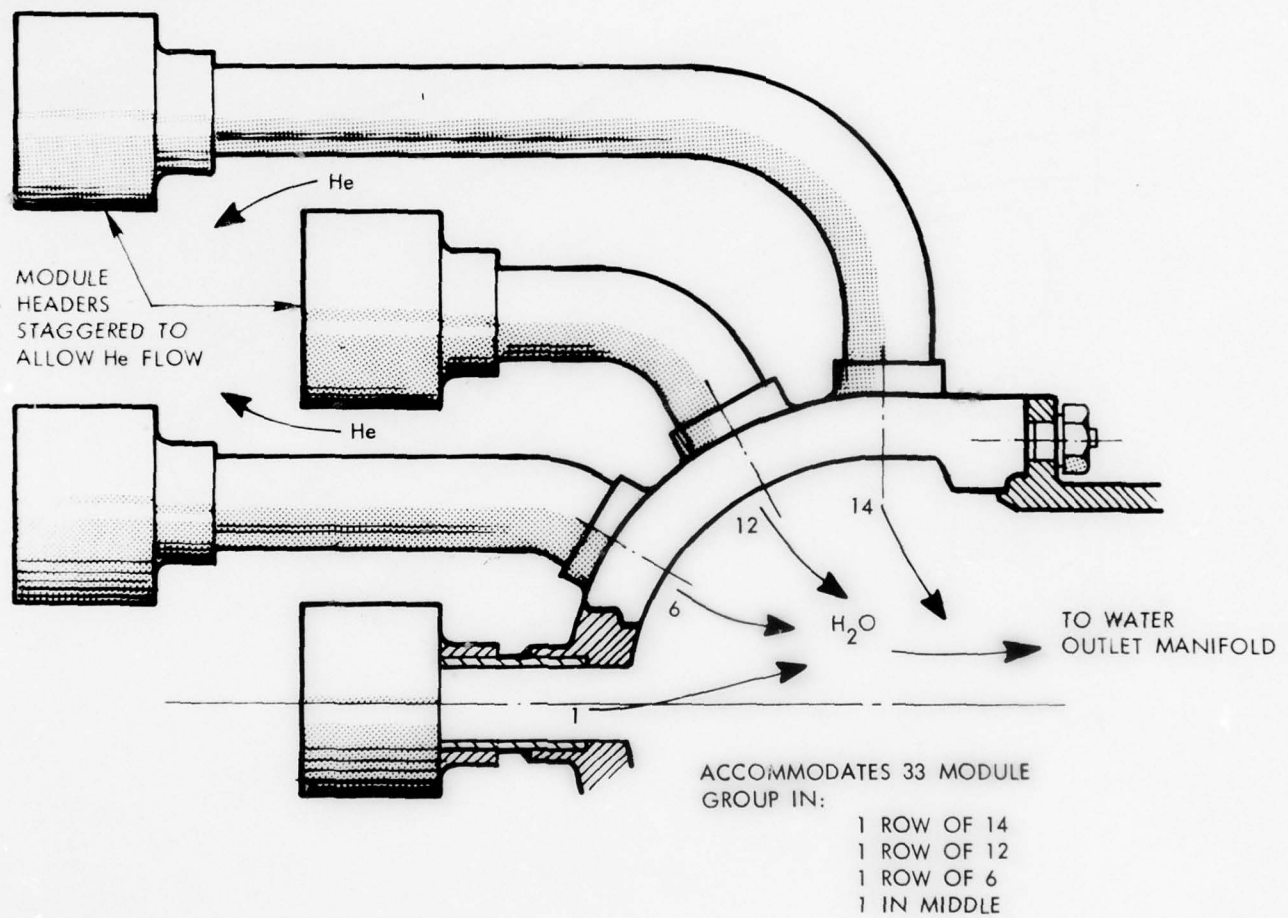


Figure 4.16 Pre-Cooler Detail of Module Headering

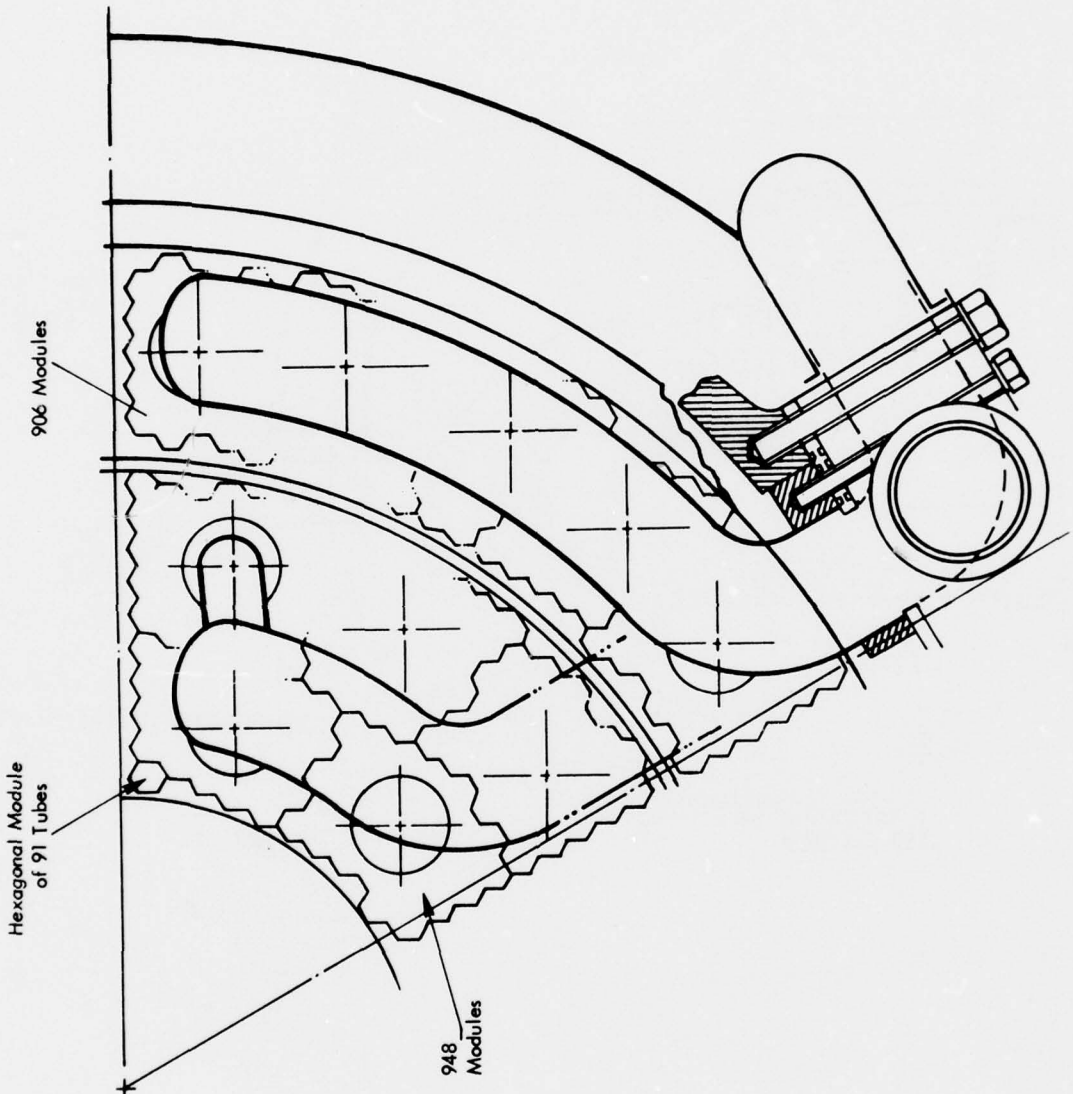


Figure 4.17 Layout of Precooler and Intercooler - Hexagonal Modular Concept

TABLE 4.5
PRECOOLER AND INTERCOOLER SHELL AND TUBE GEOMETRY

	Precooler	Intercooler
Tube OD-inch	0.100	0.100
Tube ID-inch	0.120	0.130
Pitch to OD ratio	1.23	1.23
Effective length-inch	50	50
Number of tubes/unit	81750	85450
Volume-ft ³	44.6	46.6

consisted of 2016 stainless steel tubes with copper fins which were joined with U-tubes to form a continuous liquid flow path.

Finned tubes, similar to the tubes used in the HSHX discussed above and shown in Figure 4.18, are commercially available in several sizes and materials. They are fabricated by winding a fin around a tube in a helical pattern and brazing.

Both finned and plain tube cross-counterflow heat exchanger concepts were investigated by considering four curved modules in an annular configuration. The gas side pressure drop ratio for the coolers and intercoolers was set at the trial design values of 0.013 and 0.008 respectively. The given ID and OD of 25 inches and 73 inches were used as the limits for packaging. A gas side effectiveness of 0.97 was selected for the analysis.

The parameters that were varied in the finned tube analysis were:

- The tube OD was varied from 0.12 to 0.2668 inch which also effected the tube spacing.
- Three fin thicknesses of 0.003, 0.004 and 0.005 inch.
- Two fin configuration - SFT 17 with a fin-to-tube diameter ratio of 1.885 and SFT 18 with a fin-to-tube diameter ratio of 1.27.
- 30 and 40 fins per inch.
- 4, 5, 6 liquid passes.

Stainless steel tubing with a wall thickness of 0.008 inch was selected to result in a minimum frontal area core design. This wall thickness is equal to that used in the cooler design described in Reference 8. Tube wall thicknesses up to 0.012 inch have been evaluated, and the results indicate that the 0.012 inch wall may be desirable to reduce the gas flow length of the cooler and intercooler and increase the frontal area. Total core volume would be about 5 percent less for the 0.012 inch thick tube designs compared with the 0.008 inch thick tube designs.



ILLUSTRATION FROM BULLETIN VB72
VOSS FINNED TUBE PRODUCTS, INC.
CLEVELAND, OHIO



Figure 4.18 Finned Tubes

Stainless steel clad copper fins were selected as a representative configuration available from Voss Finned Tube Products, Inc. Voss makes copper finned tubing which could also be used. Use of pure copper fins would reduce the core volume by 2 percent. There appears to be no major design advantage for either fin material. Differences in fabrication, cost and/or handling may be the basis for a final selection.

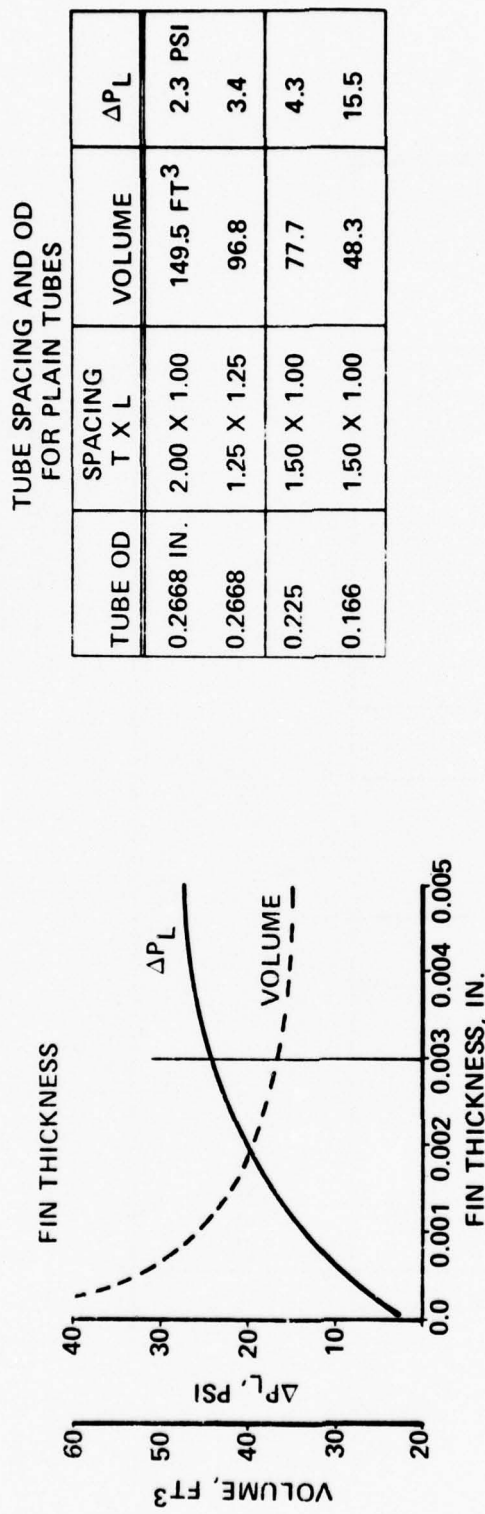
Different fin thicknesses were investigated to determine the effects on liquid side pressure drop (ΔP_L) and core volume. As shown on Figure 4.19, the 0.003 inch thick fin yields the best results.

The analysis indicated that the SFT 18 (short fin configuration) with a fin density of 30 fins per inch, an OD of 0.225 inch, and a transverse and longitudinal spacing of 0.445 inch and 0.223 inch, respectively, yielded the best cooler and intercooler package.

In packaging the coolers, both modular and helical packaging concepts were studied. The helical packaging concept resulted in lower liquid side pressure drops and reduced the total number of discrete tubes from 35,792 to 7,956, when compared to the modular packaging concept. This is an important advantage when considering potential single point failures and fabrication costs. As shown in Figure 4.20, both the helical and modular designs package within the cooler and intercooler envelope.

The results of the analysis for the helical packaging concept are summarized below:

	<u>Cooler</u>	<u>Intercooler</u>
Core Volume, ft ³	29.3	35.6
Core Weight (including coolant), lb	1773	2161
Outside Diameter, in.	67.8	61.5
Gas Flow Length, in.	20.3	31.1
No. of Liquid Passes	4	4



$$\begin{aligned}\delta_T/OD &= 1.98 \\ \delta_L/OD &= 0.99 \\ DIA_f/OD &= 1.27\end{aligned}$$

Figure 4.19 Cooler/Intercooler



Westinghouse

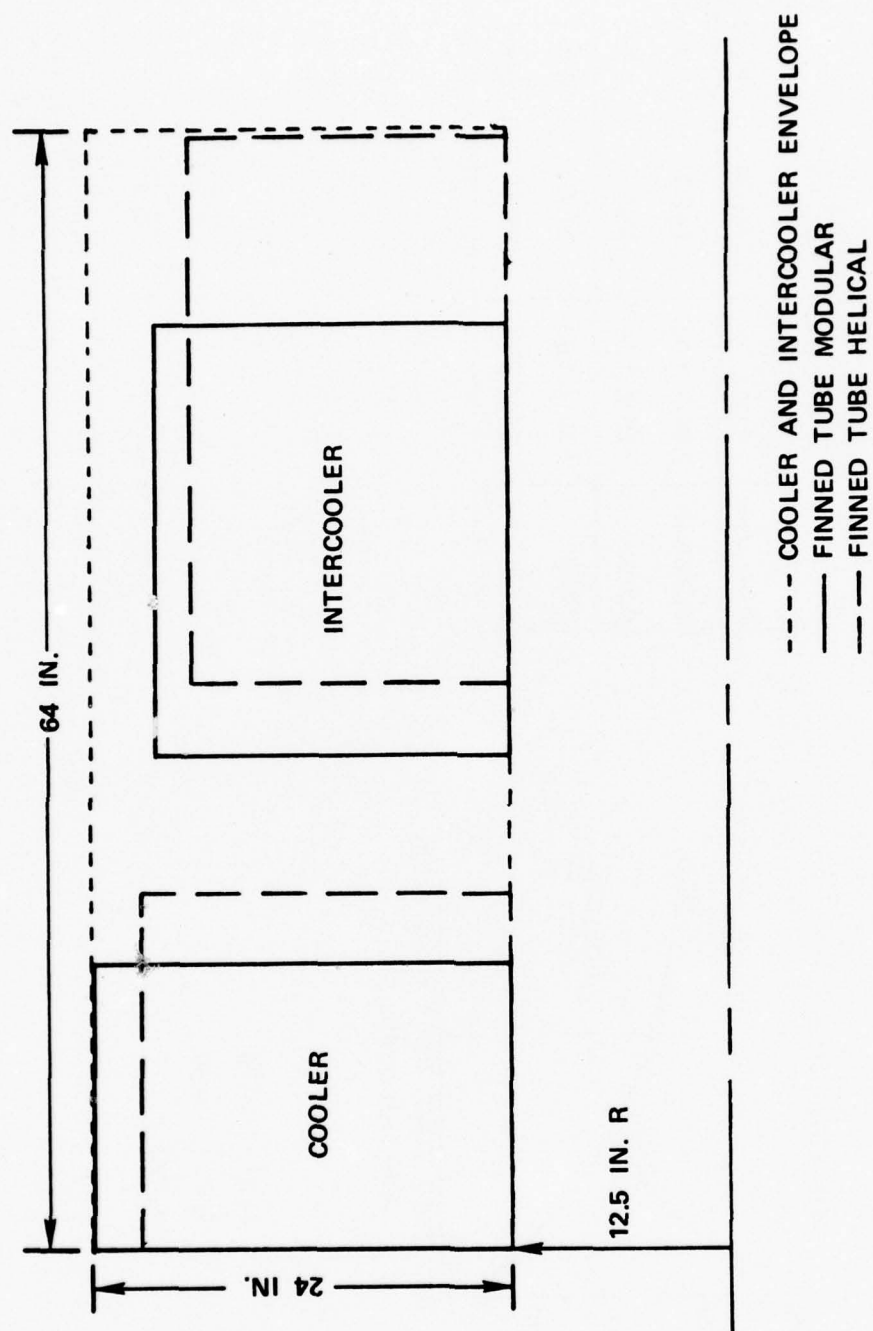


Figure 4.20 Cooler/Intercooler Packaging

The cooler and intercooler are designed as four tube bundles in a helical cross-flow configuration as shown in Figures 4.21 and 4.22. The coolant would enter the coolers radially through four pipes located 90 degrees apart and exit the same way on the opposite side. There would be two main feed pipes and one common exit pipe located outside the containment vessel in an annular configuration. The gas flow through the coolers would be axial and the coolers would share the same inlet duct. It should be noted that the gas flow length for the modular cooler/intercooler design would be equivalent to the active flow length of the helical design, therefore the modules would be shorter. However, the modules would be larger in diameter due to the space required for the coolant ducting between the modules.

Adequate tube support structure must be designed to withstand the imposed vibration due to structure-borne and fluid-induced noise. These support structures will be similar to those required in the cooler assembly described in Reference 8 but will be of a lighter weight design since the tube-type heat exchangers are to be packaged within the engine envelope that also provides gas containment.

The heat exchanger core and support structure can be designed to survive significant shock loads as described in Reference 8. The loads imposed on the heat exchangers may be different (either higher or lower), depending upon the support structure for the entire engine system.

4.1.2.3 Plate-Fin Cooler and Intercooler

AiResearch has formed a high technology base for plate-fin heat exchangers as discussed in Section 4.1.1.2. These heat exchangers have been used in many applications in which liquid-to-gas leakage was not critical.

Several plate-fin cooler and intercooler cases were investigated. Due to the cross flow configuration, these heat exchangers were modeled as six rectangular modules since they cannot reasonably be fabricated in a curved configuration. The fin geometry that resulted in the best cooler and intercooler design is listed below:

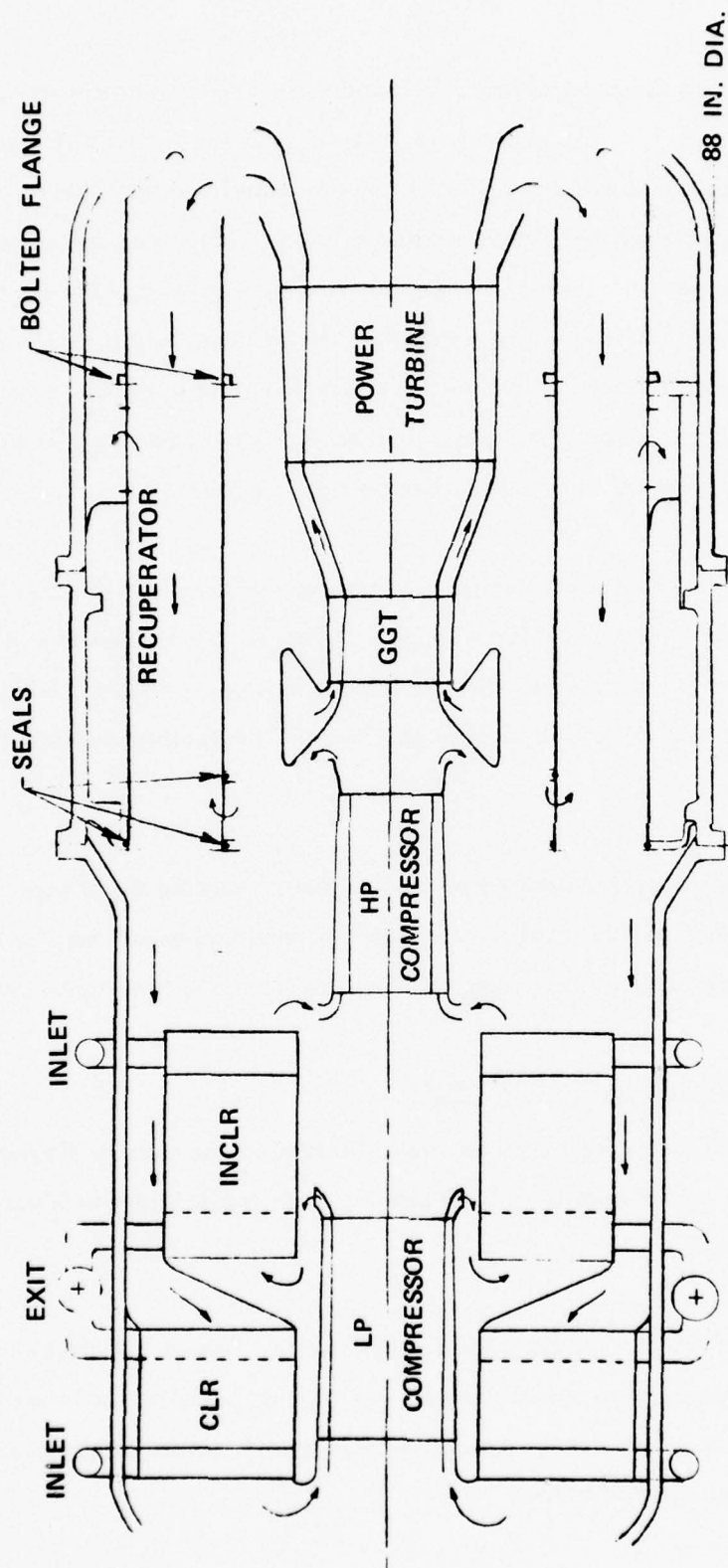


Figure 4.21 Flow Path Through Heat Exchangers

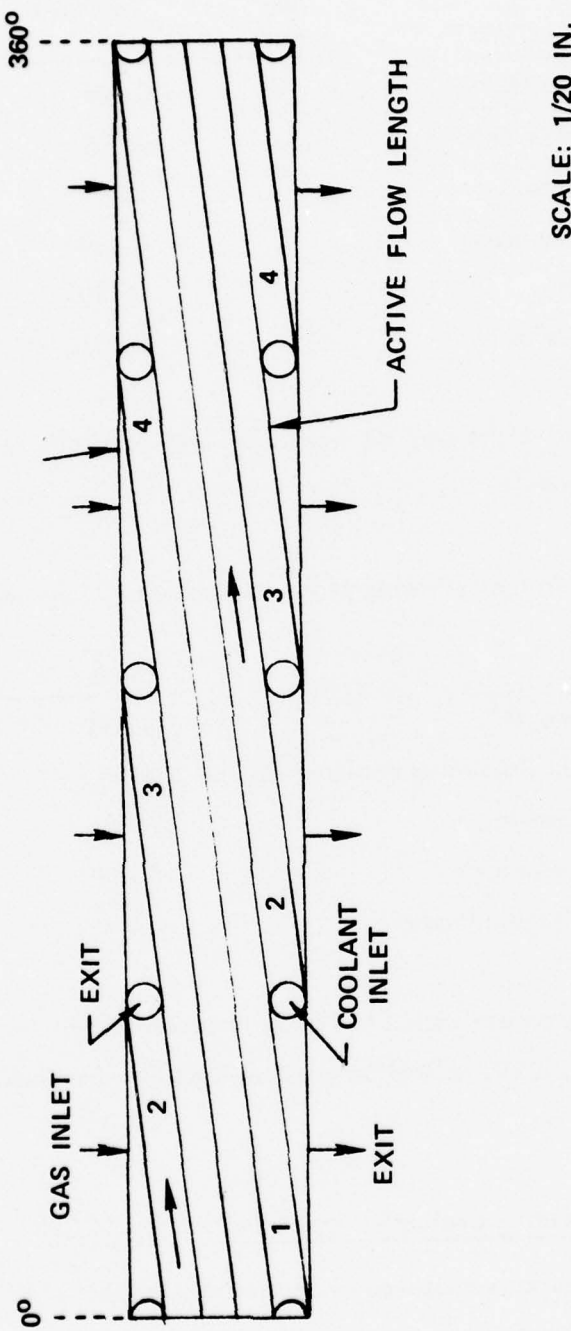


Figure 4.22 Unwrapped View of the Cooler



Westinghouse

	Fins Per Inch	Thickness In.	Spacing In.
Cross Flow Side	12	0.004	0.125
Through Flow Side	16	0.004	0.100
Splitter Plates		0.010	
Wrap-up Material		0.100	
Spacer Bars		0.100	
Braze Material		0.001	

The plate-fin material used in the analysis was nickel with a density of 0.321 lb/in³ and a conductivity of 38 Btu/hr-ft-°F.

This fin geometry resulted in the following plate-fin cooler and intercooler design.

	Cooler	Intercooler
Core Volume, ft ³	30.34	30.15
Core Weight (including coolant), lb	4195	4130
Outside Diameter, in.	69.8	62.11
Gas Flow Length, in.	22.04	32.08
Number of Liquid Passes	4	4

This plate-fin design will package within the allowed cooler and intercooler envelope, but is not recommended for the CCCBS application because liquid-to-gas leakage is a point of concern.

4.1.2.4 Comparative Evaluation and Selection for CCCBS

Evaluation of the design concepts consisted of comparing a number of characteristics of the two types of heat exchangers, each of which met the design point performance. The criteria used in the evaluation of the heat exchangers for the CCCBS application are shown in Table 4.2 with their corresponding weighting factors.

The recuperator is placed in an annular region around the free power turbine and the recuperator frontal area then determines the diameter of the turbomachinery/heat exchanger module. This module diameter then determines the containment vessel diameter in a nuclear powerplant.

The recuperator frontal area has a significant effect on powerplant weight and volume. However, as long as the precooler/intercooler packaging does not increase the module diameter, the powerplant volume is not affected and the type of intercooler/precooler has only a secondary effect on powerplant weight. Therefore, the impact on powerplant weight and volume for the various types of coolers is judged to be about equal.

Compatibility with other powerplant components is taken to mean heat exchanger compatibility with the other trial design components or compatibility with a new trial design configurations in the components. The primary compatibility consideration is that of sealing between the recuperator discharge flow and the low pressure compressor discharge flow. This sealing consideration is shared by all the cooler concepts. However, the plate-fin concept utilizes rectangular modules which are not compatible with the annular envelope and this concept is therefore downgraded in this area (see Table 4.6).

Reliability is the probability that a device will perform its required function under given environmental conditions for a specific operating time within the prescribed limits of precision and accuracy. The area of concern in the design of these coolers is the brazed or welded joints which, experience indicates, is the most likely place for failure if one were to occur. The number of inches of brazed joint exposed to significant pressure differences is considered to be one measure of the reliability of the designs. The shell and tube concept has about 125,000 inches of brazed joint, the helical configuration has about 11,000 inches of joint, the cross counter flow from about 12,000 to 48,000 inches of joint and the plate-fin has approximately 152,000 inches of joint. The tubular concepts were judged to have lower thermal stresses and thermal strain cycling than the plate-fin concept. Therefore the cross flow and helical concepts were rated high in the reliability area (Table 4.8), the shell and tube was downgraded due to the large number of tubes, and the plate-fin was downgraded due to the number of inches of brazed joint.



Westinghouse

TABLE 4.6
COOLER CONCEPT EVALUATIONS

	<u>Cross Counterflow</u>	<u>Helical</u>	<u>Shell and Tube</u>	<u>Plate-Fin</u>
• Impact on Powerplant Weight		Equal		
• Impact on Powerplant Volume		Equal		
• Compatibility with other Powerplant Components	10	1		5
• Reliability	10		4	3
• Malfunction Suitability	10			5
• Technology Base	10	9	8	8
• Development Cost	10	9	8	9
• Fabrication Cost	8	7	4	
• Maintainability	9	5	9	9
Total with Weighting Factors	472	448	374	278

The plate-fin coolers are more susceptible to over stress failure within the core due to a high pressure difference spike. A failure of this type could be caused by either overpressurizing the system above the mechanical design maximum pressure or by an increased compressor pressure ratio at a high compressor discharge pressure. Cooler failures of this type would be minimized by careful fabrication development. Note however, that small areas within a module could have incomplete brazing and most likely would not be detected with non-destructive inspection and testing.

The tubular concepts would be more tolerant of thermal stresses in the course of transients that might occur in emergencies or as a consequence of operator error. The plate-fin concept therefore was judged lower in the malfunction suitability area.

All of the concepts were rated relatively high in technology base, with the shell and tube concept degraded slightly due to the large number of small tubes and the plate-fin concept downgraded slightly due to the higher than normal pressure difference for this concept.

Development costs are expected to be reasonable for all concepts due to the relatively high technology base. The shell and tube and plate-fin were slightly downgraded for the reasons given in the technology base discussion.

Only rough estimates of fabrication costs can be obtained at this time. The plate-fin concept was judged to be the most economical of the concepts due to flat stock being less expensive than tubing. The shell and tube was judged to be the most expensive due to the large number of small tubes.

Cooler maintainability is assumed to mean module replacement if failure occurs. All concepts except the helical concept, have modules of about the same size. Therefore, the helical concept was downgraded in this area.

Table 4.6 lists the relative evaluations in each of the categories discussed in the preceding sections. The total evaluation value given at the bottom of the table utilizes the weighting factors given in Table 4.2.

These studies have indicated that three types of heat exchangers could meet the requirements (cross counterflow, helical and shell and tube). Thus feasibility of the CCCBS could be demonstrated with the selected type or with either of the two alternates. Based on these results, it was concluded that the cross counterflow tubular concept has the greatest promise and was selected for incorporation into the design concept and associated further study.

4.2 HIGH PRESSURE (GAS GENERATOR) TURBINE

The first stage of the high pressure turbine is the most limiting stage of the turbomachinery. Its capabilities and configuration determine to a large extent the configuration and characteristics of the turbomachinery as a whole. Therefore, an early task was established to investigate specifically the first turbine stage as input to the design concept definition.

4.2.1 Blade State-of-the-Art

4.2.1.1 Materials Currently Available

Commercial open cycle gas turbines, using uncooled turbine blades in air, are currently operating at turbine inlet temperatures in the region of 1600°F. The Westinghouse 251AA gas turbine, as an example, uses nickel based Udimet 500 cast or Udimet 710 forged first stage blade material. This machine is a simple open cycle turbine using air as the working fluid. The blade metal temperature is reduced to approximately 1500°F by the temperature drop through the first nozzle vanes. Creep properties for the Udimet 710 material are shown in Figure 4.23 (developed from Reference 9) and indicate a temperature capability of about 1540°F for 100,000 hours to rupture at 17,000 psi which is representative of the centrifugal stress at the blade root in this particular machine.

Obviously, an assessment of the blade stress situation and material situation for large air cycle gas turbine blades is oversimplified but it does provide useful information. The centrifugal stress varies along the blade span, generally reducing towards the tip. The temperature along the blade is not constant, but is affected by the combustor outlet temperature profile which generally results in a maximum temperature in the midspan region reducing towards the root and tip. The blade also experiences gas bending stresses which, to some extent, can be balanced by leaning the blade to introduce an opposing moment due to the offset centrifugal force. Bending stresses also result from manufacturing tolerances in the blade root fixing which affect the amount the blade leans in one direction or the other. Additional stresses arise as a

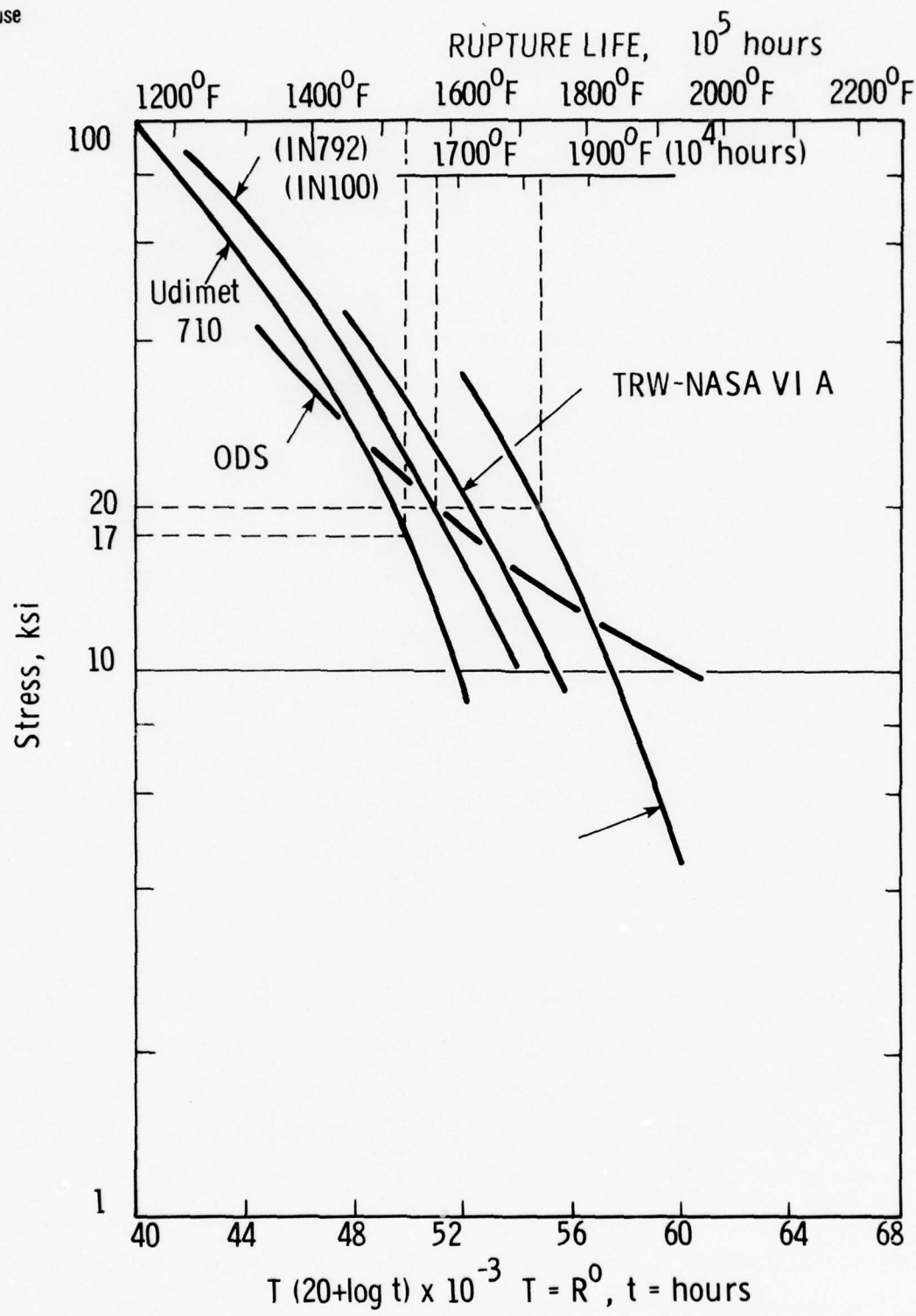


Figure 4.23 Stress Rupture Data (Larson-Miller Plot) for Selected Nickel Base Alloys

result of thermal gradients and vibration. Thermal gradients in uncooled blades generally occur under transient conditions, such as start up and shut down, and are caused by the differing cooling and heat up rates of the mid-chord region of the blade and the less massive leading and trailing edges. Life is limited by cracking at the leading and trailing edges resulting from this effect and augmented by corrosion caused by sulphur, vanadium and other contaminants in the combustor fuel. Vibration results from the excitation of blade natural frequencies by various forcing frequencies such as upstream nozzle vanes, wakes from support structure and distortion of the flow distribution into the blading by asymmetrical inlet piping arrangements, etc.

All of these secondary influences tend to degrade the potential temperature capability of the turbine which is determined by the centrifugal blade stress and the material creep rupture strength for the operating life of interest.

In inferring the potential temperature capability of Closed Brayton Cycle helium turbines from state-of-the-art air breathing machines, some recognition of the relative magnitude of these degrading influences in the two types of turbine is appropriate.

The blades in commercial air breathing gas turbines generally fail as a result of cracking and corrosion rather than creep rupture. The corrosion is caused by contaminants in the fuel, such as sulphur and vanadium which will not be present in the Closed Brayton Cycle helium environment. In this respect the helium working fluid presents a much more benign environment than air.

The elimination of the combustor also tends to improve the uniformity of the temperature distribution into closed cycle turbines, resulting in a reduced maximum blade metal temperature for a given average inlet temperature. Problems due to hot streaks and hot starts which frequently result from fuel injection nozzle and igniter defects are also eliminated.



Westinghouse

The use of helium instead of air may cause other problems, however which must be considered. Some evidence has been obtained, in the limited testing performed to date in helium, that the creep rupture properties of certain superalloy materials are significantly reduced. This effect appears to be the result of intergranular attack caused by selective internal oxidation of aluminum and titanium strength additives. The addition of niobium, tungsten and tantalum has been shown to decrease the extent of the attack. The effects of impurities in the helium are not clear at the present time and a considerable amount of material testing will be required to resolve these questions. Testing has been accomplished as part of this CCCBS study at Westinghouse using ultra-high purity helium to provide a base line for future tests incorporating various impurities. The results of the tests to date are reported in Section 6.0.

In inferring the potential temperature capability of CCCBS helium turbines from the state-of-the-art air breathing machines, any degrading effects due to the helium are anticipated at the present state of knowledge to be no worse than the combustion related effects of the air breathing machines.

The helium closed cycle turbomachinery designed for GT-HTGR powerplant (Reference 12) has a turbine inlet temperature of 1500°F which, allowing for the smaller temperature drop in the first stage nozzles characteristic of helium turbines and its substantially higher operating life assumption of 280,000 hours, is generally consistent with the state-of-the-art as represented by the Westinghouse 251AA machine. If the design life requirement is substantially reduced, below that of the 251 AA machine, (100,000 hours) to that of the CCCBS (10,000 hours at full power or 40,000 total hours), the permissible turbine inlet temperature can be increased accordingly. The use of a somewhat superior blade material can further raise the turbine inlet temperature.

It should be noted that these potential temperature improvements cannot necessarily be exploited in closed cycle machines which employ heat source heat exchangers due to the temperature limitations of the energy source heat exchanger. An example of such a closed cycle machine

is the Oberhausen closed cycle gas turbine in which the turbine inlet temperature is limited to 1380°F when operating on fossil fuel although this machine was actually designed for a higher temperature consistent with nuclear operation.

One of the candidate nickel-base blade alloys currently being considered for the Closed Brayton Cycle turbine (IN 100) is approximately 50° to 75°F better than the Udimet 710 material on a stress rupture basis (Figure 4.23). If the centrifugal stress estimated at the root of the preliminary concept study first stage turbine blade (19,874 psi) is equated with the 10,000 hours rupture curve derived from Figure 4.23, the resulting allowable metal temperature is 1670°F .

Actual blade metal temperature in the case studied is 1632°F (turbine inlet temperature of 1671°F reduced by a 39°F drop across the first stage nozzle). A margin of 38°F is available in this case, compared with the 40°F value estimated for the Westinghouse 251 AA machine. Thus the helium turbine design for 10,000 hours full power life exhibits a degree of conservatism similar to the 251 AA machine for 100,000 hours.

The IN100 material used in this illustration is by no means the only candidate for use in first stage turbine blades. IN792 has creep strength similar to IN100 (see Figure 4.23) and is a promising candidate for the small size blading of the Closed Brayton Cycle helium turbine. Other currently available state-of-the-art superalloy candidates are IN738 and IN713LC. The Westinghouse materials testing program using ultra high purity helium currently includes the IN100 and IN713 LC materials.

The above blade material candidates are currently being used in aerospace turbines and can be considered readily available production alloys. Therefore, if the current test program verifies their suitability for operation in a helium environment, as is expected, the requirements of the 1700°F Closed Brayton Cycle first stage turbine can be met with state-of-the-art nickel based superalloy materials.

4.2.1.2 Materials - Expected Developments

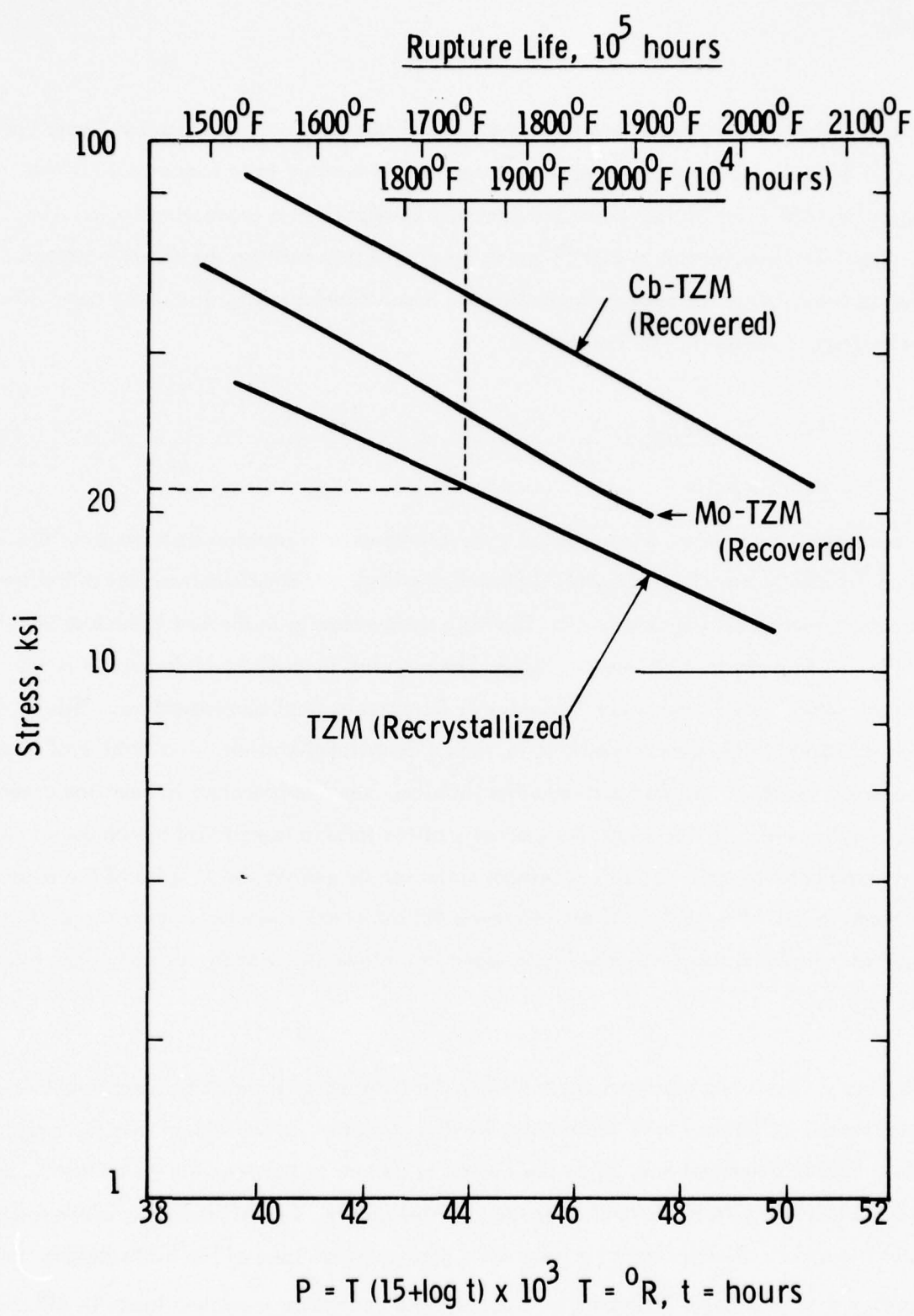
More advanced superalloy materials are currently under development. One such alloy is TRW-NASA VI A (see Figure 4.23). This material is approximately 50° to 75°F better than the IN100 and IN792 alloys from the standpoint of creep rupture. This alloy probably represents the highest temperature capability it is possible to obtain by conventional investment-casting of nickel based superalloys.

Other techniques, such as mechanical alloying may result in further extensions of the temperature range of "near" conventional superalloys. An yttria dispersion-hardened alloy with a base composition derived from IN792 produced using this technique has demonstrated improved strength and corrosion resistance.

Eutectic superalloys consisting of a superalloy-type matrix reinforced by a high temperature intermetallic such as Ni₃Nb or TaC are also under investigation. Currently, the strongest material of this class is the $\gamma^1 - \delta$ (Ni₃Al-Ni₃Nb)composite. Stress rupture data for the material is illustrated on Figure 1 for comparision with the more established superalloy materials.

Fiber-reinforced superalloys probably have the highest strength and temperature capability of any metal systems with a potential temperature capability approaching 2000°F for the W-Re-Hf-C superalloy composite. However, these materials, together with the eutectic composites introduce new problems resulting from the mismatch in the coefficients of expansion of their constituents. Thermal fatigue is an area of major concern in such materials.

The freedom from oxidation in the Closed Brayton Cycle helium working fluid allows the refractory metal alloy Mo-TZM to be considered. Mo-TZM has demonstrated the excellent forgeability required to produce the required airfoil shapes and has a potential temperature capability between 1800 and 1900°F. The properties of Mo-TZM are shown on Figure 4.24 (developed from Reference 9).



$$P = T (15 + \log t) \times 10^3 \quad T = {}^{\circ}R, t = \text{hours}$$

Figure 4.24 Stress Rupture Data for Selected Refractory Alloys

To summarize the materials state-of-the-art applicable to the Closed Brayton Cycle uncooled turbine blading, nickel base superalloys capable of a turbine inlet temperature in the region of 1700°F for 10,000 hours are currently available on a production basis. The potential for development to 2000°F exists by substituting existing refractory materials such as Mo-TZM or the more advanced nickel based developments, including composite technology, foreseen in the near future.

4.2.1.3 Design

Hub/Tip Ratio

In evaluating the current and expected state-of-the-art of uncooled first-stage turbine blades as applicable to the closed Brayton cycle power plant, certain characteristics of helium turbomachinery must be considered. The high sonic velocity in the low molecular weight gas results in a tendency to employ higher blade speeds in order to minimize the number of stages. Blade speed tends to be limited only from mechanical considerations. This tendency towards higher blade speeds results in increased centrifugal stresses, in a turbine of given geometry, which in turn forces a reduction in blade metal temperature to meet the creep life requirement. If, however, the geometry of the turbine is modified by the use of an increased hub/tip ratio, a low centrifugal stress can be maintained in spite of the increase in blade speed. Figure 4.25 (from Reference 10) shows the variation of centrifugal stress with hub/tip ratio for a fixed value of blade speed in a blade designed for an early open cycle marine gas turbine.

Obviously, there is a practical upper limit to hub/tip ratio, imposed by considerations of aerodynamic efficiency and, ultimately, by disc stresses. As hub/tip ratio is increased, blade length is reduced and, since the operating clearance between the tip of the blade and the stationary liner cannot be reduced proportionally, the tip clearance/blade length ratio increases. As tip clearance becomes a greater percentage of the blade height, the tip leakage effects become increasingly important and contribute increased losses in efficiency. Also, as hub/tip ratio is increased, disc rim speed increases for a given value of blade speed.

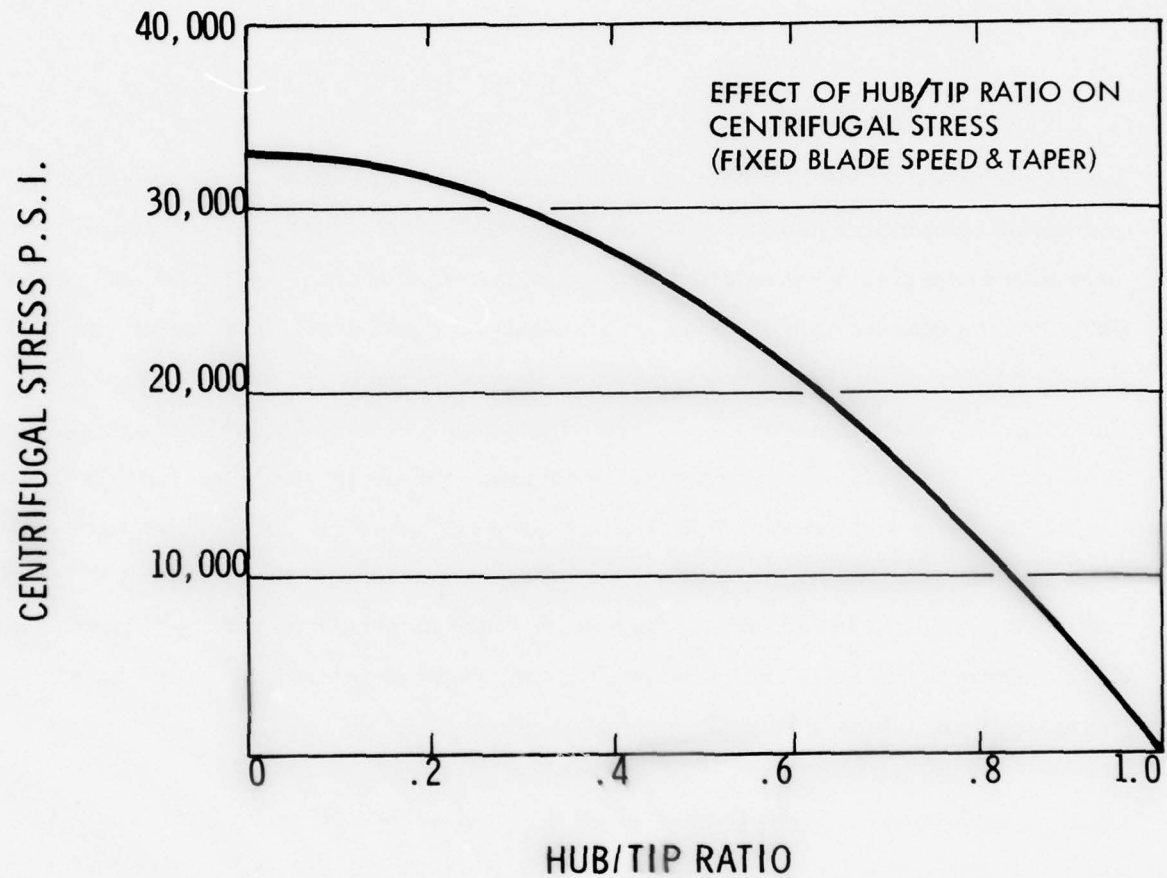


Figure 4.25 Variation of Centrifugal Stress with Hub/Tip Ratio

Therefore, although blade speed might be raised indefinitely, if efficiency effects could be ignored, by progressively increasing hub/tip ratio to maintain blade stress at an acceptably low value, disc stresses would rapidly increase and ultimately limit the blade speed. The hub/tip ratio is therefore a compromise between the desire for high blade speed and temperature capability, on the one hand, and for acceptably low blade tip losses and disc stresses on the other.

Rotor Blade Shrouds

Testing performed by Westinghouse on large closed cycle gas turbine stages with shrouded and unshrouded rotor blades (Reference 11) demonstrated that shrouding conferred no efficiency advantage at tip clearances below 0.0017 in/in of rotor diameter. At 0.0025 in/in of rotor diameter, the unshrouded turbine had an efficiency of 0.898 while the shrouded version was slightly superior at 0.902. The 0.0025 in/in of rotor diameter, when related to the CCCBS first stage turbine tip diameter of 17 inches, corresponds to a tip clearance of approximately 0.043 inch. This value should probably be adjusted to allow for the higher hub/tip ratio of the Brayton Cycle turbine relative to the test turbines (0.8 versus 0.718) which results in a blade approximately 30 percent shorter as a percentage of rotor diameter. If the 0.043 inch clearance is adjusted in the ratio of the relative blade heights, the resulting clearance is approximately 0.030 inch. This clearance is not unreasonably small and should be achievable in practice in a turbine of this size.

Shrouds are difficult to justify in the first stage high pressure turbine even at much higher efficiency differentials. The centrifugal force of the shroud substantially increases the centrifugal stresses in the blade, forcing the turbine inlet temperature to be substantially reduced. The reduction in cycle temperature tends to reduce plant thermal efficiency and nullify the effect of the higher efficiency shrouded blade turbine. The reduction in turbine temperature associated with shrouded turbine blades has an even more serious effect on specific power, resulting in substantially increased plant size and weight for a given power output. This consideration is especially important in plants which are designed for minimum

size and weights. The situation in the power turbine is somewhat different due to the lower temperatures and centrifugal stress levels. Here the use of rotating shrouds might be justified to provide bending support for long slender blades.

Extended Blade Roots

Extended blade roots provide a thermal barrier between the hot blade airfoil section and the rim of the disc. As a result the operating temperature at the disc rim and the temperature gradient between the rim and the hub can be substantially reduced. Cooling gas bled from the compressor stages is directed to the disc rim for most economical use of the gas. Rim temperature can easily be reduced sufficiently to permit the use of a ferritic material.

Within certain limits, set by the hub/tip ratio and blade speed, the centrifugal stresses along the blade can be varied by adjusting the taper ratio. Taper ratio is merely the ratio of the blade cross section area at the root to the area at the tip. Obviously the higher the taper ratio, the lower will be the centrifugal stress at the root. Taper ratio is limited in practice, however, by the minimum blade thickness and chord which can be permitted at the tip and the maximum thickness and chord which can be allowed at the root.

The blade tip thickness/chord ratio tends to be limited to a minimum value of about 6 percent by considerations of local vibration in the tip region of the blade. The thickness/chord ratio at the root tends to be limited to a maximum value of about 26 percent by aerodynamic flow path considerations concerned with the avoidance of adverse pressure gradients and diffusing flow. Thus, the ultimate effectiveness of taper ratio as a means of reducing centrifugal stresses is limited by these practical considerations.

In combustion gas turbines using uncooled blades, the maximum metal temperature tends to occur near the midspan due to the peaked combustion outlet temperature profile. This results in the need for a blade with a large amount of taper from the tip to the midspan, to minimize the centrifugal stress at this location. The taper from the midspan to the root can be adjusted to permit the centrifugal stress to increase towards the cooler root section.

In the CCCBS helium turbine, however, the temperature profile at inlet to the turbine is expected to be much flatter than in air breathing turbines. As a result, the mid-span region can be expected to be very little hotter than the root. In this case the blade should be provided with less taper from tip to midspan and more taper from midspan to root than the combustion turbine blade. In other words the helium turbine blade would be expected to be relatively thinner at the midspan region.

Chord

Blade chord is normally a compromise between the requirements of compactness, on the one hand, and low bending stresses in the blade, on the other. Figure 4.26 (obtained from Reference 10) shows the variation of bending stress with blade chord for an early marine gas turbine design of the open cycle type. The bending stress varies inversely as the square of the chord. In the first stage turbine blade of the CCCBS machine the bending stress at the blade root is approximately 20,000 psi for a blade chord of 1.0 inch. This stress is estimated to be in the right range for the CCCBS turbine.

The question of the maximum gas bending stress permissible in the turbine blade is a difficult one to answer. Conservative judgement suggests that the blade gas bending stress be limited to the region of 15,000 to 20,000 psi to provide for the magnification of cyclic stresses which can occur under certain near resonance conditions. These conditions can result from excitation of the blade natural frequency by various sources in the flow path of the machine. Every effort is made in the design to avoid the most serious resonant conditions in the normal running range, such as the excitation of the first cantilever bending modes by low engine order frequencies. An extensive program of design, analysis and testing is normally undertaken during development to provide the least vibration prone design possible. The resulting interference diagrams generated in such programs superimpose the vibration frequencies of the various blade modes of interest on a plot of the various engine order excitation frequencies throughout the operating range. The scope available for tuning out undesirable interferences, by adjustments in blade stiffness or design changes to modify forcing frequencies, is thus clearly defined. Blade chord adjustments and appropriate changes in the number of blades can then be detailed in the early design stages.

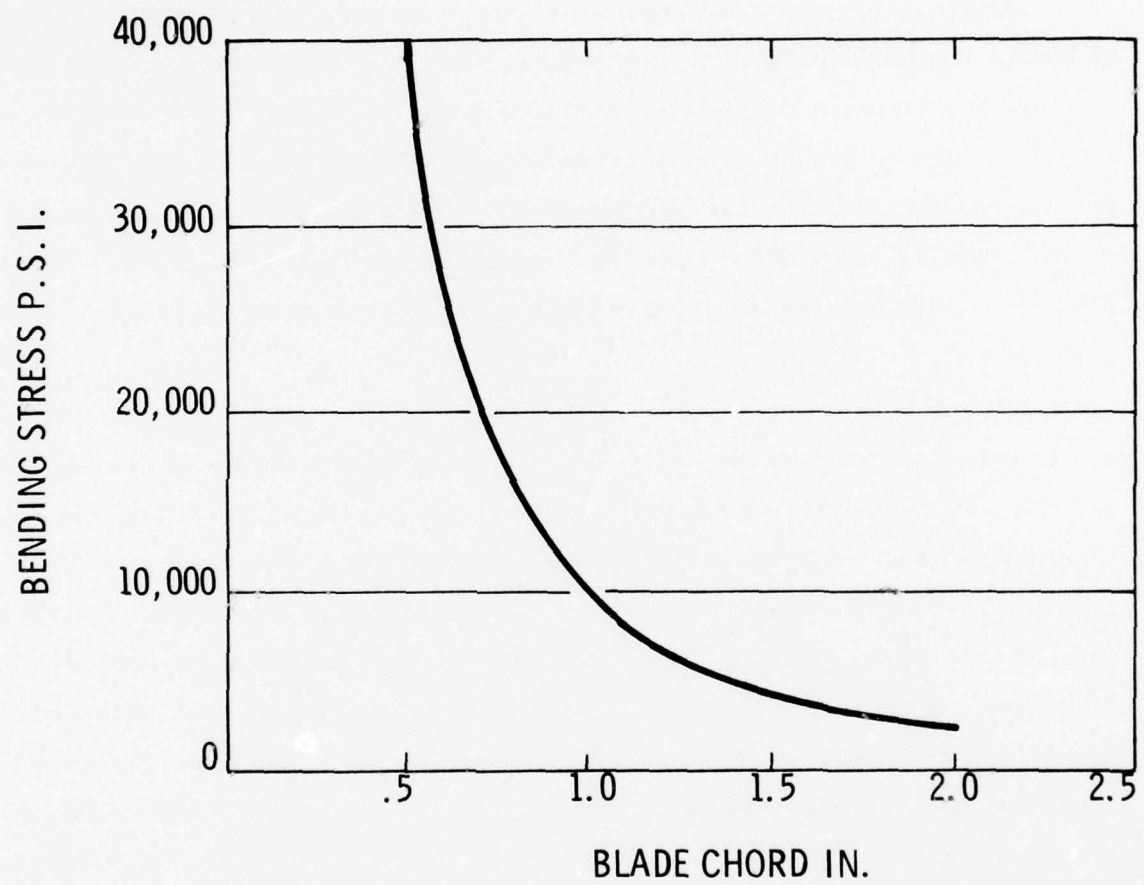


Figure 4.26 Variation of Bending Stress with Blade Chord



Westinghouse

4.2.2 Disc State-of-the-Art

4.2.2.1 Materials - Currently Available

Disc materials can be generally classed as either austenitic or ferritic.

The Westinghouse 251 open cycle gas turbines, which are representative of the current state-of-the-art of commercial air-cycle gas turbines, employ ferritic turbine discs. The material is an iron based nickel-chrome-molybdenum steel similar to AISI 4340 steel but having improved fracture toughness. The use of ferritic discs is made possible by extended root turbine blades and disc cooling which results in low disc operating temperatures. The disc rim operates in the 600° to 650°F temperature range. The body of the disc is approximately 50°F cooler. High pressure air, bled from the compressor at 600°F and cooled to approximately 300°F, is used to cool the discs.

Earlier open cycle machines used discs made of the Westinghouse developed Discalloy austenitic material. This material has sufficient alloying constituents (25 percent Nickel, 15 percent Chromium and small percentages of other elements) to provide good creep strength in the region of 1000°F, consistent with the disc rim temperatures associated with earlier blading design which did not employ extended root fixings. However this material and the generally similar A286 have a higher coefficient of expansion than typical ferritic materials. This characteristic and the higher rim temperature resulting from the omission of the root extension feature, give rise to appreciable thermal expansion. Disc cooling is difficult to apply without overcooling the body of the disc in relation to the rim. The low blade to disc heat flow impedance tends to result in radial temperature gradients and thermal stresses in highly cooled discs. Disc cooling air should be confined as much as possible to the disc rim only.

The use of ferritic discs offers a number of advantages to the CCCBS. Ferritic materials generally have substantially lower thermal expansion coefficients than austenitic materials. The combination of the reduced operating temperature, achieved by the use of extended root blading, and the low coefficient of expansion of ferritic discs can result in a worthwhile reduction in

disc expansion. This significantly reduces the amount of total rotor thermal growth, especially in high hub/tip ratio rotors and assists in achieving minimum tip clearance during operation. Table 4.7 illustrates the various contributions to total rotor expansion which might be expected in the Closed Brayton Cycle first stage turbine rotor.

TABLE 4.7

 CONTRIBUTIONS TO TOTAL TURBINE ROTOR EXPANSION
 17 INCH TIP DIAMETER CLOSED BRAYTON CYCLE FIRST STAGE ROTOR

<u>Radial Growth (in)</u>		<u>Radial Growth (in)</u>	
(No extended blade root A286 austenitic disc - 800°F rim)		(Extended blade root AISI 422 ferritic disc - 600°F rim)	
Disc	0.048	Disc	0.020
Blade	0.022	Blade	0.029
Disc	0.012	Disc	0.012
Blade	0.001	Blade	0.0015
0.083 Total tip growth (in)		0.0625	

The combination of reduced temperature gradient and reduced expansion coefficient in ferritic discs used with extended root blading also results in substantially reduced disc thermal stresses which, in turn, have a beneficial effect on rotor cyclic life. The reduction in the maximum disc temperature is especially effective in limiting the temperature gradient and thermal stress which can be produced during transient conditions. The reduced temperature range through which the disc has to operate tends to reduce the sensitivity of the rotor to rapid temperature changes.

The AISI 422 ferritic material used in Table 4.7 for comparison with A286 is of the 12Cr variety and has a particularly low coefficient of expansion. However, its conductivity, although higher than that of A286, is lower than that of the 4340 type material. The AISI 422 possesses



Westinghouse

some degree of corrosion resistance and is superior to 4340 in this respect. The AISI 422 has been used successfully in steam turbine discs. However, the relative suitability of the two materials in a helium environment has not been established.

The use of A286 as the austenitic material representative in the Table 4.7 comparison may be somewhat unfair, in that superior austenitic materials have become available in recent years. Inconel 718 is an example of such a material and would be an extremely capable disc material. Its creep strength and tensile properties at 1000°F are both superior to those of A286 and, in addition, it has a lower expansion coefficient. However, the lower alloy materials such as AISI 422 may prove to be competitive in the low temperature environment anticipated for the Closed Brayton Cycle turbine discs. In this low temperature requirement, creep is not a problem and the low alloy disc materials can be heat treated to develop high tensile strengths. Also, as discussed previously, low expansion coefficient is beneficial in minimizing rotor growth and tip clearance.

4.2.2.2 Materials - Expected Developments

The material properties of currently available disc materials are not expected to influence performance of the CCCBS helium turbine as directly as the uncooled blade material properties. Discs used in turbines having extended blade roots are easily cooled to temperatures which allow high creep, yield and fatigue strength to be developed. While the tendency in the CCCBS helium turbomachinery will be to resort to high blade speeds in order to minimize the number of stages, this tendency is likely to be limited by considerations of compactness and blade tip efficiency losses at high values of hub/tip ratio rather than by the limitations of disc materials properties.

Obviously disc materials having low coefficient of expansion and high modulus of elasticity are advantageous in minimizing the tip clearance necessary in high hub/tip ratio turbines. This is also true for the blading materials and suggests advantages in this respect for the Mo-TZM refractory material. However, consistent with the choice of nickel based superalloy material

for the CCCBS turbine blades, the initial disc design studies concentrate on the more conventional iron based materials, exploiting the use of effective cooling methods used with extended root blading, to achieve a stable rotor system.

Materials developments in conventional iron based disc materials are not expected to result in substantially improved structural capability. In any event, turbine temperature capability is less dependent on disc material properties than on blade material properties at the present time so that new materials are not expected to be required for feasibility.

4.2.2.3 Design

Attachment of Blades

Gas turbine blades are most often attached to the disc rim by "firtree" fixings. The firtree, in addition to providing an efficient distribution of shear, bearing and tensile area, provides surface area for heat dissipation and relieves the tangential thermal stress which tends to be produced in the rim of the disc. The firtree fixing also contributes mechanical damping, helping to suppress blade vibration.

Several small gas turbines have employed integral blade and disc rotors. This can result in economy using the investment casting process. The disc portion of the rotor in this case does not necessarily have the material properties best suited to its function, the material selection being influenced by the blading requirements. Also, individual blade replacement is impossible using this arrangement. The integral blade and disc arrangement is probably best suited to turbines substantially smaller than the CCCBS helium unit.

The use of separate disc with extended root blades allows the disc to be made of ferritic material suitably cooled to minimize thermal growth and stresses and is believed to be a more appropriate design approach for the CCCBS turbine. Individual blade replacement capability is also a very desirable feature in service. Firtree slots are normally machined into

the disc rim by broaching. The broaching should be as nearly axial as possible to avoid additional components of stress due to bending introduced in the firtree fixings in highly staggered designs.

Blades can be located axially in the firtree grooves in a number of ways. Deformable lugs can be provided at each end of the blade footing and peened radially inward onto the disc rim. Alternatively, separate sheet metal locking strips can be inserted into the bottom of the firtree groove and deformed onto both the blade and disc. Occasionally, the axial location locking feature is made an integral part of the design features provided in the extended root region of the blade for controlling the flow of cooling gas in the blade root region. Obviously the particular location method chosen must recognise the high g-field at the blade root which can cause high stresses in poorly designed components.

Attachment to Rotor

Turbine discs can be attached to their rotors in a variety of ways. A shrink fit between the disc and shaft is used in many steam and heavy industrial gas turbines. The interference between the shaft and the disc bore is arranged to be greater than the growth of the bore of the disc under centrifugal stress and thermal expansion influences.

Shaft and disc construction can also be designed to avoid the need for shrink fits. Appropriately designed extensions of the disc hub and shaft can be arranged to tighten the fit provided between them as the rotor is brought up to speed. Close fitting bolts can be used to transmit torsional shear in these arrangements. Alternatively a splined extension of the disc hub can engage with a mating spline on the shaft.

Turbine discs have also been attached to their shafts by radially disposed pins. The radial arrangement of the pins provided some freedom for radial growth of the disc relative to the shaft but maintained accurate alignment.

A favored method is the curvic coupling. Curvic couplings consist of radial teeth which are machined onto axial extensions of the discs. The discs are then clamped together axially, using a number of tie bolts arranged around the disc or alternatively a single central tie bolt or tube. The resulting built up rotor is stiff in bending but allows freedom for radial expansion in the individual components. The torsional moment is carried through the radial teeth, the tie bolts merely providing sufficient clamping force to hold the rotor together.

A logical development of the curvic coupling rotor would be a welded rotor, in which the curvic couplings would be eliminated and the discs butt welded together at their extensions using electron beam welding. This development would eliminate the need for bolt holes in the discs. The central hole could also be eliminated. The resulting reduction in stress concentration at the holes should greatly improve the cyclic fatigue life of the rotor or permit the use of a higher average tangential stress for a given fatigue life.

4.2.3 Concept Design for CCCBS

4.2.3.1 General

In order to investigate more fully the applicability of the turbine state-of-the-art, discussed in the previous sections, to the closed Brayton cycle turbomachinery and to define the first stage turbine in sufficient detail to permit the evaluation of blade stresses against the available material candidates at the required operating temperatures, a design concept for the high pressure turbine was developed. Figure 4.27 illustrates the resulting concept.

The turbine is a 5 stage machine with 50 percent reaction at the mean blade height. The hub and tip diameters are 13.671 inches and 16.887 respectively at entry and 12.95 and 17.61 at exit, resulting in a mean blade speed of 1200 ft/sec at 18,000 RPM. The maximum hub/tip ratio is 0.81 in the first stage, representing a compromise between the requirements for reasonably low blade centrifugal stresses on the one hand and reasonably low tip losses and good efficiency on the other. The design evolved from earlier 24,000 RPM trial designs which were less optimum in this respect.



Westinghouse

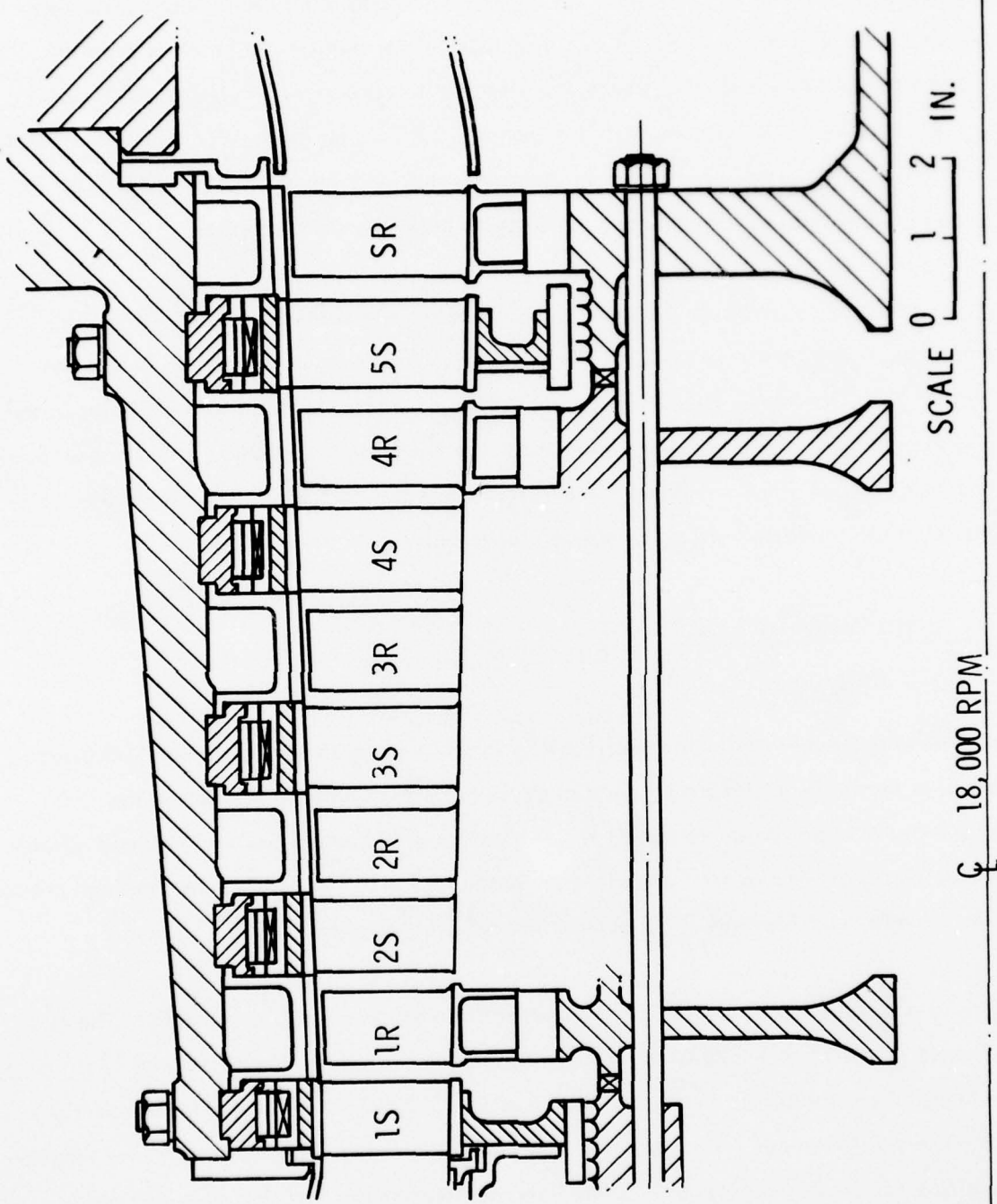


Figure 4.27 5 Stage HP Turbine

4.2.3.2 Blade Design

The first stage rotor blades are made of IN 100 nickel base superalloy. The properties of this material and other possible candidate materials are described in Section 4.2.1.1 and, as discussed in that section, indicate a lifetime capability on the order of 10,000 hours at maximum power conditions (1671°F inlet temperature at 18,000 RPM). Substantially increased life, using IN 100 material, can be obtained at reduced power conditions by a nominal reduction in turbine inlet temperature. (100°F reduction results in a ten fold increase in life at the same stress level or speed). Other, more advanced materials, are currently under development which, as they become available, could permit the turbine inlet temperature to be increased from the 1671°F used in this study, to the region of 2000°F . Some of these possibilities are discussed in Section 4.2.1.2.

The rotor blades in the high pressure turbine are unshrouded since rotating shrouds would not confer a significant efficiency advantage at a tip clearance below approximately 0.030 inch. It is expected that a typical clearance/diameter ratio of 0.0015 will be achieved in practice, resulting in an operating tip clearance of approximately 0.023 inch. Rotor and casing growth contributions will be approximately 0.065 inch and 0.035 inch respectively, necessitating a cold tip clearance of about 0.053 inch. The increased cold clearance provides margin for bearing eccentricity and rotor thermal bending in the non-rotating condition after shutdown. Essentially all of the operations of the closed Brayton cycle high pressure turbine will be at relatively high temperature conditions, resulting in a minimum of tip clearance variation over the normal operating range.

The high pressure turbine rotor blades have extended root fixings which provide a thermal barrier between the hot airfoil section and the firtree attachment at the disc. Cooling gas, at approximately 300°F , bled from the compressor outlet, is directed at the firtree attachment and disc rim to maintain a disc rim temperature in the 600° to 800°F range permitting the use of ferritic disc material. A candidate ferritic material is AISI 422, a 12Cr type stainless steel, which has a low coefficient of expansion, minimizing disc thermal growth and stresses.



Westinghouse

The blade axial chord width at the root was set at approximately one inch to limit the gas bending stress to less than 20,000 psi. A highly tapered blade design was developed to minimize centrifugal stress. This and the aerodynamic design work result in a first stage rotor complement of 113 blades. The blade complement is somewhat tentative at this preliminary stage of the design and is subject to change as the design matures and the blading is tuned to avoid vibration generating interferences. The stress analysis of the blades is discussed in Section 4.2.3.5.

4.2.3.3 Disc Design

The turbine rotor illustrated in Figure 4.27 is built up from discs which have curvic couplings machined onto cylindrical extensions from their front and rear faces. The discs are clamped together axially, using through-bolt construction. The bolts attach the built-up turbine rotor assembly to the compressor drive shaft which is similarly attached to the built up compressor rotor assembly. The complete high pressure compressor/turbine rotor is supported in two bearings one at the compressor inlet and the other at the turbine outlet. The overall rotor assembly is illustrated in the Design Concepts described in Section 3.5.

Cooling gas (at 300°F) is introduced into the high pressure turbine rotor through a "vortex reducer" arrangement which forms an integral part of the compressor/turbine drive shaft. A number of radial holes drilled in the shaft constrain the inwardly flowing gas and prevent its forming a free vortex which could result in substantial pressure losses. The cooling gas passes through the central holes in the turbine discs and is metered to the interstage seal regions for cooling the later stage disc rims.

Multi-stage labyrinth seal grooves are machined into the outer diameter of the curve coupling cylinders. The labyrinth seals follow the practice described by Dr. E. S. Moul in his paper "Seals for Rotating Shafts" published on page 727 of "Engineering", September 1975. The labyrinth fins operate at close clearance within the bores of the turbine stator diaphragm assemblies. The stationary seal members are designed to be abradable by the labyrinth fins

and can employ metal honeycomb, "feltmetal" or other materials. Various composite materials, sintered and sprayed, are being developed as ablatable seals for high temperature turbine applications. The rubbing characteristics of the candidate seal materials, while satisfactory in an oxygen rich combustion turbine environment, will have to be re-evaluated for the helium environment of the closed Brayton turbine.

4.2.3.4 Stator Assembly

The stator vane assemblies illustrated in the concept design of Figure 4.27 are of the diaphragm type which employ fabricated outer and inner ring and vane assemblies split diametrically. The half diaphragm assemblies are radially keyed to the turbine casing halves to locate them concentrically in the casing while accommodating relative thermal growth in the radial direction. The outer ring halves are saw cut at appropriate intervals to relieve the relative thermal expansion between the inner and outer rings. The radial keys which locate the diaphragm halves in the casing are formed in the heads of bolts which attach several machined segmented rings to the casing. The segmented rings, in turn support the segmented stationary turbine shrouds. The shroud segments have axial extensions at their outermost radii which engage with machined grooves in the segmented rings. Ablatable material such as honeycomb, "feltmetal" or some other sintered or sprayed material is applied to the inner surfaces of the shroud segments to accommodate potential blade tip rubs.

The resulting stator assembly accurately defines the turbine shroud and diaphragm seal radii, minimizing leakage at the blade tips and interstage seals, while providing freedom for the individual components to expand and contract. The segmented shroud region insulates the turbine casing from the hot gas passage and minimizes the temperature gradient to which each component part is exposed. The turbine casing is cooled by compressor outlet gas at approximately 300°F which is circulated around it. Some of this gas can be bled into the segmented shroud region through small holes in the casing, if additional cooling should be required. A complete half casing and half stator assembly can be removed without disassembling the rotor to facilitate inspection of the blading.

Candidate stator materials are MAR 509 vanes, Type 321 stainless steel ring segments and diaphragm halves and low expansion Ni-resist cast turbine casing. Alternatively the turbine casing could be fabricated from 2-1/4 Cr. 1 Mo plate. Stator assemblies can be fabricated by welding or brazing. Haynes stellite 31 vanes, microbrazed to 18-8 stainless steel ring segments and diaphragms have been used in combustion gas turbines. The particular high pressure turbine design illustrated in Figure 4.27 lends itself to the use of a low expansion cast Ni-resist casing because the casing is maintained in a state of circumferential compression by the high pressure compressor outlet gas which surrounds it. This arrangement eliminates any possibility of catastrophic tensile failure in the cast material and minimizes the stresses in the bolted flange at the axial split line. The use of low expansion material in the high pressure turbine casing, minimizes thermal distortion due to local temperature gradients in addition to minimizing total casing growth. Both of these effects help to minimize the tip clearance required.

The diaphragm type of construction described achieves good interstage sealing by permitting the use of a multistage labyrinth seal and minimizing the relative thermal expansion of the rotor and stator components of the seal. The advantages of diaphragm construction are particularly significant when the turbine shaft diameter can be kept small in relation to the blade root diameter. In this respect the power turbine provides a somewhat more suitable application for this type of construction than the high pressure turbine. In the high pressure turbine a large diameter shaft is employed to maximize the rotor bending stiffness. The resulting geometry restricts the radial space available at the hub to accommodate the diaphragm type of structure. As a result, alternatives to diaphragm construction will receive more consideration in the high pressure turbine than in the power turbine. One such alternative would support the stator vanes from the casing as a series of individually cantilevered vanes or as a series of multi-vane segments. This arrangement eliminates the structural problems of the diaphragm but tends to result in poorer interstage sealing. Relative thermal expansion of the rotor and stator components of the seal may be increased due to the inward motion of the stationary seal which can result from the vane growth. However this effect is less important in a machine having an essentially constant operating temperature such as the CCCBS turbine. The quantitative evaluation of the

magnitude of the various expansion effects and the structural capability of the various design candidates must await the more detailed design phases. The selection of the preferred design approach can then be made from the results of trade studies supported by more extensive and analytical work.

4.2.4 Aerodynamic Design Considerations

The temperature and pressure conditions assumed in this study of the high pressure turbine are 1671°F and 1487.9 psia respectively at inlet and 1277°F and 836.9 psia at outlet. The helium mass flow through the turbine is 130.6 lb/sec.

The design of a helium turbine differs from that of an air cycle gas turbine because of the higher specific heat and lower molecular weight for helium. The result is that coupled with the need for compactness, the tendency is to drive the design toward higher rotative speeds, more stages and higher load coefficients.

Since several stages are indicated for the high pressure turbine, it is convenient to consider an average or mean stage design. Alterations to this mean stage would be made for the axial (or other) inlet velocity, and to reduce the exit swirl. The reaction or proportion of stage enthalpy drop occurring within the rotating blade row was chosen as 50 percent, as is customary in gas turbine design practice.

The stage load coefficient is defined as the stage enthalpy drop divided by the enthalpy equivalent of the blade velocity or:

$$\psi = \frac{\Delta h/\text{stage}}{U^2/2 g J} \quad (1)$$

For the high pressure turbine, the mean blade speed at 18,000 RPM was chosen to be 1200 ft/sec. This value is somewhat high but is within mechanical design capabilities as verified by stress calculations discussed in Section 4.2.5.

The enthalpy drop for the high pressure turbine is 488.8 btu/lb. The number of stages was limited to five to achieve a compact assembly, resulting in an enthalpy drop per stages of 97.8 btu/lb. The corresponding value of load coefficient is 3.39. This is higher than that corresponding to maximum efficiency (≈ 2.0) but the reduction in efficiency is only about 1 percent and the higher load coefficient seems appropriate in the interest of obtaining a small machine.

The flow coefficient is defined as the axial component of velocity divided by the blade velocity, i.e.,

$$\phi = \frac{V_a}{U} \quad (2)$$

The value chosen is 0.78 which is slightly above the optimum value for a load coefficient of 3.39 to favor a short blade and thus minimize centrifugal stresses.

The efficiency to be expected may be estimated by relating the above design parameters to published performance curves. Smith (Reference 13) has correlated turbine test efficiency with stage load coefficient and flow coefficient. Figure 4.28 is a plot of Smith's curve as portrayed on page 127 of J. H. Horlock's book, "Axial Flow Turbines - Fluid Mechanics and Thermodynamics", 1966, Butterworth and depicts the design points of both the high pressure and low pressure turbines. Horlock's definition of stage load coefficient has one half the value defined in Equation (1) above. The coefficients for the HPT are $\psi = 1.7$ and $\phi = 0.78$. This design point falls at an efficiency of 92.7 percent which must be adjusted for leaving loss and leakage. The axial leaving velocity is 936 ft/sec corresponding to 17.5 btu/lb. Assuming a diffuser recovery of 50 percent and relating the remainder to the overall heat drop of 488.8 btu/lb the leaving loss is 1.8 percent ($\eta_{LL} = 0.982$). To estimate the leakage the clearance/diameter ratio may be assumed to be 0.0015 (typical). The actual tip clearance would be 0.0015×15.279 inches or 0.023 inch.

AD-A044 413

WESTINGHOUSE ELECTRIC CORP PITTSBURGH PA ADVANCED ENE--ETC F/6 21/5
COMPACT CLOSED CYCLE BRAYTON SYSTEM FEASIBILITY STUDY. (U)

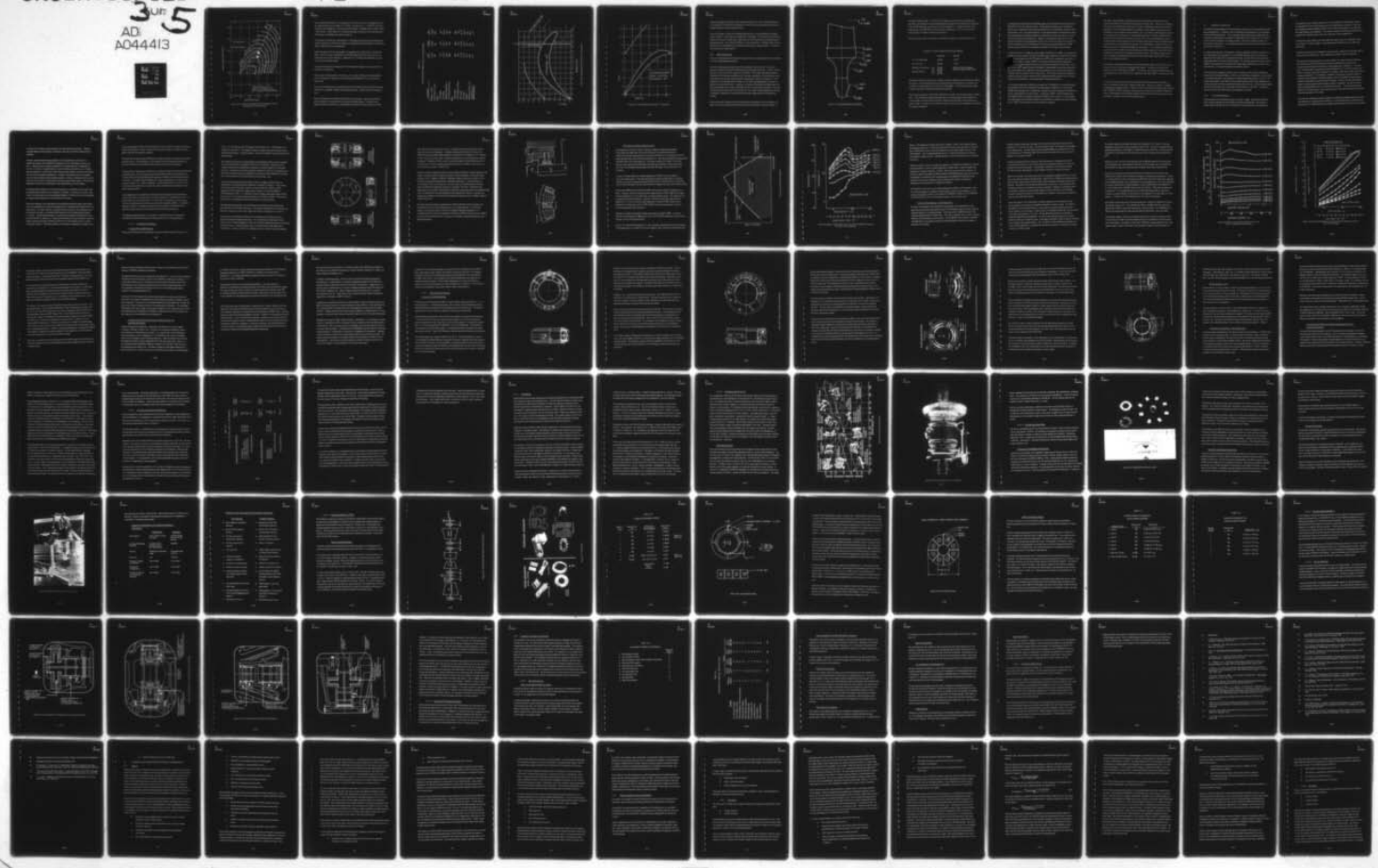
JUL 77 R E THOMPSON, G H PARKER, R L AMMON N00014-76-C-0706

UNCLASSIFIED

3ur 5
AD
A044413

WAES-TNR-233

NL



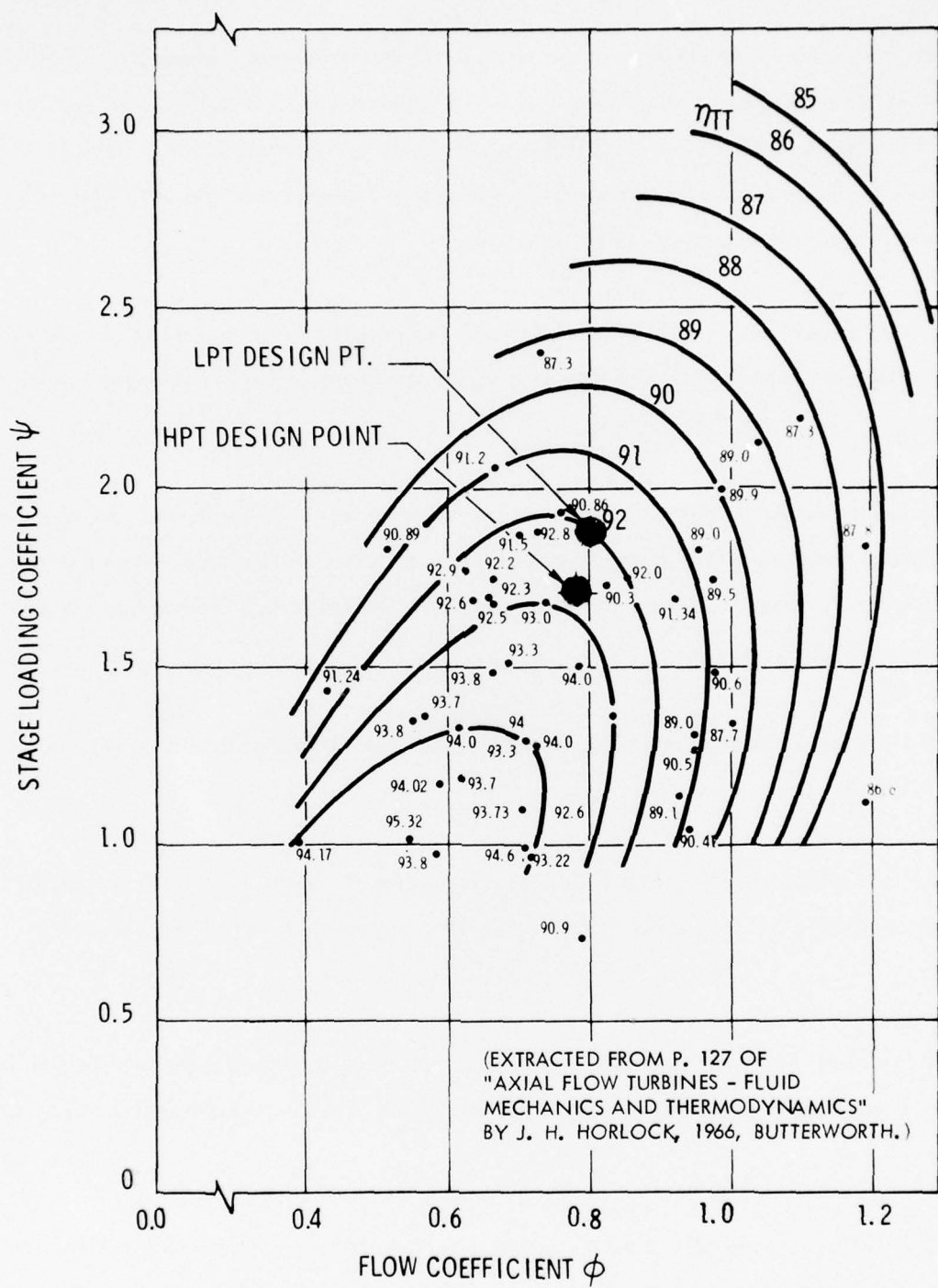


Figure 4.28 Correlation of Measured Turbine Stage Efficiencies
(Corrected for Zero Tip Leakage)

Using a mean blade height of 1.97 (average of first and last rows) and a blade gaging of 0.50 the clearance/area ratio is $0.023/(1.97 \times 0.50) = 2.3$ percent ($\eta_{LL} = 0.977$) which is representative of the leakage loss. The resulting net efficiency is therefore $0.927 \times 0.982 \times 0.977 = 88.9$ percent. These results for a non-optimized design indicate that the desired efficiency of 90 percent is reasonable and should be achieved.

This estimate of the efficiency achievable in a well designed turbine having the selected load and flow coefficients is believed to represent a reasonable compromise between the conflicting goals of high efficiency and compactness.

Table 4.8 presents the first stage geometry corresponding to this blade path and includes the blade width/pitch ratios corresponding to a Zweifel coefficient of 0.8 which results in the blade spacing for optimum efficiency. (Reference 14). The Table 4.8 information was used to layout the rotor blade profiles.

Figure 4.29 illustrates the development of the first stage rotor blade root section profile from the Table 4.8 information.

Usually when the blade profile is first laid out, the number of blades is not well established and it is convenient to develop a non-dimensional profile based on unit pitch as shown in Figure 4.29.

The nose of the blade has been extended beyond the 0.8 Zweifel line and the profile has been made as thick as possible consistent with good flow profiles, in order to achieve a large base area.

Figure 4.30 depicts the tip profile resulting from the same process. Here a thin profile has been developed to minimize the section area and centrifugal loading. The blade width, approaching the 0.8 Zweifel line, could probably be reduced still more at the tip to further

TABLE 4.8
HIGH PRESSURE TURBINE STAGE 1 BLADE GEOMETRY

LOCATION	HUB	MEAN	TIP
Diameter - inches	13.671	15.279	16.887
Axial Velocity - ft/sec	936	936	936
Nozzle			
Inlet Angle	90°	90°	90°
Exit Angle	27.4°	30.1°	32.6°
Gaging (Throat/Pitch)	.460	.501	.539
Exit Tangential Velocity	1808	1618	1464
Blade			
Wheel Speed	1074	1200	1326
Inlet Tangential Velocity	734	418	138
Inlet Angle	51.9°	65.9°	81.6°
Exit Angle	31.3°	30.1°	28.9°
Gaging	.519	.501	.481
Relative Exit Tang. Vel.	1541	1618	1704
Width/Pitch for .8 Zweifel Coefficient	2.12	1.36	1.14

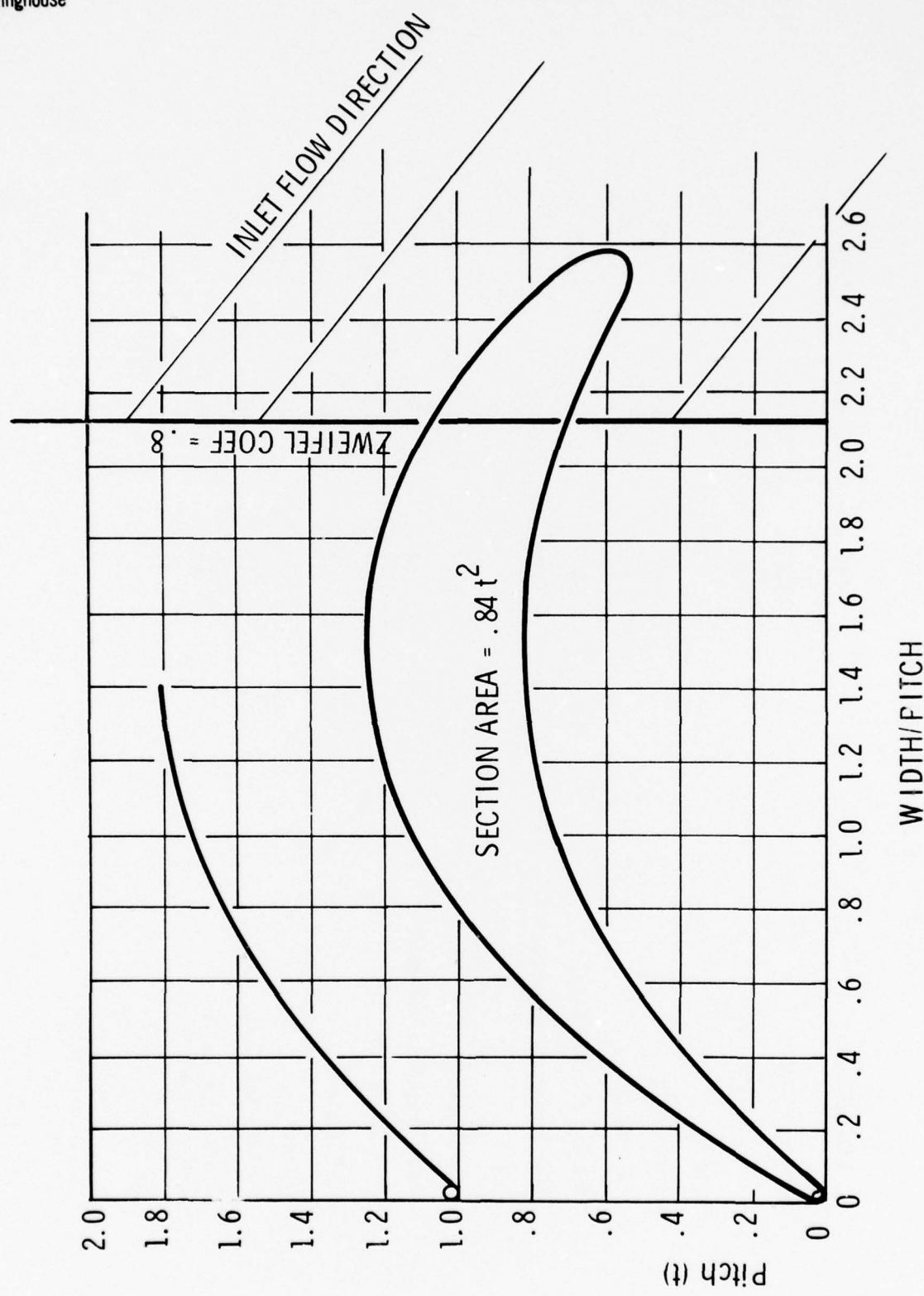


Figure 4-29 High Pressure Turbine Row IR - Base Section

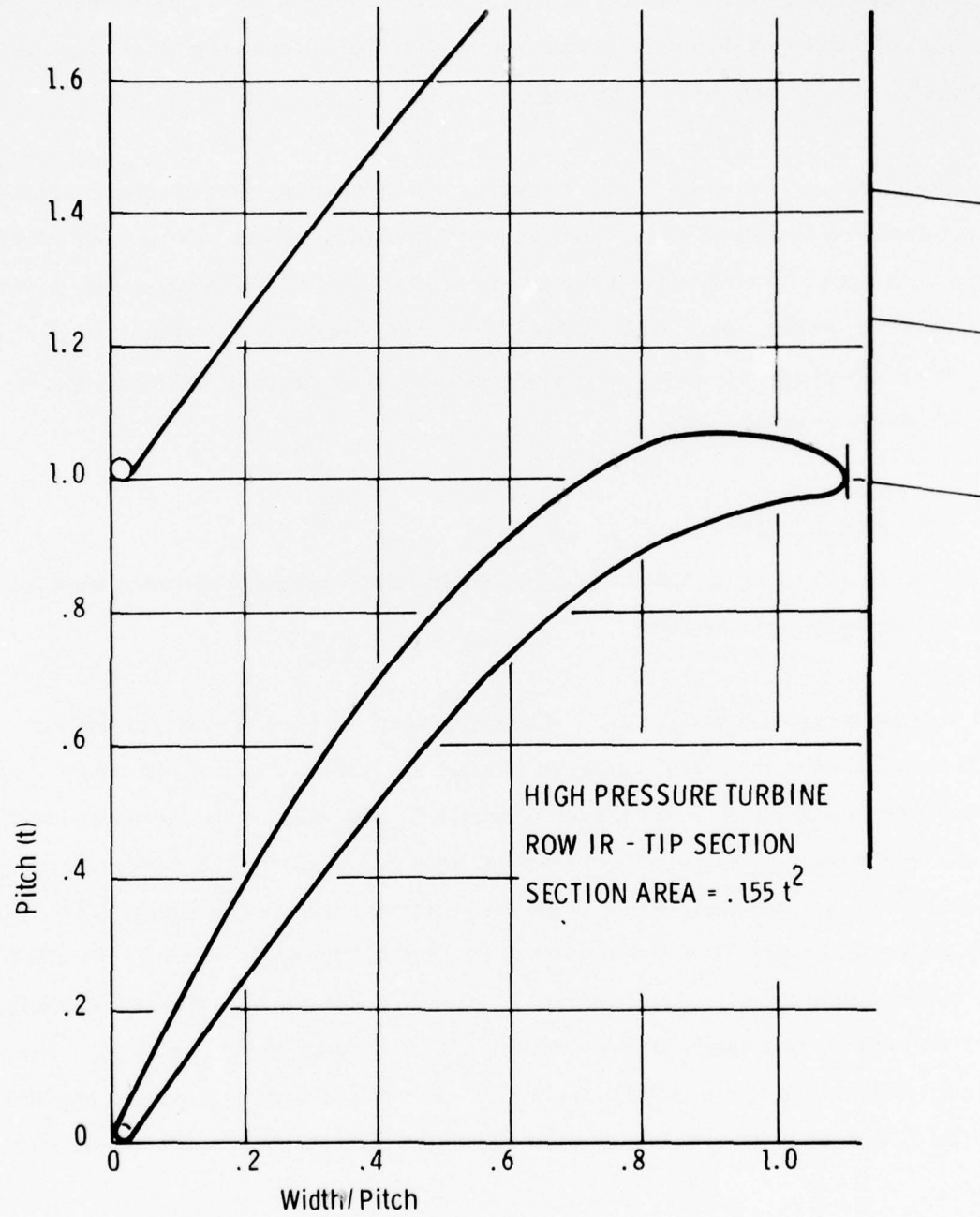


Figure 4.30 High Pressure Turbine Row IR - Tip Section



Westinghouse

reduce centrifugal stress without unduly compromising efficiency since a Zweifel coefficient in the region of 0.8 would then be obtained over most of the mid span region as the width and Zweifel coefficient increase toward the root.

In sizing the blades, a root width of approximately one inch, using the geometry developed above, resulted in a first stage rotor complement of 113 blades. This blade size was tentatively selected on the basis of a preliminary stress check which indicated that an acceptable level of gas bending stress, in the region of 20,000 psi, should be obtained. The blade design was then subjected to the Westinghouse gas turbine blade stress analysis computer program. The results of this analysis are reported below.

4.2.5 Blade Stress Analysis

Two of the Westinghouse Power Generation Systems Division's computer programs were employed in the first stage blade stress analysis.

The first of these programs takes as input the coordinates of the tip and root sections and generates coordinates of several intermediate sections along the blade span. A linear variation between root and tip sections is assumed in the analysis. The program also generates section properties of the blade and extended root from the input coordinates. The extended root input coordinates for this purpose were derived from the geometry illustrated in Figure 4.31. This geometry has not been optimized with respect to the conflicting requirements for thermal impedance and structural efficiency. However, it provides a sufficiently valid representation of the lower temperature root region of the blade for use in the stress analysis program. The input coordinates for the blade root and tip sections with their output section properties are included in Appendix C together with computer plots of the output blade profiles and extended root sections.

The second computer program uses the section properties, generated in the first program, together with the input gas loads (assumed uniformly distributed along the blade) and RPM, to

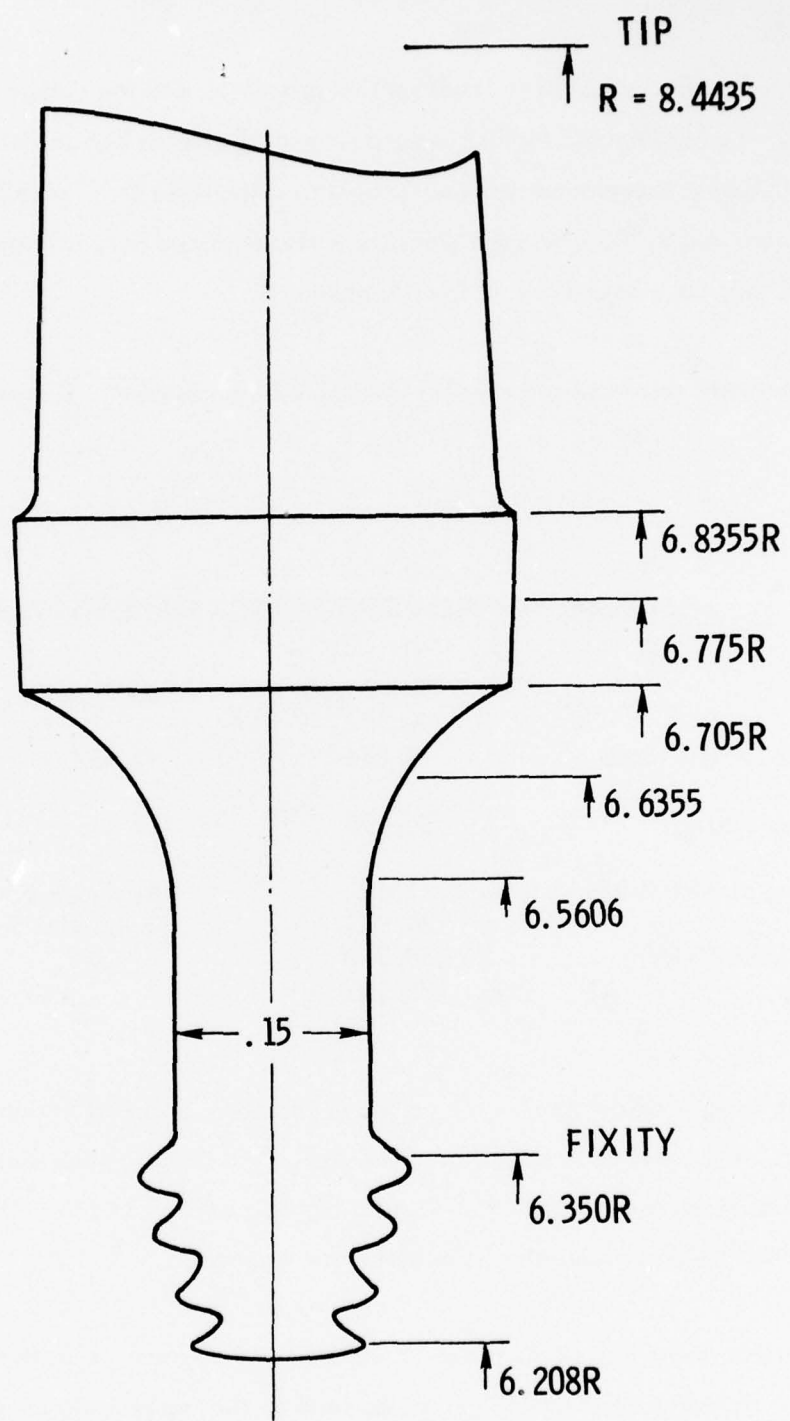


Figure 4.31 Extended Blade Root and Platform



Westinghouse

calculate the blade stresses. The input section properties and the output centrifugal forces and stresses, the leading and trailing edge gas bending stresses and the blade natural frequencies at the 18,000 RPM speed condition are included in Appendix C. Computer printouts of the stresses at zero and 9,000 RPM conditions were also obtained but, in view of the low stress levels obtained, have been omitted from Appendix C.

The most pertinent results of the analysis, extracted from Appendix C are summarized below.

SUMMARY OF FIRST STAGE ROTOR BLADE STRESSES

	Stress (psi)	Load (lb)
C. F. At Airfoil Base	19,874	2,457
C. F. at Fixity	36,695	4,416
Bending at Airfoil Root	L. E. 17,669 T. E. 20,907	Maximum Power Condition (Rotational Speed 18,000 RPM)
Bending at Fixity	L. E. 35,379 T. E. 35,306	

The bending stresses calculated by the computer include an approximation of the dynamic effects of vibration. The bending stresses due to the steady gas bending load alone are somewhat less (15,070 psi at leading edge and 19,270 psi at trailing edge). In calculating bending stresses, a uniform distribution of load along the blade was assumed.

The first natural frequency of the blade (1810 CPS) is very near the sixth engine order at 18,000 RPM. If the interference diagrams generated later in the design program should indicate this to be a problem, the blade would be tuned by modifying the dimensions of the extended root. Some increase in the blade chord might also be made in conjunction with changes to the extended root design or separately.

In evaluating the significance of these blade stresses, the centrifugal stress at the root of the blade airfoil is the most significant value. The gas bending stresses are not considered as additive to the centrifugal values since bending effects can be substantially reduced by leaning the blade. This is an oversimplification, in that speed variations and the effects of manufacturing tolerances and assembly clearances complicate the situation and result in a continuously varying detail stress distribution. However, the centrifugal stress level is the most pertinent indicator of the average level of stress in the critical root section of the blade. By comparing the value of the centrifugal stress with the creep rupture strength of the blade material a good indication of the temperature capability of the blade can be obtained.

IN 100 material has a 10,000 hour rupture strength of 20,000 psi at 1670°F . This temperature capability must be compared with the actual blade metal temperature of 1632°F (resulting from a turbine inlet temperature of 1671°F reduced by a 39°F drop in temperature across the first stage nozzle vanes). A margin of 38°F is thus available between the blade temperature capability at its operating stress level and the actual metal temperature of the blade. This is less than the 100°F margin allowed in the design of Westinghouse combustion gas turbines but the turbine blades of the combustion machines are exposed to much more arduous operating conditions than are expected in the CCCBS turbine. The thermal transients and temperature gradients caused by adverse combustor outlet temperature profiles should not occur in helium closed cycle turbomachinery, to the great benefit of blade operating life.

It is therefore judged that an effective full power life of 10,000 hours is an achievable goal. Total operating life can be substantially increased beyond 10,000 hours, to the required 40,000 total operating hours, by operating at reduced turbine inlet temperature and RPM over the port power regions of the duty profile. A reduction of 100°F in turbine temperature is worth approximately a one order of magnitude increase in life to rupture. It is also judged from these results that the desired lifetimes can be achieved at a design turbine inlet temperature of 1700°F with optimization of turbine materials and design.



Westinghouse

Obviously, these estimates of temperature and lifetime capability are approximate only, since they are based on limited preliminary design and analysis work. However, it is believed that future more refined detail design work will result in significantly reduced critical blade stress levels. This will be made possible by adjustments in the gradation of blade chord and thickness from tip to midspan and from midspan to root. The linear variation between root and tip, assumed in this initial analysis is not necessarily optimum. Obviously, blade chord and thickness could be maintained constant and equal to the minimum values selected at the tip for some distance inward towards the root of the blade, deferring the section increases necessary towards the root to limit the blade root stresses. This more parabolic, rather than linear, distribution can result in reduced blade weight and root stresses. This is especially advantageous in turbines which have fairly flat radial temperature profiles is expected in the CCCBS turbine. Combustion turbines would not generally be expected to permit such slender midspan sections due to the higher gas temperature prevailing over the midspan region resulting from the combustor outlet temperature profile.

The stresses in the extended root portion of the blade, although higher than at the airfoil root, are less critical due to the lower temperature environment. IN 100 has a 10,000 rupture strength in excess of 100,000 psi at 1200°F. The maximum centrifugal and bending stresses in the extended root, which will operate at temperatures well below 1200°F, are less than 37,000 psi.

In view of the less critical nature of the extended root and firtree regions of the blade, no effort was expended to optimize the design in these areas. However, no problem is foreseen in developing an adequate design. Similarly, the disc rim will be well cooled to approximately 600° to 800°F by 300°F cooling gas, allowing the use of a ferritic disc material at high stress levels. The development of the detailed design of the blade root fixing and disc are such that no problem is foreseen in achieving an adequate design.

4.3 BEARING EVALUATIONS

The achievable characteristics of the turbomachinery bearings can have a significant impact upon turbomachinery. In addition, both oil lubricated and gas bearings can be considered for the CCCBS turbomachinery. The fundamental nature of the bearings necessitated early evaluations of bearings and a comparison of capabilities of the two types so that a selection could be made for inclusion in the design concept. The results of these evaluations are documented in this section. The comparative evaluations and the bearing type selection are summarized in Section 4.3.3.

In evaluating the practical characteristics of bearing assemblies suitable for application to the closed Brayton cycle powerplant, it is immediately apparent that the thrust bearings, especially for the high speed compressor/turbine rotor, are more likely to require special development effort than are the journal bearings. This situation results from the high helium pressure levels employed in the cycle which produce large unbalanced thrust loads, in the axial direction, in the small high speed turbomachinery rotors.

The thermodynamic properties of helium allow the machinery to be small in diameter and permit high blade tangential speeds. (Mach number limitations are generally not encountered in the rotating assemblies, the limitation on rotational speed being solely mechanical.) The resulting combination of high RPM and high unbalanced thrust load in small diameter rotors must be reconciled with the practical thrust bearing state of the art. This will require careful attention to thrust balancing, using rotating balance pistons or "dummies", to reduce the net thrust carried by the thrust bearings to acceptably low levels.

4.3.1 Oil Lubricated Bearings

Thrust bearings of the hydrodynamic type vary widely in design, ranging from simple flat thrust collars to tapered land and Kingsbury type tilting pad bearings. Anti-friction or rolling contact bearings will not be considered for the closed Brayton cycle powerplant.

The statistical nature of rolling bearing life, with the possibility of isolated early failures is inconsistent with the long life requirement of the closed Brayton cycle plant. Also, the low temperature starting capability inherent in the rolling contact bearing is not required in the closed Brayton cycle powerplant. The inherent longevity of hydrodynamic bearings when supplied with a reliable source of clean oil makes their choice unquestionable.

The flat thrust collar bearing is the least capable of carrying load and is generally limited to low loads (< 75 psi) and speeds. It has generally been limited to low cost, light duty applications.

Tapered land bearings can be designed to carry high loads (> 500 psi) and have been used as turbomachinery thrust bearings. These bearings are somewhat sensitive to alignment.

Tilting pad thrust bearings are the most widely used form of hydrodynamic thrust bearings. The individual pad and self adjusting load equalizing arrangement employed on the Kingsbury type bearing allows the design to accommodate some misalignment. In the last two or three years some very pertinent test data (References 15, 16 and 17) have been published on Kingsbury type bearing operated at high speeds, while carrying high loads (400 psi. average pad pressure). This information is extremely encouraging in providing empirical evidence of the capability of standard Kingsbury bearings in the speed and load regime of interest to closed Brayton cycle power plant designers. However, the data must be extrapolated to bearings approximately 30 percent smaller in diameter in the case of the high speed compressor/turbine rotor in the CCCBS turbomachinery. The power turbine thrust bearing in the closed Brayton cycle turbomachinery is in the same size range as the smallest of the test bearings (10-1/2 inches).

The recent test information probably represents the highest demonstrated current state of the art performance in hydrodynamic thrust bearings. This indicates that the unbalanced axial gas forces in the CCCBS turbomachinery require careful balancing of the thrust in both rotors

to reduce the net thrust to values consistent with these state-of-the-art data. Unless an adequate degree of thrust balancing is achieved, the loads on the thrust bearings will be excessive.

However, improved thrust bearing capability can almost certainly be achieved in a development program which addresses the requirements of the closed Brayton cycle power plant. Approaches which might be considered are "directed lubrication" (References 18 and 19), in which oil is supplied directly to each individual pad rather than to a flooded bearing compartment, and the use of improved pad bearing materials, permitting the development of higher pad operating temperatures. Benefits to be expected from such a program would be improved bearing load and speed capability, resulting in reduced sensitivity of the bearing to thrust balancing variations and providing improved safety margins. Thrust bearing development should have a high priority in the closed Brayton cycle work program.

The state-of-the-art situation for the journal bearings is quite different and very little need for developmental extension of basic capability is foreseen. Rig testing in this area is more likely to be concerned with the more peripheral aspects of oil sealing which can be expected to impose stringent requirements on the bearing and its housing.

The journal bearings in the closed Brayton cycle machinery experience quite nominal loads which are unaffected by the high helium pressure levels, being essentially determined by the rotor weights. The need to transmit a substantial amount of power to the compressors and to the external load results in substantial shaft diameters and low average bearing pressures (≈ 100 psi). Journal bearing problems in gas turbines are generally associated with a lack of load rather than an excess of it. Simple journal bearings running at high speed under light loading conditions are prone to develop oil film whirl or whip instability which can result in damaging vibration. Fortunately problems of this nature can generally be avoided by the



Westinghouse

use of bearing designs which have been developed to help minimize rotor bearing instabilities. These include elliptical, lobed, nutcracker and tilting pad bearings. Of these, the tilting pad has been the most generally successful.

Tilting pad journal bearings are available from a number of domestic and foreign manufacturers as standard items. The closed Brayton cycle turbomachinery bearing operating speeds and loads are well within the permissible operating ranges covered by the manufacturer

Tilting pad journal bearings are available from a number of domestic and foreign manufacturers as standard items. The closed Brayton cycle turbomachinery bearing operating speeds and loads are well within the permissible operating ranges covered by the manufacturers catalog information. The design details employed by the various manufacturers to locate the pads, provide oil sealing, etc., differ considerably. Journal bearing selection is more likely to be influenced by a preference for a particular design detail than by any difference in basic load or speed capability.

Ample reassurance on the suitability of tilting pad journal bearings for the closed Brayton cycle turbomachinery was obtained in a test program performed by Westinghouse for the U. S. Maritime Administration (Reference 32). In this program the compatibility of the bearings with the lubrication system and helium environment was successfully verified. No problems relating to operation in a helium environment were encountered in the testing and the lubrication system was shown to be relatively free from aeration and foaming.

The following paragraphs discuss, in more detail, the state of the art in tilting pad oil lubricated thrust and journal bearings and characteristics for the CCCBS application.

4.3.1.1 Tilting Pad Thrust Bearings

Commercially Available Bearings

Tilting pad thrust bearings are manufactured by several companies throughout the world. In

the U. S. A. the bearings made by Kingsbury Machine Works, Inc., of Philadelphia are probably the best known. The Kingsbury company manufactures standard bearings and also special bearing designs for specific purposes. Figure 4.32 illustrates a typical standard thrust bearing design.

The Kingsbury company has a bearing research and development facility which is equipped with a gas turbine driven rig capable of 1100 HP and 17,500 RPM. Using this facility, Kingsbury personnel have generated test information on bearing capability at high speeds and loads. This information has been published in References 15 and 17 and probably represents the most pertinent test data, defining the current state of the highspeed thrust bearing art, of direct relevance to the closed Brayton cycle turbomachinery.

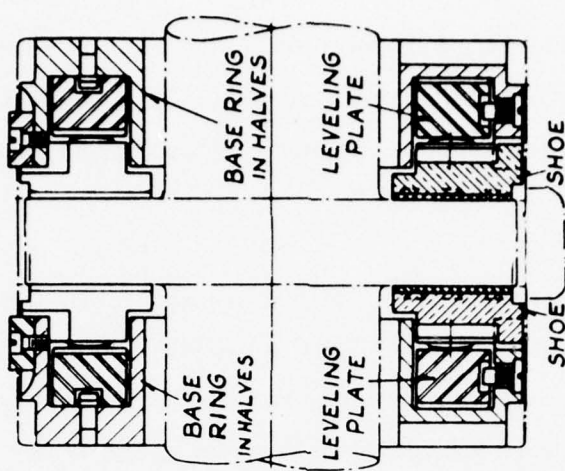
Tilting pad thrust bearings of similar design to those of Kingsbury Machine Works are manufactured by Waukesha Bearings Corporation of Waukesha, Wisconsin. Their catalog load and power loss information is based on the use of light oil of 150SSU at 100°F operating at 135°F whereas the Kingsbury data is based on Oil of 250 to 300SSU at 100°F operating at 125°F. It is noteworthy that the Kingsbury high speed testing of references 15 and 17 was conducted using light turbine oil of 150SSU at 100°F. The light oil is probably the more appropriate for the closed Brayton cycle turbomachinery.

Waukesha Bearing Corporation also has laboratory test facilities and has published test data (Reference 19) on tilting pad bearings. Unfortunately the Reference 19 information was obtained at substantially lower collar speeds than the date of References 15, 16 and 17.

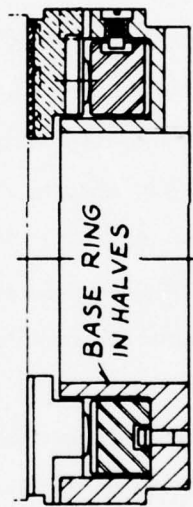
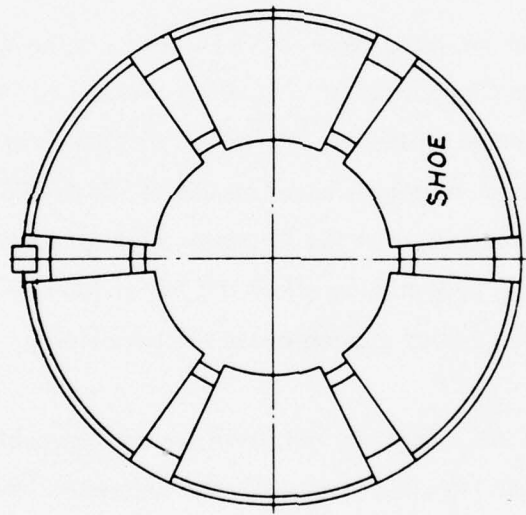
Both Kingsbury and Waukesha tilting pad thrust bearings employ self leveling or load equalizing mechanisms supporting the pads. Also, both bearing manufacturers normally employ similar oil feed arrangements in which oil is flooded through the bearing in a relatively undirected manner. Flooded operation results in high power loss at high speeds due to churning and, in order to minimize this, Kingsbury uses an oil control ring at the periphery



Westinghouse



STYLE JJ
(Double, Split)
Vertical or Horizontal



STYLE J
(Single, Split)
Vertical or Horizontal

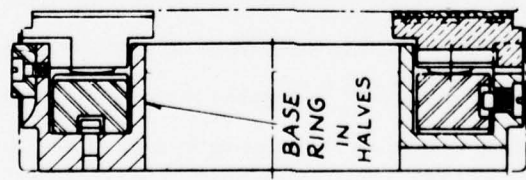


Figure 4.32 Kingsbury Tilting Pad Thrust Bearing

which diverts the oil away from the collar in a tangential direction and directs it into the drain with a minimum of resistance. Kingsbury also prescribes a reduced "oil flow ratio" (GPM/HP Loss) at the higher speeds resulting in reduced power loss (Reference 17). Reduced oil flow ratio does, however, cause increased pad temperature and must therefore be applied cautiously. The optimum oil flow rate is a compromise between the conflicting demands for minimum power loss and acceptable pad operating temperature ($\approx 266^{\circ}\text{F}$ in the babbitt material used almost exclusively - Reference 21).

The power loss/pad temperature conflict has been handled differently in Europe (Reference 18) where a successful method of directed lubrication has been developed. The Glacier Metal Company, Ltd., of Alperton, Wembley, Middlesex, England incorporate this device in the tilting pad bearings they manufacture for high speed applications. In these bearings the oil is directed, in the form of spray jets, onto the collar at the leading edge of each pad. Free circumferential drainage for the used oil is provided. The claim is made that power loss reductions on the order of 50 percent are obtainable using directed lubrication (Reference 20). This is accompanied by lower pad temperature and increased film thickness. Test data from another source (Reference 19) also indicate reduced pad temperature with a different design of directed lubrication.

The tilting pad thrust bearings manufactured by Glacier differ from those of Kingsbury and Waukesha in that a pad load levelling device is not normally provided. The technical position of the company seems to be that the Kingsbury/Waukesha arrangement is not completely effective and that the expense of providing an effective device cannot be justified for most applications (Reference 22). Figure 4.33 illustrates a Glacier thrust bearing with directed lubrication.

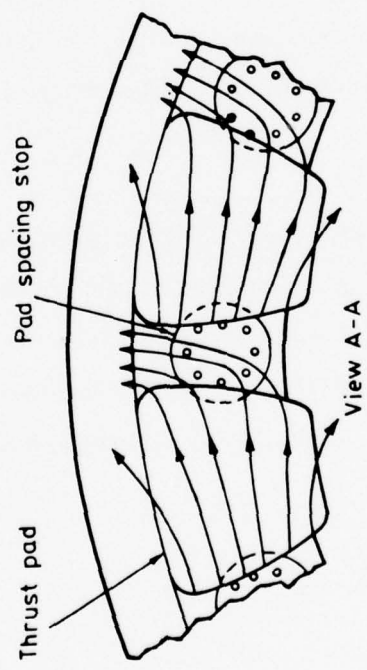
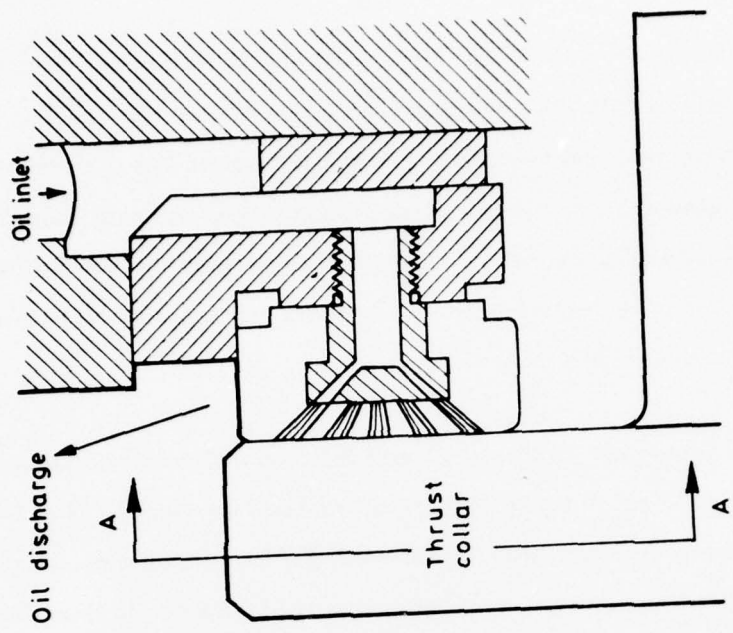


Figure 4.33 Thrust Bearing with Directed Lubrication

Tilting Pad Thrust Bearing Operating Limits

Pad temperature is the basic criterion of bearing integrity at high operating speeds. At low speeds and high loads, minimum film thickness is the dominating criterion. Additional constraints are imposed by the structural limitations set by reasonable mechanical design geometry and by the collar bursting speed limit. Figure 4.34 obtained from Reference 23, illustrates these limits of safe operation. The range of operation of interest in the closed Brayton cycle turbomachinery high speed thrust bearing is bounded by the pad temperature limit line. The allowable pad temperature has been the subject of some discussion in the literature.

A typical tin based babbitt has a melting temperature of 462°F but starts to weaken at much lower temperatures. It has been determined from tests that deformation in a bearing is likely to occur if its temperature exceeds 320°F and this is normally taken as the absolute limit at which bearings can be run without permanent damage to the pad surface (Reference 22).

Other sources (References 24 and 25) give 300°F as the maximum operating temperature for babbitt. However, some test failures have been experienced in the 260 to 280°F pad temperature range (Reference 19) in the high load, low speed operating regime. The temperature limit is apparently somewhat dependent on operating conditions since the high speed testing of References 15, 16 and 17 achieved a pad temperature in excess of 290°F without failure. References 21 and 22 quote a limit of 130°C (266°F) for the calculated value of maximum continuous operating babbitt temperature.

Reference 31 quotes limiting babbitt temperatures ranging from 268 to 390°F. One of the discussers of the Reference 31 paper gave a current limit of 275°F (measured) for steam turbine bearings in Navy main propulsion plant.

Figure 4.35, extracted from Reference 15, shows the babbitt temperatures which were measured in high speed tests on a standard 10-1/2 inch Kingsbury 6 pad, centrally pivoted double thrust

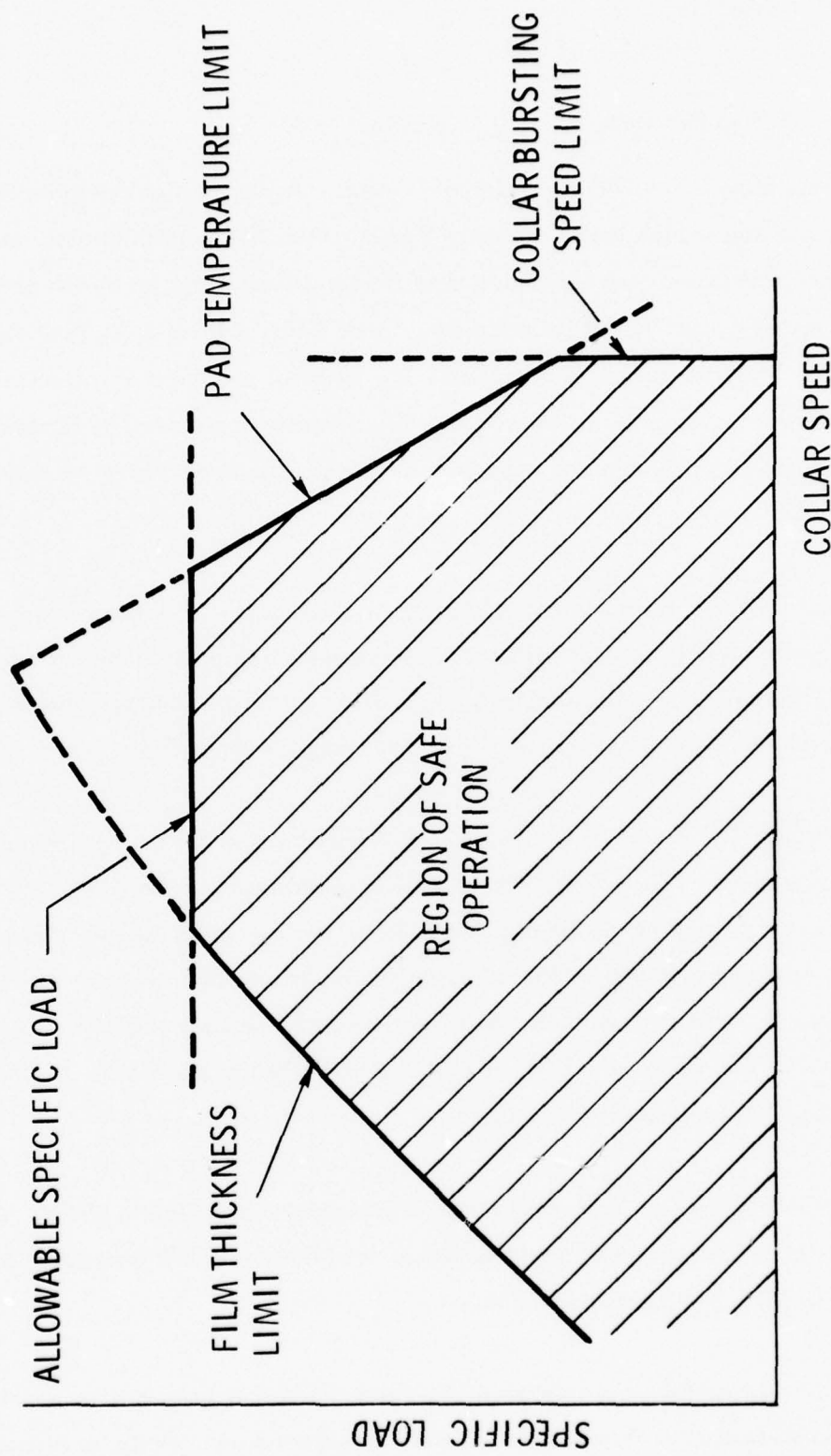


Figure 4.34 Limits of Safe Operation

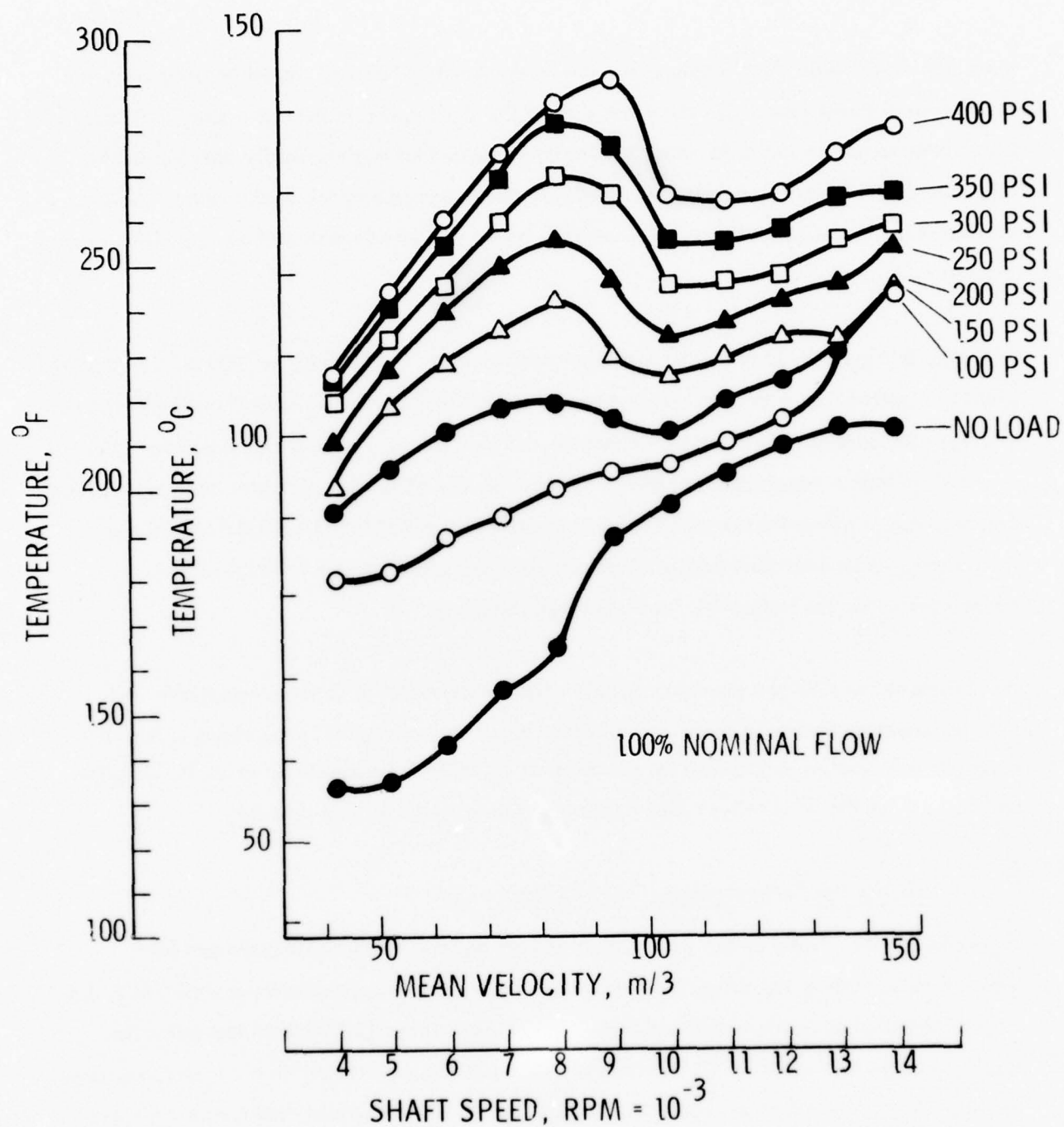


Figure 4.35 Effect of Shaft Speed and Load on Maximum Babbitt Temperature
(10-1/2 Inch Thrust Bearing)

bearing. The double thrust bearing consists of a loaded or "active" thrust bearing carrying the measured thrust load. On the other side of the shaft collar is the slack side or "inactive" thrust bearing which serves to carry any transient loads that might possibly develop in the other direction. The two bearings (loaded and slack) comprising the double thrust bearing are identical in design and size. The bearing tested was of conventional design with standard dimensions.

Referring to Figure 4.35 it can be seen that operation at 14,000 RPM and 400 psi average pad pressure resulted in a maximum babbitt temperature of 280°F which is somewhat higher than desirable for continuous operation. However, failure did not occur at this condition, nor at the even higher temperature of 290°F recorded at the 9000 RPM speed under the same load. The reduction in temperature with increasing speed above 9000 RPM is explained by the transition from laminar to turbulent oil film conditions which results in reduced pad temperature and, theoretically, increased film thickness.

If it is desired to limit the maximum babbitt temperature to 265°F (a more reasonable value for continuous operation) a reduction in either speed or load would be necessary. A pad minimum temperature of 265°F is encountered at 12,000 RPM and 400 psi or at 14,000 RPM and 350 psi for the 10-1/2 inch size bearing tested as shown in Figure 4.35.

Tilting Pad Thrust Bearing - CCCBS Application

This data can be related to the 18,000 RPM closed Brayton cycle turbomachinery high speed rotor by setting the turbomachinery thrust collar diameter to retain the same collar tip tangential speed as in the tested bearings. In the case of the 12,000 RPM test point the resulting tangential speed is 32,986 ft/min. This value is achieved with a 7 inch in diameter bearing in the closed Brayton cycle machine. The 14,000 RPM point results in a tip speed of 38,484 ft/min. and would be achieved in the closed Brayton machine with a bearing diameter of 8.17 inches.

Standard Kingsbury double thrust bearings of the six-shoe self aligning equalizing type are available in 7 inch and 8 inch sizes. The net pad areas are 24.5 and 32 square inches respectively (Reference 26). The permissible loads are therefore 9800 pounds (400×24.5) for the 7 inch bearing and 11,200 pounds (350×32) for the 8 inch bearing if the pad maximum temperature is to be limited to 265°F.

It should be recognized that the validity of this scaling process is somewhat questionable in that test data obtained on a 10-1/2 inch bearing is not directly relatable to 7 and 8 inch bearings at the same collar speed. In this process, size effects, such as Reynolds number and other important characteristics, which change as a bearing is scaled, are ignored.

Preliminary estimates of the axial thrust loads in the high speed compressor/turbine rotor indicate a net unbalanced thrust of 85,200 pounds. Reducing this to 10,000 pounds (approximately) will obviously require careful control of balance piston diameters and operating pressure differences. The sensitivity of the resulting bearing load to variations in cycle pressures under off-design conditions and transients must also be considered. Therefore, any measures which can be taken to improve the load carrying capability of the thrust bearing will be highly desirable by reducing the sensitivity of the bearing to unforeseen circumstances and generally improving operating safety margins.

One of the aspects of the CCCBS power conversion assembly which is favorable to thrust bearing operation is the power control system using helium inventory control. This results in the operation of the turbomachinery at or near a fixed non-dimensional design point from about 15 percent up to full power. Power changes in this operating regime are made by adjusting the helium gas pressure in the cycle. The gas generator turbomachinery operates at essentially fixed RPM and temperatures. As a result thrust bearing loads are low at power levels from start-up to 15 percent power, in the region where RPM is reduced and film thickness tends to become the limiting criterion. Thus, the RPM at which hydrodynamic operation becomes initially established is correspondingly reduced and operation in the region of boundary lubrication is further limited.

This mode of operation also allows the bearing to be operated in the "valley" of low pad temperature caused by the onset of turbulence (Figure 4.35). The area of increased bearing operating temperature at lower speed is avoided during power reductions, since bearing load is reduced to a small fraction of the full power level, prior to reducing the turbomachinery RPM.

Power loss in the 7 inch and 8 inch bearings at the 18,000 RPM speed of the closed Brayton cycle high speed rotor was estimated to be 80 HP and 130 HP respectively by extrapolating the data given on Figure 24 of the Waukesha tilting pad thrust bearing catalog W-3A.

Power loss, estimated by scaling the measured test data obtained in the Kingsbury tests (Figure 4.36) on the 10-1/2 inch bearing in proportion to the bearing surface areas, resulted in a value of 120 HP for the 7 inch bearing and 220 HP for the 8 inch bearing when operating at the 18,000 RPM speed of the closed Brayton cycle high speed rotor. Scaling was performed at constant tip speed (and oil shearing speed) by using 12,000 RPM data from Reference 15 for 7 inch bearing and 14,000 RPM data for the 8 inch bearing. These data are reproduced in Figure 4.36. It is recognized that neither of these scaling approaches is rigorous but should give a rough indication of the power loss to be expected in the high speed rotor thrust bearing. (≈ 100 HP and 175 HP respectively for the 7 and 8 inch bearings).

The nominal oil flow rates used in the testing are given in Figure 4 of Reference 15 and are reproduced in Figure 4.37. At 14,000 RPM and 400 psi, 43 GPM were fed to the active bearing and 26 GPM to the inactive bearing for a total of 69 GPM. At 12,000 RPM and 400 psi the corresponding flow rates were 40 GPM and 20 GPM for a total of 60 GPM.

Scaling these values in the ratio of the bearing areas for the 7 and 8 inch bearings results in total flows of 27 GPM and 40 GPM respectively for the 18,000 RPM CCCBS high speed rotor thrust bearing. The resulting "flow ratios" (GPM/HP) of approximately 0.2 are in the reduced range of nominal values used in the high speed Kingsbury testing (Reference 17).

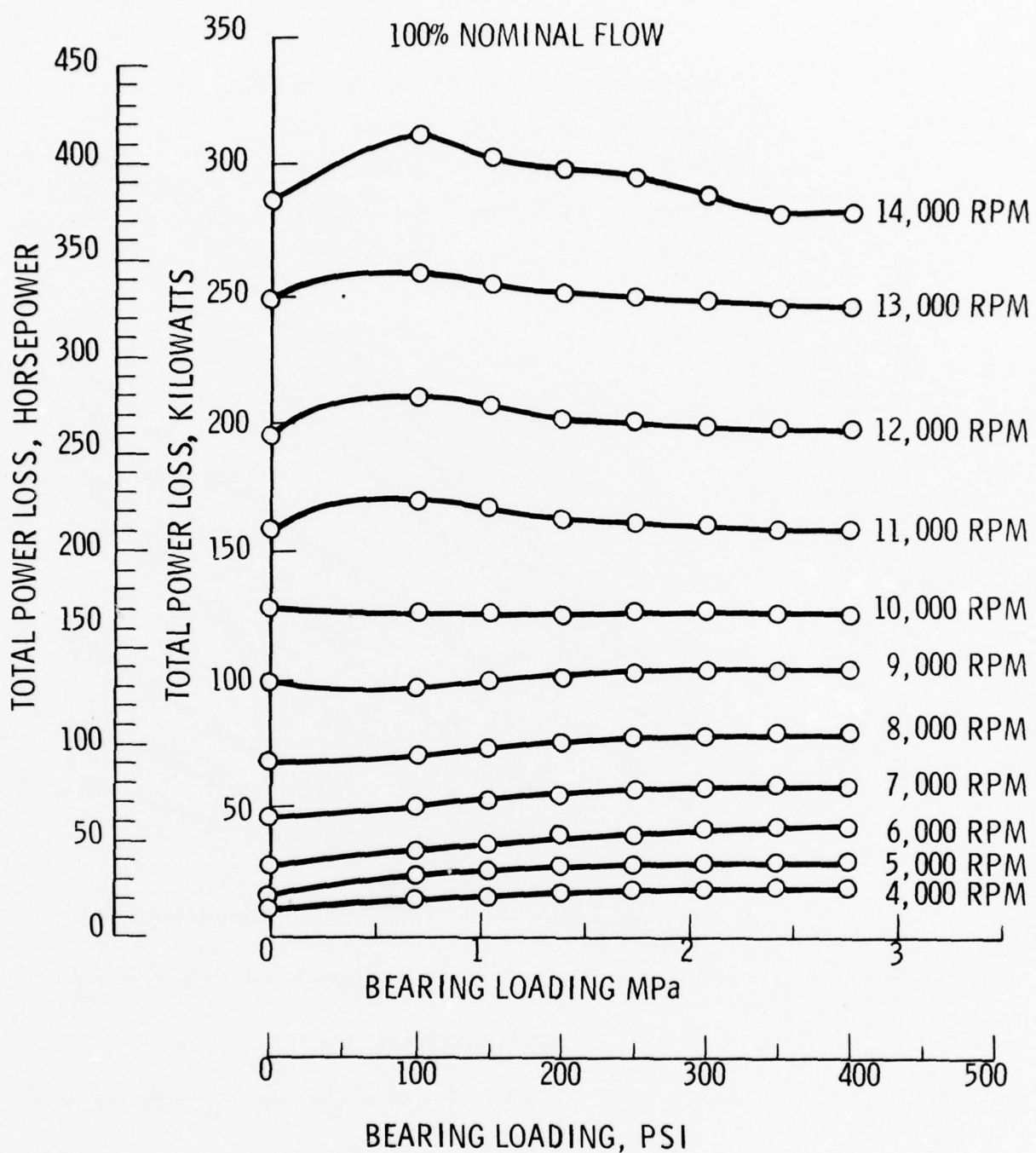


Figure 4.36 Effect of Load and Shaft Speed on Power Loss
(10-1/2 Inch Double Thrust Bearing)

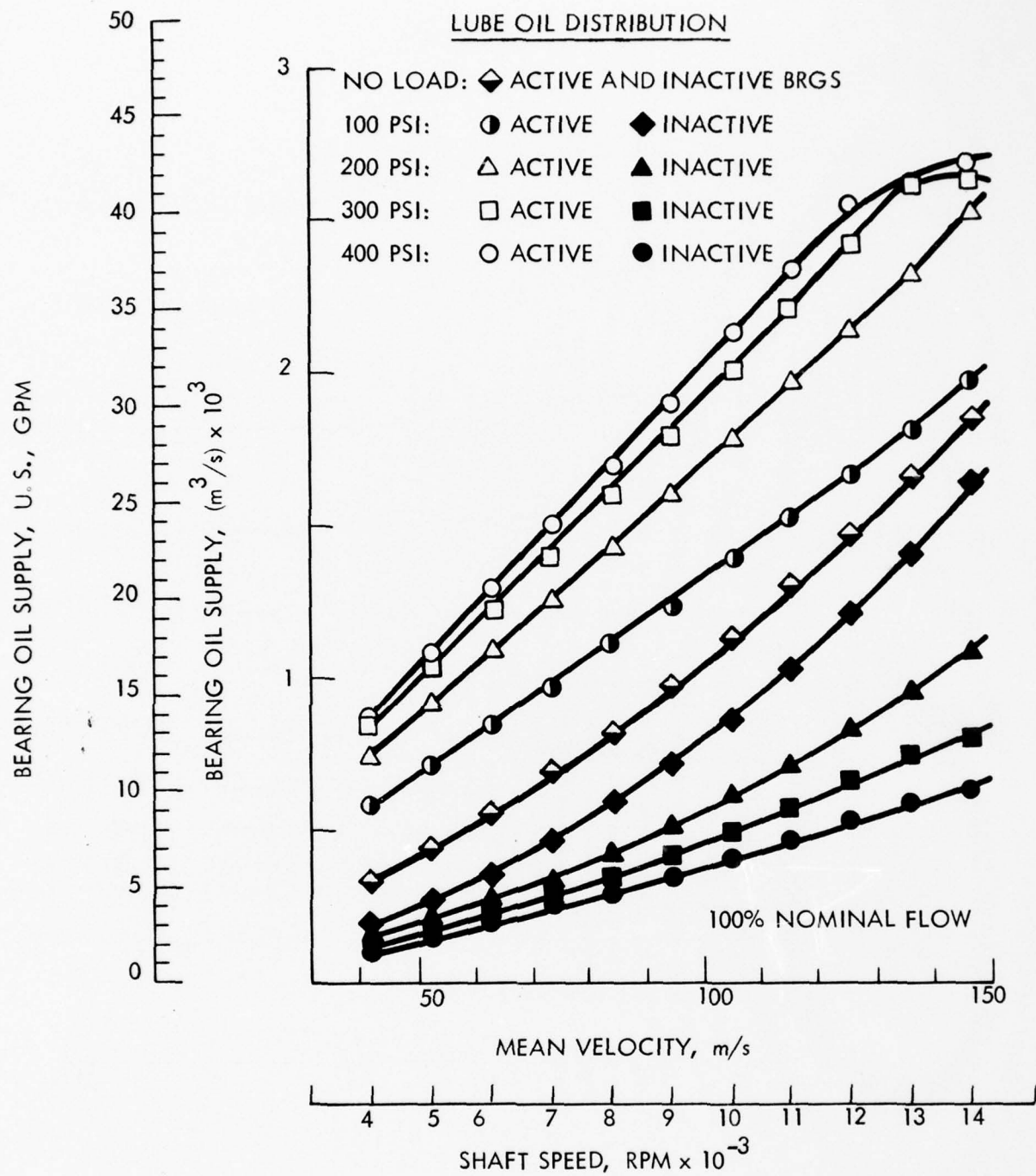


Figure 4.37 Lube Oil Distribution to Active and Inactive Elements of 267-mm
(10-1/2 Inch Bearing)

Scaling these values in the ratio of the bearing areas for the 7 and 8 inch bearings results in total flows of 27 GPM and 40 GPM respectively for the 18,000 RPM CCCBS high speed rotor thrust bearing. The resulting "flow ratios" (GPM/HP) of approximately 0.2 are in the reduced range of nominal values used in the high speed Kingsbury testing (Reference 17).

It is evident from this study that power loss is highly sensitive to speed and relatively insensitive to load (Figure 4.36). Thus bearing developments which result in increased pad pressure loading capability and permit the use of small bearing diameter are certainly desirable from the standpoint of minimizing the lubrication system component sizes (lines, sump volumes, pump and cooler sizes, etc.) The effect of the bearing power loss on cycle efficiency is probably insignificant (200 HP versus 70,000 HP output).

The situation in the power turbine of the CCCBS turbomachinery is less critical than in the gas generator rotor. The lower speed (6,000 RPM) and the available space will permit the use of a 10-1/2 inch thrust bearing which can carry an average pad pressure of 400 psi at a pad temperature of less than 260°F (Figure 4.35). The net pad area of the 10-1/2 inch bearing is 55.1 square inch (Reference 26) and the resulting allowable thrust load at 400 psi is 22,040 pounds. This must be compared with the power turbine unbalanced thrust of approximately 140,000 pounds. Obviously a balance piston is needed but the percentage of the unbalanced load which must be cancelled by the balance piston is significantly smaller than in the gas generator rotor. However, technology developments to increase thrust bearing load capability, although more urgently needed for the gas generator rotor thrust bearing, could also be exploited in the power turbine thrust bearing.

Power loss in the power turbine thrust bearing at the 6,000 RPM speed of the CCCBS output shaft was estimated to be 52 HP using the Waukesha catalog horsepower loss data (Figure 24 of Reference 30).

Power loss using the Kingsbury test data given in Figure 4.36 was 60 HP for the 10-1/2 inch bearing at 6,000 RPM and 400 psi pad pressure.

The required oil flow rate can be read directly from Figure 4.37. The active bearing received 20 GPM and the inactive bearing 6 GPM at the 6,000 RPM and 400 psi test condition. It is notable that the flow ratio of .43 resulting from the total flow of 26 GPM and the 60 HP measured power loss is substantially greater than that of the high speed rotor bearing (.2) and corresponds to the profile of reducing oil flow ratio with increasing speed used by Kingsbury in their testing (Reference 17).

Thus the 10-1/2 inch diameter power turbine thrust bearing has a power loss of about half that of the 7 inch diameter compressor/turbine thrust bearing and requires a somewhat smaller flow of lubricant. The use of an 8 inch diameter bearing in the high speed rotor increases the power loss by about 75 percent and the oil flow requirement by 50 percent. Any technology developments which can increase the pad pressure capability and thus minimize the size of the high speed bearing will therefore be most helpful in reducing the size of the lubrication system components in the closed Brayton cycle powerplant.

Tilting Pad Thrust Bearing Technology Developments Which Can Reasonably Be Expected

Standard tilting pad thrust bearings, commercially available from the various vendors (Kingsbury, Waukesha, Glacier, etc.) invariably have centrally pivoted pads in order to permit operation in either direction of rotation. In a machine such as the CCCBS power conversion assembly, which is required to run in one direction only, the use of standard bearings may unnecessarily restrict bearing performance. Pads with offset pivots have been demonstrated to operate at lower temperatures than those with center pivots. Tests on a 6 inch diameter bearing at 8000 RPM (reported in Reference 19) indicated a 40°F reduction in pad temperature using offset pivots. This effect increases at higher speeds (Reference 22). Directed lubrication, in which a stream of oil is directed onto the collar at the leading edge

of each pad, also results in reduced pad operating temperatures (References 19 through 22). Temperature reductions of 10-20°C (18-36°F) are reported in testing described in Reference 27. An important additional advantage of directed lubrication is the reduction in power loss which is achieved.

Improved pad materials can increase bearing capability. In the tests described in Reference 19 the standard steel backing material of the babbitt pads was replaced by copper. The copper backed pads showed a reduction in babbitt temperature of approximately 20°F. By substituting copper for the steel backing material, thermal distortions are reduced which is quite beneficial in high speed bearings where thermal distortions may otherwise be large.

With center pivots, pad crowning works in conjunction with viscosity variations to provide substantial load capacity where theory shows that the flat center pivot pad (no crowning) with isothermal conditions in the lubricant has zero load capacity (Reference 28). Crowning results from thermal and pressure gradients in the pad. In general, at high speeds the thermal effects dominate. Thus, the coefficient of expansion, conductivity and Young's modulus of the backing are important factors in determining the amount of crowning distortion produced. Although some distortion is desirable in a centrally pivoted pad, the problem generally is to limit the amount. By substituting copper for steel backing material, thermal distortions are reduced, benefiting the high speed capability of the bearing.

The use of all aluminum pads results in a further increase in high speed bearing capability. This results from an additional improvement in thermal distortion compared with a babbitt and copper combination (Reference 19).

In addition to these approaches, which are aimed at reducing the operating temperature of the bearing, it is also possible to increase the temperature capability of the bearing by substituting higher temperature materials for the babbitt normally used. Copper-Lead is an example of such a material and has a maximum operating temperature some 50°F higher than that of babbitt (Reference 24). Other candidate materials are lead-bronze, tin-bronze, barium-bronze and silver. These materials have substantially higher operating temperature capabilities (in the region of 450°F and above).

Kingsbury have recently been performing comparison tests on bronze and babbitt materials and believe that barium bronze can be used at pressures as high as 600 psi in high speed bearings. This is made possible by the reduced pad crowning experience with barium-bronze (Reference 30). Kingsbury bearings are currently running at 500 psi and 30,000 feet/minute collar tip speed in commercial steam turbines using babbitt faced (1/16 inch thick) steel backed pads.

Replacement of babbitt by higher strength materials, unfortunately, is accompanied by a deterioration in compatibility which is a measure of the anti-weld and anti-scoring characteristics of the material. This is of interest mainly during startup, when the hydro-dynamics film has not become fully developed. Conformability and embeddability are also reduced in the higher strength materials. Conformability is the ability to compensate for misalignment. Embeddability is the ability to absorb dirt and other foreign particles to avoid scoring and wear. The reduced corrosion resistance of the stronger materials when compared with babbitt can also cause problems. Some of these corrosion problems are caused by oxidation products which may not be a problem in the closed Brayton cycle helium environment.

A program of thrust bearing development, directed toward the closed Brayton cycle requirements would logically seek to exploit the potential improvements outlined in the foregoing paragraphs, with the aim of developing a bearing having substantially improved capability (in speed, load or both). Such a program would require experimental work supported and guided by theoretical analysis. The successful development of improved thrust bearing capability would reduce the sensitivity of the turbomachinery to variations in thrust balancing conditions during operation and provide a greater margin of safe operation.

4.3.1.2 Tilting Pad Journal Bearings

Commercially Available Bearings

Tilting pad journal bearings are available in several standard designs produced by U. S. and foreign companies. As mentioned previously, and in contrast to the thrust bearing situation, the required operating conditions of the closed Brayton cycle turbomachinery, with respect to speed and load, are well within the range of the manufacturers catalog data.

Waukesha Bearings Corporation claim to be the major supplier of tilting pad journal bearings in this country and that they have more bearings in operation and have accumulated more operating experience in their design than any other bearing supplier. This experience ranges from 1 inch bearings operating at 70,000 RPM to 17 inches at 36000 RPM. The corporation has engineering, computer design programs, and research laboratories equipped with journal bearing test facilities. Figure 4.38 illustrates a Waukesha standard tilting pad journal bearing.

The standard design has a length to diameter ratio of 0.4. The bearing assembly consists of five centrifugally babbitted steel backed pads held in place by hardened steel locating dowels and by bolted on aluminum or bronze end plates. The pads are made with an outside radius of curvature considerably smaller than the bore of the hardened shell into which they are installed. The claim is made that this feature provides a friction-free rocking pivot not found in restricted pin or knuckle type designs.

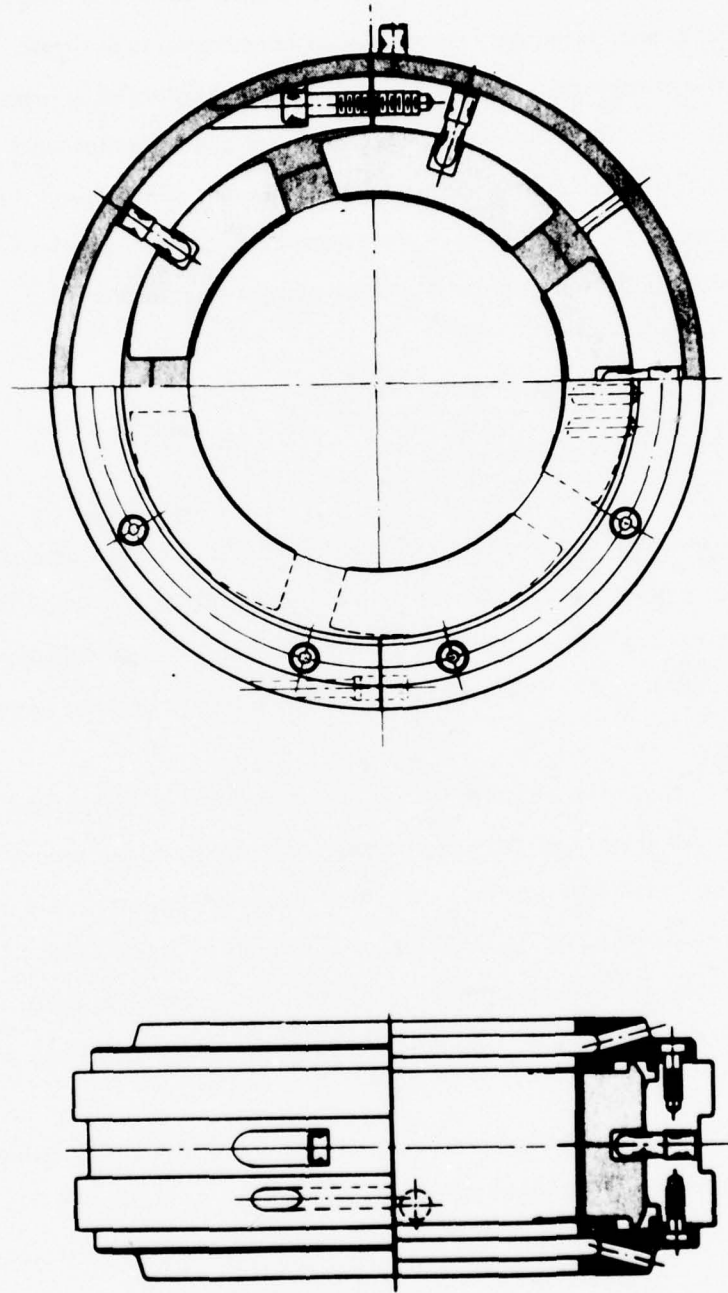


Figure 4.38 Waukesha Tilting Pad Journal Bearing

Lubricant is fed into the pad cavity through a single hole and floods the chamber. The oil then leaves the chamber axially through the small radial clearances between the bolted on end plates and the shaft. Circumferential grooves machined in the end plates collect the oil and channel it to a number of drain holes at the bottom of the bearing. Presumably some of the oil in the circumferential collecting grooves also leaks axially along the second radial clearance to the outside of the bearing. The design of the housing for the bearing must provide suitable drainage for this leakage oil and the necessary seals to prevent oil leakage from the housing.

Kingsbury, Inc., also makes tilting pad journal bearings. Their design differs from that of Waukesha in the method used to locate the pads. The pads are pivoted on pins, pressed into the ends of the pads, which are inserted into jig bored holes in the shoe retaining plates. Figure 4.39 illustrates a Kingsbury tilting pad journal bearing.

Lubricant is fed into the pad cavity through a hole for each pad. The oil leaves the chamber axially through the shaft to shoe retaining plate radial clearance. Circumferential grooves are machined into the inner diameters of the shoe retaining plates but the grooves do not appear to be provided with drainage holes. Thus all the oil leaving the bearing must exit in an axial direction along the shaft. This arrangement can be expected to result in the presence of more oil in the vicinity of the bearing housing shaft seal than in the Waukesha design, which may be a disadvantage from the standpoint of minimizing oil loss through the seals.

Two of these Kingsbury tilting pad journal bearings, 5.0 inches in diameter by 2-1/4 inches long, were used to support the shaft in the thrust bearing testing (Reference 15) to 14,000 RPM described earlier. This represents a surface velocity comparable to that of the 4.0 inches diameter bearing which will be required in the closed Brayton cycle turbomachinery high speed rotor.



Westinghouse

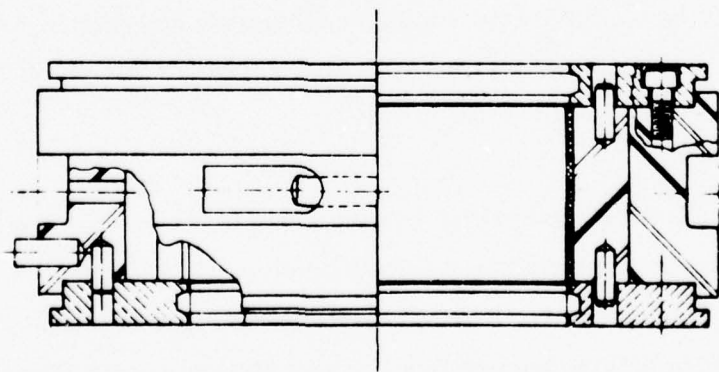
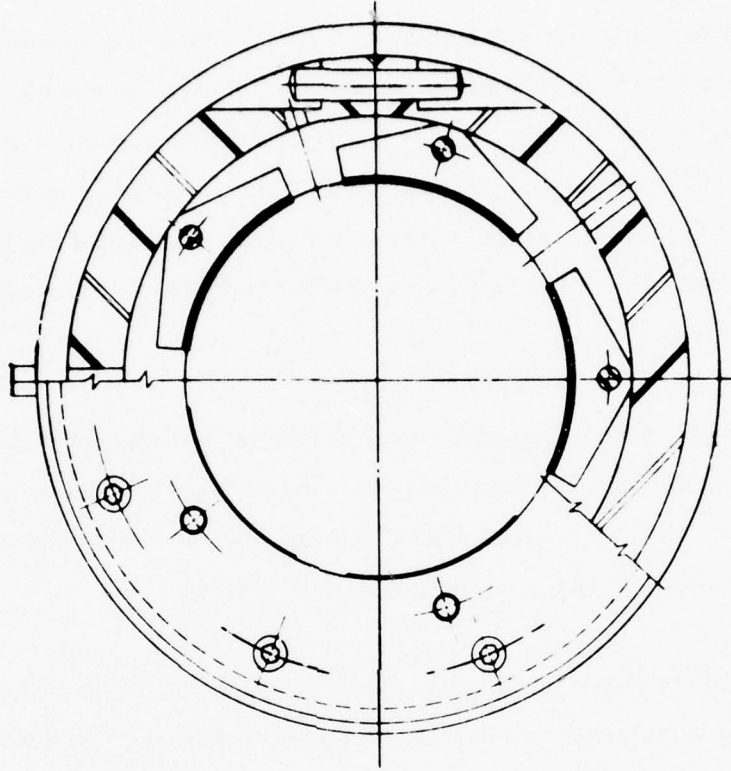


Figure 4.39 Kingsbury Tilting Pad Journal Bearing

Pioneer Motor Bearing Company of South San Francisco, California, makes tilting pad journal bearings which use a three pad design. The pads are located by simple stop pins at their ends. In operation, each pad is supported on a self-generated hydrostatic oil film which is created by tapping off a small portion of the pad hydrodynamic oil film to pressurize a central recess on the back of each pad. The hydrodynamic oil flow, in turn, is supplied by direct pressure lubrication from the machinery housing through the bearing shell to spreader grooves on the leading and trailing edges of each pad. Figure 4.40 shows a bearing operation schematic which illustrates this concept.

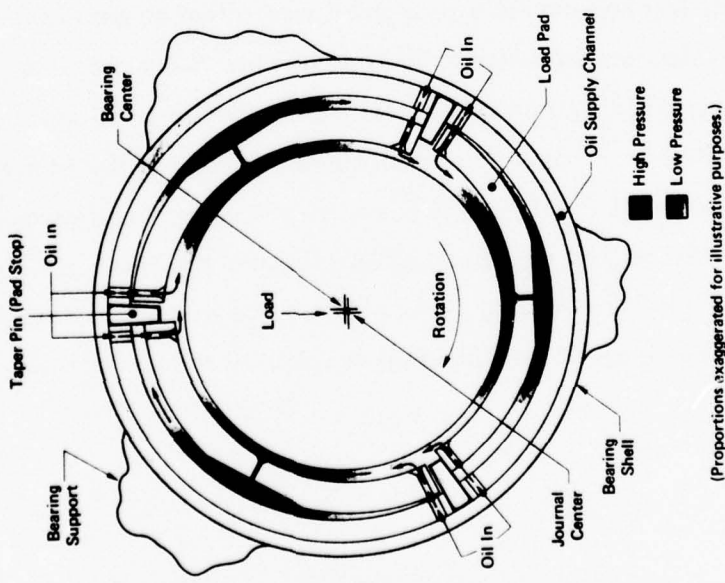
The pads are free to respond to the action of the oil films acting on them. The formation of a hydrostatic film on the back of each pad allows it to lift, pitch and tilt axially in response to misalignment, until force and moment equilibrium is attained for any particular operating condition. This pad action was predicted by an advanced computer analysis performed for Pioneer by Mechanical Technology, Inc., and has also been observed repeatedly on Pioneer's test stand with proximity probes.

Pioneer claim that this bearing has a good stabilizing effect on the rotor, particularly at high speeds and light loads, due to the generation of high pad recess pressures. Also claimed is substantially higher damping than mechanically pivoted tilting pad bearings, especially at light load and high speed. Power loss in the bearing is reduced due to the elimination of churning losses associated with flood lubricated bearings. End seals are not required or desired as the lubricant is introduced directly to the leading and trailing edges of each pad. It is claimed that the Fluid Pivot bearing exhibits only 40-60 percent of the power loss of comparable flood-lubricated tilting pad journal bearings and that oil requirements are correspondingly reduced.

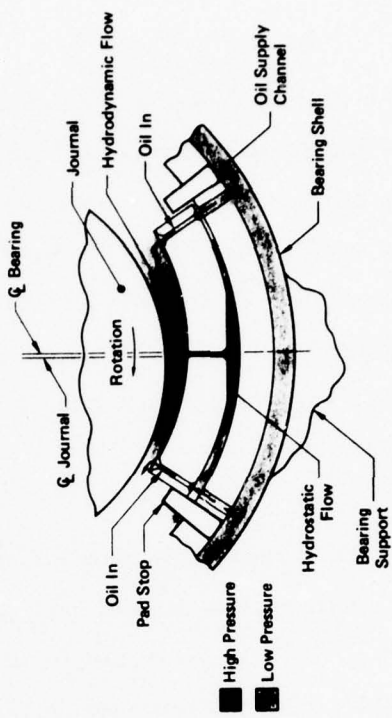
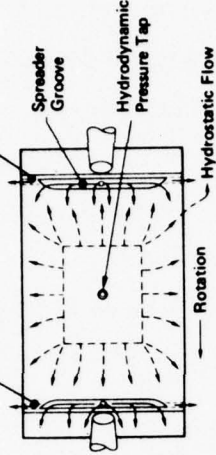


Westinghouse

Bearing Operation Schematic



Auxiliary Bleed Grooves if Req'd
to Achieve Additional Cooling



(Proportions exaggerated for illustrative purposes.)

Figure 4.40 Pioneer Tilting Pad Journal Bearing (Fluid Pivot)

Pioneer bearings are available with oil baffle rings at the ends of the bearings to direct the lubricant leaving the bearing away from the bearing housing seals. A drain slot is provided at the bottom of the bearing to allow the baffled oil to drain into the housing sump.

Pioneer is also licensed to produce the bearing designs of the Glacier Metal Company, Ltd., of Wembly, England. The Glacier tilting pad journal bearing is similar in design to the Waukesha in that it has five pads which rock on their outside radii. The Glacier pad locating pins are at the ends of the pads, however, and are made hollow to serve as oil inlet ports. Drained circumferential grooves are provided in the end plates, as in the Waukesha design.

Orion Corporation of Grafton, Wisconsin, manufactures a five shoe tilting pad journal bearing which is equipped with floating seal rings at each end of the bearing. The rings are split, the split halves being held together radially by a garter spring which is also split, allowing the ring to be replaced without disturbing the shaft. The pads in this bearing are provided with projections on their back surfaces which are seated in machined grooves in the casing. The projections are contoured appropriately to allow the pads to self align to compensate for shaft angularity. Figure 4.41 illustrates this design.

The lubrication system is somewhat different than the other bearings described in that the used oil is removed from the top of the casing through drilled holes which connect with circumferential grooves in the outer diameter. The amount of oil which leaks axially from the bearing is small, because of the oil seal rings.

This bearing design would appear to have advantages over the other bearings in that the drainage oil is confined to the immediate vicinity of the bearing. There should be less oil ejected in the direction of the housing seals resulting in improved oil loss characteristics. In addition, the confinement of the oil to the bearing by the oil seal rings should improve the chance of the bearing surviving a temporary interruption in the oil supply.



Westinghouse

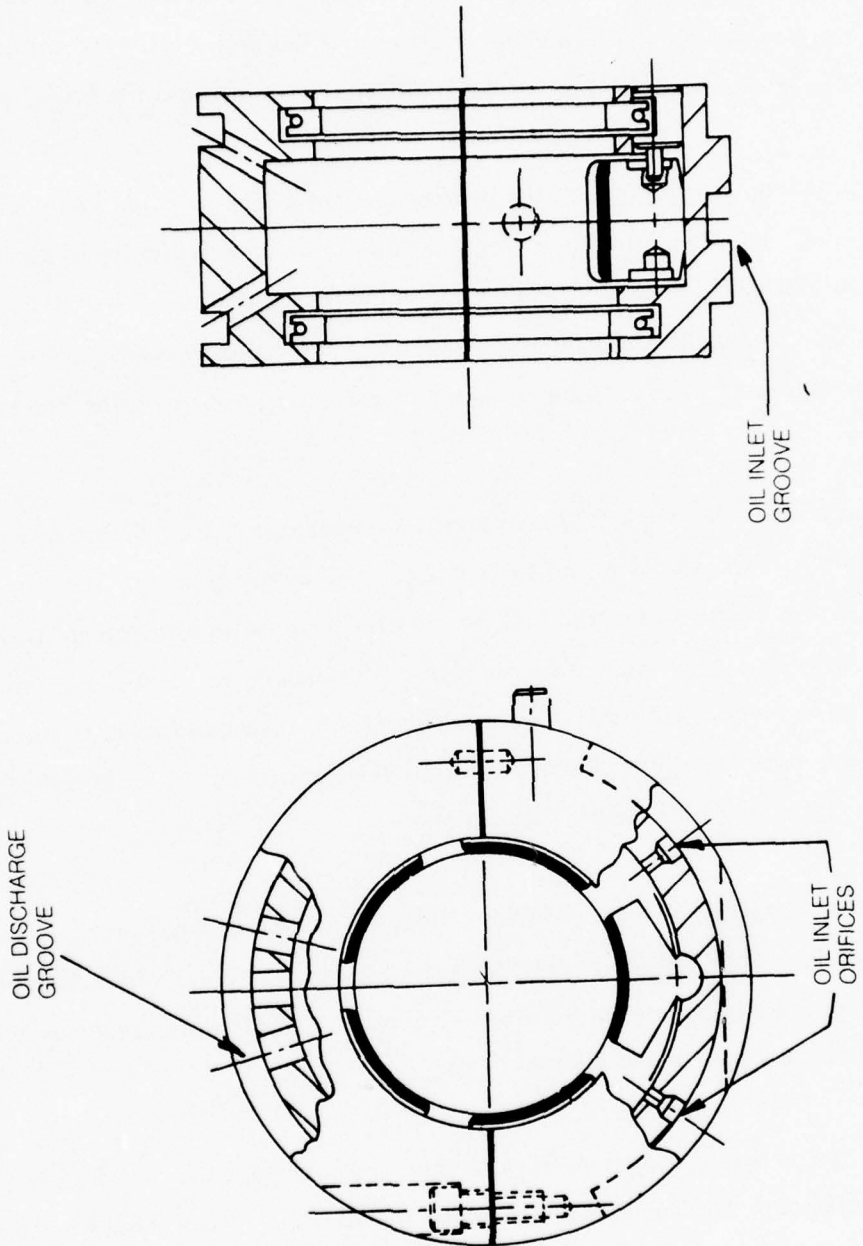


Figure 4.41 Orion Tilting Pad Journal Bearing

These bearings have been used successfully since 1960 by various manufacturers of turbines and compressors. (Allis-Chalmers, Solar, etc.) No problem has been experienced with the integrity of the split seal ring at high speeds. This feature was used in a 1 inch bearing at 100,000 RPM. However, the bearing power loss is somewhat higher than in the other bearings described.

Bearing Operating Limits

Pad temperature, the basic criterion of integrity at high operating speeds is of far less concern in the journal bearing than the thrust bearing. This situation results from the reduced pressure level and surface velocity in the journal bearing. The average journal bearing pad pressures in the CCCBS turbomachinery will be on the order of 100 psi using narrow bearing geometry. All of the manufacturers data extend beyond the anticipated load and speed requirements of the closed Brayton cycle powerplant.

Low speed operation is of some concern in the journal bearings which have to support the 100 psi (approximate) load due to rotor weight from a standing start, in contrast to the thrust bearings which are essentially unloaded at zero speed. This concern has been largely dispelled by discussions with the bearing manufacturers on the subject of providing hydrostatic jacking during startup. The feeling was generally expressed that hydrostatic jacking would not be necessary with babbitted bearings at the low Brayton cycle bearing pressures ($\simeq 100$ psi).

Tilting Pad Journal Bearings - CCCBS Application

In the high speed compressor/rotor, the need to transmit the driving torque ($\simeq 170,000$ inches/pounds) to the LP compressor results in a minimum shaft size of about 3 inches in diameter. Practical design considerations, resulting from the need for transmitting the torque through driving splines in a conveniently assembled machine, will tend to increase the shaft diameter at the bearings to perhaps 4 inches at the inter-compressor location. The journal bearings at LP compressor inlet and HP turbine outlet may possibly be as small as 3 inches in diameter since the shaft load at these locations is nominal. These estimates are based on preliminary judgment not yet confirmed by design layout.

Using the Waukesha tilting pad journal bearing catalog (Reference 16) the clearance selection guide gives a minimum recommended diametral clearance of .008 for a 4 inch diameter bearing at 18,000 RPM. The horsepower loss of 20 HP for the 4 inch bearing with 0.002 inch in diameter clearance at 100 psi loading and 18,000 RPM. This estimate is based on the use of 150 SSU of oil at 100°F with an outlet temperature of 150°F. The recommended oil flow for an inlet temperature of 125°F is $0.500 \times \text{HP}$ or, in this case, 10 gpm. It is of interest that the normal maximum design load of the 4 inch bearing is 1200 pounds at 100 RPM and 1650 pounds at 18,000 RPM. The maximum bearing load in the closed Brayton cycle high speed rotor will be about 700 pounds.

The power turbine bearings will probably have to be about 5 inches in diameter in order to accommodate a shaft capable of transmitting the torque (810,000 inches/pounds). Journal loads in the power turbine will be somewhat higher (\approx 900 pounds) than in the high speed rotor.

The recommended minimum diametral clearance for a 5 inch bearing at 6000 RPM is 0.008. The horsepower loss is 6.5 HP for the 5 inch bearing with a 0.0015 inch in diameter clearance at 100 psi loading and 6000 RPM. The recommended oil flow is about 3 gpm. The normal maximum design radial load at 1000 RPM is 2000 pounds, more than twice the actual load of 900 pounds expected in the closed Brayton cycle powerplant.

Tilting Pad Journal Bearing Technology Developments Which Can
Reasonably Be Expected

The journal bearing requirements in the CCCBS turbomachinery are judged to be far less demanding than those of the thrust bearings. This is the result of pad pressures and speeds which are substantially lower in the journal bearings than in the thrust bearings. Technology developments to improve bearing load and speed capability are therefore more likely to be applied to the improvement of the thrust bearing than the journal bearing. Since the commercial bearing manufacturers tilting pad journal bearing designs show every indication of being

perfectly adequate for direct application to the closed Brayton cycle turbomachinery, with little or no modification, there will be little incentive to change them.

The developments described in Section 4.3.1.1 to lower pad operating temperature could possibly find additional application in the journal bearings in solving an unforeseen problem. On the other hand, the developments to raise the allowable operating temperature, by the substitution of higher temperature materials for the babbitt normally used, are unlikely to be applied in the journal bearings. The boundary lubrication situation which exists in the journal bearings at start up is best handled by babbitt at the present state of the art. The unloaded condition of the thrust bearing in this situation, on the other hand, allows materials having poorer compatibility, conformability and embeddability to be considered. The use of these materials in the journal bearings might result in excessive wear during startup, unless hydrostatic jacking of the shaft were provided. The use of high temperature pad materials and hydrostatic jacking to improve bearing load capability could possibly be justified in specialized applications such as navy ships subject to high bearing loads under battle conditions. In most applications of the closed Brayton cycle powerplant, however, the almost universally used babbitt should provide a quite adequate journal bearing pad material.

Technology development in the journal bearing area is more likely to be directed at the oil sealing problem in the CCCBS turbomachinery. It is especially important to eliminate oil loss in closed cycle machines for a number of reasons. Oil loss causes fouling of compressor blading, leading to losses in efficiency. Cleaning of the blading in a closed cycle plant is less conveniently achieved than in simple open cycle machinery. Also, the oil lost to the cycle helium will tend to coke in the heat source heat exchanger and other hot areas of the cycle. In reactor systems, the cleanup system could be loaded up with oil leaking from bearing housing seals. These possibilities must be carefully considered in the design of the overall lubrication system. Also, a thorough test program of the lubrication and seal gas systems must be followed to ensure that these concerns are eliminated. In this context the efficiency of the journal bearing design in limiting the amount of oil ejected in the direction of the housing

seals is quite important. Technology developments in the bearing design which achieve the greatest isolation of the lubricant from the helium gas, which allow the amount of helium injected through the seals to be minimized and which result in the minimum of aeration of the oil by the helium are desirable. Journal bearing development is more likely to be concerned with these goals than with increasing the basic load carrying capability of the bearings.

4.3.1.3 Lubrication System Design Consideration

Having evaluated the current bearing state of the art and its application to the closed Brayton cycle turbomachinery, it is appropriate to summarize the lubrication system requirements which result from the characteristics of the various bearings required in the plant. The oil flow and heat removal requirements are shown in Table 4.9.

The lubrication system, in its simplest form must provide means of circulating the oil, remove the heat deposited in the oil by the bearings and the local turbomachinery, remove the helium gas entrained by the oil and remove particulate matter by filtration.

Deaeration of the oil is normally effected by providing a dwell time in the oil tank. The tank capacity in an aircraft or marine unit, where space and weight considerations limit the amount of oil, provides a dwell period of from about 30 seconds up to about one minute. This is generally the minimum time in which satisfactory deaeration can be effected. (Reference 24). Generally if a substantially larger dwell period can be provided, this is beneficial. Thus with a total oil circulation of 89 GPM, a minimum tank capacity of about 100 gallons will be necessary. It is expected that a tank capacity substantially larger than this can be provided in a closed Brayton cycle powerplant.

Deaeration rate is extremely dependent on oil viscosity and temperature, with low viscosity and high temperature causing increased deaeration rates (Reference 39). For this reason the hotter the oil temperature during its residence in the tank, the better the conditions for rapid deaeration. For this reason the oil cooler should not be placed in the drain line from the turbomachinery bearings to the tank.

TABLE 4.9
OIL FLOW AND HEAD REMOVAL REQUIREMENTS

<u>Compressor/Turbine Rotor (18,000 RPM)</u>	<u>Power Loss (HP)</u>	<u>Oil Flow (GPM)</u>
Thrust Bearing	- 7 In. Dia.	27
L. P. Comp. Inlet Journal	- 4 In. Dia.	10
L. P. Comp. Outlet Journal	- 4 In. Dia.	10
H. P. Turbine Outlet Journal	- 4 In. Dia.	10
Total (High Speed Rotor)	160	57

<u>Power Turbine Rotor (6,000 RPM)</u>	<u>Power Loss (HP)</u>	<u>Oil Flow (GPM)</u>
Inlet Journal	- 5 In. Dia.	6.5
Outlet Journal	- 5 In. Dia.	6.5
Thrust Bearing	- 10-1/2 In. Dia.	60.0
Total (Power Turbine Rotor)	73.0	32

Total Per 70,000 HP Unit	233 HP	89 GPM
--------------------------	--------	--------



Westinghouse

The simplest lubrication system would preferably allow free drainage, by gravity from the bearing compartments to the oil tank. Helium drawn into the bearing compartments through the seals would be separated from the oil in the tank. The oil would then be pumped from the tank through an oil cooler, filtered and returned to the bearings.

The simple system would, preferably, have a fairly uniform level of ambient gas pressure at all the bearing compartment seals to ensure proper control of breathing from the bearing compartments to the oil tank. This circumstance arises naturally in the compact closed cycle Brayton turbomachinery in three of the four bearing compartments, as a result of the thrust balancing and turbine cooling provisions which must be made. The means of suitably pressurizing the fourth bearing compartment (at LP compressor inlet) should not cause any excessive complication or result in a severe performance penalty.

Provisions for conveying the breather gas from the tank back into the helium closed cycle will require careful consideration from the standpoint of removing oil mist and vapor. This may require the use of a special breather circuit using electrostatic precipitators and cold traps. Failure to remove essentially all of the oil from the breather gas will cause the cleanup system in a nuclear installation to be loaded up with oil. In this respect the importance of a thorough program of development testing of all components of the lubrication and seal gas management system is obvious.

In a nuclear installation it is envisaged that the oil tank could be mounted beneath the turbomachinery units, inside the containment. A hot oil line would run from the tank to the pump, which would be mounted outside the containment. Filters, coolers, pressure relief valves, etc., would all be external to the containment. A single return line would convey the cold oil to the turbomachinery. In the event that a breather cleanup circuit were deemed necessary, the breather line from the tank to the de-oiling system and the return line to the turbomachinery

closed gas cycle would also penetrate the containment. Means for replenishing the oil system from an oil storage tank through a charging pump would be provided outside the containment. Charging with oil would be performed on demand from a level indicator in the oil tank inside the containment. Such a system would result in most of the critical oil system components being external to the containment for ease of maintenance.

4.3.2 Gas Bearings

Closed Brayton Cycle engines impose some unique bearing requirements not normally associated with conventional open cycle turbomachinery. One of the desirable features of closed cycle turbomachinery is derived from the freedom to choose the cycle gas to optimize the heat transfer characteristics and aerodynamic components. Another feature is the ability to vary the pressures in response to power requirements and, thereby, operate the turbine at constant temperature and high efficiency over the entire power range. Pressures are frequently varied over a 10:1 range to achieve the desired power levels. Still another feature is that all heat input and waste heat removal is accomplished through high effectiveness heat exchangers requiring low levels of contamination or fouling for continued high efficiency.

These three factors combine to place stringent requirements on the turbomachinery bearings, lubrication, and sealing systems. The bearings of a closed cycle turbomachine must operate reliably over a wide range of ambient pressures and dynamic loads. Bearing lubricant and cooling must be provided under these varying conditions, and effective sealing of the lubricant from the gas loop must be maintained under all conditions of static and dynamic operation.

Gas bearings, utilizing the cycle gas as a lubricant, eliminate the problem of loop contamination and greatly simplify the requirements and design of the sealing system. They are capable of operation under varying temperatures, pressures, and related conditions of a closed cycle gas turbine and provide a high degree of reliability and long life. A wide variety of gas bearing designs covering both radial and thrust bearings has been developed. Several closed Brayton cycle engines have been successfully operated on solid geometry and compliant type gas bearings. A production model of an air cycle cooling turbine used in the DC-10 aircraft has accumulated a total of over 14,000,000 hours of operation on compliant type gas bearings.

Designs have been developed for hydrostatic, hydrodynamic, and hybrid types of operation. Gas bearing designs include all the conventional liquid bearing types such as plane journal, pocketed, tilting, pad, elliptical, lobed, stepped sector, spiral grooved, etc. and also

manifest the same or related problems. Compliant type gas bearings do, however, eliminate or greatly reduce many of the conventional liquid bearing problems. Gas bearings are generally larger than their liquid counterparts due to the difference in the fluid densities.

The characteristic properties of a gas, such as compressibility, density, specific heat, viscosity, thermal conductivity, etc., are utilized to design bearings to meet specific requirements of load, speed, pressure, temperature, stability, shock, vibration, and rotor dynamics. Due to the viscosity increase with increasing temperature characteristic of gases, gas bearings can operate at high temperatures and actually provide increased load capacity and stability as bearing temperatures increase.

Gas bearing sizing, as with liquid lubricated bearings, is strongly influenced by the viscosity of the fluid. As an example, the viscosity of air is 1/50th of that of water and 1/3500th of the viscosity of 10 weight oil. As a consequence, gas bearings are relatively larger than their liquid bearing counterparts, operate at smaller fluid film thicknesses, and are lower in power losses.

The concept of gas bearings was first documented by G. Hirn in 1854, but little or no effort was directed toward development of a functional bearing until approximately 1897 when A. Kingsbury released the results of his experiments with an air lubricated journal bearing. Thrust bearing designs were subsequently investigated, and the efforts ultimately resulted in the well known Kingsbury thrust bearing. Numerous investigators, in the intervening years, have added to the knowledge and development of functional air bearings. Analysis has reached a high degree of refinement. In most applications, however, the low viscosity of gases and other restrictive characteristics have limited the use of gas bearings to small specialized applications, such as: precision grinders, turboexpanders, cryogenic turbines, and precision inspection equipment. Only in the past twenty years has the technology been extended to production turbomachinery of any appreciable size and rotor weight. The extension of this gas bearing technology to large turbomachinery can now be accomplished.

4.3.2.1 Gas Bearing State of the Art

As a consequence of the past limited need for gas bearings, almost all of the gas bearings in commercial use or under development are the product of an isolated bearing support requirement. It has been the practice to use gas bearings only when conventional bearing systems cannot be made to function properly, or a special requirement dominates and forces the selection of a gas bearing. The technology base for gas bearings is very limited in comparison to that of liquid film bearings, primarily due to the more complex relationships of a compressible medium and the ultimate factor of limited investment. Gas bearing technology, within any given manufacturer's organization, is generally limited to his specific needs, i.e. Ampex incorporates gas bearings in film or tape transport, and machine tool manufacturers support precision grinders on gas bearings. Some of these companies have acquired a broader technology base through company and government sponsored R and D work. Computer programs have been developed to analyze and design the various types of gas bearings. The solid geometry bearing designs have the broadest technical base because the fixed geometry can be most easily analyzed. Compliant gas bearing computer programs have also been developed but are relatively crude due to lack of knowledge as to how the compliant bearings actually change geometry in operation.

Gas Bearing Machines

The state-of-the-art of gas bearings relevant to the support of larger turbomachinery is best illustrated by examples of gas bearing supported machines in use and under development. The machines, shown on Figure 4.42, represent some of the turbomachinery produced by AiResearch and supported on compliant foil type gas bearings. The DC-10 three wheel air cycle machine with a 9 pound rotor weight has a service history of over 14,000,000 hours of commercial operation. The BRU-F, shown in Figure 4.43, with a rotor weight of 21 pounds is a closed Brayton cycle 15 kW_e engine equipped with compliant hydrodynamic foil gas bearings. A similar unit, designated as the BRU and equipped with solid geometry tilting pad gas bearings, has been tested by the NASA in excess of 27,000 hours of closed cycle operation. The largest

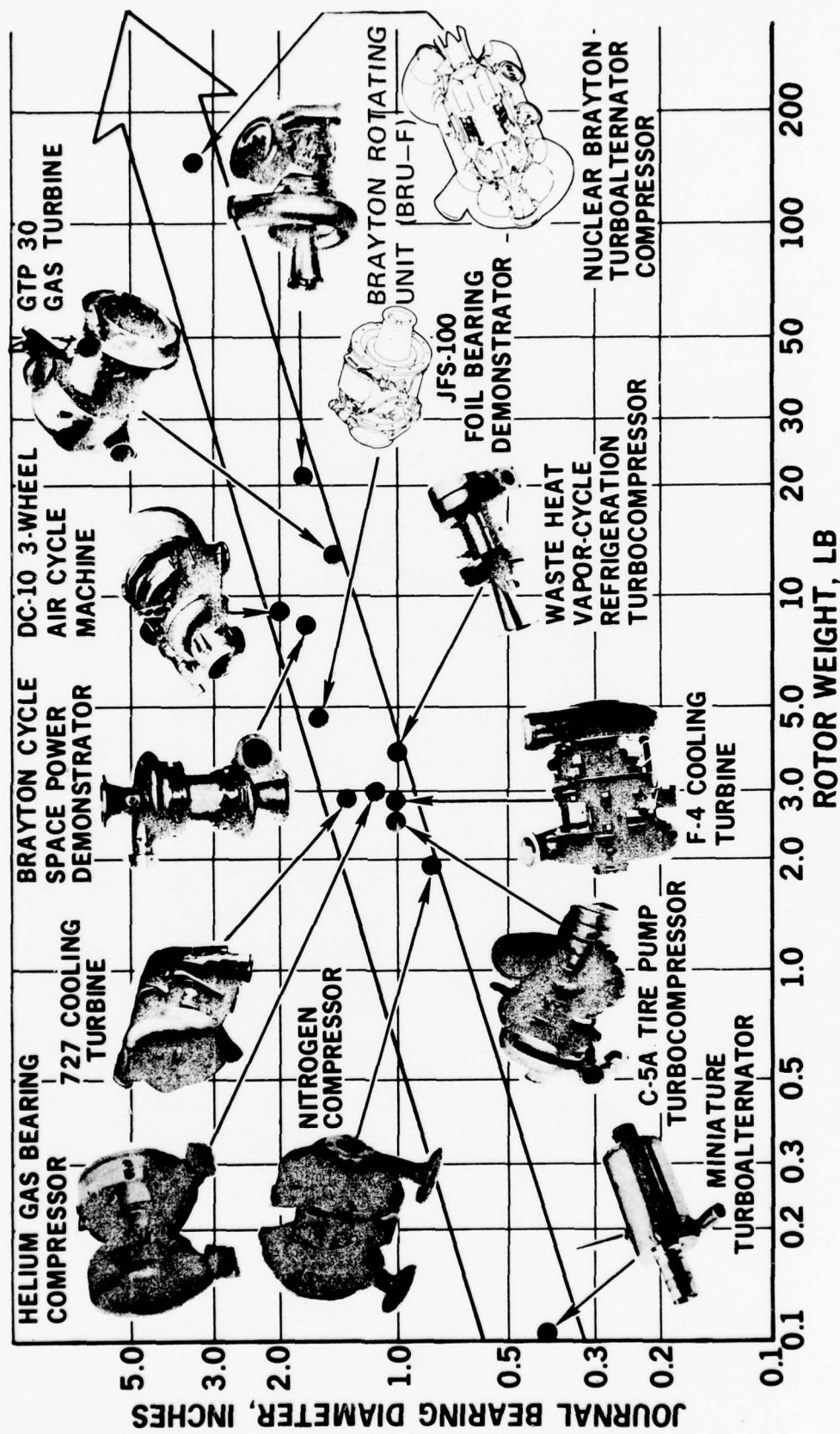


Figure 4.42 Foil Bearing Applications



Westinghouse

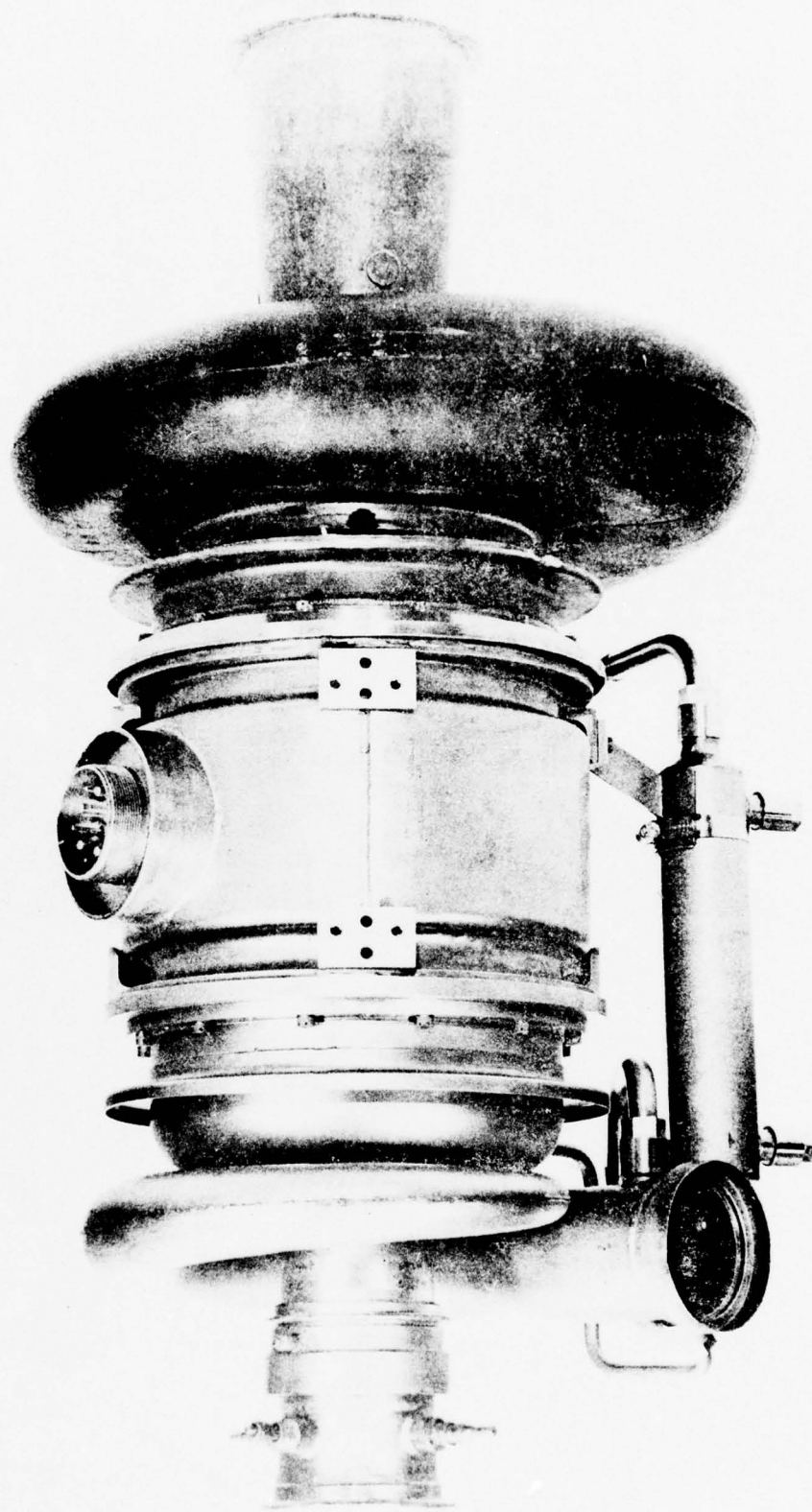


Figure 4.43 Brayton Rotating Unit - Foil (BRU-F)

machine operated with hydrodynamic gas bearings is designated the turboalternator compressor (TAC). This machine has a 142 pound rotor and operates at 24,000 rpm. One of the smallest machines is a turbocompressor operating at 540,000 rpm. The foil bearing system for this machine is shown in Figure 4.44 (scale is in inches).

Clearly, gas bearing technology is sufficiently advanced to permit realistic design and development of bearing systems for turbomachinery. The technology has been limited in use to relatively small turbomachines; however, there does not appear to be any reason that the technology cannot be extended to large turbomachines with rotors weighing thousands of pounds.

4.3.2.2 Gas Bearing Characteristics

The use of a compressible gas film as a bearing lubricant results in certain inherent characteristics of gas bearings. Primarily, the relatively low viscosity of a gas does not provide the high load capacity, damping, or stability normally desired of any bearing. Gas bearing designs are, then, a compromise of characteristics to meet the desired bearing requirements. Hydrostatic, hydrodynamic, and hybrid combinations constitute the gas bearing design technology currently in use.

Hydrodynamic Gas Bearings Characteristics

Hydrodynamic gas bearings, which generate a supporting gas lubricant film by virtue of the relative velocities of the bearing and the viscosity of the gas, operate ideally at very thin gas films on the order of 0.0005 to 0.0008 in. thick. Thinner gas films present mechanical problems while thicker films result in low film spring stiffnesses which in turn cause bearing instabilities of a number of varieties. It becomes obvious that with the small gas film thicknesses required for stable bearing operation, the bearing geometry must be very accurate or mechanical interference will occur. With the exception of very small turbomachinery, it is generally



Westinghouse

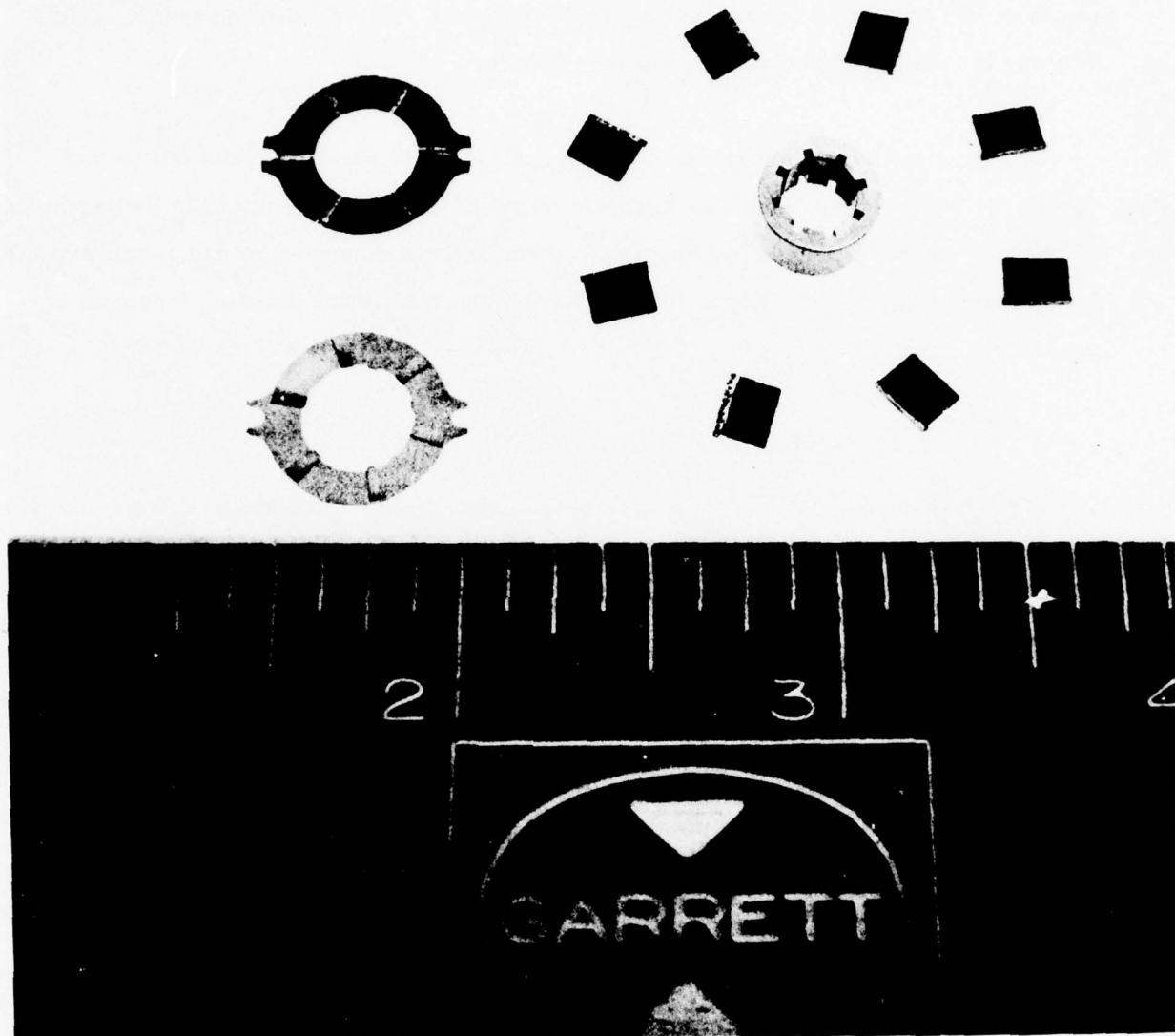


Figure 4.44 540,000 RPM Foil Bearing System

impractical to maintain the required system accuracy without resorting to bearing designs that provide for rotor transient excursions, misalignment, thermal and centrifugal distortion, and a means of maintaining the gas film within acceptable limits.

Hydrodynamic bearings are limited in load capacity by their ability to generate gas film pressures. The viscosity of the gas used, the geometry of the bearing and the leakage paths from the pressurized area of the bearing are the limiting factors of a hydrodynamic bearing.

A hydrodynamic bearing is generally stable over a wide range of speeds due to the fact the generated bearing pressures change in relation to the speed, and a near optimum film thickness is maintained. The effective spring stiffness of the gas film ranges from 40,000 to 80,000 pounds per inch for an optimum hydrodynamic air bearing.

Full hydrodynamic air bearing systems can be successfully started and stopped providing the specific loading is kept below two pounds per square inch, bearing surfaces are treated, and the rotor inertias are kept low. Every hydrodynamic gas bearing has a critical speed below which a gas film cannot be generated or maintained. Operation below this critical speed results in direct contact and wear of the bearing surfaces. Highly loaded hydrodynamic gas bearings usually incorporate some form of hydrostatic gas bearing for starting and stopping.

Hydrostatic Gas Bearing Characteristics

Hydrostatic gas bearings provide relatively high load capacity as a function of the externally supplied gas pressure. Optimum gas film thicknesses for hydrostatic bearings range from 0.0005 to 0.0015 inch, but due to the external pressurization, the effective gas film spring stiffness is much higher than for a hydrodynamic bearing. Spring rates may exceed 1,000,000 pounds per inch and cause the support of the bearing to be the determining factor in rotor bearing critical speeds. Hydrostatic bearings inherently provide little in the way of damping and generally require careful design and development to control this characteristic.

The ease of starting and stopping hydrostatic gas bearing systems is one of the outstanding features of this concept. A gas film is maintained at all times within the bearing, and friction and wear are at a minimum. Heavy rotors with large inertias can easily be started, stopped, and operated on these bearings.

Bearing stability of hydrostatic gas bearings operating over a wide range of speeds is a problem usually requiring control of the hydrostatic gas pressures as a function of the loads and speeds.

As with the hydrodynamic gas bearing, a hydrostatic gas bearing also requires good accuracy of the bearing components for reliable operation.

Common Characteristics

Hydrodynamic and hydrostatic gas bearings share some common characteristics. Both types of bearings are capable of operation at high temperatures and over a wide range of temperatures. The load capacity of gas bearings actually increases with increasing temperatures due to a corresponding increase in gas viscosity.

Light bearing loads tend to encourage gas bearing instabilities. As a consequence, most stable gas bearing designs incorporate provisions for preloads and/or a progressive loading device to keep the bearing in a stable region of operation. In some cases of very heavy rotors, the weight of the rotor is sufficient to maintain stable bearing operation, even to the point that the top half of a journal bearing is not required.

Shock and vibration are not easily tolerated by rigid or fixed geometry gas bearings. The tolerance to shock and vibration is greatly improved by providing flexible mounts and compliant bearing surfaces. The BRU-F foil bearing machine, shown in Figure 4.45, has sustained

(W)
Westinghouse

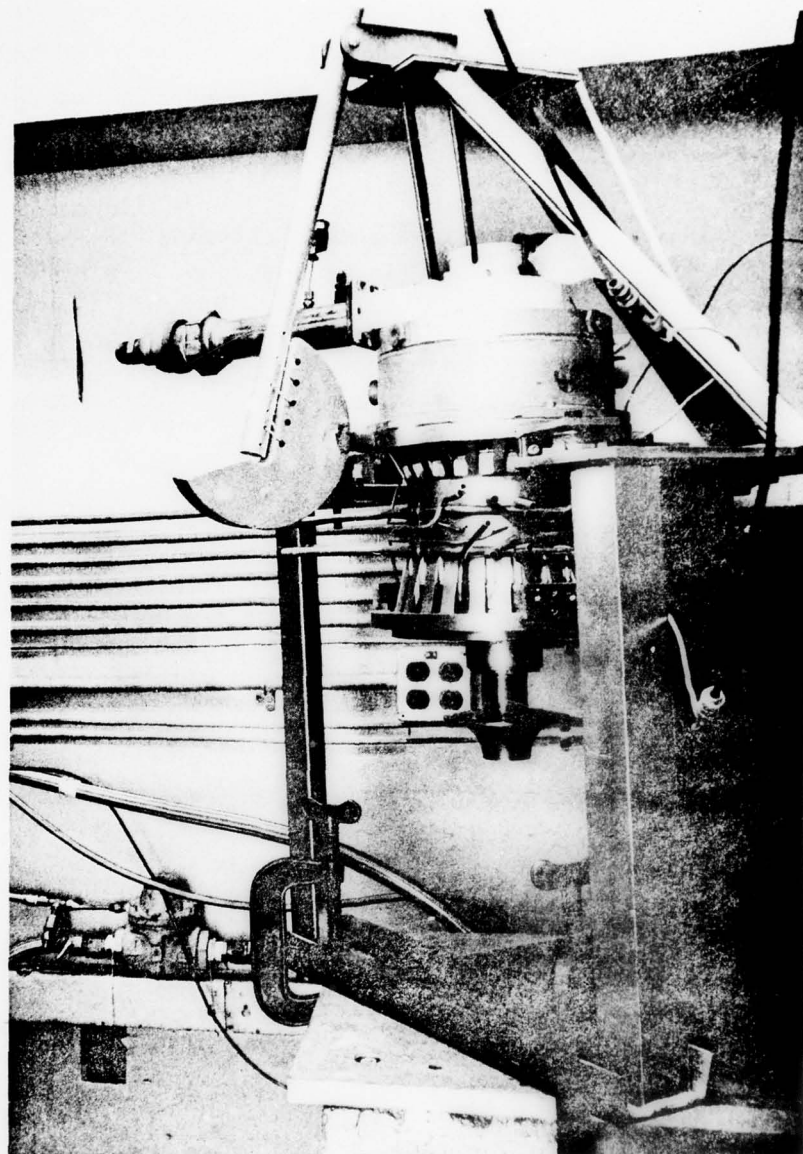


Figure 4.45 BRU-F Foil Bearing Machine Shock Tests



Westinghouse

repeated shocks up to 500 g's without failure. Rigid gas bearings are not tolerant of misalignment, thermal or centrifugal induced gradients unless some form of flexibility is incorporated in the bearing system design.

Comparison of Hydrodynamic and Hydrostatic Gas Bearing Characteristics

	<u>Hydrodynamic</u>	<u>Hydrostatic</u>
Load Capacity	Low-limited by viscosity of gas	High-Adjustable Function of Gas pressure
Starting and Stopping Capability	Limited to light bearing loads and low inertia rotors	Excellent
Stability	Good-over broad speed range	Fair-speed range limited
Power Loss	Low	Very Low
Tolerance to Shock and Vibration	Low to High	Low to High
Tolerance to Misalignment	Low to High	Low to High
Tolerant to Thermal and Centrifugal Distortion	Low to High	Low to High

Comparison of Solid and Compliant (Foil) Geometry Gas Bearings

<u>Solid Geometry</u>	<u>Compliant Geometry</u>
● Easier design for hydrostatic operation	● Requires extra shaft seals for hydrostatic operation
● Requires less hydrostatic gas flow	● Requires 50 to 100 percent more hydrostatic gas flow
● Provides close control aerodynamic clearances	● More allowance for aerodynamic clearances required
● Provides maximum load capacity	● Lower load capacity
● Low power loss	● Slightly higher power loss due to smaller film thicknesses
● Intolerant of thermal gradients, misalignment	● Tolerant of thermal gradients, misalignment
● Intolerant of momentary rubs	● Tolerant of momentary rubs
● Intolerant to shock vibration	● Tolerant to shock and vibration
● Requires hydrostatic starting and stopping except for very light loads	● Can be started and stopped hydrodynamically under twice the loads of a solid geometry bearing
● Less stable operation over wide speed range	● Stable operation over wide speed range
● Less stable operation with combined hydrostatic/hydrodynamic operation	● Stable operation with combined hydrostatic/hydrodynamic operation
● High fabrication costs	● Moderate fabrication costs

4.3.2.3 Gas Bearing Designs for CCCBS

The feasibility of operating a large scale (70,000 HP) closed Brayton cycle turbine on helium gas bearings was investigated by evaluating two basic gas bearing concepts as applied to supporting the turbomachinery shown schematically in Figure 4.46. Solid geometry and compliant geometry bearings, similar to those shown in Figure 4.47, were selected for comparison. All bearing evaluations were made on the basis of maintaining the CCCBS engine aerodynamic flow paths and rotor bearing spacing unchanged from the basic oil lubricated bearing CCCBS engine design.

Baseline Gas Bearing Design

Hydrostatic gas bearings were selected as the baseline gas bearing concept because they provide the highest load capacity gas bearing system and result in an acceptable envelope.

The bearing can be incorporated within the same cavity as the oil lubricated bearing with only minor changes to the engine shafting. In addition, hydrostatic gas bearing systems provide the necessary means for starting and stopping large inertia rotors such as those under consideration in this application. The hydrostatic bearing sizes tentatively established for the 70,000 HP CCCBS engine are shown in Table 4.10

The basic journal bearing design is shown in Figure 4.48. The bore of the bearing housing is divided into four pads by axial relief slots. Centered in each pad is a pressure pocket 0.005 to 0.010 in. deep and supplied by high pressure gas through an orifice. The pressure pocket area is approximately 1/9th the surface area of the pad. Ideally, in a functional bearing designed for all the known rotor dynamics, speeds, pressures, and temperatures, the four pads would be separated and individually resiliently mounted to accomodate the misalignment, thermal distortion, and transient conditions inherent of any bearing system.

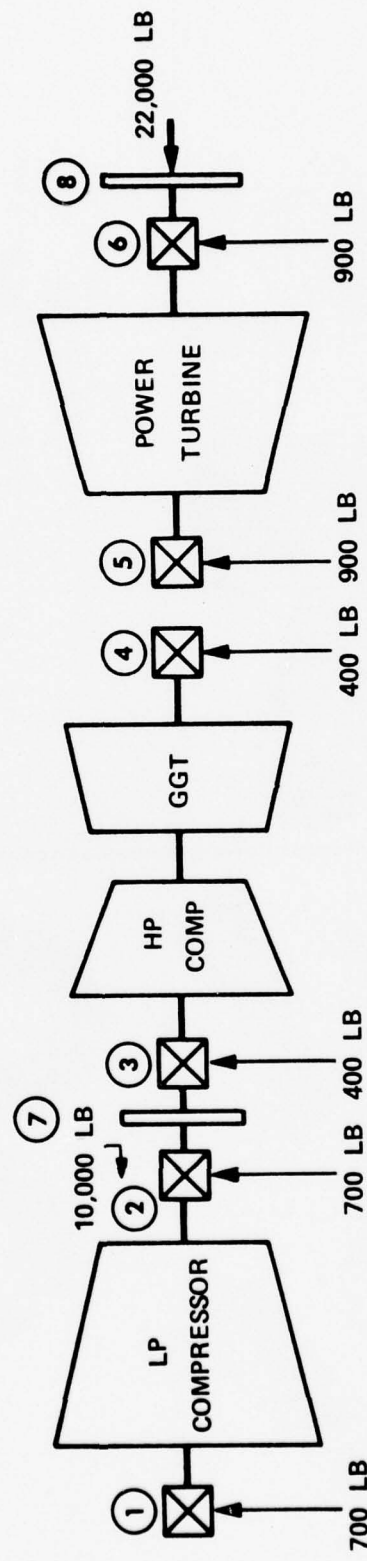


Figure 4.46 70,000 HP CBC Engine Bearing Support Schematic



Westinghouse

SOLID GEOMETRY

JOURNAL BEARING



COMPLIANT GEOMETRY

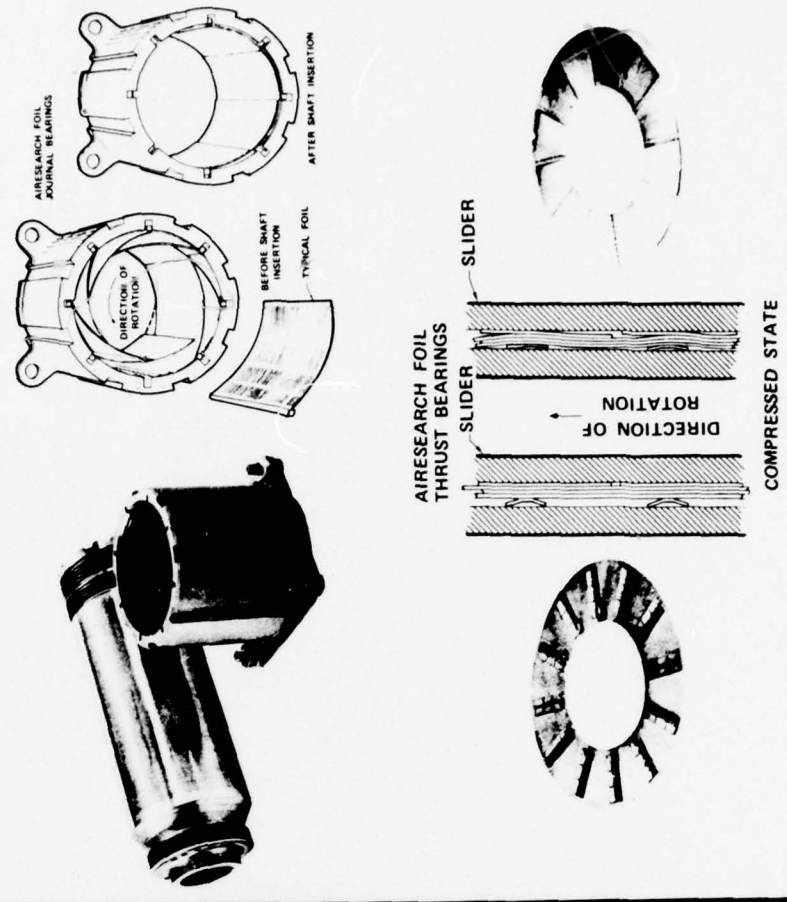


Figure 4.47 Gas Bearings

TABLE 4.10
HYDROSTATIC BEARING SYSTEM

Bearing No.	Bearing Load lb	Bearing Size Dia x Length in.	Helium Flow lb/sec
1	700	4 x 3.94	0.00420
2	700	4 x 3.94	0.00420
3	400	4 x 2.25	0.00420
4	400	4 x 2.25	0.00420
5	900	5 x 4.05	0.0190
6	900	5 x 4.05	0.0190
7	10,000	10.05 x OD x 3.5 ID	0.070
8	22,000	15.0 OD x 5.5 ID	0.070
		Total He Flow lb/sec or lb/min	0.1948 11.688



Westinghouse

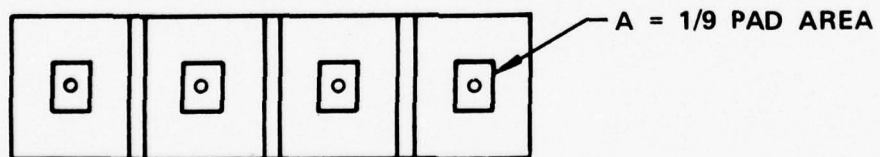
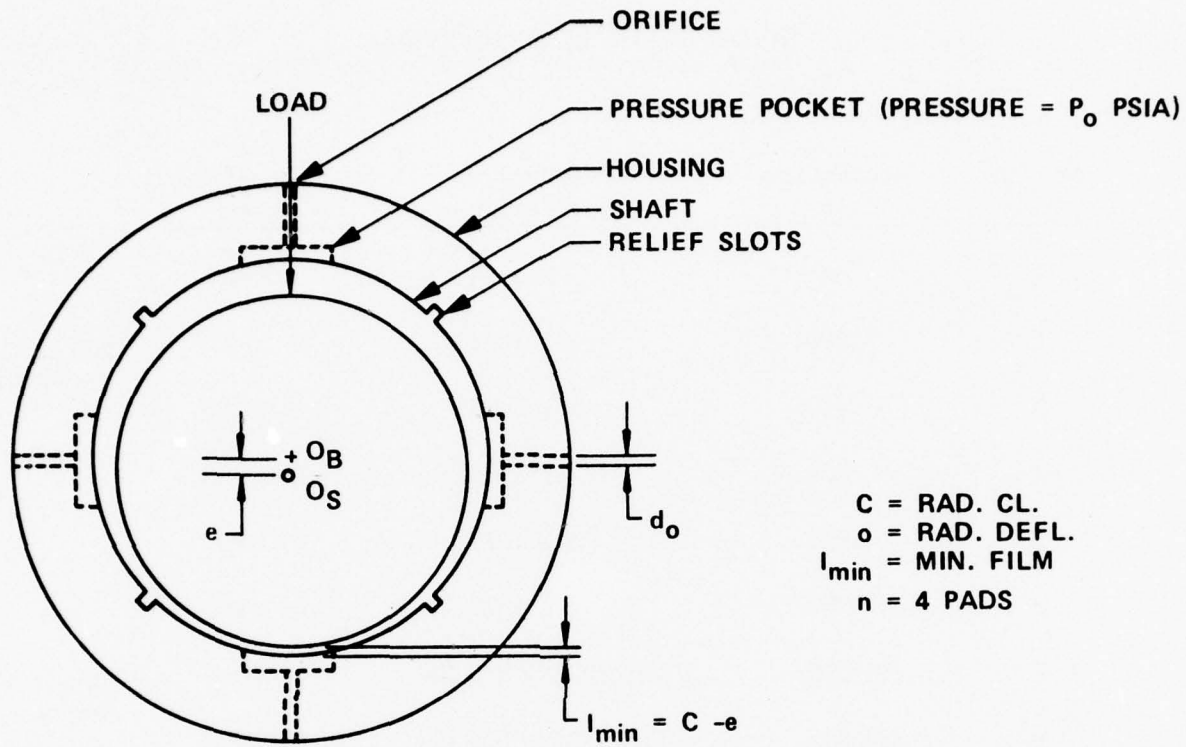


Figure 4.48 Journal Bearing Design

The basic thrust bearing design is shown in Figure 4.49. The flat stator of the thrust bearing is similar to the bearing housing of the journal bearing in that it is also divided into pad areas by radial slots. Each pad contains a pressure pocket and orifice similar to that in the journal bearing design. In the case of large thrust bearings operating with small clearances, the stator of the thrust bearing must be resiliently or flexibly mounted to accommodate normal dimensional variations. Pads can be individually mounted or connected as in the conventional Kingsbury design, or the entire stator may be gimbaled to follow the thrust runner.

The bearings were sized using the following rationale. It was assumed that helium could be supplied to each bearing so that a differential pressure of 200 psi could be maintained across each journal bearing orifice and 400 psi across each thrust bearing orifice. This means that, for all practical purposes, each bearing cavity would be maintained 200 or 400 psi below the helium supply pressure. Each thrust bearing would be a bi-directional design incorporating a hydrostatic side to carry the normally unidirectional aerodynamic thrust loads and hydrodynamic thrust side to position the rotor and accommodate thrust reversals due to starts/stops or load transients.

The high pressure helium required to support the gas generator rotor, including thrust loads, would be approximately 0.0868 lbs/sec, while the power turbine bearing system would require approximately 0.108 lb/sec, or a total flow of 0.1948 lb/sec for the complete engine bearing system. Helium flow can be reduced significantly by increasing the temperature from 200°F to 400°F or other temperatures acceptable from a thermal analysis or distortion standpoint.

Hydrostatic helium for the bearings can be supplied by bleed from the engine compressor or a separate compressor. For purposes of starting and stopping the machine, a storage tank or separate motor driven helium compressor would be recommended. Alternatively, the bearing gas supply system could be integrated with the engine gas management system.



Westinghouse

8-PAD HYDROSTATIC THRUST BEARING BASIC GEOMETRY

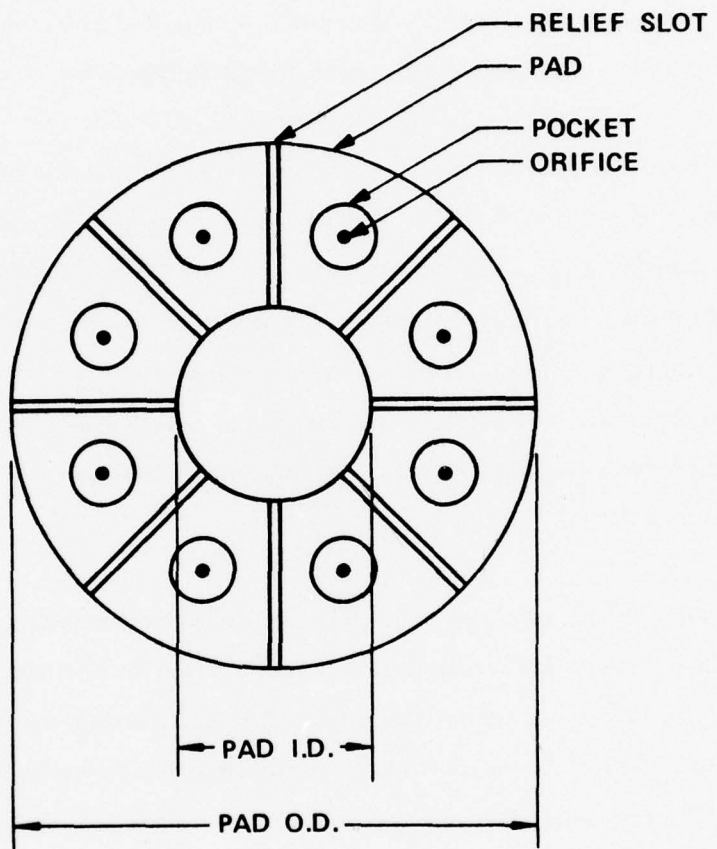


Figure 4.49 Thrust Bearing Design

Optional Gas Bearing Designs

With due consideration to the characteristic operation of pure hydrostatic gas bearings, several hydrodynamic gas bearing designs with superior stability were also selected for evaluation.

Standard overlapping hydrodynamic foil bearings of the configuration shown in Figure 4.47 were investigated and tentatively sized to support the turbomachinery. The concept provided hydrostatic starting to 50 percent design speed. The results are summarized in Table 4.11. Obviously, the resulting large bearing sizes would, if incorporated in the engine, necessitate a major redesign of the gas generator and power turbine and would also generate excessive bearing losses. For this application, the limited load capacity of overlapping hydrodynamic foil gas bearings results in unacceptably large bearings.

A recently developed improved version of the segmented foil journal bearings was also evaluated. The improved bearing incorporates a bump type spring system similar in purpose to the MTI Hydrosil bearing, but maintains the high damping of individual foil segments. This bearing design results in a three fold increase in load capacity compared to the standard overlapping foil bearing design. Use of the improved foil bearing design would decrease the journal bearings to the sizes shown in Table 4.12. These bearings could easily be incorporated within the basic CCCBS design.

The load capacity of compliant hydrodynamic thrust bearings has reached near optimum values. Consequently, hydrodynamic gas thrust bearings would be extremely large and impractical for applications such as the 70,000 HP CCCBS engine with thrust loads between 10,000 and 22,000 lbs. The only practical gas thrust bearing for this application is a hydrostatic design with large adjustable load capacity and relatively small size.



Westinghouse

TABLE 4.11

HYDRODYNAMIC FOIL BEARINGS

100 PSI AMBIENT PRESSURE

Bearing Number	Bearing Load lb	Bearing Size in.
1 Journal	700	8.375 dia x 10.47 long
2 Journal	700	8.375 dia x 10.47 long
3 Journal	400	6.74 dia x 8.47 long
4 Journal	400	6.75 dia x 8.47 long
5 Journal	900	16,000 dia x 12.80 long
6 Journal	900	16,000 dia x 12.80 long
7 (Gas Gen. Thrust)	10,000	21.5 OD x 6 ID
8 (Power Turbine Thrust)	22,000	31.4 OD x 7 ID

TABLE 4.12

IMPROVED INTEGRATED FOIL
JOURNAL BEARING DESIGN

<u>Bearing Number</u>	<u>Bearing Load Lb</u>	<u>Bearing Size - inch</u>
1	700	6.24 dia x 6.24 long
2	700	6.24 dia x 6.24 long
3	400	4.71 dia x 4.71 long
4	400	4.71 dia x 4.71 long
5	900	7.05 dia x 7.05 long
6	900	7.05 dia x 7.05 long

4.3.2.4 Gas Bearing Recommendations

Since hydrostatic starting and stopping provisions must be included in gas bearings capable of supporting turbomachinery in the 70,000 HP class, a hybrid hydrostatic/hydrodynamic foil bearing system appears to be the optimum gas bearing design. Such a hybrid bearing system would provide the load capacity of a hydrostatic system and the stability and mechanical tolerance of a compliant foil bearing system. Thrust bearings would be primarily hydrostatic in operation with backup provisions for hydrodynamic operation during engine transients. Journal bearings would be jointly operated hydrostatically and hydrodynamically to provide the ultimate load capacity and mechanical tolerance to rotor dynamics. The journal bearings would be sized to carry the full load hydrodynamically.

The recommended gas bearings for the 70,000 HP CBC engine are shown in Figures 4.50 through 4.53. Each figure defines a separate bearing cavity for the gas generator LP spool, HP spool and the power turbine. The cavities lie within the aerodynamic flow passages established for the trial design 70,000 HP CCCBS engine. Labyrinth shaft seals would be required to maintain the bearing cavity pressures below the hydrostatic supply by a suitable margin.

4.3.2.5 Ancillary Equipment

The use of hydrostatic gas bearings requires a source of pressurized gas. For starting and stopping of the 70,000 HP CCCBS engine, a storage tank of pressurized helium would be required. Suitable regulators, valves, and controls would be required to introduce and modulate the hydrostatic pressures as a function of loads and speeds. The helium storage tank could be a part of the CCCBS gas management system or a separate tank and motor driven compressor.

Once the CCCBS engine is started and brought to design speed, the required hydrostatic gas could be bled from the main CCCBS engine compressor. The thrust bearing hydrostatic pressures could be allowed to float with the CCCBS engine power level and the corresponding closed loop

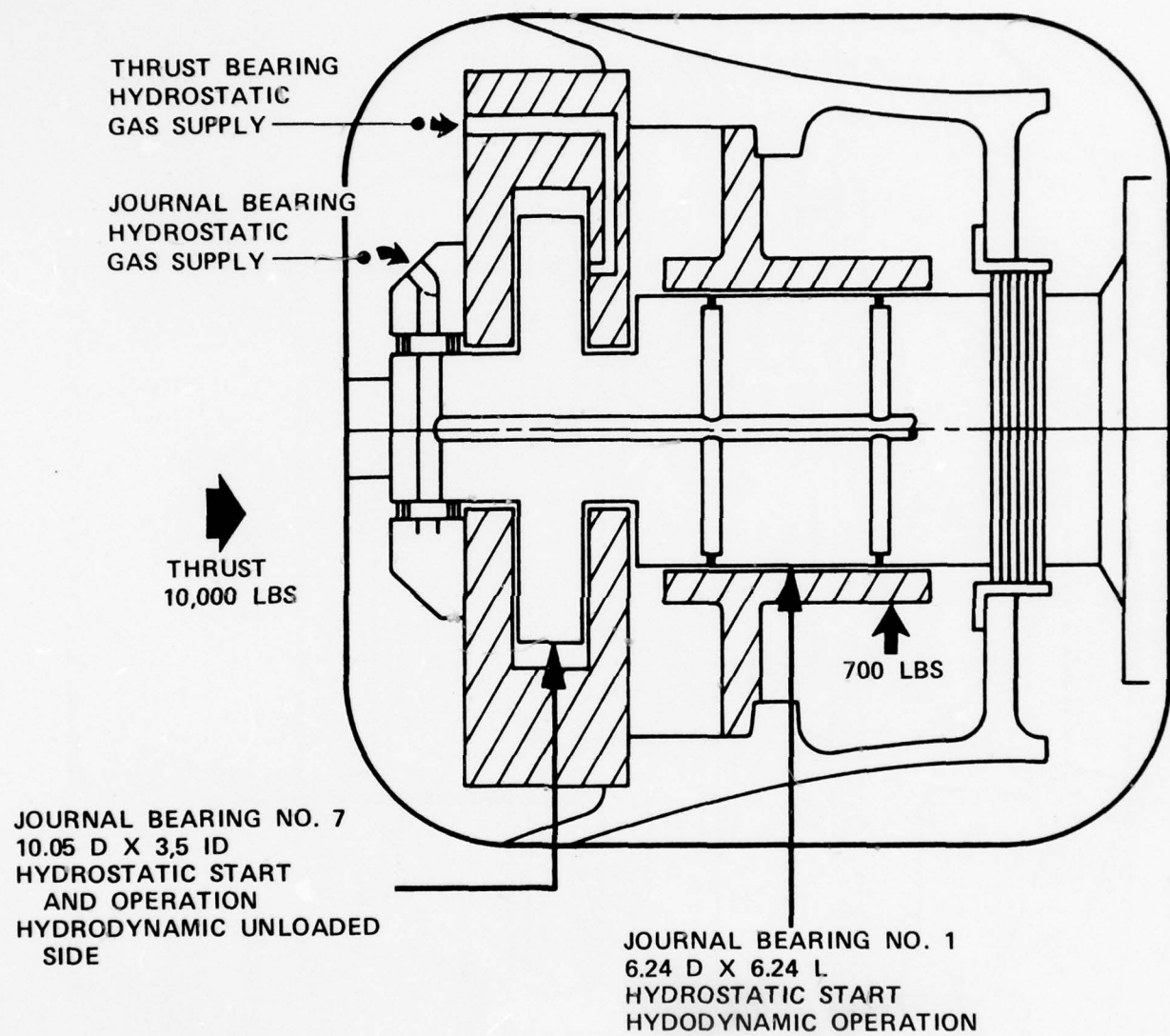


Figure 4.50 Gas Generator L.P. Compressor Thrust and Journal Bearings



Westinghouse

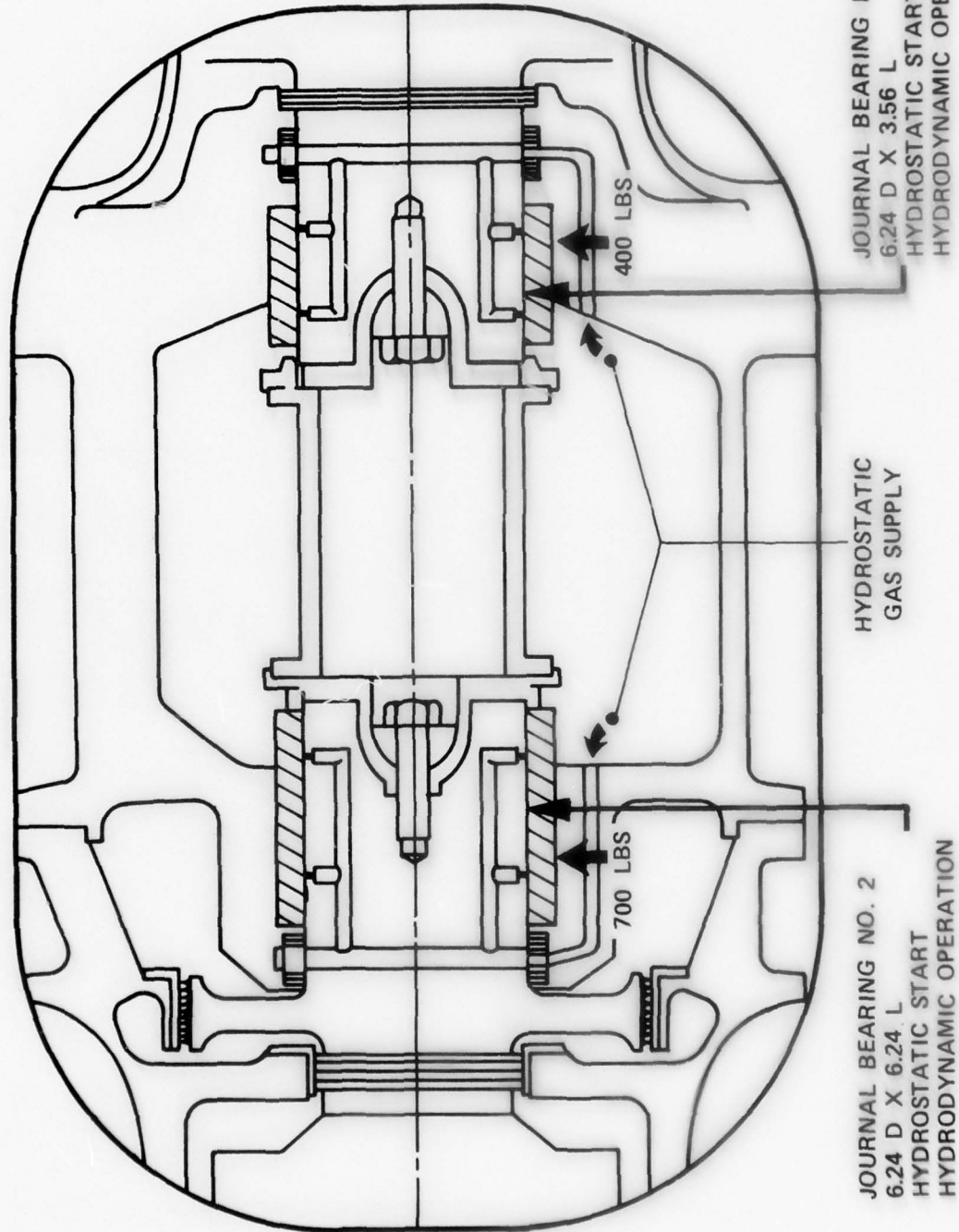


Figure 4.51 Gas Generator L.P. and H.P. Speed Journal Bearings

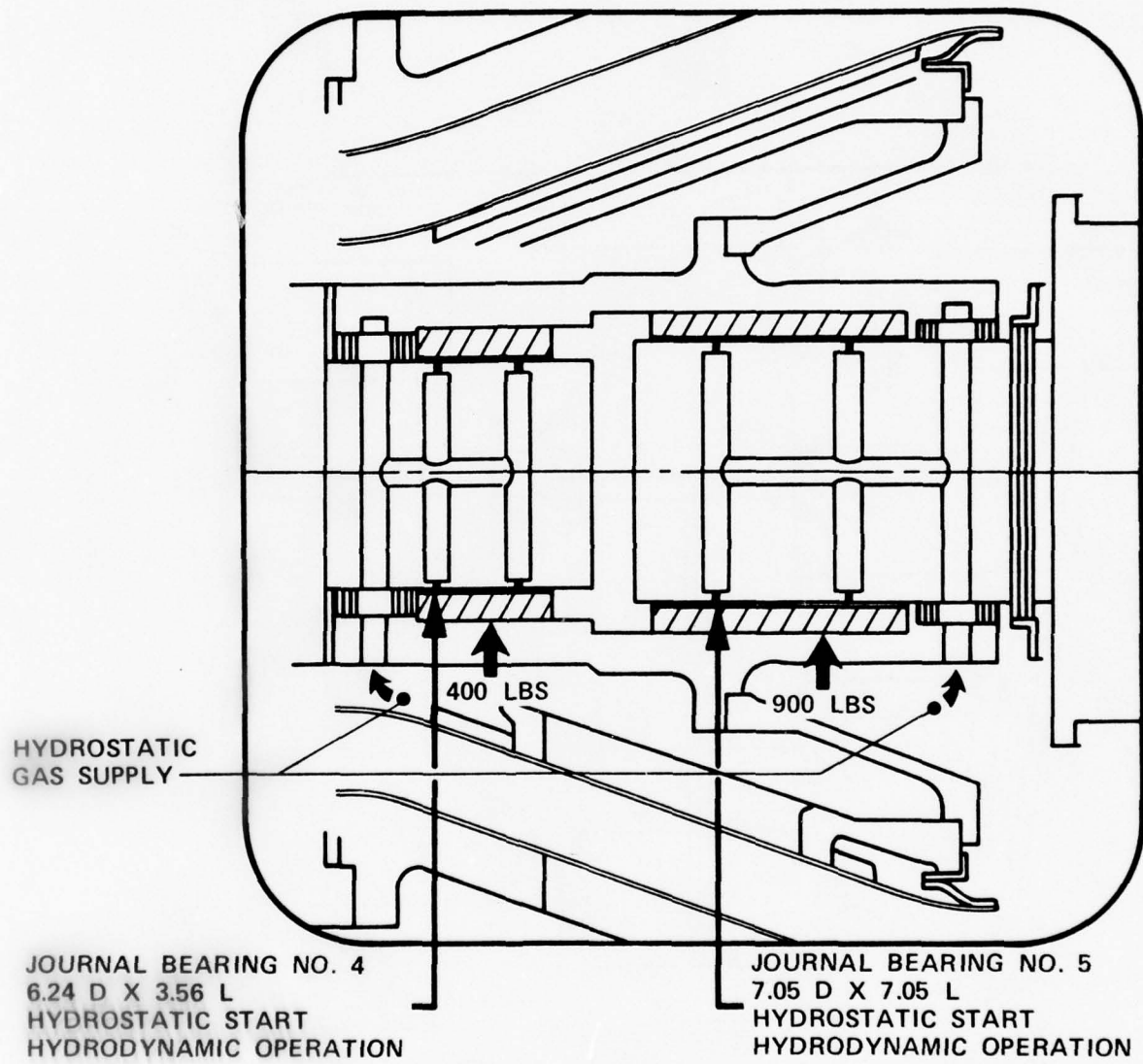


Figure 4.52 Gas Generator/Power Turbine Journal Bearings



Westinghouse

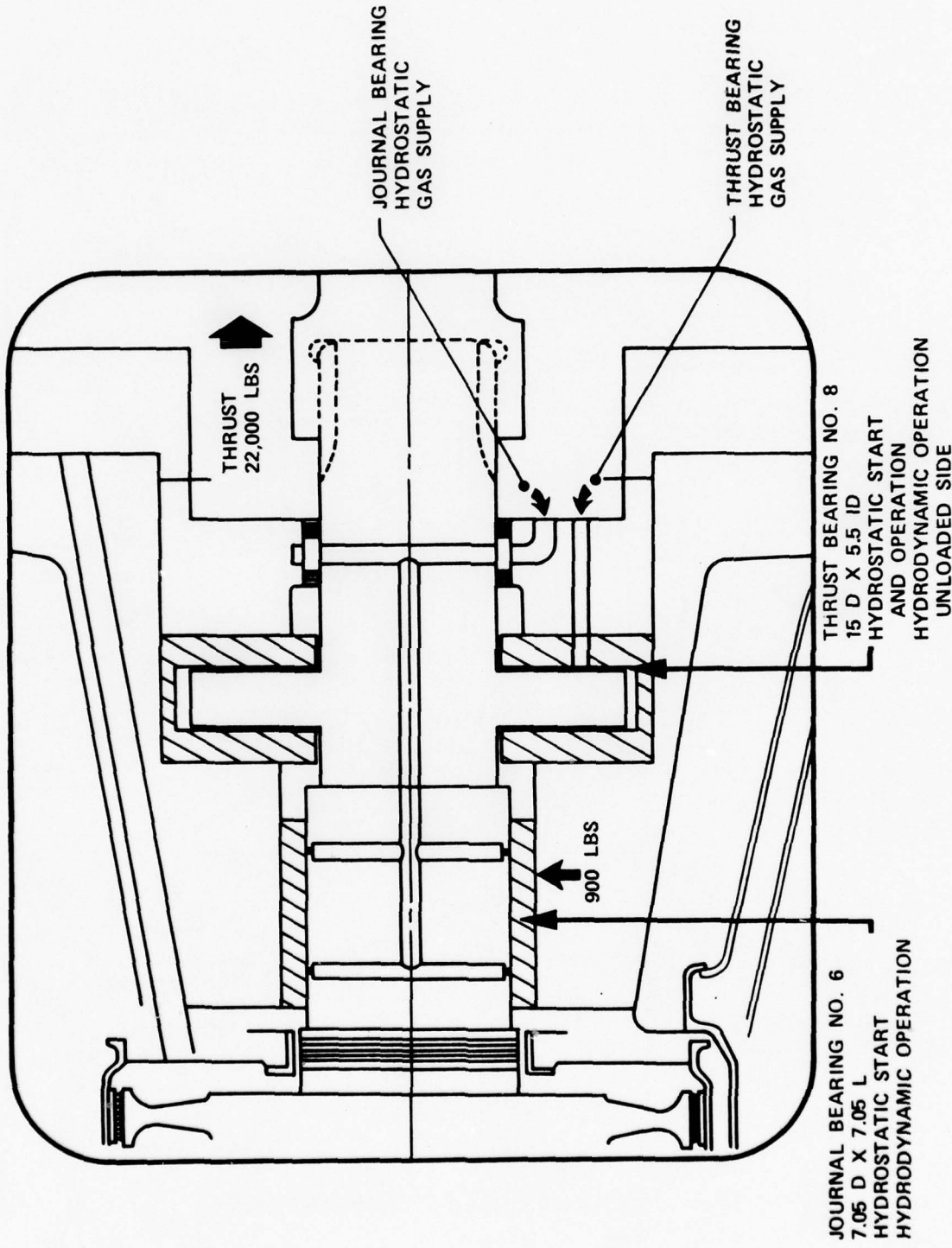


Figure 4.53 Power Turbine Journal and Thrust Bearings

pressures. This approach is practical because the aerodynamic thrust loads also vary in phase and in proportion to the changes in loop pressure; i.e., low power, low loop pressures correspond to low aerodynamic thrust loads, and the hydrostatic pressures to the thrust bearings can be correspondingly reduced. Since the journal bearings would be designed to carry the full radial loads in a hydrodynamic mode, variations in hydrostatic pressures would be of no concern. In fact, the hydrostatic gas could be turned off to the journal bearings at all times except during starting and stopping of the CCCBS engine.

Due to the extremely low friction losses of hydrostatic gas bearings and the high inertia rotating groups of the CCCBS engine, the roll down to a full stop would take many minutes, even with a cold engine heat source. A 70,000 HP CCCBS engine shut down from full or partial load would conceivably take hours to stop due to the stored energy in the heat source heat exchanger and recuperators. Supplying hydrostatic gas to the bearings from a storage tank during a prolonged roll down becomes impractical unless a make up compressor can supply the required flow. Aside from the prolonged need for hydrostatic gas supply, it does not appear reasonable or practical to tolerate a multihour shut down of the engine. Therefore, a means to load and brake the CCCBS engine rotating groups to a stop in a reasonable time compatible with the hydrostatic storage tank supply should be considered. As a matter of practice, other closed Brayton engines have utilized a loaded generator to absorb as much stored energy as possible prior to applying mechanical or pneumatic braking. This approach minimizes the thermal soak back into the engine and protects the heat exchangers equipment from large transients.

4.3.2.6 Gas Bearing Technology Development

Recent gas bearing development tests for other small CCCBS engines have indicated that current gas bearing theories do not correlate well with actual bearing performance when mono atomic gases are used at high pressures. AiResearch is currently conducting a company sponsored research and development (R and D) program to investigate the apparent discrepancies. It is noted that the R&D work is directed toward small bearings initially and that scaling to large bearings may introduce additional unknown factors. Initial results of the R and D program will be analyzed, and a course of action established for R and D on large gas bearings.

4.3.3 Comparative Evaluation and Selection

The evaluation of the oil and gas bearings consisted of rating the candidates with respect to a number of criteria. The criteria used in the evaluation are shown in Table 4.13 with their corresponding weighting factors and are discussed in the following paragraphs. The weighting factor is an estimate of the importance of the criterion or the influence the choice of bearing system has on the attribute being used as the criterion. The rating factor is an estimate of the degree to which each bearing type being evaluated satisfies the criterion in comparison to the type which best satisfies it. The weighting and rating factors are assigned numbers up to 10. Since a comparison such as this is between candidates which, by definition, meet all fundamental requirements, the methodology requires that the best alternate be assigned a rating of 10. The weighted ratings (i.e., the product of weighting and rating factors) for all criteria are summed for each bearing type to give a measure of the overall merit of each bearing type with respect to the criteria (Table 4.14). The gas bearings rated in this evaluation are the rigid geometry type because of the more extensive specific information regarding this type of gas bearing.

4.3.3.1 Bearing Comparisons

Impact on Powerplant Weight and Volume

Although powerplant weight and volume are important characteristics in themselves, the effect of the choice of turbomachinery bearings on either of these characteristics was determined to be small. A low weighting factor was therefore assigned.

In rating the bearings, consideration was given to the volume of the tankage, deaeration, cooling and filtration systems associated with oil bearing systems which would not be required if gas bearings were used. This resulted in a small rating penalty for the oil bearings with respect to powerplant volume. Since the weight contribution of either system is negligibly small in relation to the overall powerplant weight, the two types were rated equal with regard to their effect on powerplant weight.

TABLE 4.13
EVALUATION CRITERIA FOR BEARINGS

	Weighting Factor
● Low Powerplant Weight	2
● Low Powerplant Volume	2
● High Compatibility with Other Powerplant Components	10
● Simple Auxiliary Systems	7
● High Malfunction Suitability	10
● High Technology Base	7
● Low Development Cost	6
● Low Fabrication Cost	3
● High Reliability	10
● High Maintainability	2



Westinghouse

TABLE 4.14
OIL BEARING/GAS BEARING TRADE-OFF-STUDY

Criterion	Weighting Factor	Ratings			
		Journal Bearing Oil	Journal Bearing Rigid Gas	Thrust Bearing Oil	Thrust Bearing Rigid Gas
Low Powerplant Weight	2	10	10	10	10
Low Powerplant Volume	2	8	10	8	10
High Compatibility with Other Components	10	4	10	4	10
Simple Auxiliary Systems	7	5	10	5	10
High Malfunction Suitability	10	10	7	10	7
High Technology Base	7	10	6	10	4
Low Development Cost	6	10	8	10	7
Low Fabrication Cost	3	10	8	10	8
High Reliability	10	10	10	10	10
High Maintainability	2	8	10	8	10
Overall Merit (Total of Weighting Factor x Rating)		487	514	487	494

High Compatibility with Other Powerplant Components

Compatibility with other powerplant components is most pertinently associated with a lack of potential for contaminating the closed cycle helium working fluid. Obviously, oil lubricated bearings are at a distinct disadvantage in this respect. In a nuclear plant, the potential for contamination of the cycle helium due to malfunctions leading to oil leakage from bearings is particularly detrimental.

For these reasons, compatibility with other powerplant components was assigned the highest possible weighting factor (10). In rating the bearings, the oil bearings were assigned very low ratings factors relative to the gas bearings.

Simple Auxiliary Systems

Simplicity of auxiliary systems was judged to be of less importance than the compatibility criterion and was therefore assigned a somewhat lower weighting factor of 7. The oil bearings were judged to require more complex auxiliary systems than the gas bearings. This is especially true in a nuclear system where buffer gas systems are employed with the bearing seal systems to prevent contamination of the lubricating oil by fission products. De-misting of the breather gas in labyrinth sealed oil lubricated closed cycle powerplants is essential since the gas must be recycled and must not be permitted to foul turbomachinery blading or load up clean up system components. Complete de-misting will probably require the use of electrostatic precipitation. The need for this additional contamination control equipment, which would not be needed with gas bearings resulted in the assignment of a low rating to the oil bearings.

High Malfunction Suitability

This criterion was considered important and was assigned a weighting factor of 10. The oil bearings were judged to be highly tolerant of momentary overloads resulting from high pressure spikes, loss of a blade, etc. and were assigned a rating factor of 10. The gas bearings

were believed to be more sensitive to momentary overload conditions and were given a rating factor of 7.

High Technology Base

The technology base was considered to be of somewhat less than major importance and was assigned a weighting factor of 7. Here the gas bearings were penalized with ratings of 6 for the journals and 4 for the thrust bearings versus 10 for the oil bearings. Oil bearings have, of course, been almost universally used since the dawn of the industrial revolution, whereas gas bearings have a good technology base but only recently found relatively limited application.

Low Development and Fabrication Cost

Bearing development and fabrication costs would be expected to form a very small part of the overall powerplant development cost and are not considered to be of the greatest importance in themselves. Development cost was assigned a weighting factor of 6 and fabrication cost a factor of 3. Fabrication cost of the production bearings in the system will obviously have very little effect on the cost of the powerplant.

The gas bearings were judged to be more costly to develop and manufacture than the oil bearings and were rated accordingly. The gas thrust bearing was rated somewhat lower than the gas journal bearing from the development cost standpoint since the capability of handling high thrust loads is a critical development requirement for the gas bearings. With respect to low development cost, the gas journal bearings were rated at 8 and the thrust bearings at 7. Rating factors of 8 were assigned to the gas bearings for low fabrication cost. The oil bearings received rating factors of 10 in both cost criteria areas.

High Reliability

Reliability is obviously of great importance and was therefore assigned a weighting factor of 10. With adequate development, the reliability of the gas bearings should be comparable to that of the oil bearings. Both types were accorded equal ratings.

High Maintainability

Maintainability was assigned a weighting factor of 2 because the usage will place the emphasis on reliability rather than maintainability. The oil bearings were judged to be less desirable from the maintainability standpoint than the gas bearings. The gas bearings in the DC-10 cabin cooling air cycle machine, which has accumulated more than 14,000,000 total hours of commercial operation, require no maintenance. Oil bearing maintainability is compromised by system complexity relative to gas bearings. Electrostatic precipitation, coolers, filters and buffer gas systems are involved. Oil bearings were accorded a rating factor of 8.

4.3.3.2 Conceptual Design Selection

The overall ratings are summarized in Table 4.13. The results indicate a slight, although not great, superiority for rigid gas bearings. The most important influence contributing to this result is the poor compatibility of the oil bearings with the other components.

The trade-offs shown in Table 4.13 are based on the assumption of the rigid geometry type of gas bearing. However, had the compliant type been used as the basis of comparison, the ratings accorded the gas bearings would probably be still higher and would not have changed the selection. Compliant gas bearings have a high technology base and would require simpler auxiliary systems than the solid geometry gas bearings. It can also be argued that the compliant bearing has a higher malfunction suitability due to its ability to operate with a large eccentricity between the shaft and bearing.

From the specific studies of oil lubricated and of gas bearings and from the above comparisons, it was concluded that either type of bearing could suitably fulfill the CCCBS requirements. Each of the two types would require essentially the same size bearing cavities. Thus, selection of one type or the other for inclusion in the Design Concept would not constrain the design. This is very important because it indicates that demonstration of CCCBS feasibility will not depend upon a specific bearing type.



Westinghouse

Based upon these study results and comparisons, gas bearings were selected for inclusion in the CCCBS Design Concept. This will enable design attention to be focused on the gas bearings which are inherently most compatible with closed cycle powerplants, especially with those utilizing nuclear heat sources, and appear to have the potential for even greater advantages in the CCCBS application.

4.4 REFERENCES

1. K. Bammert, et. al., "Highlights and Future Development of Closed-Cycle Gas Turbines," ASME Paper No. 74-GT-7.
2. C. F. McDonald, "Gas Turbine Recuperator Technology Advancements," ASME Paper No. 72-GT-32.
3. H. R. Cox, Gas Turbine Principles and Practice, D. Van Nostrand Company, Inc. 1955.
4. K. Bammert, et. al., "Layout and Present Status of the Closed Cycle Helium Turbine Plant Oberhausen," ASME Paper No. 74-GT-132.
5. A. J. Wheeler, et. al., "Small Gas Turbine Engine Component Technology Regenerator Research," USAAV LABS Technical Report 66-90, January 1967.
6. I. Amato, et. al., "Brazing of Stainless Steel Heat Exchangers for Gas Turbine Applications," Paper presented at sixth AWS-WRC Brazing Conference Cleveland, Ohio, April 1975.
7. I. Stambler, "Working on 5000 - Cycle Trouble-Free Regenerator," Gas Turbine World, Vol. 6, No. 3, July 1976.
8. J. D. Duncan, "Brayton Heat Exchanger Unit Development Program (Alternate Design) Final Design Report, NASA CR-121269, August 1973.
9. D. E. Thomas, D. M. Moon, S. C. Singhal, F. G. Arcella, R. E. Witkowski, B. R. Rossing, T. Vojnovich, F. J. Harvey, II and A. R. Vaia, Energy Conversion Alternatives Study (ECAS), Westinghouse Phase I Final Report, Volume II Materials Considerations, 76-9E9-ECAS-Rw2, Westinghouse Research Laboratories, February 12, 1976.
10. F. R. Spurrier, Designing the Marine Gas Turbine, Mechanical Engineering, September 1957.
11. Maritime Gas Cooled Reactor Project Engineering Report No. EC-142 on Turbine Model Test as authorized by U.S. Maritime Administration Contract MA-2795, June 1962.
12. Technical and Economic Assessment of the Direct Cycle Gas Cooled Reactor Plant. ERDA-109, September 1975.
13. S. F. Smith, A Simple Correlation of Turbine Efficiency, Jour. Aeronaut. Sci. 69 (1965) 468.



Westinghouse

14. O. Zweifel, "The Spacing of Turbomachine Blading, Especially with Large Angular Deflection," Brown Boveri Review, December 1945.
15. J. W. Capitao, R. S. Gregory and R. P. Whitford, "Effects of High Operating Speeds on Tilting Pad Thrust Bearing Performance," ASME Paper No. 75-LubS-6, 1975.
16. J. W. Capitao, "Performance Characteristics of Tilting Pad Thrust Bearings at High Operating Speeds," ASME Paper No. 75-LubS-7, 1975.
17. R. S. Gregory, "Performance of Thrust Bearings at High Operating Speeds, ASME Paper No. 73-LubS-16, 1973.
18. N. H. New, "Experimental Comparison of Flooded, Directed and Inlet Orifice Type of Lubrication for a Tilting Pad Thrust Bearing," ASME Paper No. 73-LubS-5, 1973.
19. W. W. Gardner, "Performance Tests on Six Inch Tilting Pad Thrust Bearings," ASME Paper No. 74-Lub-13, 1974.
20. A. J. Leopard, "Directed Lubrication for Tilting Pad Thrust Bearings," Tribology, November 1970.
21. A. J. Leopard, "Thrust Bearings for Gas Turbines," ASME Paper presented at Gas Turbine Conference and Products Show, Houston, Texas, March 1971.
22. A. J. Leopard, "Tilting Pad Bearings - Limits of Operation," ASLE Meeting, Atlanta, May 5-8, 1975.
23. Glacier Load Capacity Guidance Chart - Design Aid No. 1.
24. D. F. Wilcock and E. R. Booser, "Bearing Design and Application," McGraw-Hill, 1957.
25. Machine Design, June 3, 1976.
26. Kingsbury Catalog EQ.
27. M. K. Bielec and A. J. Leopard, "Tilting Pad Thrust Bearings: Factors Affecting Performance and Improvements with Directed Lubrication," Proceedings of I. Mech. E., Vol. 184, Pt3L, 1970.
28. A. A. Raimondi and J. Boyd, "The Influence of Surface Profile on the Load Capacity of Thrust Bearings with Centrally Pivoted Pads," Trans. ASME, Vol. 77, pp 321-330, 1955.

29. Telephone Communication with W. Chambers, Kingsbury Machine Works, Philadelphia.
30. Waukesha Tilting Pad Journal Bearing Catalog, W-2A.
31. E. R. Booser, F. D. Ryan and C.L. Kinkinhoker, "Maximum Temperature for Hydro-dynamic Bearings under Stead Load," July 1970, Lubrication Engineering, pp 226-235.
32. "Maritime Gas Cooled Reactor Project - Engineering Report No. EC-167 on Development of Turbomachinery," Westinghouse Electric Corporation, Lester, Pa., June 1963.
33. T. J. Fowle, "Problems in the Lubrication Systems of Turbomachinery," Proc. Inst., Mech. Engrs., Vol. 186 60/72.

5.0 CCCBS/ PROPULSION PLANT INTERFACES

5.1 ELECTRICAL POWER TRANSMISSION INTERFACE CONSIDERATIONS

5.1.1 General

Compact electric power transmission systems are recognized to be candidates for some of the Navy ships of the future. Although such systems are external to the power conversion system scope as defined for this feasibility study, the impact of the characteristics of this type of load as they effect the interfaces with the gas turbine is of importance. Application of electric power transmission systems to a compact closed cycle Brayton powerplant could introduce interface considerations which do not exist in other installations. Therefore, studies were conducted to identify and address those considerations which could possibly have an important impact upon gas turbine/powerplant design characteristics or upon power-plant/ship interfaces that must be considered in the subsequent evaluations of the study.

Interest in electrical propulsion systems has been justified by the inherent ability to provide a satisfactory speed reduction between a high speed, efficient, lightweight prime mover and a slower, efficient propulsor. As well, certain flexibility of design regarding plant choice and arrangement yields rewards to the naval architect and owner. Rapid maneuvering control is advantageous to the ship operator. Briefly summarized, the advantages of electrical propulsion include:

- Flexibility of ship arrangements due to freedom of location of major components relative to prime movers.
- Economy of operation with multiple prime movers to reduce the high fuel rate at part load.
- Flexibility, availability, and interchangeability among multiple prime movers.
- Use of high efficiency unidirectional prime movers.



Westinghouse

- Optimum maneuverability through relatively simple control systems.
- Capability to provide higher torques at reduced speeds.
- Ease of adaptation to automated plant control.
- Possible reduction in crew size through automated control of machinery.
- Low maintenance cost of electrical transmission system.
- Ease in providing pilot house and remote controls.
- Reliability of operation of overall system.
- Reduced vibration and structure-borne noise.

These manifold advantages of electric drive are related to specific applications. Further, the advantages and merits of one system over another are in complex relationship among the following variables:

- Horsepower level and rpm required in the ship concept under study.
- Desired maneuvering requirements and the minimum maneuvering requirements acceptable.
- Alternative uses of main propulsion power anticipated in the ship system.
- Proportion of weight fraction that can be allotted to the propulsion system.
- Geometrical constraints of the hull-propulsion system interface.

The excellent reliability of electrical propulsion systems and the flexibility provided by the ability to separate prime mover from propeller shafting have been significant in the history of marine propulsion. In particular, the advent of superconducting electrical machinery suitable for ship propulsion has indicated great reductions in weight and volume. This is

particularly evident for high performance ships -- including hydrofoil and Surface Effect Ships, where the use of light-weight electrical propulsion apparatus will allow the unusually high horsepower required to be delivered from the prime mover to the thrusters usually located remote from the powerplants. This is an attractive alternative to right angle gearing which experiences low endurance and reliability in the marine environment. The hydrofoil motor can be contained within a propulsion pod due to its small diameter and the SES can be propelled by super-cavitating props or water jets. In summary, the application of superconduction electrical machinery to ship propulsion will result in an increase of flexibility, system efficiency, and a decrease of volume and weight relative to conventional systems.

The use of superconducting transmission bus, however, is not practical at this time for ship propulsion systems, thus generators and motors are the most feasible candidates for superconducting technology. Systems under consideration are presently all ac, all dc or hybrid combinations of ac and dc. Certain applications to high speed propeller ships such as hydrofoils and SES, which do not require reversal, appear naturally suited for ac synchronous installations. Other installations are not so easily defined as to the optimum propulsion plant. The traditional high maneuverability aspect of dc propulsion that has been in service in tugs, ferries and icebreakers may be difficult to achieve in certain installations of superconducting homopolar generators and motors, due to the extremely high magnetic energy stored in the fields and the requirements that they be varied in very short time intervals.

Many electrical propulsion installations have used generator field control coupled with control of governing of prime mover speed. The importance of prime mover and load scheduling will increase as the need is recognized for good fuel consumption.

In many propulsion applications utilizing electrical components, control of motor speed is achieved through variations of several parameters:

- Generator output voltage by speed control of prime mover, generator excitation, or combinations of both.



Westinghouse

- Field of propulsion motor.
- Input voltage to the motor terminals through control circuitry.

The required power level is determined by the torque demanded at specific propulsor speeds as a function of ship speed. This torque is generally proportional to the current drawn by the propulsion motor, and the field strength which is related functionally to the speed of rotation.

Several cases of ship propulsion have been surveyed, with information gathered to determine feasibility of concept application over the power and rpm range involved. Some of these applications will require reversal and operation at various rpm in both forward and reverse directions. In some instances, the reversals are required quickly, possibly in rapid succession and in minimum time.

A number of ship propulsion applications involve high powers at revolutions much higher than those of conventional displacement ships. These include advanced marine vehicles such as hydrofoils, surface effect ships, and certain types of planing hull vessels. In these types of installation, reversal is not required for the high power shaft and these ship types are the most likely to use the compact CCCBS power source. For use in the nonreversing high rpm propulsion system, superconducting ac synchronous generators and motors, seem more attractive combinations. Indeed, the use of homopolars, superconducting or not, for SES thrust and lift would be difficult due to distribution problems of the low voltage, high current power to lift fans and propulsion thrusters through extraordinarily heavy copper bus bars. Higher voltage dc generators to alleviate this problem have to be considered but they lead to other design problems discussed later.

With regard to variation of field current and flux parameters, it will suffice here to note that typical dc electrical propulsion applications utilize variation of generator excitation to achieve voltage control over the range from zero output to saturation voltage output at the minimum speed of the prime mover. The remaining system voltage is generated by increase

of prime mover speed from the minimum to maximum speed. In a ship propulsion application, this variation of voltage will vary the motor speed in a reasonably linear fashion, with the increased torque loading drawing current as required by the characteristics of the load.

Typical ac electrical propulsion installations rely on simultaneous control of excitation, prime mover, and phase interconnections. In typical synchronous ac installations, switch-gear or contactors are used to interconnect the phase order of power into the synchronous motor for directional control. The prime mover is brought from set power to a low value to permit the interchange of phases. Simultaneous control of excitation is required, decreasing to enter the asynchronous induction mode of operation. Over excitation of generators and run-up of prime movers will lock the motor into synchronism in the reverse direction.

The steady state and transient response of superconducting electrical machines must be completely defined prior to successful shipboard implementation. The naval ship propulsion system must be capable of reliable operation under a wide range of typical marine environment operating conditions that represent transient motion of the naval vessel, including:

- Conventional speed and course changing maneuvers
- High-speed turns
- High-speed reversals
- Ship twisting maneuvers
- Any combination of the above

These maneuvers introduce transient departure from steady state conditions into the electro-mechanical power transmission system, transients which must either be accepted or attenuated, as they manifest themselves in certain instances as ac rotor losses. The general thermal transients introduced into the cryogenic superconducting field system will be realized as heat. As the machine must be maintained in the superconducting mode, the quench situation must

be avoided. The transients under consideration could generate inception of quench (normalization) in the superconductor if they are not understood and considered. This combination of transients, reflected from the thruster element of the ship propulsion transmission system, is manifest as electrical and mechanical phenomena in the system, and is ultimately transmitted to the prime mover through the electromechanical network.

These transients will reflect themselves into motions departing from the electromechanical steady state and manifest themselves as certain ac losses in the superconductor field winding. These losses must be compensated for in the design with sufficient helium flow for the field winding or eliminated by sufficient shielding by damper attenuating windings or by electromagnetic shielding coils. While these losses must be tolerated in some sense, they will essentially determine the refrigeration sizing in propulsion systems.

5.1.2 Electrical Equipment System Considerations

This section will consider the factors influencing the selection of various components and subsystems, and the resulting identifiable parameters and characteristics of the system.

The selection of systems requires the investigation of the alternative ac, dc, and hybrid combinations; the influence and significant consequence of candidate propulsor types; and the optimization of the liquid helium refrigeration system configuration for a given ship concept.

System composition may then be detailed into identification of such major components as motors, generators, and refrigeration, as well as essential subsystems of excitation, cables and current transmission, control, power conditioning, switchgear, and protection circuitry. The characteristics of available prime movers, and the requirements of significant auxiliaries will be discussed.

System parameters such as voltage, temperature, overload capacity, and ventilation must be considered, as well as an examination of the critical speed range in the propulsor-shaft-motor elastic mass system.

A large number of candidate systems for electric ship propulsion applications can be separated into three distinct families:

- Alternating current (ac) systems
- Direct current (dc) systems
- Hybrid combinations of ac and dc components

These basic systems will be discussed and further classified in order to identify significant parameters in the systems selection process.

5.1.2.1 AC Systems

AC systems can be divided into two types according to the frequency characteristics of each type:

- Constant frequency
- Variable frequency

Constant frequency ac power transmission systems utilize constant speed prime movers. This permits the use of the propulsion prime movers to supply ship's service power, auxiliary power and propulsion power, either from separate generators connected in tandem with the propulsion generators, or directly from the propulsion generators.

Where a constant frequency system is used in conjunction with a propulsor, propulsion motors would be of the wound rotor induction type; with speed control achieved by rotor external resistance control. However, with constant voltage and rotor external resistance control,

considerable power is lost as heat in the resistance whenever the propeller operates at less than rated speed. Thus, the use of wound rotor motors and external resistance speed control is normally limited to ships requiring only low amounts of propulsion power, or to ships where slow speed operation of the propeller is very limited. While the case could be made, in certain circumstances, for use of an induction motor, such a requirement eliminates the application of superconducting technology to the motor. The use of superconducting materials in rotating electrical machinery is thus limited. In certain cases the option of a constant speed prime mover may be realized. This occurs in systems utilizing frequency variation of power fed to the motor and is accomplished by means other than prime mover speed variation, or in systems where propulsor thrust is varied independent of speed such as nozzle control of waterjets.

Another optimum use of the constant frequency ac system is with a controllable reversible pitch propeller. With this arrangement, the propeller can be operated constantly at rated speed, with the load controlled by varying propeller pitch. Provision is often made for operation at discrete speeds and variable pitch/power levels. Use of constant frequency permits use of the propulsion generators for the supply of ship's service power, thereby eliminating the need for separate ship's service prime mover-generating sets. The propulsion motor can be either a squirrel cage induction motor or a synchronous motor. While the induction motor could be used in a specific case, the synchronous motor with superconducting windings offers numerous advantages over the induction motor system.

In summary constant frequency ac systems can be used in many ways:

- With constant speed prime movers.
- With fixed pitch propellers and induction motors only when low propulsion power or minimum operation at low speed is required.
- With variable duct control of waterjet propulsors.
- With controllable reversible pitch propellers where propulsion power is appreciable, or considerable operation and maneuvering is required.

- With induction motors for fixed pitch propellers.
- With either induction or synchronous motors with controllable-reversible pitch propellers.
- To simultaneously supply ship's service and propulsion power from prime mover.

Variable frequency ac power transmission systems are generally used with variable speed prime movers. This situation does not permit optional use of the propulsion prime mover to supply ship's service power under all operating conditions. This is desirable for economic reasons, but is often overruled in favor of redundancy and reliability, and may not be a significant feature in systems selection for naval vessels.

Variable frequency systems are used with either fixed pitch or controllable pitch propellers. The motors are of the synchronous type and would utilize superconducting field windings controlled by dc excitation. The synchronous motor is generally designed to operate as an induction motor during start-up and to provide propeller speed control for speeds below the corresponding minimum operating speed of the prime mover. This operation as an induction motor during start and reversal, with fixed pitch propeller, causes a heavy current-low power factor load on the generators. Under this condition, the generator must be provided with considerably more excitation than when the system is in synchronism. In conventional propulsion systems, the exciter must be capable of three to nine times rated power under these conditions. In the case of superconducting electric machinery systems, a certain benefit may be theoretically realized from the persistent flow of current in the field winding. The excitation requirements may then be simplified in certain situations, but in practice, the omnipresent ac losses prevent total persistent operation. For reasons of economy, based on shared power utilization, it is common in conventional propulsion systems to supply the field requirements for generators and motors from a common power supply. This takes advantage of the unused synchronous motor field power and supplies generator field excitation when the motor is in the



Westinghouse

induction mode. This situation may be applied to the superconducting machine system if desired.

The most widely-used variant of the variable frequency case occurs when prime mover speed control is utilized to provide variable frequency power. Basically, the motor and propeller speed are determined by the frequency of the applied voltage and the number of motor poles, as given in Equation 5.1.

$$\text{rpm}_{\text{motor}} = \frac{120 \times \text{frequency applied}}{\text{No. of motor poles}} \quad (5.1)$$

In the previous case, with a synchronous generator, the line frequency is determined by the prime mover speed and number of generator poles, as in Equation 5.2.

$$\text{line frequency} = \frac{\text{rpm}_{\text{prime mover}} \times \text{no. of gen poles}}{120} \quad (5.2)$$

For a given application, a propeller and motor speed is directly related to prime mover speed as a function of the ratio of motor and generator poles. A general expression for motor speed is given below:

$$\text{rpm}_{\text{mover}} = \frac{\text{rpm}_{\text{prime mover}} \times \text{no. gen poles}}{\text{No. motor poles}} \quad (5.3)$$

With this system, reversal is generally accomplished with control of excitation, control of prime mover, use of the motor in the induction mode, and interchanging the order of connections in the three-wire propulsion bus. The fixed-pitch propeller is reversed in this manner. Recent acceptance of the synchronous motor with the controllable pitch propeller has led to a minimum cost installation on a class of merchant tankers. Control and propeller reversal with the mechanical system is expected to have response equal to that of the all-electric system with the fixed pitch propeller, with elimination of certain elements of the control subsystem, including reversal switch gear and dynamic braking apparatus.

Some major configurations of the variable frequency ac systems do not rely principally on prime mover speed control for frequency variation. In these systems the motor speed is related to input voltage frequency as before. The major difference lies in the technique with which the frequency of voltage applied to the propulsion motor is generated and varied. Two basic systems are possible: (1) those systems where frequency of generated voltage is varied by control of frequency of the excitation voltage, and (2) those systems whose frequency of generated voltage is varied by power electronic sampling and recombination of the generated voltage.

This variable frequency power is then fed into the synchronous motor, with control of low-power signals controlling the much higher systems power.

The first basic system generally consists of a dc generator whose excitation is powered by an ac source. This condition is tolerable for a certain range of ac, due to losses, up to perhaps 20 Hz. The output of the dc generator is essentially modulated by the variable frequency ac excitation. This modulated dc, effectively ac power, is fed to a synchronous motor of optimized performance and minimum size. As the basic relationship of Equation 5.1 is valid in this case, excitation of 3 or 6 Hz and power output of 3 or 6 Hz from the generator may be delivered to a 2 or 4 pole synchronous motor for a speed of 180 rpm. Variation of shaft speed from reverse to forward is accomplished by variation of exciter frequency and phase. Furthermore, in these systems, excitation frequency and machine frequency are essentially independent of prime mover speed. The maneuvering response of such a system is ideal; reversal is accomplished by variation of the phase of the generated ac. In conventional synchronous ac propulsion systems, the reversal requires "plugging" or switching between stator phases at the propulsion motor. With this concept, the low power excitation phasing is controlled to yield desired output. The propulsion motor will be a synchronous ac motor, with superconducting dc field windings. The ac excited-dc machine used to generate power may be either heteropolar or homopolar, superconducting or non-superconducting.



Westinghouse

The second basic system uses power electronic circuitry typically in the form of a cyclo-converter to choose a desired frequency, reconfigured from the generated ac power. This system has two options:

1. Use of high-power cycloconverter systems to configure the total generated power as desired.
2. Use of low and medium power cycloconverter systems to configure low maneuvering power, with normal synchronous ac control above a minimum power level.

These propulsion systems will be dependent upon the availability and economic feasibility of the power electronic circuitry.

Most early work on the application of superconducting electric propulsion systems to naval vessels required the cycloconverter in order to provide quick response to maneuvering, avoiding the induction motor-asynchronous operation of the superconducting synchronous propulsion motor. Practical cycloconverters have most recently reached the 6000 hp industrial rating for use in similar variable speed drive applications. Such subsystems will require economic justification, as well as considerations of their cooling requirements, volume, weight, and availability.

These two cases of variable frequency systems are ideal for control of installations where the controllable-reversible pitch propeller is unacceptable. A detailed analysis of system economics would be required to determine the ideal combination of propeller and superconducting electrical machinery when propeller type was not predetermined.

Finally, variable frequency systems described above are enhanced by the option of full economy that is available from following the ideal operating characteristics of the prime mover. In this configuration, the power required for a certain motor and propeller speed is essentially decoupled from the speed requirement of the generator prime mover combination.

This allows maximized performance of existing marine prime movers and suggests the use of higher efficiency systems with the prime mover designed around a specific power application. In summary, the uses of the variable frequency system are:

- With variable or fixed speed prime mover.
- With fixed or controllable-reversible pitch propeller.
- With synchronous propulsion motors.
- To supply ship's service power in some cases.

5.1.2.2 DC Systems

Direct current propulsion power transmission systems comprise three basic types with regard to operating voltage and current characteristics:

- Constant voltage
- Variable voltage
- Constant current

Direct current constant voltage systems require the use of constant speed prime movers. The generator is configured to provide constant voltage under all load conditions. With fixed pitch propellers, speed control is provided by a combination of armature voltage variation achieved by varying resistance in series with the motor armature, and by variation of the strength of the field of the propulsion motor. Reversal of direction of motor rotation is usually achieved by reversal of polarity of the power supply to the motor armature. The constant voltage system has the disadvantage of considerable loss of power in the armature series resistors when operating at low propeller speeds. One way of eliminating a major portion, or all, of this armature series resistance loss is to arrange to have more than one generator, and to use a double armature propulsion motor. By varying the connections between the generators and the motors, a number of propulsion system voltages can be provided to the motor armatures and the required speed control can be obtained by means of motor field variation. For example,

AD-A044 413

WESTINGHOUSE ELECTRIC CORP PITTSBURGH PA ADVANCED ENE--ETC F/G 21/5
COMPACT CLOSED CYCLE BRAYTON SYSTEM FEASIBILITY STUDY. (U)
JUL 77 R E THOMPSON, G H PARKER, R L AMMON N00014-76-C-0706
WAES-TNR-233 NL

UNCLASSIFIED

4 OF 5
AD
A044413





Westinghouse

if each generator armature were rated 500 V, and each motor armature were rated 1000 V, the following motor armature voltages could be obtained:

- Generator armatures in parallel and motor armatures in series give 250 V on each motor armature.
- Generator armatures in series and motor armatures in series give 500 V on each motor armature.
- Generator armatures in series and motor armatures in parallel give 1000 V on each motor armature.

Full power of connected prime movers is available to the propeller by means of motor field adjustment.

Use of a constant voltage dc system with a controllable-reversible pitch propeller or variable duct waterjet eliminates the requirement for multiple generator armatures and double armature motors, but would have no other particular advantages over a constant voltage ac system.

The utilization of the dc constant voltage system can be stated as:

- For use only with constant speed prime movers.
- Use should be restricted to low power systems where considerable low speed propeller operation is required unless either using more than one generator armature on double armature motors.
- For use with controllable-reversible pitch propellers where considerable low power operation is required thus eliminating need for more than one generator armature and double armature motors.
- For use with variable duct waterjets.

- Reversal of fixed pitch propeller rotation is achieved by reversal of polarity of voltage at the motor armature.
- Full power of each prime mover is available under all operating conditions.

Variable voltage dc propulsion power transmission may be used with either variable speed or constant speed prime movers. Variable voltage dc systems are generally used with fixed pitch propellers. Since full range propeller speed control is inherent to the system there is no advantage to using a controllable reversible pitch propeller. Where the prime mover is of the variable speed type, generator voltage is increased from zero to full strength, by increasing excitation of the field while the prime mover is operating at minimum speed. This provides propeller speed control from zero to a speed proportional to the minimum speed of the prime mover. Further speed control of the propeller is obtained by increasing the speed of the prime mover. Where the prime mover is of the constant speed type, full propeller speed control is obtained only by variation of generator field strength. The propulsion motor field strength is basically maintained at a constant value, thus motor speed control is by variation of the armature voltage. Reversal of propeller direction of rotation is obtained by reversing the polarity of the voltage from the generator, hence reversal of the generator field supply voltage. This requires detailed study of response, due to high rates of change desired in the field which may be detrimental if the field is superconducting because of the associated losses in the superconducting coils under these conditions.

Operation of the variable voltage system is inherently stable under all conditions, without the use of generator or motor regulators. The motor with basically constant field is inherently self-protecting against dangerous overspeeds should propeller load be suddenly removed. In order to permit more rapid operation of propeller speed control operating handles, and hence more rapid propeller and ship response to maneuvering requirements, a regulator is used to prevent dangerous overloads to the propulsion system. This regulator measures the system current, and if during a maneuver this current attempts to exceed the safe allowable value, the



Westinghouse

regulator operates to reduce the generator field strength. Hence generator voltage and propeller speed are reduced until the propeller operates at a load within the capability of the propulsion system. Thus, this regulator is required to operate only during rapid maneuvers. Operation of the regulator is not required under steady state conditions. Where prime movers are not capable of supplying full rated torque at reduced operating speeds the system current operating point of the regulator is varied to limit the propeller load to the power available from the prime mover.

Where the ship operating requirements include the necessity of operating the ship propeller at other than ship free running load, such as towing condition, or icebreaking, the motor is usually provided with a regulator which varies the motor field which in turn varies the propeller speed and available torque to permit full prime mover power utilization for any propeller operating condition between ship bollard and ship free running. While field adjustment could be made manually, the regulator provides for automatic unattended operation.

With the variable voltage system, the generator field, and/or the motor field can be readily re-calibrated as prime movers are connected to, or disconnected from, the propulsion power system, such that full power of all connected prime movers may be utilized by the propeller.

Variable voltage dc systems may be arranged for generators to be connected in series or in parallel to supply prime mover power to the propulsion motors. Series connection of generators provides easier control of load sharing than is available with parallel systems. However, in the series arrangement, each generator must carry the full current in the system, whereas in the parallel system, each generator carries only its share of the total system current. This will influence the length of cable run from generator to switchboard, as well as the number of switch units required to connect or isolate machines from the line.

The utilization of the variable voltage system may be summarized as:

- Can be used with any type of variable or constant speed prime mover.

- Full range of speed control is available.
- Reversal of rotation is achieved by reversal of polarity of power supply to generator field or by reversing the polarity of the bus at low load.
- System is inherently stable and capable of manual control.
- System current limit regulator can be used to increase ship maneuverability and reduce manual operation.
- System variable current limit regulator can be used to prevent overloading at any prime mover operating speed.
- Continuous operation of system regulator not required.
- Motor field regulator can be used to assure full power to the propeller over a range of speed.
- Motor field regulation can be manual or automatic.
- Motor field can be adjusted to permit full utilization of power of prime movers connected to system.

Constant current propulsion power transmission systems, are based on the maintenance of full rated current in the system power circuits at all times. Generators and motors are connected in one continuous series loop. Due to the limitation in allowable maximum system voltage to ground, the generators and motors in this system are usually connected in a "series sandwich" arrangement, to utilize generators of the highest possible voltage and lowest possible current for any particular power. Regardless of which system is used, the generators, motors, cables and switches must be designed to carry continuously the system rated full power current, resulting in large equipment and full load heat losses at all times. Each time that the propeller stops, it is necessary to disconnect the propulsion motor armature from the loop circuit, otherwise commutator overheating and ultimate destruction will occur. Disconnection of a motor,

or generator, armature from the loop circuit requires that an armature bypass switch be closed before the armature can be disconnected. This necessitates a large number of power circuit control switches.

An advantage of the constant current system is the ability to share the load of two propellers equally between an odd number of propulsion generators.

The system cannot be subjected to overloads. Unfortunately, this apparent advantage is also a disadvantage, resulting from the fact that, because the regulator must operate to maintain the current constant, it is very difficult to provide suitable short circuit protection for the system. If regulator response time is sufficiently slow, an instantaneous overcurrent relay can be used to detect instantaneous short circuit occurrences. However, if the regulator response is so fast as to limit the short circuit current to a little more than the controlled constant current, the overload relay will not operate. Further, if the short circuit develops slowly, the fault current does not rise above the controlled value and a sustained fault occurs.

Propeller speed control in a constant current system is based on maintaining a balance between the propeller load torque and the motor output torque. Since motor armature current is constant, then motor output torque must be controlled by variation of motor field strength. Motor torque will increase as field strength increases. Reversal of direction of rotation of the motor is achieved by reversing the polarity of the motor field, hence reversing polarity of the field power supply.

The constant current system, while having some advantages, has a considerable number of disadvantages. Since current must be maintained constant for all propeller loads and load changes, then the voltage of the generators must be varied accordingly. This requires that the generator field be continuously controlled by means of a regulator to assure constant current. If this regulator should fail at any time, complete loss of propulsion power on the ship will result. Since all generator fields must be simultaneously controlled, protection must be provided to prevent the reversal of a prime mover if loss of prime mover torque occurs. This requirement

is due to the fact that any generator will operate as a motor should the mechanical input torque be reduced while current flows in the armature windings. Not only will the generator become a motor, but since the voltage across the armature is now reversed, the generator will attempt to operate as a motor in the opposite direction of rotation and thus attempt to reverse the prime mover. Therefore, underspeed protective devices must be provided on each prime mover to prevent reversal or loss of torque output. Furthermore, since a small reduction in torque from one prime mover as compared to another, could result in complete loss of power from that generator, it is usual to install prime movers with a torque capability considerably in excess of the full required power torque.

The constant current system also involves inherent instability of the balanced torque system. To provide positive propeller speed control, a motor field regulator must be provided, and must operate continuously, to vary the motor torque in accordance with the variation of propeller load torque which can occur. Further, this regulator is required to prevent propulsion motor speeds from increasing to a destructive speed when propeller torque is suddenly reduced from a high torque to a low torque.

In summary, the operating parameters of the constant current system are:

- Full power heat loss occurs due to constant current.
- Motors must be disconnected or shorted out each time they are stopped.
- Generators, motors, cables, and switches carry rated current continuously.
- Considerable switching is required to disconnect or connect motors and generators in the circuit.
- Constant speed prime movers must be used.
- Prime movers should be capable of supplying more than rated load torque.
- Short circuit protection is difficult to provide.



Westinghouse

- Current control regulator must operate continuously; failure means loss of all propulsion power on the ship.
- Motor torque regulator must operate continuously; failure could result in destructive motor speeds.
- Prime mover underspeed protection is required to disconnect a generator when engine torque is reduced.
- System inherently prevents overloads from occurring.
- Ship's service generators can be driven by propulsion prime movers.
- An odd number of prime movers can equally supply power to two or more propulsion motors.
- Motor rotation is reversed by reversing the polarity of the power supply to the motor field, thus providing excellent maneuverability.
- Full power from any prime mover can be utilized by either or both propulsion motors.

5.1.2.3 AC/DC Systems

Combined systems utilize ac generators, dc motors, and a rectification subsystem to convert the generated ac power to dc power for use by the dc propulsion motors. The advantage of this approach is that for equal power ratings, ac generators can be smaller, lighter, generally less expensive, and of higher voltage than dc generators. The systems implications are significant in the transmission of large dc power as generated by low voltage homopolar machines and high voltage heteropolar dc machines.

One theory is that the dc motor will have a wide range of propeller speed control and ease of propeller reversal not readily available with ac motors. While true of conventional ship propulsion machinery, the implications of the total system, including refrigeration and excitation equipment, have not yet been compared in the superconducting system. A significant

excitation requirement has been seen necessary for prompt reversal. In a systems context, the use of an ac/dc hybrid combination is seen as a suitable solution to propulsion applications where the added complexity of rectification and solid state control is viewed as a necessity for the operational torque-speed requirements of the vessel. This case would apply to systems wherein a high-speed turbine drives a suitable matched ac synchronous generator, and the power is fed through rectification to a solid-brush dc heteropolar propulsion motor.

Combined ac/dc systems can be divided into two basic types, depending upon the operating characteristics of the ac side of the system: (1) variable ac voltage and (2) constant ac voltage. Both of the combined systems utilize variable dc voltage to the propulsion motor armature for the propeller speed control. Reversal of direction of rotation of the propeller can be achieved by simply reversing the field supply to the motor, by utilizing switches to reverse the polarity of the power supply to the motor armature, or by using more complex controls and equipment to provide reversal of armature power supply polarity in the static rectifying equipment. Regenerative power from the propeller can be absorbed in resistors, or, inverters can be used in the static power unit to convert the regenerated power to ac for subsequent absorption in the ac system. Thus, the two systems differ only in the control of the ac portion of each system, and in the type of rectifying equipment used.

Variable AC Voltage System

The variable ac voltage combined ac/dc system is the simpler, less costly system of the two combined types. It utilizes a simple static rectifier to supply dc voltage to the motor.

Variation of the dc voltage is achieved by variation of the ac voltage to the rectifier unit. The frequency of the ac voltage can be varied if it is advantageous to vary the speed of the prime mover. Used with constant speed gas turbines, the frequency would not vary. Thus, the variable ac voltage combined system would provide operating characteristics very similar to those of the variable voltage dc system while using the higher speed ac generators.

Constant AC Voltage System

The constant ac voltage combined ac/dc system operates at constant frequency ac, and thus uses a constant speed prime mover. This simplifies the prime mover control which can thus be provided with a constant speed governor, and the generator can be provided with a constant voltage regulator. Variation of the dc voltage to the propulsion motor armature is achieved by utilizing a static rectifier unit having a variable controlled firing point.

The constant ac voltage system will have the same operating characteristics as a variable voltage dc system. In addition to permitting the use of smaller ac generators, the system has the important advantage that ship's service power can be provided by the constant voltage, constant frequency ac propulsion generators.

Hybrid System

The current size limit in shipboard hybrid electrical systems is near 15,000 HP per motor armature, limited essentially by the size of conventional dc motors. The use of superconducting generators and motors will allow an increase in the horsepower, providing the motor can sustain the high currents involved at higher horsepowers. This system will offer an overall weight advantage, with favorable torque characteristics at the propeller and with suitable matching to the high speed turbine prime mover.

System parameters, such as voltage, are chosen to suit the type and rating of the motor, with a maximum dc voltage of 1000 V in use in the U.S. For higher voltage generators, the use of transformers may be an attractive alternative to matching certain types of motors and generators.

In this type of hybrid system, the speed of the propulsion motor is controlled by varying the ac generator excitation and speed of the prime mover or both. The direction of rotation is controlled by the polarity of motor field or polarity of applied armature voltage. In the case of superconducting field machines, the excitation must be capable of reversing the field in

short intervals, and may be difficult to achieve without cost penalty of the superconducting windings.

Unlike conventional dc propulsion, the use of a one-way rectifier blocks the transfer of power from motor to generator. While dynamic braking is not normally required with dc installations, it may be necessary to absorb the energy from a windmilling propeller in transition from forward to reverse. A resistance must be switched into the armature circuit to absorb this energy and limit dc armature current.

5.1.3 Candidate Propulsor Types

Propellers are of three distinct types: fixed pitch propellers, controllable pitch propellers, and waterjets. Distinction is often made between controllable pitch (CP) propellers and controllable-reversible pitch (CRP). Waterjets typically are of variable speed and may include nozzle vectoring.

The fixed pitch and controllable pitch propeller have essentially the same basic speed-torque-power characteristics. An essential difference is that instead of having one rated torque and power demand at rated speed, the controllable pitch propeller demand will vary from zero torque and power at rated speed and zero pitch, to rated torque and power at rated speed with maximum pitch. Thus by controlling propeller pitch any limited amount of prime mover power can be absorbed by the propeller. The controllable-reversible pitch propeller requires only reversal of propeller pitch to initiate ship reversal. This action, accomplished with minimum delay, provides ship stopping times which are comparable with fixed-pitch electric propulsion installations and generally superior to fixed pitch gear driven systems.

The efficiency of a CRP propeller approaches the efficiency of fixed pitch propellers at the same design point. The slight degradation of 2 to 3 percent is due to the larger propeller hub that contains control mechanism for the CRP. At conditions off the original design point, the CRP propeller efficiency is less than that of a fixed pitch propeller designed for the new



Westinghouse

condition, but often superior to the off-design performance of the fixed pitch propeller designed for the original operating point.

The CRP propeller is of greater weight, complexity, and cost than the simpler fixed pitch propeller. These facts and a lack of operating experience at large horsepower have been largely responsible for its lack of general acceptance in the past. With the need for a reversal device in propulsion systems utilizing the unidirectional gas turbine, the CRP propeller has become the optimum solution. This is confirmed by its acceptance in the U.S. Navy after years of experimentation and observation by the merchant fleet after economic analysis showed clear advantage on reduction of life-cycle costs.

As the complexity of superconducting electrical propulsion systems has not yet been defined in detail it is appropriate to view both fixed and controllable reversible pitch propellers in the propulsion system synthesis. Until otherwise proven uneconomical or technically unfeasible for the particular naval ship application under study, they should be viewed as likely candidates. The use of certain arrangements of ac and dc propulsion systems utilizing generators and motors and the CRP propeller to vary power and ship speed could provide an ideal ship propulsion system. The CRP propeller system should be viewed as a viable alternative from the outset of the design process.

Various naval ship applications imply different ranges of rotative shaft speeds. These applications are separated into two basic groups for purposes of discussion: displacement ships and lift-augmented ships.

5.1.3.1 Types for Displacement Ships

The reversal capability of a naval vessel is of considerable importance. It is a prime determinant of the vessel's maneuverability quality. Electric drive has traditionally provided a rapid means for reversal of the propeller shaft and the timely application of reverse power. In contrast to the mechanically geared ship, reversal times are generally much shorter with

electric drive. The controllable pitch propellers now in service offer shaft reversal times on the order of the electric drive ships now in service.

Studies of anticipated superconducting electric drive systems indicate that the high levels of magnetic stored energy in certain types of superconducting field electrical machinery will resist being "swung" or varied in amplitude and direction by the excitation control. This electrical variation of current and/or voltage has been the normal manner in which the speed or direction of rotation of the propeller will be changed in dc and ac propulsion schemes. This action will weigh heavily in designing the fields and the sizing of the refrigeration plant. The level of sophistication and power rating required for excitation and refrigeration equipment in a superconducting electrical propulsion installation will most likely be determined by this reversal requirement.

5.1.3.2 Types for Lift Augmented Ships

The concept of fixed or specific design propeller pitch is generally considered more suitably applied to naval displacement ship applications than it is to surface-effect ships or hydrofoils. This follows because the CRP propeller is favorably disposed to operation in a system that experiences various loads, such as tow boat which must operate efficiently both with and without a towed cargo. A direct analog exists between the ship that operates at two different powerspeed regimes, such as the surface effect ship or hydrofoil. These craft operate in two basic conditions, displacement and flying.

The operating schedule for SES is similar to that of the hydrofoil. A large thrust requirement exists at low speeds, the so-called hump condition. Ideally, however, the propeller should also operate at maximum rpm and maximum power at maximum speed. These conditions are generally difficult for a fixed pitch propeller, and thus supercavitating propellers are typically used for these types of craft. Waterjets, although slightly lower in efficiency than supercavitating propellers, are also utilized because of simplicity of arrangement and ease of control.



Westinghouse

Several conclusions for SES (and similar hydrofoil) operation are:

- A major difference in design conditions exists between takeoff and cruise flight.
- A smaller disparity exists between cruise flight and high speed flight.
- Proper allowance must be maintained to provide thrust margin for acceleration through takeoff.
- Controllable pitch propellers, supercavitating propellers or waterjets, for these installations offer the distinct possibility of efficiency, savings, and a light weight superconducting electrical propulsion system.

5.1.4 Refrigeration System Configuration

The single most critical auxiliary in the superconducting propulsion system is the cryogenic refrigeration subsystem.

The superconducting windings will require an environment at a temperature near that of liquid helium at one to three atmospheres of pressure, in the range 3.7 to 4.2°K. Basically, this may be achieved in three ways:

- By a continuous operating refrigerator.
- By providing a cryogenic reservoir of sufficient capacity to effect cooldown and sustain superconducting operation for the duration of the mission.
- By initial system cooldown by transfer of liquid helium from a base supply and through maintaining a low temperature with refrigeration equipment.

The capacity of the refrigeration system is based on two factors, the quantity of liquid helium required for cooling the machines during continuous operation and that required for rapid cooldown. The latter usually predominates, since most requirements call for fairly rapid cooldown of the machines from ambient to 4.2°K which may require several times the normal

continuous helium flow. Thus most superconducting installations use dual compressors to provide sufficient capacity for the cooldown conditions and then utilize only one unit for continuous operation. This inherently supplies a redundant unit for standby in case of failure of the first unit. The machinery arrangement also dictates the type of helium distribution. Typically the helium compressors are located in the machinery room and high pressure, ambient temperature helium is piped to individual refrigerators located near the superconducting machines. This permits short lengths of the vacuum insulated piping to the machinery. It also provides for redundancy in the use of refrigerators when machines are located near each other as usually one refrigerator may be easily switched out of service after initial cooldown enabling one refrigerator to serve two machines. Cross connections of the high pressure helium lines and the liquid helium lines improve reliability and insure that each machine can be provided with sufficient helium flow.

The amount of liquid helium required for steady state cooling of the machine is a function of the machine design. In one configuration, for example, the heart of the machine is the superconducting field winding which must be maintained at or near 4.2°K using liquid helium as a coolant. The field winding is supported within the dewar vessel by a torque tube and a flexible support structure. The torque tube transmits the machine torque to the rotor drive coupling. The flexible support structure supports the exciter end of the field winding while accommodating the thermal contraction between the inner structure and dewar wall. Radiation shields are provided to shield the field winding from thermal radiation from the ambient temperature dewar walls. The field winding excitation leads provide the necessary current from the machine slip rings. In order to minimize the coolant flow required due to the low temperature, careful design attention must be directed toward minimizing heat leaks into the low temperature zone. All three modes of heat transfer, radiation, convection, and conduction, must be considered in evaluating heat leaks into the low temperature region.

The helium flow rate represents the mass flow rate, in equivalent liquid liters, required to cool the structure, leads, and radiation shields. The heat losses represent the heat leaks into the cold zone that must be removed at 4.2°K . These will be removed by the latent heat of the

liquid helium injected into the machine. The total heat removal capability for each machine can be determined by calculating the latent heat of vaporization of the total machine flow. Excess heat removal capacity is available in each machine. The excess capacity can, if necessary, be utilized to remove heat generated in the winding due to ac flux penetration of the winding.

5.1.5 Excitation Systems

The excitation subsystem must be capable of providing controllable amounts of exciter power to superconducting dc generators and motors. Marine applications will generally require separate excitation of propulsion machinery, in order to provide flexible response and sufficient reliability. In the dc system, either variable or constant voltage, changes in motor speed and directions are accomplished through magnitude and polarity control of generator output. This corresponds to control of the excitation subsystem in magnitude and polarity of output.

In many installations the excitation power is supplied by either rotary dc generators, driven by the prime or an auxiliary mover or solid state power sources.

With larger plants, excitation power is connected to the ship's service power system's vital bus. A certain redundancy is required to insure the reliability of this circuitry. On most systems, ship service power is 440 volts 60 Hz ac, requiring conversion to controllable voltage dc for the exciter. The use of motor generator sets is being replaced by static conversion devices. Silicon rectifier with control and gating circuits provide for easily controlled excitation power, current regulation limiting and inherent protection circuitry within the exciter subsystem. Redundancy is generally required, with one standby generator or motor exciter for each two generator or motors.

The excitation systems for superconducting ac propulsion systems are directly related to the type of ac system proposed, the main consideration being whether reversal of the propulsor motor is or is not required.

A separate exciter is generally utilized in ac propulsion machines, due to wide speed variation of prime mover on most installations and the requirement for overexcitation voltage during certain control modes. Generally a rapid response double amplification rotating machine or solid state device is used, with the latter accomplishing regulation and limiting control functions. Amplidyne and rototrol devices have been commonly used, but are giving way to static solid state power electronic subsystems. Under steady state conditions, excitation must be sufficient to avoid pulling out of step due to torque variations at the propeller induced by sea conditions or by turning. The inherent torque margin requires continuous maximum normal field current in conventional machines. The high level of magnetic field anticipated in the superconducting propulsion machines predicts a "stiff" machine system. With the need for excitation control, the possibility of less regulation firmly exists.

The excitation system and the field circuits may often provide for equal loading of multiple generators when two generators are supplying one motor for all positions of the control lever with the prime mover speeds equal. A vernier voltage adjusting device can be installed for each regulator on the propulsion console to manually balance the loads. A similar function will exist for more than two prime movers.

The excitation system and the generators may be designed so that, with the generator fields deenergized, no voltage is generated due to residual magnetism.

In most installations the motor field is changed only while in maneuvering, specifically reversal. As the motor function is an induction motor in that mode of operation, the field must be secured. This is the essential control with motor field. Generator field must allow for overexcitation, as well as maintaining a constant volts per cycle function on the output voltage.

5.1.6 Switchgear

A major technical development required in switchgear for advanced electrical propulsion systems, apart from making high power ac switchgear suitable for marine applications, is one



Westinghouse

of switching very large dc currents. On large dc segmented magnet homopolar and superconducting homopolar systems the rated current may be as high as 100,000 A. At present, there are only a few identifiable technical directions which will lead to the successful development of a high current dc circuit breaker. System design will offer the possibility of eliminating the need for these breakers in certain types of installations.

The absence of a dc circuit breaker may result in some systems which use other methods of clearing the faults, such as rapid quenching of the generator superconducting winding.

Most ship propulsion systems to date have protection/control devices that sense overcurrents or grounds and act to disconnect field circuitry, rather than attempting to open armature or main propulsion bus lines.

In a certain ship concept of high power, where use of auxiliary electric power from the propulsion bus is of interest, voltage ratings of 13,800 V have been proposed. In this application it is also proposed to use 13,800 V switchgear for the allocation of generated power to the propulsion units and for overload and short circuit protection of the power system. These systems also may use field-killing switchgear to ensure utmost protection.

For these cases of high voltage, typical industrial switchgear is utilized, consisting of circuit breaker cells for each generator and each motor-bus combination. A cell of this equipment, capable of handling the 70,000 HP output of the generator weighs approximately 2400 pounds. The switchgear requirement for a 50,000 HP motor weighs about 2200 pounds while the breaker for a 5000 HP motor weighs about 2000 pounds.

The circuit breaker cells, using type 150 DHP 500, drawout, air break circuit breakers for use in a three phase ungrounded system, has a 500 MVA interrupting capacity at 15 kV, a stored energy closing device for operation from a separate 115 Vac power supply, and an auxiliary switch for operation of remote control and indicating devices. Provision for manual closing and tripping is made for emergency conditions.

The cell would contain numerous elements, including:

- Current transformer
- Potential transformer
- Circuit breaker indicating lights
- Automatic synchronizing controls
- Overcurrent relays as necessary
- Anticondensation heaters and controls
- Insulated bus
- Wiring and terminal blocks

The field switchgear is also cubicle-enclosed, each capable of connecting main or standby excitation to field windings, containing a generator field discharge device. A typical cubicle for excitation control of the propulsion machine would weigh about 2000 pounds and enclose a volume 8 feet x 3 feet x 3 feet. This cubicle contains on the order of 1000 A, 250 V dc, fixed, airbreak, circuit breakers for connection of the generator field to either the main or standby excitation unit. The system would include closing and trip coil for operation from a separate 115 Vac supply, auxiliary control circuit contacts, and provision for manual tripping and closing in emergency.

As well, a number of elements would be contained in the cell:

- Field overload relay
- Field ground relay
- Field discharge resistor
- Circuit breaker position lights
- Shunts for remote field ammeter



Westinghouse

- Anticondensation heater and control
- Insulated bus
- Control wiring and terminal blocks

It has become popular in recent years to assemble several functions in the master switchboard:

- All field control switches to be interlocked so they cannot make or break field currents.
- Control transfer switches interlocked with the generator set-up switches so that the control system can be connected to the correct control level as required by the position of the generator set-up switch.
- Generally one set-up switchboard will be provided for each shaft system of the propulsion plants.
- Modular construction of each switchboard has been found to provide for easiest maintenance.
- The rear of each switchboard includes removable louvered metal panels.

Each switchboard includes three sections: a generator section, generator exciter section, and motor section designed to perform necessary functions.

One of the switchboards includes additional components and functions for emergency use:

- Field exciter "On"- "Off" selector switch
- "Manual", "Automatic" selector switch
- Rheostat for manual operation

5.1.7 Instrumentation

A sufficient number of sensors should be placed in and about the superconducting generator and motor to monitor pertinent data as to how the machine is functioning during actual operating conditions. Some of these devices will probably have to be embedded in position during construction, thus becoming integral parts. They must be so placed that they will not violate the electrical integrity of the apparatus.

The utmost care should be exercised in selecting the proper detector to perform any given task. Temperature and field measurements are difficult whenever they are interrelated or coexist, as they will be in the cryogenic field winding. The devices used to monitor these phenomena are themselves affected by field and temperature, respectively. Most of these sensors are also pressure sensitive. Pressure gradients will be established due to mass weight, thermal contractions, and centrifugal forces in rotating field windings. All these perturbations will have to be extracted from any data collected.

For measuring low temperatures one has the option of using semiconductor, carbon, or wire wound sensors along with the Au-Fe thermocouple. Each has its limitations. The semiconductors are thermal cycle stable, but are mechanically weak, magnetoresistive, and strain sensitive. Carbon sensors are not too reproducible after thermal cycling and they, too, are strain and magnetosensitive. Wire wound elements can be cycled and have quantitatively lower magnetoresistance. However, their main detriment is that they require relatively high currents to produce reasonable readout potentials. When higher currents are used, the joule heating could become a source of thermal drain upon the cryogenic requirements. The Au-Fe thermocouple is also highly thermocyclic and strain sensitive, but does have acceptable readout values. Thermocouples also exhibit a small amount of magnetoresistance.

The magnetic field can be measured by essentially using any one of the devices previously mentioned as thermometers. Only the calibration makes the difference as to how it should be used. A Hall effect device would be the most desirable however, it is sensitive to field

orientation and thus not too usable in a fixed position where the field direction may vary.

Any sensor placed internally in rotating field structure machines must be connected to the external circuitry through slip rings. The performance of these rings at high rotational speeds will have to be carefully evaluated, mainly because the signals being conducted will be of very low current or voltage levels. Monitoring will be less complicated in stationary dewar field windings.

Efficiency, torque, power dissipation, windage, reactance, vibration, and cooling rates can all be determined by using conventional instrumentation connected external to the machine.

The electric propulsion will have a master control and indication console. As an estimate of the number of functions that will be monitored, in addition to the special requirements of superconducting machines previously mentioned, the following list has been prepared for guidance.

- Indicating instruments: ammeters; voltmeters, temperature, torque, speed, and control indicators.
- Indicating lights (direction, position, control overload imbalance, etc.).
- Control circuit breakers.
- Controllers (trip-off-close; adjustment; test, emergency).
- Automatic sequence system for controlling speed and direction.

5.1.8 Size and Weight of Machines

To determine approximate sizes of machines for this study, several computer codes (priorly developed by Westinghouse) were utilized. The aim was to ascertain the approximate diameters, lengths, weights and efficiencies of superconducting machines capable of generating power at an assumed level of 70,000 HP and powering assumed loads of 50,000 HP and 5,000 HP. These

power levels were assumed in order to take advantage of previous work performed on high performance class vehicles at these levels as both a reference and a base for extrapolation to higher or lower power levels. Since one of the goals of the Compact Closed Brayton Cycle System (CCCBS) Study was to utilize electrical machinery that was small and of low weight and yet capable of delivering the stated powers, it was anticipated that there would exist optimum machines to fulfill this goal. With the realization that these machines would be used for ship propulsion systems, and without a specification of either the type of ships on which they would be installed or the types of propulsors on these ships, some basic assumptions had to be made. It was therefore assumed that since small, lightweight machinery was desired, these electrical propulsion systems would be used on high performance ships such as hydrofoils or Surface Effect Ships where size and weight are primary concerns. It was considered that their application to conventional displacement type ships would be of secondary importance. It was further assumed that since the CCBBS would most likely be used on these high performance ships, high speed propulsors typified by supercavitating propellers or waterjet pumps would be utilized. Required power was assumed to vary as the cube of the speed for supercavitating propellers while duct control was assumed for thrust control of the waterjet. Until a specific ship type and control method is specified, the electrical equipment arrangement assumed must be considered only in general terms. In addition the dimensions and weights given here must be considered approximate as complete designs were not made since it was out of the content of this study. They are all, however, developed under the same general guidelines and include the essential electrical, magnetic and mechanical components and probably reflect the actual machine weights and dimensions within 10 percent. Such components as shaft extensions, pedestal, brush supports and mounting feet are not included, nor are any internal or external cooling devices.

In all systems, ship's service power was assumed to be obtained from an auxiliary generator and not from the main power source. This was done to allow higher speed main generators. Thus for the AC system, main power could be at a frequency higher than 60 Hz, allowing more compact generators and propulsion motors while ship's service power could be generated at 440 volt, 60 Hz to comply with the loads.

5.1.8.1 Superconducting Generator

Investigating the effects of changing output voltage and speed of the main superconducting ac generators while varying the rotor diameter indicated that output voltage did not have a great impact on machine size. Figure 5.1 shows the trend in machine weight and efficiency as rotor diameter is varied. As the plot indicates, speed has a decided impact on weight of the generator of approximately 6000 pounds between the 12,000 RPM and 6000 RPM designs. Efficiency is also improved by approximately one-tenth of 1 percent, although this slight improvement may not be significant. Thus if weight were the prevalent parameter, the optimum design would be the 12,000 RPM design. However if compactness is considered, all of the optimal weight designs tend towards small diameters and long lengths, being more pronounced at the 6000 RPM design than the 12,000 RPM design. Figure 5.2 indicates the stator OD and the bearing-to-bearing length variations plotted against rotor OD. By comparing Figures 5.1 and 5.2, it is seen that the lowest weight machines are in the range of rotor diameters of 7-1/2 inches to 8 inches which are still on the steep part of the length to rotor diameter curve. Thus if compactness is desired, a rotor diameter of about 9 inches to 10 inches, at a slight weight penalty might be a better choice. The stator outside diameter curve increases linearly with increased rotor diameter. If the optimum designed machine is defined as that machine with the highest efficiency, then machines in the range of 9 inches to 12 inches would be selected, again however, at a penalty in weight.

As stated previously, the optimum machine in terms of size, weight and efficiency is better at 12,000 RPM than at 6000 RPM. There are however some design problems associated with the higher speed machines, particularly in regard to the helium flow for rotor cooling, bearings and rotor deflection stresses that would require more development effort before they can be proven to be economically and technically feasible at the smaller rotor radii.

For a 70,000 HP DC generator of the SEGMA II design, voltage is a much more critical parameter, particularly as it determines the current output. The highest voltage that was considered practical was a 2000 volt machine which gave an output current of 26,100 amps. This large

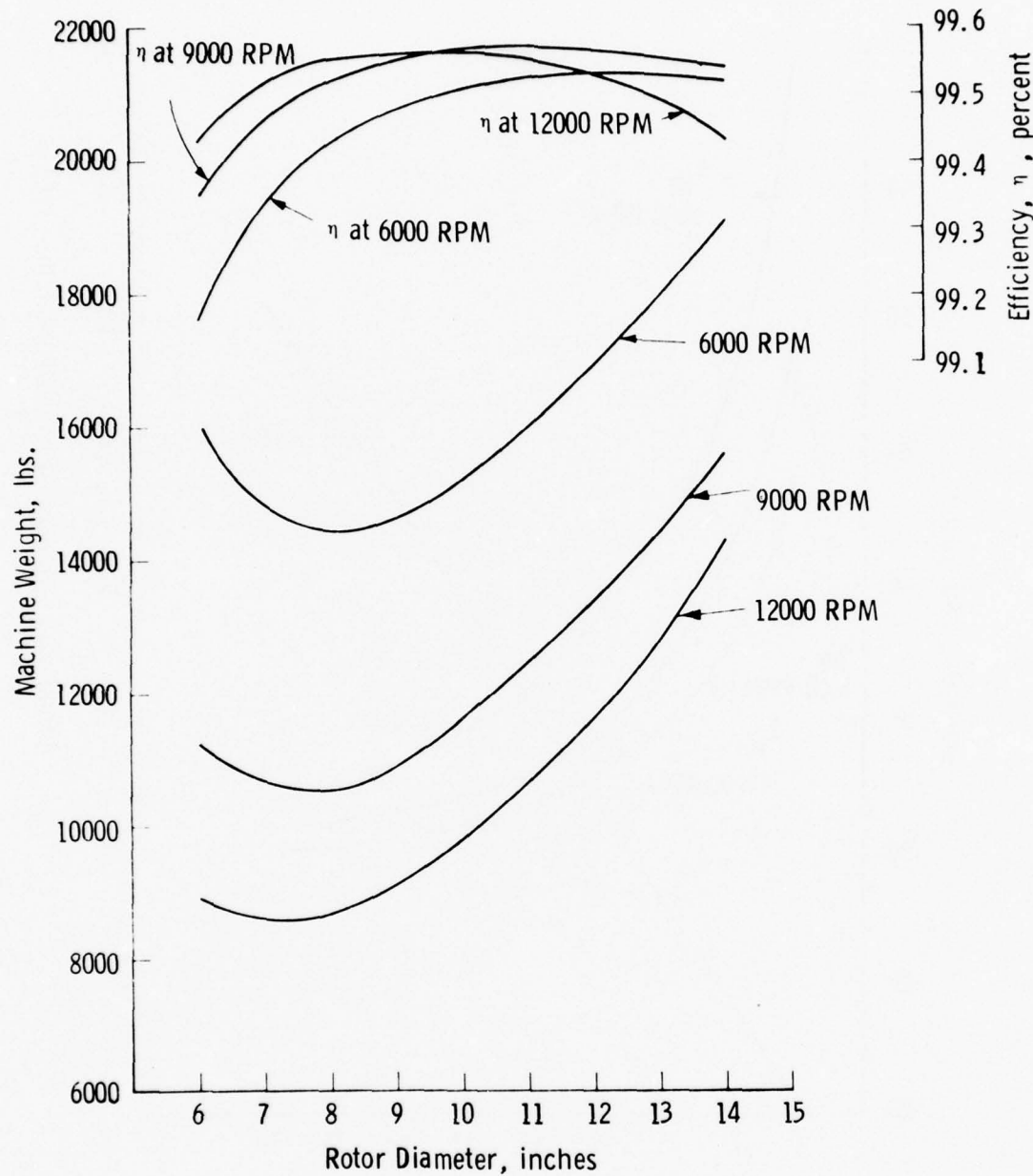


Figure 5.1 70 KHP (52.5 MVA) Generator 13.8 KV



Westinghouse

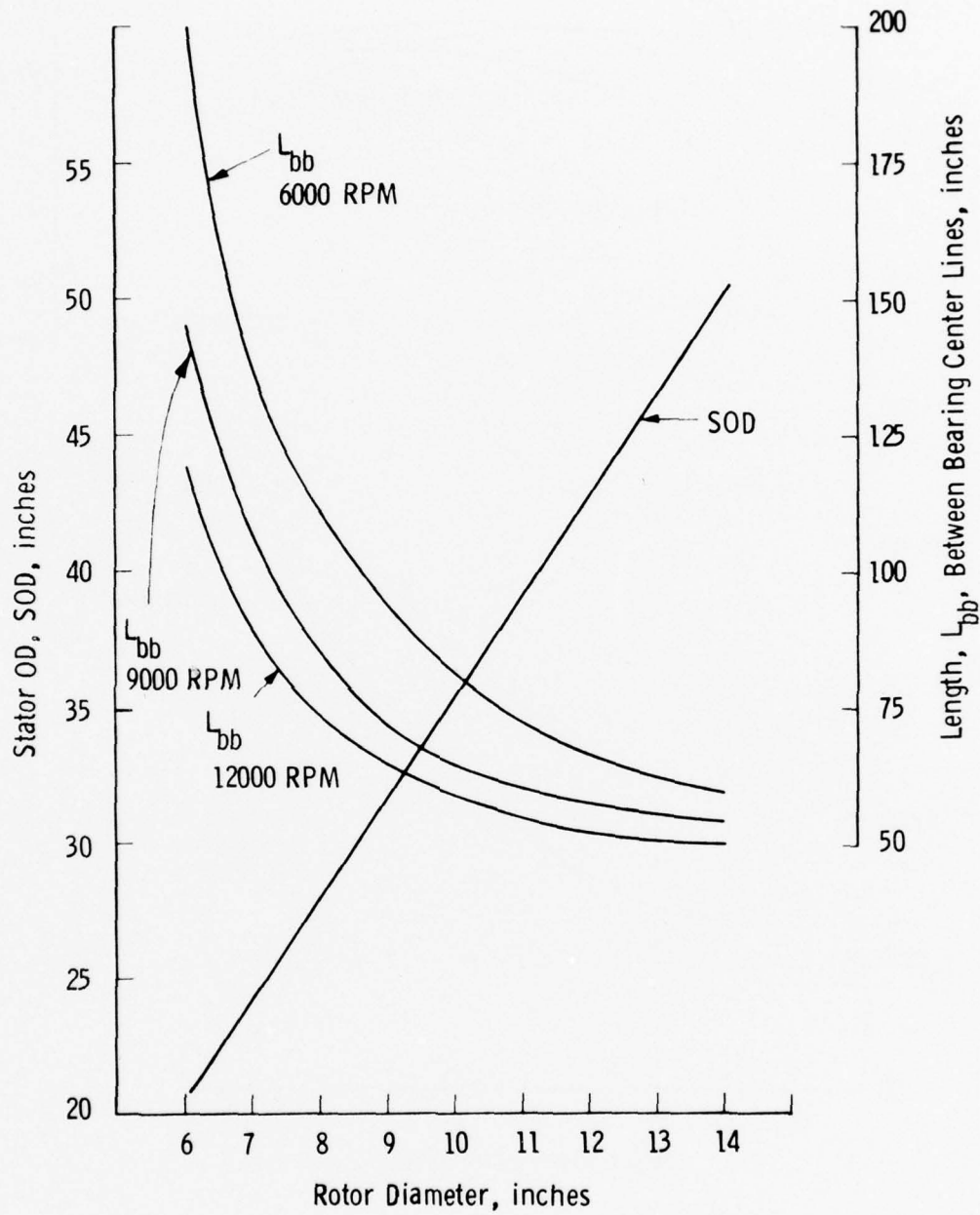


Figure 5.2 70 KHP (52.5 MVA) Generator 13.8 KV

current required large conductor cross-sectional areas and because of the limited circumferential length of the 15-3/4 inch rotor diameter led to deep bars which increased the magnetic gap of the machine and a larger number of ampere turns for excitation. Lowering the system voltage intensified this problem and raising it led to current collector bar voltages that were excessively high. Going to larger rotor diameters alleviated the excitation ampere turns; however, the tip velocities of the collector bar/brushes interface became excessively high. Even with the 15-3/4 inch rotor diameter, tip speeds at the brush interface are considerably higher than conventionally accepted values. The length of the machine between bearings is approximately 240 inches which would present critical speed problems. With a stator outside diameter of 42.5 inches and a total machine weight of 62,000 pounds. This dc generator could not be considered small, compact or lightweight and hence was dropped from further consideration. The only feasible machine design at this power rating would be at a much slower speed and therefore larger, heavier generator; however, since this slower speed reflects back to a slower, larger power turbine it was not further considered.

5.1.8.2 Superconducting Motors

Although the ac motor speed was assumed to be driving a 50,000 HP, 1200 RPM load, the parametric variations of superconducting generator speed resulted in changing the number of poles of the motor to accommodate the different frequencies. At 6000 RPM and 12,000 RPM generator speed, the number of motor poles were 10 and 20 respectfully; however at the 9,000 RPM generator speed the number of motor poles was 16, resulting in a motor speed of 1125 RPM which is the closest speed match to 1200 RPM possible. In the optimization process, the higher number of poles results in lighter weight machines at slightly higher rotor diameters due to the improved pole-face to pole-pitch ratio. This is shown on Figure 5.3 which indicates minimum weights at rotor diameters of 38, 52 and 60 respectfully for the 100, 150 and 200 Hz motors. As in the case of the generators, machines of minimum weight are not necessarily the most compact, as shown on Figure 5.4 where the length (between bearing centerlines) is plotted for each motor. The more compact machines in terms of length and stator outside diameter



Westinghouse

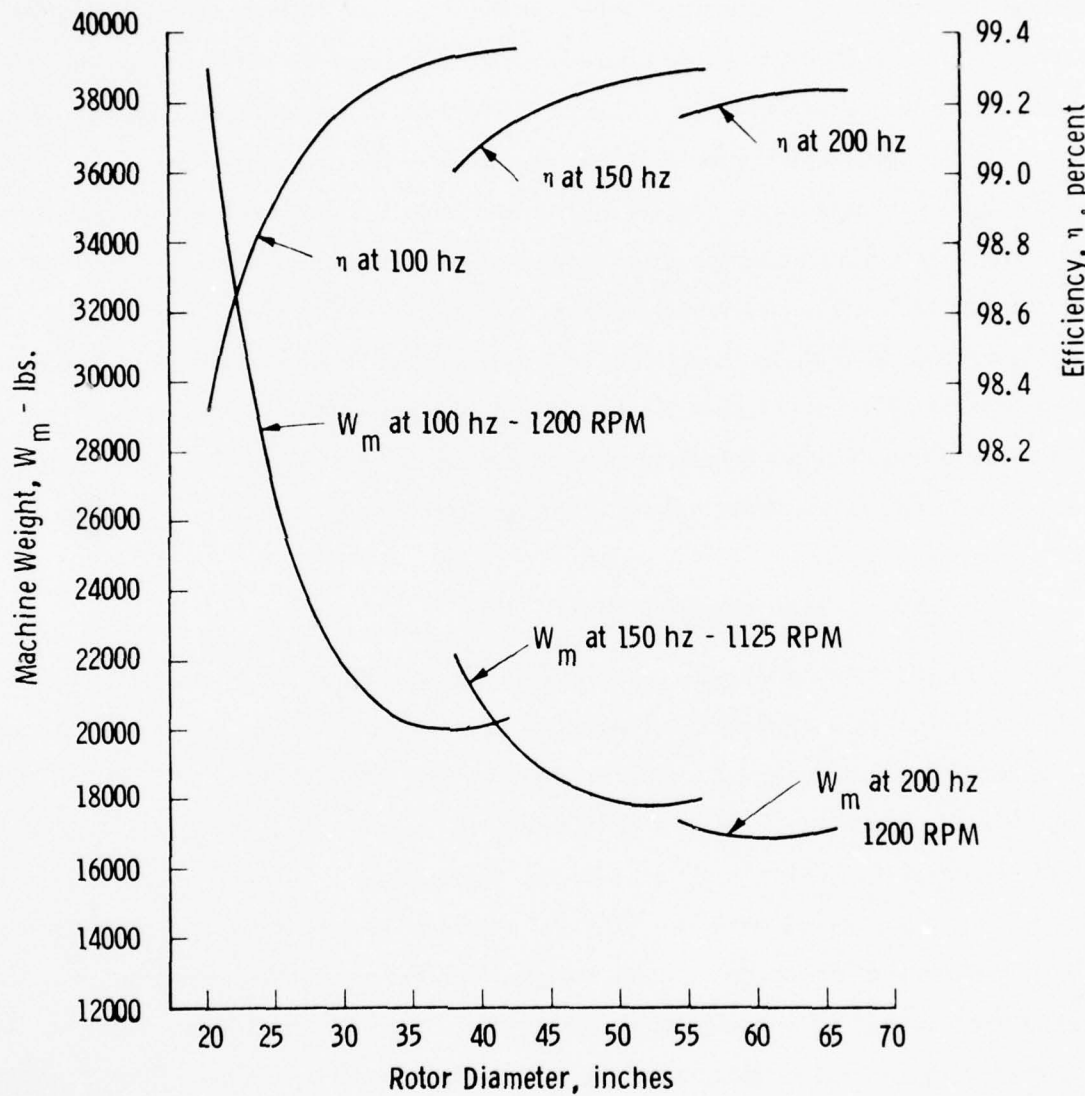


Figure 5.3 50,000 HP Motor

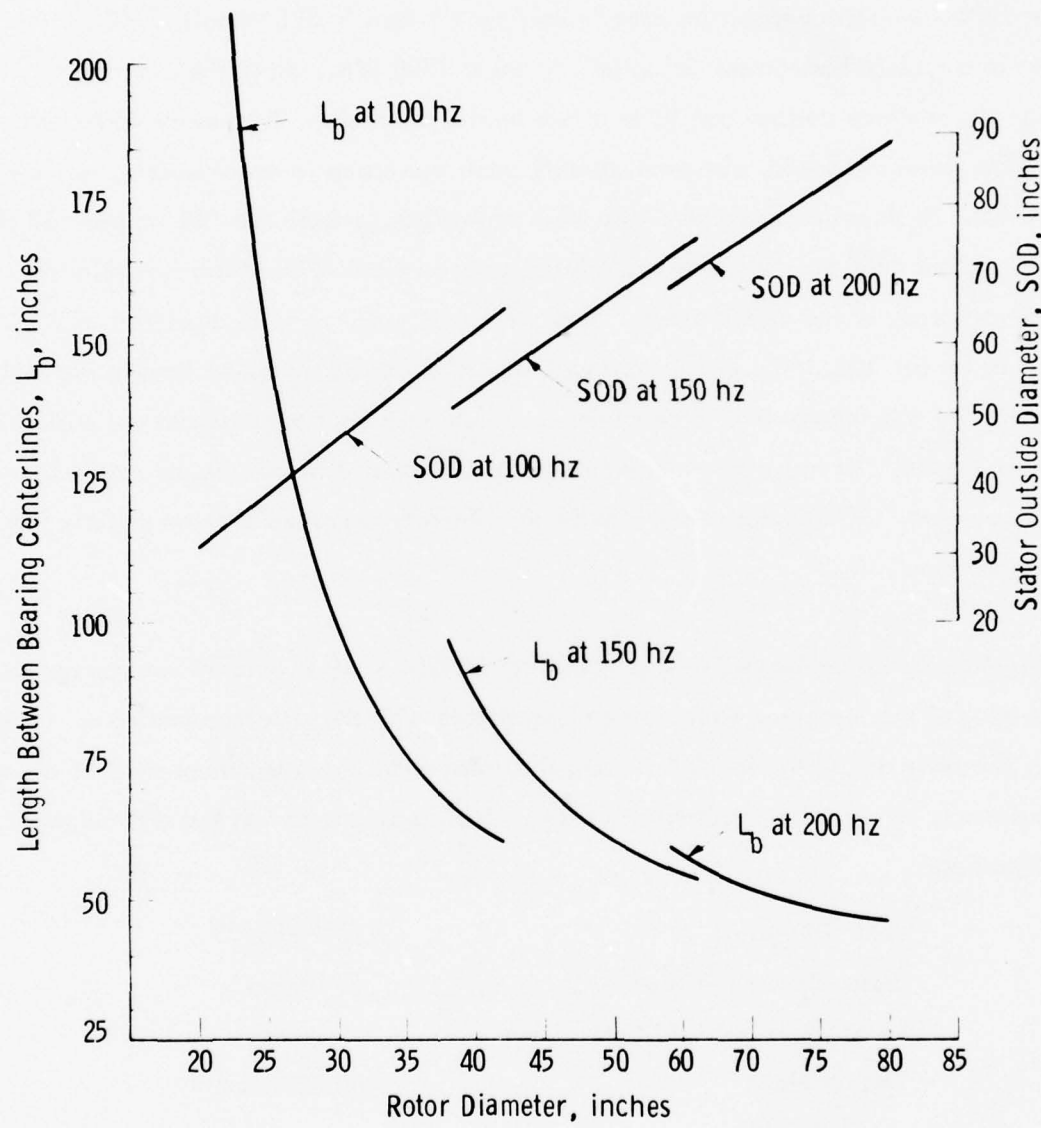


Figure 5.4 50,000 HP Motor



Westinghouse

tend toward the higher rotor diameters at a slightly higher weight penalty. Peak efficiencies also tend to favor the higher rotor diameter designs.

For ac motors of lesser capacities, usually used for lift fans in SES vessels, 5000 HP was chosen as a typical horsepower rating at a speed of 1500 RPM. As in the other ac machines, varying the machine voltage had little effect on the motor size. Frequency variations, dependent on the generator speed, also produce only small variations in motor weight, as shown on Figure 5.5. As shown on this figure, the minimum weight for both the 100 Hz and 150 Hz motors is about 4400 pounds while the 200 Hz motor is about 4700 which is within the 10 percent accuracy of the calculations. These minimums occur at rotor diameters of 20, 28 and 34 inches for the 100, 150 and 200 Hz machines respectively. Machine lengths are plotted on Figure 5.6 which show that these minimum weight machines are near but not quite at the optimum lengths. For more compact motors, rotor diameters 4 inches greater would be more nearly optimum. Efficiencies would also be significantly improved at these slightly larger rotor diameters.

Investigating dc motors for delivering 50,000 HP at 1200 RPM, it quickly became apparent that the weights of the machines would not be comparable with the superconducting ac machines. This is primarily due to the lower flux densities inherent in these machines and the amount of iron necessary to carry the required flux. The principle parameters of the most promising design developed are:

Rotor Diameter	45 inches
Stator Outside Diameter	67 inches
Length Between Brg. Centerlines	149 inches
Total Weight	105,000 pounds

Parametric variations of rotor diameter around 45 inches had no appreciable effect on the machine weight. Since this weight was five times greater than the ac motor and also since the corresponding dc generator was similarly large and heavy, further investigative effort on dc motors seemed unwarranted.

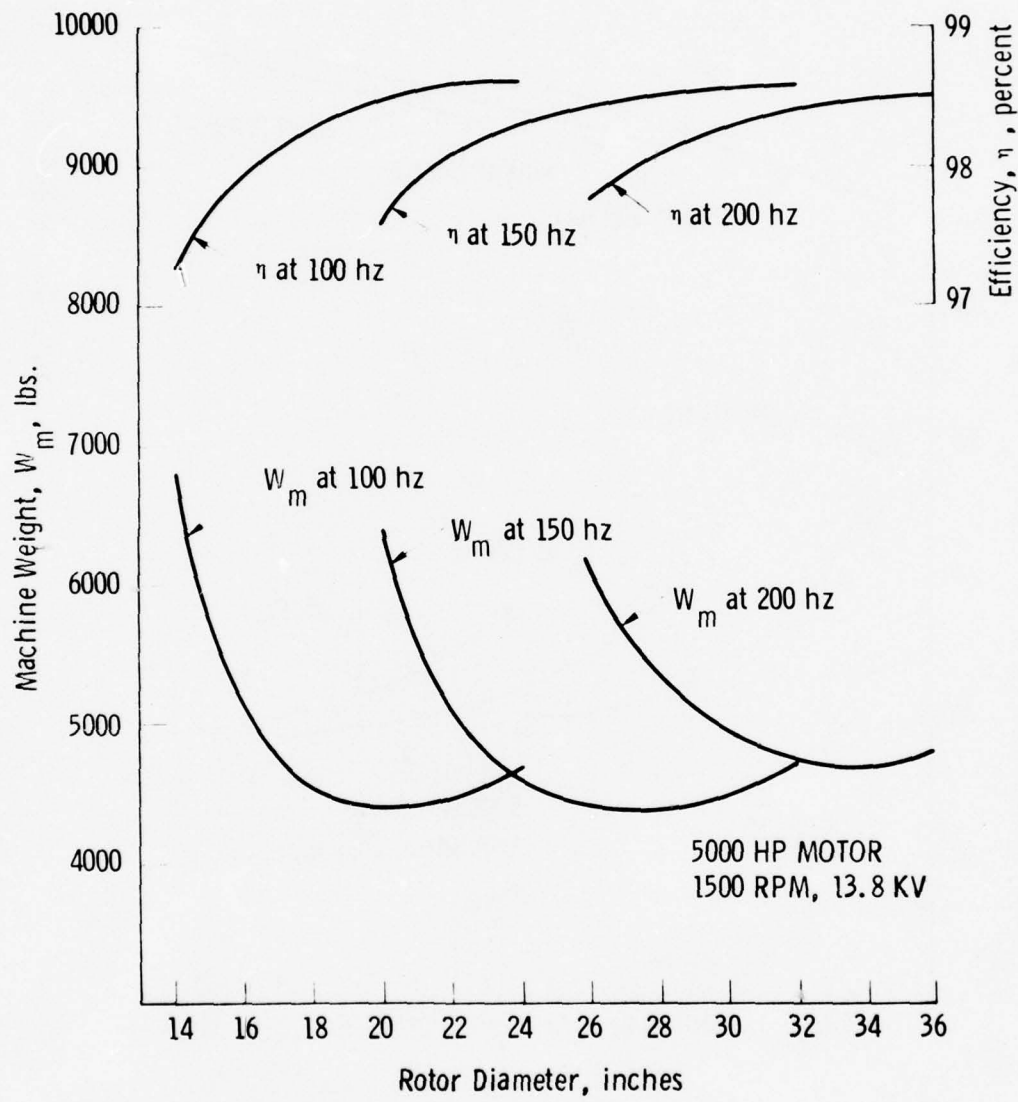


Figure 5.5 5000 HP Motor 1500 RPM, 13.8 KV

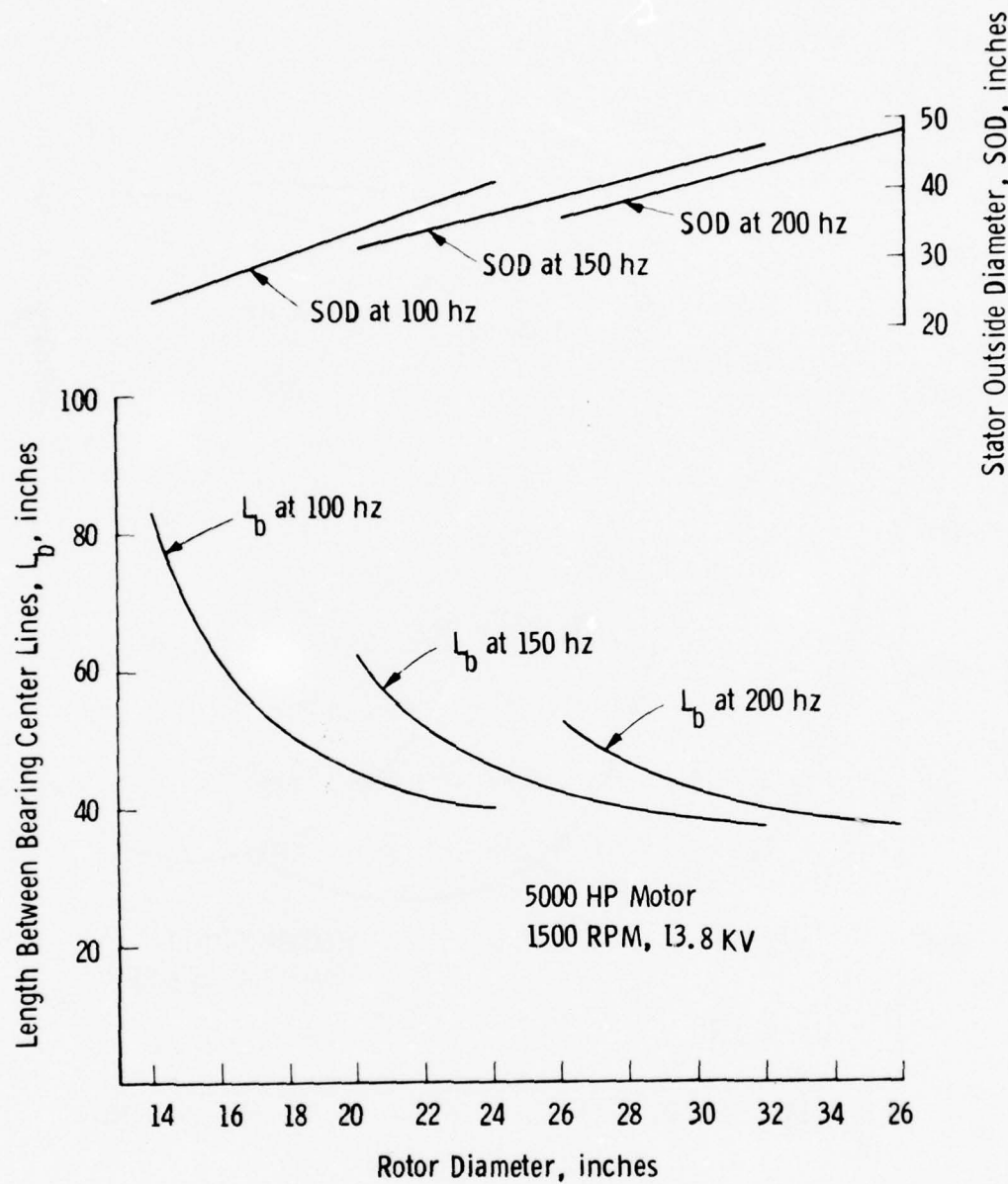


Figure 5.6 5000 HP Motor 1500 RPM, 13.8 KV

By observing the plots of ac machines, one can pick designs which are the lightest weight, most compact or the most efficient depending on which criteria is used in defining the most optimum machine. It would appear however that machines with rotor diameters slightly greater than those with minimum weight would be more nearly optimum in terms of compactness and efficiencies with only slightly greater weight penalties. Systems incorporating these machines (assuming 13.8 KV machine voltages) would utilize exciters, switchgear and control equipment of approximately the same size and weight and therefore total system weight would be dependent on the generator speed-chosen. For example if it is assumed that a system consists of four propulsion generators, two propulsion motors and four lift-fan motors, total machine weights would be as follows:

	Wt. at 100 Hz		Wt. at 200 Hz	
	Minimum	Penalty	Minimum	Penalty
Generators	58,000 lbs.	2,800 lbs.	34,400 lbs.	2,400 lbs.
Prop. Motors	40,000	800	34,000	600
Lift	17,600	200	18,800	400
	115,600	3,800	87,200	3,400

Selecting the 12,000 RPM generators over the 6000 RPM design would then result in a system machinery weight advantage of about 28,400 pounds if minimum weight machines were selected. If a weight penalty is accepted in order to achieve compactness and slightly higher efficiencies, this weight advantage would decrease to 25,000 pounds. It must be reiterated here that this weight advantage may not be achievable due to the problems of the 12,000 RPM generator as discussed in Section 5.1.8.1. A much more detailed design of the generator would be required to determine its feasibility. However, based upon these and other studies, it appears that a speed of 9,000 RPM for the ac superconducting generators should be acceptable and can be assumed for CCCBS interface conditions.

5.2 ENERGY SOURCE HEAT EXCHANGER INTERFACE CONSIDERATIONS

As discussed in Section 1.0, the results of the overall CCCBS study are to be as generally applicable as possible and the scope of the CCCBS power conversion system therefore does not include a specific energy source. The CCCBS power conversion system is considered to interface with, but not include, either a fossil fired heat exchanger or a gas cooled nuclear reactor wherein the energy is added to the closed Brayton cycle. This system definition permits studies and evaluation of the system with consideration given to the alternate heat sources which the Navy may desire to use without constraining the studies by the characteristics of a single fuel and heat exchanger assumption.

Evaluations of the power conversion system must, however, recognize and give proper consideration to the expected ranges of fossil fired energy source heat exchanger characteristics to insure that the results are appropriate for applications which may be selected. An early study was therefore required to provide the necessary consideration of power conversion system/energy source heat exchanger interfaces. In this study the state-of-the-art of heat exchangers was evaluated to identify and quantify the interfaces of importance and the requirements placed upon the power conversion system from energy source heat exchanger considerations. These results therefore provide input to the Design Concept definition and later evaluation of feasibility.

5.2.1 Heat Exchanger Design Considerations

The state-of-the-art survey to evaluate representative heat exchangers and their performance limits is constrained by several factors that must be considered in the design of a fossil fuel fired CCCBS. A principal requirement for high temperature heat exchangers is that they must operate for long periods and high temperatures with large pressure differentials between the gas streams. For compact lightweight propulsion systems, the energy source heat exchanger must provide high effectiveness with a minimum impact on overall system volume and weight and must be capable of withstanding the high shock environment required for naval propulsion powerplants. To minimize significant performance penalties, leakage between the gas streams

must be minimized. The characteristics of the combustion gas stream also impose additional considerations such as oxidation resistance and susceptibility to flow stoppage.

Table 5.1 summarizes generalized candidate configurations and potential advantages and disadvantages. The tube and shell configuration is inherently more suited for this application compared to the plate/fin configuration because it is better suited to withstand high stress loadings and to minimize leakage and plugging of the combustion products.

For high temperature heat exchangers, material temperature limits provide a major constraining factor. Superalloys have been utilized in most high temperature metallic concepts and the design and fabrication of superalloy heat exchangers is a well developed technology. In addition, superalloys are oxidation resistant. A major drawback is their limited maximum temperature capability. Refractory metals have high temperature strength capability, but are difficult to fabricate and have little resistance to oxidation, thus precluding their use as the energy source heat exchanger. Graphite is an excellent high temperature structural material; however, its permeability to low molecular weight gases and the lack of a high integrity joining process make its use unlikely. Ceramics also are excellent high temperature structural materials that are oxidation resistance and low in cost, but are brittle. Permeability and fabrication of ceramic heat exchangers are design problems. The considerable development efforts currently being applied to ceramic heat exchangers should lead to a solution to these problems for stationary powerplants. The material candidates that offer the best potential for near term and, eventually, long term consideration, therefore, are the superalloys and ceramics, respectively.

As a result of these considerations, the state-of-the-art survey was concentrated on tube and shell designs incorporating superalloys and ceramics.



Westinghouse

TABLE 5.1
BASIC DESIGN CONSIDERATIONS

<u>CONFIGURATION:</u>	<u>ADVANTAGES</u>	<u>DISADVANTAGES</u>
Tube and Shell	Leak Tight High Stress Loading	Headering
Plate Fin	Lower Material Cost for Equivalent Surface Area to Volume Ratio	Stress Load Capability Lack of Leak Tightness Susceptible to Plugging of Combustion Gases
MATERIALS:		
Superalloys	Low Cost Oxidation Resistance Fabrication Experience	Temperature Limited to 1750°F for Long Life Limited Long Life Experience
Refractory Metals	High Temperature Strength Capability	High Cost, No Oxidation Resistance Difficult Fabrication Little Experience in Long Life
Ceramics	High Temperature Capability Oxidation Resistance Low Cost Material	Brittle Questionable Permeability Limited Fabrication Capability
Graphite	High Temperature Capability Low Material Cost Fabrication Experience	No Oxidation Resistance High Permeability Brittle

5.2.2 Results of State-Of-The-Art Survey

The state-of-the-art survey consisted of evaluating heat source heat exchangers, intermediate heat exchangers and recuperators which have been designed for several technologies and have been carried to various states of development ranging from conceptual design to operational.

Applications considered included:

- Closed Cycle Gas Turbines Systems
- Process Industry Systems
- High Temperature Gas Cooled Reactor (HTGR) Systems
- Central Plant Topping Cycles
- Magnetohydrodynamics Systems
- Rankine Cycle Systems

The characteristics of several metallic heat exchangers at various stages of development are shown in Tables 5.2a and 5.2b. For heat exchangers presently in operation, peak wall temperature up to 1580°F have been noted with process gas temperatures up to 1450°F. The pressure level for these designs have ranged from 50 to approximately 500 psia. Commonly used tube materials have included the superalloys Inconel 807, Incoloy 800, and Haynes 188. Tube diameters have ranged from 0.25 inch to 2.0 inches.

The upper limits in temperature and pressure for the Inconels presently used today is a wall temperature of approximately 1650°F with pressure differentials in the 500 to 1000 psi range. In a practical design, a process gas temperature of 1500°F could be achieved within these material limits. Other Inconels such as Inconel 617 have been considered (References 4 and 9) in designs which can be operated at a peak wall temperature of 1750°F with a pressure differential of 1000 psia. This offers a potential of achieving a process gas exit temperature as high as 1600°F. However, the technology for Inconel 617 operating in an oxygen environment of these temperatures is not as firm as for the Incoloy 800 or Inconel 807 materials.

TABLE 5.2a
METALLIC HEAT EXCHANGERS FROM VARIOUS TECHNOLOGIES

Type	Gas Fired Heater	Heat Exchanger	Air Heater for Fluidized Bed	IHX for VHTR Application
Function	Closed Cycle Helium Turbine Plant	ANP	Closed Cycle Gas Turbine	Process Heat
Development Status	Designed in 1972 for Test in 1974	Small Scale Testing in 1960	Detail Design	Conceptual Design
Fluids	Comb Gas/He	Salt/Nak	Comb Gas/Air	He/He
Configuration	Cross Parallel Tube in Shell	Counterflow Tube and Shell	Counterflow	Counterflow
Tube Material	Inconel 807	Inconel	Tubular Arrangement	Tube and Shell
Tube O.D.	2.0 Inches	0.23 Inch	Inconel 800	Inconel 617
Process Gas	1382°F	-	0.5 Inch	0.6 Inch
Exit Temperature	1382°F	-	1450°F	1600°F
Peak Wall Temperature	1472°F	1540°F	1580°F	1750°F
Pressure Level	409 psi	-	-	600 to 1000 psi
Pressure Differential	~400 psi	50 psi	130 psi	600 to 1000 psi
Δ P/P	4.2%	-	-	3%
Effectiveness	0.92	-	-	0.9
Q/V	-	-	-	0.3 MW/Feet ³
Advantages	Proven Technology in Fabrication and Joint Design	Proven Technology in Fabrication and Joint Design	Based on Technology for Industrial Processes	Based on Proven Technology in Joint Design and Fabrication
Disadvantages	-	Experienced Failures During Cyclid Thermal Test	-	Needs Design Development
Reference	1	2	3	4

TABLE 5.2b
METALLIC HEAT EXCHANGERS FROM VARIOUS TECHNOLOGIES

Type	Gas or Oil Fired Potassium Boiler	HTGR Recuperator	Heat Source Heat Exchanger	Primary Heat	Helium Heater
Function	Central Plant Topping Cycles	Nuclear Powered Closed Cycle Gas	Mini Brayton Cycle	Liquid Metal MHD System	Helium Direct Cycle CTF
Development Status	Built and Under Construction	Under Development	Conceptual Design	Detailed Design	
Fluids	Gas/K	He/He	He/Xe	Argon/Liquid Metal	Combustion Gas/He
Configuration	Counterflow Tube and Shell	Counterflow Tube and Shell	Tubular	-	Dual Concentric Tube
Tube Material	SS-304	2-1/4 Cr-1 Mo/316 SS	Columbium Alloy	Haynes 188	Inconel 617/ Incoloy 800
Tube O.D.	1.0 Inch	0.44 Inch	-	2.0 Inches	1.5 Inches
Process Gas	-	930°F	1600°F	1500°F	1500°F
Exit Temperature	1580°F	970°F	1600°F +	~1500°F	1600°F
Peak Wall Temperature	-	-	-	-	-
Pressure Level	-	960 psi	58 psia	1200 psia	1000 psia
Pressure Differential	120 psi	550 psia	~58 psia	-	950 psia
Δ P/P	-	1 to 2%	0.5%	9%	1.5%
Effectiveness	-	0.89	-	-	-
Q/V	-	-	-	-	-
Advantages	Fabrication Joint Design Established	Fabrication Joint Design and Stress Design Established	Demonstrates Design and Fabrication Facility	-	Demonstrates Design and Fabrication Feasibility
Disadvantages	-	Low Temperature Limit	-	Needs Design Development	Not
Reference	5	6	7	8	9

Current day tube technology indicates that tubes with diameters considerably smaller than 0.25 inch are readily available; however, at smaller diameters plugging of the combustion gas products may become significant.

Table 5.3 summarizes the characteristics of several designs incorporating ceramic tubes. Reference 11 discusses an operating recuperator that uses ceramic tubing. This particular design utilizes spring loaded metallic headering. As a result, the peak gas temperature on the heat removal side (which would be equivalent to the working gas temperature in the energy source heat exchangers) is limited to 1800°F although the silicon carbide tubing can withstand wall temperatures up to 2500°F. Furthermore, this particular heat exchanger was designed for a low pressure differential. It is anticipated that with a significant pressure differential, considerable leakage between gas streams would occur in this design. Conceptual designs (References 10 and 12) indicate a potential for achieving wall temperatures as high as 2500°F and process gas temperatures of approximately 2250°F. Pressure differentials of the order of 500 psia appear achievable. Presently, the ceramic heat exchanger is a developing technology with major questions of the fabrication of leak tight headering and permeability characteristics. Developmental work is in progress, however, which indicates probability of successful development for stationary powerplants.

Representative characteristics of the heat source heat exchanger are summarized in Table 5.4. In this table, current technology represents heat exchangers now in operation or in detail design. The near term development category represents performance estimates which should be achievable with moderate technology development. The long range development category represents performance levels that require significant technology development.

5.2.3 Conclusions

For assessing feasibility of CCCBS with fossil heat sources, the most promising characteristics of the energy source heat exchanger are those that can be achieved with moderate technology development. Based on the results of the state-of-the-art survey and reasonable design practices,

TABLE 5.3
STATE-OF-THE-ART OF CERAMIC HEAT EXCHANGERS (CONTINUOUS FLOW TYPES)

Type	Coal Fired Heat Exchanger	Recuperator	Heat Source Heat Exchanger
Function	Process Heat	Slot Furnace	Closed Brayton Cycle
Development Status	Conceptual Design	Built and Tested	Under Development
Fluids	Comb Gas/Helium	Comb Gas/Argon	Comb Gas/He-Xe
Configuration	Counterflow, Tube and Shell	Cross-Counterflow Tube and Shell	Cross-Counterflow Tube and Shell
Tube Material	Ceramic/Superalloy	SiC	SiC
Tube O.D.	-	-	-
Process Gas Exit Temperature	2250°F	1800°F	2250°F
Peak Wall Temperature	2500°F	2500°F	2500°F
Pressure Level	500 psi	Low	500 psi
Pressure Differential	~500 psi	Low	~500 psi
ΔP/P	2 to 3 %	-	-
Effectiveness	~0.8	0.55	~0.5
Q/V	-	-	-
Advantages	Metal-Sealing Ceramic Stress	Simple Design Simple Fabrication	Simple Design
Disadvantages	<ul style="list-style-type: none"> • Complex Design • Unproven Fabrication • Permeability Unproven 	<ul style="list-style-type: none"> • Ceramic Metal Spring • Loaded Seals • Questionable Shock Resistance • Questionable Stress Capability • Low Effectiveness (55%) 	<ul style="list-style-type: none"> • Fabrication Capability • Not Fully Developed • Permeability Capability • Not Fully Developed • Low Effectiveness



Westinghouse

TABLE 5.4

HEAT SOURCE HEAT EXCHANGER
STATE-OF-THE-ART

	CURRENT TECHNOLOGY	NEAR-TERM DEVELOPMENT	LONG RANGE DEVELOPMENT
Configuration	Counterflow	Counterflow	Cross Counterflow
	Tube and Shell	Tube and Shell	Tube and Shell
Tube Materials	Inconel, Stainless Steel, Hastelloy	Inconel	Silicon Carbide
Peak Wall Material	1600° F	1650 to 1700° F	2500° F
Process Gas	1500° F	1550 to 1600° F	~2250° F
Outlet Temperature			
Pressure Level	500 psi	600 to 1000 psi	~500 psi
Tube Outside Diameters	0.25 to 0.5 Inch	0.25 to 0.5 Inch	~0.5 Inch
$\frac{\Delta P}{P}$ (Working Fluid)	1 to 4%	1 to 3%	1 to 3%

representative interface characteristics that can be expected using superalloy materials are:

• Maximum Wall Temperature	~1700°F
• Maximum Gas Temperature	1500-1550°F
• Pressure Level	1000 psi
• Effectiveness	0.8 - 0.9
• $\frac{\Delta P}{P}$ (Working Fluid)	1 - 3%

These interface conditions are consistent with the study guidelines and are judged to be sufficiently conservative to support conservative assessments of CCCBS feasibility. The constraints associated with the limitation to superalloys has been imposed because of the recognition of the high shock and vibration capabilities required for naval propulsion powerplants and because of the relative maturity of superalloy heat exchanger technology. It should be recognized, however, that on-going developments of very high temperature heat exchangers can, when successfully completed and adapted for naval powerplants, further enhance the performance of fossil fired closed Brayton cycle systems.

5.3 REFERENCES

1. Bammert, K. and Deustes, S., "Layout and Present Status of the Closed Cycle Helium Turbine Plant Obenhausen," 1973.
2. Fraas, A. P., "Design Precepts for High Temperature Heat Exchangers," Nuclear Science and Engineering, Volume 8, No. 1, July 1960.
3. Fraas, A. P., et al, "Design Study for a Coal-Fueled Closed Cycle Gas Turbine System for MUIS Applications," 10th IECEC, August 1975.
4. "Very High Temperature Reactor Engineering Design Studies," WAES-TME-2800, Westinghouse AESD, September 1976.
5. Fraas, A. P., "Preliminary Assessment of a Potassium-Steam Gas Vapor Cycle for Better Fuel Economy and Reduced Thermal Pollutions," ORNL-NSF-EP-6, ORNL, August 1, 1971.
6. McDonald, C. F., et al, "Heat Exchanger Design Considerations for Gas Turbine HTGR Power Plant," ASME Paper 76-GT-53.
7. Kenney, W. D., "Brayton Isotope Power System Ground Demonstration," 11th IECEC, August, 1976.
8. Holman, R. R., Lippert, T. E., "Liquid Metal Magnetohydrodynamic System Evaluation," Paper 769180, 11th IECEC, August 1976.
9. Larson, V. R., et al, "Helium Heater Design for the Helium Direct Cycle Component Test Facility," AIAA Paper No. 75-1262, Rocketdyne, September 1975.
10. "Proposal to Electric Power Research Institute for a Coal Fired Prototype High Temperature Continuous Flow Heat Exchanger," WANL-M10-0513, Westinghouse Advanced Energy Systems, May 1975.
11. Bjerklic, J. W. and LaHayne, P.S., "A Practical Ceramic Recuperator System for High Temperature Furnaces," Hague International, 11th IECEC, May 1976.
12. Fayrweather, D. J., et al, "Advanced Marine Closed Brayton Engines," AiResearch, Paper No. 76-312002, September 1976.

6.0 MATERIALS TESTING AND EVALUATION

6.1 INTRODUCTION AND BACKGROUND

In the proposed closed cycle Brayton system, the highest combination of stress and temperature occurs in the first row turbine blades. First stage stator vanes and blades are expected to operate at elevated temperatures for a system life in the range of 10,000 to 40,000 hours. The working fluid will be an inert gas, helium, with equilibrium concentrations of various impurities. Based on past helium turbine design technology, such as that from the Westinghouse closed Brayton turbomachinery development under contract with the U. S. Maritime Administration, and based on expected materials properties, it has been concluded that a turbine inlet temperature on the order of 1700°F pushes but does not exceed the state-of-the-art for uncooled turbine blades and stators in inert gas. This conclusion regarding materials capability, however, is based on engineering extrapolation of materials properties data obtained in inert gas at lower temperature and on properties data at comparable temperature in air for shorter test time periods. In order to demonstrate material performance feasibility, material testing is necessary to confirm properties and to provide baseline data for feasibility evaluation.

Historically, superalloy alloy development has been aimed at problems associated with aviation and land gas turbines where hot corrosion and oxidation are the primary factors which limit component life. While creep-rupture behavior is an important design consideration in such systems, hot component life is limited to a large degree by materials compatibility with combustion products, including fuel impurities such as sulfur compounds and catalytic agents, vanadium pentoxide, from fuel processing. In the case of CCCBS, creep behavior is expected to be a primary design consideration for turbine components. Minor amounts of active contaminants in the inert working fluid are expected to produce surface reactions which may or may not influence creep behavior. Most superalloys are designed for and are tested in air and

fossil fuel combustion products and, as a result, are optimized for these environments. This is particularly true with respect to creep-rupture properties.

The objective of this test program, which involves a three year effort, is to determine the feasibility of component materials to function under CCCBS conditions for the design life of the system. To achieve this objective a number of candidate turbine alloys were selected for creep-rupture testing. Five ultra-high vacuum creep-rupture test units were modified for ultra-high purity helium (UHP-He) operation. Initial testing during the first year of the study was initiated to establish baseline data under ultra-high purity helium environmental conditions for the feasibility evaluation.

In the remaining two years of the Materials Evaluation task, confirmatory data for candidate materials will also be obtained under the expected system environmental conditions. The actual system helium working fluid is expected to contain active gas impurities such as H_2 , CH_4 , H_2O , CO , and CO_2 from various sources within the closed powerplant system. These impurities can be carburizing, reducing, or oxidizing depending on the temperature and chemical potential as determined by the ratio of certain impurity species. For example, the oxygen potential is established by the H_2/H_2O and CO/CO_2 ratios, carbon by the H_2/CH_4 ratio and also by the CO/CO_2 ratio. Thus interaction of active impurity gases with metal surfaces can occur which may in some cases alter the mechanical properties of the material. These effects will be investigated in subsequent phases of the materials feasibility evaluation.

6.2 TEST EQUIPMENT AND PROCEDURE

Creep testing was carried out in five ultra-high vacuum creep test units modified for ultra-high purity helium atmosphere operation. The creep units are illustrated in schematic in Figure 6.1 and are pictured in Figure 6.2. Ultra-high vacuum creep test operation of these units is described in detail elsewhere⁽¹⁾. The cogent system characteristics which made these units ideally suited for ultra-high purity helium atmospheric testing are summarized as follows:

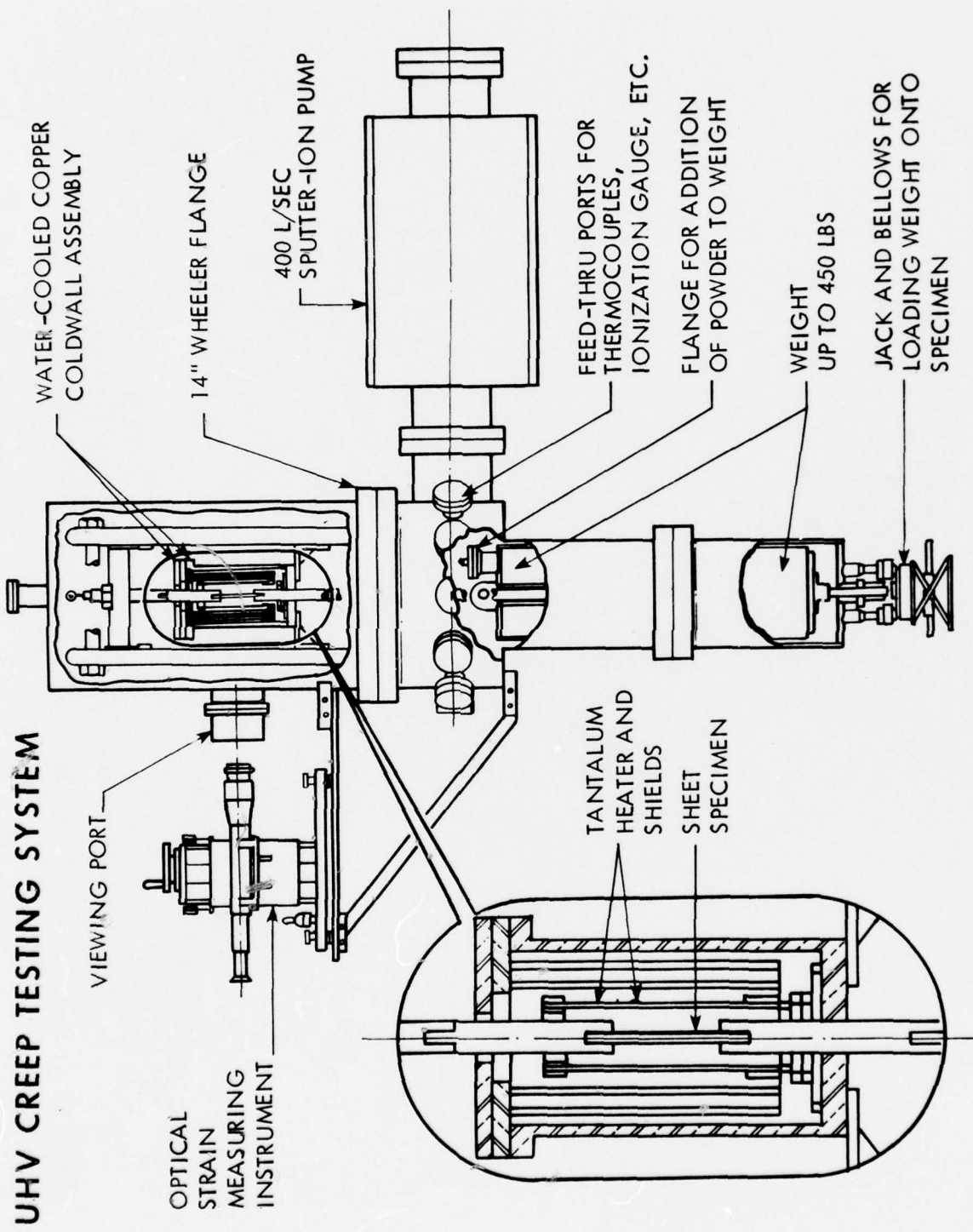


Figure 6.1 Schematic Diagram of Modified Ultra-high Vacuum Creep Units

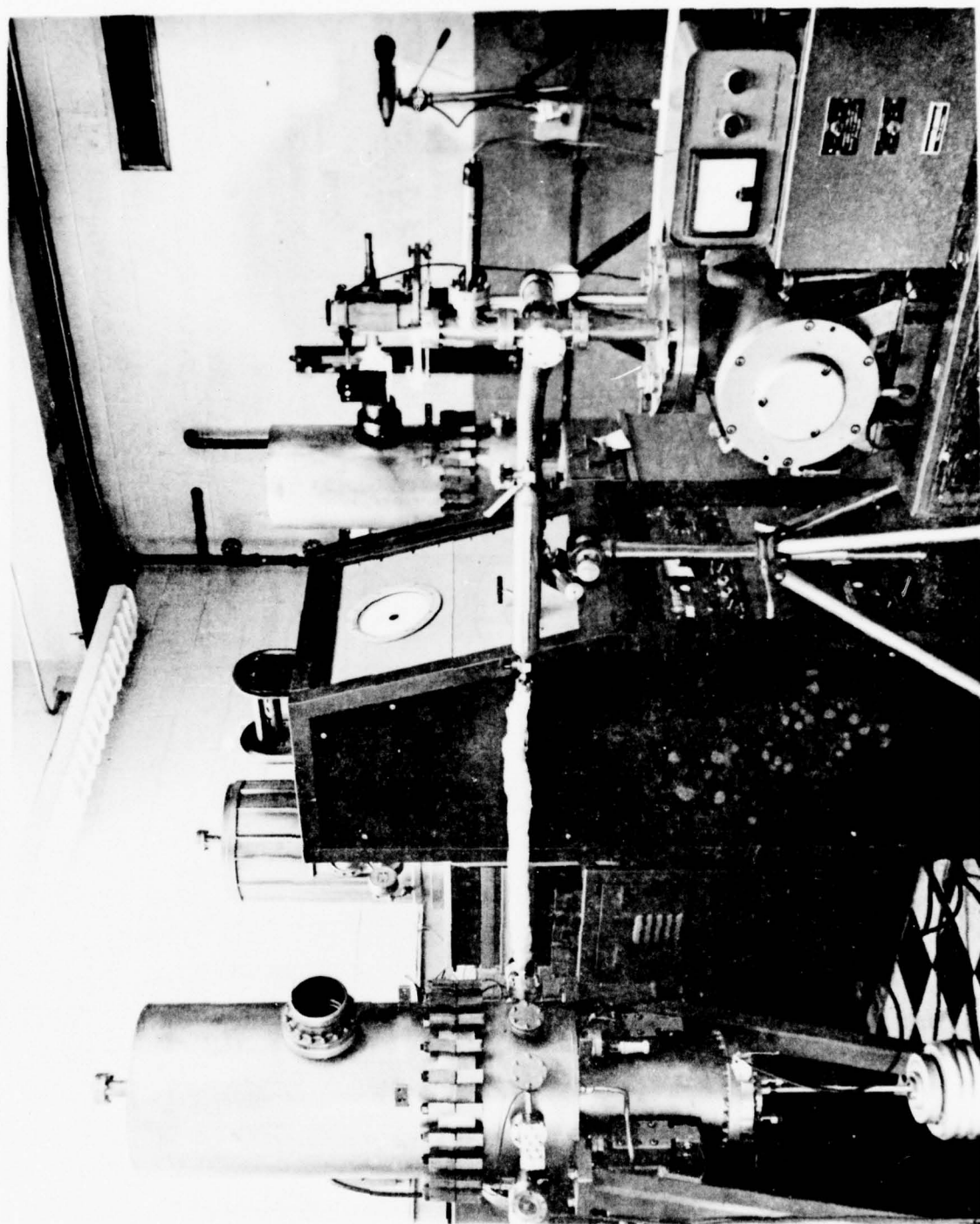


Figure 6.2 Photograph of Modified Ultra-high Vacuum Creep Units

- The all metal system construction utilizes crushable copper gasket seals which permits evacuation to pressures below 1×10^{-7} torr while the entire system is baked at 400°F. This operation removes adsorbed moisture and gases from all internal surfaces.
- The specimen is heated by radiation from a split tantalum resistance heating element insulated by tantalum radiation shields. Tantalum at temperatures above 1000°F is an active "getter" of oxygen, thus the test specimen is exposed to an environment with a very low oxygen level.
- The specimen is deadweight loaded internally by weights contained in the system. External loads are transmitted to the specimen through a stainless steel bellow seal.
- Specimen strain is measured optically directly off the gage section. This feature plus deadweight loading eliminates systematic error.

6.2.1 Helium Gas Analysis

Helium gas used for the creep testing atmosphere was Matheson Purity 99.9999% min. helium. Gas analysis was conducted using a one liter sample bottle which was attached to the system through a bakeable valve. The sample bottle, which was baked out under dynamic vacuum conditions, was permitted to equilibrate with the static helium environment within the test chamber. The helium in the sample bottle was analyzed using a technique developed at the Westinghouse Research and Development Center^(1,2). The helium in the sample bottle is drawn through a liquid helium cooled freeze-out trap which condenses out and effectively concentrates all gaseous impurities. The preconcentrated trapped gases are then warmed to room temperature. The resulting gas pressure in the cryogenic trap with a known volume is measured. The gases are then expanded into the inlet system of a mass spectrometer and analyzed quantitatively. Determination of water level is qualitative due to the limited size of the gas sample and difficulties which are inherent in the quantitative analysis

of water in the low ppm range. In all cases no distinction could be made between sample moisture level and mass spectrometer background which varied from the high ppb to the very low ppm level.

6.2.2 Test Procedure

A suitably prepared and thermocoupled test specimen was inserted into the test chamber shown previously in Figure 6.1. The grips were attached to the upper support member and weight train by means of pinned joints. The thermocouple leads were fed to the outside by means of a ceramic feedthrough assembly. Extreme care was exercised during loading of the system to prevent the introduction of any foreign matter, such as dirt, oil, etc., which would compromise system operation.

Personnel handled all hardware inside the vacuum envelope with lint free gloves. After the necessary internal connections were made the bell jar was put in place, all openings sealed, and the system evacuated. Pumpdown from atmospheric pressure was accomplished by means of a turbo-molecular pump to eliminate the possibility of contamination due to backstreaming of oil from the mechanical or diffusion pumps which employ organic pumping media. When the system pressure reached 1×10^{-5} torr the sputter ion pump was energized. After sufficient time to allow for pump outgassing and pump startup, the system was isolated from the turbo-molecular pump. After the ion pump startup, the system pressure decreased rapidly and after approximately one hour, was less than 1×10^{-6} torr. At that time the system was leak checked. After it was determined that the system was leak free, the system was baked to remove the adsorbed gas moisture from the walls of the test chamber. This was accomplished by enclosing the vacuum system within a two piece portable oven. The ion pump contains its own internal heater. Both pressure and temperature are used to control the amount of heat input during bakeout. During the initial portion of bakeout, a system pressure upper limit of 1×10^{-6} torr regulated the power input to the bakeout heaters. After removal of the major adsorbed gas load, the maximum temperature of the wall of the vacuum envelope is

limited to approximately 400 to 500°F by thermostats attached to the exterior surface of the vacuum system. After a bakeout of 12-24 hours, the system was cooled to room temperature and the bakeout oven removed. The system pressure after bakeout at room temperature was less than 5×10^{-10} torr. At this point, the helium backfill system, illustrated in Figure 6.3, was attached to the test chamber through a bakeable microvalve. All lines were stainless steel, and all connections were made using crushable copper gasketed flanges. The gas lines and gas sampling bottle were fitted with trace heating tapes. The backfilling procedure consisted of attaching the fill lines to the evacuated test chamber, connecting the turbo-molecular pump to the system, and placing a gas sample bottle in the system. The lines between the helium supply bottle and the test chamber were heated along with the gas sample bottle to 300°F while being evacuated by the turbo-molecular. A two to three hour bakeout was accomplished at a pressure of 1×10^{-6} torr or less, prior to release of the helium from the supply bottle into the backfill system and into the test chamber. The test chamber was filled to a pressure of 0.95 atmospheres. The gas sampling bottle valve was closed and the sample was removed for analysis.

Gas samples were taken at the beginning and at the conclusion of a creep test. Typical analytical results are reported in Table 6.1. Hydrogen was the most prominent active gas with concentration levels which varied from initial values of 0.35 ppm to maximum values as high as 4.0 at the end of testing. All other active gases were either not detected or were present in levels which were consistently less than 1.0 ppm.

The test specimen was heated to temperature; and once stabilized, the weight was applied. When internal loading was utilized, the weight was supported through a bellows assembly. A partial load of several hundred psi was maintained on the specimen at all times. As soon as the test temperature was reached and thermal equilibrium established, the total load was applied to the specimen by retracting the support platform. Measurements were made of the specimen gage length to establish the l_0 at temperature. Periodically during the test duration the change in l_0 , Δl , was measured to establish the time-elongation curve.



Westinghouse

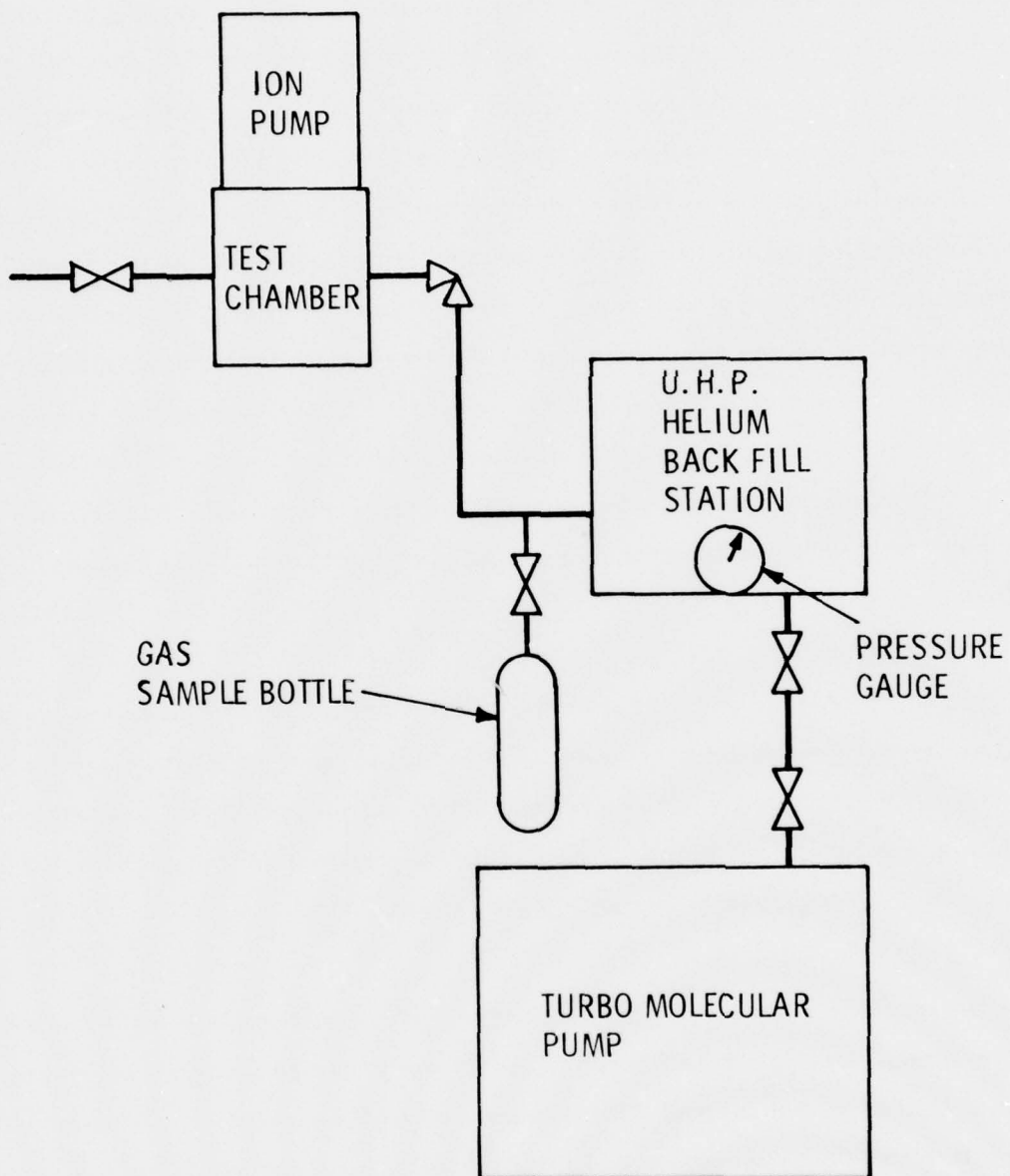


Figure 6.3 Schematic Diagram of Ultra-High Purity Helium Creep Test Unit with Helium Charging and Vacuum Evacuation Units in Place

TABLE 6.1
TYPICAL HELIUM GAS ANALYSIS

	Typical He Analysis (ppm)						
	H ₂	O ₂	N ₂	CO	CO ₂	THC	Ar
Final	1.0	0.04	0.9	ND	0.2	0.04	1.4
Initial	0.3	ND	0.07	ND	0.2	0.04	0.01
Initial	0.5	0.1	0.2	ND	0.4	0.10	0.01
Final	4.0	ND	ND	1.3	0.2	0.05	0.1
Initial	2.2	ND	ND	0.1	2.3	0.2	0.01

Final analyses were taken for tests run for >1000 hours. It must be noted that reported values at or below the 1 ppm level are at the limits of detectability and most likely represent background levels of the sampling and analytical equipment.

ND - Not Detected

THC - Total Hydrocarbons

Creep strain was determined by direct measurement of the separation of fiducial scratches applied to the extremes of the uniform gage section of the test specimen. The separation of the fiducial marks was followed by a horizontal telescope which moves vertically along a hollow column. The telescope is moved vertically by a 0.050 inch pitch precision micrometer screw and nut assembly mounted inside a dust tight column. The readings are made with a vertical reference scale and 100 part drum equipped with a 10 part vernier. The instrument, manufactured by Gaertner Scientific Corporation, can be read to 0.000050 inch.

Helium gas samples were also taken during and/or at the conclusion of the creep test. The helium backfill system (Figure 6.3) was reconnected to the test chamber and prepared as previously described. The test chamber valve was opened to allow the helium from the test system to enter the sample bottle. Sufficient time was allowed to permit pressure equilibration between the test chamber and sample bottle volume. After closing the valves to the test chamber and the sample bottle, the bottle was removed for analysis.

Creep testing in air was conducted in conventional lever arm test units equipped with resistance wound radiation heaters. In these units, strain is measured by means of a dial gage detecting lever arm motion.

Because of the location of the dial gage, deflections in the entire load train are detected. This arrangement can lead to possible larger indicated primary creep strains. Secondary creep rate and rupture life, however, are not affected.

6.3 ALLOY SELECTION, PROCUREMENT, AND CHARACTERIZATION

6.3.1 Alloy Selection

The alloys selected for the initial phase of the materials testing program are listed in Table 6.2. The first three alloys were selected on the basis of their commercial status and their particular applicability to the Compact Closed Brayton System requirements. Alloys 713LC,

TABLE 6.2
SELECTED ALLOYS AND NOMINAL COMPOSITIONS

Alloy	Density (lbs/in ³)	Composition (wt. %)
1. Alloy 713LC	0.289	Ni-12Cr-4.5Mo-2Cb-5.9Al-0.6Ti-0.05C
2. IN100	0.280	Ni-10Cr-15Co-3Mo-4.7Ti-5.5Al-0.9V-0.18C
3. MAR-M509	0.320	Co-23.5Cr-10Ni-7.0W-3.5Ta-0.2Ti-0.5Zr-0.6C
4. MA 754	0.300	Ni-20Cr-0.5Ti-0.3Al-0.6Y ₂ O ₃ -0.05C
5. TZM	0.368	Mo-0.5Ti-0.08Zr-0.02C



Westinghouse

IN100, and MAR-M-509 are commercially available alloys which have been used extensively in gas turbine applications over the past 10 to 15 years. Their history of metallurgical development and mechanical behavior are well documented. Thermal stability as determined by microstructural behavior on thermal exposure at elevated temperature is also well known and recorded. Alloy 713LC is one of a few nickel-base superalloys which does not contain cobalt as an intentional alloying addition. There are applications where cobalt is an objectionable alloying addition, and its presence is undesirable. IN100 is a "workhorse" turbine blade material designed to have a relatively low density combined with excellent creep resistance up to 1900°F. The alloy has been successfully cast and utilized in a variety of shapes from turbine blades, vanes, and nozzles to integral wheels. Cobalt alloys are generally used as vanes, nozzles, and other static hot structures because of their excellent hot corrosion (sulfidization) resistance. Cobalt alloys, however, are not generally used for rotating parts due to their lower creep and oxidation resistance compared to nickel-base alloys. MAR-M-509 has good creep strength, resistance to thermal stressing, and resistance to crack propagation. The alloy can be used in the as-cast condition; no heat treatment is required. It can be successfully welded and joined both to itself and to many dissimilar metals by conventional techniques.

MA 754 is a recently developed nickel-chromium alloy produced by mechanical alloying which uniformly disperses yttrium oxide for dispersion strengthening at temperatures to the alloys' melting point. MA 754 exhibits excellent stress-rupture properties which are equivalent to or superior to cast alloys. MA 754 is currently being used as vanes in gas-turbine engines where high temperature strength is required. The superior creep-rupture properties of MA 754 provides high temperature growth potential for CCCBS turbine components.

TZM, a molybdenum-base alloy, is a refractory metal alloy which has demonstrated compatibility with inert gases at elevated temperatures and has superior creep strength at 1800°F and above. TZM provides system growth to higher temperature capability.

6.3.2 Procurement

Alloy 713LC, IN100, and MAR-M-509 were obtained as "as-cast" creep specimens from Jet Shapes, Inc., of Rockleigh, NJ. Alloy 713LC was purchased according to a Westinghouse specification, since no formal published specification for the alloy could be found in the open literature. The specification was modeled after AMS 5391 for alloy 713C. The only difference being a lower carbon level, 0.05 percent for the LC version vs 0.12 percent for the "C" alloy designation. IN100 specimens were cast according to AMS 5397 and MAR-M-509 to a Pratt and Whitney specification PWA 647E. Cast specimens were examined by x-ray analysis to insure sound porosity free gage sections.

MA754 test material was procured from Huntington Alloys as solution annealed bar stock 3-1/2 in. x 1-1/4 in. by 5 in. long. No specification exists at this time for this material. A Huntington data sheet supplied with the material indicated the solution annealing heat treatment to be 1/2 hour at 2400°F followed by air cooling.

The TZM test specimens were machined from forged and stress relieved material which was part of a NASA sponsored creep test program. Processing information and chemical analysis were supplied by TRW, Cleveland, Ohio, the contractor to NASA⁽⁴⁾. The TZM alloy was obtained from Climax Molybdenum of Michigan (now AMAX) in the form of 11 inch diameter disc forging. The material was vacuum arc-melted to 11-1/2 in. diameter ingot, extruded to a 6-1/4 in. diameter, then upset forged to final size at 2200°F after heating to 2700°F. The material was then stress relieved one hour at 2700°F. Creep specimens were cut in a radial direction from the forged disc with the gage section parallel to the wrought microstructure. Chemical analyses of the test materials are given in Table 6.3.

6.3.2.1 Microstructure of Starting Material

The microstructures of the starting materials are shown in Figures 6.4, 6.5, 6.6, 6.7, and 6.8. Cross sections of the specimen gage sections of alloy 713LC and IN100 are shown to give an indication of the typical as-cast grain size. The microstructures shown at higher magnification

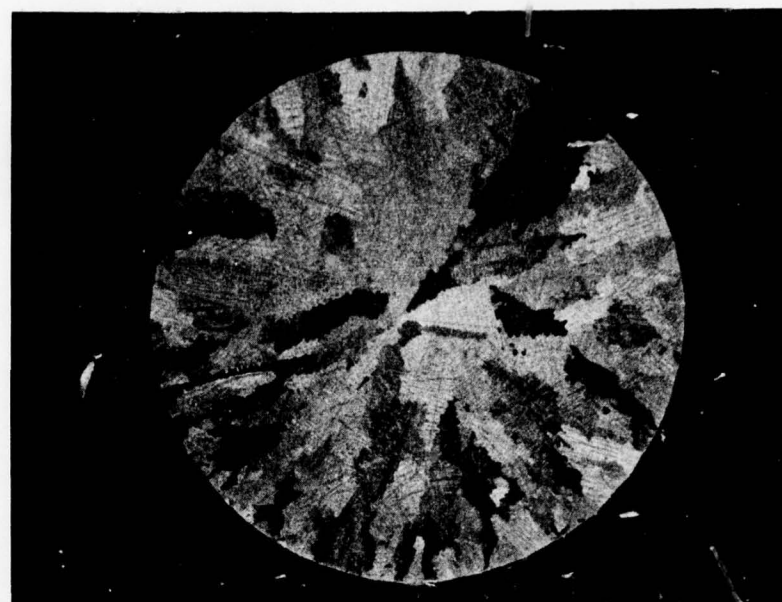
TABLE 6.3
CHEMICAL ANALYSIS OF TEST MATERIAL*
(PERCENT)

Alloy	Heat No.	C	Mn	P	S	Si	Ni	Cr	Mo	Co	Fe	Ti	Al	B	Zr	Other
713LC	8553	.06	<.1	<.01	.003	<.1	bal.	11.4	4.0	.1	.05	.6	5.75	.015	.13	Cu-.04; Cr-.199
IN 100	8747	.16	<.01	-	.004	.01	bal.	8.9	3.0	14.1	.2	.91	4.75	5.44	.001	V-.91
MAR-M509	8716	.621	.042	<.005	.005	.058	10.51	23.39	-	bal.	.408	.205	-	.0073	.467	Ta-3.47; W-7.24
MA 754**	DT0074B2-2	.02	-	-	-	-	bal.	20.0	-	-	.44	.3	-	-	-	Y ₂ O ₃ -.6
TZM	7502	.01	-	-	-	-	bal.	-	-	.5	-	-	-	.1	O ₂ -.002; N ₂ -.01; H ₂ -.001	

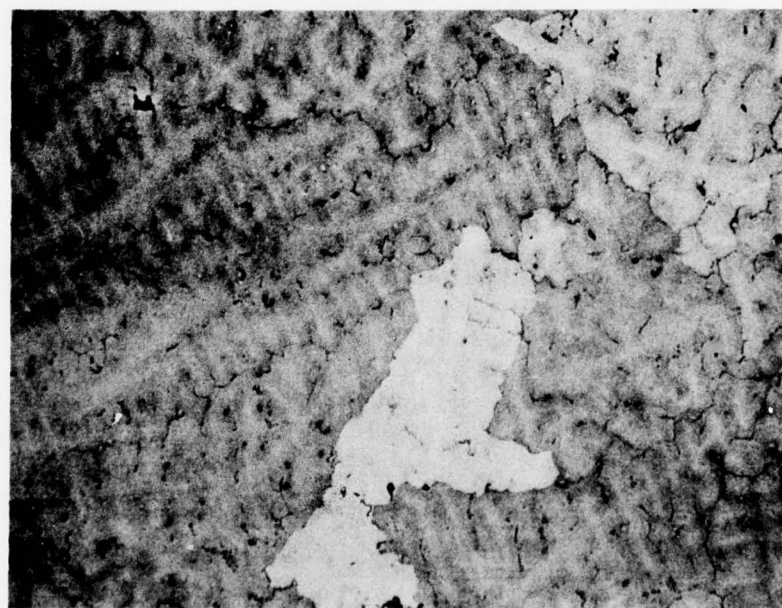
* Certified analysis by supplier

** Typical analysis

Alloy 713LC, IN 100, and MAR-M509 supplied by Jet Shapes, Inc.,
MA 754 by INCO, and TZM by AMAX.



12X



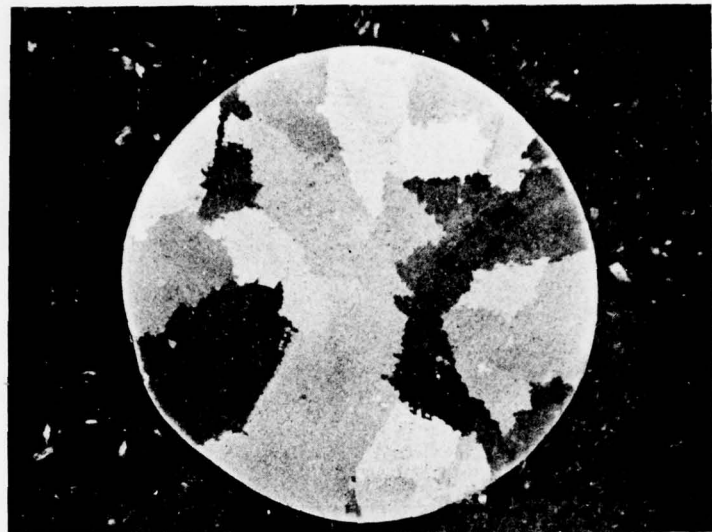
100X

Figure 6.4 Microstructure of As-cast Alloy 713LC

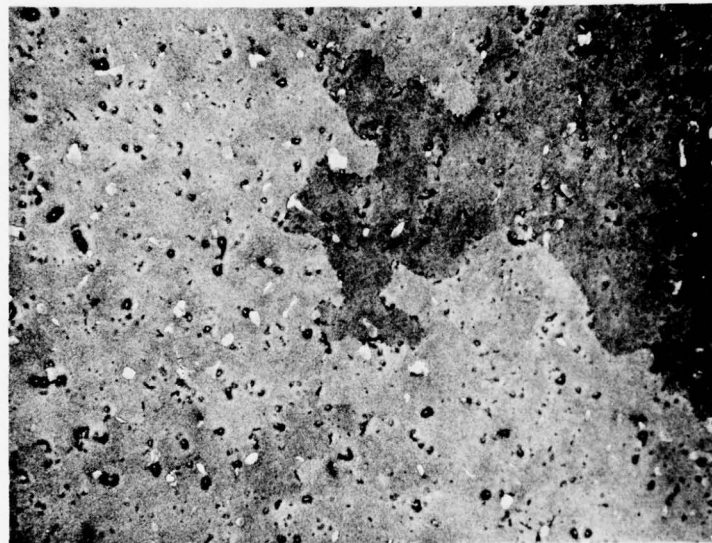
W

Westinghouse

A

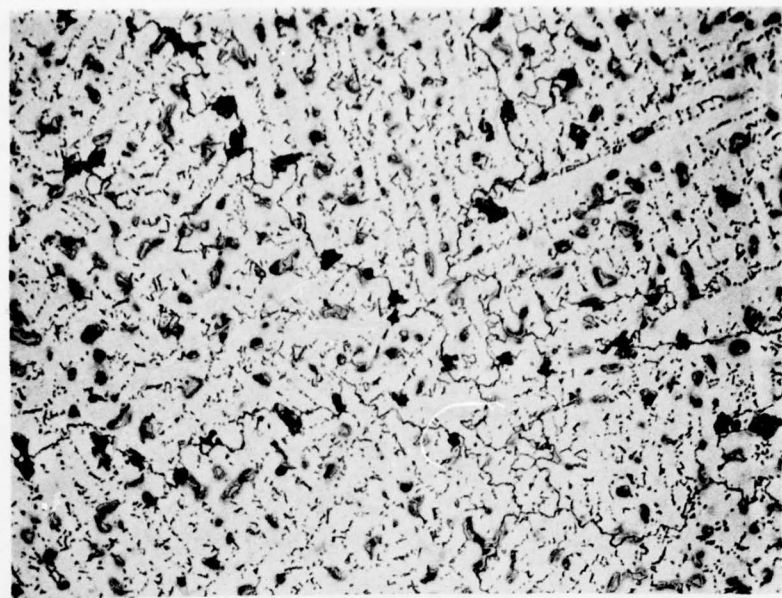


B

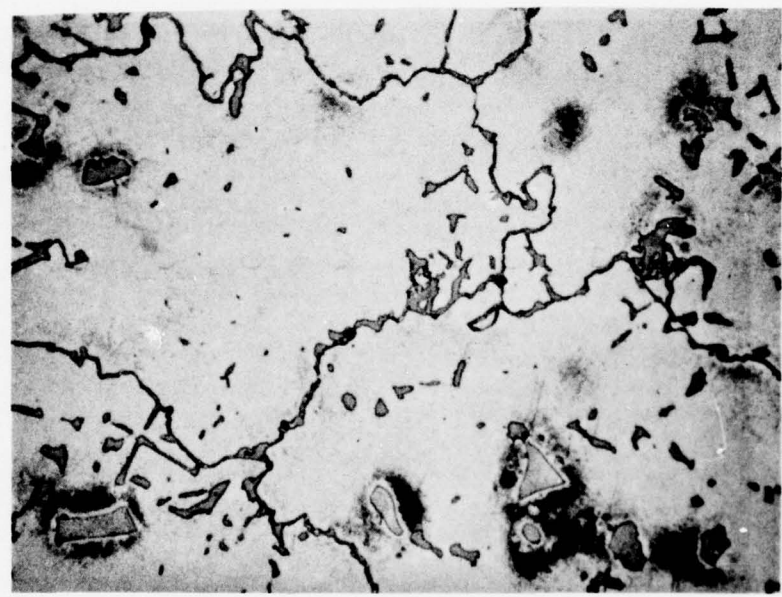


12X

Figure 6.5 Microstructure of As-cast IN100



100X

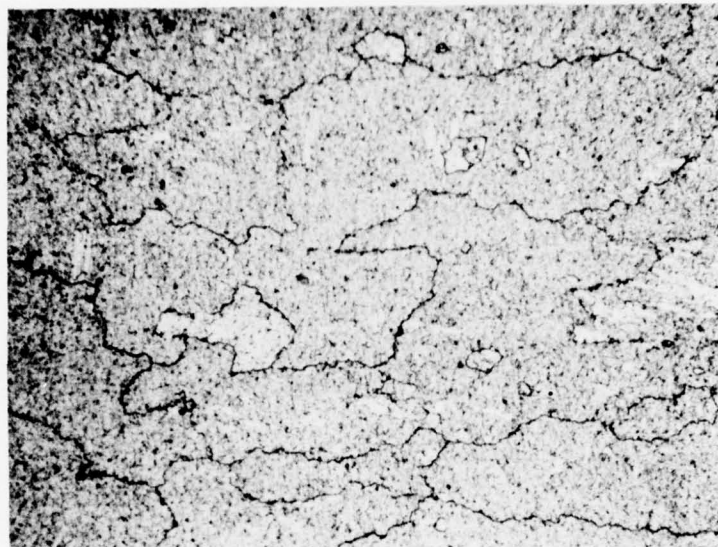


500X

Figure 6.6 Microstructure of As-cast MAR-M509

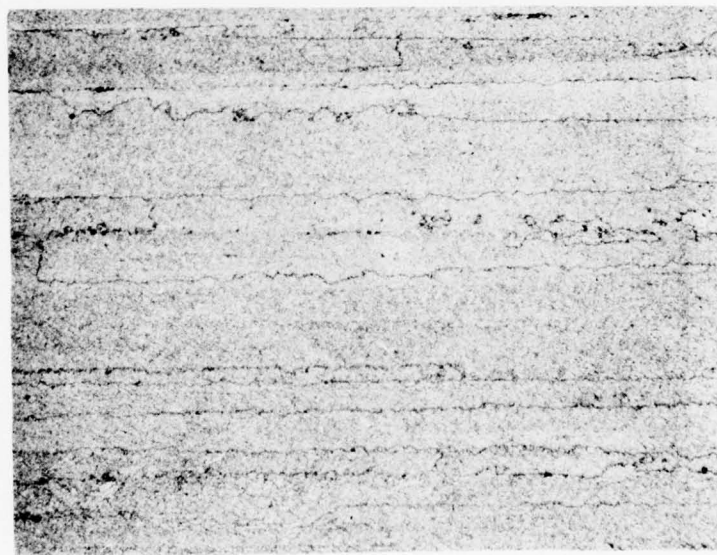
W
Westinghouse

A
Transverse



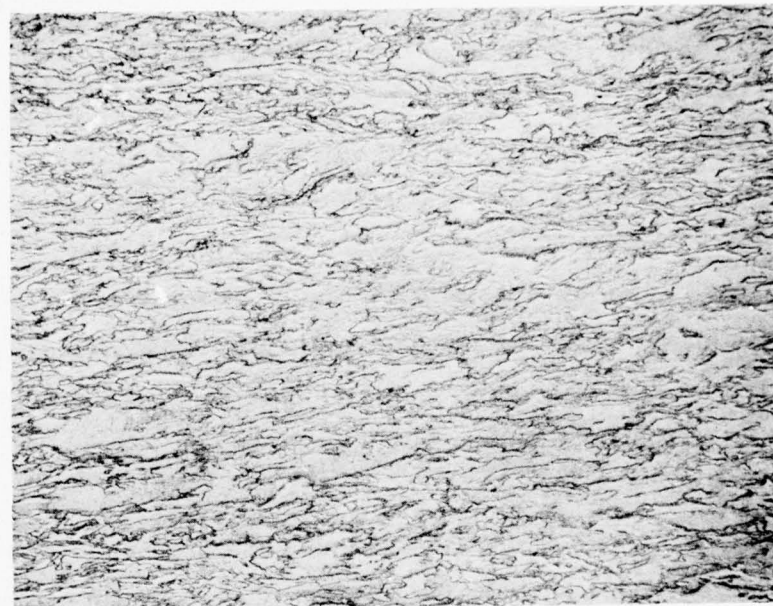
500X

B
Longitudinal



500X

Figure 6.7 Microstructure of MA 754



Longitudinal

100X

Figure 6.8 Microstructure of Stress-Relieved TZM

are typical of cast superalloys. Alloy 713LC displays a dentritic type appearance. The low carbon modification of Alloy 713 resulted from desire to improve low temperature ductility by reducing massive MC formation during solidification. The resulting microstructure is relatively clean with some $M_{23}C_6$ located at the grain boundaries. MC and $M_{23}C_6$ are carbide phases which precipitate from the matrix and have a pronounced effect on mechanical properties. The microstructure of IN100 contains nodular gamma prime, γ' , an intermetallic compound primarily Ni_3Al , throughout the matrix, white appearing particles, along with MC and $M_{23}C_6$ carbide phases. The MAR-M509 alloy is a cobalt-base alloy which contains $M_{23}C_6$ and MC phases. Tantalum, titanium, and zirconium tend to dominate the monocarbide, MC. The $M_{23}C_6$ tends to form massive blacks in the interdendritic zones and at the grain boundaries.

The MA 754 alloy displayed a microstructure typical of oxide-dispersion strengthened material. In the transverse direction grains are irregular, while in the longitudinal direction (parallel to working direction) the microstructure exhibited a large grain aspect ratio with interlocking grain boundaries pinned by finely dispersed Y_2O_3 .

The TZM alloy exhibits a wrought microstructure with no evidence of recrystallization as a result of the stress relieve anneal. The test specimen blanks were cut parallel to the radii of "pancake" forging and thus exhibit a high aspect ratio wrought structure which resulted from the upset forging operation.

6.3.2.2 Test Specimen Geometry

The creep-rupture test specimen geometries, which were used, are shown graphically in Figure 6.9. Actual test specimens are shown in Figure 6.10. The cast materials, Alloy 713LC, IN100, and MAR-M509, were received as cast-to-size specimens. The specimens had a nominal 1/4 inch diameter gage section 1-1/4 inch long with 1/2-13 threaded ends. The as-cast specimens were machined to produce a round uniform diameter along the gage length as

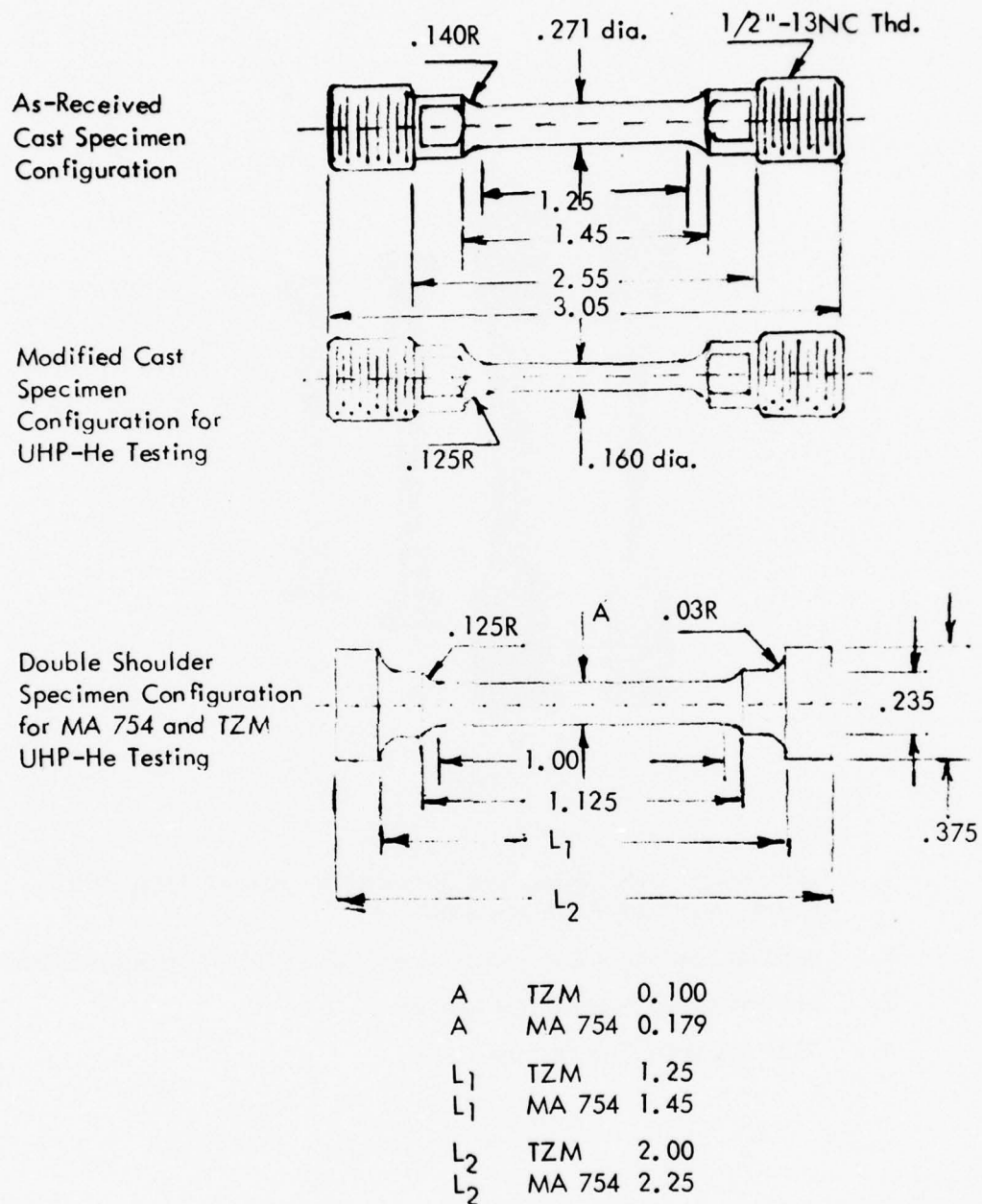
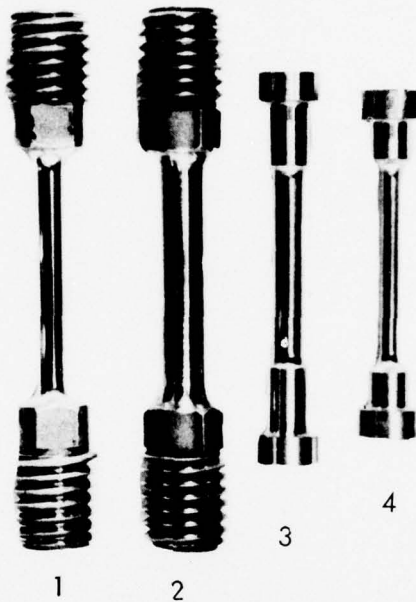


Figure 6.9 Creep-Rupture Specimen Geometries for Various Test Materials



1. Ultra-high Purity Helium Test Specimen for As-cast Alloy 713LC, IN100, and MAR-M509 Material
2. Air Test Specimens for As-cast Alloy 713LC, IN100, and MAR-M509
3. MA 754 Creep Rupture Test Specimen
4. TZM Creep Rupture Test Specimen

Figure 6.10 Photographs of Creep-Rupture Test Specimens

shown by specimen 2 in Figure 6.10. These specimens were used for the air tests because the cross sectional area was compatible with the load capacity of the lever arm test machines. For the deadweight loaded tests in ultra-high purity helium, the cross sectional area of the gage section was reduced to a diameter of 0.160 in. as illustrated by specimen 1 in Figure 6.10. The gage diameter for each material was adjusted to accommodate the physical volume of the load required to achieve the desired stress levels and remain within the equipment limitations. Double shoulder-type creep specimens with differing gage diameters were used for the MA 754 and TZM materials as shown by specimens 3 and 4 in Figure 6.10. The MA 754 specimen gage diameter was 0.180 in., and the TZM specimen diameter was 0.1 in.

6.3.2.3 Tensile Properties of Test Materials

In order to more completely characterize the creep-rupture test materials, a limited number of tensile tests were conducted. The number of tensile tests conducted was dependent on the availability of extra test specimens. The results are given in Table 6.4 along with test data from the alloy developer or other available services. Tests were conducted at room temperature and at 1700°F and at other elevated temperatures where possible. No tensile tests of TZM alloy were conducted.

6.4 CREEP-RUPTURE TEST RESULTS AND EVALUATION

Creep-rupture testing of five selected turbine materials in an ultra-high purity helium environment was initiated during this the first year of a three year study to assess the feasibility of the closed cycle Brayton system. Supplementary creep-rupture tests in air were also carried out for Alloy 713LC, IN100, MAR-M509, and MA 754. The status of the creep-rupture test program at end of the year of effort is summarized in Table 6.5. During the first year approximately 29,000 hours of creep-rupture test hours in ultra-high purity helium were also accumulated. A number of air and ultra-high purity creep-rupture tests were still in progress at the end of the first year. These tests were permitted to continue to completion as part of



Westinghouse

TABLE 6.4
TENSILE PROPERTIES OF TEST MATERIALS

Material	Test Temp.	0.02 Yield Strength (ksi)	Ultimate Strength (ksi)	Elong. (%)	R. A. (%)	Comment*
713LC	RT	120.4	146.0	8.0	7.8	INCO Data
	RT	124.2	148.8	8.8	8.7	
	RT	109.0	130.0	15.3	20.9	
	1600	87.9	102.5	8.3	7.2	
	1700	69.0	80.8	8.8	12.9	INCO Data
	1700	71.1	85.3	11.2	17.8	
	1700	66.9	94.2	6.0	12.0	
	1800	50.6	59.7	11.3	9.6	
IN100	RT	125.9	141.3	8.8	15.2	INCO Data
	RT	123.0	147.0	9.0	11.0	
	1600	104.8	112.3	4.0	6.4	
	1700	86.4	94.9	4.8	4.8	
	1700	73.0	107.0	6.0	7.2	
	1800	67.3	72.5	4.6	5.6	
	1800	67.3	72.5	4.6	5.6	
MAR-M509	RT	92.8	114.6	1.6	2.1	W GTED
	RT	61.0	90.0	6.0	-	
	1600	46.8	56.9	21.6	25.2	
	1700	39.7	45.3	21.6	32.7	W GTED
	1700	30.0	37.0	35.0	-	
	1800	32.5	36.2	25.6	32.7	
MA 754	RT	97.6	144.4	21.0	31.7	
	1700	32.4	34.4	15.0	33.4	

* All data are for material evaluated on this current program, except where noted.

Strain Rate - 0.05/min.

W GTED - Westinghouse Gas Turbine Engine Division

INCO - International Nickel Corporation - Data Brochure



Westinghouse

TABLE 6.5
CREEP-RUPTURE DATA FOR SELECTED CCCBS MATERIALS AT 1700°F

Material	Stress (ksi)	Test Atmos.	Time to % Strain			Total Strain (%)	Rupture Time (hrs)	Reduction in Area (%)	Status
			0.5%	1.0%	3.0%				
Alloy 713LC	20.0	He	84	192	268	6.4	269	16.7	Completed
	20.0	He	260	495	691	8.0	755	22.0	Completed
	18.0	He	128	943	1522	4.8	1527	8.4	Completed
	15.0	He	1060	2500	3150	5.6	3182	10.2	Completed
	20.0	Air	212	395	572	9.6	623	25.8	Completed
	20.0	Air	8	86	324	10.4	397	8.7	Completed
	18.0	Air	29	119	405	9.6	476	8.3	Completed
	15.0	Air	100	740	1870	5.6	1959	8.1	Completed
	22.5	He	700	1170	1982	16.0	2271	17.6	Completed
	16.0	He	--	--	--	--	2416	--	In progress
IN 100	30.0	Air	8	70	211	6.4	271	6.7	Completed
	30.0	Air	22	93	285	7.2	334	8.5	Completed
	25.0	Air	1	7	490	7.2	685	4.3	Completed
	22.5	Air	110	550	1130	8.5	1346	6.0	Completed
	18.0	Air	1460	2890	2985	7.2	3110	12.1	Completed
	16.0	Air	--	--	--	--	430	--	In progress
	15.0	He	--	--	--	--	2500	--	In progress
	12.5	He	--	--	--	--	693	--	In progress
	18.0	Air	2	5	264	21.6	618	34.1	Completed
	15.0	Air	1	570	1910	16.8	2507	19.6	Completed
MAR-M509	12.5	Air	5	25	--	--	2330	--	In progress
	18.0	Air	--	--	--	--	5455	--	In progress
	15.0	Air	--	--	--	--	5957	--	In progress
	12.5	Air	--	--	--	--	1559	--	In progress
MA 754	20.0	He	--	--	--	--	5378	--	In progress
	22.0	Air	--	--	--	--	6937	--	In progress
	20.0	Air	70	3480	--	--	--	--	In progress
TZM	60.0	He	220	425	1095	12.0	1483	98	Completed
	55.0	He	450	1010	2000	14.5	2256	98	Completed
	52.5	He	790	--	--	--	5115	--	In progress
							8854		

the following year's effort. Tests in progress are indicated in Table 6.5 under the "status" column. With five ultra-high purity helium creep test units available and an objective of 26,000 test hours for the first year's effort, a nominal goal of 5200 hours appeared to be a reasonable partition of the effort. The test results for each alloy are described and evaluated individually in the following discussions.

6.4.1 Alloy 713LC

Four creep-rupture tests of Alloy 713LC were conducted in ultra-high purity helium for a total of 5700 test hours. Test times ranged in duration from 269 to 3182 hours. All tests were completed. Four air tests at corresponding stress levels were also conducted. The test results, rupture life vs stress level, are plotted in Figure 6.11. In order to provide a basis for comparison, a computer printout of creep-rupture data for Alloy 713LC was obtained from the Mechanical Property Data Center (MPDC) Traverse City, Michigan. The MPDC is a DOD supported materials information center. The Alloy 713LC printout contained data for 831 creep-rupture tests, which were carried out in air in the temperature range 1350 to 2200°F. The data were gathered from many sources, primarily Government-sponsored programs. Of the 831 creep-rupture test results reported, 507 were carried out at 1800°F at a stress level of 22 ksi. These test conditions are apparently used for heat qualification. Only three tests of > 10,000 hours were reported, and they were conducted at 1500°F or lower. Sixteen creep rupture tests of greater than 1000 hours were reported. These comments are made to illustrate the dearth of long term high temperature creep-rupture data available in the open literature for a widely used, relatively old, commercial superalloy.

The solid reference curve in Figure 6.11 was generated from a Larson-Miller plot of the MPDC data. Logarithmic curve fit and linear regression analysis were used to produce a best fit curve for 61 data points representing the rupture life of Alloy 713LC in the stress range 12.5 to 30 ksi and test temperatures in the range 1600 to 1800°F. The air and ultra-high purity helium environment test data for material evaluated on this program compares favorably with

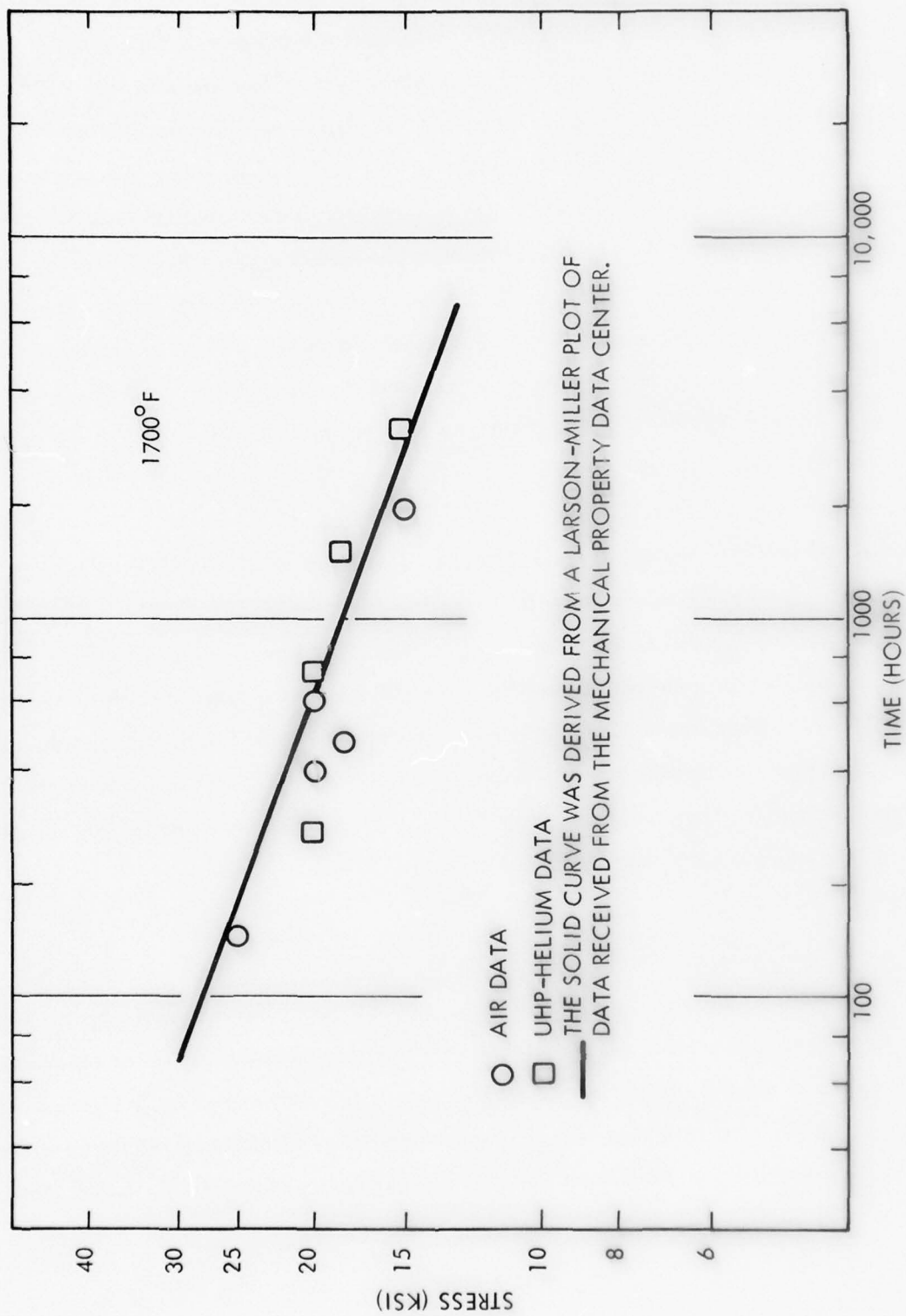


Figure 6.11 Creep Rupture Life of Alloy 713 LC

the reference curve. At the 20 ksi stress level, four tests were conducted two under each environmental condition. The actual creep-rupture curves are shown in Figure 6.12. The specimens tested in ultra-high purity helium exhibited rupture times ranging from 269 to 755 hours with fracture strains of 6.4 and 8.0 percent, respectively. The two air tests had rupture times of 397 and 623 hours with slightly higher fracture strains of 10.4 and 9.6 percent. At the lower stress levels, Figure 6.13 and 6.14, the ultra-high purity helium tests exhibited significantly longer rupture times compared to tests conducted in air. The test results for both environmental conditions, however, fall within a reasonable scatter band. The lack of test data prevent definitive conclusions to be drawn, although a trend to improved rupture life of Alloy 713LC in ultra-high purity helium appears as a possibility. Additional tests preferably at times of 10,000 hours or longer are required to definitely establish the validity of the observed trend.

One additional comment regarding the stress rupture behavior of Alloy 713LC relevant to CCCBS requirements involves the projected stress required to give a 10,000 hour rupture life. Initial published data by INCO in which a limited number of rupture tests of less than 3500 hours, indicated an extrapolated rupture life of 10,000 hours at a stress of slightly higher than 15 ksi at 1700° F.⁽⁷⁾ Data from MPDC involving many more test results indicate that the extrapolated 10,000 hour rupture life may be closer to 12 ksi at 1700° F. Actual creep-rupture behavior for long term tests greater than a few thousand hours may be affected by air oxidation resulting in a reduced stress for 10,000 hour life.

6.4.2 Alloy IN100

Five air tests were completed, and one was in progress at end of the first year effort. Two ultra-high purity helium tests were also conducted. One test was completed, and the second was still in progress at the end of the first year. The rupture life data are given in Figure 6.15. The reference curve was generated from a Larson-Miller plot of data received from the Mechanical Property Data Center. As pointed out in the discussion of Alloy 713LC, 6.4.1, the

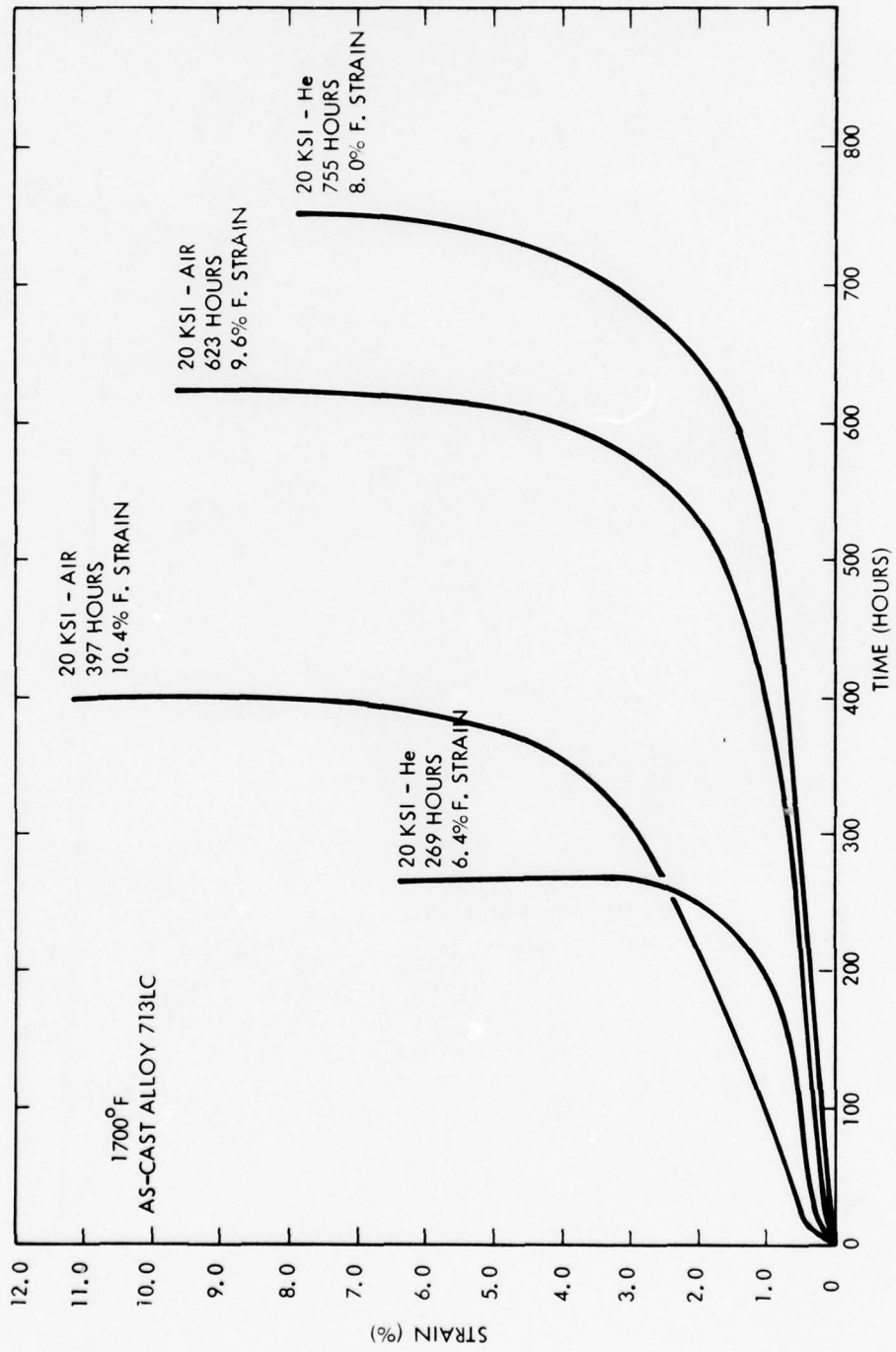


Figure 6.12 Creep-Rupture Curves for As-Cast Alloy 713 LC



Westinghouse

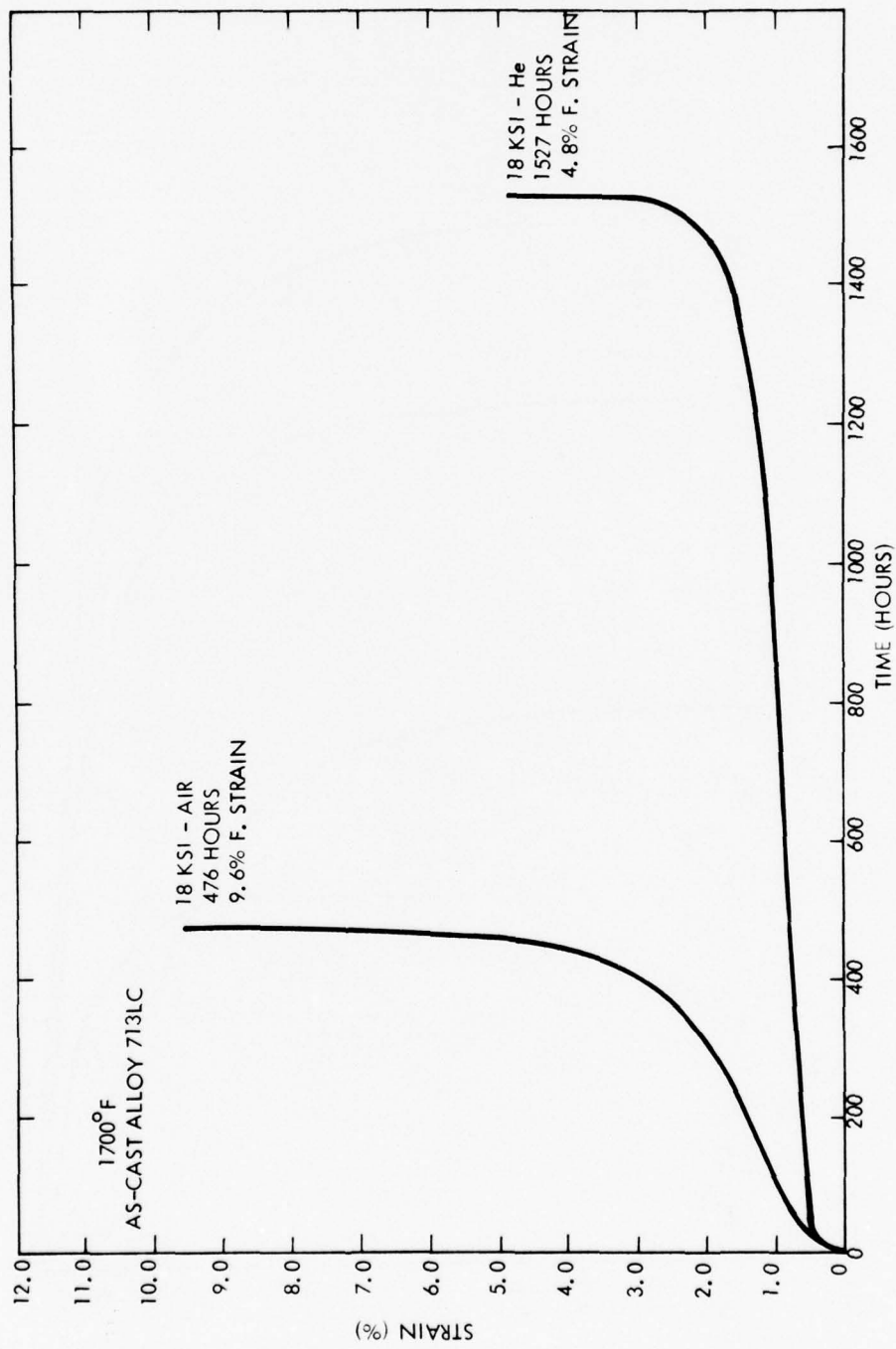


Figure 6.13 Creep-Rupture Curves for As-Cast Alloy 713 LC

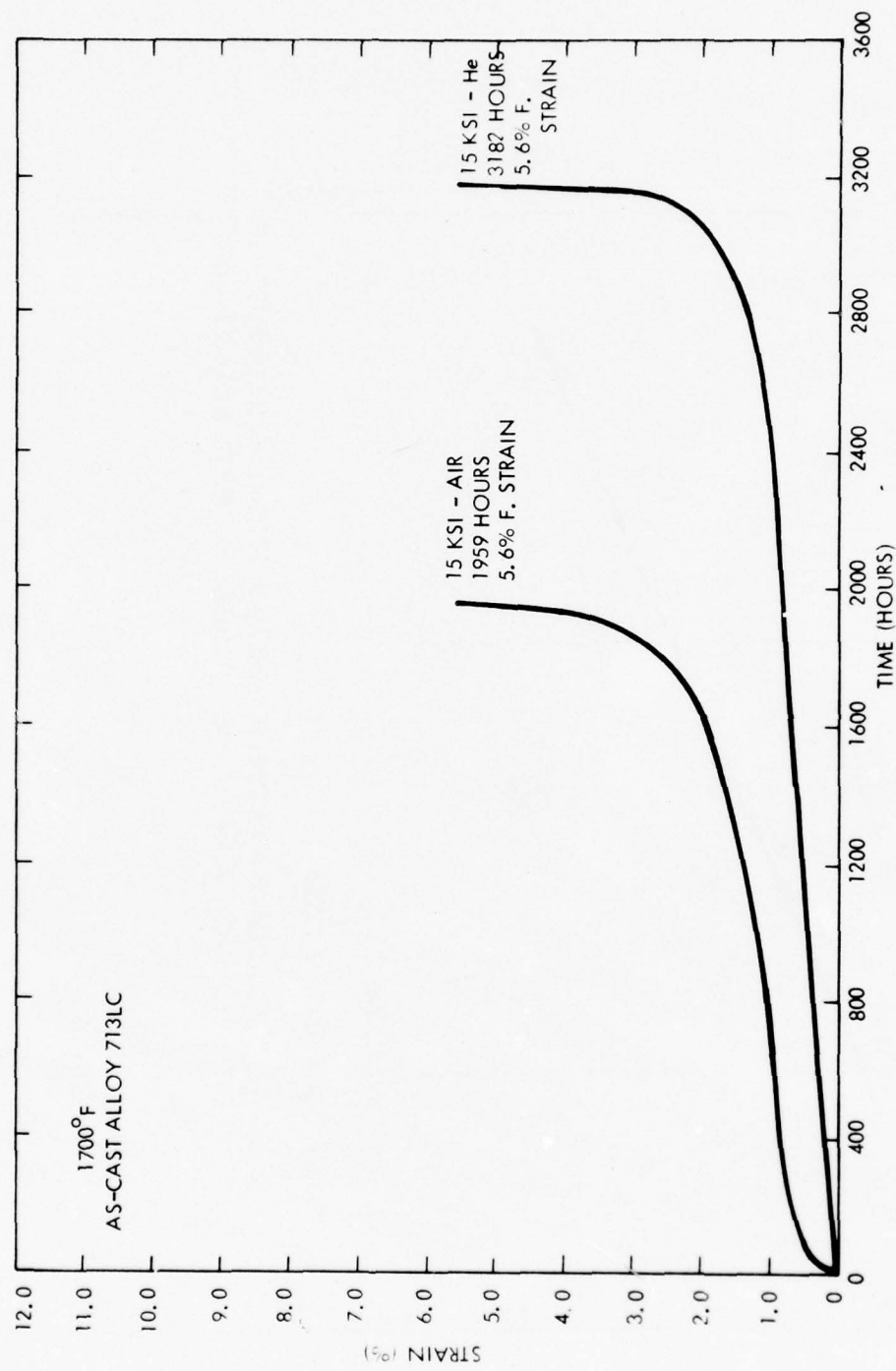


Figure 6.14 Creep-Rupture Curves for As-Cast Alloy 713 LC

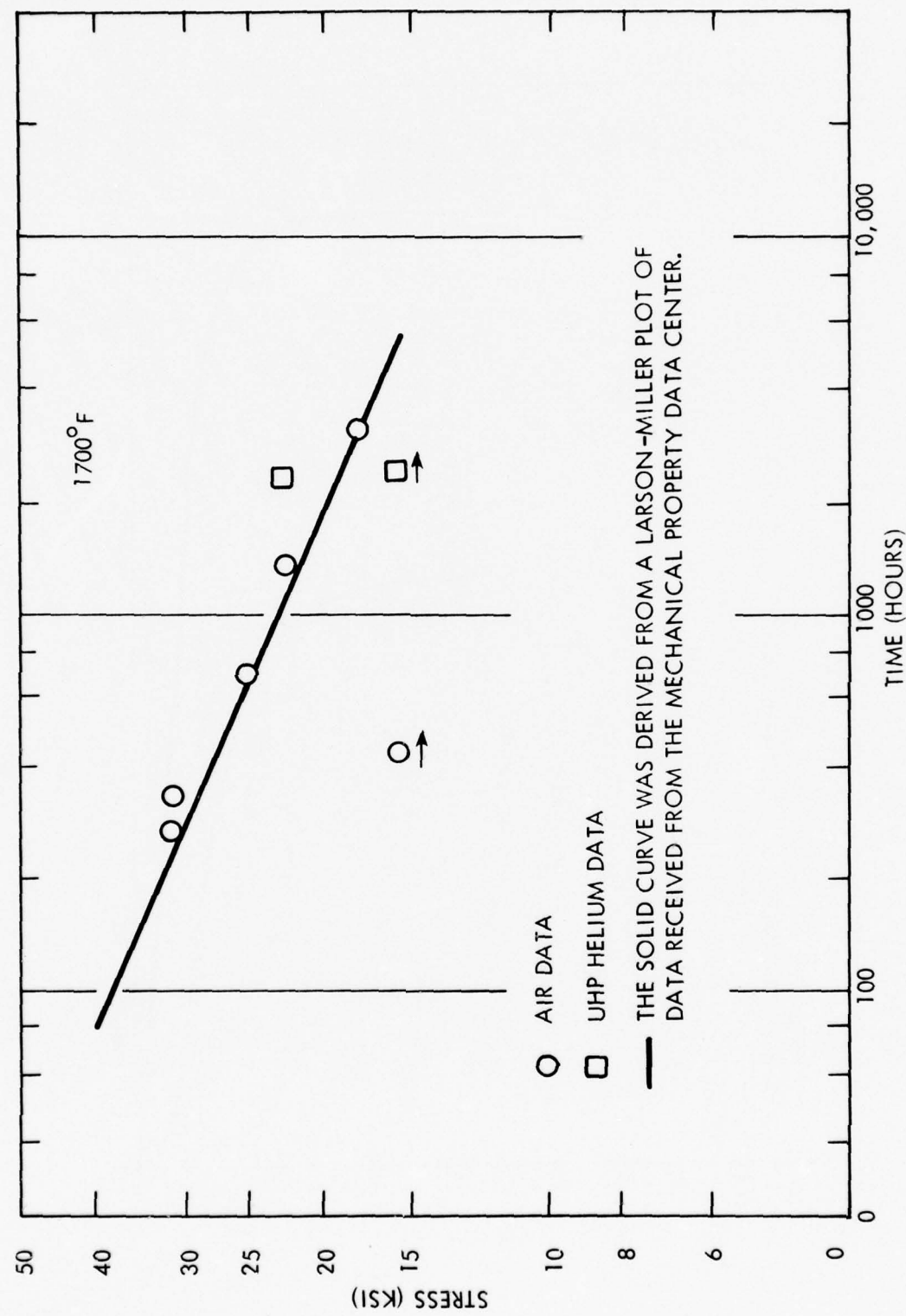


Figure 6.15 Stress Rupture Life of IN 100

number of long term tests conducted at temperatures above 1600°F was very limited. Of the 573 reported test results, only 22 tests of greater than 1000 hours were reported. There were no test results in the 1600 to 1800°F test temperature range of greater than 4700 hours. A total of 52 data points were used to develop a Larson-Miller curve from which the reference curve in Figure 6.15 was produced. The air data show excellent correlation with the reference data. Creep-rupture curves for the tests conducted at a stress level of 22.5 ksi are shown in Figure 6.16. The ultra-high purity helium test specimen exhibited more than twice the rupture strain compared to the air test and nearly twice the rupture life. The 16.0 ksi stress level test in helium was approaching the reference life indicating no significant deleterious environmental effect at that time.

It should be noted that the reference curve in Figure 6.15 derived from MPDC data varies from other published data regarding the expected stress to produce 10,000 hour rupture life at 1700°F⁽⁸⁾. The extrapolated stress to produce a 10,000 hour rupture life at 1700°F is approximately 12 ksi. The ultra-high purity helium environment may possibly extend the 10,000 hour rupture stress to some higher level. Additional creep-rupture tests at lower stress levels will be required to confirm this possibility.

6.4.3 Alloy MAR-M509

Five creep-rupture tests of alloy MAR-M509 were initiated, three in air and two in ultra-high purity helium. One helium and two air tests were completed. The remaining tests were still in progress at the end of the first year test program. Limited air test results indicate that the creep-rupture behavior of this particular heat of material compares favorably with the reference curve produced from MPDC data plotted in Figure 6.17. Creep-rupture curves for the 15 ksi tests are shown in Figure 6.18. The air test, which exhibited an unusually high strain on loading, failed after 2507 hours at a strain of 11.8 percent while the ultra-high purity helium test continued at a relatively low creep rate after 2500 hours. The high loading strain is believed to be associated with load train and the method of strain measurements used on the air tests rather than attributed to the creep behavior of the alloy. The tests in progress at 12.5 ksi have not produced results which can be discussed at this time.

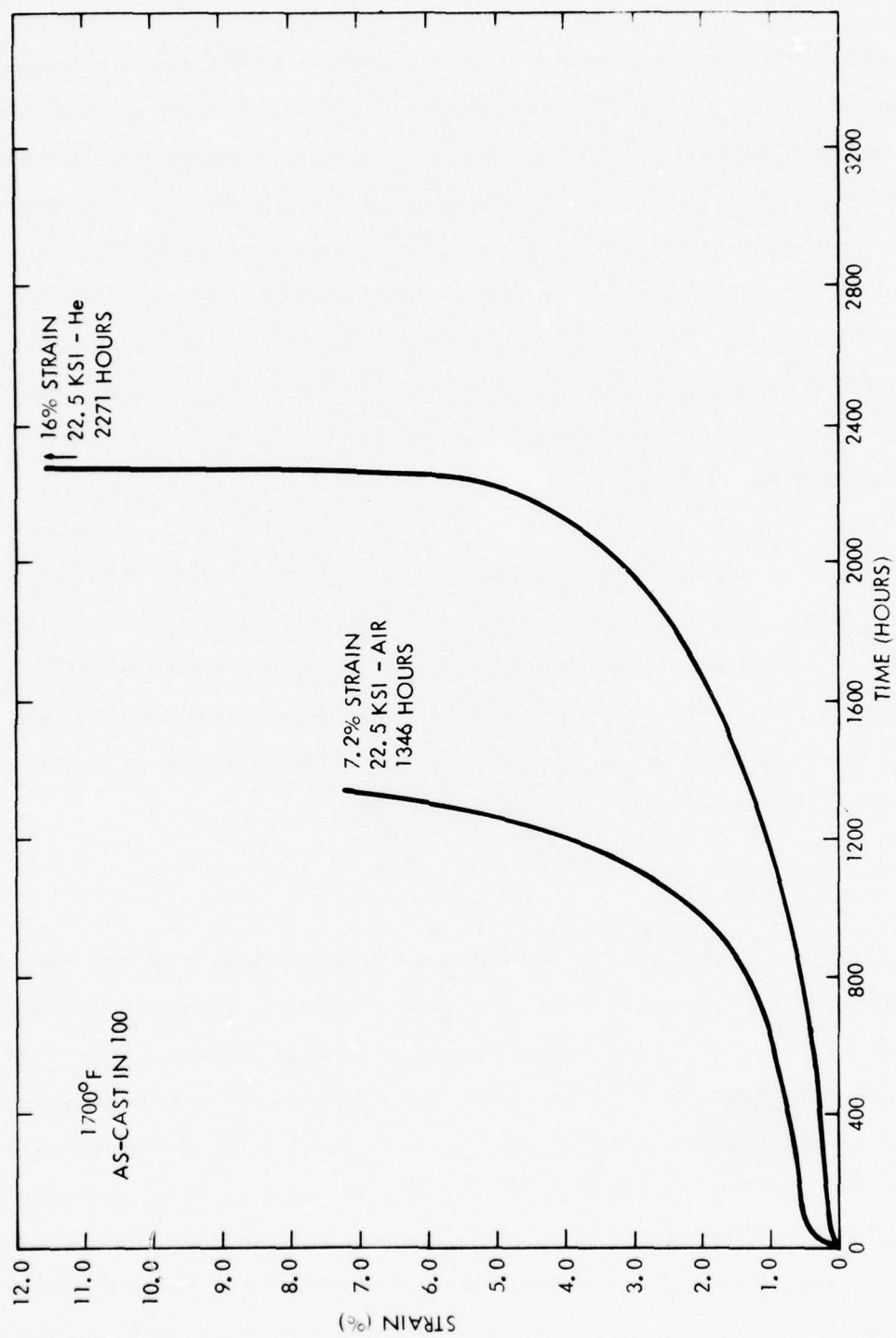


Figure 6.16 Creep-Rupture Curves for As-Cast IN 100

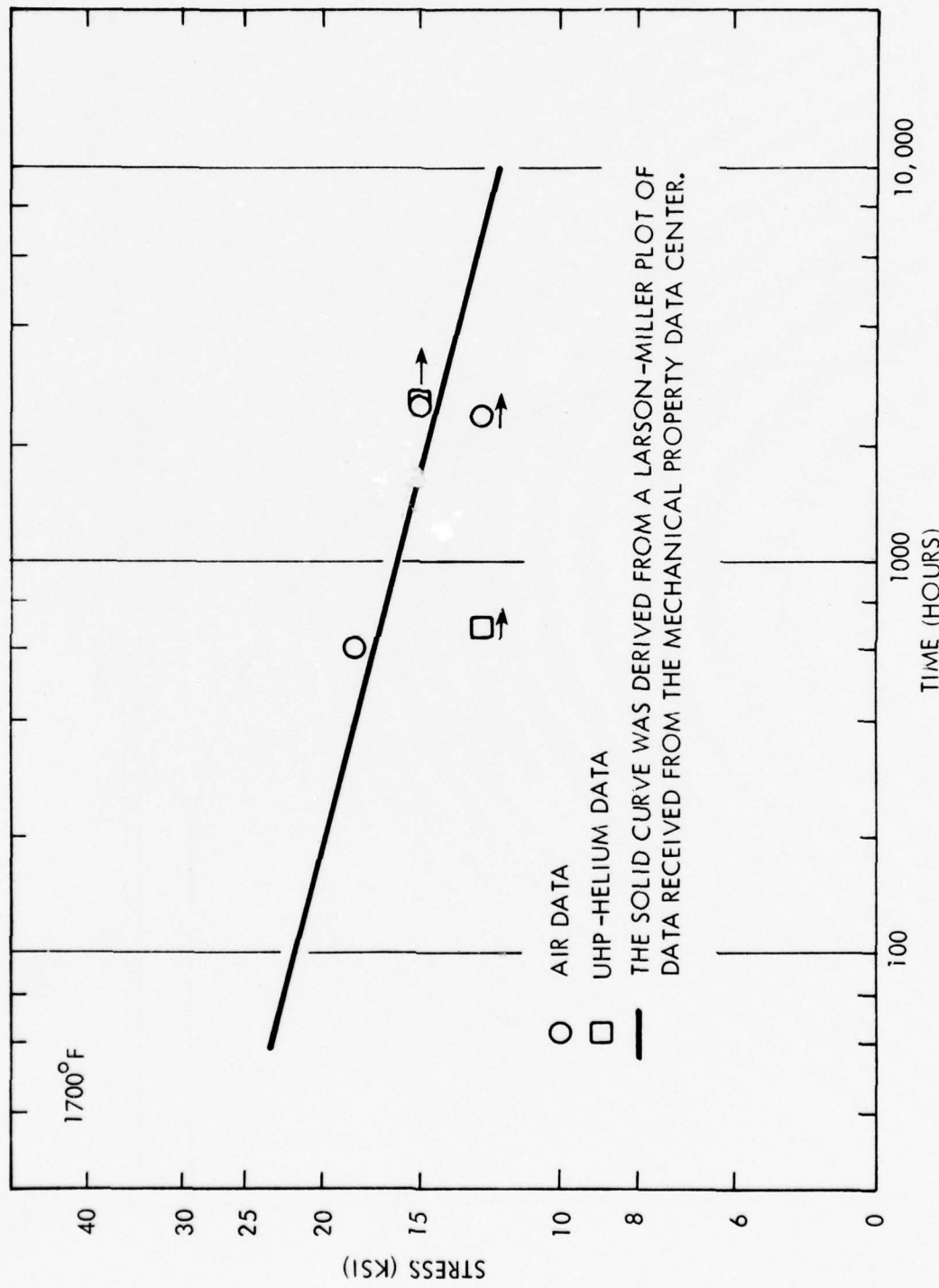


Figure 6.17 Creep-Rupture Life of MAR-M-509

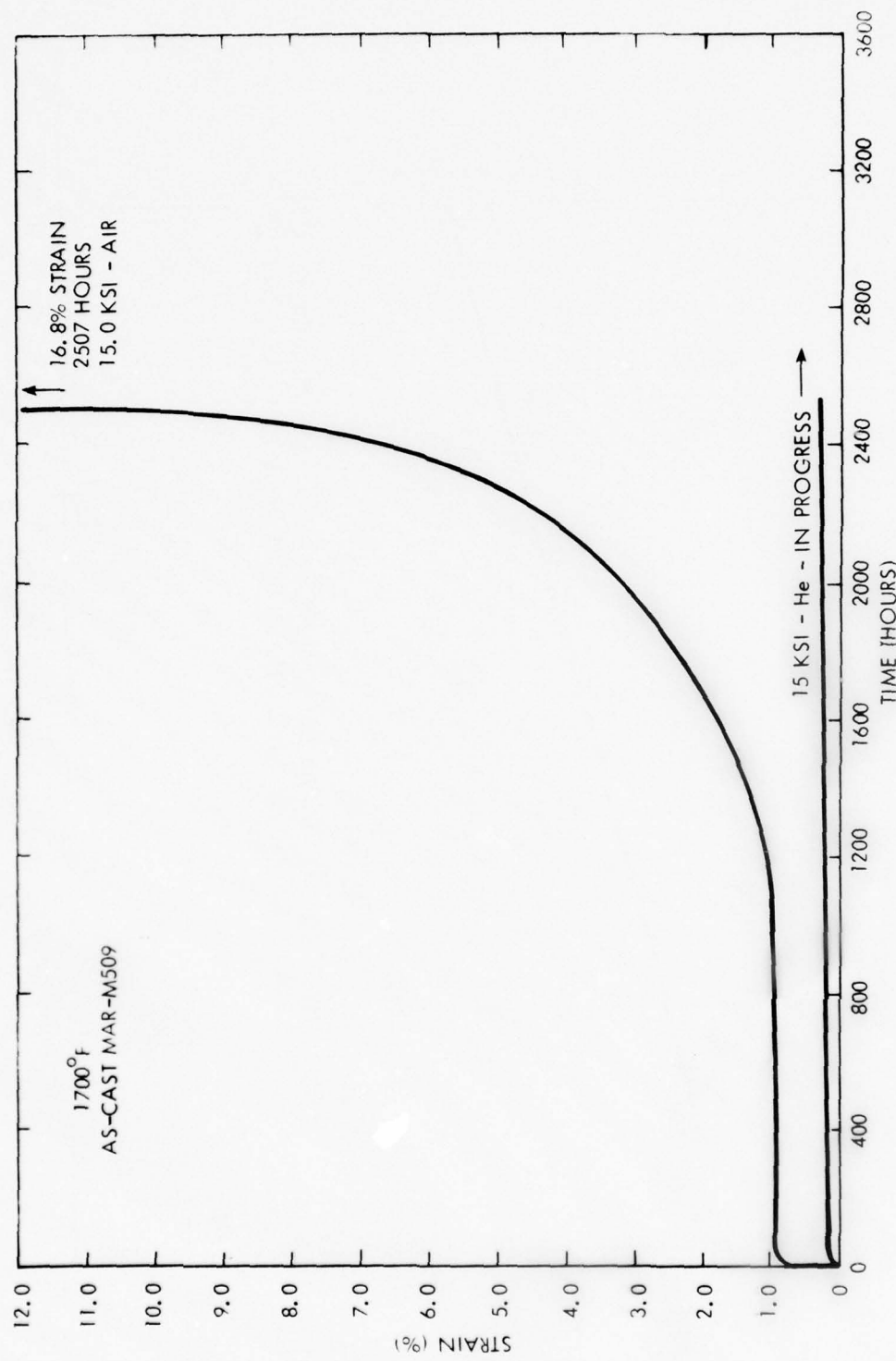


Figure 6.18 Creep-Rupture Curves for As-Cast MAR-M-509

6.4.4 Alloy MA-754

A total of three tests of alloy MA-754 were initiated, two in air and one in ultra-high purity helium. All tests were still in progress at the end of the first of year. The status of tests at the end of the report period is shown in Figure 6.19, along with a reference curve produced by extrapolation of 2000°F creep rupture data⁽⁵⁾. Because of the alloy's recent development, very limited data are available. The tests at 20 ksi stress level for both air and ultra-high purity helium environments have surpassed 5000 hours. Creep-strain in both cases was low, well below 0.5 percent for the UHP helium and slightly above 1.0 percent for the air environment. The difference in strain is possibly due to the difference in measuring technique. In the UHP helium test, strain is measured directly off the specimen gage. While in the air test, lever arm movement is monitored by a dial gage.

6.4.5 Alloy TZM

Three TZM creep-rupture tests were initiated in ultra-high purity helium during the initial year of the feasibility study. Two were completed, and the third was in progress. The status of TZM creep-rupture tests is shown in Figure 6.20. The reference curve was generated from very meager short time rupture data produced under vacuum test conditions⁽⁶⁾. The creep-rupture curves are shown in Figure 6.21. The continuing test at 52.5 ksi has accumulated over 5,000 hours with no instabilities. A concern associated with the long term testing of wrought-stress relieved material is the possibility of recrystallization. This phenomena, which is time and temperature dependent, can introduce gross instability when it occurs during creep deformation. There appears to be no sign of instability for the particular lot of TZM under test on this program. Metallographic examination of the test material upon completion of the creep-rupture test will be used to confirm the status of the TZM microstructure.

6.5 ACCOMPLISHMENTS

During the first year of a three year feasibility study to investigate the suitability of five selected materials -- Alloy 713L, IN100, MAR-M509, MA 754, and TZM -- to serve in

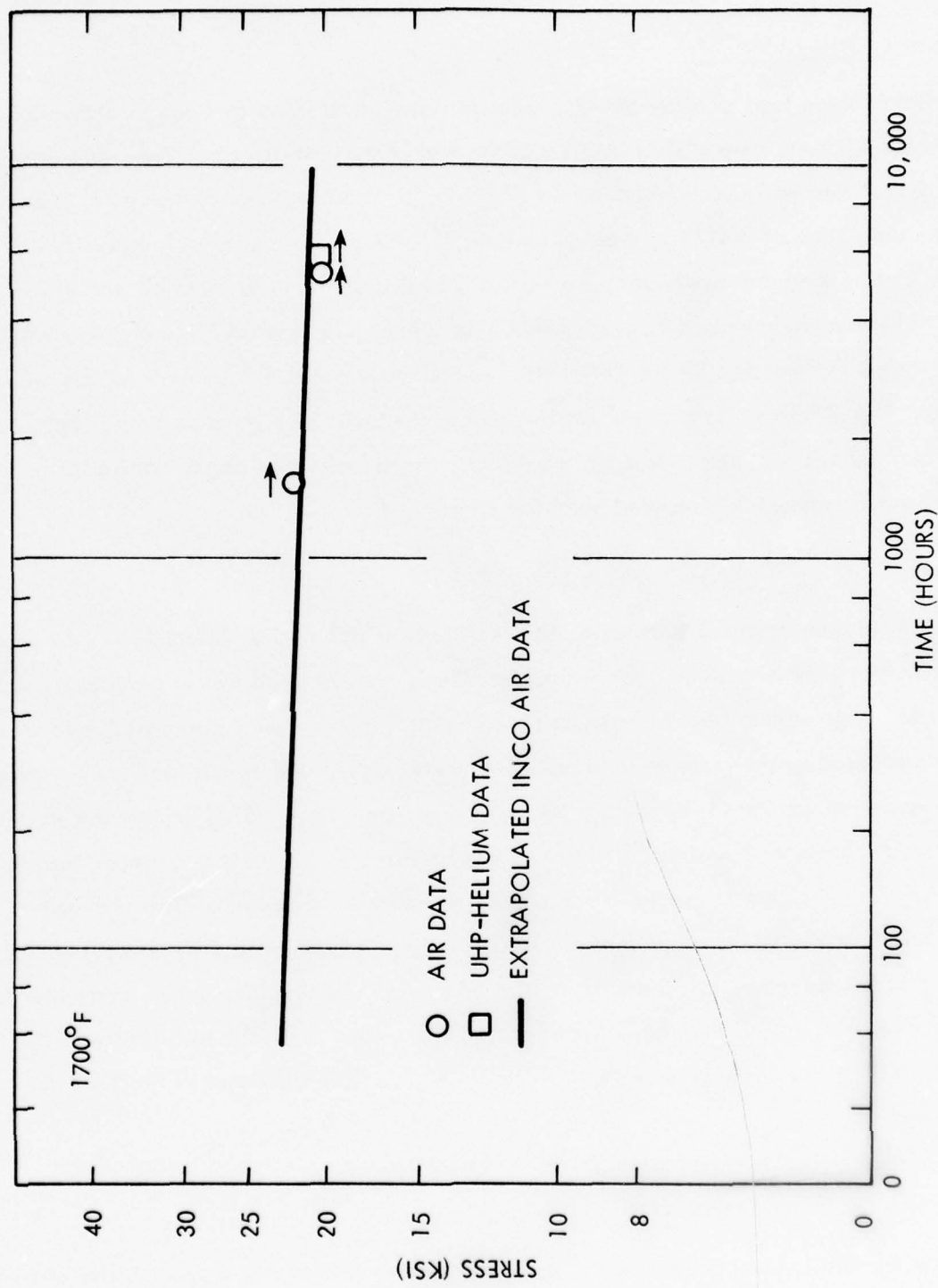


Figure 6.19 The Creep-Rupture Life of MA 754

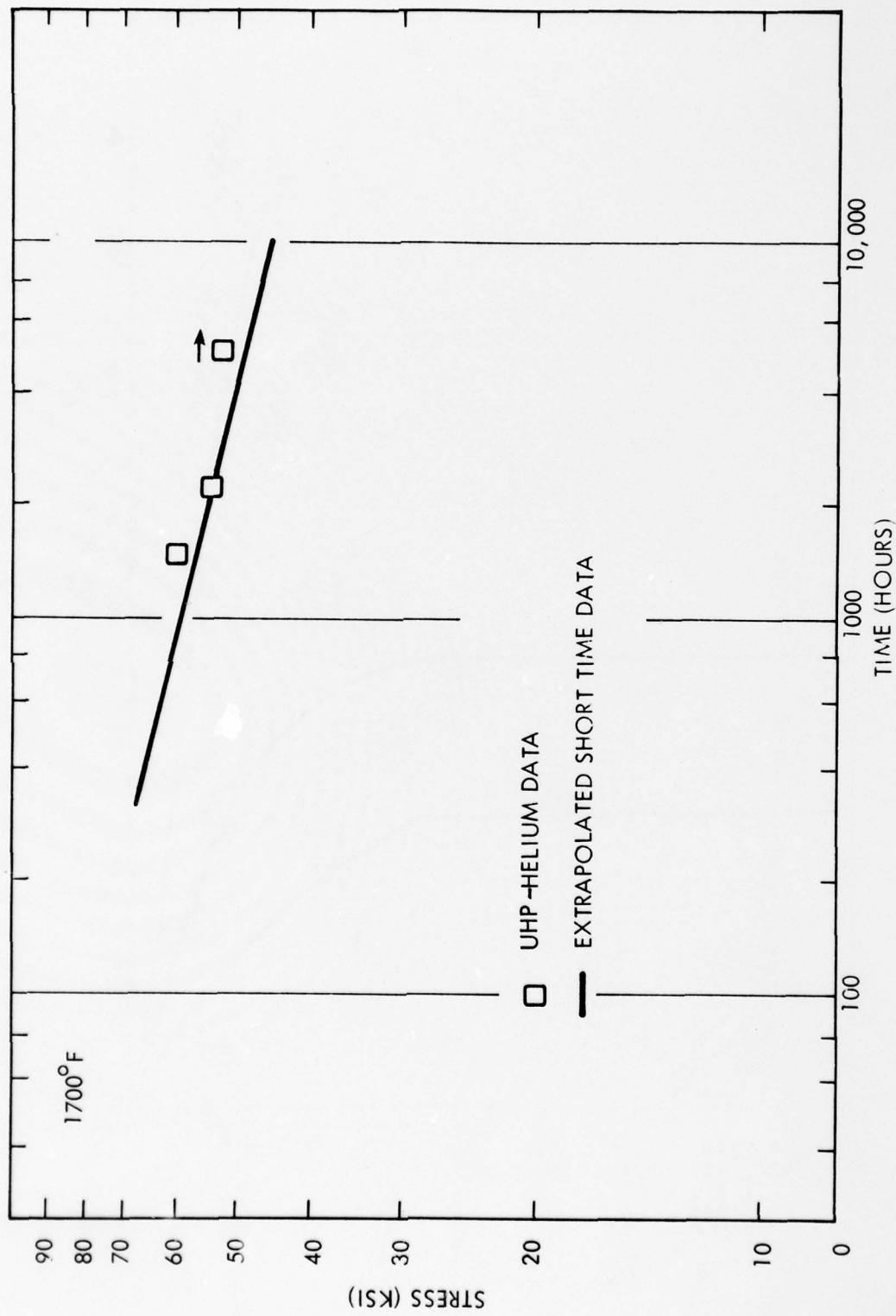


Figure 6.20 Creep-Rupture Life of TZM

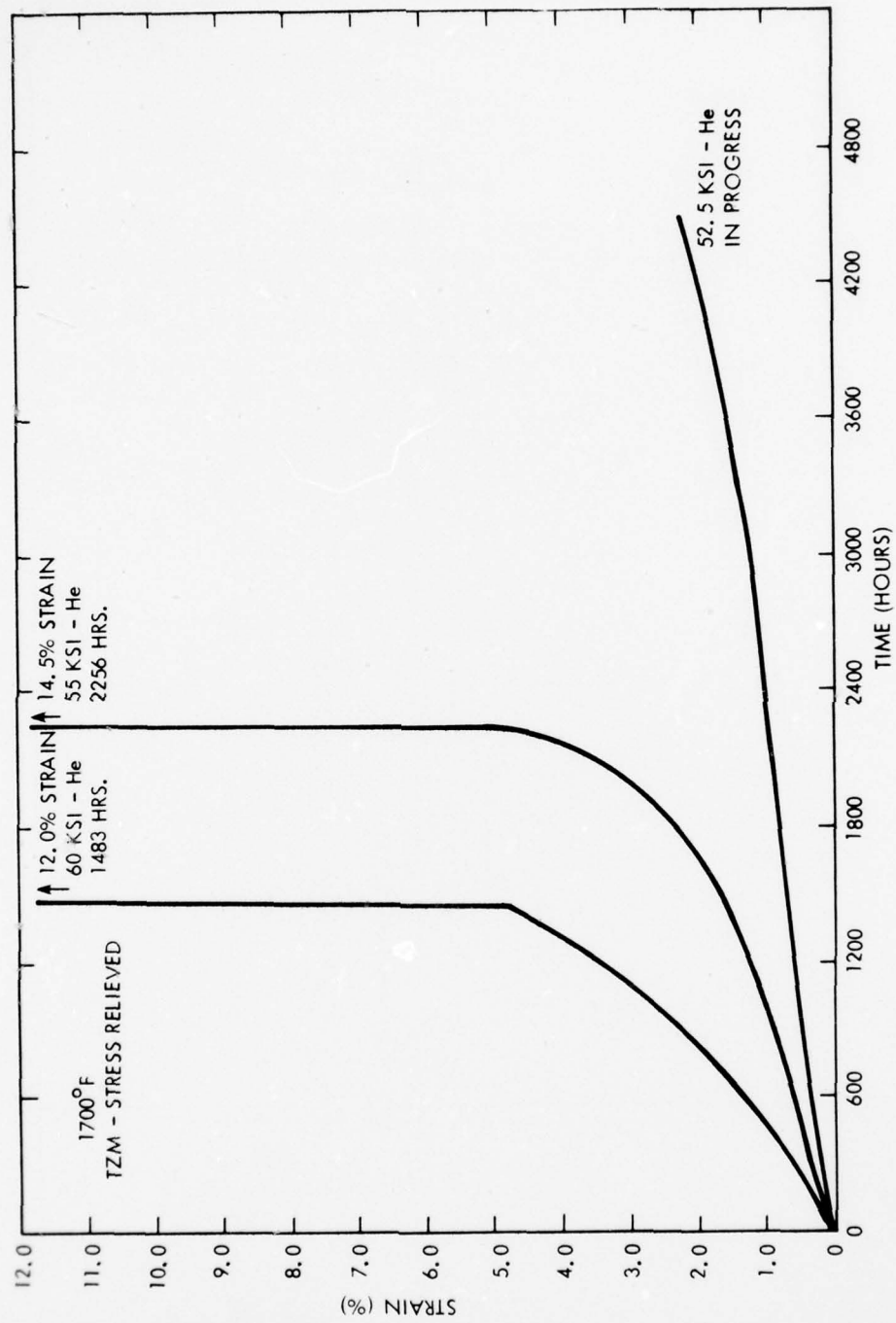


Figure 6.21 Creep-Rupture Curves for Stress Relieved TZM

critical components of a compact closed cycle Brayton system, creep-rupture testing of all five materials in an ultra-high purity helium environment was initiated. Tests in air for four of the selected materials were also initiated to characterize the creep-rupture behavior of each particular heat of material to provide a basis for comparison with published air creep-rupture data.

Five ultra-high vacuum creep units were modified for ultra-high purity helium operation, and a total of 29,000 hours of creep-rupture test time was accumulated. In addition, 22,000 hours of air creep-rupture test time was also accumulated. Based on the limited results produced during the first year of effort, the following tentative conclusions can be drawn:

- There has been no gross deleterious effect of the ultra-high purity helium environment on the creep-rupture behavior of the five selected materials; Alloy 713L, IN100, MAR-M509, MA 754, and TZM, for the temperature and time periods of the creep-rupture tests.
- Creep-rupture data obtained from the Mechanical Property Data Center for three relatively old standard gas turbine superalloys, confirm that a dearth of published creep-rupture data exists for materials at temperatures above 1600°F and for test times greater than 1,000 hours.

6.6 REFERENCES

1. R. W. Buckman and J. S. Heatherington, "Apparatus for Determining Creep Behavior Under Conditions of Ultra-high Vacuum," The Review of Scientific Instruments, Vol. 37, No. 8, August 1966.
2. W. M. Hickam, "Proceedings of the 9th Annual Conference of Mass Spectrometry," ASTM Committee E-14, Chicago, Ill. 346 (1966).
3. W. M. Hickam, "Cryogenics Applied to Mass Spectrometric Trace Gas Analysis," Analytical Chemistry, Vol. 45, p. 315, February 1973.
4. J. C. Sawyers and E. A. Stiegerwald, "Generation of Long Time Creep Data on Refractory Alloys at Elevated Temperatures," Final Report NASA Contract NAS3-2545, June 1967, TRW Cleveland, OH.
5. Huntington Alloys Data Sheet, "Inconel Alloy MA 754," 3M-9-75S-51.
6. R. L. Salley and E. A. Kovacevick, "Materials Investigation, SNAP 50/SPUR Program, Creep-Rupture Properties of Stress Relieved TZM Alloy", Report APL-TDR-64-116 Part I, Garrett Corporation, AiResearch Manufacturing Division, October 1964.
7. INCO Data Brochure, "Alloy 713LC - Low Carbon Alloy 713C", Preliminary Data, July 1964 - 1M 6-68-4290.
8. INCO Data Brochure, "Engineering Properties of IN 100 Alloy", 2M9-69 5073.

APPENDIX A

APPENDIX A

BRAYTON CYCLE ANALYSIS

The assumptions used in this Brayton cycle analysis are given in Section 3.4.2. Both the compressor and turbine efficiencies are about 2 percent less than that obtained in the MGCR program. The assumption of no bleed flows, produces slightly higher cycle efficiencies, but should have negligible effect on the comparisons of the different Brayton cycles. The cooling water inlet temperature of 95°F allows an approach temperature difference of 10°F with the seawater inlet temperature of 85°F. In this study the pressure loss in the heat exchanger increases as heat exchanger effectiveness increases and the pressure loss increases as more heat exchangers types (adding intercooling for example) are added to the cycle, these assumptions are judged to be more realistic than the usual assumption of fixed cycle pressure losses independent of cycle type and heat exchanger effectiveness.

For gas to gas heat exchangers with flow stream capacity rate ratios of one (recuperators, intermediate heat exchangers), the heat exchanger effectiveness (ϵ) is a function of the number of heat transfer units (NTU)

$$\epsilon = \frac{\text{NTU}}{1 + \text{NTU}} \quad (1)$$

or

$$\text{NTU} = \frac{\epsilon}{1 - \epsilon} = \frac{UA_s}{WC_p} = \frac{USL}{WC_p} \quad (1a)$$

From the assumptions given in Table I, the heat exchanger length (L) is proportional to effectiveness



Westinghouse

$$L \sim \frac{\epsilon}{1 - \epsilon} \quad (2)$$

With that assumption that the ratio of flow rate (w) to free flow area (A_c) is constant, the pressure drop to pressure level ratio is proportional to:

$$\frac{\Delta P}{P} \sim \frac{\epsilon}{(1 - \epsilon) P_p} \quad (3)$$

For gas to water heat exchangers the flow stream capacity rate ratio is assumed to be 0.18, and the heat exchanger effectiveness is:

$$\epsilon = \frac{1 - e^{-NTU(1 - .18)}}{1 - .18e^{-NTU(1 - .18)}} \quad (4)$$

or

$$NTU = 1.22 \ln \left(\frac{1 - .18}{1 - \epsilon} \right) \quad (4a)$$

Therefore, the heat exchanger length is proportional to:

$$L \sim 1.22 \ln \left(\frac{1 - .18}{1 - \epsilon} \right) \quad (5)$$

and the pressure loss to pressure level ratio is:

$$\frac{\Delta P}{P} \sim \frac{1.22}{P_p} \ln \left(\frac{1 - .18\epsilon}{1 - \epsilon} \right) \quad (6)$$

In estimating the weight trends of the various Brayton cycle powerplants, only two major weights were considered, the nuclear subsystem and the turbo-compressor heat exchanger

containment. These two components normally make up about 70 percent of the total power-plant weight. For the fixed output power assumption, the power transmission and auxiliaries weights are constant and make up about 20 percent of the powerplant weight. This then leaves the turbo-compressor heat exchange package and control gas storage that make up the remaining 10 percent of the powerplant weight which is variable.

The weight of the nuclear subsystem is estimated by the following relationship

$$W_T = 82460 (Q)^{0.353} \quad (7)$$

The pressure loss through the reactor subsystem (shield inlet to plug shield exit) was approximated by

$$\Delta P = \frac{51.2}{\rho} \left(\frac{W}{Q} \right)^2 \quad (8)$$

In this study six types of Brayton cycles were investigated. The temperature entropy diagrams for the six cycle types are shown in Figure A.3. In all cycle types, two turbo-compressor units are assumed to be located in the containment with the heat exchangers wrapped around the turbo-compressor units. The heat exchangers are assumed to effectively utilize 75 percent of the annulus area around the turbo-compressors. The spacing between the turbo-compressor units is assumed to be 12 inches. A 6 inch clearance between the turbo-compressor unit and the containment inner wall. In the first four types of cycles the cylindrical length of the containment is assumed to be 216 inches, and for the last two cycles (BB and PBB) the cylindrical length is assumed to be 144 inches since the superconducting generator (length 72 inches) is located external to the containment. In all cases the containment is assumed to be a right circular cylinder with 2 to 1 elliptical heads.

For the simple Brayton cycle (Type S) the precooler is assumed to be wrapped around the compressor, so that the turbo-compressor heat exchanger package diameter is determined from the compressor diameter and the heat exchanger frontal area. This package has a minimum diameter of 50 inches, since the generator diameter is 50 inches. Figure A.1 shows the efficiency curve for the Type S cycle and has no surprises. The peak efficiency for a 1700°F turbine inlet temperature is about 29.5 percent and occurs at a turbine pressure ratio between 4.5 and 5.0 for helium. The reactor subsystem and containment weight minimize for the 1700°F turbine inlet temperature at about 880,000 pounds at a turbine pressure ratio of 4.5 (see Figure A.2).

Figure A.3 shows the efficiency curves for a type R (generator) Brayton cycle. These curves are similar to conventional regeneration curves. This figure does show that the growth potential for the cycle with increased turbine inlet temperatures is poor, if the reactor inlet temperature is limited to below 1000°F , since the peak efficiency cannot be utilized. Figure A.4 shows the cycle efficiency for a 1700°F inlet turbine temperature with recuperator effectiveness a parameter. These curves are not conventional due to the pressure loss being a function of effectiveness. This figure shows that there is very small gain in cycle efficiency due to increasing the recuperator effectiveness beyond 0.8. The reactor subsystem and containment weight versus turbine pressure ratio is shown in Figure A.5 with turbine inlet temperature a parameter. The reactor inlet temperature locus of 1000°F shows that the minimum weight cannot be effectively utilized at the higher turbine inlet temperatures. The system weight is not significantly influenced by recuperator effectiveness as shown in Figure A.6.

The recuperated and intercooled Brayton cycle (Type RI) efficiency versus pressure ratio is shown in Figure A.7. The intercooling allows more effective use of recuperation, producing higher cycle efficiencies than the recuperated (Type R) cycle. This cycle (Type RI)

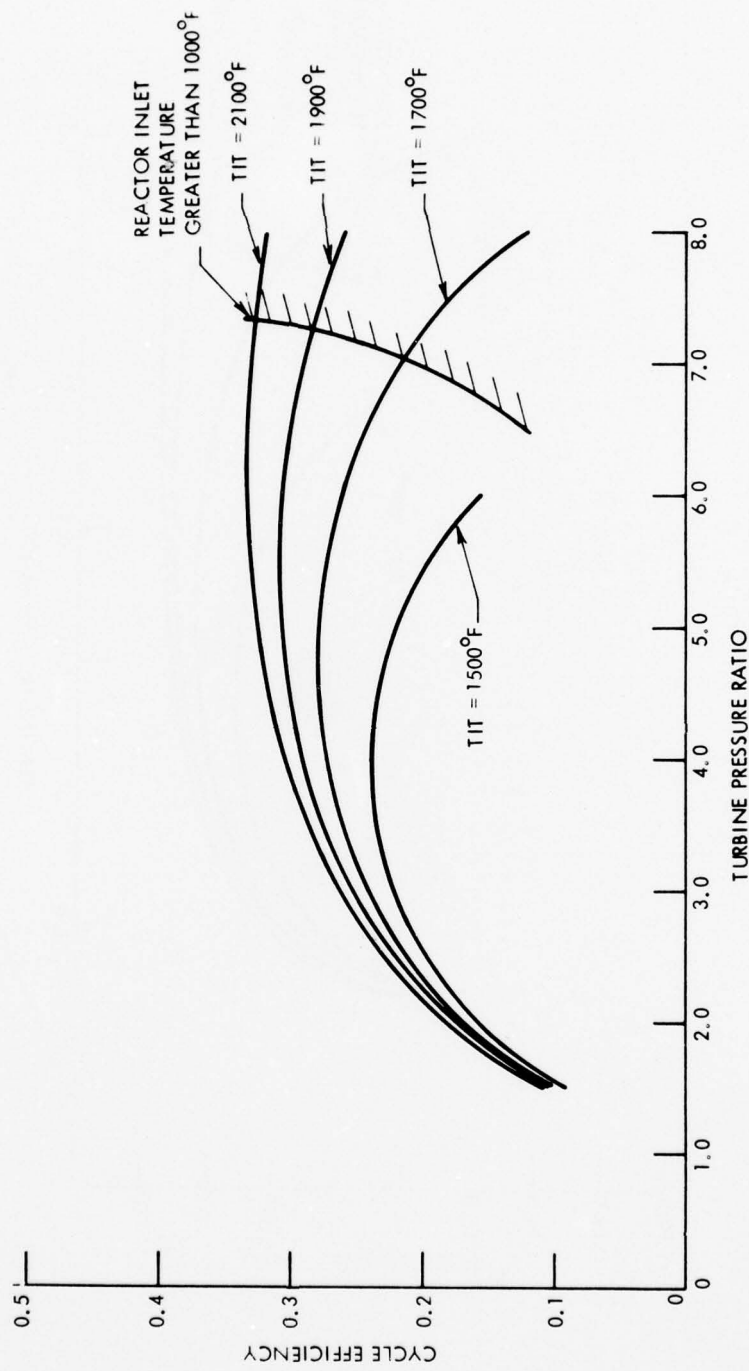


Figure A.1 Simple Brayton Cycle (S)



Westinghouse

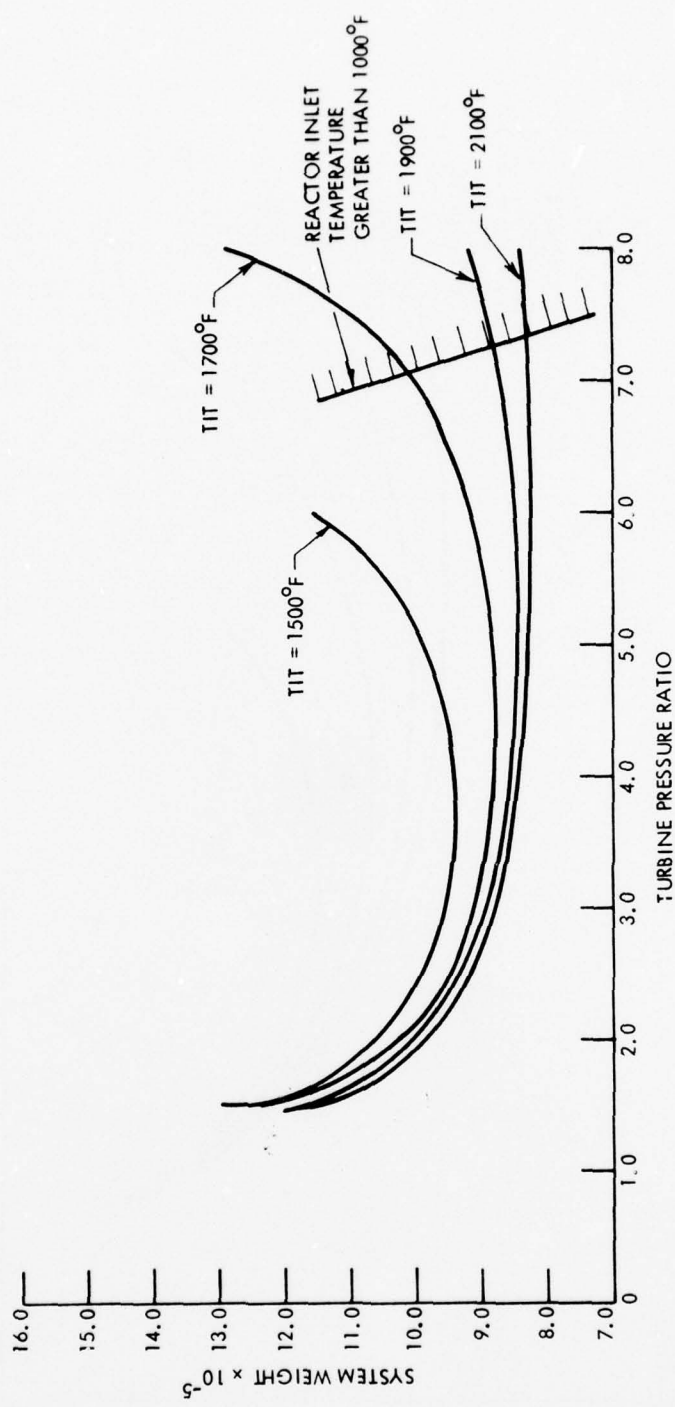


Figure A.2 Simple Brayton Cycle (S)

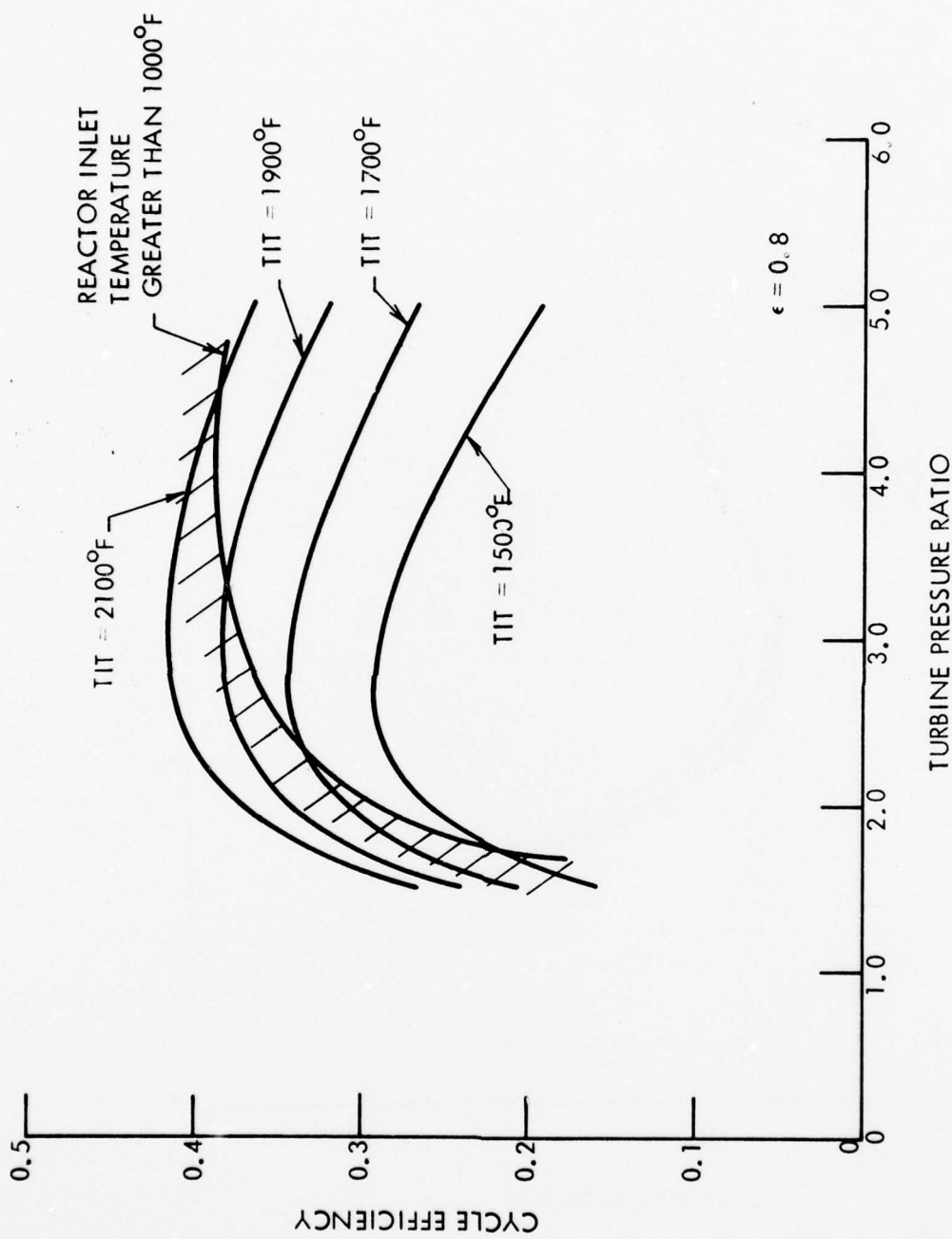


Figure A.3 Recuperated Brayton Cycle (R)



Westinghouse

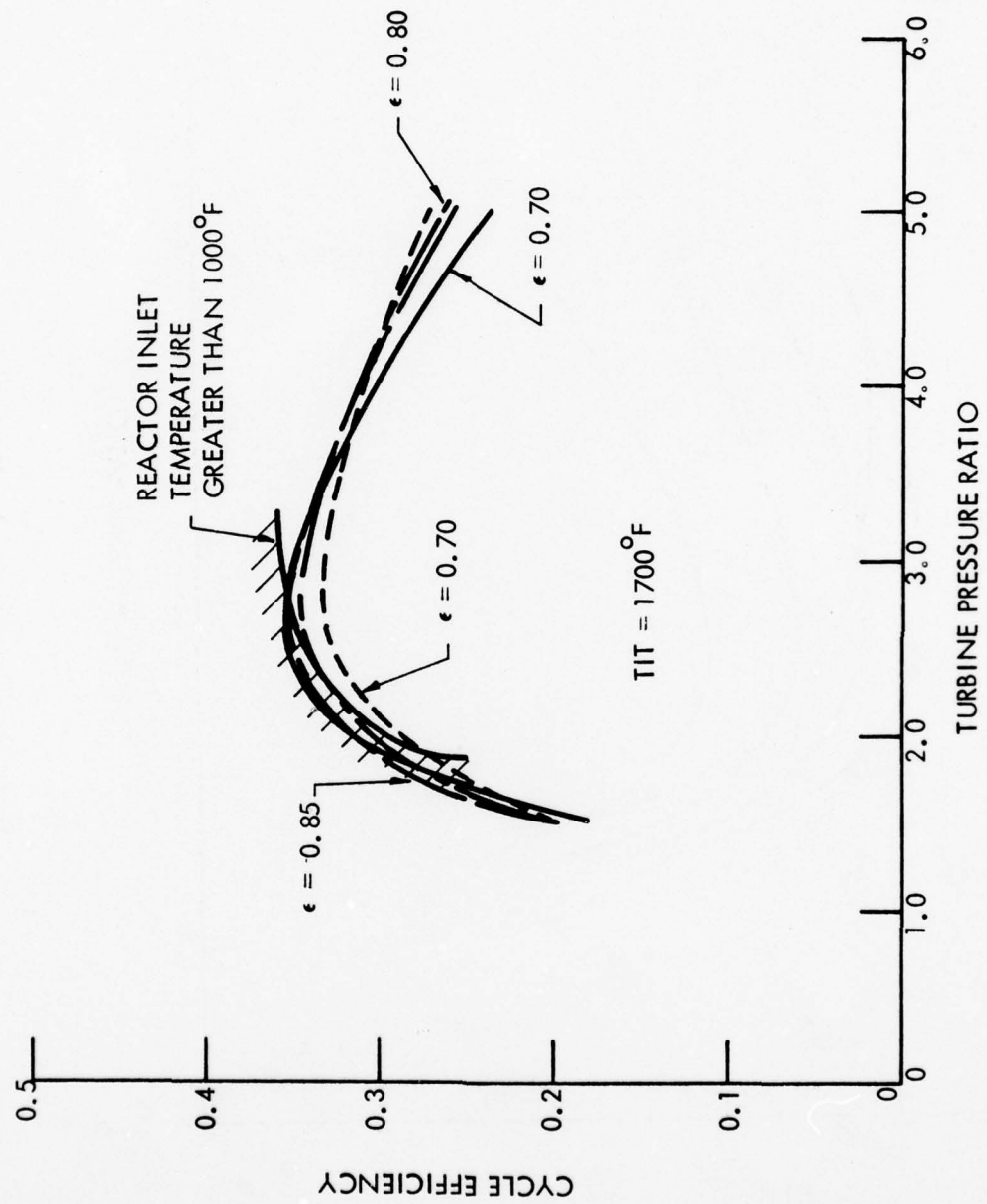


Figure A.4 Recuperated Brayton Cycle (R)

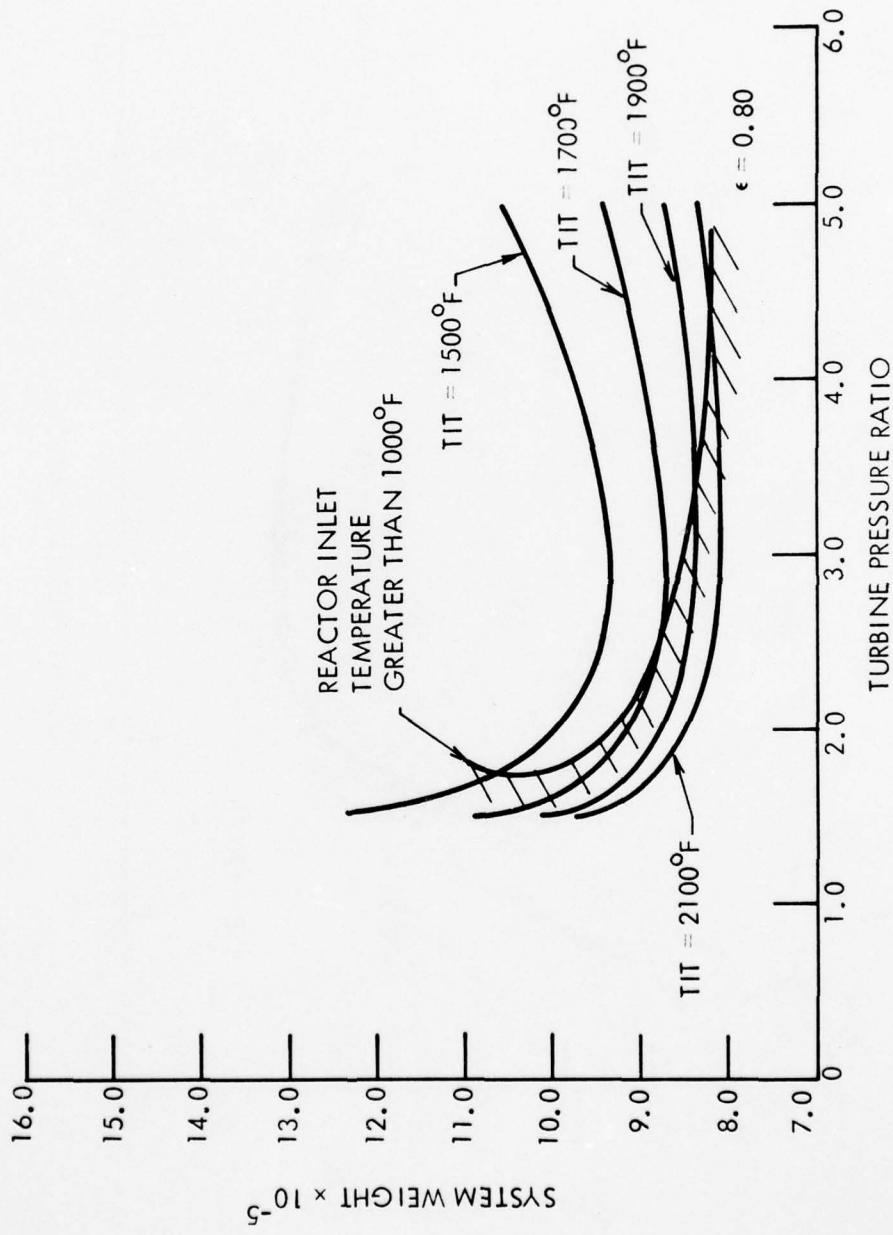


Figure A.5 Recuperated Brayton Cycle (R)

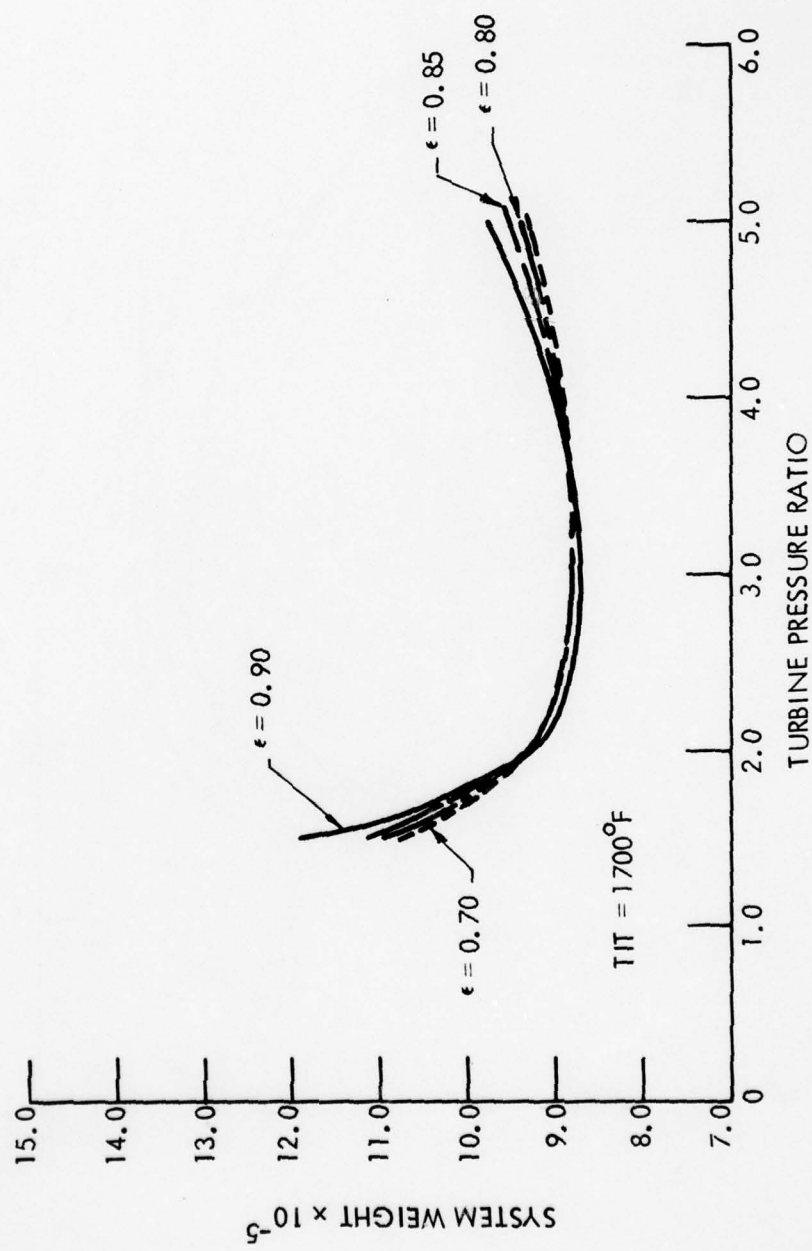


Figure A.6 Recuperated Brayton Cycle (R)

AD-A044 413

WESTINGHOUSE ELECTRIC CORP PITTSBURGH PA ADVANCED ENE--ETC F/G 21/5
COMPACT CLOSED CYCLE BRAYTON SYSTEM FEASIBILITY STUDY.(U)
JUL 77 R E THOMPSON, G H PARKER, R L AMMON N00014-76-C-0706

WAES-TNR-233

NL

UNCLASSIFIED

5 OF 5
AD
A044413



E
IC

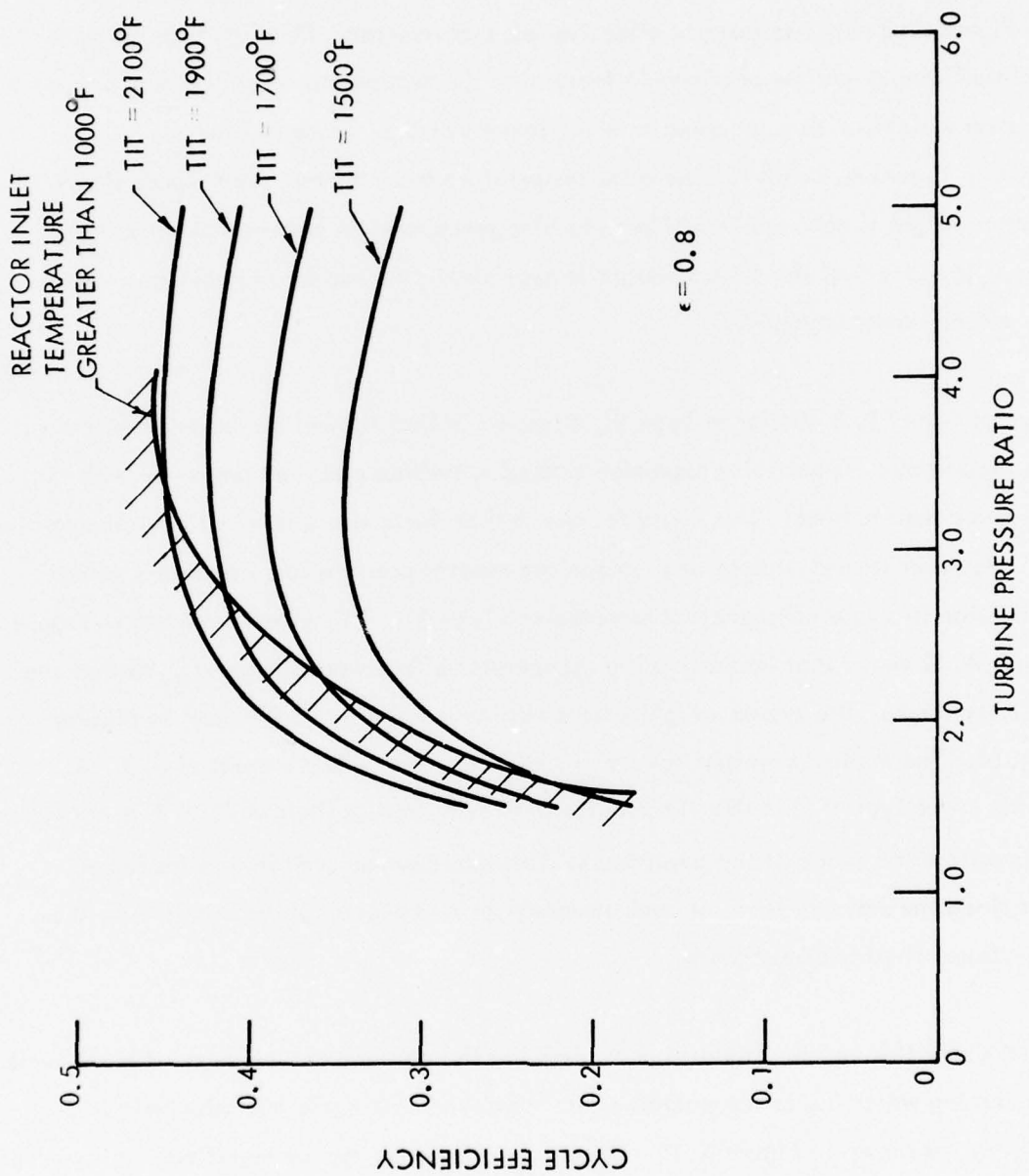


Figure A.7 Intercooler Brayton Cycle (R1)

can also effectively use higher turbine inlet temperatures before the reactor inlet temperature becomes a limiting factor. The cycle efficiency at a turbine inlet temperature of 1700°F is shown in Figure A.8 with recuperator effectiveness a parameter. This figure shows some gain in cycle efficiency can be obtained in increasing the recuperator effectiveness beyond 0.8. The system weight, with a recuperator effectiveness of 0.8, versus turbine pressure ratio is shown in Figure A.9 with turbine inlet temperature a parameter. This figure shows that the system weight is not very sensitive to turbine pressure ratio between about 2.5 to 5.0. Figure A.10 shows that the system weight is negligibly effected by increasing the recuperator effectiveness beyond 0.8.

The next cycle, Type RT, is similar to Type RI, differing in that the helium, after passing through the recuperator, is partially expanded through a turbine and then passes through the heat source and power turbine. This cycle feature is that the pressure level at peak temperature is reduced. However with a nuclear heat source the reactor pressure loss increases, which causes a reduction in cycle efficiency as compared to Type RI. This effect is shown in Figure A.11. Figure A.12 shows that increasing the recuperator effectiveness beyond 0.85 that the cycle efficiency drops. The system weight versus turbine pressure ratio is shown in Figures A.13 and A.14. The minimum weight occurs with a recuperator effectiveness of 0.8. A feature of this cycle Type (RT) is that the reactor inlet temperature limit of 1000°F is not reached within the investigation range of the parameters. This cycle appears attractive for fossil heat sources since the pressure level at peak temperature is reduced, which should ease the design of the fossil fired heat exchanger.

The BiBrayton cycle (BB) has the features of minimizing the components inside the containment, and not introducing water inside the containment. However, this cycle has relatively low cycle efficiency, as shown in Figure A.15. This cycle efficiency can be significantly increased by increasing the intermediate heat exchanger effectiveness (Figure A.16). Figures A.17

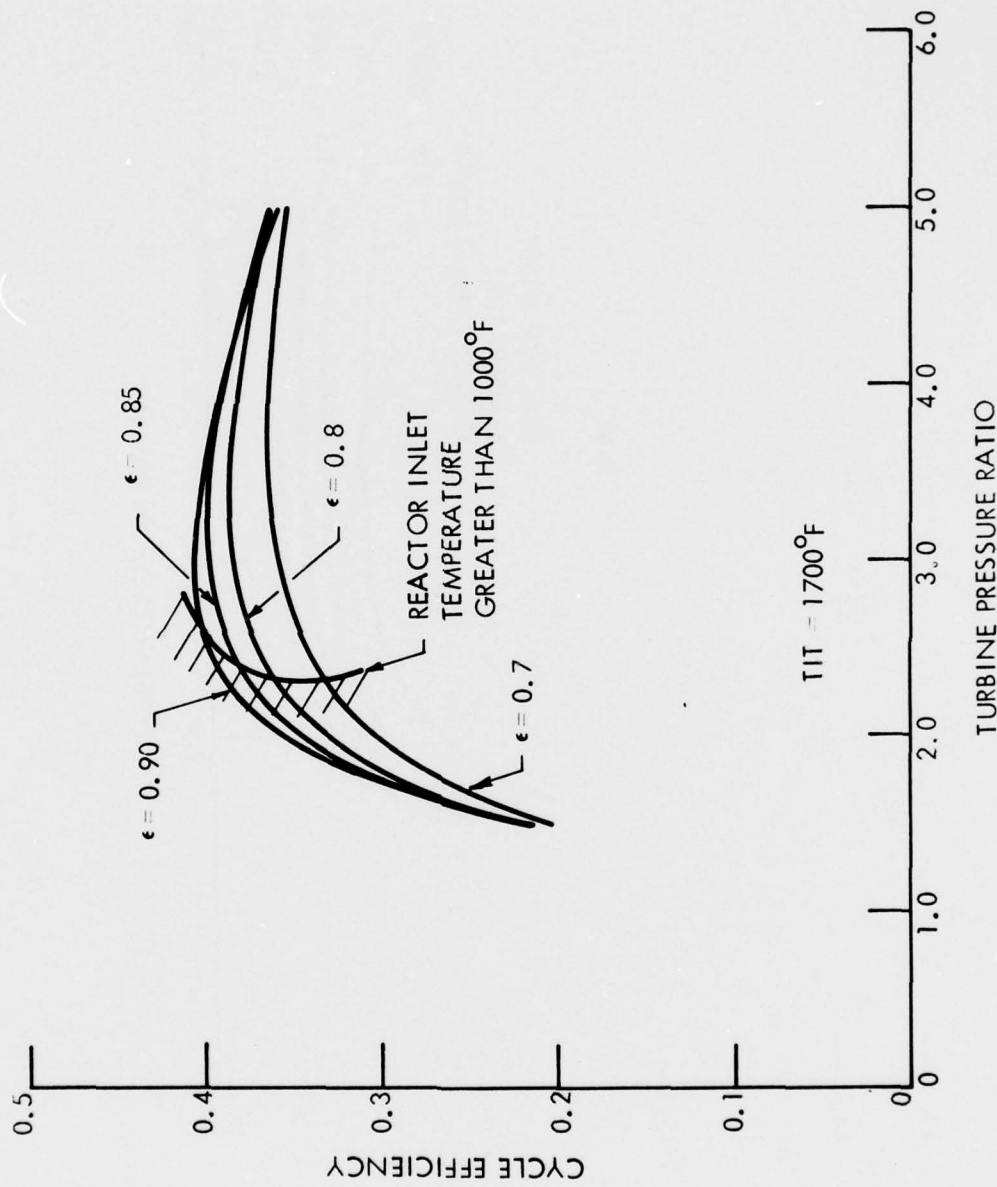


Figure A.8 Intercooled Brayton Cycle (RI)



Westinghouse

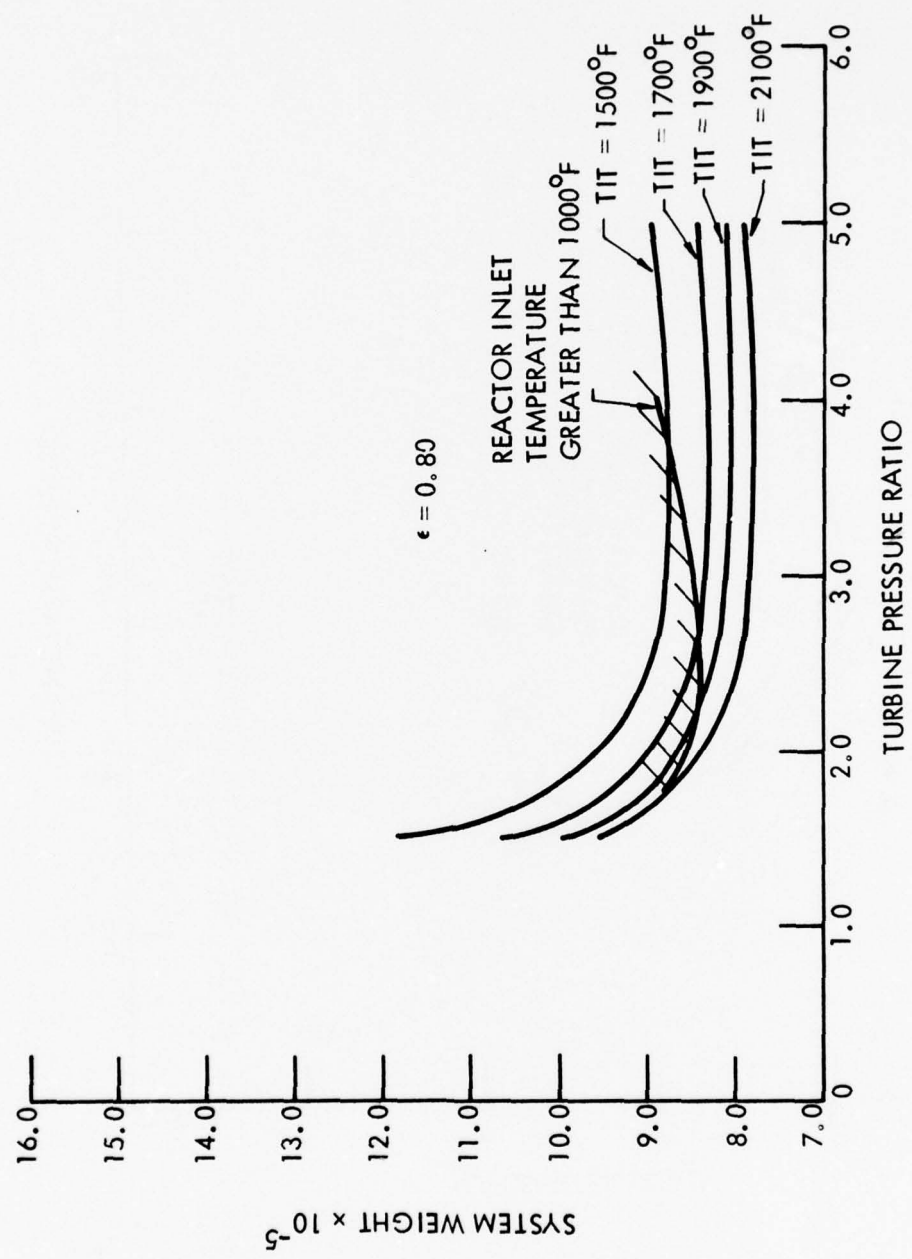


Figure A.9 Intercooled Brayton Cycle (RI)

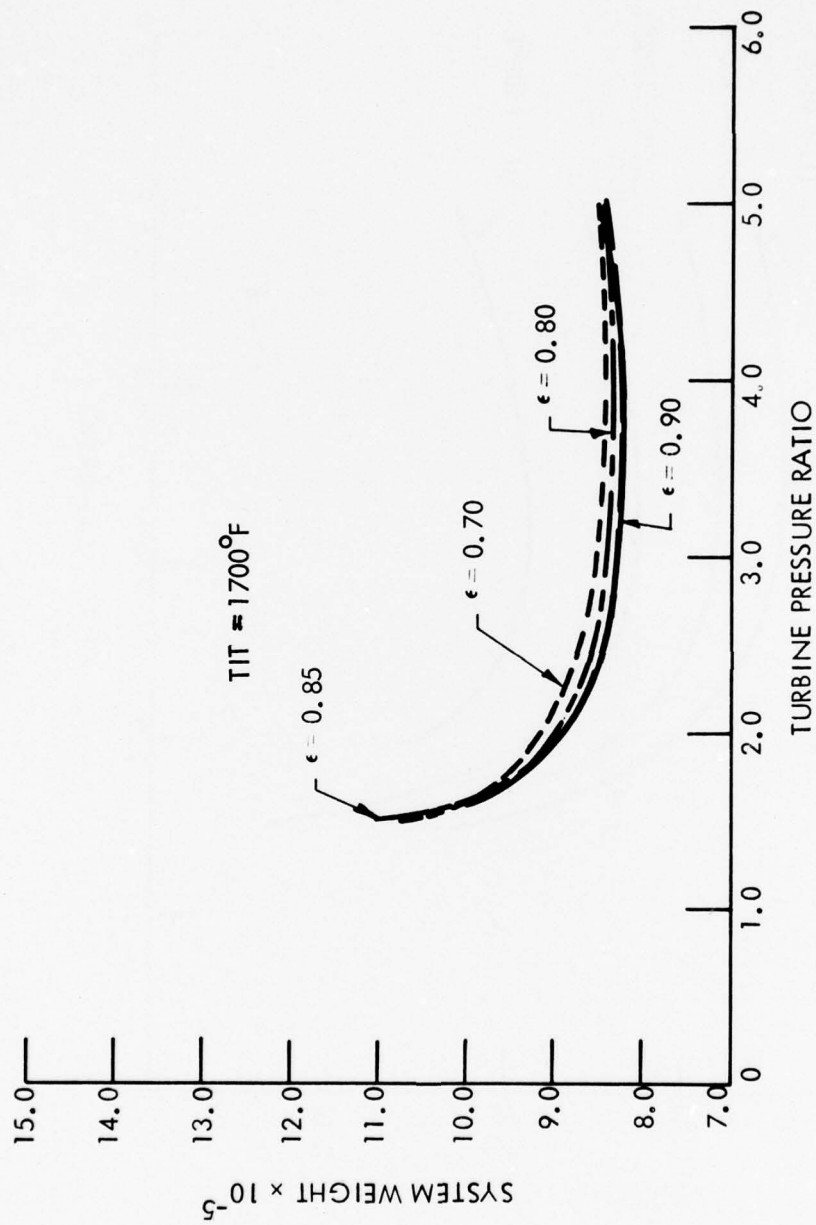


Figure A.10 Intercooled Brayton Cycle (RI)



Westinghouse

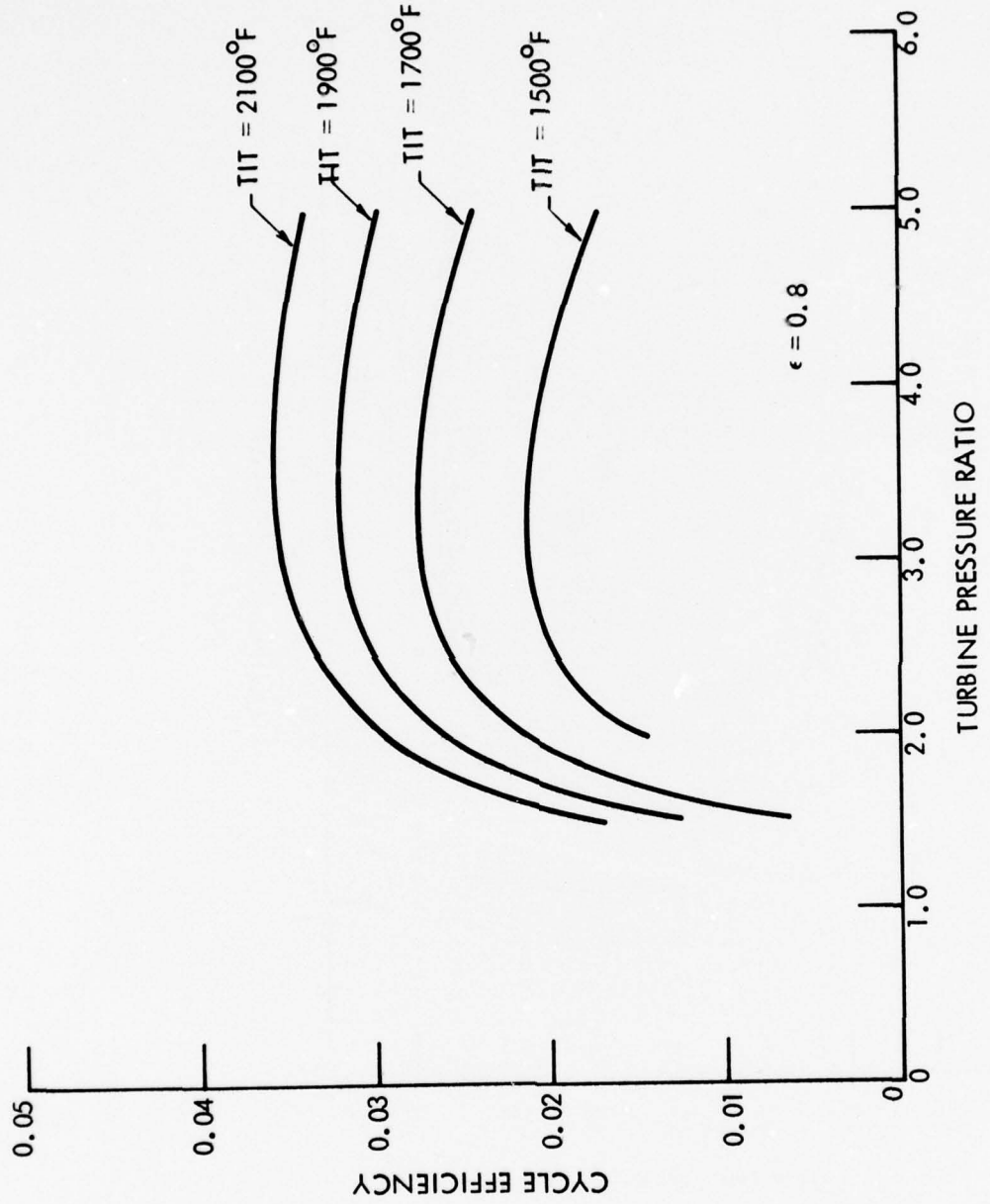


Figure A.11 Expanded Brayton Cycle (RT)

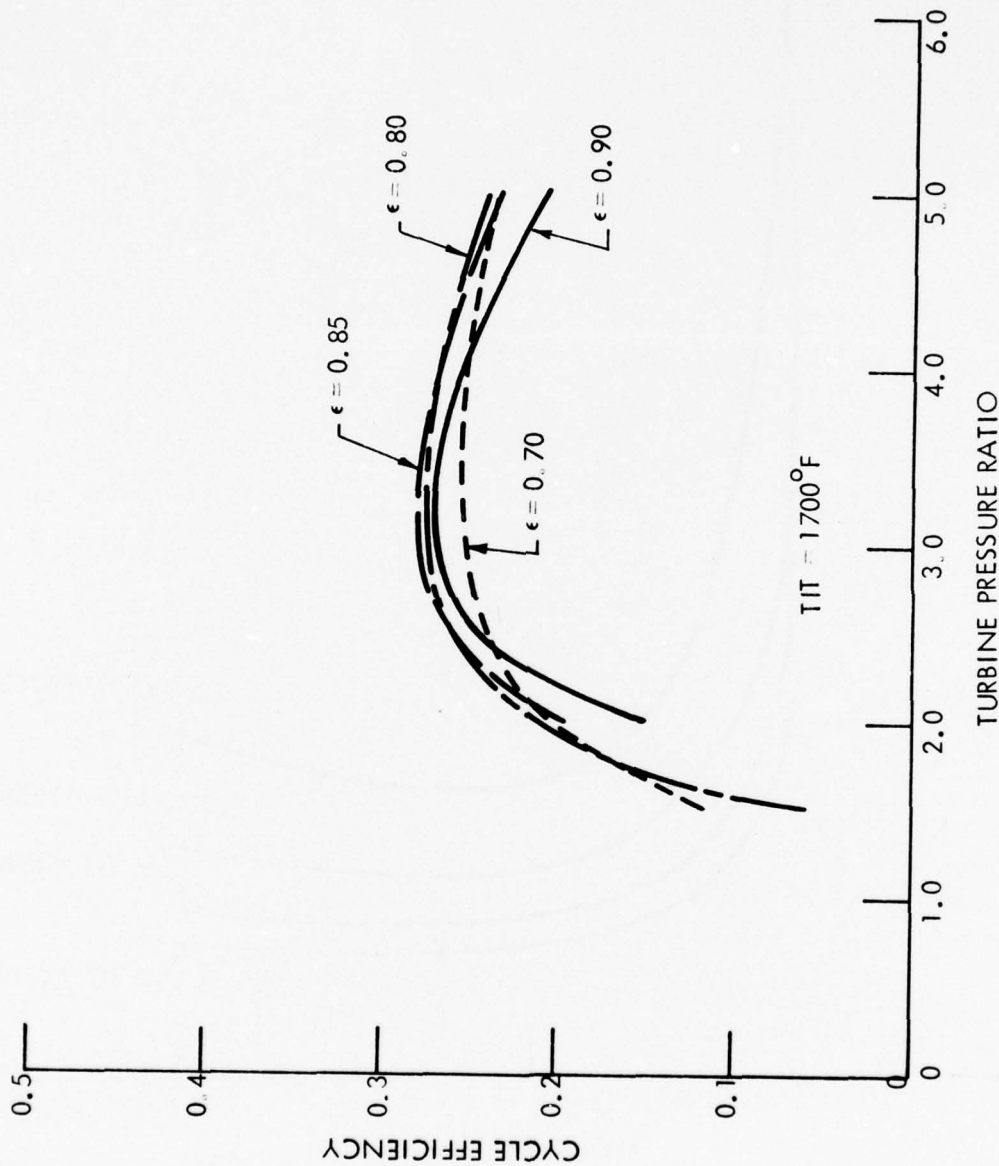


Figure A.12 Expanded Brayton Cycle (RT)

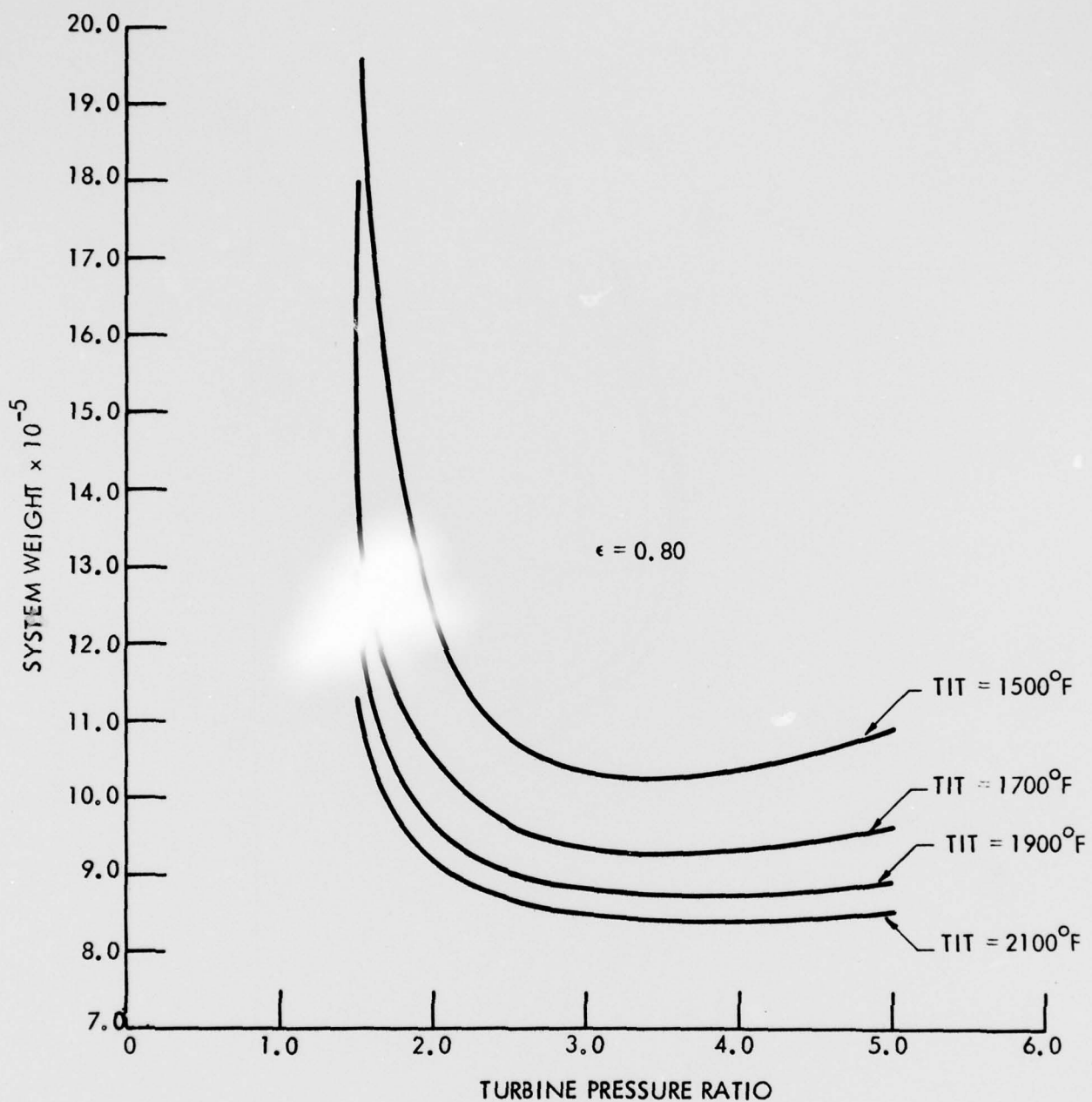


Figure A.13 Expanded Brayton Cycle (RT)

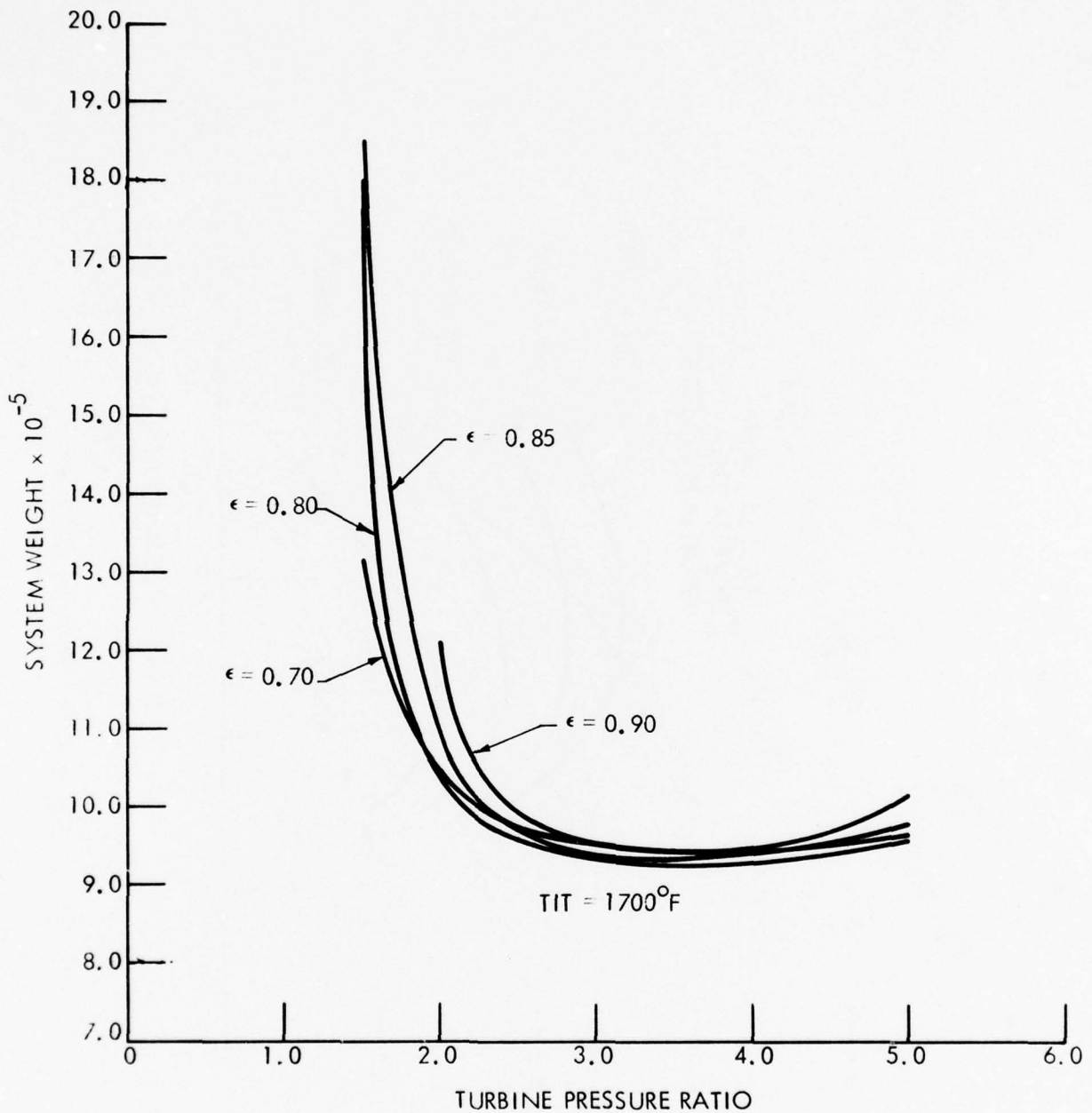


Figure A.14 Expanded Brayton Cycle (RT)

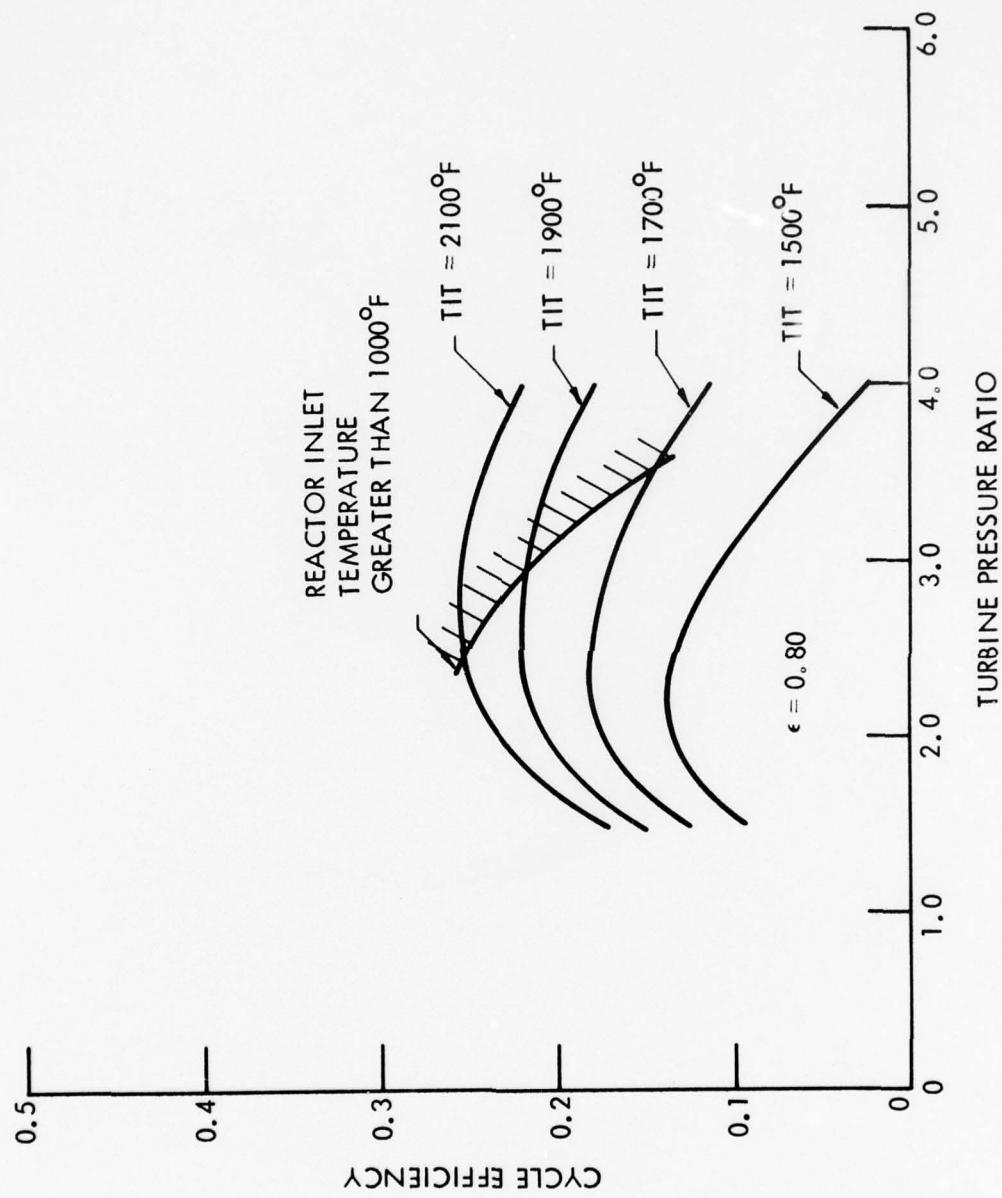


Figure A.15 BiBrayton Cycle (BB)

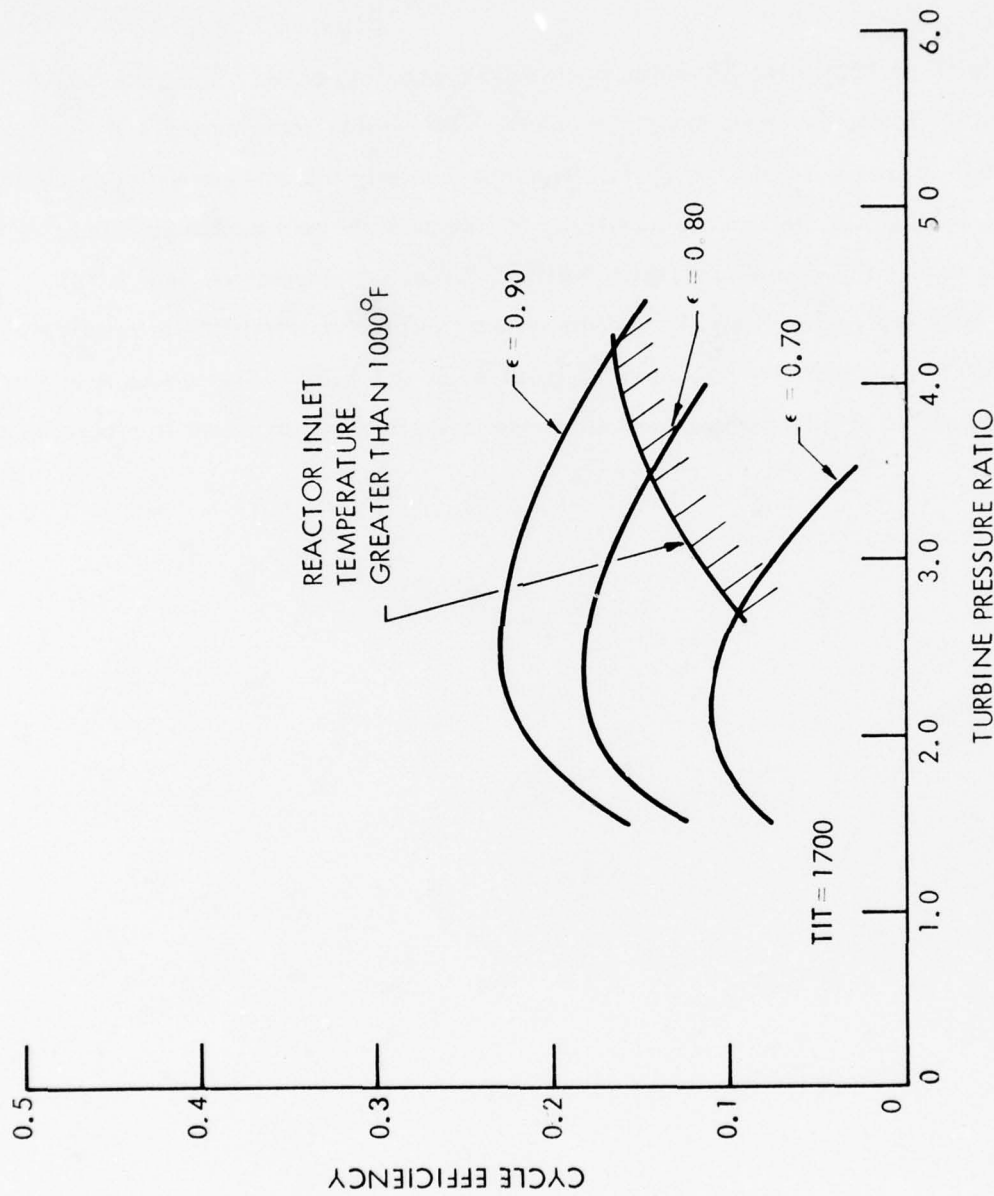


Figure A.16 BiBrayton Cycle (BB)

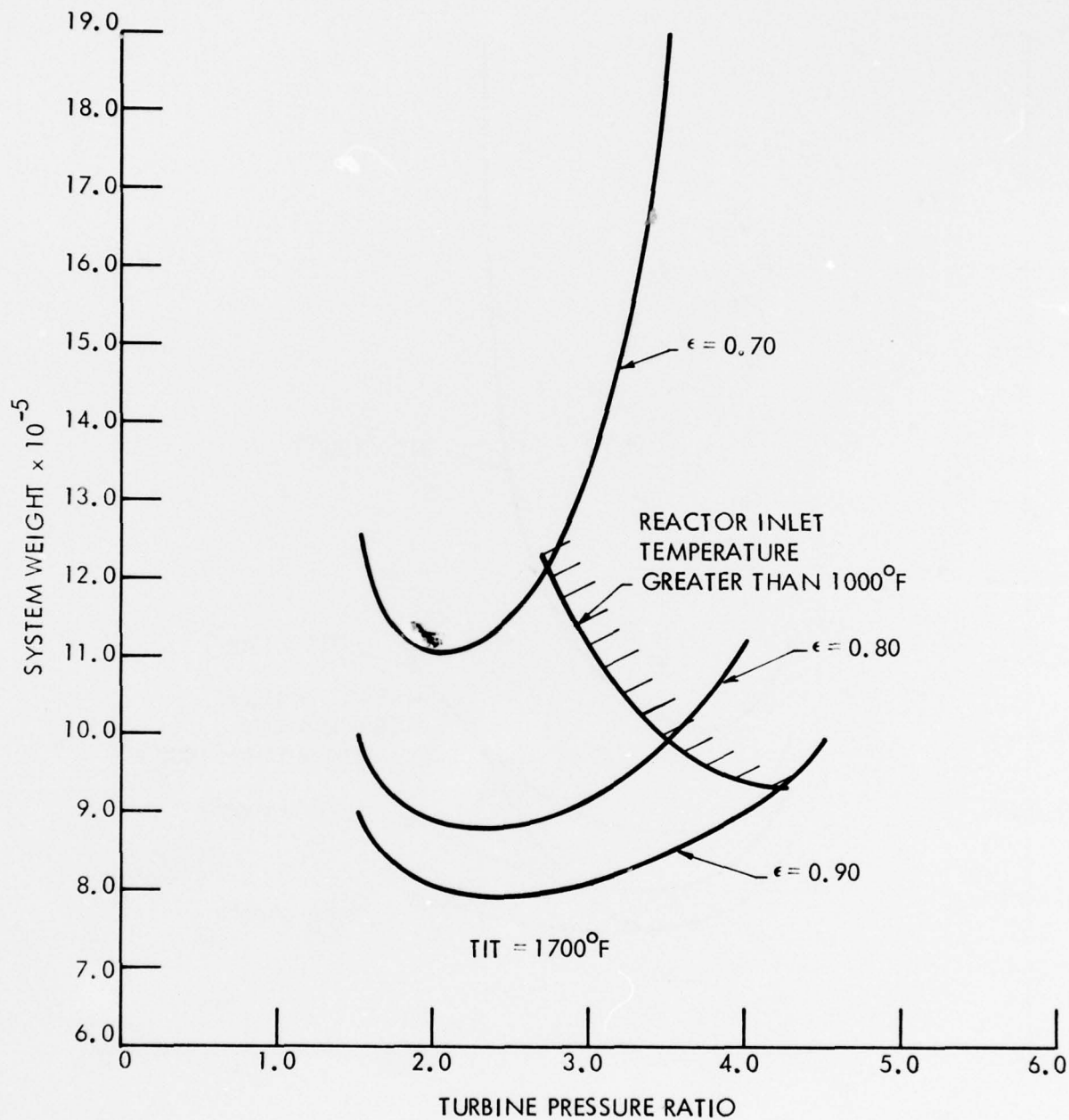


Figure A.17 BiBrayton Cycle (BB)

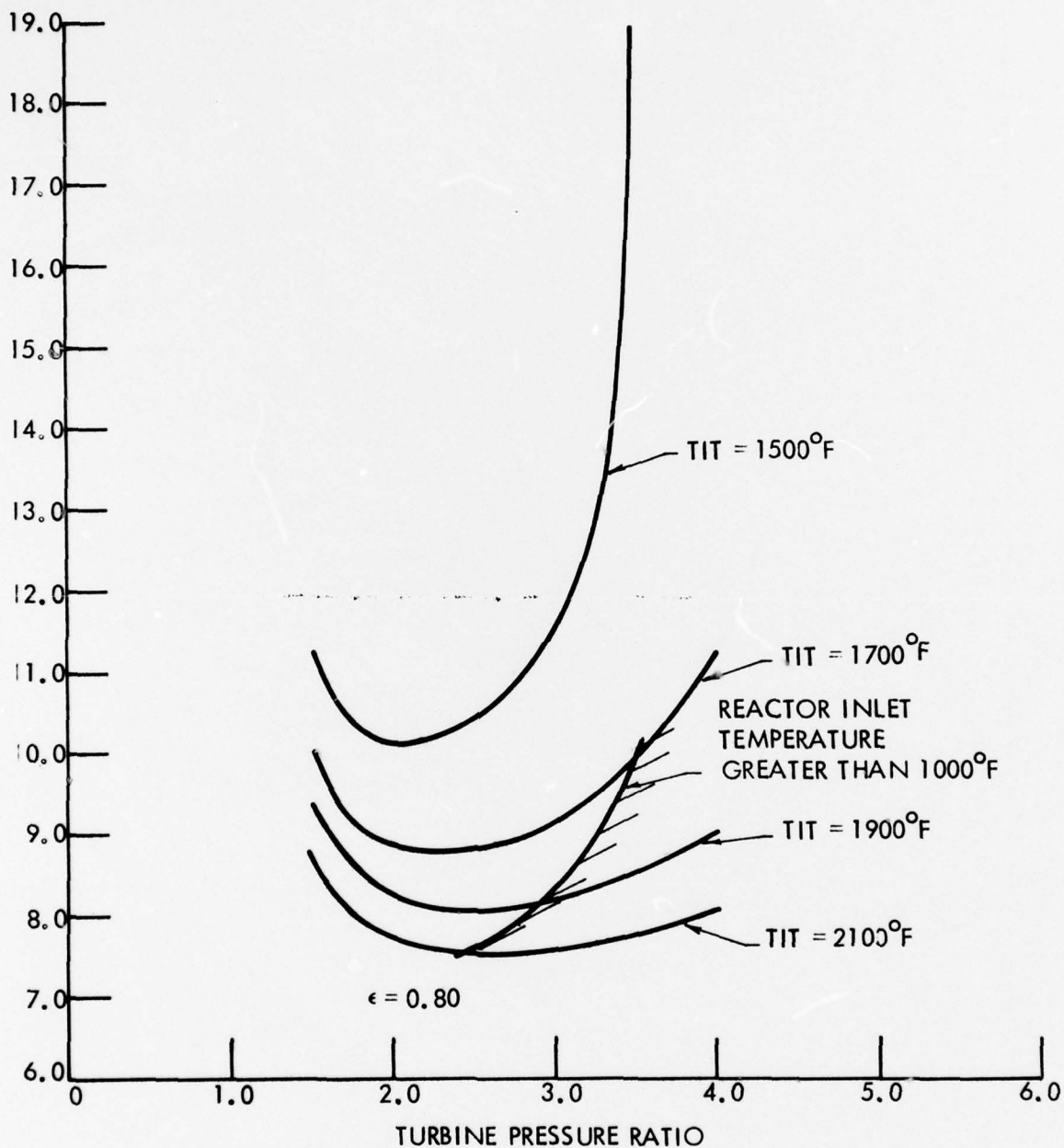


Figure A.18 BiBrayton Cycle (BB)

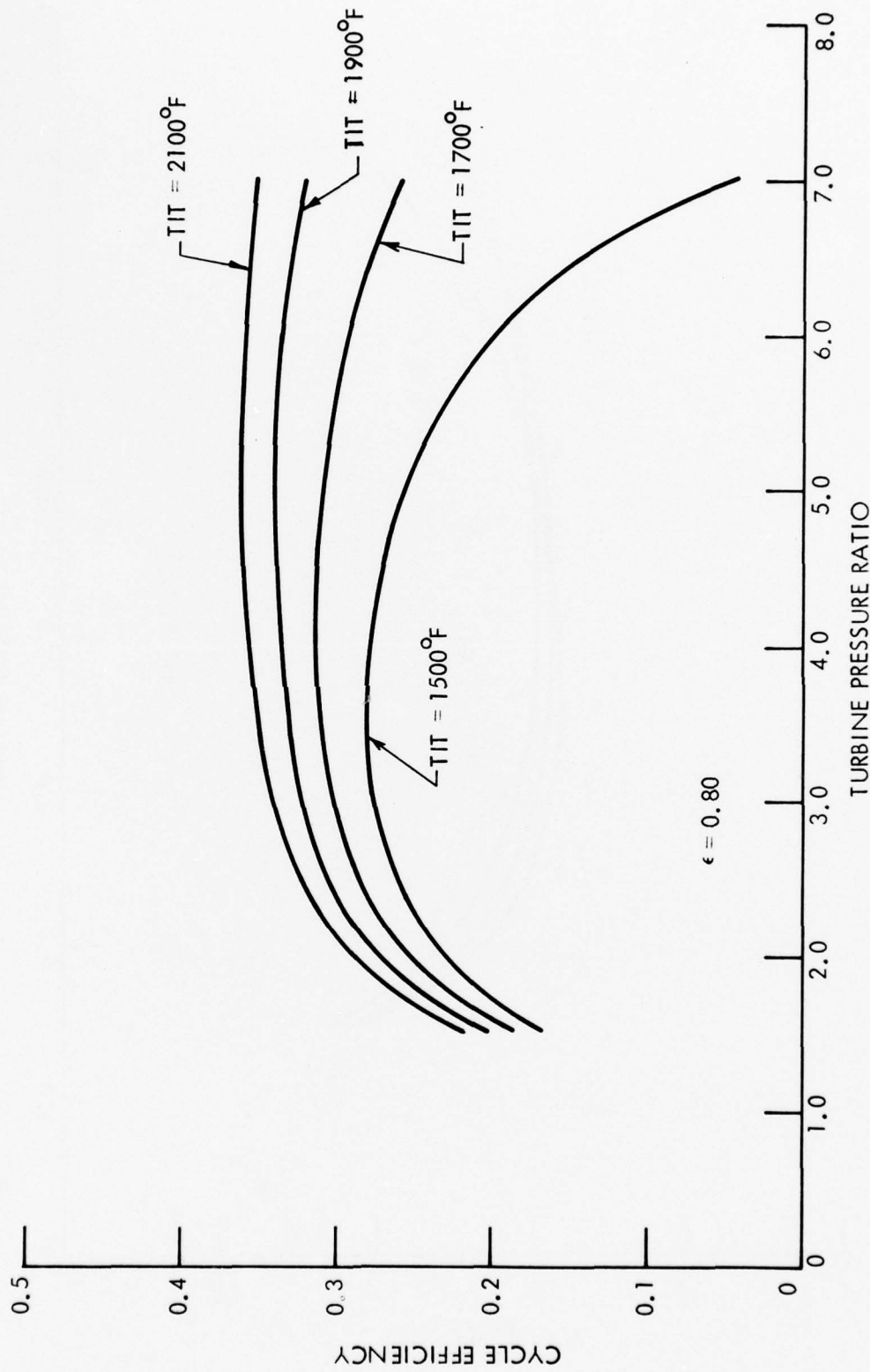


Figure A.19 BiBrayton with Precooler (BBP)



Westinghouse

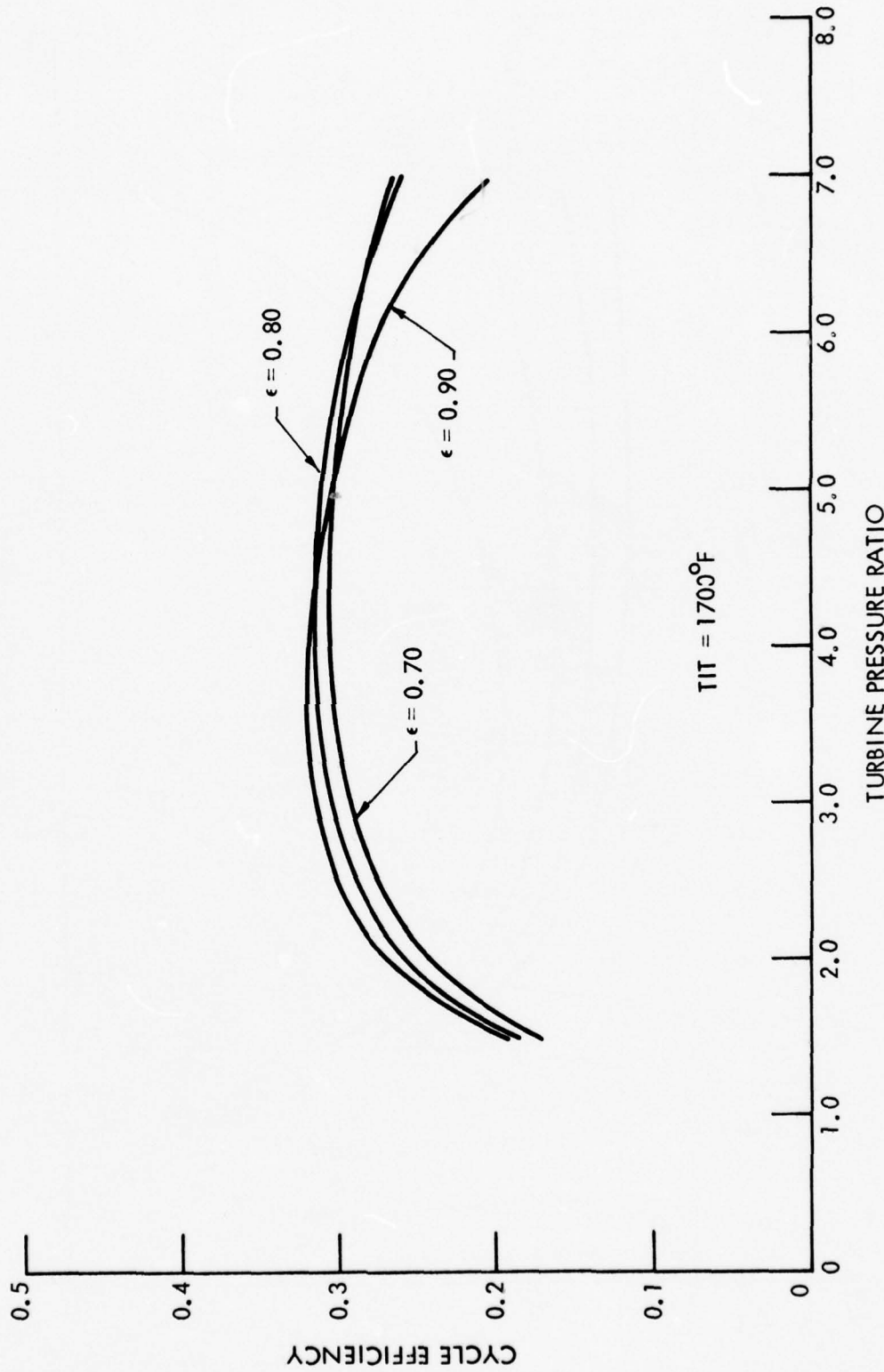


Figure A.20 BiBrayton Cycle with Precooler (BBP)

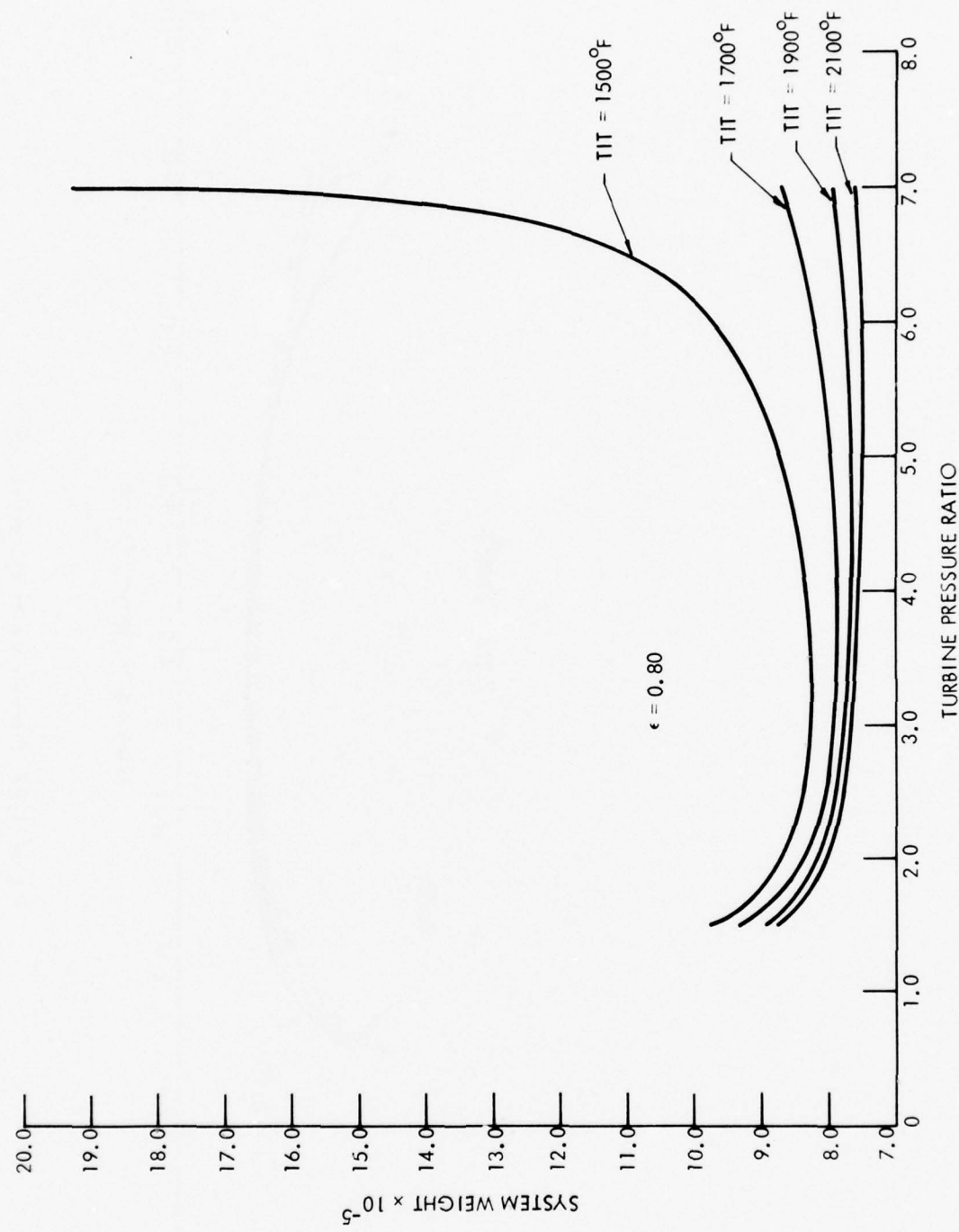


Figure A.21 BiBrayton Cycle with Precooler (BBP)



Westinghouse

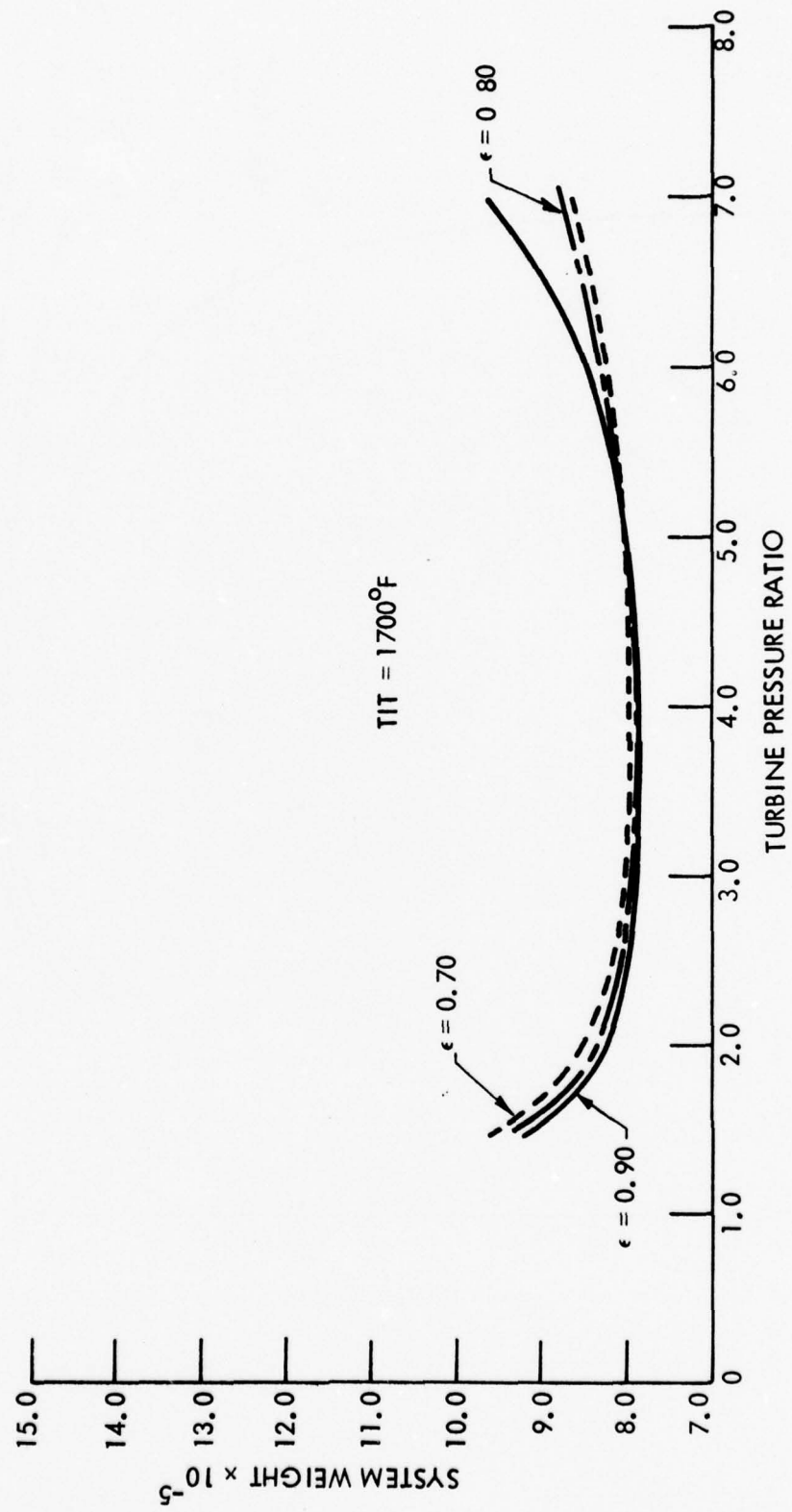


Figure A.22 BiBrayton with Precooler (BBP)

APPENDIX B

APPENDIX B

FRONTAL AREA CHARACTERISTIC OF TUBE AND SHELL RECUPERATORS

In tube and shell heat exchangers, the flow cross section is round on the tube side, and corresponds to a square or triangular lattice on the shell side. The correlations given below have been found for round channels, however application of a given correlation to the shell side can be made by introducing the hydraulic diameter

$$d = \frac{4 AL}{F} \quad (1)$$

The resulting pressure drop or heat transfer coefficient will give (in the turbulent flow region) a good approximation of the real conditions. The heat transfer coefficient may be expressed utilizing the Colburn factor (j)

$$h = j \frac{W}{A} C_p / P_r^{2/3} \quad (2)$$

Substituting equation 1 into equation 2

$$hF = \frac{j}{P_r^{2/3}} C_p \frac{4LW}{d} \quad (3)$$

The pressure drop equation using the Moody friction factor

$$\Delta P = \frac{fL}{d} \left(\frac{W}{A} \right)^2 / 2g\rho \quad (4)$$

Combining equations 3 and 4, the heat exchanger frontal area contribution due to one side is:

$$A = \sqrt{\frac{f}{i} \frac{hF W P_r^{2/3}}{\Delta P 8\rho g C_p}} \quad (5)$$

Since

$$hF = \frac{Q}{\Delta T} = \frac{W C_p \delta T}{\Delta T} \quad (6)$$

Then by substituting equation 6 into equation 5

$$A = W \sqrt{\frac{f}{i}} \sqrt{\frac{\delta T P_r^{2/3}}{\Delta T \Delta P 8\rho g}} \quad (7)$$

For a given flow rate, pressure loss temperature range and difference, the heat exchanger frontal area is proportional to the square root of the ratio of the friction factor to Colburn modulus. This ratio versus Reynolds number is shown in Figure 4.3. Therefore to minimize the heat exchanger frontal area, one would utilize a Reynolds number in the range of 10,000 to 20,000 for slightly rough surfaces (resulting from the fabrication process).

Substituting equation 6 into equation 3 and rearranging

$$d = \frac{i 4L \Delta T}{P_r^{2/3} \delta T} \quad (8)$$

The required tube diameter may be then be determined for specified effective tube length and heat exchanger effectiveness, with the Colburn factor evaluated at the appropriate Reynolds number.



Westinghouse

APPENDIX C

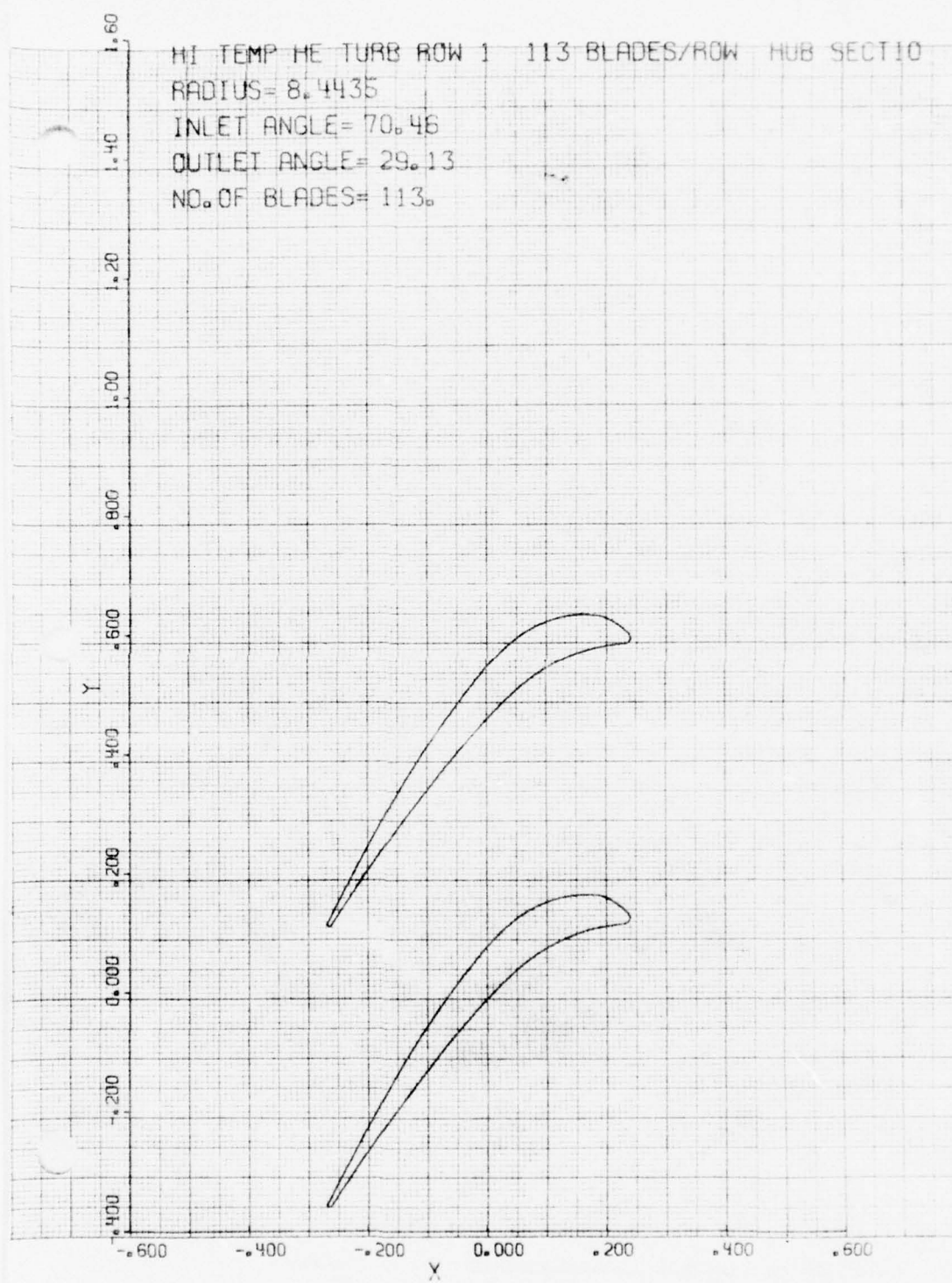
FIRST STAGE ROTOR BLADE STRESS ANALYSIS COMPUTER PRINTOUTS

BAR 1	X	000931	BAR 1	X	001185
	C MIN	013086		C MIN	236405
	C MAX	013086		C MAX	565912
	Z MIN	018448		Z MIN	013514
	Z MAX	026088		Z MAX	292106
	C MAX	005134		C MAX	008259
	Z MIN	005134		Z MIN	960000
	BAR D	001127		BAR D	960000
	X	000756		X	

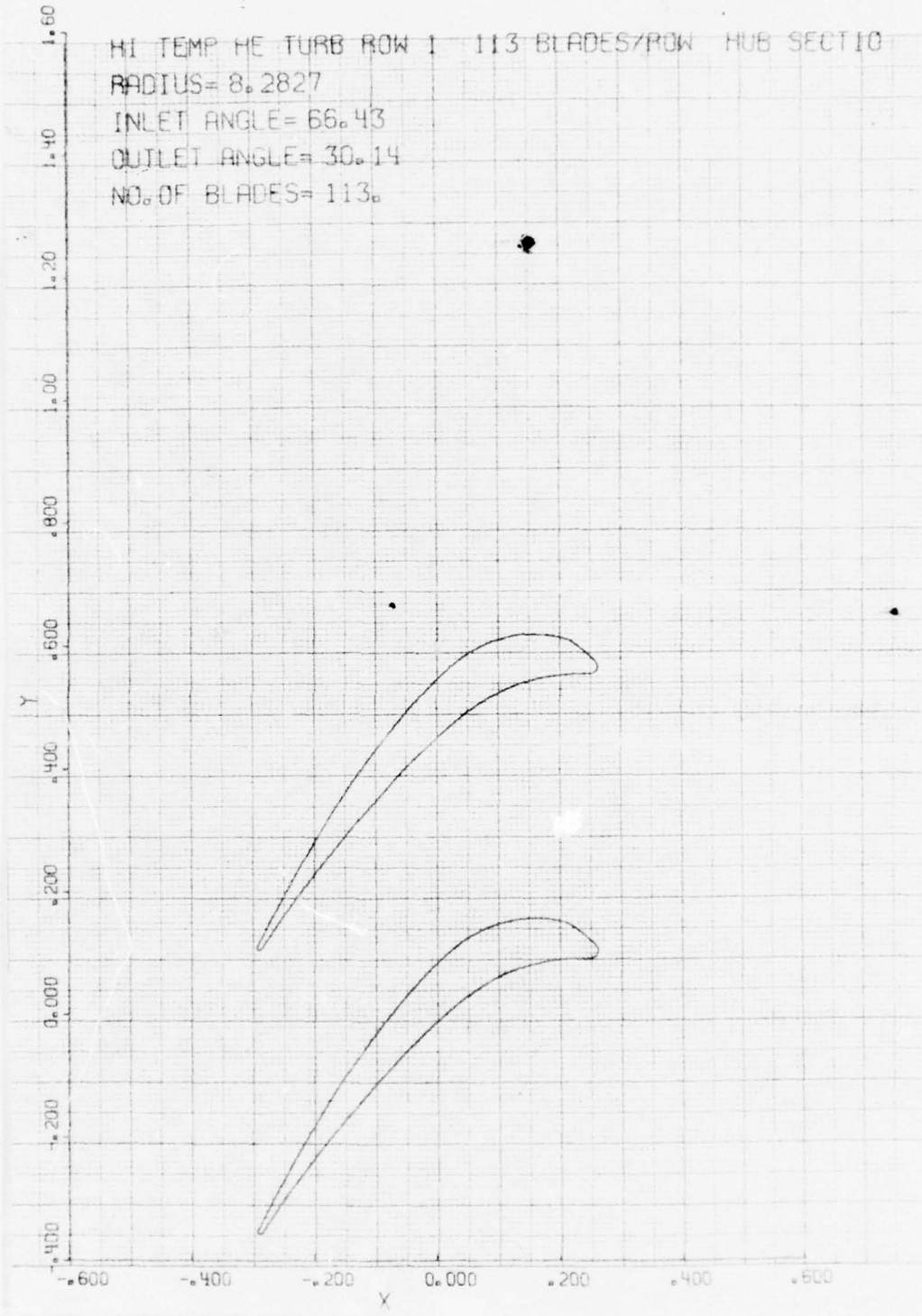
BAR 1	X	0007411	BAR 1	X	000317
	C MIN	0193630		C MIN	0003725
	C MAX	0193630		C MAX	0140513
	Z MIN	0003725		Z MIN	000317
	Z MAX	0140513		Z MAX	520207
	C MAX	000317		C MAX	520207
	BAR B	000317		BAR B	
	BAR X	520207		BAR X	

BAR B	" .000043	BAR C	" .000075	BAR D	" .000071	CHORD	" .703150
BAR X	".267993	BAR Y	".358717	X	".000027	WIDTH	".507500

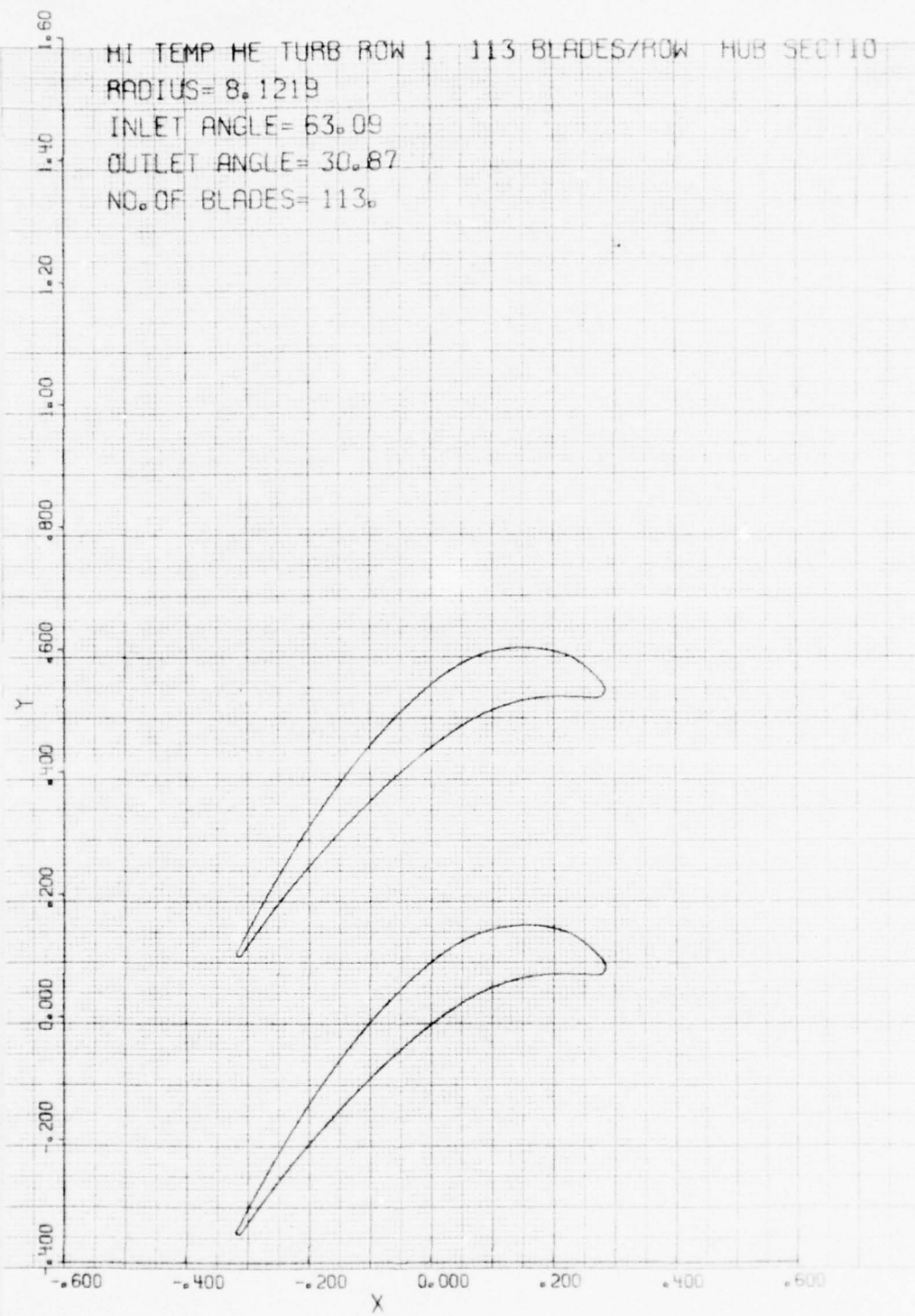
HI TEMP HE TURB ROW 1 113 BLADES/ROW HUB SECT 10
RADIUS = 8.4435
INLET ANGLE = 70.46
OUTLET ANGLE = 29.13
NO. OF BLADES = 113.

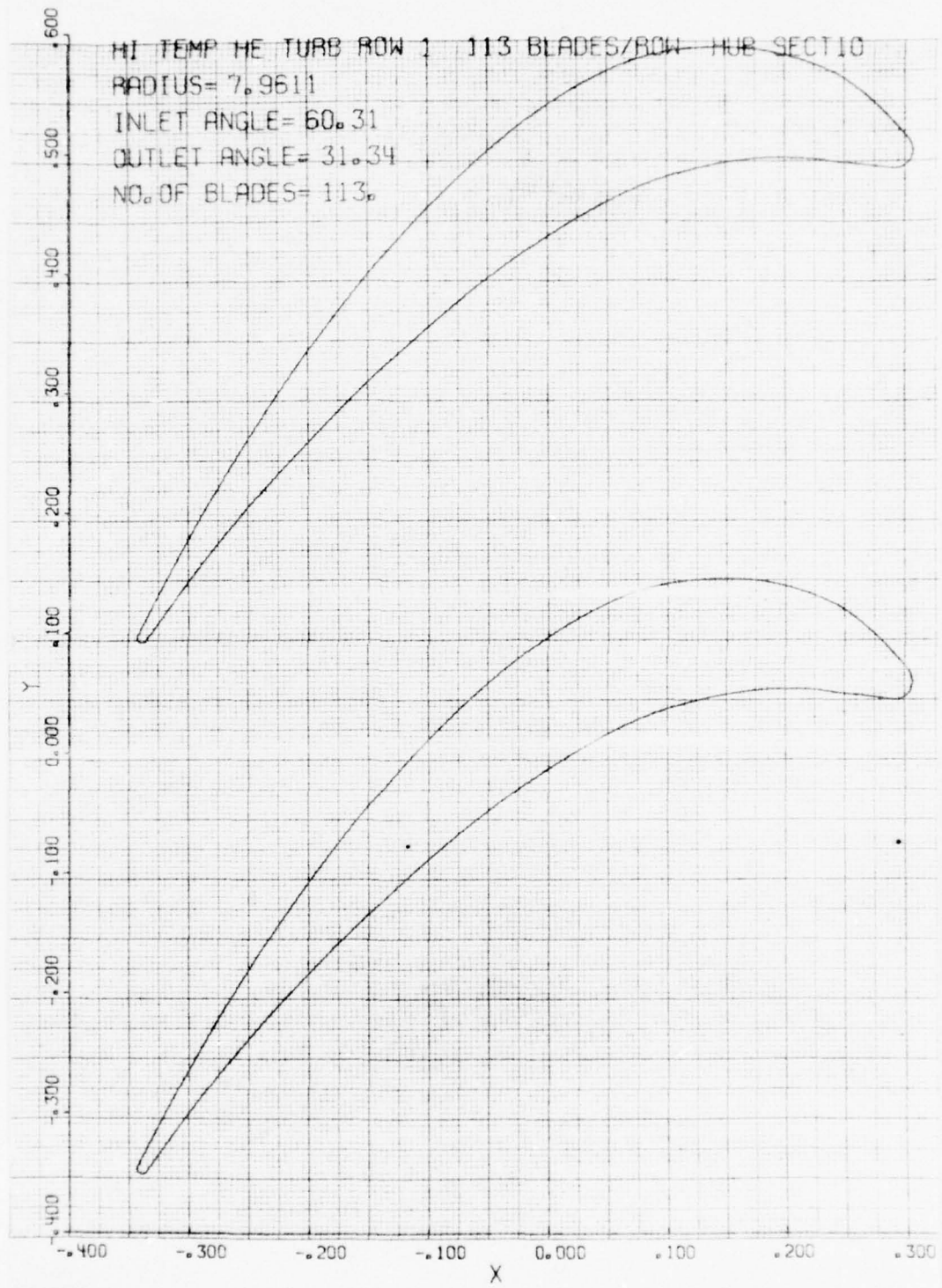


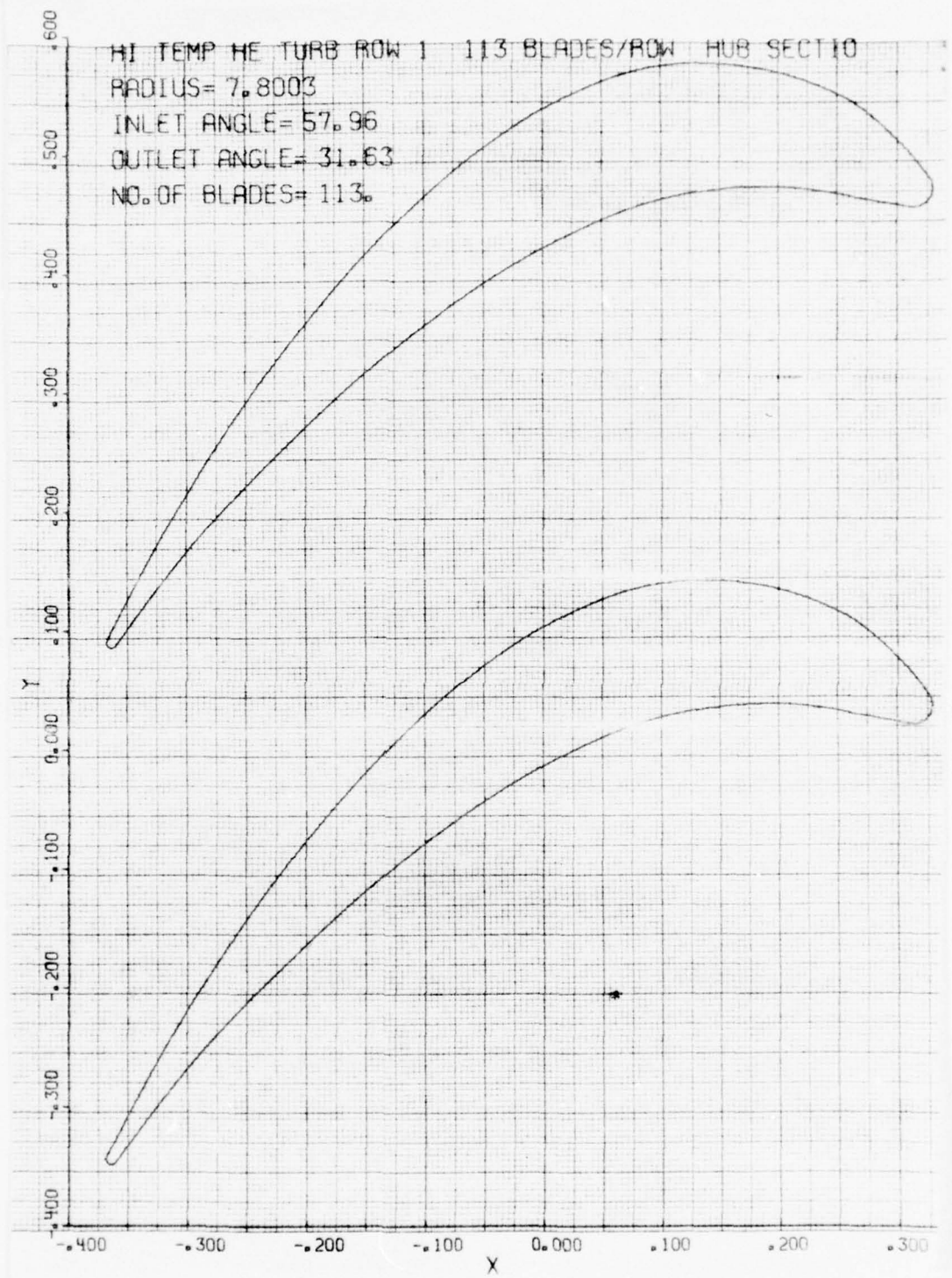
HI TEMP HE TURB ROW 1 113 BLADES/ROW HUB SECT 10
RADIUS= 8.2827
INLET ANGLE= 66.43
OUTLET ANGLE= 30.14
NO. OF BLADES= 113.

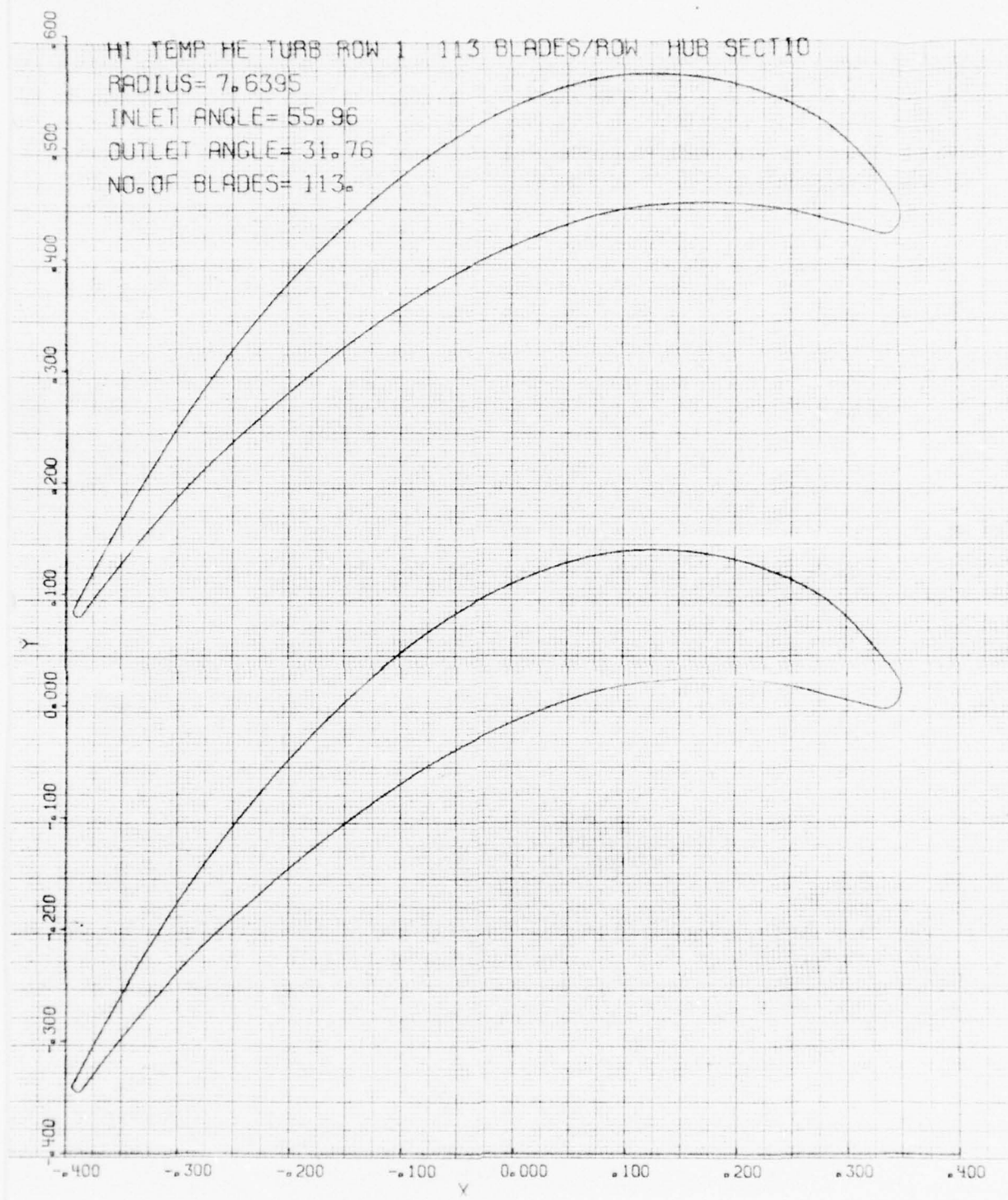


HI TEMP HE TURB ROW 1 113 BLADES/ROW HUB SECTION
RADIUS = 8.1219
INLET ANGLE = 63.09
OUTLET ANGLE = 30.87
NO. OF BLADES = 113.

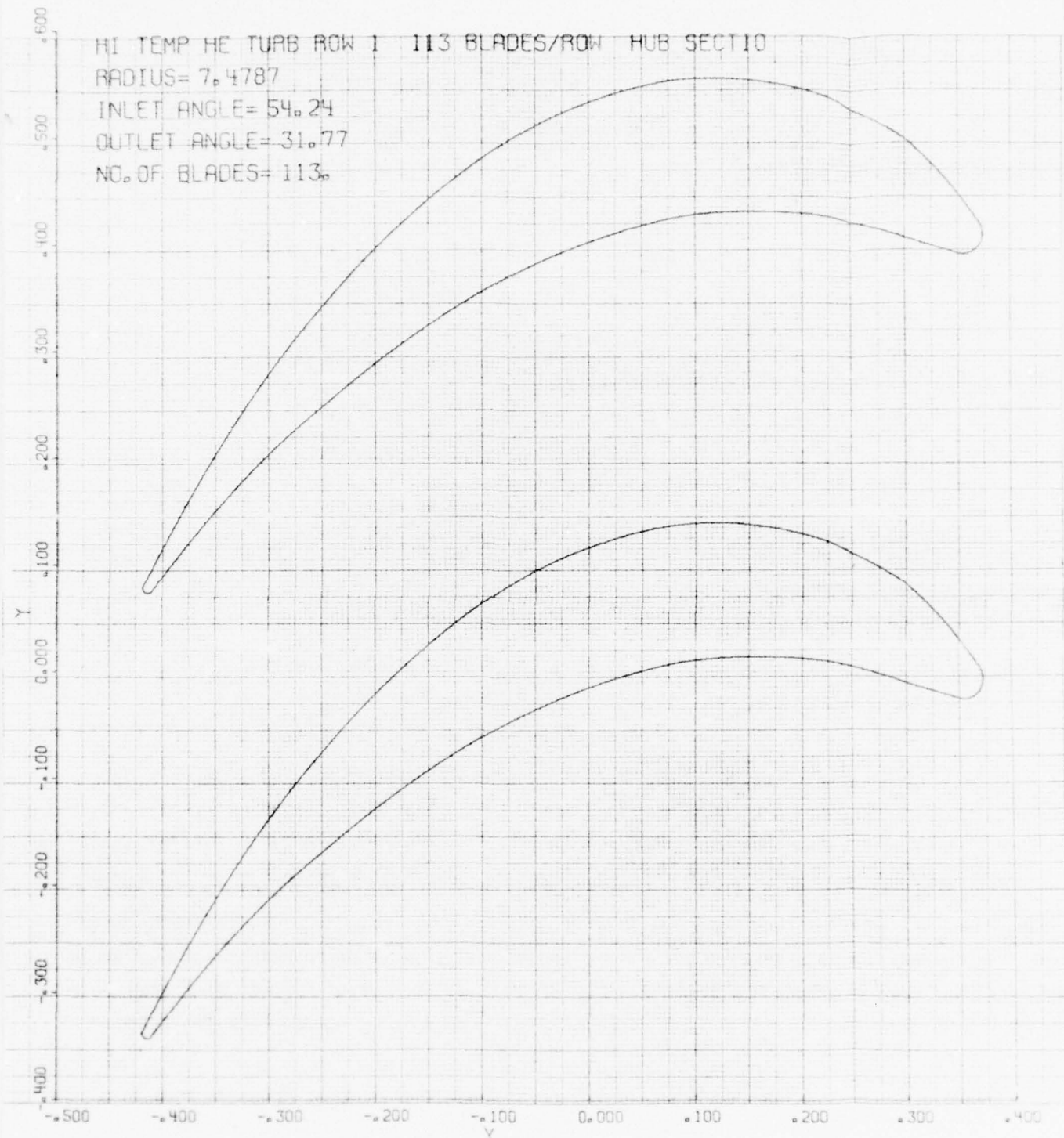




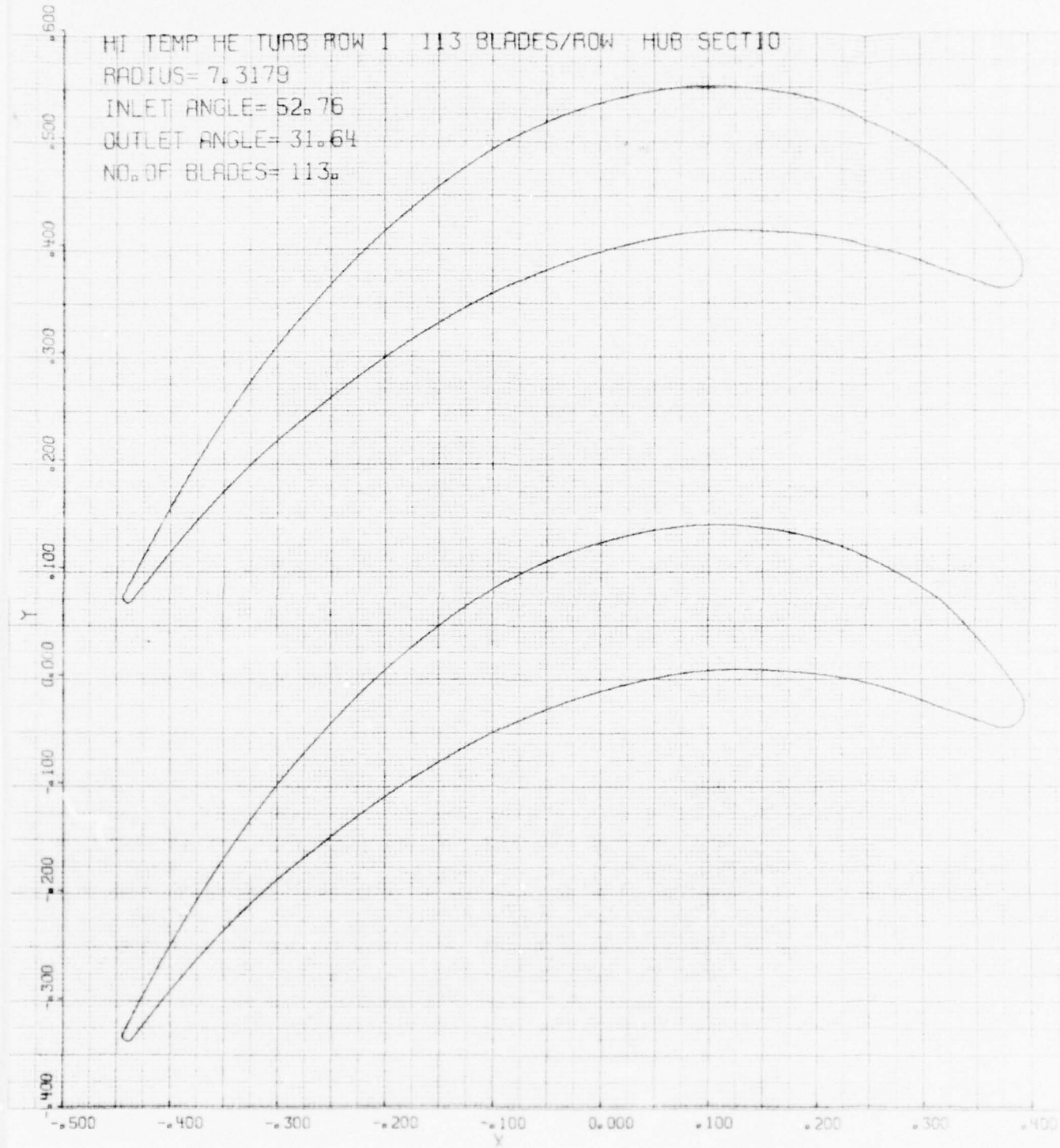


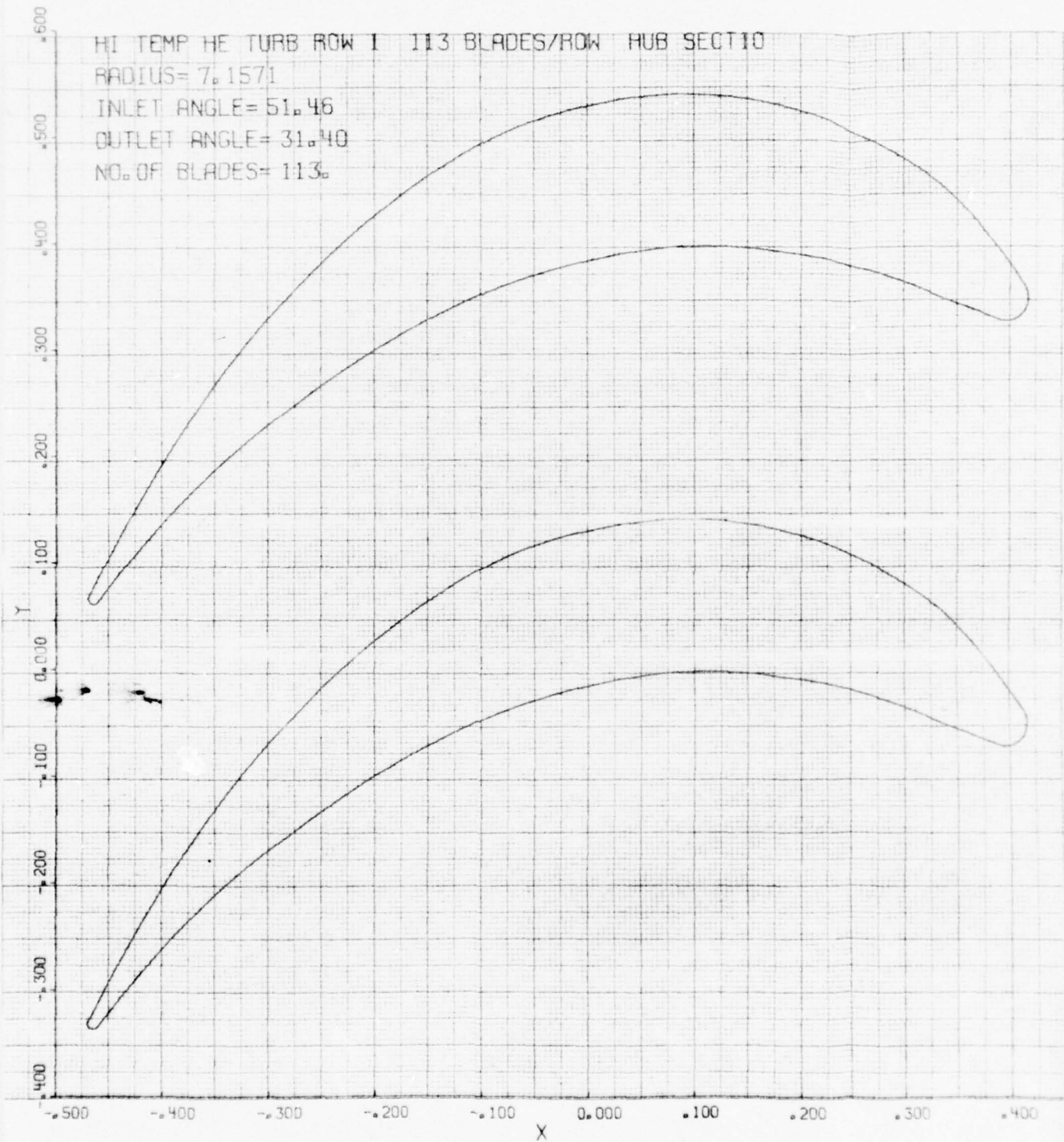


C-10

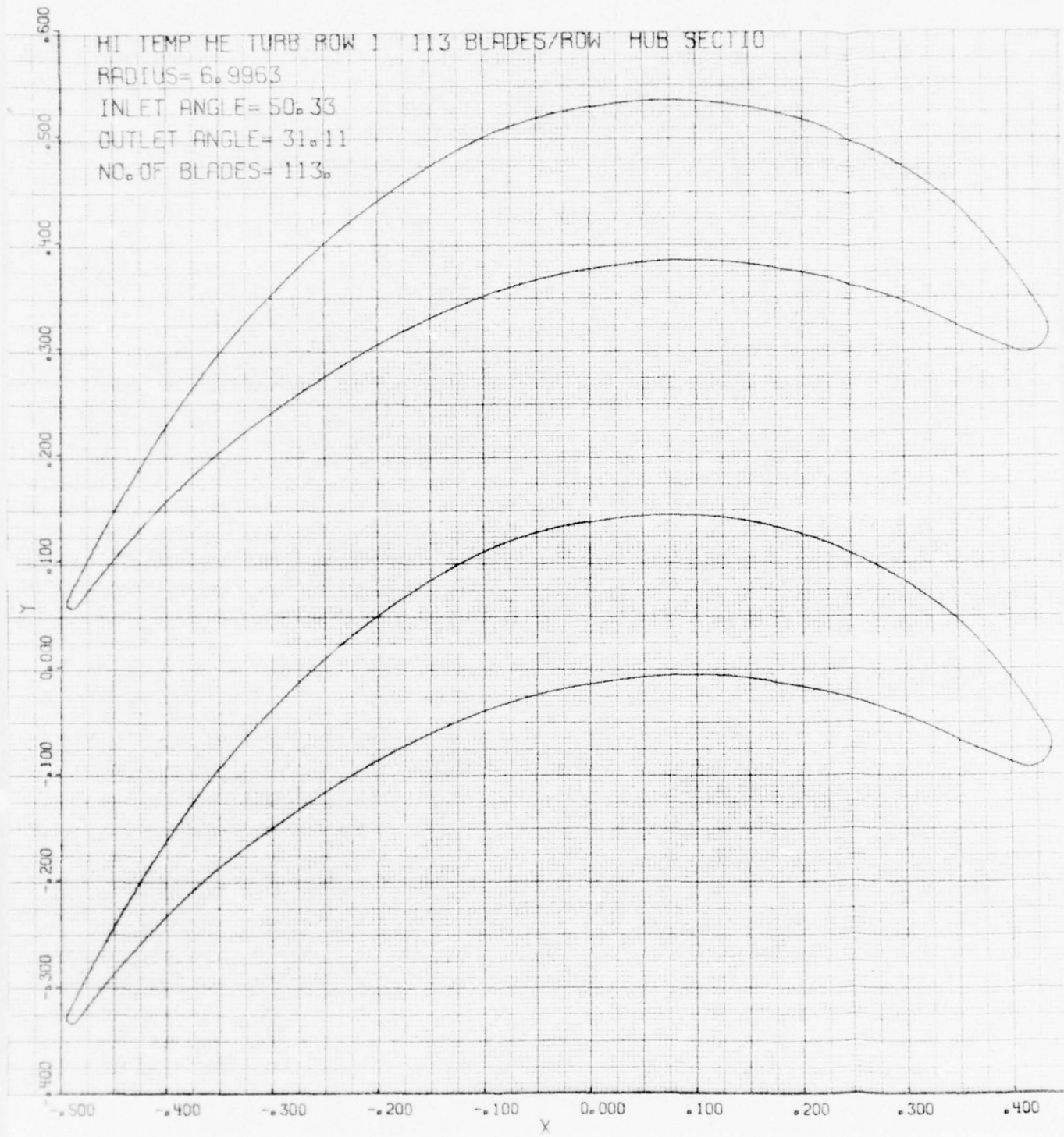


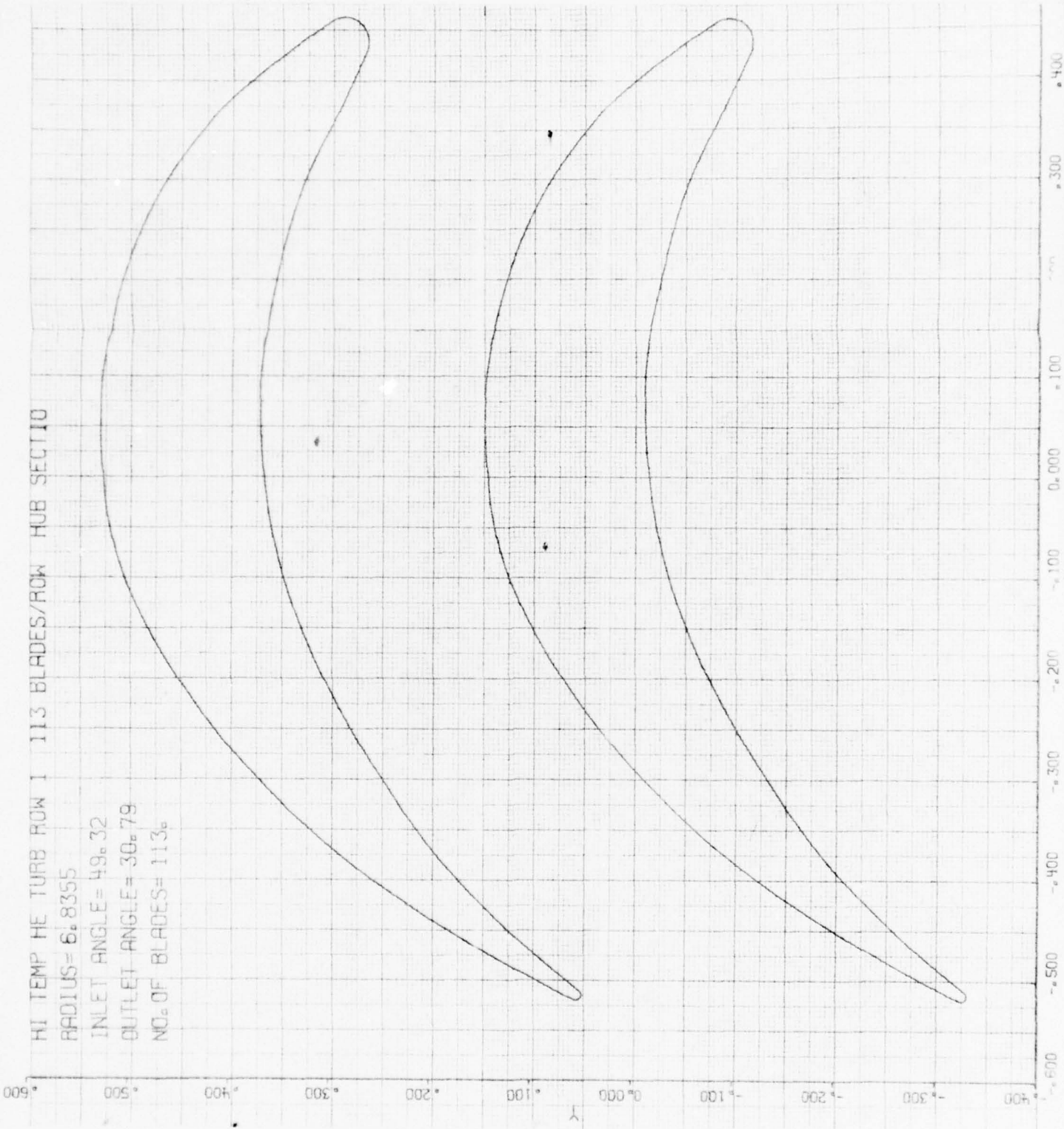
HI TEMP HE TURB ROW 1 113 BLADES/ROW HUB SECTION
RADIUS= 7.3179
INLET ANGLE= 52.76
OUTLET ANGLE= 31.64
NO. OF BLADES= 113.



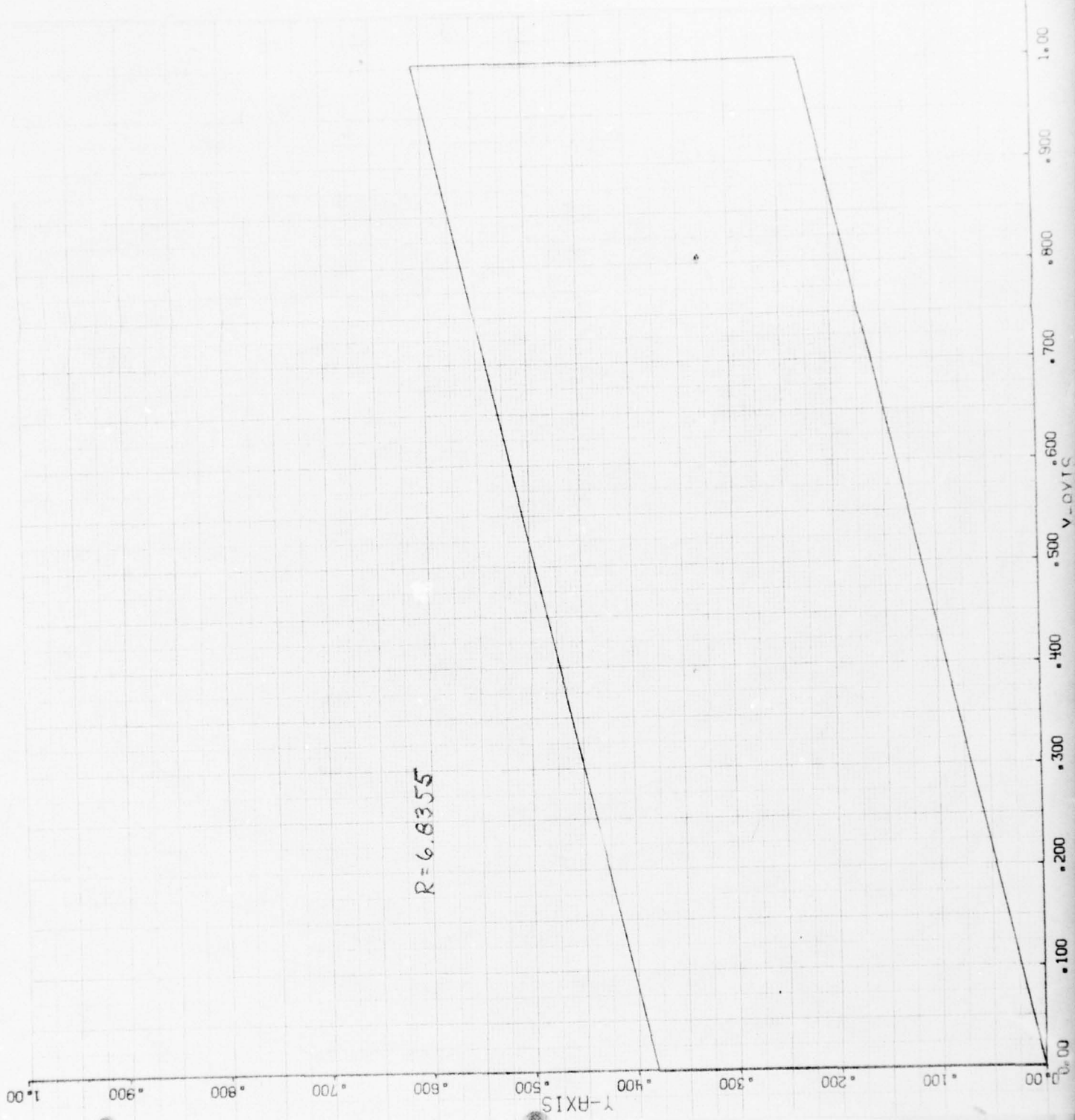


C-13

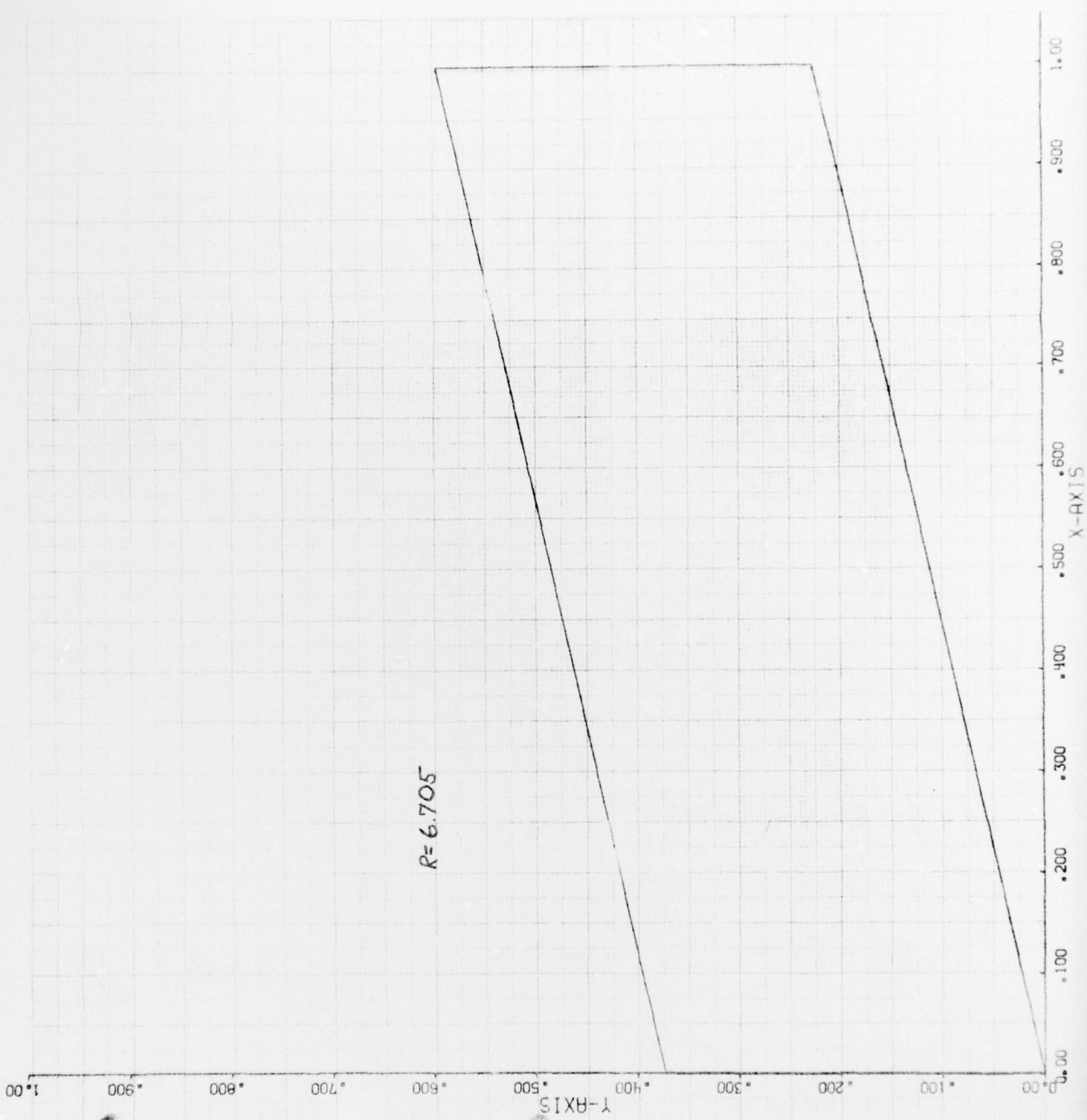




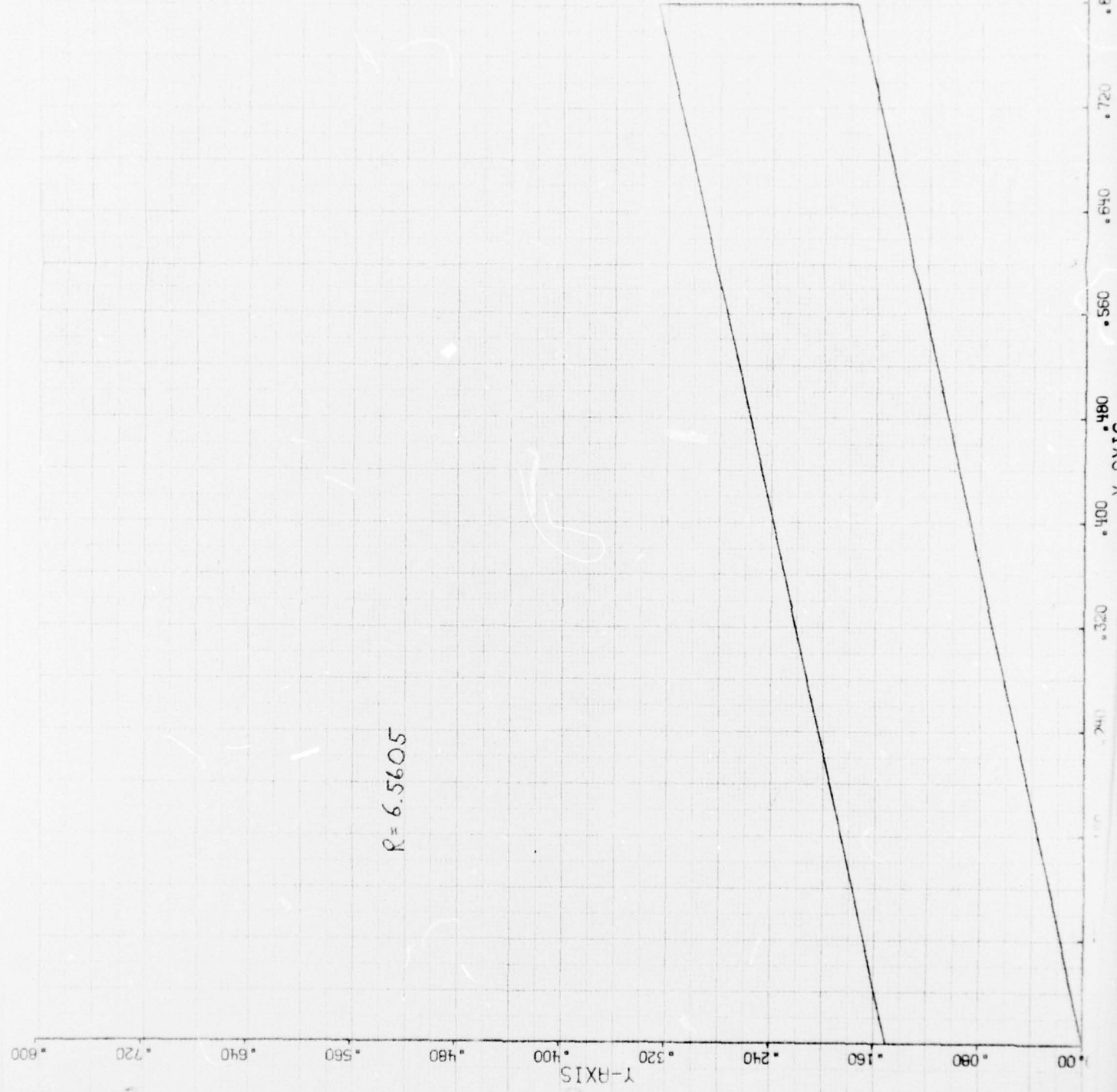
C-15



C-16



C-18



C-19

6.6355 * 1204 390, 5000 4594, 8000 1014, 8000
 6.3500 * 1204 390, 5000 4594, 8000 1014, 8000

INPUT FLEXIBILITY ALPHAS ARE ALREADY COMPUTED FOR ALL RADIUSES

STATISTICS ARE REQUESTED

RADIUS	Z MIN L.E.	Z MAX L.E.	Z MIN T.E.	Z MAX T.E.	ALPHA
8.44	* 000270	* 003930	* 000440	* 002230	45.400000
8.122	* 000560	* 005800	* 000750	* 003510	45.400000
7.900	* 001010	* 001160	* 001160	* 004800	29.804920
7.479	* 001660	* 010820	* 001670	* 006870	22.416030
7.157	* 002540	* 014160	* 002550	* 009690	15.453880
6.836	* 003680	* 016240	* 003030	* 013430	10.439260
6.835	* 023500	* 07100	* 023500	* 063100	14.971000
6.705	* 022600	* 069700	* 02600	* 056500	14.625000
6.350	* 002947	* 017200	* 002947	* 015800	13.439000
6.350	* 002947	* 017200	* 002947	* 015800	13.439000

7.479	-1.51402
7.157	-0.74256
6.856	-0.40071
6.435	-0.07504
6.705	+0.19305
6.350	+2.36244
6.350	+2.36244

-1.51402	-2.231905
-0.74256	-2.209928
-0.40071	-1.62731
-0.07504	-0.24077
+0.19305	+0.24096
+2.36244	+0.15903
+2.36244	+0.15903

ROTATING SPEED = 3000.0 CPS.

RADIUS	ACTUAL CENTRIFUGAL FORCE AND STRESS VS. RADIUS AT THIS ROTATING SPEED	
	CENTRIFUGAL FORCE (LBS.)	CENTRIFUGAL STRESS (PSI.)
6.4435	0.0000	0.0000
6.1219	244.1544	6526.7312
7.8003	671.1096	16912.5519
7.4787	1156.6756	14659.2352
7.1571	1736.6289	17413.9744
6.8355	2456.6611	19870.2967
6.5545	2661.6894	6482.5612
6.7050	3347.6774	9093.5006
6.6355	5796.1259	31469.9125
6.3500	4916.4321	356693.5205

C-22

THE COMPUTER IS TAKING FIVE STEPS OF (.1 CPS) STARTING AT 200.0 CPS. (STEP = 50.000, PLATEAU)

FREQUENCY NO. 1 AT THE 300.0 CPS SPEED = 1100.5 CPS. (STEP = -2.7622E-10)

$$\frac{1609.6 \text{ CPS}}{16000 \text{ CPS}} = 6.0H$$

RADIUS	TANGENTIAL MODE SHAPES	SPECIFICATIONS
6.4435	1.00000	0.00041
6.1219	1.625627	0.00124
7.8003	9.72752	0.00205
7.4787	4.61034	0.00240
7.1571	7.95955	0.00355
6.8355	7.56644	0.00354
6.5545	5.54747	0.00375
6.7050	5.52525	0.00341
6.3500	1.12562	0.00045

2, 55)

• 0.00025

• 0.00000

• 0.00005

RADIUS	MODE N	SHAPES
6.444	0.00000	• 0.00000
8.122	• 0.99995	• 296149
7.600	• 0.00011	• 250648
7.479	• 0.00025	• 201450
7.157	• 0.00043	• 180905
6.836	• 0.00065	• 132619
6.835	• 0.00065	• 132507
6.705	• 0.00075	• 130244
6.350	• 0.00105	• 000000
6.350	• 0.00105	• 000000

AXIAL EDGE SHAPES

STRAIN	DEFLLECTIONS
• 0.00011	• 112406
• 0.00052	• 512755
• 0.00052	• 223770
• 0.00052	• 150447
• 0.00052	• 091751
• 0.00055	• 044155
• 0.00055	• 044012
• 0.00075	• 026645
• 0.00105	• 000000
• 0.00105	• 000000

INTEGRATION RESULTS

$$S_x = 236314.3530 \quad S_y = -36946.4747 \\ \text{INTEGRAL OF } Y_x = -58.1282 \quad \text{INTEGRAL OF } Y_y = 58.1282 \\ \text{SUM OF INTERVALS} = 0.726$$

No. IUS

LEADING EDGE RELATIVE	LEADING EDGE VIBRATORY	TRAILING EDGE RELATIVE	TRAILING EDGE VIBRATORY
0.444	0.00000	0.00000	0.00000
8.122	• 0.016270	• 0.015655	• 3609.587478
7.800	• 0.042246	• 0.040724	• 9625.732545
7.479	• 0.059847	• 0.053074	• 14405.277486
7.157	• 0.070353	• 0.078776	• 18615.967458
6.836	• 0.074900	• 0.088472	• 20407.184905
6.835	• 0.011544	• 0.011696	• 2763.954577
6.705	• 0.013804	• 0.013939	• 3294.066759
6.350	• 0.149714	• 0.149401	• 35505.692242
6.350	• 0.149714	• 0.149401	• 35505.692242

C-23

LOOKING FOR FREQUENCY NO.	2 AT THE	300.000 RPS. ROTATING SPEED
FREQUENCY NO. 2 AT THE 300.000 RPS. SPEED = 6467.4642 CPS. (ABSOLUTAL = 5.054415)		

TANGENTIAL MODE SHAPES

RADIUS	DEFLECTIONS
8.444	1.000000
8.122	0.999959
7.800	0.999976
7.473	0.999961
7.157	0.999957
6.836	0.999962
6.835	0.999962
6.705	0.999965
6.350	0.999983
6.350	0.999983

MOMENT/E	SLOPES
0.000000	0.981152
0.000086	0.791182
0.000309	0.500965
0.000638	0.269526
0.001058	0.129436
0.001484	0.049951
0.001485	0.049830
0.001675	0.043169
0.002218	0.000000
0.002218	0.000000

RADIUS	DEFLECTIONS
8.444	0.999972
8.122	0.999969
7.800	0.999968
7.473	0.999967
7.157	0.999967
6.836	0.999967
6.835	0.999967
6.705	0.999967
6.350	0.999967
6.350	0.999967

AXIAL MODE SHAPES	SLOPES
0.000000	0.814056
0.000086	0.513954
0.000309	0.289876
0.000638	0.151002
0.001058	0.072330
0.001484	0.029690
0.001485	0.029619
0.001675	0.021704
0.002218	0.000000
0.002218	0.000000

INTEGRATION RESULTS
 SXE = 20441.2972
 INTEGRAL OF YE = 6.6660
 INTEGRAL OF XE = 15.3209
 SE = -11547.3917
 INTEGRAL OF F = 0.000000
 SYE = 6895.9055
 INTEGRAL OF VYE = 0.0146

RADIUS	PLATE STRESS CALCULATIONS	TRAILING EDGE	LEADING EDGE	RELATIVE	VIBRATORY	TRAILING EDGE	STREAM
8.444	0.000000	0.000000	0.000000	0.000000	1.069	0.440116	0.000000
8.122	-0.151043	-0.092617	-0.141537	-0.141537	1.634	3.84679	1.069
7.800	-0.246192	-0.095690	-0.052555	-0.052555	1.116	5.16335	1.634
7.473	-0.252559	-0.1607	-0.17740	-0.17740	0.60	6.77017	1.116
7.157	-0.161697	-0.175615	-0.19179	-0.19179	-1.359	5.92801	0.60
6.836	-0.074427	-0.242120	-0.242120	-0.242120	-2.21	4.65759	-1.359
6.835	-0.074299	-0.240667	-0.240667	-0.240667	-3.24	4.226249	-2.21
6.705	-0.026060	-0.245344	-0.245344	-0.245344	-2.632	4.020596	-3.24
6.350	-0.039907	-0.245344	-0.245344	-0.245344	-2.632	4.020596	-2.632
6.350	-0.039907	-0.245344	-0.245344	-0.245344	-2.632	4.020596	-2.632

LOOKING FOR FREQUENCY NO. 3 AT THE 300,000 RPS. ROTATING SPEED
 FREQUENCY NO. 3 AT THE 300,000 RPS. SPEED = 7822.0126 CPS. RESIDUAL = -7.4107 -1.4

TANGENTIAL MODE SHAPES

RADIIUS	MOMENT/E	SLOPES	DEFLECTIONS	SPLIT AREA/E
6.444	0.000000	1.000000	-536591	-0.01264
6.122	0.000083	-0.51531	-224393	-0.00542
7.800	0.00252	-0.536766	-0.014049	-0.00514
7.479	0.000414	-1.92991	-1.34918	-0.00217
7.157	0.000483	-0.74573	-0.157637	-0.00215
6.836	0.000419	-0.234760	-0.102955	-0.00375
6.655	0.000419	-0.234962	-0.192715	-0.00586
6.705	0.000347	-0.239144	-0.071261	-0.00934
6.350	0.000028	-0.000000	-0.000000	-0.00934
6.350	0.000028	-0.000000	-0.000000	-0.00934

AXIAL MODE SHAPES

RADIIUS	MOMENT/E	SLOPES	DEFLECTIONS	SPLIT AREA/E
6.444	0.000000	-345801	-0.061669	-0.00030
6.122	0.000010	-220363	-0.157235	-0.00225
7.800	0.000083	-0.43115	-0.195532	-0.00551
7.479	0.000260	-0.68898	-0.175499	-0.00933
7.157	0.000557	-1.40644	-0.125067	-0.01274
6.836	0.000961	-1.34536	-0.066045	-0.01576
6.635	0.000962	-1.34489	-0.065691	-0.01514
6.705	0.001156	-1.31050	-0.046747	-0.01740
6.350	0.001765	0.000000	0.000000	-0.01740
6.350	0.001765	0.000000	0.000000	-0.01740

INTEGRATION RESULTS

INTEGRAL OF X	S = 11765.1820	SX = 14472.4861	INTEGRAL OF Y = 7.8752	INTEGRAL OF Y = 1.4732	SUM OF INTEGRALS =	SY = -2707.3042
---------------	----------------	-----------------	------------------------	------------------------	--------------------	-----------------

RADIUS	LEADING EDGE RELATIVE	BLADE STRESS CALCULATIONS	TRAILING EDGE RELATIVE	TRAILING EDGE VIBRATORY
--------	-----------------------	---------------------------	------------------------	-------------------------

DISTRIBUTION LIST

LCDR W. R. Seng (3)
Scientific Officer
Office of Naval Research
Code 473
800 N. Quincy Street
Arlington, VA 22217

Commander, Defense Contract Admin. (1)
Services District, Hartford
96 Murphy Road
Hartford, CT 06114

Director, Naval Research Lab. (6)
Attn: 2627
Washington, DC 20375

Office of Naval Research (6)
Department of the Navy
Attn: Code 102 IP
Arlington, VA 22217

Commanding Officer (1)
Office of Naval Research Branch Office
495 Summer Street
Boston, MA 02201

United States Naval Post Graduate School (1)
Dept. of Mechanical Engineering
Attn: Dr. R. H. Nunn
Monterey, CA 93940

Defense Advanced Research Projects Agency (1)
Director of Tactical Technology
Attn: Dr. Robert Moore
1400 Wilson Blvd.
Arlington, VA 22209

Defense Advanced Research Projects Agency (1)
Attn: CAPT Cox
1400 Wilson Blvd.
Arlington, VA 22209



Westinghouse

DISTRIBUTION LIST (Continued)

United States Coast Guard Research & Technology (1)
Attn: CAPT D. B. Flanagan
400 7th Street SW
Washington, DC 20590

Dr. Larry W. Noggle (1)
ASD/XRD
Wright Patterson AFB
Dayton, OH 45402

Mr. Robert Ziem (1)
Director Defense Research & Engineering
Pentagon 3D1089
Washington, DC 20350

Mr. James Remson (1)
Headquarters, Naval Material Command
(MAT) 033
Washington, DC 20360

Mr. Zel Levine, Director (1)
Office of Advanced Ship Development
Department of Commerce
Maritime Administration
Rm. 4610, Code 920
14th & E. Streets, NW
Washington, DC 20230

Mr. Frank Welling (1)
NSEC, 201
Center Building
3700 East-West Highway
Prince Georges Plaza
Hyattsville, MD 20782

Mr. H. D. Marron (1)
NSEC, 202
Center Building
3700 East-West Highway
Prince Georges Plaza
Hyattsville, MD 20782

DISTRIBUTION LIST (Continued)

Dr. Robert Allen (1)
David W. Taylor
Naval Ship Research & Development Center
Code 012
Bethesda, MD 20084

Dr. Earl Quandt (1)
David W. Taylor
Naval Ship Research & Development Center
Code 272
Annapolis, MD 21402

Dr. F. R. Riddell (1)
Institute for Defense Analyses
Room 9A11
400 Army & Navy Drive
Arlington, VA 22202

Mr. Charles Miller (1)
Naval Sea Systems Command 03
Crystal City
National Center No. 3
Washington, DC 20360

United Technologies Research Center (1)
Attn: Dr. Simion C. Kuo
East Hartford, CT 06108

Mechanical Technology Incorporated (1)
Attn: Mr. Tom Ivsan
968 Albany-Shaker Road
Latham, NY 12110

General Atomic Company (1)
Attn: Dr. Leon Green
Suite 709
2021 K Street, NW
Washington, DC 20002



Westinghouse

DISTRIBUTION LIST (Continued)

Defense Documentation Center (12)
Bldg. No. 5, Cameron Station
Alexandria, VA 22314